

Alma Mater Studiorum – Università di Bologna

DOTTORATO DI RICERCA IN  
SCIENZE DELLA TERRA

Ciclo: XXXI

**Settore Concorsuale di Afferenza: 04/A1**

**Settore Scientifico Disciplinare: GEO/08**

Geochemistry of C-bearing gas compounds in natural fluids under crustal  
conditions: insights into deep and shallow processes

**Presentata da:** Andrea Ricci

**Coordinatore Dottorato**

Prof. Giulio Viola

**Supervisore**

Dr. Stefano Cremonini

**Co-supervisori**

Prof. Franco Tassi

Prof. Orlando Vaselli

Prof. Jens Fiebig

**Esame finale anno 2019**



# Abstract

The PhD research project was aimed to improve the scientific knowledge of the origin and fate of C-bearing gas compounds released from active volcanoes, hydrothermal systems and tectonically active sedimentary basins. The first goal was to investigate the primary source(s) of CH<sub>4</sub> and light hydrocarbons in volcanic-hydrothermal gases under crustal conditions. This objective was achieved by comparing the composition of low molecular weight organic fraction (C<sub>1</sub>-C<sub>4</sub>) and associated CO<sub>2</sub> and H<sub>2</sub>O in fumarolic gases and geothermal wells from different study areas around the world. We demonstrated that these hydrocarbons derive from biotic sources, i.e., predominantly from the thermal decomposition of organic matter. Meteoric waters and seawater circulating through the crust shuttle organic matter from Earth's surface into the reservoir rocks. There, high temperature pyrolysis of organic matter and open system degassing generates n-alkanes with isotopic compositions previously classified as being indicative for abiogenesis. These results led us to question the dogma of crustal production of abiotic hydrocarbons and highlighted the potential of n-alkanes to become sensitive indicators of life on habitable (exo)planets. The second goal was to study the secondary processes affecting the composition of CO<sub>2</sub>, CH<sub>4</sub> and light hydrocarbons in natural fluids during their uprising from the deep reservoirs to the surface in different geologic setting, ranging from active volcanoes to sedimentary basins. Under magmatic-hydrothermal conditions, catalytic organic reactions may strongly affect volatile organic compounds, drastically changing alkanes-alkenes-aromatics relative abundances and isotopic composition of C<sub>1</sub>-C<sub>4</sub> hydrocarbons. At peripheral areas of volcanic systems and tectonically active sedimentary basins, composition of CO<sub>2</sub> and CH<sub>4</sub> in interstitial soil gases and dissolved gases in groundwater are mainly controlled by supergene mechanisms, such as calcite precipitation and microbial-driven processes. These secondary processes likely play a major role in regulating the ultimate release of C-bearing gas compounds into the atmosphere.



# Contents

<b>1 Introduction</b> .....	<b>1</b>
<b>2 Origin and fate of C-bearing gas compounds in Earth's crust</b> .....	<b>9</b>
2.1 Introduction .....	9
2.2 Carbon species in Earth degassing .....	9
2.3 Origin of hydrocarbons: geological sources and processes .....	12
2.3.1 Thermogenic hydrocarbons from deep environment .....	12
2.3.1.1 Thermal cracking .....	14
2.3.1.2 Catalytic reforming .....	16
2.3.2 Abiotic hydrocarbon formation in crustal environments .....	22
2.3.2.1 Chemical and physical conditions for hydrocarbon formation in the crust .....	25
2.3.2.2 Synthesis of hydrocarbons by Fischer-Tropsch-type reactions: evidences from hydrothermal experiments .....	28
2.3.2.3 Isotopic fractionation during FTT synthesis. ....	36
2.3.2.4 Implications for abiotic hydrocarbon formation by FTT synthesis within the crust. ....	39
2.3.3 Alternative pathways for hydrocarbon formation in the crust .....	41
2.4 Biogenic processes .....	45
<b>3 Abiotic hydrocarbons in the Earth's crust: a phantom</b> .....	<b>49</b>
<b>4 Extreme isotopic and chemical variations in light hydrocarbons in magmatic and hydrothermal gases from Vulcano Island (southern Italy): insights into deep source(s) and post-genetic processes</b> .....	<b>74</b>

<b>5 Fractionation processes affecting the stable carbon isotope signature of thermal waters from hydrothermal/volcanic systems: the examples of Campi Flegrei and Vulcano Island (southern Italy)</b> .....	<b>121</b>
<b>6 Carbon isotopic signature of interstitial soil gases reveals the potential role of ecosystems in mitigating geogenic greenhouse gas emissions: Case studies from hydrothermal systems in Italy</b> .....	<b>133</b>
<b>7 Methane in groundwaters of Emilia Plain (northern Italy): sources and sinks</b> .....	<b>145</b>
<b>8 Conclusions</b> .....	<b>208</b>
<b>References</b> .....	<b>211</b>

# 1 Introduction

Carbon displays remarkable chemical flexibility and thus is unique in the diversity of its biogeochemical roles. Carbon has the ability to bond to itself and to more than 80 other elements in a variety of bonding topologies, most commonly in 2-, 3-, and 4-coordination. With oxidation numbers ranging from  $-4$  to  $+4$ , carbon is observed to behave as a cation, as an anion, and as a neutral species in phases with an astonishing range of crystal structures, chemical bonding, and physical and chemical properties. This versatile element concentrates in dozens of different Earth repositories, from the atmosphere and oceans to the crust, mantle, and core, including solids, liquids, and gases as both a major and trace element (Holland, 1984; Berner, 2004; Hazen et al., 2012).

The origin of carbon on Earth, similar to many other volatile elements, is debated (Marty et al., 2013). Although carbonaceous chondrite is commonly used as the model for the terrestrial building block because of their compositional similarities with the solar photosphere (Lodders, 2003), geochemical arguments for other types of chondrites and non-chondritic compositions, likely with quite different and lower abundance of carbon, also exist in modern literature (e.g., Alard et al., 2000; Javoy et al., 2010; Caro, 2011; Warren, 2011; Campbell and O'Neill, 2012; Morbidelli et al., 2012). The key information on the fate of carbon during early Earth differentiation is how the element was partitioned between various reservoirs: core, mantle (magma ocean), and proto-atmosphere. Magma ocean processes must have set the initial distribution of carbon and conditions for further development of Earth's deep carbon cycle and have forced Earth to evolve differently compared to the planet Mars (Kuramoto, 1997). The carbon cycle post magma ocean crystallization was modulated by the thermal vigor of solid state convection and plate tectonic cycles. The most important potential consequences of plate tectonics on carbon cycle relate to subduction of carbon, notably carbon-rich sediments. The sequestration of carbonates and organic matter has undoubtedly played, and continues to play, a major and evolving role in Earth's carbon cycle (Hayes and Waldbauer, 2006; Kah and Bartley, 2011; Dasgupta, 2013). Plate tectonic cycle also generated, for the first time, buoyant continental crust that resulted in substantial amounts of subaerially exposed crust, as well as potentially extensive shallow marine continental shelves. The evolution of Earth's near-surface carbon mineralogy is intertwined with the origin and evolution of life. In this respect, the co-evolving geosphere and biosphere transformed Earth

through three main episodes: (i) the emergence of chemolithoautotrophic microbial communities, (ii) the rise of photosynthetic organisms and finally (iii) the innovation of skeletal biomineralization.

The onset of plate tectonic and the emergence of life strongly shaped dynamics and timing of the global carbon cycle. Dasgupta (2013) argued that the upper mantle geotherm of the past billion years is sufficiently cool for subducted carbonates to remain largely sequestered in the mantle; a situation that contrasts with prior eons of Earth history. Burton et al. (2013), cataloging all known volcanic emissions of carbon and concluded that these varied sources collectively represent only a small fraction of the carbon that is being subducted. Taken together, these observations suggest a possibly dramatic Phanerozoic increase in the amount of subducted carbon that remains sequestered in the mantle. The geologic history of Earth led to the concentration of carbon into reservoirs interconnected by pathways of exchange. Subduction is considered as a factory for the recycling of elements such as carbon between the Earth's interior and surface, linking the shallow and the deep carbon cycle. Presently, the major reservoirs of carbon at the surface of our planet are carbonates in marine and continental sedimentary rocks, reduced carbon in the biosphere and in fossil hydrocarbons, dissolved inorganic carbon in the oceans and gaseous C species, notably CO<sub>2</sub>, in the atmosphere. Carbonates occur as continental massive units from ancient oceanic platforms, as oceanic sediments, and as veins and alteration phases in the oceanic crust (Hazen et al., 2013). The amount of reduced carbon is lower than the carbonate reservoir by about a factor of ~4 to 5. Current estimates of the total amount of carbon at Earth's surface are around  $7-11 \times 10^{21}$  moles (Ronov and Yaroshevskiy, 1976; Javoy et al., 1982; Holser et al., 1988; Hayes and Waldbauer, 2006).

Throughout Earth's crust and upper mantle, fluids play the dominant role in transporting and concentrating Earth's energy and chemical elements (Liebscher and Heinrich, 2007). Furthermore, the flux of fluids, which act as both reaction media and reactants, strongly influences the genesis and evolution of different rocks. Among the different types of fluids, those containing volatile carbon, hydrogen and oxygen (C-H-O) species tend to dominate in the lithosphere. Carbon can be a major constituent of crustal and mantle fluids, occurring both as dissolved ionic species (e.g., carbonate ions or organic acids) and molecular species (e.g., CO<sub>2</sub>, CO, CH<sub>4</sub>, and more complex organic compounds). The chemistry of dissolved carbon changes dramatically with pressure (P) and temperature (T). In aqueous fluids at low P and T, molecular carbon gas species such as CO<sub>2</sub> and CH<sub>4</sub> saturate at low concentration to form a separate phase. With modest increases in P and T, these molecular species become fully

miscible with H<sub>2</sub>O, enabling deep crustal and mantle fluids to become highly concentrated in carbon. At such high concentrations, carbon species play an integral role as solvent components and, with H<sub>2</sub>O, control the mobility of rock-forming elements in a wide range of geologic settings. The mobility of C species from deep reservoirs to shallow environments on Earth supply pre-biotic molecules and nutrients to the biosphere, to gas reservoirs and to the atmosphere and oceans. Hence, the migration of carbon-bearing crustal and mantle fluids contributes to Earth's carbon cycle; however, the mechanisms, magnitudes, and time variations of carbon transfer from depth to the surface remain least understood parts of the global carbon budget (Berner 1991, 1994; Berner and Kothavala, 2001). At crustal conditions, carbon-bearing gas compounds can be primarily produced by geological and biological processes. Magma degassing and carbonates metamorphism are both geogenic sources of C gas species mainly in the form of CO<sub>2</sub>. On the contrary, thermal decomposition of sedimentary organic matter produces CH<sub>4</sub> and volatile organic compounds and only minor amounts of CO<sub>2</sub> during the early stages of kerogen's evolution via decarboxylation of pre-existing carboxylic acids. Recent observations of hydrocarbons emanating from non-sedimentary systems (abiogenic), such as mid-ocean ridge hydrothermal systems or occurring within some crystalline rock-dominated Precambrian shield environments have challenged the view that organic rich sediments provide the only significant source of crustal hydrocarbons (Potter and Konnerup-Madsen, 2003; Sleep et al., 2004; Sherwood Lollar et al., 2006; McCollom, 2013; Sephton and Hazen, 2013). Geopressured-geothermal regimes contain C-H-O fluids with vast energy potential in the form of methane and hot water at high pressure. Even fluid inclusions from both metamorphic and igneous terrains record the presence of methane-bearing fluids reflecting reduced redox state conditions of formation. It is becoming increasingly clear that organic molecules present as gas species, in aqueous and volatile fluids play major roles in controlling geochemical processes, not just at Earth's surface, but also deep within the crust. Biosphere heavily shapes the global carbon cycle, being the source of CO<sub>2</sub> and CH<sub>4</sub> by plant and animal respiration and methanogenesis, respectively. Methanogenic microbial consortia have been found at basinal temperatures up to 75 °C and down to 3 km depth (Rice and Claypool, 1981; Inagaki et al., 2015). Biogenic gases are produced ubiquitously in near-surface environments (Rice and Claypool, 1981; Faiz and Hendry, 2006) and can commingle with geogenic gases, forming gas of mixed origin. A grand challenge in carbon sciences is developing criteria to accurately discriminate between biogenic and abiogenic processes. In ecosystems near the limits of habitability some of the classical discriminants for life, e.g. organic carbon compounds, are also potentially produced

by abiotic processes (Sephton and Hazen, 2013). Due to the overlap of biogenic and abiogenic processes, and complex physiological adaptations of microbial populations (e.g. under carbon limitation), several geologic contexts present a challenge to deciphering biogenic from abiogenic carbon sources.

Once formed through geological or biological processes in the subsurface, C-bearing gas compounds such as CO<sub>2</sub> and CH<sub>4</sub> may be transported within the Earth's crust as a free gas phases or dissolved in water, forming secondary carbon reservoirs, fostering shallow biosphere and ultimately being released into the atmosphere. Upon leaving the formation zone, C species may experience post-genetic processes during their geologic pathways throughout the crust, such as: dissolution of CO<sub>2</sub> into shallow aquifers and subsequent carbon segregation in carbonate minerals (e.g. Inguaggiato et al., 2005; Chiodini et al., 2015), microbial oxidation of methane in oxic and anoxic environments by methanotrophic activity (e.g. Templeton et al., 2006; Sivan et al., 2007) and biodegradation of C<sub>2+</sub> volatile organic compounds (e.g. Alexander, 1994). Accordingly, the chemical speciation of carbon in natural gas samples is the result of source and supergene processes and information about the primary source (genetic mechanism and physico-chemical conditions) can be totally or partially preserved or completely altered by secondary phenomena. The comprehension of both (i) the primary processes on C-bearing gas compounds occurring in deep reservoirs at crustal conditions and (ii) the secondary processes occurring during the uprising of fluids toward the surface, are crucial for a reliable estimation of the global carbon budget.

The latter processes have a limited effect on the pristine fluid composition when the uprising of the deep-originated C species is relatively fast. Hence, gases from high-flux natural emissions may be considered the best proxy of the deep reservoirs. However, CO<sub>2</sub>, CH<sub>4</sub> and light hydrocarbons are emitted not only through punctual degassing vents, but also diffusively through the Earth surface. Soil diffuse degassing significantly contributes to the atmospheric emissions of carbon (e.g. Cardellini et al., 2003; Chiodini et al., 2004; Granieri et al., 2010; Viveiros et al., 2010; Tassi et al., 2013). The chemical features of C species in interstitial soil gases from diffuse degassing areas are likely controlled by secondary processes as fluids are uprising towards the surface. Gas fluxes from soil, depending on the pressure gradient, and on the structure, porosity and permeability of the media encountered during the ascent towards the surface (e.g. Cardellini et al., 2003; Chiodini et al., 2010), is orders of magnitude lower than those characterizing punctual discharges (e.g. Aiuppa et al., 2013). Thus, it is reasonable to suppose that the composition of the gases released as diffuse emissions significantly depends on chemical and physical processes (e.g. oxidation reactions, water vapor

condensation, interactions with shallow aquifers), favored by the strong changes in physico-chemical conditions, which are particularly effective when fluids slowly approach the surface, i.e. within the soil (Tassi et al., 2013). Similarly, secondary processes driven by microorganisms (Bacteria and Archaea), inhabiting soils and aquifers at shallow depths, may affect the C-bearing compounds of fluids (e.g. Huber et al., 2000; Norris et al., 2002; D'Alessandro et al., 2011; Gagliano et al., 2014). The establishment of pathways of fluid migration in natural environments is particularly effective in volcanic and tectonic areas where structural configuration allows fluid channeling along faults and fracture enhancing the transport speed of carbon from deep to shallow reservoirs.

Investigating the geochemistry of C-bearing gas compounds in natural fluids can shed light on their origin and evolution and on the history of the transporting media but many aspects are still pending a solution. For example, based on the  $\delta^{13}\text{C}$  and  $\text{CO}_2/{}^3\text{He}$  ratios measured in volcanic gases from convergent plate boundaries volcanic centers, Sano and Marty (1995) inferred that up to 20 % of the carbon is derived from a MORB-type source, while the major fraction of the gases has been attributed to  $\text{CO}_2$  produced by decarbonation of subducted marine limestone slab carbonate. However, shallow processes such as mixing of deep gases with meteoric water and calcite precipitation may strongly mask the deep  $\delta^{13}\text{C}$ - $\text{CO}_2$ , making deciphering the origin of  $\text{CO}_2$  in volcanic contexts a challenging task. In the last decades organic geochemistry has been extensively used in order to unravel the sources of methane and light hydrocarbons in natural fluids. It has been generally presumed that thermogenic, biogenic, and abiogenic hydrocarbons should differ in their carbon isotopic composition. Typical reference values of  $\delta^{13}\text{C}$  ( $\text{CH}_4$ ) are -70‰ to -60‰ for a biological production, -60‰ to -40‰ for a thermogenic origin, -30‰ to -20‰ for geothermal hydrocarbons, and -20‰ to -5‰ for MORs (Schoell, 1988; Bradley and Summons, 2010), but this division is being debated (e.g., Sherwood Lollar and McCollom, 2006; Ueno et al., 2006a, 2006b). As for hydrocarbon gases ( $\text{C}_1$ - $\text{C}_4$ ), it has been suggested that a slight decrease in  $\delta^{13}\text{C}$  with increasing carbon number could be an indication of an abiotic catalytic formation, while a thermogenic origin has always shown a strongly positive correlation (Des Marais et al., 1981; Sherwood Lollar et al., 2002; Pan et al., 2006). This isotope reversal trend has been attributed to kinetic isotope fractionation effects during surface-catalyzed polymerization reactions of methylene units (e.g., Schoell, 1983; Jenden, 1993; Fu et al., 2011). As the trend is weak to almost flat, it was even suggested that no fractionation occurs during polymerization. However, hydrocarbon gases produced experimentally via abiogenic reactions do not consistently produce inverse or flat trends, and results are rather heterogeneous (e.g.,

McCollom and Seewald, 2006; Fu et al., 2007; Taran et al., 2007, 2010a; McCollom et al., 2010). Experiments reported in the literature to date were carried out under various physical and chemical conditions. This definitely indicates that carbon isotope fractionation of hydrocarbons is controlled by their formation processes and kinetics, which in turn may differ according to temperature, pressure, and redox conditions (McCollom and Seewald, 2006; Fu et al., 2011). Whether the experiments were conducted in a gas and/or water phase and in a closed or flow-through reactor are other possible influencing factors. In addition, several thermogenic gases do show reversals of the kind attributable to abiotic reactions (e.g., Burruss and Laughrey, 2010). The reverse or flat trend has generally been observed for hydrocarbon gases in ultramafic-hosted hydrothermal systems and terrestrial volcanic-hydrothermal systems, but no clear evidence of their abiogenic origin has been brought forth (Proskurowski et al., 2008; Charlou et al., 2010). Clearly, it will be even more difficult to determine the origin of longer n-alkanes and other organic compounds detected in natural fluids from non-sedimentary environments. Notwithstanding the complexity of carbon cycle, understanding the mechanisms and rates of C-bearing gas compounds formation and alteration under crustal conditions is very promising not only for geochemical studies, but also in the framework of industrial applications and green chemistry (Shipp et al., 2014) and it opens fascinating and appealing perspectives in studies on the origin of life on the Early Earth and astrobiology (e.g. Wächtershäuser, 1988; Russel and Martin, 2004; Sherwood Lollar, 2004; Williams et al., 2005).

The current PhD project was aimed to improve the scientific knowledge of the origin and fate of C-bearing gas compounds released from active volcanoes, hydrothermal systems and tectonically active sedimentary basins, covering most of the issues previously described. In the framework of the 3-year research project, several sampling campaigns were carried out from different sites. The selection of the study areas was dictated by the need to investigate the geochemistry of carbon-bearing gas compounds under a wide range of conditions and geologic contexts to understand the primary origin and fate of these compounds in the Earth's crust. Sampling strategies and analytical techniques were adopted in order to determine the chemical and isotopic composition of carbon species in high-flux emissions (fumaroles, boiling and bubbling pools), interstitial soil gases, shallow aquifers and natural gas reservoirs. The first goal was to investigate the primary source(s) of CH<sub>4</sub> and light hydrocarbons in volcanic-hydrothermal gases under crustal conditions. This objective was achieved by comparing the composition of low molecular weight organic fraction (C<sub>1</sub>-C<sub>4</sub>) and associated CO<sub>2</sub> and H<sub>2</sub>O in fumarolic gases and geothermal wells from different study areas around the

world. The second goal was to study the secondary processes affecting the composition of CO<sub>2</sub>, CH<sub>4</sub> and light hydrocarbons in natural fluids during their uprising from the deep reservoirs to the surface in different geologic setting, ranging from active volcanoes to sedimentary basins. The scientific objectives of this thesis are documented within five individual manuscripts, including data already presented at national and international scientific conferences (Appendix B) and published in (or under submission to) peer-reviewed international scientific journals (Appendix A). The results of these studies are presented and discussed in chapters 3-7.

The first manuscript (submitted to *Nature Geoscience*) investigates the primary origin of methane and light normal-alkanes in hydrothermal gases associated to subaerial volcanic systems. In this context, the origin of the organic fraction was debated, and two main genetic mechanism are often invoked: thermal decomposition of organic matter or abiogenesis. Results suggest that high temperature pyrolysis of organic matter and open system degassing are the processes most likely responsible for the observed chemical and isotopic composition of n-alkanes in hydrothermal gases. Furthermore, our findings challenge the dogma of crustal production of abiotic hydrocarbons.

The second manuscript (in preparation, under internal review) focuses on the primary origin and fate of light hydrocarbons in high-temperature magmatic gases and low-temperature hydrothermal gas emissions discharged at Vulcano Island (southern Italy). Vulcano Island was the perfect case study to investigate the behavior of light hydrocarbons in natural fluids under a wide range of temperatures and redox conditions. Moreover, the primary origin of methane in high temperature magmatic gases has been also studied. Results suggested that secondary processes possibly catalyzed by minerals or inorganic gas species, heavily shape the isotopic composition of the organic fraction, challenging the use of geochemical parameters used commonly to discriminate between biotic and abiotic sources.

The third (published in *Journal of Volcanology and Geothermal Research*) and fourth (published in *Science of Total Environment*) manuscripts investigate the effects of secondary processes on CO<sub>2</sub> and CH<sub>4</sub> in soils affected by hydrothermal alteration and shallow aquifers from Vulcano Island, Solfatara crater (Pozzuoli, southern Italy) and Monterotondo Marittimo (Larderello geothermal field, central Italy). In soils, gas diffusion and microbial activity seemed to highly affect the carbon isotopic composition of CO<sub>2</sub> and CH<sub>4</sub>. While in shallow aquifers, our results suggested that calcite precipitation, affecting hydrothermal fluids during their underground circulation, rather than two endmember biogenic-hydrothermal mixing, is

the process responsible for the observed variations of the  $\delta^{13}\text{C}$  of dissolved  $\text{CO}_2$  and TDIC (Total Dissolved Inorganic Carbon).

The fifth manuscript (in preparation; under internal review) explores the origin and fate of  $\text{CH}_4$  in the Southern Po River Basin, a tectonically active sedimentary basin of central-northern Italy, highlighting the key role of microbial activity in regulating the ultimate release of methane into the atmosphere. In the study area, migration of deep hydrocarbons, enhanced by the structural configuration of the strata, allowed them to reach shallower levels and pervasively contaminate near-surface aquifers. Our geochemical investigation suggested that methane fluxes from shallow aquifers to atmosphere is controlled by the microbial consumption of methane at aerobic conditions by methanotrophic bacteria.

# **2 Origin and fate of C-bearing gas compounds in Earth's crust**

## **2.1 Introduction**

Carbon-bearing compounds are of specific importance to many geochemical processes on Earth and other planets. Not only are volatile species ( $\text{CO}_2$ ,  $\text{CO}$ ,  $\text{CH}_4$  and light hydrocarbons) important components of biological systems, but they might also be a manifestation of deep-seated geologic processes. In this chapter, a compendium of the current state of knowledge about: (i) carbon species in Earth degassing; (ii) genetic mechanisms of hydrocarbons in the deep subsurface under crustal conditions and (iii) biological processes of formation/consumption of C-bearing compounds in shallow environments is presented in order to provide a suitable background to the main topics of this PhD thesis. First, an overview on the main hypotheses about the origin of organic compounds in natural systems is described. These sections, shedding light on processes occurring at depth, are preparatory to the results and discussions presented in the manuscript. Finally, the potential role played by biogenic processes at shallow depth on the origin and fate of C-bearing gas compounds rising toward the surface is discussed through the description of the main microbial metabolic pathways involving these compounds.

## **2.2 Carbon species in Earth degassing**

Earth is unique among the terrestrial planets in our solar system in having a fluid envelope that fosters life. The secrets behind Earth's habitable climate are well-tuned cycles of carbon (C) and other volatiles. While on time-scales of ten to thousands of years the chemistry of fluids in the atmosphere, hydrosphere, and biosphere is dictated by fluxes of carbon between near surface reservoirs, over hundreds of millions to billions of years it is maintained by chemical interactions of carbon between Earth's interior, more specifically the mantle, and the exosphere (Berner, 1999). This is due to the fact that the estimated total mass of C in the mantle is greater than that observed in the exosphere (Sleep and Zahnle, 2001; Dasgupta and Hirschmann, 2010) and the average residence time of carbon in the mantle is between 1 and 4 Ga (Sleep and Zahnle, 2001; Dasgupta and Hirschmann, 2006).

Over long periods of time (~Ma), we may consider the oceans, atmosphere and biosphere as a single exospheric reservoir for CO<sub>2</sub>. The geological carbon cycle describes the inputs to this exosphere from mantle degassing, metamorphism of subducted carbonates and outputs from weathering of aluminosilicate rocks (Walker et al., 1981). A feedback mechanism relates the weathering rate with the amount of CO<sub>2</sub> in the atmosphere via the greenhouse effect (e.g., Wang et al., 1976). An increase in atmospheric CO<sub>2</sub> concentrations induces higher temperatures, leading to higher rates of weathering, which draw down atmospheric CO<sub>2</sub> concentrations (Berner 1991). Atmospheric CO<sub>2</sub> concentrations are therefore stabilized over long timescales by this feedback mechanism (Zeebe and Caldeira, 2008). This process may have played a role (Feulner et al., 2012) in stabilizing temperatures on Earth while solar radiation steadily increased due to stellar evolution (Bahcall et al., 2001). In this context the role of CO<sub>2</sub> degassing from the Earth is clearly fundamental to the stability of the climate, and therefore to life on Earth. Notwithstanding this importance, the flux of CO<sub>2</sub> from the Earth is poorly constrained. The uncertainty in our knowledge of this critical input into the geological carbon cycle led Berner and Lagasa (1989) to state that it is the most vexing problem facing us in understanding that cycle. Notwithstanding the uncertainties in our understanding of CO<sub>2</sub> degassing from Earth, it is clear that these natural emissions were recently dwarfed by anthropogenic emissions, which have rapidly increased since industrialization began on a large scale in the 18th century, leading to a rapid increase in atmospheric CO<sub>2</sub> concentrations. While atmospheric CO<sub>2</sub> concentrations have varied between 190-280 ppm for the last 400,000 years (Zeebe and Caldeira, 2008), human activity has produced a remarkable increase in CO<sub>2</sub> abundance, particularly in the last 100 years, with concentrations reaching ~390 ppmv at the time of writing. This situation highlights the importance of understanding the natural carbon cycle, so that we may better determine the evolution of the anthropogenic perturbation. The main sources of carbon are active and inactive volcanism from arcs and rift zones and metamorphism of crustal carbonates. The main sinks for geological carbon are silicate weathering and carbonation of oceanic crust. Knowledge of both the total magnitude of carbon capture during subduction and carbon released from volcanism and metamorphism would allow quantification of the evolution and relative distribution of volatiles in the crust and mantle (Dasgupta and Hirschmann, 2010). CO<sub>2</sub> released directly from active volcanoes has three main sources, CO<sub>2</sub> dissolved in the mantle, recycled CO<sub>2</sub> from subducted crustal material (e.g., Marty and Tolstikhin, 1998) and decarbonation of shallow crustal material (e.g., Troll et al., 2012). Separating the relative proportions of mantle and crustal carbon is possible through investigation of the isotopic composition of emitted carbon (e.g., Chiodini et

al., 2011) and is increasingly important given that during eruptions magmatic intrusions may interact with crustal material, strongly enhancing the CO<sub>2</sub> output of the volcanic system (Troll et al., 2012), at least temporarily. The magnitude of diffuse mantle CO<sub>2</sub> can also be identified isotopically in mixed metamorphic and magmatic gases using Carbon (Chiodini et al., 2011) or Helium isotopes as a proxy for deep mantle sources in both major fault systems (Pili et al., 2011) and crustal tectonic structures (Crossey et al., 2009). Diffuse CO<sub>2</sub> degassing from both volcanic and tectonic structures is a large contributor to the global geological CO<sub>2</sub> emission, but is difficult to measure due to the large areal extent that may be in play, and the large number of degassing sites throughout the globe. Measuring the CO<sub>2</sub> degassing rates into volcanic lakes and from submarine volcanism have significant technical challenges.

CO<sub>2</sub> is not the only carbon-containing molecule emitted from the Earth. In order of decreasing emitted amounts, CO<sub>2</sub>, CH<sub>4</sub>, CO, OCS and VOCs (*Volatile Organic Compounds*) all contribute to the total carbon budget. Mörner and Etiope (2002) estimated that the global emission of CO<sub>2</sub> from Earth degassing was ~600 million tons of CO<sub>2</sub> per year (Mt/yr, 1 Mt = 10<sup>12</sup> g), with ~300 Mt/yr produced from subaerial volcanism, and another 300 Mt/yr produced from non-volcanic inorganic degassing, mostly from tectonically active areas (Chiodini et al., 2005). For comparison, Cadle (1980) estimated that volcanic activity produces 0.34 Mt/yr of CH<sub>4</sub>. Mud volcanoes in Azerbaijan were estimated to produce ~1 Mt/yr of CH<sub>4</sub>, however the global flux from mud volcanism is not known. Hydrocarbon seepage of CH<sub>4</sub> globally is estimated to produce between 8 and 68 Mt/yr (Hornafius et al., 1999). Etiope et al. (2008) estimated that global CH<sub>4</sub> emissions from geological sources to be 53 Mt/yr, a significant proportion of the geological C output. CH<sub>4</sub> from geological sources is commonly emitted along with minor amounts of higher hydrocarbons and heteroatomic organic compounds. Within this large group of compounds, ethane is the most abundant non-methane hydrocarbon in the atmosphere. Nicewonger et al. (2016) estimated that global geologic emission of ethane was 0.002-0.003 Mt/yr in the Preindustrial era. CO is emitted directly from volcanoes, with a CO<sub>2</sub>/CO ratio that varies between ~10 and ~1000 depending on the oxygen fugacity and temperature of the fluid co-existing with melt prior to outgassing. OCS is also directly emitted within volcanic plumes, but in even smaller relative amounts than CO, typically 1000-10,000:1 for CO<sub>2</sub>: OCS (Mori and Notsu, 1997; Burton et al., 2007; Oppenheimer and Kyle, 2008; Sawyer et al. 2008). OCS is the most abundant S bearing gas species in the atmosphere, contributes to stratospheric sulfuric acid aerosol generation (Crutzen, 1976) and is an efficient greenhouse gas (Brühl et al., 2012). Its budget is dominated by emissions from oceans and anthropogenic processes. From a total global output

of ~1.3 Mt/yr of OCS only 0.03 Mt is estimated to arise from volcanism (Watts, 2000). CS<sub>2</sub> is the final trace carbon gas emission from volcanoes, with a similar flux and chemistry to OCS.

## **2.3 Origin of hydrocarbons: geological sources and processes**

### **2.3.1 Thermogenic hydrocarbons from deep environment**

Deep hydrocarbons include a rich diversity of organic chemical compounds in the form of petroleum deposits, including oil and gas in various reservoirs, bitumen in oil sands, coal and clathrate hydrates. The major gaseous hydrocarbons are the alkanes methane (natural gas, CH<sub>4</sub>), ethane (C<sub>2</sub>H<sub>6</sub>), propane (C<sub>3</sub>H<sub>8</sub>), and butane (C<sub>4</sub>H<sub>10</sub>). Liquid components of petroleum include a complex mixture primarily of linear and cyclic hydrocarbons from C<sub>5</sub> to C<sub>17</sub>, as well as numerous other molecular species, while solid hydrocarbons include such broad categories as paraffin waxes (typically from C<sub>18</sub> to C<sub>40</sub>). Water-based clathrates, also known as gas hydrates or clathrate hydrates, are an important emerging source of deep methane that deserve special notice in the context of deep hydrocarbons. These remarkable crystalline water-cage compounds, which form at low temperatures (< 0 °C) and elevated pressures (> 6 MPa), have potential applications both as a major methane source and as model materials for efficient energy storage (Buffett, 2000; Boswell, 2009; Koh et al., 2009, 2011). “Methane ice,” by far the dominant natural clathrate hydrate mineral, forms in permafrost zones below a depth of ~130 meters and in marine sediments on the outer continental shelves (Max, 2003; Guggenheim and Koster van Groos, 2003; Koh et al., 2011). The extent of methane hydrate is remarkable, with total estimated methane storage of  $2 \times 10^{16} \text{ m}^3$  (Kvenvolden, 1995; Milkov, 2004). Methane ice thus represents a potential energy source that is orders of magnitude greater than the proven traditional natural gas reserves (Allison and Boswell, 2007), and which may exceed the energy content of all known fossil fuel reserves (Kvenvolden, 1995; Grace et al., 2008). It is well established that methane-bearing hydrate clathrates arise from H<sub>2</sub>O-CH<sub>4</sub> fluids subjected to low-temperature and high-pressure (Buffett, 2000; Hyndman and Davis, 1992; Max, 2003), at which conditions an H<sub>2</sub>O framework crystallizes around the CH<sub>4</sub> template molecules. Subsurface methanogenic microorganisms represent one significant source of methane (and to lesser extent low-molecular weight hydrocarbons) generated at relatively low temperatures (Chapelle et al., 2002; D’Hondt et al., 2004; Hinrichs et al., 2006; Jorgensen and Boetius, 2007; Roussel et al., 2008; Schrenk et al., 2010, 2013; Mason et al.,

2010; Menez et al., 2012; Colwell and D'Hondt, 2013). At higher temperatures and pressures, thermal maturation of organic matter followed by migration of hydrocarbons to surficial environments is another important contributor to the formation of reservoirs. The more conventional view of petroleum formation is that it formed when selected aliquots of biomass from dead organisms were buried in a sedimentary basin and subjected to diagenesis through prolonged exposure to microbial decay followed by increasing temperatures and pressures. Oxygen-poor conditions, produced by exhaustion of local oxygen levels by biomass decay and often sustained by physical barriers to oxygen recharge, are obvious enhancers for fossil organic matter preservation and passage into the geosphere. The major organic components in life are large, high molecular weight entities and the most resistant of these units are preserved in sediments, augmented by cross-linking reactions that polymerize and incorporate smaller units into the complex network. The high molecular weight sedimentary organic matter is termed kerogen. It is worth noting that not all of life's organic matter is reflected in kerogen. Even under relatively favorable conditions less than 1% of the starting organism, representing the most resistant chemical constituents, may be preserved (Demaison and Moore, 1980). The chemistry of kerogen depends strongly on its contributing organisms and several different types are formed. Type I forms from mainly algae, Type II from a mixture of algae and land plants, and Type III primarily from land plants. Irrespective of kerogen type, increased temperature and pressure leads to thermal dissociation or "cracking" and produces petroleum. Owing to their intrinsic chemical constitution, Type I and Type II kerogens are predisposed to generate oil while Type III kerogens produce gas. At more extreme temperature and pressures, petroleum can undergo secondary cracking reactions that result in significant quantities of the light hydrocarbons. Petroleum reservoirs often comprise porous and permeable sedimentary rock (Selley, 1985). Resilient compounds derived from plants (lignin) and microbes (long-chain carboxylic acids) progressively transform on burial. There are many pathways for these transformations, and a host of products. Oxidation of organic carbon and decarboxylation of preexisting carboxyl groups in organic matter yield CO<sub>2</sub>. Small organic acids are released during petroleum and coal formation (followed, perhaps, by their decarboxylation). Hydrolytic disproportionation processes transform hydrocarbons. Alkanes, alkenes, alcohols, ketones, aldehydes, and other compounds are generated through aqueous organic transformation reactions. Finally, methane and other small organic compounds are released during the final steps of maturation of organic matter.

Thermogenic processes are a series of reactions involving pre-existing organic compounds and occurring at temperatures >120-150 °C. They refer to both (i) thermal degradation of

large organic molecules (e.g. proteins, lipids, DNA) to smaller and simpler ones and (ii) rearrangement of compounds under high temperature and pressure conditions (Konn et al., 2015). In analogy with processes used in petroleum refining industry, Capaccioni et al. (1993, 1995) referred to these processes as (i) thermal cracking and (ii) catalytic reforming (including polymerization processes).

### ***2.3.1.1 Thermal cracking***

Thermal decomposition of organic matter (or thermal cracking, also referred to as pyrolysis) is considered the most important source of hydrocarbons in the deep subsurface of sedimentary basins. Thermal cracking defines a series of reactions involving the breaking of bonds in organic molecules, i.e. C-C, C-H or C-R bonds (where R refers to any heteroatom, such as O, S, N or halogens, or group of atoms), resulting in the fragmentation of molecules into smaller structures (Capaccioni et al., 1993, 1995; Guéret et al., 1997). The molecule fractionation preferentially occurs by breaking of C-C bonds as the result of the larger dissociation energy of the C-H bonds (Guéret et al., 1997). For instance, the cracking of normal-alkanes, during which the C-C or C-H bonds are broken, leads to the formation of an alkane and/or an alkene (Guéret et al., 1997). Consequently, ethane may decompose to ethene, propane to propene or ethene, butanes to methane, ethane, ethene, propene and 1-butene (Gunter, 1978).

The dissociation reaction is highly endothermic; hence, it requires high temperatures. The standard free energy of formation (Figure 1) provides an indication of the stability of each hydrocarbon molecule. At a given temperature, the most stable compound has the lowest  $\Delta G_f^0$ . The stability of hydrocarbons generally decreases with increasing temperatures, except for ethyne (Figure 1). Methane is the most stable hydrocarbon up to 1300 K, where benzene becomes more stable than methane (Guéret et al., 1997). In fact, the stability of aromatics increases faster as a function of temperature. However, hydrocarbons in Figure 1 are unstable for all T relative to C and H<sub>2</sub>, except for methane and ethane at T lower than 800 K and 400 K, respectively (Guéret et al., 1997).

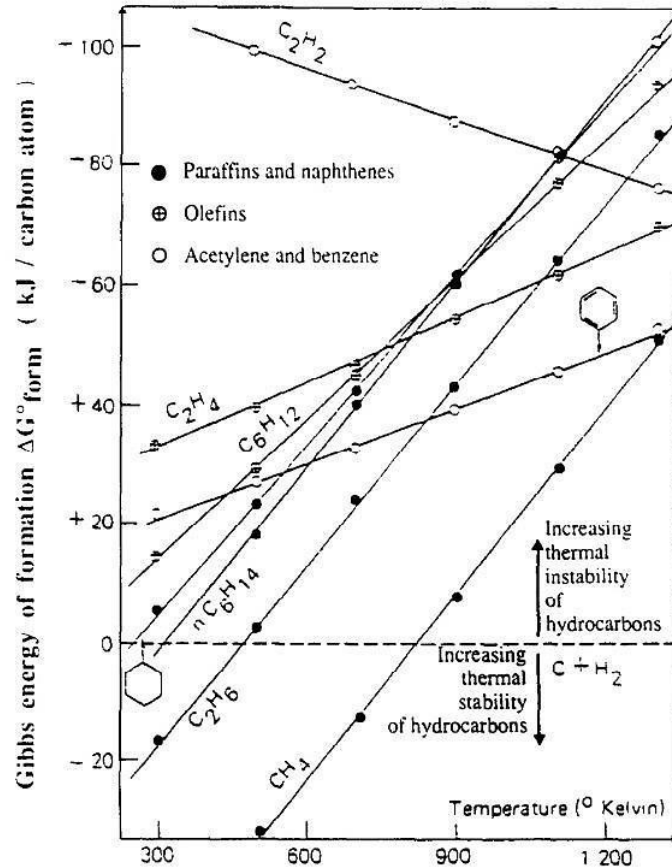


Figure 1: Thermodynamic stability of hydrocarbons (after Guéret et al., 1997). The standard Gibbs energy of formation is related to a carbon atom to facilitate comparison.

To prevent the decomposition of hydrocarbons into C and H the reaction has to be stopped (quenched) at a certain time (or reaction progress), i.e. before C is formed (Holmen et al., 1995; Guéret et al., 1997). The rates of cracking reactions are considered negligible at temperatures below 350 °C (Capaccioni et al., 1995). At temperatures from 150 to 350 °C, catalytic reforming processes prevail (Capaccioni et al., 1995). The traditional paradigm of kerogen-cracking limits the generation of oil-associated gas to the 'oil window' (vitrinite reflectance  $R_o = 0.6$  to  $1.0$  %), whereas the onset of gas generation in the 'gas window' is typically associated with  $R_o$  of  $1.0$  to  $1.3$  % and terminates around  $3.0$  % (Higgs, 1986; Jarvie et al., 2007). However, in a series of laboratory experiments, Wei et al. (2018) were successful in generating large amounts of methane along with minor contents of  $C_2$ - $C_3$  alkanes by long-term heating kerogen-containing rocks at low temperatures (60 and 100 °C). High experimental methane yields, up to 5-11 orders of magnitude higher than those theoretically predicted by kinetic models of hydrocarbons generation, strongly suggest a contribution of catalytic methanogenesis, providing evidences that high amounts of organic

matter can be converted to relatively dry natural gas over tens of thousands of years in sedimentary basins at temperatures as low as 60 °C.

### 2.3.1.2 Catalytic reforming

In reforming processes, catalytic agents, rather than temperature and pressure, play the most important role (Capaccioni et al., 1993). A catalyst is a substance that increases the rate of a chemical reaction by providing an alternative pathway for breaking and making of bonds without undergoing a permanent chemical change itself in the process (Killops and Killops, 2005; Brown et al., 2012). The catalyst partially bonds to the reactants, weakening one or more of the bonds that are to be broken (Killops and Killops, 2005).

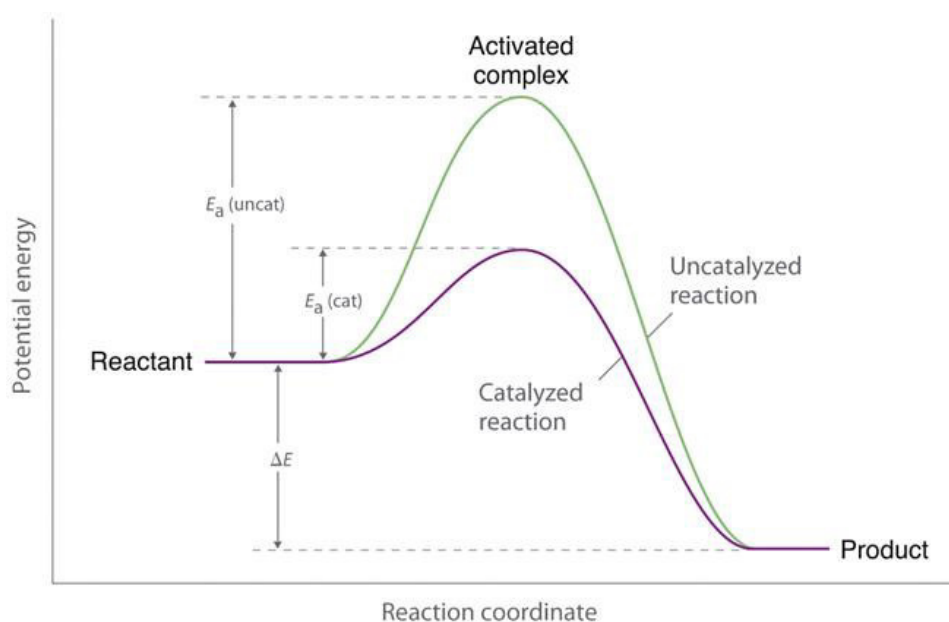


Figure 2: Effect of a catalyst on the activation energy of a reaction

In other words, a catalyst lowers the overall activation energy for a specific chemical reaction (Figure 2), without being involved as a reactant, and allows the reaction to proceed faster. Catalyst may be present in the same phase of the reacting molecules (homogeneous catalyst) or in a different phase (heterogeneous catalyst), usually as a solid in contact with either gaseous or liquid reactants. The distinction between hetero- and homo-catalytic processes is important. While homogeneous catalyzed reactions are subject to the probability (clearly small under dilute conditions) of favorable reactant collision in solution, heterogeneous catalysts scavenge dilute solutions for reactants through surface adsorption, significantly enhancing the reaction rate (Cody et al., 2004). Heterogeneous catalysis usually starts with adsorption of reactants, i.e. reactant molecules bind to the catalyst surface. Adsorption occurs

because atoms and ions at the surface of a solid are extremely reactive as they have unused bonding capability that can be used to bond molecules from the gas or liquid phase to the surface of the solid (Brown et al., 2012). Catalytic agents may enhance a series of structural transformations of organic molecules, including e.g. polymerization (addition to make larger molecules) and many organic functional interconversions (e.g. by condensation, cleavage, cyclization, hydrolysis, oxidation and hydrogenation reactions; Shock et al., 2013 and references therein). An example of catalytic reforming reaction is metathesis, consisting in interconversions among homologues, as follows:



For instance, propene may undergo metathesis reaction to form ethene and butene, by breaking and making C=C double bonds and redistributing carbons to new compounds, as follows:



Other examples include (i) the metathesis of methane, ethane and propane (Mango et al., 2009), as follows:



(ii) the dehydrogenation of alkanes to the corresponding alkenes (Capaccioni et al., 1995), as follows:



The prevailing of catalytic processes as source of organic compounds in gases originated at temperature lower than 350 °C is confirmed by the achievement of thermodynamic equilibrium among light hydrocarbons in natural gases, as argued by Mango et al. (2009). Equilibrium requires the easy exchange of carbon atoms between organic compounds, i.e. C-C and C-H  $\sigma$  bonds broken and reformed with overall bond conservation. This is unlikely in thermal reactions, which are generally under kinetic control and whose products are then far from thermodynamic equilibrium; contrarily, catalytic reactions are often under thermodynamic control and the products may approach a complete equilibrium (i.e. metastable equilibrium; Mango et al., 2009 and references therein). The possibility for organic compounds to approach equilibrium under hydrothermal conditions is a crucial point. If the relative abundances of some compounds were controlled by thermodynamic equilibria (and hence by physical and chemical variables such as temperature, redox, pressure),

measurements of the concentrations of these compounds would be potentially powerful tools for evaluating chemical conditions in subsurface environments (McCollom et al., 2001). The attainment of metastable equilibrium among organic compounds under hydrothermal conditions was demonstrated both theoretically (Shock, 1990b) and experimentally (Seewald, 1994). Empirically, studies on fumarolic gases (Taran and Giggenbach, 2003) have shown that alkane/alkene pairs can approach equilibrium in natural environments and that their relative concentrations in volcanic gases are controlled by reversible reactions, enhancing the use of ethane/ethene and propane/propene pairs as geothermometers (e.g. Capaccioni and Mangani, 2001; Taran and Giggenbach, 2003; Capaccioni et al., 2004; Tassi et al., 2005a,b; Agosto et al., 2013). Hence, the achievement of metastable equilibrium among organic compounds is possible because of the presence of specific catalysts. Organic reactions are known to be catalyzed by a variety of transition metals. Nickel, palladium, copper, rhodium, etc. are commonly used for organic synthesis in technological applications in chemical and refining industry. However, these catalysts are rarely observed in natural environments. Instead, catalytic activity on organic reactions is known to be exerted by both hot water and minerals in hydrothermal systems. Organic hydrocarbons in waters are expected to be rather unreactive. However, the physicochemical properties of water change as temperature increases. In particular, the solvent properties of liquid water (density, dielectric constant) at high temperature become similar to those of polar organic solvents at room temperature, thus enhancing (more than expected for the effect of temperature) the solubility of organic compounds and their reactions in an environmentally friendly medium (Katritzky et al., 1996; Siskin and Katritzky, 2000). Laboratory experiments have demonstrated that water participates to organic reactions not only as a solvent, but also as reactant and catalyst (Katritzky et al., 1996; Siskin and Katritzky, 2000; Seewald, 2001; Shipp et al., 2013). In fact, the increase in the dissociation constant allows water at high temperature to act as an acid, base or acid-base biocatalyst (Katritzky et al., 1996; Siskin and Katritzky, 2000). Minerals were demonstrated to catalyze organic reactions as well (e.g. Soma and Soma, 1989; Dale Ortego et al., 1991; Seewald, 2001, 2003; Ferris 2005; Fu et al., 2008; Shipp et al., 2014; He et al., 2015). Al-silicates, such as zeolites and clays (e.g. smectites), are known to act as catalysts for organic reactions (Soma and Soma, 1989; Capaccioni et al., 1995; Williams et al., 2005). Owing to its sorbent and catalytic properties, montmorillonite has extensively been used in organic chemical applications for technological and environmental purposes (e.g. selective removal of organic pollutants; Dale Ortego et al., 1991 and references therein). The reducing capability of the FeS/FeS<sub>2</sub>-system was experimentally demonstrated by Kaschke et

al. (1994). Recent experiments by Shipp et al. (2014) demonstrated that sphalerite significantly favors the breaking and making of C-H bonds. Similarly, magnetite was found to catalyze oxidation/reduction reactions (He et al., 2015). Moreover, since many organic reactions involve changes in the oxidation state of carbon, the relative stability of organic compounds may be strongly dependent on the redox state of the system which in turn is buffered by mineral assemblages (e.g. Seewald, 2001). Evidences from experimental studies suggest that the reaction pathways among organic compounds consist of stepwise reversible and irreversible processes (e.g. oxidation/reduction, hydration/dehydration, carboxylation/decarboxylation) resulting in functional group interconversions (e.g. Seewald, 2001; Shipp et al., 2013). Seewald (2001, 2003) proposed a general reaction scheme (Figure 3) connecting alkane to carboxylic acids through a series of reversible and irreversible functional group interconversions: alkanes interconvert with alkenes, followed by hydration of alkenes to alcohols, dehydrogenation to ketones, and conversion to carboxylic acids, which can undergo decarboxylation and/or oxidation reactions to produce CO<sub>2</sub> and shorter-chain saturated hydrocarbons. This model was based on hydrothermal experiments focusing on specific functional group reactions.

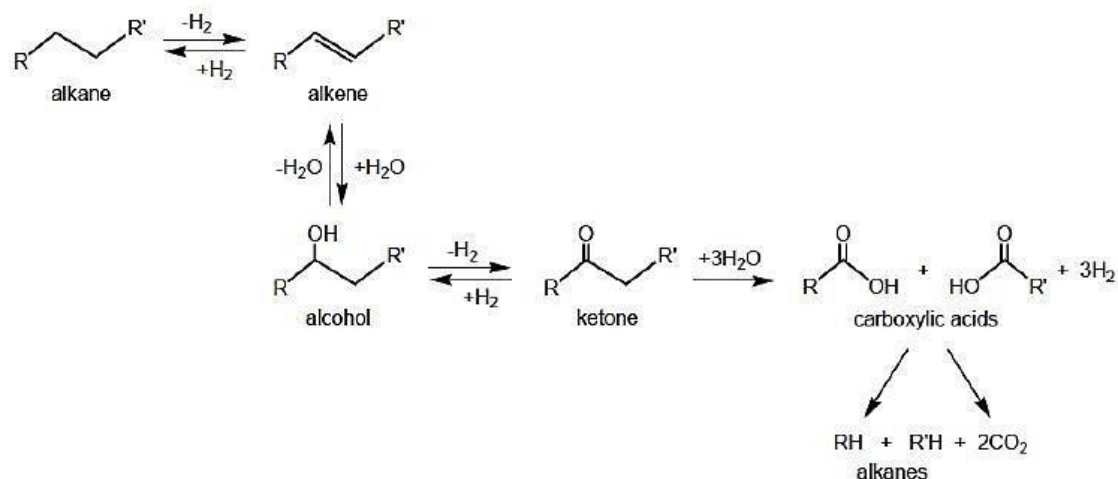


Figure 3: Reaction scheme of functional group interconversions, as proposed by Seewald (2001, 2003), involving reversible hydration/dehydration, hydrogenation/dehydrogenation and C-C bond cleavage reactions (after Shock et al., 2013).

The stepwise reactions in Figure 3 mainly consist of hydrogenation/dehydrogenation and hydration/dehydration reactions, in which the reactants and products were experimentally shown to approach metastable equilibrium states (Seewald, 1994, 2001; McCollom and Seewald, 2003). Shipp et al. (2013) found that the reaction path connecting alkanes to ketones

is completely reversible under hydrothermal conditions (300 °C, 100 MPa) and that the various functional group interconversions exhibit quite different rates. The reactivity was found to decrease in the following order: diene > alcohol > alkene > ketone > alkane. Hydrogenation/dehydrogenation reactions are common among organic compounds during geochemical processes (Shock et al., 2013 and references therein). In hydrogenation reactions, a carbon atom in an organic compound gains a bond to hydrogen and loses a bond to a heteroatom (or to another carbon atom), resulting in higher electron density on the carbon atom (hydrogen is the least electronegative element). Thus, hydrogenation consists of a reduction of the organic molecule. Conversely, during dehydrogenation reactions, a carbon atom loses a bond to hydrogen and gains a bond to a heteroatom (or to another carbon atom), resulting in an overall loss of electron density, i.e. oxidation. Common hydrogenation/dehydrogenation reactions include the alkane-alkene (e.g. Seewald, 1994; Shipp et al., 2013) and the alcohol-ketone (e.g. Leif and Simoneit, 1995; Seewald, 2001) interconversions. The reversibility of these redox reactions was observed in hydrothermal experiments, demonstrating that reactants and products can approach metastable equilibrium states (Shock et al., 2013 and references therein). For instance, Seewald (1994) experimentally proved the reversibility of the reaction between ethane and ethene in water at 325 °C and 350 bar:



Considering the equilibrium constant  $K$  for this reaction, it can be derived that:

$$\log a_{\text{H}_2} = \log K - \log (a_{\text{C}_2\text{H}_4}/a_{\text{C}_2\text{H}_6})$$

Setting the activities of the hydrocarbons equal, the corresponding equilibrium activity of hydrogen can be computed from  $\log K$  (Shock et al., 2013) (Figure 4). Alkanes show relatively high stabilities at redox conditions common to many mineral assemblages, being consistent with the higher abundance of saturated hydrocarbons relative to alkenes in natural systems (Shock et al., 2013). Moreover, dehydrogenation (i.e. oxidation) of alkanes to alkenes is thermodynamically enhanced at increasing temperatures (Shock et al., 2013) (Figure 4). Based on hydrothermal experiments.

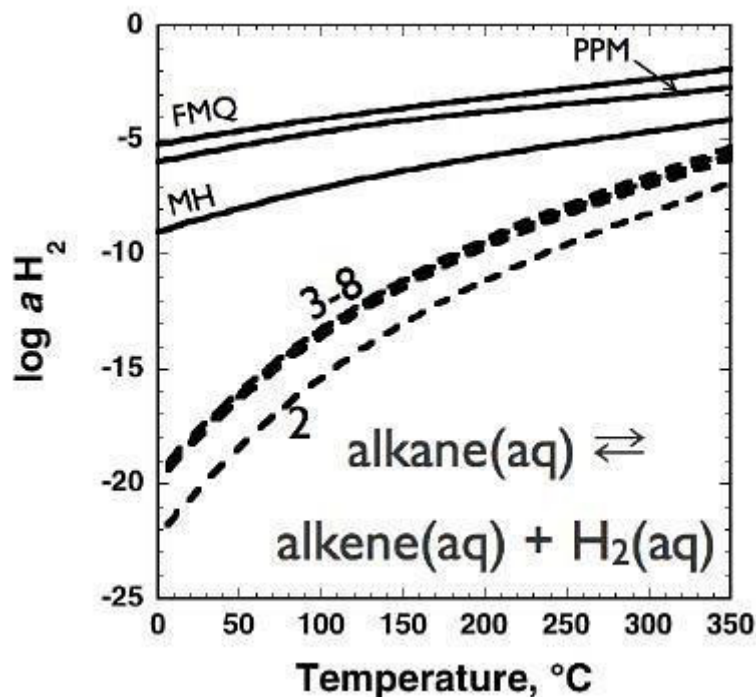


Figure 4: Equilibrium values of  $a_{H_2}$  corresponding to (i) equal activities of alkanes and alkenes (dashed curves; numbers refer to number of carbon atoms in the alkane and alkene), or (ii) mineral assemblages (solid curves; MH = magnetite-hematite; PPM = pyrrhotite-pyrite-magnetite; FMQ = fayalite-magnetite-quartz) as a function of temperature at PSAT (after Shock et al., 2013).

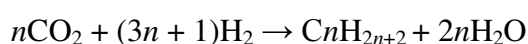
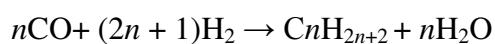
Hydration/dehydration reactions consist of the addition/removal of  $H_2O$  in the organic molecule. The reversible hydrothermal hydration reaction of alkenes to form alcohols is well known (e.g. Leif and Simoneit, 1995; Seewald, 2001; Akiya and Savage, 2001). The alkene/alcohol ratios increase at increasing temperatures (up to 5 orders of magnitude from 0 to 350 °C), highlighting the existence of a thermodynamic drive towards dehydration at high T, whereas hydration is thermodynamically favored as temperature decreases. Hence, as fluids cool, hydration of alkenes to alcohols may compete with hydrogenation of alkenes to alkanes (Shock et al., 2013). Dehydration reactions may also lead to the production of larger molecules through condensation of smaller organic compounds (Shock et al., 2013 and references therein). Some of the transformations described above involve parallel processes. For instance, for the cyclic structures, aromatization processes may compete with the other functional group interconversions. Shipp et al. (2014) found that the formation of aromatic structures may dominate the product distribution for alkylated cyclohexanes at hydrothermal conditions (300 °C and 100 MPa), eventually prevailing over the reaction path connecting alkanes to ketones. Aromatization of alkanes consists of a dehydrogenation reaction, highly endothermic and favored at high temperatures, likely proceeding through the formation of alkenes and dienes as by-products (Crittendon and Parsons, 1994; Shipp et al., 2013).

Transition metals are known to be heterogeneous catalysts for aromatization at high temperature conditions (Crittendon and Parsons, 1994 and references therein).

### **2.3.2 Abiotic hydrocarbon formation in crustal environments**

The hypothesis that at least some components of petroleum have a deep abiotic origin in the lower crust or mantle has a long history, with influential support and elaboration by Russian chemist and mineralogist Dimitri Mendeleev (Mendeleev, 1877) and astronomer and mathematician Fred Hoyle (Hoyle, 1955). The deep-Earth gas hypothesis proposes that abiogenic methane reflects a cosmic organic inheritance that is subsequently released by the mantle and migrates towards the surface utilizing weaknesses in the crust such as plate boundaries, faults, and sites of meteorite impacts. The deep sourced methane polymerizes *en route* to higher molecular weight hydrocarbons that ultimately form petroleum deposits. Members of the so-called “Russian-Ukrainian School” pursued this model with theory, experiments, and field observations (Kudyratsev, 1951; Glasby, 2006; Safronov, 2009). Superficial support for this theory is provided by the increase in abundance of methane with depth in petroleum-containing basins. However, it is known that the higher temperatures associated with greater depths in Earth’s subsurface promotes the cracking of high molecular weight hydrocarbons to produce lower molecular weight units, the ultimate product of which is methane. Hence, enhanced methane concentrations with depth are most effectively explained as an organic response to the geothermal gradient rather than closer proximity to a mantle source of methane. Yet the position that petroleum is primarily abiotic in origin is still held by some advocates (Gold, 1992; Kenney et al., 2001). The abiotic petroleum hypothesis first gained significant exposure outside the Soviet Union during the 1977 gasoline crisis, when Cornell astrophysicist Thomas (Tommy) Gold published an editorial in the *Wall Street Journal* (Gold, 1977) in which he claimed that most deep hydrocarbons are generated abiotically in the mantle and migrate to the crust, where they act as an energy source for microbes producing a deep microbial ecosystem (“Deep Hot Biosphere”) that may rival the surface biosphere in mass and volume. The organic remains of microbes in the deep hot biosphere represent the source of biological molecules in petroleum as a biological overprint onto an abiogenic organic mixture (Gold and Soter, 1980, 1982; Gold, 1992, 1999; Hazen, 2005). Gold presented several lines of evidence for abiotic petroleum, including (1) the presence of clearly abiotic hydrocarbons and other organic molecules in meteorites and on

other solar system bodies; (2) plausible synthetic pathways for mantle hydrocarbon production; (3) the association of hydrocarbon deposits with helium and other trace gases, presumably from mantle sources; (4) the existence of extensive deep microbial communities that impart an overprint of biomarkers onto the abiotic petroleum; (5) the tendency of hydrocarbon reservoirs to occur at many depths in a single locality, implying an underlying deep source; (6) the distribution of hydrocarbon deposits related to underlying mantle structures; (7) the distribution of metals and other trace elements in petroleum, which correlate more strongly with chondrite compositions than presumed crustal sources; and (8) the occurrence of hydrocarbons in non-sedimentary formations such as crystalline rocks. While compelling evidence for the abiotic synthesis of petroleum is lacking, there is experimental, theoretical, and field evidence for deep abiotic origins of some hydrocarbons (McCollom, 2013). Remote observations indicate that the Universe is replete with organic compounds produced without the influence of biology. Studies of the absorption spectra of dense molecular clouds reveal more than 150 small molecules (Ehrenfreund and Charnley, 2000; Kwok, 2009). The greatest amounts of hydrocarbons in our solar system are associated with the gas giant planets and their satellites, where significant amounts are present in atmospheres and on icy surfaces. Carbonaceous meteorites contain percentage levels of organic matter that were generated in the absence of biology (Sephton, 2002). The widespread presence of organic matter in the Cosmos suggests that no exotic mechanism therefore need be invoked to propose abiogenic hydrocarbons on Earth. In fact, the biogenic origin of some hydrocarbons on Earth is, thus far, a unique observation in an abiotic hydrocarbon-rich Universe. In contrast to our Cosmic environment, organic matter on Earth is associated primarily with biological processes. Industrial processes achieved abiotic synthesis under controlled conditions through the conversion of carbon monoxide or carbon dioxide to hydrocarbons.



These processes are broadly known as Fischer-Tropsch synthesis (Fischer and Tropsch, 1926). During FTT synthesis, CO or CO<sub>2</sub> is reduced to organic compounds through a series of steps on the surface of a catalyst (Figure 5).

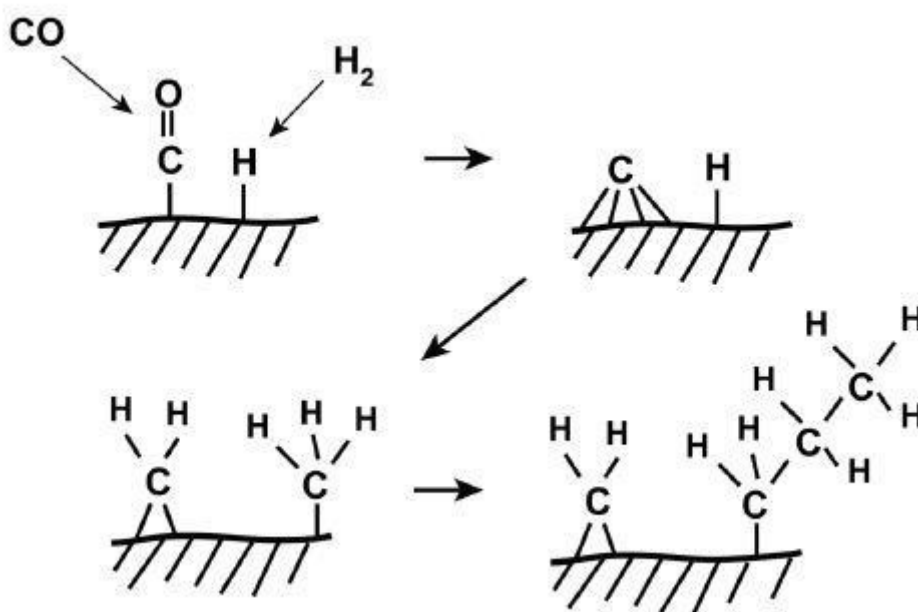


Figure 5: Generalized reaction mechanism for Fischer-Tropsch synthesis of hydrocarbons. The reaction starts with binding of CO to the catalyst surface to form a carbonyl unit ( $-\text{CO}$ ), which then undergoes sequential reduction to surface-bound carbide ( $-\text{C}$ ), methylene ( $-\text{CH}_2$ ), and methyl ( $-\text{CH}_3$ ) groups. Chain growth occurs as methylene groups polymerize to one another and terminates when the growing chain combines with a methyl group or surface-bound H rather than another methylene.

Typically, the primary products of the reaction are  $\text{CH}_4$  and a homologous series of linear alkanes that show a regular decrease in abundance with increasing number of carbons (Schulz-Flory distribution, Salvi and Williams-Jones, 1997). However, the process also generates lesser amounts of other compounds, including alkenes, branched hydrocarbons, and oxygen-bearing compounds including alkanols and alkanolic acids (e.g., Anderson and White, 1994; McCollom et al., 1999). If a source of nitrogen is present, the synthesis can also generate amino acids, amines, and other N-bearing compounds. The Fischer-Tropsch reaction was originally developed as a means of converting coal-bed gases to petroleum, and over the years it has been the subject of hundreds of experimental studies directed at optimizing yields of hydrocarbons and other industrial products. Unfortunately, most of this vast literature has no clear relevance to the study of formation of carbon compounds within Earth because the reaction conditions are not directly comparable to geologic environments. Although elegant and efficient reactions exist that can produce substantial amounts of hydrocarbons from simple precursors in the absence of biology, care must be taken when extrapolating data to natural settings.

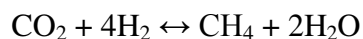
In recent years, methane and other light hydrocarbons with an apparently abiotic origin have been identified in an increasing number of geologic fluids on Earth. These compounds have been found in a variety of geologic settings, including seafloor hydrothermal systems, fracture

networks in crystalline rocks from continental and oceanic crust, volcanic gases, and gas seeps from serpentinized rocks (e.g., Abrajano et al., 1990; Kelley 1996; Sherwood Lollar et al., 2002, 2008; Fiebig et al., 2007, 2009; Proskurowski et al., 2008; Taran et al., 2010b; Etiope et al., 2011, 2018; Potter et al., 2013; Suda et al., 2014). Understanding the origin of these compounds has significant implications for range of topics that includes the global carbon cycle, the distribution of life in the deep subsurface (Gold, 1992), and the origin of life (Martin et al., 2008). Conceptually, there are two potential major sources of abiotic hydrocarbons to fluids in Earth's crust. First, abiotic hydrocarbons could migrate to the crust from deeper sources within Earth, through processes such as convective transport, grain boundary diffusion, or release of magmatic volatiles. Second, abiotic hydrocarbons could form *in situ* within the crust through reduction of inorganic carbon sources. Potential substrates for carbon reduction include CO<sub>2</sub> and CO in circulating fluids, and carbon-bearing solids such as carbonate minerals and graphite. In either case, the ultimate source of the inorganic carbon may be primordial (i.e., from the mantle) or recycled from Earth's surface. This chapter summarizes some of the recent laboratory experimental studies conducted to investigate potential pathways for the abiotic formation of methane and light hydrocarbons in subsurface geologic environments under crustal conditions.

### ***2.3.2.1 Chemical and physical conditions for hydrocarbon formation in the crust***

The prevailing oxidation state of source regions of magmas in the upper mantle dictates that carbon speciation in pristine magmatic-derived fluids should be dominated by CO<sub>2</sub>, with very little CH<sub>4</sub> present (e.g., Mathez, 1984; Kelley, 1996). This observation appears to be consistent, for example, with chemical analyses of magmatic volatiles trapped in vesicles within seafloor basalts, which are characterized by very high CO<sub>2</sub>/CH<sub>4</sub> ratios (e.g., Pineau and Javoy, 1983). At the same time, oxidizing conditions at Earth's surface ensure that CO<sub>2</sub> and bicarbonate are the predominant forms of dissolved carbon in seawater, in fracture-filling groundwater, and in shallow pore waters. Consequently, the predominant inputs of carbon to Earth's crust from both above and below are in highly oxidized forms. Accordingly, any hydrocarbons found in fluids circulating in Earth's crust that do not derive from deep within in the mantle or from biologic sources must therefore be formed by non-biological reduction of inorganic carbon within the crust itself. In general, two sets of conditions favor the reduction of inorganic carbon to hydrocarbons within the crust (McCollom and Seewald,

2007; McCollom, 2008). At the elevated temperatures and oxidation states that prevail in environments deep within the crust, CO<sub>2</sub> is thermodynamically stable relative to CH<sub>4</sub>. However, decreasing temperatures increasingly favor the stability of CH<sub>4</sub> relative to CO<sub>2</sub>. This trend is illustrated in Figure 6a, which shows that the log K for the reaction:



becomes increasingly positive with decreasing temperature, indicating that lower temperatures favor the compounds on the right side of the reaction relative to those on the left side. As shown in Figure 6b, this means that CO<sub>2</sub> predominates relative to CH<sub>4</sub> at equilibrium for high temperatures (>~200 to 350 °C, depending on oxidation state), but CH<sub>4</sub> is the more thermodynamically stable compound at lower temperatures. Similar relationships can be shown for other hydrocarbons relative to CO<sub>2</sub>. Therefore, cooling of high-temperature fluids that contain dissolved CO<sub>2</sub> and H<sub>2</sub> will thermodynamically favor reduction of the CO<sub>2</sub> to CH<sub>4</sub> and other hydrocarbons (e.g., Shock, 1990, 1992).

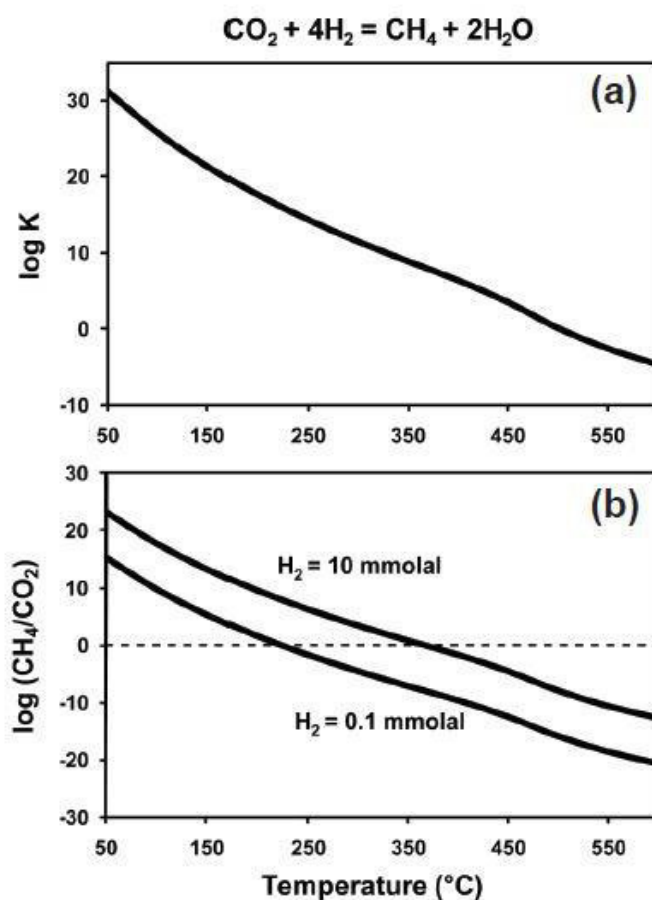
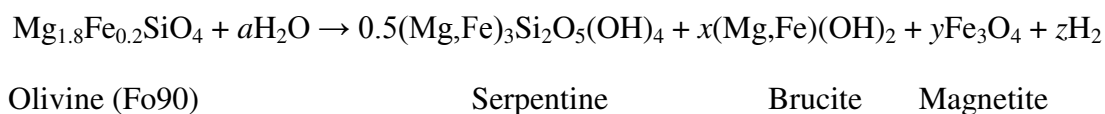


Figure 6: Thermodynamic relationships between dissolved CO<sub>2</sub> and CH<sub>4</sub> at elevated temperature and pressure. (a) Log K for reduction of CO<sub>2</sub> to CH<sub>4</sub>. (b) Calculated equilibrium (CH<sub>4</sub>/CO<sub>2</sub>) ratios as a function of temperature at two values of H<sub>2</sub> concentration that bracket those found in reducing environments within the crust. Data

shown are for a pressure of 50 MPa. Values for log  $K$  calculated using thermodynamic data from SUPCRT92 and Shock et al. (1989).

A second set of circumstances that can promote reduction of inorganic carbon within Earth's crust is the generation of reducing environments through fluid-rock interactions. These interactions are typically manifested by increasing abundances of  $H_2$  as fluid-rock interactions proceed, shifting the equilibrium of reactions like the one written above towards the compounds on the right side. Hence, the predominant equilibrium carbon species can shift from  $CO_2$  to  $CH_4$  as fluids interact with rocks, even without a change in temperature. Because the interaction of aqueous fluids with ultramafic rocks is known to generate particularly large amounts of  $H_2$ , fluids circulating through these rocks have become the focus of many studies of abiotic hydrocarbon formation. For example, hydrothermal fluids circulating through ultramafic rocks below the seafloor have measured  $H_2$  concentrations up to 15 mmol/kg, and evidence suggests that light hydrocarbons in these fluids have an abiotic origin (Charlou et al., 2002, 2010; Kelley et al., 2005; Proskurowski et al., 2008). Hydrous alteration of ultramafic rocks, which are composed predominantly of olivine and pyroxene, is known as serpentinization, owing to precipitation of the mineral serpentine as the primary alteration product (Schrenk et al., 2013). Serpentinization can be summarized by the general reaction:



The exact stoichiometry of this reaction, and thus the amount of  $H_2$  generated, is dependent on a number of factors that affect partitioning of Fe among the reaction products, including temperature, rock composition, and water/rock ratio (e.g., Seyfried et al., 2007; McCollom and Bach, 2009; Marcaillou et al., 2012). While ultramafic rocks have become a focal point for studies of abiotic hydrocarbon formation, serpentinization is by no means the only fluid-rock reaction that can produce sufficiently reducing conditions to favor carbon reduction, and many other rock types and reactions may be involved in  $H_2$  production within Earth's crust (e.g., Charlou et al., 1996; Potter et al., 2004; Sherwood Lollar et al., 2006, 2007). Although thermodynamic factors can favor reduction of inorganic carbon to hydrocarbons under circumstances like those outlined above, kinetic inhibitions can still prevent the reactions from occurring. In contrast to the experimental results obtained at mantle temperatures, which show rapid equilibration among carbon species, reactions involved in the reduction of inorganic carbon at temperatures and pressures relevant to environments in Earth's crust are susceptible to kinetic inhibitions (e.g., Seewald et al., 2006). Laboratory experiments provide a means to evaluate which conditions within the crust can allow carbon reduction to proceed.

### ***2.3.2.2 Synthesis of hydrocarbons by Fischer-Tropsch-type reactions: evidences from hydrothermal experiments***

The most widely invoked pathway for the formation of hydrocarbons and other organic compounds in geologic environments is the Fischer-Tropsch synthesis. Accordingly, this process has also received the greatest attention in experimental studies. As originally described, Fischer-Tropsch synthesis refers to the surface-catalyzed reduction of CO by H<sub>2</sub> in gas mixtures. However, the term is often used in a broader context in the geological literature to refer to reduction of an inorganic carbon source to form organic compounds, regardless of the nature of the carbon source, the medium in which the reaction occurs, or the identity of the reductant. In many cases, dissolved CO<sub>2</sub> is inferred to be the primary carbon source for abiotic organic synthesis in geologic systems. In this section the geologic convention will be adopted, and the term Fischer-Tropsch-type (FTT) synthesis use to refer in general to any surface-catalyzed reduction of an inorganic carbon source to organic matter. The challenge for experimental geochemists is to understand the extent to which FTT reactions can proceed at conditions that more closely resemble subsurface geologic environments. One key question is whether FTT type reactions can proceed in environments where reactants are dissolved in sub- or supercritical aqueous fluids. Another critical question is which naturally occurring minerals, if any, are effective in catalyzing the reaction, and under what circumstances. Some catalysts used in industrial Fischer-Tropsch synthesis are found in natural systems, but for industrial purposes their catalytic properties are typically enhanced in ways that may not occur in natural settings. For example, magnetite has long been employed as a catalyst for industrial Fischer-Tropsch studies, but it is usually pre-treated with a stream of H<sub>2</sub> and CO prior to use in these applications. This process generates pockets of highly reactive native Fe or Fe-carbides on the surface that appear to be active sites for catalysis (e.g., Dictor and Bell, 1986; Satterfield et al., 1986). These kinds of sites would likely be destroyed very rapidly in natural systems, especially if H<sub>2</sub>O is present. To address these issues, recent experimental studies concerning the potential contribution of FTT synthesis to hydrocarbon occurrences in geologic systems have largely focused on exploring the capacity for naturally occurring minerals to catalyze the reaction, and on evaluating the effectiveness of the reactions under hydrothermal conditions. Several recent laboratory experiments indicate that FTT synthesis can indeed proceed readily under hydrothermal conditions in some circumstances (e.g., McCollom et al., 1999, 2010; McCollom and Seewald, 2006). In these studies, CO or formic acid (HCOOH) and water were heated to temperatures of 175 or 250 °C and pressures ranging

from steam-saturation to 25 MPa, with  $H_2$  supplied by decomposition of formic acid ( $HCOOH \rightarrow CO_2 + H_2$ ) or of native Fe included in the reaction vessel ( $Fe + H_2O \rightarrow Fe_3O_4 + H_2$ ). Over periods of hours to days, a significant portion of carbon is reduced to typical Fischer-Tropsch reaction products. These products include  $CH_4$  and other light hydrocarbons, as well as long-chain *n*-alkanes, alkanols, and alkanolic acids (Figure 7). The products exhibit a regular decrease in abundance with increasing carbon number that is characteristic of Fischer-Tropsch products.

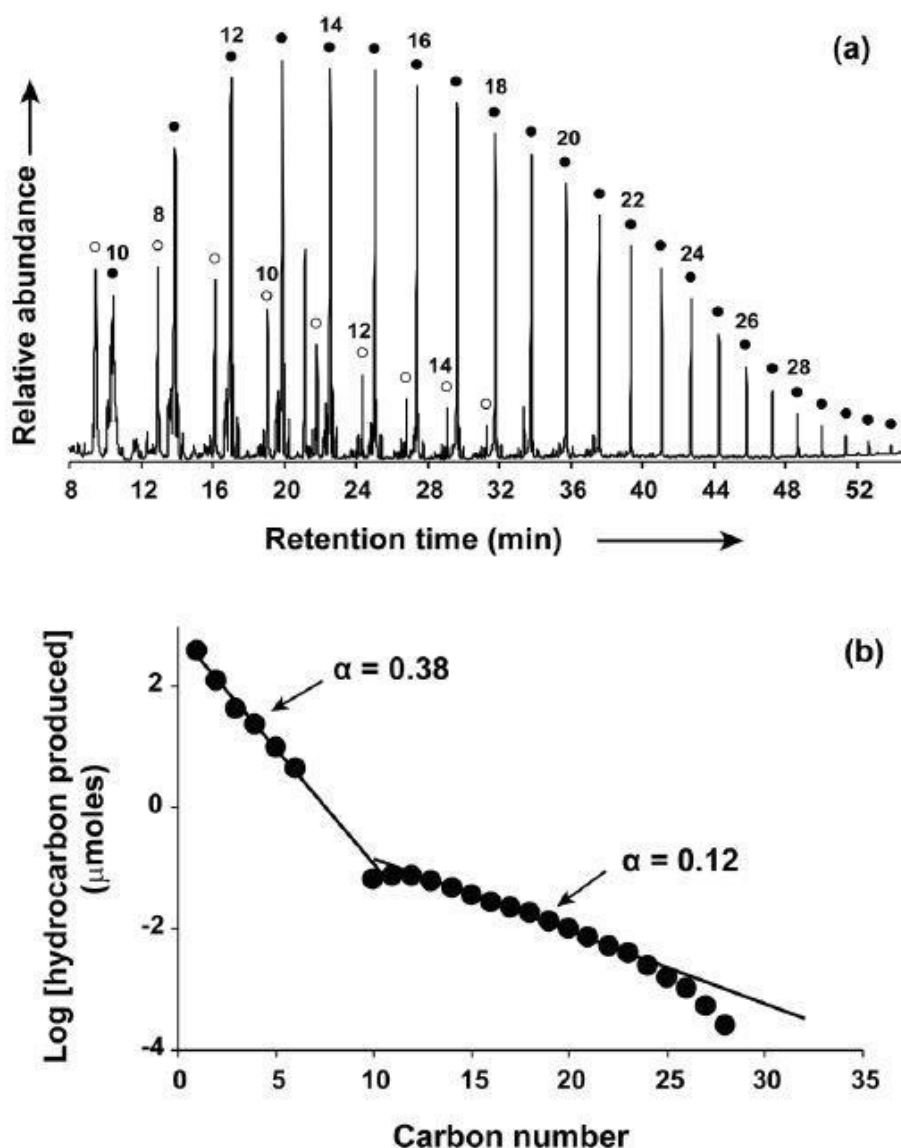


Figure 7: Example of typical products of Fischer-Tropsch-type synthesis. (a) Gas chromatogram of nonvolatile products, showing predominance of linear saturate hydrocarbons (*n*-alkanes; filled circles) and alcohols (*n*-1-alkanols; open circles). (b) Relative abundance of saturated hydrocarbons (*n*-alkanes) as a function of carbon number, showing typical log-linear decrease. The slope of the decrease ( $\alpha$ ) is a gauge of the relative probabilities of continued growth of the carbon chain versus chain termination. The break in slope at carbon number around 10 is common for iron-based catalysts. Figure shows data from McCollom and Seewald (2006).

While these experiments show that FTT synthesis is not necessarily inhibited by hydrothermal conditions, a couple of considerations may limit their direct applicability to natural systems. First, the synthesis in these experiments was probably catalyzed either by native Fe included in the reaction vessel, or by the walls of the steel tube used in some of the experiments. Thus, they may not represent catalysts present in natural environments. Second, it appears likely that the synthesis reactions took place either in the vapor headspace for reactions performed in fixed-volume tube reactors (McCollom et al., 1999) or in H<sub>2</sub>-rich vapor bubbles formed on the surfaces of the solids in reactions performed at higher pressures (McCollom and Seewald, 2006; McCollom et al., 2010). Consequently, while these experiments show that the presence of water-saturated vapors do not preclude efficient FTT synthesis, they do not indicate that the reactions can proceed for compounds dissolved in aqueous liquid. In addition, H<sub>2</sub> was also present in these experiments at very high levels (>200 mmol/kg) that are probably rarely approached in natural environments within Earth's crust. The prospect that abiotic hydrocarbons might form during serpentinization of ultramafic rocks led to experimental investigation of the capacity for minerals found in serpentinites to catalyze carbon reduction reactions. The first study to focus on this possibility was that of Berndt et al. (1996), who monitored the production of light hydrocarbons during reaction of Fe-bearing olivine with an aqueous solution containing dissolved bicarbonate at elevated temperature and pressure (300 °C, 50 MPa). The experiment utilized a flexible-cell reaction apparatus, which allows reactions to proceed without a vapor phase present and also provides a means to monitor concentrations of compounds dissolved in the fluid as reactions proceed. Dissolved concentrations of H<sub>2</sub> and several light hydrocarbons (CH<sub>4</sub>, C<sub>2</sub>H<sub>6</sub>, and C<sub>3</sub>H<sub>8</sub>) were observed to increase steadily during the experiment as the serpentinization reaction progressed, while the concentration of total dissolved CO<sub>2</sub> (CO<sub>2, aq</sub> + HCO<sub>3</sub><sup>-</sup>) declined. The authors interpreted the small amounts of hydrocarbons generated over the course of the experiment to represent products of Fischer-Tropsch synthesis through reduction of dissolved CO<sub>2</sub>. Magnetite formed in the experiments as a product of serpentinization was suggested to be the catalyst. The groundbreaking results of Berndt et al. (1996) suggested that reduction of dissolved inorganic carbon to hydrocarbons could proceed readily with minerals common in hydrothermal systems serving as catalysts. Further investigation, however, showed that hydrocarbon formation at the conditions of their experiments was much more limited than initially thought. McCollom and Seewald (2001) performed an experiment under essentially identical conditions to those of Berndt et al. (1996), except that <sup>13</sup>C-labeled bicarbonate (99%

$\text{H}^{13}\text{CO}_3^-$ ) was substituted as the inorganic carbon source to trace the origin of carbon in the hydrocarbon products. While the experiment yielded similar amounts of  $\text{H}_2$  and  $\text{C}_1\text{-C}_3$  hydrocarbons to those reported by Berndt et al. (1996), isotopic analysis of the hydrocarbon products indicated that only a small fraction of the  $\text{CH}_4$  contained the  $^{13}\text{C}$  label (2-15%), while none of the  $\text{C}_2\text{H}_6$  or  $\text{C}_3\text{H}_8$  was labeled. This result indicated that, except for a small fraction of the  $\text{CH}_4$ , the  $\text{C}_1\text{-C}_3$  hydrocarbons generated in the experiments were not the product of reduction of dissolved  $\text{CO}_2$ , but were instead generated from thermal decomposition of other sources of reduced carbon already present among the reactants at the start of the experiment. It is worth emphasizing that, at the  $\text{H}_2$  concentrations attained in both experiments (up to 158 mmol/kg), reduction of inorganic carbon to  $\text{CH}_4$  and other hydrocarbons was strongly favored by thermodynamics, and essentially all the dissolved  $\text{CO}_2$  present should have been converted to  $\text{CH}_4$  to attain equilibrium. Yet, only a very small fraction ( $\ll 1\%$ ) of the available carbon was reduced to  $\text{CH}_4$ , even after nearly three months of heating at 300 °C. Thus, the results clearly demonstrated that reduction of dissolved inorganic carbon to light hydrocarbons is kinetically sluggish even at 300 °C. Furthermore, although magnetite was formed in abundance in both experiments as a product of serpentinization, the lack of significant hydrocarbon formation suggests that it is not a very effective catalyst for reduction of dissolved inorganic carbon in natural systems. Otherwise, a much larger fraction of the inorganic carbon present in the experiments would have been converted to  $\text{CH}_4$  or other organic compounds. In a series of follow-up experiments also using  $^{13}\text{C}$ -labeled carbon sources, it was found that dissolved  $\text{CO}_2$  (or  $\text{HCO}_3^-$ ) was rapidly reduced by  $\text{H}_2$  to  $\text{HCOOH}$  and  $\text{CO}$  under hydrothermal conditions (Seewald et al., 2006). In contrast to  $\text{CH}_4$ , these compounds attained thermodynamic equilibrium within a few days, even at temperatures as low as 175 °C and in the absence of mineral catalysts. Methanol was also found to accumulate but did not reach equilibrium proportions. As in the serpentinization experiments,  $^{13}\text{C}$ -labeled  $\text{CH}_4$  was produced in small amounts (mmolar concentrations) during these experiments, along with larger amounts of unlabeled  $\text{CH}_4$  and other light hydrocarbons. Overall, the experimental results demonstrated that partial reduction of dissolved inorganic carbon proceeds rapidly and spontaneously to  $\text{HCOOH}$  and  $\text{CO}$  under hydrothermal conditions, but complete reduction to  $\text{CH}_4$  proceeds only very slowly without catalysis. Several other experimental studies have focused on evaluating the catalytic potential of individual minerals found in serpentinites, including NiFe-alloys, magnetite, chromite, and Nisulfide (pentlandite). Awaruite, a Ni-Fe alloy with compositions between  $\text{Ni}_2\text{Fe}$  and  $\text{Ni}_3\text{Fe}$ , occurs in many serpentinites as a by-product of the highly reducing conditions that can

develop as a result of H<sub>2</sub> production during serpentinization (Frost, 1985; Klein and Bach, 2009). Horita and Berndt (1999) examined the reduction of dissolved CO<sub>2</sub> in the presence of NiFe-alloy, magnetite, water, and highly elevated H<sub>2</sub> concentrations (170-300 mmol/kg). Experiments were conducted at temperatures of 200-400 °C and 50 MPa. In contrast to the small amounts of CH<sub>4</sub> produced in the earlier experiments of Berndt et al. (1996), nearly complete conversion of CO<sub>2</sub> to CH<sub>4</sub> was observed in the 300 °C experiments in two weeks or less, and >40% conversion was observed after 3 months of reaction at 200 °C. Moreover, rates of conversion were found to increase when greater amounts of NiFe-alloy were included, and no CH<sub>4</sub> was generated in a control experiment in the absence of the alloy, demonstrating that the NiFe-alloy had catalyzed the production of CH<sub>4</sub>. No C<sub>2</sub>H<sub>6</sub> or C<sub>3</sub>H<sub>8</sub> were found in the experiment, indicating that the catalysis exclusively promoted CH<sub>4</sub> synthesis. Lesser amounts of conversion of CO<sub>2</sub> to CH<sub>4</sub> were observed at 400 °C, which was attributed to passivation of the catalyst at higher temperature. The experiments of Horita and Berndt (1999) provided the first documentation that the kinetic inhibitions to reduction of dissolved CO<sub>2</sub> to CH<sub>4</sub> could be effectively overcome by naturally occurring minerals, and that NiFe-alloy was a very effective catalyst in promoting the reaction. The experiments also showed that pure CH<sub>4</sub> could be produced by an abiotic process in hydrothermal environments, which was contrary to the widely held notion that only methanogenic microorganisms can produce nearly pure CH<sub>4</sub> in geologic systems (e.g., Whiticar 1990). Although the alloy present in the experiments of Horita and Berndt (1999) was significantly enriched in Ni relative to awaruite found in natural serpentinites, there is no obvious reason to doubt that natural awaruite would have similar catalytic properties. The catalytic potential of chromite and magnetite has been investigated in experiments by Foustoukos and Seyfried (2004). Two experiments were performed under hydrothermal conditions at 390 °C and 40 MPa, one containing chromite plus magnetite and the other including only magnetite, with both minerals synthesized from Fe and Cr oxides. A <sup>13</sup>C-labeled inorganic carbon source was used (99% H<sup>13</sup>CO<sub>3</sub><sup>-</sup>) to assess the origin of carbon in reaction products, and high levels of H<sub>2</sub> (>100 mmol/kg) provided conditions favorable for carbon reduction. During heating for 44 to 120 days, <sup>13</sup>CH<sub>4</sub> was observed to accumulate at concentrations up to 192 mmol/kg. Much smaller, but detectable, levels of <sup>13</sup>C-labeled C<sub>2</sub>H<sub>6</sub> and C<sub>3</sub>H<sub>8</sub> were also observed. In each case, the labeled compounds represented only a small fraction of the total concentrations of C<sub>1</sub>-C<sub>3</sub> hydrocarbons observed in the experiments. A key finding of this study was that C<sub>2+</sub> hydrocarbons could be produced from reduction of dissolved reactants, demonstrating that higher hydrocarbons as well as CH<sub>4</sub> could be generated without a vapor phase present in

subsurface and hydrothermal environments. Although yields were low (<0.1% of added inorganic carbon), the concentrations attained were comparable to those of hydrocarbons in deep-sea hydrothermal systems thought to have an abiotic origin (e.g., Proskurowski et al., 2008; Charlou et al., 2010). The results show that it is possible for light hydrocarbons to be generated from reduction of inorganic carbon in subsurface environments even when there is no vapor phase present. Owing to the high levels of unlabeled hydrocarbons in the experiments, which apparently derived from traces of background reduced carbon included among the reactants, the use of labeled carbon source was a critical factor in the authors ability to demonstrate that the hydrocarbons were derived from reduction of inorganic carbon. Foustoukos and Seyfried (2004) inferred that the minerals catalyzed formation of the hydrocarbons and, based on the observation that yields of labeled hydrocarbons were higher in the experiment that contained chromite than in the experiment that contained only magnetite, the authors inferred that chromite was more effective than magnetite in promoting the hydrocarbon formation. However, subsequent studies have not observed any catalytic effect for the reduction of dissolved CO<sub>2</sub> by naturally occurring chromite (Lazar et al. 2012; Oze et al. 2012), and alternative explanations for the differences observed by Foustoukos and Seyfried (2004) are possible. In particular, the chromite-bearing experiment contained higher H<sub>2</sub> than the magnetite-only experiment (~220 mmol/kg vs. ~120 mmol/kg) and was also performed at a substantially lower pH (4.8 vs. 8.8, which changes the predominant carbon species from CO<sub>2</sub>(aq) to HCO<sub>3</sub><sup>-</sup>), either of which may have affected the rate of reduction of inorganic carbon to hydrocarbons independent of any mineral catalysis. As a consequence, the capacity for chromite to catalyze the reduction of inorganic carbon to CH<sub>4</sub> and other light hydrocarbons under natural hydrothermal conditions remains uncertain. Because the physical properties of water undergo substantial changes near the critical point (404 °C, 29 MPa for seawater salinity; Bischoff and Rosenbauer, 1985), the near-critical conditions of the Foustoukos and Seyfried (2004) experiments might have had a role in allowing the reduction of carbon to occur. However, a more recent study by Ji et al. (2008) reported the reduction of dissolved <sup>13</sup>CO<sub>2</sub> to C<sub>1</sub>-C<sub>5</sub> hydrocarbons in experiments at 300 °C and 30 MPa with a cobalt-enriched magnetite catalyst. The authors reported isotopic analyses only for the C<sub>3</sub>-C<sub>5</sub> hydrocarbons, but the results showed that at least 50% of carbon in linear alkanes was <sup>13</sup>C, while branched C<sub>4</sub> and C<sub>5</sub> alkanes contained none of the added <sup>13</sup>C. Yields of hydrocarbons in these experiments were an order of magnitude greater than those of Foustoukos and Seyfried (2004), although uncertainties in the abundance and isotopic composition of CO<sub>2</sub> and CH<sub>4</sub> preclude direct comparisons. In any case, the results of Ji et al. (2008) provide further

evidence that synthesis of at least short-chain hydrocarbons is possible in the absence of a vapor phase. The potential of magnetite to promote abiotic production of hydrocarbons under hydrothermal conditions was further investigated by Fu et al. (2007), who heated solutions of CO<sub>2</sub> and H<sub>2</sub> in the presence of magnetite at 400 °C and 50 kPa. In order to avoid background contributions of hydrocarbons from magnetite, the minerals were scrupulously treated prior to the experiments to reduce carbon contents, and control experiments without an added carbon source did not generate detectable levels of CH<sub>4</sub> or other light hydrocarbons. In contrast, when a carbon source was injected into the experiments (as CO<sub>2</sub> or HCOOH) together with H<sub>2</sub>, concentrations of CH<sub>4</sub>, C<sub>2</sub>H<sub>6</sub>, or C<sub>3</sub>H<sub>8</sub> were found to increase over time. On the order of 0.2- 0.3% of the inorganic carbon added to experiments was converted to hydrocarbons, comparable to the conversion amounts observed by Foustoukos and Seyfried (2004) at similar pressure and temperature. Based on a carbon imbalance in their experiments, Fu et al. (2007) also suggested that a large fraction of the inorganic carbon reactant was converted to additional unidentified organic products, although no supporting evidence was provided. While the experiments of McCollom and Seewald (2001), Fu et al. (2007), and Foustoukos and Seyfried (2004) resulted in the synthesis of CH<sub>4</sub> and, in some case, other light hydrocarbons in the presence of magnetite, it must be pointed out that none of these studies provide definitive evidence that magnetite efficiently catalyzed the reactions. Using similar methods, experiments conducted by Seewald et al. (2006) with no minerals present generated small amounts of CH<sub>4</sub> comparable to those observed in magnetite-bearing experiments, and it seems possible that other hydrocarbons might be produced as well. Definitive studies showing that the presence of magnetite increases the production of hydrocarbons over that observed for the same conditions without magnetite have not yet been published. Additionally, in the experiments of Horita and Berndt (1999), the catalytic properties of NiFe-alloy was demonstrated by showing that CH<sub>4</sub> production increased with the amount of alloy present, but no similar set of experiments with variable amounts of magnetite have yet been published. Consequently, whether magnetite can catalyze carbon reduction in hydrothermal environments should be considered an unresolved question. The potential for hydrocarbon synthesis in the presence of pentlandite (an Fe-Ni sulfide mineral) has also been explored by Fu et al. (2008), using similar conditions (400 °C, 50 MPa) and experimental methods to those of previous experiments with chromite and magnetite. The source of inorganic carbon in the experiment, and also of H<sub>2</sub>, was <sup>13</sup>C-labeled HCOOH. During several weeks of reaction, μmolar concentrations of labeled <sup>13</sup>CH<sub>4</sub>, <sup>13</sup>C<sub>2</sub>H<sub>6</sub>, and <sup>13</sup>C<sub>3</sub>H<sub>8</sub> accumulated in the fluid, along with much higher levels of unlabeled compounds. Overall conversion of inorganic carbon was

<0.01%, and  $^{13}\text{CH}_4$  yields were an order of magnitude lower than observed in the previous magnetite and chromite experiments (Foustoukos and Seyfried, 2004). More recently, Lazar et al. (2012) reported that  $^{13}\text{CH}_4$  generation was faster during experiments using natural komatiite and  $\text{H}^{13}\text{COOH}$  as reactants at 300 °C than in parallel experiments with synthetic komatiite. The authors inferred that the increased rates were attributable to the presence of pentlandite in the natural sample. These studies suggest that Ni-bearing sulfides are another potential catalyst for reduction of inorganic carbon to hydrocarbons in subsurface hydrothermal environments. While most of studies described above were performed at temperatures of 300 °C or above, several recent studies have explored the production of  $\text{CH}_4$  during reaction of olivine with water at lower temperatures (Jones et al. 2010; Neubeck et al. 2011; Oze et al. 2012). In a series of experiments using methods similar to those of Berndt et al. (1996) and McCollom and Seewald (2001), Jones, Oze, and colleagues (Jones et al., 2010; Oze et al., 2012) reacted olivine and chromite with fluids containing variable amounts of  $\text{HCO}_3^-$  at 200 °C and 30 MPa. Steadily increasing levels of  $\text{H}_2$  were observed during the experiments, resulting from serpentinization of olivine. Methane concentrations increased in parallel with the  $\text{H}_2$ , which was inferred by the authors to be an indication that the  $\text{CH}_4$  was generated by FTT synthesis reactions catalyzed by magnetite. After reaction for up to 1321 hours, dissolved concentrations of 5-12 mmol/kg  $\text{H}_2$  and 56-120  $\mu\text{mol/kg}$   $\text{CH}_4$  were attained. Although these authors inferred that the  $\text{CH}_4$  observed in their experiments was the product of magnetite-catalyzed reduction of dissolved inorganic carbon, results from previous experiments suggest that this inference must be viewed with caution. As described above, numerous experimental studies have demonstrated that minerals and other sources can produce background  $\text{CH}_4$  during hydrothermal experiments in comparable amounts to the  $\text{CH}_4$  concentration reported by Jones et al. (2010) and Oze et al. (2012). Furthermore, most of their experiments generated  $\text{CH}_4$  even though no inorganic carbon source was included among the reactants, and dissolved inorganic carbon was below detection limits throughout the experiments. Methane generation decreased when an inorganic carbon source was added, opposite to expectations for carbon reduction. Since Jones et al. (2010) and Oze et al. (2012) did not assess background levels of  $\text{CH}_4$  in their experiments, it is not possible to evaluate the actual source of the  $\text{CH}_4$ . However, based on results of other studies, it is likely that only a very small fraction of the  $\text{CH}_4$  observed, if any, was derived from reduction of inorganic carbon during the experiments. Neubeck et al. (2011) employed a totally different experimental approach to examine  $\text{CH}_4$  generation from olivine at 30-70 °C. These investigators reacted olivine with a bicarbonate solution in partially filled glass vials, sealed

with rubber stoppers and flushed with N<sub>2</sub>. The headspace of the vials was monitored for production of H<sub>2</sub> and CH<sub>4</sub>, and over nine months of reaction these compounds were found to accumulate at low nanomolar amounts, with higher yields observed with increasing temperature. Based on lower CH<sub>4</sub> production in mineral-free experiments and apparent absence of alternative carbon sources, Neubeck et al. (2011) inferred that the CH<sub>4</sub> observed in their experiments was derived from reduction of the dissolved HCO<sub>3</sub><sup>-</sup>, with trace amounts of magnetite or chromite serving as catalysts. If the results of Neubeck et al. (2011) are taken at face value, it would suggest a possible widespread source of CH<sub>4</sub> within the crust from low-temperature serpentinization of ultramafic rocks. However, as suggested by Jones et al. (2010) and Oze et al. (2012), the claim of abiotic CH<sub>4</sub> formation in these experiments must be viewed with some caution. Neubeck et al. (2011) did not report any effort to assess background levels of CH<sub>4</sub> in their experiments, and the amounts of CH<sub>4</sub> produced in experiments that included no inorganic carbon source among the reactants were nearly identical to the levels generated in experiments performed with bicarbonate solutions. As a result, this study provides no evidence directly linking the CH<sub>4</sub> observed to reduction of bicarbonate, and previous results suggest that most, if not all, of the CH<sub>4</sub> observed may have been derived from reduced carbon sources among the reactants. Furthermore, based on experimental evidences, McCollom and Donaldson (2016) highlighted that reactor material (glass bottles and rubber stoppers) commonly used in low-temperatures experiments, releases H<sub>2</sub> and CH<sub>4</sub> upon heating at 90 °C. Consequently, the potential for abiotic CH<sub>4</sub> production during low-temperature alteration of ultramafic rocks remains uncertain. Consistent with previous high-temperature studies, McCollom (2016) provided evidence that abiotic formation of CH<sub>4</sub> from reduction of dissolved inorganic carbon during the experiments is extremely limited, with nearly all the observed CH<sub>4</sub> derived from background sources. However, McCollom (2016) observed more extensive production of CH<sub>4</sub> in one experiment performed under conditions that allowed an H<sub>2</sub>-rich vapor phase to form, suggesting that shallow serpentinization environments where a separate gas phase is present may be more favorable for abiotic synthesis of CH<sub>4</sub>.

### ***2.3.2.3 Isotopic fractionation during FTT synthesis.***

The carbon and hydrogen isotopic compositions of CH<sub>4</sub> and other light hydrocarbons have increasingly become key elements of efforts to identify hydrocarbons with an abiotic origin in natural systems (e.g., Sherwood Lollar et al. 2002, 2008; Fiebig et al. 2007; Proskurowski et al. 2008; Taran et al. 2010a). The potential for isotopes to be used as criteria for identification

of abiotic hydrocarbons has led to renewed interest in recent years in experimental study of isotopic fractionation during FTT synthesis. The isotopic compositions of FTT reaction products have been reported for a number of laboratory experiments performed under a variety of reaction conditions, including CO/H<sub>2</sub> gas mixtures in flow-through reactors (Taran et al. 2007, 2010a; Shi and Jin 2011), gas mixtures in closed reaction vessels (Lancet and Anders 1970; Hu et al. 1998), and hydrothermal reactions (McCollom and Seewald 2006; Fu et al. 2007; McCollom et al. 2010). A variety of Fe-, Co-, and Ru-bearing catalysts have been used in these experiments. The isotopic compositions of the light hydrocarbons generated in the various experiments exhibit both some similarities and some substantial differences. Nearly all the hydrocarbons generated in the experiments are depleted in <sup>13</sup>C relative to the initial carbon source. However, the magnitude of the depletion varies considerably among the different experiments, and varies substantially within individual experiments as a function of reaction times and for compounds with different number of carbon atoms. These trends are illustrated in Figure 8, which shows the carbon isotopic composition of a few selected examples of experimental reaction products. It should be noted that these examples represent only a portion of the full range of isotopic compositions that have been reported for experimental products. Within this selected set of results, however, <sup>13</sup>C depletions of the products relative to the carbon source range up to 33‰, while other results show no fractionation or even a slight enrichment in <sup>13</sup>C. Among the experiments, the isotopic compositions of hydrocarbons exhibit a wide variety of different trends as a function of carbon number.

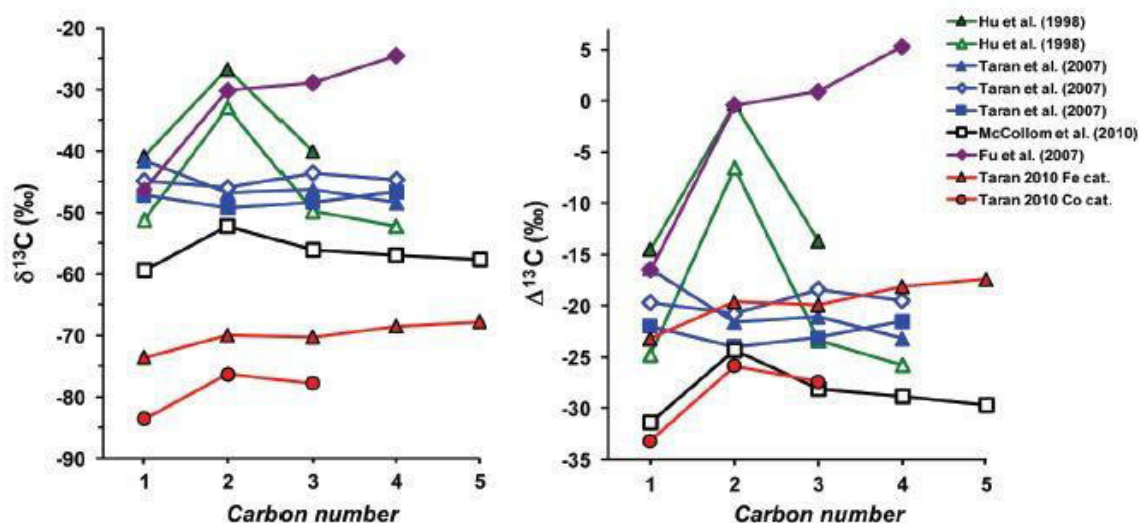


Figure 8: Carbon isotopic composition of CH<sub>4</sub> and C<sub>2</sub>-C<sub>5</sub> alkanes for selected experimental FTT reaction products. Values are shown both as measured values (*left*) and relative to the composition of the initial carbon source (*right*) ( $\Delta^{13}\text{C} = \delta^{13}\text{C}_{\text{product}} - \delta^{13}\text{C}_{\text{source}}$ ).

At present, however, no obvious explanation for the variation in trends among experiments has emerged, and there does not appear to be any consistent variations in trends with factors such as catalyst composition, reaction temperature, or closed- versus open-system reactions. Although not strictly a FTT reaction because no carbon-carbon bonds are formed, the reduction of dissolved CO<sub>2</sub> to CH<sub>4</sub> catalyzed by NiFe-alloy also results in a substantial depletion in <sup>13</sup>C, with depletions of 42-49‰ at 200 °C and 15-29‰ at 300 °C reported for the experiments of Horita and Berndt (1999). Much less data is available on the hydrogen isotope composition of experimental FTT reaction products (Fu et al. 2007; Taran et al 2010a; McCollom et al. 2010). However, the limited data that are available for hydrogen isotopes show somewhat more consistent trends among experiments than the data for carbon isotopes. For the most part, these data show that CH<sub>4</sub> is depleted in <sup>2</sup>H by -35 to -80‰ relative to the initial H<sub>2</sub>, and exhibit a regular trend of increasing <sup>2</sup>H abundance with increasing number of carbon atoms. The data of Fu et al. (2007) deviate somewhat from this trend, but the CH<sub>4</sub> in this experiment may include some contribution from background sources. In addition to the lack of consistency among isotopic trends observed among experimental products, the presently available experimental data do not show close agreement with isotopic trends observed for natural samples of light hydrocarbons that are thought to have an abiotic origin. Although this might be construed to be an indication that the hydrocarbons in the natural samples do not really have an abiotic origin, a more likely explanation would appear to be that the experimental conditions employed to date do not accurately simulate the conditions of hydrocarbon formation in natural systems. At this point, however, it is not immediately apparent which aspects of the natural system are not adequately represented in the laboratory experiments. While there are clear discrepancies among the broader datasets for experimental and natural systems, a consistent explanation may be emerging for at least a subset of those data. Sherwood Lollar et al. (2008) proposed a model to explain the isotopic composition of light hydrocarbons in deep fracture fluids from ancient Precambrian Shield settings that involves isotopic fractionation during formation of the first C-C bond that initiates chain growth, but subsequent additions of carbon atoms to the hydrocarbon backbone are non-fractionating. The outcome is an isotopic trend that shows a sharp fractionation between CH<sub>4</sub> and C<sub>2</sub>H<sub>6</sub>, while higher hydrocarbons converge towards the isotopic value of CH<sub>4</sub>. McCollom et al. (2010) inferred a similar scenario to explain the carbon isotopic trend observed for C<sub>1</sub>-

C<sub>5</sub> hydrocarbons generated in their laboratory FTT synthesis experiments performed under hydrothermal conditions. These two trends exhibit a difference in direction of isotopic fractionation between CH<sub>4</sub> and C<sub>2</sub>H<sub>6</sub>, but a similar convergence towards the isotopic composition of methane with increasing carbon number for C<sub>2+</sub> compounds. The opposing directions of the initial step may be caused by different reaction mechanisms or conditions effecting the fractionation during the chain initiation.

#### ***2.3.2.4 Implications for abiotic hydrocarbon formation by FTT synthesis within the crust.***

Several indications can be drawn from the experiments described in the previous sections that are particularly relevant to evaluation of the production of abiotic hydrocarbons within Earth's crust. A number of experiments demonstrate that pathways exist for the reduction of dissolved CO<sub>2</sub> (or HCO<sub>3</sub><sup>-</sup>) to CH<sub>4</sub> and other hydrocarbons. However, except when a NiFe-alloy was present, the amount of carbon converted to hydrocarbons was only a very small fraction (<<1%) of the inorganic carbon present in the experiments, even with very high temperatures and dissolved H<sub>2</sub> concentrations that in many cases are an order of magnitude higher than those observed in natural systems. In each of the experiments, thermodynamic constraints indicate that most or all of the carbon should have been converted to hydrocarbons to approach equilibrium, yet the reaction only proceeded to a very limited extent. While it is possible that the minerals present in these experiments (magnetite, chromite, pentlandite) promoted the reactions to some degree, none of these minerals could have been very effective in catalyzing the conversion of inorganic carbon to hydrocarbons, or much greater yields would have been attained. Thus, while industrial Fischer-Tropsch processes may conceptually invoke rapid synthesis of organic compounds, FTT reactions in natural systems may require significantly longer reaction times and produce a more limited range of compounds. The same gradual reduction reaction rates observed in the experiments may prevail in natural systems as well. For instance, although CH<sub>4</sub> and other hydrocarbons with an apparent abiotic origin have been observed in high-temperature (>350 °C) ultramafic-hosted deep-sea hydrothermal systems (e.g., Charlou et al., 2002, 2010), the concentrations of CH<sub>4</sub> in these fluids are much lower than expected for thermodynamic equilibrium with the measured levels of dissolved CO<sub>2</sub> and H<sub>2</sub> in the fluids (McCollom and Seewald, 2007; McCollom, 2008). Consequently, while some reduction of inorganic carbon has apparently occurred as the fluids circulated

through the hydrothermal system, the reactions remain far from equilibrium. Nevertheless, concentrations of CH<sub>4</sub> and other light hydrocarbons produced in the experiments are similar to those observed in fluids from the natural system. The slow rates of reduction of dissolved inorganic carbon are in strong contrast to the rapid reaction rates and high hydrocarbon yields (typically >50%; e.g., Taran et al., 2010a) obtained in conventional gas-phase Fischer-Tropsch studies using transition metal catalysts. Rapid reaction rates and relatively high conversions (1-10%) have also been observed for FTT reactions in the presence of a water-saturated vapor phase (McCullom and Seewald, 2006; McCullom et al., 2010; McCullom, 2016), although these reactions were probably catalyzed by native Fe. This comparison suggests the possibility that the presence of a vapor phase may facilitate rapid reduction of inorganic carbon to hydrocarbons at crust temperatures, although it remains to be determined whether naturally occurring minerals can promote the reaction to the same degree as native transition metals. Vapor phase reactions might occur, for instance, during ascent of magmatic fluids to the surface. Alternatively, an H<sub>2</sub>-rich vapor phase could develop in fluids circulating through the crust as a result of fluid-rock interactions that consume H<sub>2</sub>O and produce H<sub>2</sub>, such as serpentinization. With respect to the latter, it may be noteworthy the mineral assemblage magnetite + pentlandite + awaruite that is found in many serpentinites requires H<sub>2</sub> concentrations that are at, or very close to, the solubility limit of H<sub>2</sub> in water (Klein and Bach 2009), suggesting that an H<sub>2</sub>-rich vapor may have exsolved locally during formation of this assemblage. An exception to the above discussion, of course, is NiFe-alloy, which has been shown to effectively catalyze reduction of dissolved CO<sub>2</sub> to CH<sub>4</sub> (Horita and Berndt 1999). Where this mineral is present, rapid reduction of CO<sub>2</sub> and equilibration with CH<sub>4</sub> can be expected at temperatures at least as low as 200 °C. The formation of NiFe-alloys requires conditions that are more strongly reducing than are commonly found in Earth's crust, but such conditions are sometimes attained during serpentinization of ultramafic rocks (Frost, 1985; Klein and Bach, 2009). Consequently, fluids circulating through serpentinites could become enriched in abiotic CH<sub>4</sub> as a result of interaction with NiFe-alloy. However, since this process appears to exclusively catalyze formation of CH<sub>4</sub>, additional processes would be required for formation of other light hydrocarbons in these environments. The high CH<sub>4</sub>/C<sub>2+</sub> ratios and <sup>13</sup>C-depleted isotopic signatures for CH<sub>4</sub> formed by NiFe-alloy catalysis are very similar to the characteristics of CH<sub>4</sub> produced during methanogenesis by autotrophic microorganisms (Whiticar, 1990), indicating that it may be difficult to confidently distinguish between abiotic and biotic sources of CH<sub>4</sub> in many subsurface settings (Horita and Berndt, 1999; Sherwood Lollar, and McCullom, 2006; Bradley and Summons, 2010).

### 2.3.3 Alternative pathways for hydrocarbon formation in the crust

While most experimental studies have focused on FTT synthesis as a possible contributor of abiotic hydrocarbons to geologic systems, it is by no means the only pathway that could generate these compounds. A few of these alternative pathways are discussed briefly in the following sections. For most alternative pathways, however, there has been little or no experimental study of the reactions at conditions relevant to Earth's crust, and certainly none have been investigated to nearly the same extent as FTT synthesis.

#### *Methane polymerization*

The process of methane polymerization discussed above with respect to the mantle (Chen et al., 2008; Kolesnikov et al., 2009) could also contribute to formation of C<sub>2+</sub> hydrocarbons in the crust, provided a source of CH<sub>4</sub> is available. However, pure CH<sub>4</sub> might arise, for instance, through NiFe-alloy catalyzed reduction of CO<sub>2</sub> in serpentinites (Horita and Berndt, 1999) or reaction of H<sub>2</sub>-rich fluids with graphite in metamorphic rocks (Holloway, 1984). To date, the potential for methane polymerization has apparently not been investigated experimentally at conditions relevant to the crust, although methane polymerization has been invoked as a possible explanation for isotopic trends in some deep-crustal fluids (Sherwood Lollar et al., 2008). Polymerization of CH<sub>4</sub> to higher hydrocarbons can be represented by the general reaction:



As pointed out earlier, thermodynamic considerations demand that some finite amount of hydrocarbons must be present at equilibrium with CH<sub>4</sub> to satisfy the type of reactions represented by this equation, albeit the amount of hydrocarbons required at equilibrium may be vanishingly small under some conditions. According to the reaction, formation of hydrocarbons will be favored by lower levels of H<sub>2</sub>, all other factors being equal.

#### *Carbonate decomposition*

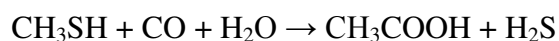
Another process that could generate hydrocarbons in the crust is thermal decomposition of carbonate minerals. Carbonate minerals precipitate in a variety of geologic settings at relatively low temperatures, and these minerals will decompose when exposed to higher

temperatures in metamorphic or hydrothermal environments. This decomposition can lead to the formation of reduced carbon compounds, particularly when the carbonates contain ferrous Fe that can serve as a reductant for the carbon (French, 1971). For example, reduced carbon coexisting with magnetite in ancient metamorphosed rocks in the Isua Greenstone Belt in Greenland has been attributed to thermal decomposition of siderite (i.e.,  $\text{FeCO}_3 \rightarrow \text{Fe}_3\text{O}_4 + \text{C}$ ; Van Zuilen et al., 2002), and decomposition of Fe-bearing carbonates has also been suggested as source of reduced carbon in Martian meteorites (Zolotov and Shock, 2000; McCollom, 2003; Steele et al., 2012). It is possible that light hydrocarbons could be produced as a by-product of such reactions. In contrast to the experiments with calcite conducted at the elevated temperatures relevant to the mantle where thermodynamic equilibrium appears to have exerted a large influence on carbon speciation, thermal decomposition of carbonates at temperatures in the crust may allow the formation of metastable organic compounds. Experimental investigations of the formation of hydrocarbons during thermal decomposition of carbonates at temperatures and pressures relevant to the crust have been limited. However, in one set of experiments, thermal degradation of siderite in the presence of water vapor at 300 °C was found to produce small amounts of organic products, predominantly alkylated and hydroxylated aromatic compounds (McCollom, 2003). Only trace amounts of  $\text{CH}_4$  and other light hydrocarbons were observed. The products of this experiment differed considerably from the typical products of Fischer-Tropsch synthesis, suggesting that an alternative reaction mechanism was responsible for the organic compounds generated. However, the actual process involved remains undetermined. The relatively small amounts of  $\text{CH}_4$  generated during siderite decomposition at 300 °C compared with the larger amounts formed in carbonate decomposition experiments performed at higher temperatures and pressures (Scott et al., 2004; Chen et al., 2008; Kutcherov et al., 2010) appears to be related to the lower H/C and H/O ratios of the experimental charge rather than to the differences in reaction conditions. Whether thermal composition of siderite might produce greater amounts of hydrocarbons under other reaction conditions, and whether other carbonates might also generate organic compounds during decomposition at crust temperatures in reducing environments, are questions that remain to be explored with further experiments.

### *Organosulfur pathways*

Abiotic synthesis reactions that proceed through organosulfur intermediates are another possible source of hydrocarbons in the crust. Scientific interest in the possibility that

organosulfur compounds might contribute to abiotic organic synthesis was initially stimulated by the origin of life theories of Gunther Wächtershäuser and others. According to these theories, reaction of carbon-bearing fluids with sulfide minerals in hydrothermal environments induced organic synthesis reactions that later evolved into primordial metabolic pathways (Wächtershäuser, 1990, 1993). The first experimental study to test this theory was that of Heinen and Lauwers (1996), who heated solid FeS with H<sub>2</sub>S, CO<sub>2</sub>, and water in glass vials at temperatures of 25 to 90 °C, and observed formation of a homologous series of C<sub>1</sub>-C<sub>5</sub> alkylthiols as major products. Reduction of carbon in this system presumably involved reaction of CO<sub>2</sub> with H<sub>2</sub> produced by the reaction: FeS + H<sub>2</sub>S → FeS<sub>2</sub> (pyrite) + H<sub>2</sub> (referred to by Wächtershäuser as “pyrite-pulled” reactions). The alkylthiols decrease in abundance with increasing number of carbons, and linear butane- and pentanethiol were more abundant than branched forms. This initial set of experiments was followed up recently by Loison et al. (2010). Using similar reaction conditions to Heinen and Lauwers (1996), but replacing the water in the reactions with D<sub>2</sub>O, these investigators showed that the alkylthiols incorporated D into their structures, thus proving they were formed during the reactions. Other reaction products identified by Loison et al. (2010) were polydeuterated C<sub>1</sub>-C<sub>4</sub> carboxylic acids. In a related study, Huber and Wächtershäuser (1997) reported formation of acetic acid during reaction of aqueous solutions of methanethiol (CH<sub>3</sub>SH) with CO gas at 100 °C in the presence of metal sulfide minerals. The overall reaction can be expressed as:



The key step in this reaction is the formation of a C–C bond, which the authors inferred took place by insertion of CO into the C–S bond on the surface of the sulfide mineral. The reaction was further investigated by Cody et al. (2000), who reacted nonanethiol (C<sub>9</sub>H<sub>19</sub>SH) with formic acid in the presence of iron sulfide at 250 °C and 50-200 MPa. Decomposition of formic acid resulted in a mixture of CO, CO<sub>2</sub>, H<sub>2</sub>, and H<sub>2</sub>O in the reaction vessel at experimental conditions. In a follow-up study testing the capacity of other sulfide minerals and native Ni to catalyze the reaction, C<sub>11</sub>-C<sub>13</sub> carboxylic acids were identified as reaction products in addition to decanoic acid (Cody et al., 2004). Although several metal sulfide minerals catalyzed the reaction, it was most strongly promoted by Ni- and Co-bearing sulfides. Results of these experiments suggest the possibility that organic compounds might be generated in subsurface environments through the sequential formation of C–C bonds involving thiols or other organosulfur as reaction intermediates, with sulfide minerals serving as a catalyst. The products of these reactions have many similarities to the products of FTT

synthesis, such as a preference for straight alkyl chains relative to branched forms, a regular decrease in abundance with increasing carbon number, and involvement of surface catalysis in the synthesis reaction. However, the apparent lack of alkane and alkene products similar to those that predominate during FTT synthesis suggests that a distinctly different reaction mechanism may be involved. Based on a series of experiments with potential reaction intermediates, Loison et al. (2010) have proposed a scenario whereby a homologous series of alkylthiols and carboxylic acids with increasing carbon number would be generated through an iterative process involving formation and reduction of thioesters. In this scenario, CO is inserted into the C–S bond of an alkylthiol to form a thiocarboxylic acid with one additional carbon, which is then either converted to a carboxylic acid or reduced to an alkylthiol, which can then undergo the same reaction cycle. McCollom and Seewald (2007) proposed a somewhat different iterative process, whereby CO is incorporated into a growing alkyl carbon chain through insertion into the C–S bond of the alkylthiol to form carboxylic acid, followed by reduction of the acid to an alcohol, which then is converted back to an alkylthiol that starts the sequence of steps over again. Whatever the actual mechanism, the outcome would be formation of series of alkylthiols and carboxylic acids that could subsequently undergo reduction to form hydrocarbons or other organic matter. If this were to occur, the process could contribute to the light hydrocarbons observed in geologic fluids. Since the canonical wisdom is that most industrial catalysts for Fischer-Tropsch synthesis are “poisoned” by sulfur (though this remains to be rigorously tested for natural geologic materials), sulfide-catalyzed reactions could provide an alternative pathway for hydrocarbon formation in sulfur-rich subsurface environments.

#### *Clay-catalyzed hydrocarbon synthesis*

Clay minerals have catalytic properties for many types of chemical reactions, which have been exploited for many years by industry. Since clay minerals are widespread in geologic environments, including altered igneous rocks and sediments, it is possible that they could play a role in the abiotic formation of hydrocarbons. This possibility was investigated in experiments by Williams et al. (2005), who reacted aqueous methanol solutions with clay minerals at 300 °C and 100 MPa. The reactions produced dimethylether (a condensation product of two methanol molecules) as the principal product, but a number of other organic products were observed including CH<sub>4</sub>, C<sub>2</sub>–C<sub>6</sub> alkanes and alkenes, along with an assortment of alkylated cyclic aromatic compounds, such as alkylbenzenes, alkylphenols,

alkylnaphthalenes, and alkylnaphthols. The predominance of alkylated aromatic compounds among the higher molecular weight reaction products distinguishes them from the linear saturated alkanes that are characteristic of FTT synthesis, suggesting either a different mechanism is involved or that alkanes were generated and then underwent secondary reactions to form aromatic compounds. The mechanism of the reaction remains to be determined, but the authors hypothesized that the organic compounds may have formed within the interlayers of the clay structure, suggesting that clay minerals may provide unique microenvironments for organic synthesis.

## 2.4 Biogenic processes

Carbon is the second most abundant element in living organisms. Carbon is present in all organic molecules, and its role in the structure of macromolecules is of primary importance to living organisms. Living organisms are connected in many ways, even between ecosystems. A good example of this connection is the exchange of carbon between autotrophs and heterotrophs within and between ecosystems by way of atmospheric carbon dioxide. Carbon dioxide is the basic building block that most autotrophs use to build multi-carbon, high energy compounds, such as glucose. The energy harnessed from the sun is used by these organisms to form the covalent bonds that link carbon atoms together. These chemical bonds thereby store this energy for later use in the process of respiration. Most terrestrial autotrophs obtain their carbon dioxide directly from the atmosphere, while marine autotrophs acquire it in the dissolved form (carbonic acid,  $\text{H}_2\text{CO}_3^-$ ). However, carbon dioxide is acquired, a by-product of the process is oxygen. The photosynthetic organisms are responsible for depositing approximately 21 percent oxygen content of the atmosphere that we observe today. Heterotrophs and autotrophs are partners in biological carbon exchange. Heterotrophs acquire the high-energy carbon compounds from the autotrophs by consuming and breaking them down by respiration to obtain cellular energy, such as ATP. The most efficient type of respiration, aerobic respiration, requires oxygen obtained from the atmosphere or dissolved in water. Thus, there is a constant exchange of oxygen and carbon dioxide between the autotrophs (which need the carbon) and the heterotrophs (which need the oxygen). Gas exchange through the atmosphere and water is one way that the carbon cycle connects all living organisms on Earth. Microorganisms are the most widespread form of life on Earth. "Microbe" is a general term that encompasses almost any microscopic organism, including bacteria and archaea, which lack a cell nucleus or other membrane-bound cellular structures,

and protists (mostly unicellular organisms that lack specialized tissues, and hence, are neither plant nor animal nor fungus). Single-celled microorganisms were the first form of life to develop on Earth and microbes can be found in almost every habitat present in nature where they are crucial for sustaining larger ecosystem life. The diversity and number of microbes in the ocean far exceed that of macroscopic life, and many employ unique life strategies not seen anywhere else on Earth. Without them, life on Earth almost certainly would not be possible. Some microbes are photosynthetic, deriving their energy from the sun. Below the photic zone, and especially at deep-ocean sites and around hydrothermal vents and seeps, microbes are chemosynthetic, meaning they derive energy from chemical reactions to drive their metabolic processes. Some microbes prey on others, some obtain carbon from inorganic sources, and some are scavengers that feed on dead organisms, fecal pellets, or other waste organic matter. Some can even consume hydrocarbons. A few, such as diatoms and foraminifera, make hard, calcite “shells” that last for thousands of years in seafloor sediments and provide clues to past climate and ocean conditions. Volatile organic compounds are strictly related to microbial activity, being consumed and/or produced by the metabolism of archaea and bacteria. For example, terrestrial soils and aqueous environments may act as a sink of VOCs due to microbe capability of degrading organic compounds under both aerobic and anaerobic conditions (Insam and Seewald, 2010; Peñuelas et al., 2014; Gennadiev et al., 2015). On the other hand, wetlands and marine sediments may be a source of VOCs (Peñuelas et al., 2014 and references therein), as these compounds may be produced by primary metabolism, as cell growth-associated by-products, and secondary metabolism, as (i) products not required for the survival of the organisms but that may serve for specific functions, (ii) competitive weapons used against other microbes, (iii) agents of symbiosis between organisms, (iv) sexual hormones, and so on.

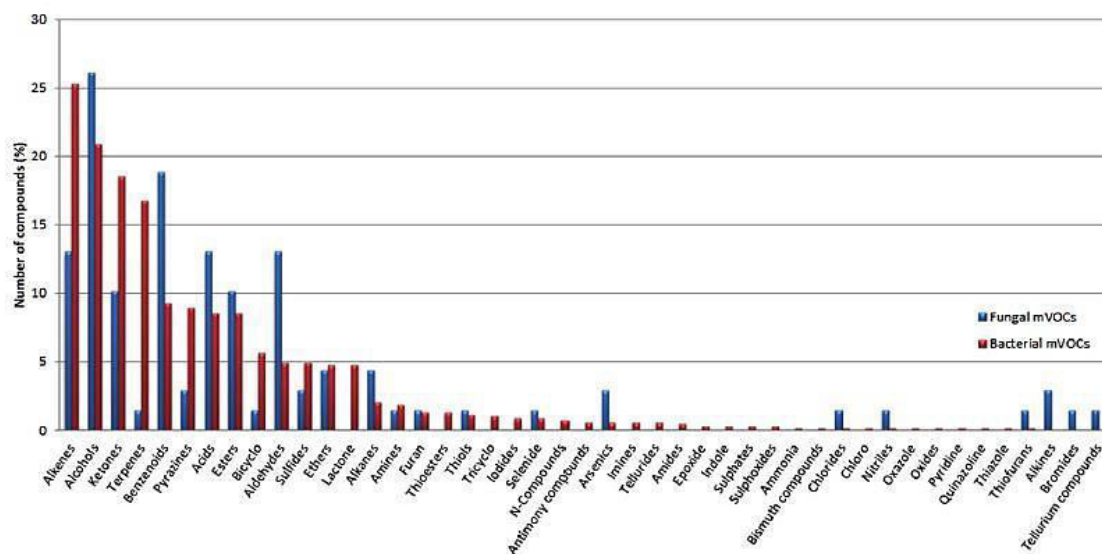


Figure 9: Distribution of microbial volatile organic compound (VOC) emission. Volatiles emitted by bacteria (red columns) and by fungi (blue columns). Chemical classes are ordered due to the number of different compounds within a class. Bacterial VOC profiles are rich in alkenes, alcohols, ketones and terpenes; fungal VOCs are dominated by alcohols, benzenoids, aldehydes, ketones and arsenics (descending order) (after Peñuelas et al., 2014)

Through metabolic pathways, living organisms convert a carbon source into the building blocks needed for the synthesis of new cellular materials. As stated above, heterotrophs are capable to break down complex organic compounds, such as carbohydrates, proteins, lipids, into simpler end-products through catabolism, i.e. the degradative phase of metabolism. The catabolic pathways consist of oxidative stepwise reactions that result in the transfer of electrons from electron donors to an electron acceptor. Energy may be obtained by (i) respiration, involving transfer of electrons to inorganic acceptors, i.e. either molecular oxygen (aerobic respiration) or other species such as  $\text{SO}_4$ ,  $\text{NO}_3$ ,  $\text{NO}_2$ ,  $\text{CO}_3$ ,  $\text{CO}_2$  (anaerobic respiration), or (ii) fermentation, involving transfer of electrons to an organic substrate. Whilst part of the energy released during these electron transfers is lost as heat, the rest is used to form electron carriers or high-energy compounds (such as ATP, NADH, NADPH and FADH<sub>2</sub>), which are the central goal of catabolism. These compounds, in particular ATP, provide energy for anabolic pathways and cell growth. Differently from heterotrophs, autotrophic organisms are capable to fix carbon atoms from inorganic species ( $\text{CO}_2$ ) into organic compounds. They may obtain energy, in the form of ATP and NADPH, from sunlight or oxidation of chemicals. Methanogenesis is the formation of methane by microbes known as methanogens, microorganisms belonging to the domain of archaea. Methanogens play a vital ecological role in anaerobic environments, removing excess hydrogen and fermentation products. Methanogens have been found in several extreme environments on Earth, making

them the most widespread VOCs-producing form of microbial life on Earth. The microbiology, ecology and biochemistry of the various bacterial CH<sub>4</sub> formation pathways have been reviewed extensively in several monographs (e.g. Garcia, 1990; Konig, 1992; Marty, 1992). Methanogens, fermentative archaeobacteria, are obligate anaerobes that metabolize only in anoxic conditions at redox levels  $E_h < 200$  mV. Methanogens form methane by pathways that are commonly classified with respect to the type of carbon precursor utilized by them. The primary methanogenic pathways are referred to as: hydrogenotrophic; acetotrophic and methylotrophic. As stated above, VOCs participate to microbial metabolism as energy and carbon sources, or products of primary or secondary metabolism. Accordingly, microbes are used, for instance, to produce biofuels and chemicals (e.g. Mukhopadhyay, 2015), and in bioremediation techniques to biodegrade VOCs in contaminated soils and waters (e.g. Megharaj et al., 2011; Lien et al., 2016). Biodegradation is defined as the biologically catalyzed reduction in molecular complexity of chemical compounds (Alexander 1994). It may occur in the presence of oxygen (aerobic conditions) or without oxygen (anaerobic conditions) through the metabolic activity of microorganisms. Chemoorganotrophic species can use a huge number of organic compounds as carbon and energy sources, some microbial species utilizing more than 100 different organic compounds (Fritsche and Hofrichter, 2008). In general, an organic compound may be (i) used by microbes as the primary carbon and energy source for cell growth and ATP production, (ii) used as an electron acceptor to aid cellular respiration (anaerobic respiration), or (iii) transformed by a microbe without nutritional benefit in the presence of a growth substrate that is used as the primary carbon and energy source (co-metabolism). For example, methanotrophs are capable to co-metabolize a variety of aromatic, aliphatic and halogenated compounds (e.g. oxidizing alkanes to organic acids, or trichloroethylene to TCE epoxide; Little et al., 1988; Fritsche and Hofrichter, 2008 and references therein) and have been applied for bioremediation of chlorinated solvents in polluted sites. The cell growth-associated degradation of VOCs may occur through cellular respiration (aerobic or anaerobic) and/or fermentative processes.

1  
2  
3  
4  
5  
6  
7  
8  
9  
10  
11  
12  
13  
14  
15  
16  
17

## Abiotic hydrocarbons in Earth's crust: a phantom

Jens Fiebig<sup>1</sup>, Andri Stefánsson<sup>2</sup>, Andrea Ricci<sup>3</sup>, Franco Tassi<sup>4</sup>, Fatima V. Viveiros<sup>5</sup>, Catarina Silva<sup>5,6</sup>, Taryn M. Lopez<sup>7</sup>, Christoph Schreiber<sup>1</sup>, Sven Hofmann<sup>1</sup> & Bruce W. Mountain<sup>8</sup>

<sup>1</sup> Institute of Geosciences, Goethe University, Altenhöferallee 1, 60438 Frankfurt/Main, Germany (Jens.Fiebig@em.uni-frankfurt.de)

<sup>2</sup> Institute of Earth Sciences, University of Iceland, Sturlugata 7, 101 Reykjavik, Iceland

<sup>3</sup> Department of Biological, Geological and Environmental Sciences, University of Bologna, Piazza di Porta San Donato 1, 40126 Bologna, Italy

<sup>4</sup> Department of Earth Sciences, University of Florence, Via La Pira 4, 50121 Florence, Italy

<sup>5</sup> Institute of Volcanology and Risks Assessment (IVAR), Universidade dos Açores, Rua da Mae de Deus, 9501-801 Ponta Delgada, Portugal

<sup>6</sup> Centre for Information and Seismovolcanic Surveillance of the Azores, Rua da Mãe de Deus, 9501-801 Ponta Delgada, Portugal

<sup>7</sup> Geophysical Institute, Alaska Volcano Observatory, University of Alaska Fairbanks, 903 Koyukuk Drive, Fairbanks, AK 99775, USA

<sup>8</sup> GNS Science, Wairakei Research Centre, 114 Karetoto Road, Taupo 3384, New Zealand

### Abstract

Abiotic formation of n-alkane hydrocarbons has been postulated to occur within Earth's crust<sup>1-6</sup>. Apparent evidence was mainly based on carbon and hydrogen isotope distribution patterns that sets methane and its higher chain homologues apart from common biotic isotopic compositions associated with microbial production and closed system thermal degradation of organic matter<sup>1-6</sup>. Here, we present the first global investigation of the carbon and hydrogen isotopic compositions of n-alkanes in volcanic-hydrothermal fluids hosted by basaltic, andesitic and rhyolitic rocks. We show that these hydrocarbons derive from biotic sources, i.e., predominantly from the thermal decomposition of organic matter. Meteoric waters and seawater circulating through the crust shuttle organic matter from Earth's surface into the reservoir rocks. There, high temperature pyrolysis of organic matter and open system degassing generates n-alkanes with isotopic compositions previously classified as being indicative for abiogenesis. These results challenge the dogma of crustal production of abiotic hydrocarbons and highlight the potential of n-alkanes to become sensitive indicators of life on habitable (exo)planets.

33

34 The ability to distinguish between biotic and abiotic hydrocarbon sources on Earth is essential  
35 to fully understand the formation of crustal hydrocarbon reservoirs, identify the origin of  
36 hydrocarbons such as methane on other planets and resolve the potential role of abiotic methane  
37 in the emergence of life<sup>1</sup>. It is well known that crustal hydrocarbons largely derive from biotic  
38 sources, i.e. from microbial production and thermal decomposition of organic matter<sup>1,2</sup>. Abiotic  
39 hydrocarbon formation (i.e., generation from pure inorganic substances, without any  
40 involvement of organic carbon) has been postulated to take place in a variety of natural systems  
41 where inorganically derived CO or CO<sub>2</sub>, water, reducing reagents and catalysts and/or heat are  
42 available. To these belong hydrothermal and low-temperature (T < 100°C) mafic and ultramafic  
43 systems, subduction-related volcanic-hydrothermal systems and igneous intrusions<sup>1,2</sup>.

44 Most prominently, the following criteria were used to identify abiotic hydrocarbon occurrences:  
45 i) methane with  $\delta^{13}\text{C} \geq -20\text{‰}$ <sup>3</sup>, ii) the occurrence of a carbon isotope reversal between ethane  
46 and methane<sup>4,5</sup> (i.e., methane more enriched in <sup>13</sup>C than ethane, contrary to what is observed  
47 for n-alkanes from confined sedimentary hydrocarbon reservoirs) and iii) methane in apparent  
48 chemical and isotopic equilibrium with inorganically derived CO<sub>2</sub><sup>6</sup>. However, laboratory  
49 experiments did not provide supporting evidence for the robustness of the carbon isotope  
50 reversal criterion<sup>7</sup>. In addition, <sup>13</sup>C-labelling of reagents revealed sluggish reaction rates<sup>8,9</sup>, and  
51 experimental setups were shown to be prone to contaminant hydrocarbons<sup>10</sup>. These results  
52 called the relevance of abiotic n-alkane production in Earth's crust into question<sup>9</sup>, especially in  
53 low temperature environments<sup>10</sup>.

54 For this study, we investigated for the first time the global-scale systematics of carbon and  
55 hydrogen isotope variations in hydrothermal fluids. We sampled two-phase well fluids (n = 29)  
56 and steam vent fumaroles (n = 61) from 28 volcanic-hydrothermal fields in New Zealand,  
57 Iceland, Argentina, USA (Alaska), Italy, Greece, Portugal (Azores) and Spain (Tenerife)  
58 (Extended Data Table 1). We analyzed the carbon isotopic compositions of methane, ethane,  
59 propane and n-butane as well as the hydrogen isotopic compositions of methane and water in  
60 these fluids (Extended Data Tables 2, 3). Sampled locations cover all types of volcanism and a  
61 wide range of reservoir temperatures (200-450°C), with the origin of external water being  
62 dominantly meteoric and/or seawater (Extended Data Table 1). Terrestrial vegetation at the  
63 sampled sites is largely dominated by C<sub>3</sub> plants<sup>11</sup>.

64 For several locations, carbon isotopes are homogeneously distributed among ethane, propane  
65 and n-butane (C<sub>2+</sub> hydrocarbons), i.e. variations in  $\delta^{13}\text{C}_{2+}$  are  $\leq 1.0\text{‰}$  (Fig. 1a). At Reykjanes,

66  $\delta^{13}\text{C-C}_{2+}$  of -16‰ (well 11) and -17 to -18‰ (well 12) overlap with the carbon isotopic  
67 composition of particulate organic matter ( $-17.5 \geq \delta^{13}\text{C-POC} \geq -22.2\text{‰}$ ) and modern  
68 sedimentary organic matter ( $-16.5 \geq \delta^{13}\text{C-SOM} \geq -19.4\text{‰}$ ) that are characteristic for the water  
69 masses surrounding the Reykjanes peninsula<sup>12</sup>. For Esguicho (Furnas village)  $\delta^{13}\text{C-C}_{2+}$  of -28  
70 to -29‰ perfectly agree with the average carbon isotopic composition of terrestrial plants  
71 growing in the Furnas caldera ( $-28.4\text{‰}$ )<sup>13</sup>. The hydrothermal reservoir at Reykjanes is  
72 predominantly fed by seawater, whereas the hydrothermal system beneath Furnas village is  
73 exclusively sourced by meteoric water (Extended Data Table 1). The same patterns - invariant  
74  $\delta^{13}\text{C-C}_{2+}$ , but absolute values changing with the source of water - is observed at Nisyros  
75 (seawater-fed hydrothermal system,  $\delta^{13}\text{C-C}_{2+}$  around -18‰), Ischia and Rotokawa well 14  
76 (both meteoric water-fed systems,  $\delta^{13}\text{C-C}_{2+}$  around -27‰) (Fig. 1a; Extended Data Table 1).  
77 These observations strongly imply that local organic matter is transported by external waters  
78 into the corresponding hydrothermal reservoirs, where it is finally subjected to high temperature  
79 pyrolysis. At these temperatures, the carbon isotope fractionation between the  $\text{C}_{2+}$  hydrocarbons  
80 and the source organic matter becomes insignificantly small and, hence, the  $\delta^{13}\text{C-C}_{2+}$  becomes  
81 indicative of the bulk organic matter decomposing at depth.

82 The majority of sampled discharges exhibits significant differences among  $\delta^{13}\text{C-C}_{2+}$  values  
83 (Extended Data Tables 2, 3). However, the carbon isotopic composition of n-butane, the longest  
84 n-alkane analyzed in this study, always occurs within the range reported for modern marine  
85 dissolved organic matter ( $-18\text{‰} \geq \delta^{13}\text{C-DOC} \geq -23\text{‰}$ )<sup>14</sup>, modern marine particulate organic  
86 matter ( $-17\text{‰} \geq \delta^{13}\text{C-POC} \geq -25\text{‰}$ )<sup>12,14</sup> and modern terrestrial  $\text{C}_3$  plants ( $-20\text{‰} \geq \delta^{13}\text{C} \geq -37\text{‰}$ ,  
87 with most data clustering between  $-23\text{‰} \geq \delta^{13}\text{C} \geq -31.5\text{‰}$  and averaging to  $\delta^{13}\text{C} = -28.5\text{‰}$ )<sup>15</sup>  
88 (Fig. 1b). Moreover, relative variations in  $\delta^{13}\text{C}$  decrease in the order ethane – propane – n-  
89 butane (Fig. 1b). These patterns are expected for thermal degradation of organic matter in which  
90 the carbon isotope fractionation between source organic matter and the evolving gaseous n-  
91 alkane decreases with the number of carbon atoms constituting the n-alkane<sup>16</sup>. These  
92 observations highlight the importance of predominant thermogenic production of  $\text{C}_{2+}$   
93 hydrocarbons in all investigated systems. In addition to the modern organic matter supplied by  
94 external waters, older organic matter contained in sediments can also contribute to overall  
95 hydrocarbon production, as becomes evident from Rotokawa  $\delta^{13}\text{C-C}_{2+}$  data (Extended Data  
96 Table 2). Although the Rotokawa hydrothermal reservoir is exclusively sourced by meteoric  
97 waters, its  $\delta^{13}\text{C-C}_4$  values range from -27‰ to -17‰, pointing to the occurrence of a marine  
98 next to a terrestrial organic source. The marine organic endmember is likely hosted in Mesozoic

99 greywacke occurring at relatively shallow depth of 1-3km depth underneath Rotokawa  
100 (Extended Data Tables 1).

101 Several lines of evidence also imply that methane predominantly derives from the thermal  
102 decomposition of organic matter that is shuttled by external waters from the surface to reservoir  
103 depth: i) Even if methane samples with an obvious microbial origin (Furnas B and Furnas Lake  
104 2, Azores (Extended Data Table 3), as indicated by relatively strong depletions in  $^{13}\text{C}$  and D)<sup>17</sup>  
105 are excluded, methane still exhibits the largest variations in  $\delta^{13}\text{C}$  of all analyzed n-alkanes (Fig.  
106 1b). ii) In  $\delta^{13}\text{C}$  vs  $\delta\text{D}$  space, methane from meteoric water- and seawater-fed hydrothermal  
107 systems plots along trends that are characteristic of open system, high temperature cracking of  
108 terrestrial and marine organic matter<sup>18</sup>, respectively (Fig. 2a). iii) In the same space, methane  
109 from volcanic-hydrothermal systems plots into a field that has a shape similar to that  
110 characteristic of thermogenic methane from confined sedimentary systems, but is, relative to  
111 the latter, shifted to higher  $\delta^{13}\text{C}$  values (Fig. 2b).  $^{13}\text{C}$ -enrichment of thermogenic methane in  
112 volcanic-hydrothermal fluids results from relatively high reservoir temperatures of 200° -  
113 450°C (Extended Data Table 1), clearly exceeding those of confined sedimentary reservoirs  
114 where methane generation mostly takes place between ~150° - 220°C<sup>19</sup>. Carbon isotope  
115 fractionations associated with organic matter degradation are, therefore, expected to be smaller  
116 in volcanic-hydrothermal systems. In addition, modern marine organic matter is enriched in  $^{13}\text{C}$   
117 by 5 to 10‰ relative to the marine organic matter of pre-Cenozoic age<sup>20</sup> that provides the source  
118 of kerogen in confined sedimentary reservoirs. iv) In Icelandic systems, which are characterized  
119 by the absence of organic sediments, DOC and POC concentrations of meteoric water and/or  
120 seawater alone are sufficiently high to balance n-alkane concentrations in the discharged fluids  
121 (Extended Data Fig. 1). v) Under steady state conditions, water recharge rates at depth should  
122 be higher in well reservoirs than in naturally degassing systems, as in well systems the reservoir  
123 fluid is continuously exploited at the surface in addition to the steam. The flux of fresh,  
124 immature organics (depleted in  $^{13}\text{C}$ ) through the reservoir should, therefore, be higher in well  
125 systems. This is consistent with the observation that well discharges display on average lower  
126  $\delta^{13}\text{C}$ -CH<sub>4</sub> values than fumaroles (Fig. 2b).

127 Two reasons may account for  $\delta\text{D}$  departing from the predicted cracking and degassing trends  
128 at high organic matter maturities characterized by  $\delta^{13}\text{C}$ -CH<sub>4</sub>  $\geq$  -20‰ (Fig. 2a). First, hydrogen  
129 isotope exchange between CH<sub>4</sub> and water might occur at the elevated temperatures  
130 characteristic of hydrothermal systems, driving CH<sub>4</sub> towards isotopic equilibrium with water at  
131  $T \geq 300^\circ\text{C}$ . (Extended Data Fig. 2a). Alternatively, the decomposing organic matter at depth

132 might be able to exchange hydrogen with the reservoir water at depth such that the hydrogen  
133 isotopic composition of the organic matter and that of the methane becomes progressively  
134 buffered by water with increasing temperature and/or increasing organic matter maturity.

135 The observation that thermogenic cracking of organic matter under open system conditions is  
136 of natural relevance has important implications for the reliability of criteria previously applied  
137 to identify abiogenic hydrocarbon occurrences. i)  $\delta^{13}\text{C}$ - $\text{CH}_4$  values exceeding those characteristic  
138 for methane from confined sedimentary systems are not indicative of abiogenesis (Fig. 2a). ii)  
139 The occurrence of a carbon isotope reversal cannot be used as evidence for abiogenic n-alkane  
140 generation either. Reversals can be obtained from thermogenic degradation and open system  
141 degassing alone (Extended Data Figs. 3), or from mixing of thermogenic n-alkanes from two  
142 or more sources of distinct organic maturity<sup>21</sup>. iii) As  $\delta^{13}\text{C}$ - $\text{CH}_4$  is controlled by the relative  
143 fluxes of organic carbon into and methane carbon out of the system, carbon isotope equilibrium  
144 between  $\text{CH}_4$  and  $\text{CO}_2$  is not attained. The apparent fractionation only fortuitously corresponds  
145 to equilibrium in some cases (Extended Data Figs. 2b, 4).

146 Although a wide variety of host rocks is involved (ultramafic, mafic, felsic),  $\delta^{13}\text{C}$  and  $\delta\text{D}$  of  
147 methane as well as  $\delta^{13}\text{C}$  of the longest chain n-alkanes (propane and n-butane) from other  
148 "abiogenic" settings<sup>1,2</sup> such as Chimaera, Zambales, Lost City, unsedimented mid-ocean ridges,  
149 Socorro, Milos, Khibina and Lovozero occur within the ranges reported in this study (Figs. 1c,  
150 2c). This may point to a thermogenic origin of methane and the  $\text{C}_{2+}$  hydrocarbons in these  
151 locations as well. Seawater and meteoric waters are cycled in large amounts through continental  
152 and oceanic crust, and large fractions of their organic matter could be sorbed to the minerals in  
153 the host rocks before thermocatalysis starts, making mass balance calculations based on organic  
154 matter content of feeding and discharged fluids difficult to interpret. Up to 70% of DOC is  
155 removed from deep seawater during its circulation through high temperature and ridge-flank  
156 hydrothermal systems<sup>22</sup>. Oceanic gabbros and serpentinites contain significant amounts of bulk  
157 organic carbon (up to 3000 ppm), whose carbon isotope composition ( $-32\text{‰} \geq \delta^{13}\text{C} \geq -8\text{‰}$ )<sup>23</sup>  
158 spreads around that of marine DOC. Abiotic production has also been proposed to occur at  
159 temperatures  $< 100^\circ\text{C}$  for n-alkanes degassing from old cratonic rocks and continental  
160 serpentinization sites associated with hypersaline spring water<sup>1,2</sup>. However, considering  
161 experimental constraints that there already is a kinetic barrier for abiogenic hydrocarbon  
162 production at temperatures as high as  $300^\circ\text{C}$  it would be remarkable if this kinetic barrier  
163 becomes less important at lower temperatures<sup>10</sup>. Experiments in which the use of rubber septa  
164 was avoided failed to produce any  $\text{CH}_4$  from reaction of carbon-bearing fluids with ultramafic

165 rocks at such low temperatures<sup>10</sup>. On the contrary, it has recently been noticed that thermogenic  
166 hydrocarbon production proceeds down to temperatures of at least 60°C<sup>24</sup>. The potential  
167 importance of thermogenic degradation of organic matter at low temperatures and microbial  
168 methanogenesis at varying availabilities of CO<sub>2</sub> and H<sub>2</sub> needs to be investigated in more detail  
169 before an abiotic origin can be assessed to these hydrocarbons. The virtual absence of abiotic  
170 hydrocarbons in Earth's crust would make methane and its higher chain homologues sensitive  
171 indicators of ancient or modern life on habitable (exo)planets, such as possibly on Mars, where  
172 locally elevated atmospheric methane concentrations of 7 ppbv cannot be explained by bolide  
173 impacts and/or photochemical degradation of exogeneously derived organic matter<sup>25</sup>.

174

#### 175 **References**

- 176 1. Etiope, G. & Sherwood Lollar, B. Abiotic methane on Earth. *Rev. Geophys.* **51**, 276-  
177 299 (2013).
- 178 2. Etiope, G. & Schoell, M. Abiotic gas: atypical but not rare. *Elements* **10**, 291-296.
- 179 3. Welhan, J. A. & Craig, H. Methane and hydrogen in East Pacific Rise hydrothermal  
180 fluids. *Geophys. Res. Lett.* **6**, 829-831 (1979).
- 181 4. Sherwood Lollar, B. et al. Abiotic formation of gaseous alkanes in the Earth's crust  
182 as a minor source of global hydrocarbon reservoirs. *Nature* **416**, 522–524 (2002).
- 183 5. Proskurowski, G. et al. Abiotic hydrocarbon production at Lost City hydrothermal field.  
184 *Science* **319**, 604–607 (2008).
- 185 6. Fiebig, J., Woodland, A. B., Spangenberg, J. & Oschmann, W. Natural evidence for  
186 rapid abiotic hydrothermal generation of CH<sub>4</sub>. *Geochim. Cosmochim. Acta* **71**,  
187 3028–3039 (2006).
- 188 7. McCollom, T. M. (2013) Laboratory simulations of abiotic hydrocarbon formation in  
189 Earth's deep subsurface. *Rev. Miner. Geochem.* **75**, 467–494 (2013).
- 190 8. Foustoukos, D. I. & Seyfried, W. E. J. Hydrocarbons in hydrothermal vent fluids: the  
191 role of chromium-bearing catalysts, *Science* **304**, 1002–1005 (2004).
- 192 9. McCollom, T. M. Abiotic methane formation during experimental serpentinization of  
193 olivine. *Proc. Natl. Acad. Sci. USA* **113**, 13965-13970 (2016).

- 194 10. McCollom, T. M. & Donaldson, C. Generation of hydrogen and methane during  
195 experimental low-temperature reaction of ultramafic rocks with water. *Astrobiology* **16**,  
196 389-406 (2016).
- 197 11. Still, C. J., Berry, J. A., Collatz, G. J. & DeFries, R. S. Global distribution of C<sub>3</sub> and C<sub>4</sub>  
198 vegetation: Carbon cycle implications. *Glob. Biogeochem. Cycl.* **17**,  
199 doi:10.1029/2001GB001807 (2003).
- 200 12. Sara, G. et al. Sources of organic matter for intertidal consumers on Ascophyllum-  
201 shores (SW Iceland): a multi-stable isotope approach. *Helgol. Mar. Res.* **61**, 297-302  
202 (2007).
- 203 13. Pasquier-Cardin, A. et al. Magma-derived CO<sub>2</sub> emissions recorded in <sup>14</sup>C and <sup>13</sup>C  
204 content of plants growing in Furnas caldera, Azores. *J. Volcanol. Geotherm. Res.* **92**,  
205 195-207 (1999).
- 206 14. Druffel, E. R. M., Williams, P. M., Bauer, J. E. & Ertel, J. R. Cycling of dissolved and  
207 particulate organic matter in the open ocean. *J. Geophys. Res.* **97**, 15639-15659  
208 (1992).
- 209 15. Kohn, M. J. Carbon isotope compositions of terrestrial C<sub>3</sub> plants as indicators of  
210 (paleo)ecology and (paleo)climate. *Proc. Natl. Acad. Sci. USA* **107**, 19691-19695  
211 (2010).
- 212 16. Tang, Y., Perry, J. K. & Jenden, P. D. & Schoell, M. Mathematical modeling of stable  
213 carbon isotope ratios in natural gases. *Geochim. Cosmochim. Acta* **64**, 2673-2687  
214 (2000).
- 215 17. Whiticar, M. J. Carbon and hydrogen isotope systematics of bacterial formation and  
216 oxidation of methane. *Chem. Geol.* **161**, 291-314 (1999).
- 217 18. Berner, U., Faber, E., Scheeder, G. & Panten, D. Primary cracking of algal and  
218 landplant kerogens: kinetic models of isotope variations in methane, ethane and  
219 propane. *Chem. Geol.* **126**, 233-245 (1995).
- 220 19. Quigley, T. M. & MacKenzie, A. S. The temperatures of oil and gas formation in the sub-  
221 surface. *Nature* **333**, 549-552 (1988).
- 222 20. Hayes, J. M., Strauss, H. & Kaufmann, A. J. The abundance of <sup>13</sup>C in marine organic  
223 matter and isotopic fractionation in the global biogeochemical cycle of carbon  
224 during the past 800Ma. *Chem. Geol.* **161**, 103-125 (1999).

- 225 21. Taran, Y. A., Kliger, G. A. & Sevastyanov, V. S. Carbon isotope effects in the open-  
226 system Fischer–Tropsch synthesis. *Geochim. Cosmochim. Acta* **71**, 4474–4487  
227 (2007).
- 228 22. Lang, S. Q. et al. Dissolved organic carbon in ridge-axis and ridge-flank  
229 hydrothermal systems. *Geochim. Cosmochim. Acta* **70**, 3830–3842 (2006).
- 230 23. Delacour, A. et al. Carbon geochemistry of serpentinites in the Lost City Hydrothermal  
231 System (30°N, MAR). *Geochim. Cosmochim. Acta* **72**, 3681–3702 (2008).
- 232 24. Wei, L. et al. Catalytic generation of methane at 60–100°C and 0.1–300MPa from source  
233 rocks containing kerogens Types I, II, and III. *Geochim. Cosmochim. Acta* **231**, 88–116  
234 (2018).
- 235 25. Webster, C. R. et al. Mars methane detection and variability at Gale crater. *Science* **347**,  
236 415–417 (2015).
- 237 26. Hayes, J. M. & Waldbauer, J. R. The carbon cycle and associated redox processes through  
238 time. *Phil. Trans. R. Soc. B* **361**, 931–950 (2006).
- 239 27. Schoell, M. Wasserstoff- und Kohlenstoffisotope in organischen Substanzen,  
240 Erdölen und Erdgasen. *Geol. Jahrb.* **67**, Reihe D, 164p (1984).
- 241 28. Clayton, C. Carbon isotope fractionation during natural gas generation from kerogen. *Mar.*  
242 *Pet. Geol.* **8**, 232–240 (1991).
- 243 29. Cramer, B., Krooss, B. M. & Littke, R. Modelling isotope fractionation during primary  
244 cracking of natural gas: a reaction kinetic approach. *Chem. Geol.* **149**, 235–250 (1998).
- 245 30. Schoell, M. Multiple origins of methane in the Earth. *Chem. Geol.* **71**, 1–10 (1988).

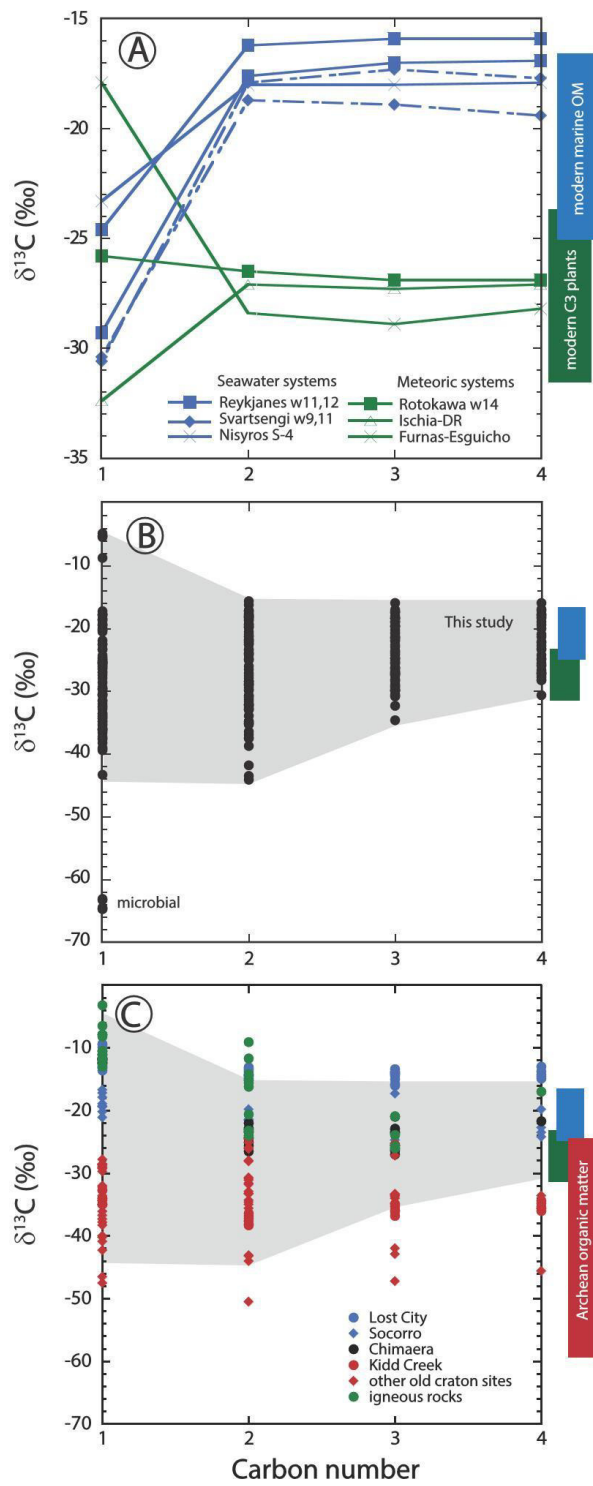


Fig., 1

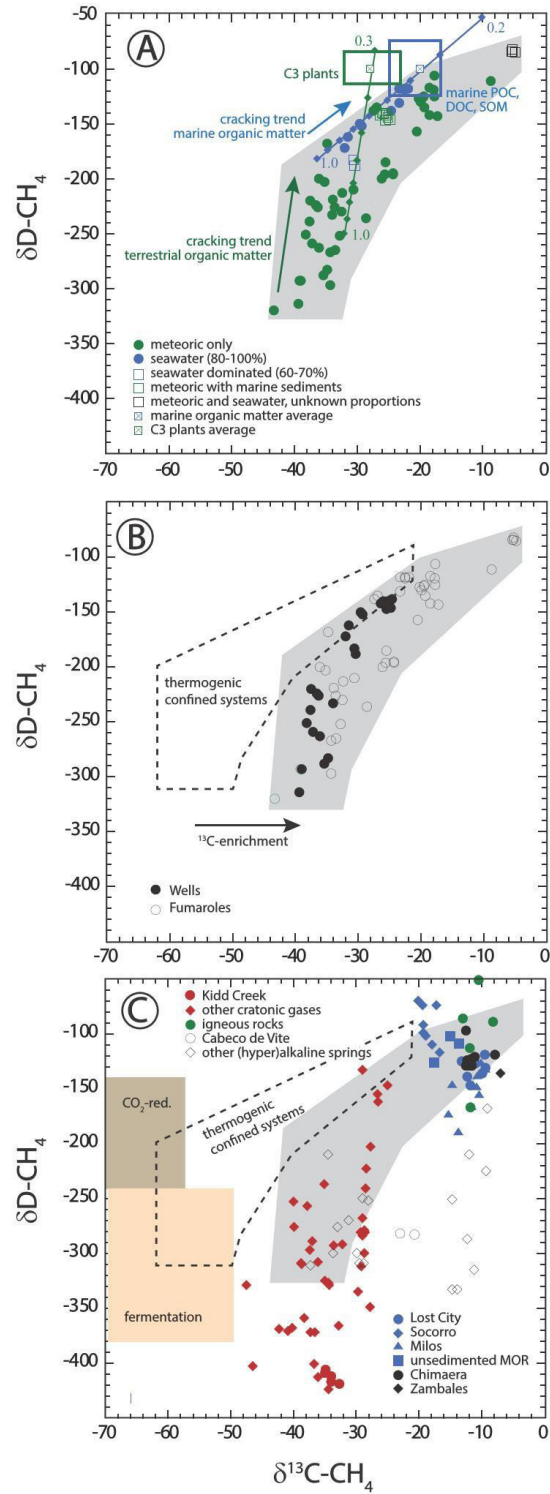


Fig. 2

1 **Figure captions**

2 **Figure 1. Plot of  $\delta^{13}\text{C}$  of individual n-alkanes against carbon number.**  $\delta^{13}\text{C}$  ranges of  
3 modern marine organic matter<sup>12,14</sup>, terrestrial  $\text{C}_3$  vegetation<sup>15</sup> and Archean organic matter<sup>26</sup> are  
4 shown for comparison. **a**, Emissions that are characterized by invariant  $\delta^{13}\text{C}\text{-C}_{2+}$ . **b**,  
5 Compilation of all n-alkane data analyzed in this study. **c**, Comparison between n-alkane data  
6 from this study (area in grey) and data available from other "abiotic" sites (see Supplementary  
7 information): hydrothermal sites (blue); ophiolite gases (black); old craton gases (red) and  
8 inclusions in igneous rocks (green).

9 **Figure 2. Plot of  $\delta\text{D}\text{-CH}_4$  vs  $\delta^{13}\text{C}\text{-CH}_4$ .** Samples with an obvious microbial origin ( $\delta^{13}\text{C}\text{-CH}_4$   
10  $< -60\%$ , Fig. 1b) are not considered. **a**, Data classified after the origin of external water feeding  
11 the hydrothermal system (Extended Data Table 1). Open system cracking and degassing trends  
12 as a function of fraction of precursor sites remaining inside the cracked organic matter were  
13 calculated for terrestrial (green) and marine organic matter (blue) using the average isotopic  
14 composition of  $\text{C}_3$  plants and modern marine organic matter<sup>27</sup> (blue), respectively, the carbon  
15 and hydrogen isotope fractionations characteristic for methane generation from xylite and  
16 Kukersite<sup>18</sup>, respectively, and the formalism of open system cracking and degassing<sup>28</sup>. The  
17 trend for marine organic matter matches the variation of  $\delta^{13}\text{C}$  and  $\delta\text{D}$  observed for seawater-  
18 fed hydrothermal systems. Trend for  $\text{C}_3$  plants corresponds to the slope described by most low  
19  $\delta^{13}\text{C}$  data points from meteoric water-fed hydrothermal systems but occurs shifted to higher  
20  $\delta^{13}\text{C}$  and  $\delta\text{D}$ . This implies that methane precursor sites in decomposing terrestrial organic  
21 matter either occur depleted in  $^{13}\text{C}$  and D with respect to the average  $\text{C}_3$  plant isotopic  
22 composition or that the corresponding carbon and hydrogen isotope fractionations ( $\epsilon_{\text{C}}$ ,  $\epsilon_{\text{H}}$ ) are  
23 larger than those obtained from xylite<sup>18</sup>, with  $\epsilon_{\text{H}} / \epsilon_{\text{C}}$  remaining unchanged. Both possibilities  
24 are in agreement with carbon isotope constraints on pyrolysis of coal<sup>29</sup>. **b**, Data classified after  
25 the style of degassing (wells vs fumaroles). **c**, Comparison between methane data from this  
26 study and data available from other "abiotic" sites (see Supplementary information): Labelling  
27 as in Fig. 1c, extended by (hyper)alkaline spring data (open symbols). Field characteristic for  
28 methane from microbial (c) and confined sedimentary systems (b, c) redrawn after Schoell<sup>30</sup>.

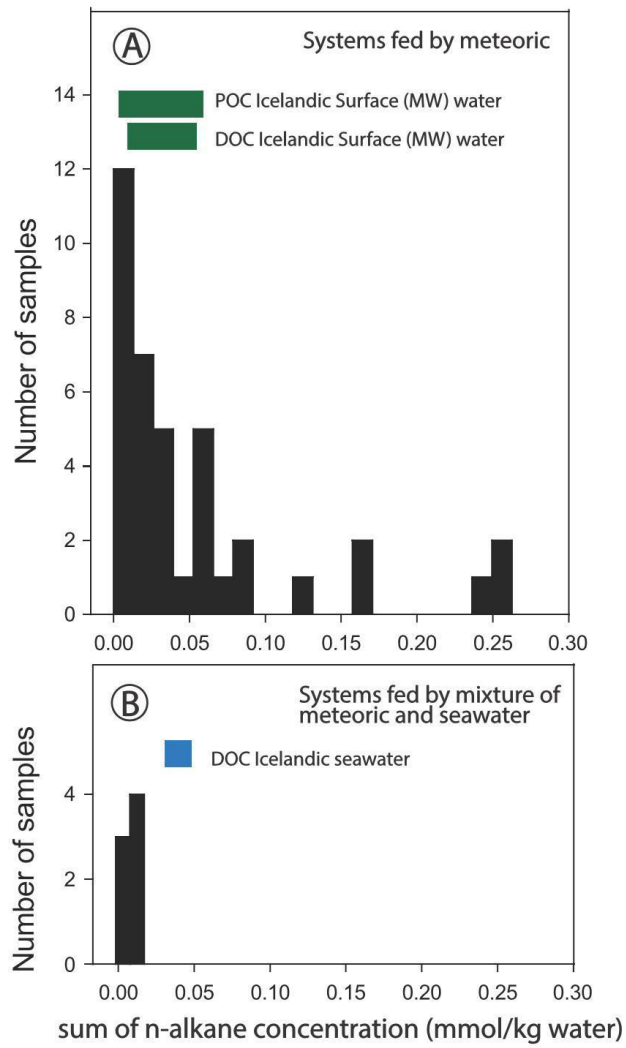
1 **Methods**

2 Well fluids, well steam and natural gas discharges were sampled following standard protocols<sup>31-</sup>  
3 <sup>33</sup>. Carbon isotope analysis of n-alkanes and CO<sub>2</sub> were performed using analytical setups and  
4 protocols described elsewhere<sup>34</sup>. External precision for carbon isotope analysis is ±0.5‰ for n-  
5 alkanes and ±0.2‰ for CO<sub>2</sub>. For hydrogen isotope analysis of CH<sub>4</sub>, a sample preconcentration  
6 system was connected to a GC/TC (Thermo), equipped with a Porapak Q column. CH<sub>4</sub> was  
7 separated from H<sub>2</sub> by keeping the column isothermal at -50°C. External precision for δD-CH<sub>4</sub>  
8 analysis was ≤ ±5‰. Internal n-alkane gas mixtures calibrated against methane#1, methane#3  
9 and ALM methane#7 (all supplied by A. Schimmelmann, Indiana University) were measured  
10 along with the samples to be able to report δ<sup>13</sup>C and δD values on the VPDB-LSVEC and  
11 VSMOW-SLAP scales. The hydrogen isotopic composition of water was analyzed using a TC-  
12 EA and internal water reference samples calibrated against VSMOW-SLAP. External precision  
13 for δD-H<sub>2</sub>O analysis was ≤ ±3‰. All isotopic data is presented in Extended Data Table 2 (wells)  
14 and Extended Data Table 3 (fumaroles).

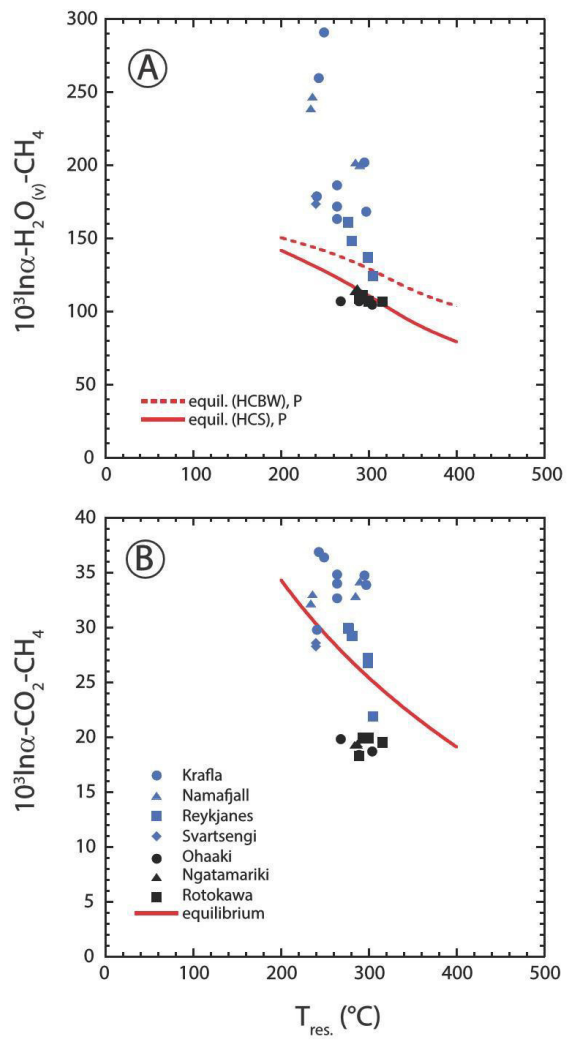
15

16 **References**

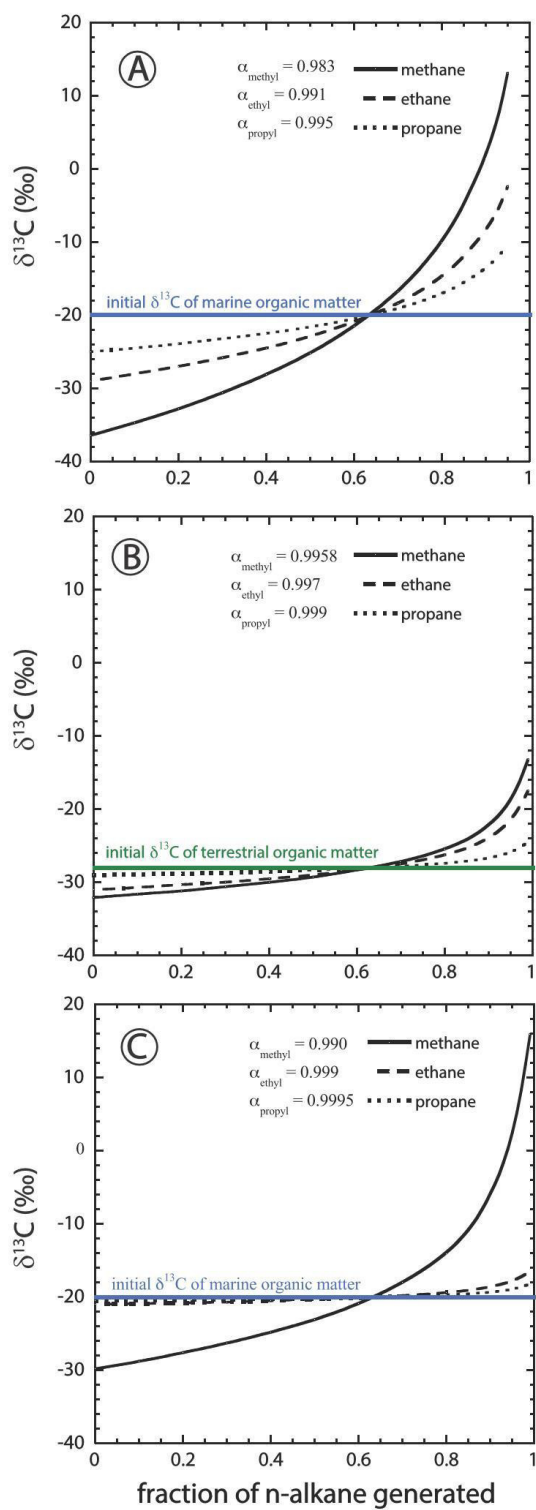
- 17 31. Arnórsson, S. et al. Sampling and analysis of hydrothermal fluids. *Geofluids* **6**, 203–  
18 216 (2006).
- 19 32. Giggenbach, W. F. A simple method for the collection and analysis of volcanic gas  
20 samples. *Bull. Volcanol.* **39**, 15-27 (1975).
- 21 33. Cioni, R. & Corazza, E. Medium temperature fumarolic gas sampling. *Bull. Volcanol.* **44**,  
22 23-29 (1981).
- 23 34. Fiebig, J. et al. Isotopic patterns of hydrothermal hydrocarbons emitted from  
24 Mediterranean volcanoes. *Chem. Geol.* **396**, 152-163 (2015).



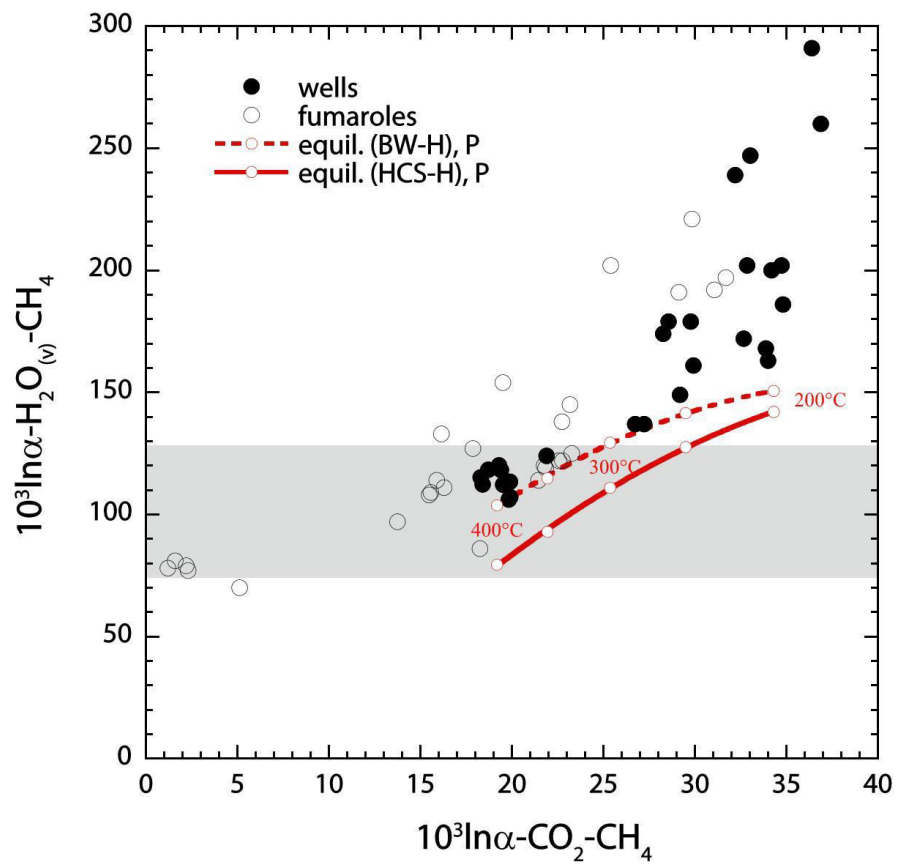
Ext. Fig. 1



Ext. Fig. 2



Ext. Fig. 3



Ext. Fig. 4

1 **Extended Data Figures**

2 **Extended Data Figure 1. The concentration of n-alkanes in volcanic-hydrothermal fluids**

3 **in Iceland.** Systems sourced by **a**, meteoric water and **b**, a mixture of meteoric water and  
4 seawater. Also shown are the ranges of concentrations of DOC in non-thermal meteoric surface  
5 waters in Iceland<sup>35,36</sup> and DOC and POC for seawater in Iceland<sup>37</sup>. Total concentrations of n-  
6 alkanes (sum of methane, ethane, propane and butane) in the hydrothermal fluids are generally  
7 below the concentrations of organic matter in the source fluids. The volcanic-hydrothermal  
8 systems in Iceland are of recent geological age and characterized by the absence of organic  
9 sediments. For more complex systems, with multiple phase relationships (vapor, liquid, brine  
10 and halite) like sub-seafloor systems, and those associated with sedimentary deposits within the  
11 reservoir, mass balances are, however, difficult to constrain.

12 **Extended Data Figure 2. Apparent isotope fractionations vs well reservoir temperatures.**

13 All well reservoir temperatures were determined from qtz-solute thermometry<sup>38</sup>. **a**,  
14  $1000\ln\alpha(\text{H}_2\text{O}_{(\text{v})}\text{-CH}_4)$  vs reservoir T. Hydrogen isotope equilibrium is marked by red lines.  
15 HCBW (red bold line) combines the theoretical  $\text{H}_2\text{-H}_2\text{O}_{(\text{v})}$ <sup>39</sup> with the experimental  $\text{CH}_4\text{-H}_2$   
16 fractionation<sup>40</sup>, whereas HCS is based on a combination of the experimental  $\text{H}_2\text{-H}_2\text{O}_{(\text{v})}$ <sup>41</sup> with  
17 the experimental  $\text{CH}_4\text{-H}_2$  fractionation<sup>40</sup>. Both the theoretical and experimental  $\text{H}_2\text{-H}_2\text{O}_{(\text{v})}$   
18 fractionations were corrected for a density effect<sup>42</sup> considering that gaseous water molecules  
19 above 200°C do not behave ideal, but form polymers. The size of the markers roughly  
20 corresponds to analytical precisions of isotope analyses. Data implies that hydrogen isotope  
21 equilibrium between  $\text{CH}_4$  and water is attained at highest reservoir temperatures of  $\geq 300^\circ\text{C}$ .  
22 Isotope fractionation associated with steam separation seems to be of minor importance only  
23 since the hydrogen isotopic composition of the steam always corresponds to that of the  
24 discharged liquid water (see Extended Data Table 2). **b**,  $1000\ln\alpha(\text{CO}_2\text{-CH}_4)$  vs reservoir  
25 temperature. Carbon isotope equilibrium<sup>43</sup> is marked by the red line. There is no indication that  
26 apparent carbon isotope fractionations vary with reservoir temperature and attain equilibrium.

27 **Extended Data Figure 3.  $\delta^{13}\text{C}$  of instantaneous methane, ethane and propane as a function**

28 **of generated fraction of n-alkane.** Methane, ethane and propane derive from different  
29 precursor sites within the organic matter, and each generated n-alkane is characterized by its  
30 own specific carbon isotope fractionation factor with respect to its precursor site<sup>18</sup>. During  
31 progressive cracking, instantaneous fractions of methane can become highly enriched in  $^{13}\text{C}$   
32 and finally even exhibit a carbon isotope reversal with respect to ethane. **a**,  $\delta^{13}\text{C}$  of the initial  
33 precursor sites corresponds with -20‰ to the average carbon isotopic composition of marine

34 DOC. Carbon isotope fractionation factors between precursor sites in the organic matter and  
35 the respective n-alkanes correspond to those determined from pyrolysis of marine Kukersite<sup>18</sup>.  
36 According to these experiments methane from marine organic matter may have the potential to  
37 become highly enriched in <sup>13</sup>C during late stage cracking (fraction of generated methane → 1).  
38 **b**,  $\delta^{13}\text{C}$  of the initial precursor sites corresponds with -28‰ to the average carbon isotopic  
39 composition of terrestrial C<sub>3</sub> plants. Carbon isotope fractionation factors between precursor  
40 sites in the organic matter and the respective n-alkanes correspond to those determined from  
41 pyrolysis of terrestrial xylite<sup>18</sup>. **c**,  $\delta^{13}\text{C}$  of the initial precursor sites corresponds with -20‰ to  
42 the average carbon isotopic composition of marine DOC. Carbon isotope fractionation factors  
43 between precursor sites in marine organic matter and the respective n-alkanes chosen to match  
44  $\delta^{13}\text{C}$  of Reykjanes n-alkanes ( $\delta^{13}\text{C}$ -CH<sub>4</sub> around -30‰;  $\delta^{13}\text{C}$ -C<sub>2+</sub> invariant and close to -20‰,  
45 Extended Data Table 2) at the very early stage of degassing (fraction of generated n-alkane →  
46 0).

47 **Extended Data Figure 4. Plot of apparent carbon (CO<sub>2</sub>-CH<sub>4</sub>) against apparent hydrogen**  
48 **(H<sub>2</sub>O<sub>(v)</sub>-CH<sub>4</sub>) isotope fractionation.** For calculation of displayed equilibrium isotope  
49 fractionations see Extended Data Figs. 2. Isotopic data for calculation of apparent isotopic  
50 temperatures is taken from Extended Data Tables 2, 3. The grey shaded field indicates  
51 hydrothermal temperatures  $\geq 300^\circ\text{C}$ , i.e. a range within which hydrogen isotope equilibrium  
52 between H<sub>2</sub>O<sub>(v)</sub> and CH<sub>4</sub> might be attained, as implied by Extended Data Fig. 2a. Within this  
53 range, the apparent hydrogen isotope fractionation between H<sub>2</sub>O<sub>(v)</sub> and CH<sub>4</sub> corresponds to  
54 reasonable hydrothermal temperatures (up to 450°C, Extended Data Table 1). Within the same  
55 range the apparent CH<sub>4</sub>-CO<sub>2</sub> isotope fractionation is largely variable and extends to very small  
56 values corresponding to temperatures exceeding 1000°C. This provides additional evidence that  
57 the apparent carbon isotope fractionation between CO<sub>2</sub> and CH<sub>4</sub> only fortuitously corresponds  
58 to equilibrium in some systems. During the stage where either the hydrogen isotopic  
59 composition of methane or that of the decomposing organic matter at depth becomes buffered  
60 by the isotopic composition of water, methane is further distilled out of the system, leaving the  
61 methane precursor sites in the organic matter and, hence, the instantaneous fractions of  
62 generated methane progressively enriched in <sup>13</sup>C.

63

#### 64 **References**

- 65 35. Eirkisdottir, E.S. *Weathering and riverine fluxes in pristine and controlled river*  
66 *catchments in Iceland*. PhD thesis, Univ. Iceland. (2016)

- 67 36. Chiffard, P. et al. Dissolved and particular organic carbon in Icelandic proglacial streams.  
68 *The Cryosphere Disc.* (2018)
- 69 37. Fontela, M. et al. Dissolved organic carbon in the North Atlantic Meridional overturning  
70 circulation. *Sci. Report* **6**, 26931 (2016).
- 71 38. Gunnarsson, I. & Arnórsson, S. Amorphous silica solubility and the thermodynamic  
72 properties of  $\text{H}_4\text{SiO}_4$  in the range of 0 to 350°C at  $P_{\text{sat}}$ . *Geochim. Cosmochim. Acta* **64**,  
73 2295–2307 (2000).
- 74 39. Bardo, R. D. & Wolfsberg, M. A theoretical calculation of the equilibrium constant for  
75 the isotopic exchange reaction between  $\text{H}_2\text{O}$  and HD. *J. Phys. Chem.* **80**, 1068-1071  
76 (1976).
- 77 40. Horibe, Y. & Craig, H. D/H fractionation in the system methane-hydrogen-water.  
78 *Geochim. Cosmochim. Acta* **59**, 5209-5217 (1995).
- 79 41. Suess, H. E. Das Gleichgewicht  $\text{H}_2 + \text{HDO} = \text{HD} + \text{H}_2\text{O}$  und die weiteren  
80 Austauschgleichgewichte im System  $\text{H}_2$ ,  $\text{D}_2$  und  $\text{H}_2\text{O}$ . *Z. Naturforsch.* **4a**, 328-332  
81 (1949).
- 82 42. Driesner, T. The effect of pressure on Deuterium-Hydrogen fractionation in high-  
83 temperature water. *Science* **277**, 791-794 (1997).
- 84 43. Horita, J. Carbon isotope exchange in the system  $\text{CO}_2\text{-CH}_4$  at elevated temperatures.  
85 *Geochim. Cosmochim. Acta* **65**, 1907-1919 (2001).

**Extended Data Table 1. The major characteristics of the various volcanic-hydrothermal systems**

Country	Geothermal system	tectonic setting	rocks	T <sub>res</sub> <sup>a</sup> (°C)	Source of external waters <sup>b</sup>	References
Alaska, USA	Trident	subduction	andesitic, dacitic	380	MW	[44]
	Mageik		andesitic, dacitic	260	MW	[44]
Argentina	Domuyo	subduction	andesitic, rhyolitic	220-240	MW	[45]
	Copahue		basaltic-andesitic, dacitic	250	MW	[46]
Azores, Portugal	Fumas	mid-ocean rifting/mantle plume	trachyte	200-275	MW	[47,48]
Greece	Nisyros	subduction	andesitic, dacitic, rhyolitic	290-340	SW	[49,50]
	Santorini		andesitic, dacitic, rhyolitic	unknown	unknown	[51]
Iceland	Reykjanes	mid-ocean rifting/mantle plume	basalts	260-345	SW	[52]
	Svartsengi		basalts	220-260	SW+MW	[52]
	Krysuvík		basalts	220-320	MW	[52]
	Krafla		basalts, rhyolites	200-440	MW	[52]
	Námafjall		basalts, rhyolites	220-320	MW	[52]
	Hengill		basalts	200-380	MW	[52]
	Hveragerði		basalts	170-230	MW	[52]
	Torfaðkull		rhyolites	260-310	MW	[52]
	Kverkfjöll		rhyolites	260-300	MW	[52]
	Kverkfjöll		basalts, rhyolites	290-350	MW	[52]
	Askja		basalts, rhyolites	160-350	MW	[52]
	Italy		Vulcano beach	subduction	leucite tephrites, trachytes, alkali-rhyolites	230
Ischia		shoshonites, alkali-trachytes	250-300		MW	[55,56]
C. Flegrei		shoshonite, phonolites, trachytes	200-360		MW	[57,58]
Vesuvio		leucite-basalts, trachytes, leucitic tephrites, leucitic phonolites	360-450		MW	[59]
Pantelleria		trachytes, peralkaline rhyolites	250		MW	[60]
New Zealand	Ohaki	subduction	rhyolites, greywacke	275-310	MW	[61,62]
	Rotokawa		andesites, dacites, rhyolites, greywacke	290-340	MW	[61,63]
	Ngatamariki		basalt, andesite, rhyolite, greywacke, tonalite	260-285	MW	[61,64]
Tenerife, Spain	Teide	mantle plume	basalt, trachytes, phonolites	285-316	MW	[65]

<sup>a</sup> reservoir temperature either measured directly or inferred from gas concentration geothermometers; <sup>b</sup> origin inferred from oxygen and hydrogen isotope data [see references]

**Extended Data Table 2. Well data:** Reservoir temperatures, sampling temperatures, carbon isotope composition of methane, ethane, propane and n-butane, hydrogen isotope composition of methane, steam and liquid water. Carbon isotope data is reported relative to VPDB, hydrogen isotope data relative to VSMOW.

Sample #	Location	Date	T <sub>res</sub> <sup>a</sup> (°C)	T <sub>s</sub> <sup>b</sup> (°C)	δ <sup>13</sup> C-CH <sub>4</sub>	δD-CH <sub>4</sub>	δ <sup>13</sup> C-C <sub>2</sub> H <sub>6</sub>	δ <sup>13</sup> C-C <sub>3</sub> H <sub>8</sub>	δ <sup>13</sup> C-C <sub>4</sub> H <sub>10</sub>	δ <sup>13</sup> C-CO <sub>2</sub> (v)	δD-H <sub>2</sub> O(v)	δD-H <sub>2</sub> O(l)
<b>Iceland</b>												
Kr w32	Krafla	27.08.15	249	178	-39.4	-314	-33.9	-28.4	-24.9	-3.8	-82	-84
Kr w16	Krafla	27.08.15	264	203	-37.6	-239	-36.4	-32.3		-3.5	-83	-80
Kr w34	Krafla	28.08.15	264	200	-37.5	-220	-28.4	-24.2		-4.2	-82	-86
Kr w37	Krafla	06.08.16	264	200	-36.3	-226	-32.9	-24.7	-22.1	-4.3	-81	-83
Kr w34	Krafla	06.08.16	295	175	-38.2	-251	-35.3	-27.3	-27.1	-4.2	-83	-81
Kr w31	Krafla	06.08.16	297	148	-36.6	-224	-27.9	-18.3		-3.4	-82	-82
Kr w36	Krafla	06.08.16	241	189	-34.0	-233	-32.8	-25.3		-4.8	-83	-86
Kr w27	Krafla	06.08.16	243	183	-39.0	-293	-34.8	-24.7	-23.2	-2.9	-83	-83
Rey w15	Reykjanes	02.09.15	281	212	-31.5	-162	-18.1	-19.0	-20.0	-2.8	-28	-12
Rey w12	Reykjanes	02.09.15	299	220	-29.6	-150	-17.1	-17.3	-18.3	-2.8	-26	-23
Rey w12	Reykjanes	12.08.16	299	207	-29.3	-152	-17.6	-17.0	-16.9	-3.0	-27	-20
Rey w18	Reykjanes	12.08.16	277	217	-32.0	-172	-19.7	-22.0	-23.3	-2.6	-27	-22
Rey w11	Reykjanes	12.08.16	305	226	-24.6	-138	-16.2	-15.9	-15.9	-3.0	-24	-20
Nam w13	Námafjall	27.08.15	290	173	-37.2	-259	-32.1	-25.0		-3.7	-95	-93
Nam w13	Námafjall	05.08.16	285	126	-36.1	-263	-32.2	-25.0		-3.9	-98	-90
Nam w9	Námafjall	27.08.15	236	184	-35.4	-288	-35.1	-23.9	-22.2	-3.0	-89	-95
Nam w9	Námafjall	05.08.16	234	175	-34.8	-283	-34.8	-22.9	-20.9	-3.2	-89	-94
Sv w9	Svartsengi	11.08.16	240	192	-30.4	-188	-18.7	-18.9	-19.4	-2.3	-29	-20
Sv w11	Svartsengi	11.08.16	240	204	-30.6	-183	-17.9	-17.3	-17.7	-2.8	-28	-19
<b>New Zealand</b>												
BR 67	Ohaki	01.03.17	304	192	-26.0	-140	-20.5	-20.2		-7.6	-45	-39
BR 56	Ohaki	01.03.17	268	174	-26.4	-142	-22.5	-23.7	-25.9	-6.9	-45	-39
BR 49	Ohaki	01.03.17	289	177	-25.3	-142	-22.2	-21.4		-7.2	-45	-39
RK 26	Rotokawa	02.03.17	293	248	-25.1	-144	-25.0	-28.1	-27.8	-5.5	-43	-44
RK 34	Rotokawa	02.03.17	289	245	-25.3	-140	-15.6	-17.5	-17.1	-7.3	-41	-44
RK 14	Rotokawa	02.03.17	316	236	-25.8	-141	-26.5	-26.9	-26.9	-6.6	-44	-42
RK 17	Rotokawa	02.03.17	300	245	-25.4	-142	-19.8	-21.2	-22.7	-5.8	-45	-44
NM 5	Ngatamariki	03.03.17	287	216	-25.5	-147	-22.5	-21.5	-21.3	-6.4	-42	-40
NM 7	Ngatamariki	03.03.17	297	224	-25.0					-6.0	-46	-42
NM 12	Ngatamariki	03.03.17	284	224	-24.8	-146	-22.0	-18.3	-17.8	-5.8	-43	-43

<sup>a</sup> T<sub>res</sub> = reservoir temperature calculated assuming adiabatic boiling and using quartz geothermometry; <sup>b</sup> T<sub>s</sub> = Sampling temperature.

**Extended Data Table 3. Fumarole data:** Vent temperatures, carbon isotope composition of methane, ethane, propane and n-butane, hydrogen isotope composition of methane and water vapor. Carbon isotope data is reported relative to VPDB, hydrogen isotope data relative to VSMOW.

Sample	Location	Date	T <sub>v</sub> (°C)	δ <sup>13</sup> C-CH <sub>4</sub>	δD-CH <sub>4</sub>	δ <sup>13</sup> C-C <sub>2</sub> H <sub>6</sub>	δ <sup>13</sup> C-C <sub>3</sub> H <sub>8</sub>	δ <sup>13</sup> C-nC <sub>4</sub> H <sub>10</sub>	δ <sup>13</sup> C-CO <sub>2</sub> (v)	δD-H <sub>2</sub> O(v)
<b>Italy</b>										
Vasca Ippo	Vulcano	Jun 16		-5.2	-82	-22.3	-26.1	-26.3	-2.9	-9
Vasca Ippo Centr.	Vulcano	04.10.16	102	-5.4	-84	-24.4	-24.6	-25.3	-3.2	-9
Vasca Ippo Est.	Vulcano	04.10.16	100	-5.2	-84	-20.1	-23.3		-3.6	-7
Vasca Vecchia	Vulcano	04.10.16	100	-4.8	-85	-17.0			-3.6	-11
FG	Pantelleria	02.10.13	98	-17.7	-125	-21.8			-4.1	-36
Pisciarelli	C. Flegrei	02.09.13	98	-20.5	-157	-19.2			-1.2	-17
BG	C. Flegrei	02.09.13	163	-17.2	-143	-17.8			-1.2	-21
BN	C. Flegrei	02.09.13	157	-18.5	-142	-17.8			-0.8	-26
FC2	Vesuvio	03.09.13	97	-17.7	-106	-17.3			0.4	-26
DR2	Ischia	04.09.13	100	-32.4	-213	-27.1	-27.3	-27.1	-3.8	-47
<b>Greece</b>										
S4	Nisyros	04.06.13	100	-23.3	-118	-18.0	-18.0	-17.9	-1.0	-4
S15	Nisyros	04.06.13	100	-22.5	-118	-18.2	-18.0		-1.0	-6
PP9S	Nisyros	05.06.13	100	-21.9	-118	-18.6	-19.6		-0.3	-7
K7	Nisyros	06.06.13	99	-22.5	-119	-18.4	-18.4		-1.3	-13
A13	Nisyros	05.06.13	99	-23.3	-131	-21.3	-19.6	-18.9	-0.4	5
Nea Kameni	Santorini	06.04.16		-31.5		-26.0	-20.8			
<b>Tenerife</b>										
FC	Teide	16.06.13		-8.7	-111	-18.2			-3.6	data from [65] -47
<b>Azores</b>										
Fumas B	Fumas village	06.01.15	65	-64.7	-309	-30.7	-29.9			-25
Fumas B	Fumas village	24.07.15	74	-63.1	-304	-31.3	-30.7		-4.1	-25
Fumas B2	Fumas village	24.07.15	74	-20.2	-127	-29.8	-29.7		-4.1	-25
Fumas B3	Fumas village	24.07.15	98	-19.4	-125	-29.0	-29.4		-4.1	-25
Fumas D	Fumas village	24.07.15	98	-19.9	-130	-29.8	-29.8		-4.2	-25
Esgulcho	Fumas village	28.11.13	95	-17.9		-28.4	-28.9	-28.2	-4.3	-25
Esgulcho	Fumas village	23.07.15	98	-18.5	-117	-28.4	-29.2			-25
Caldeira Seca	Fumas village	28.11.13	99	-18.7		-28.8	-27.1	-27.5	-4.2	-25
Caldeira Seca	Fumas village	06.01.15		-17.8	-119	-28.4	-27.0			-25
Caldeira Seca	Fumas village	23.07.15	97	-19.5	-126	-28.8	-27.5		-4.1	-25
Dos Vimes	Fumas village	24.07.15	94	-19.3	-135	-29.4	-30.8			-25
Fumas Lake	Fumas lake	28.11.13	97	-35.9		-23.3	-26.2		-4.8	-23
Fumas Lake	Fumas lake	06.01.15	97	-34.8	-168	-22.1				-23
Fumas Lake	Fumas lake	25.07.15	98	-26.9	-135	-22.1	-23.6		-4.5	-23
Fumas Lake 4	Fumas lake	25.07.15	96	-27.4	-138	-22.1	-23.8		-4.5	-23
Fumas Lake 2	Fumas lake	28.11.13	89	-64.7		-24.8	-26.8		-6.9	-23
Fumas Lake 2	Fumas lake	06.01.15	97	-64.5	-241	-24.3				-23
Fumas Lake 2	Fumas lake	25.07.15	93	-63.3	-238	-24.0	-26.5		-4.4	-23
<b>Iceland</b>										
15-AS-01	Krýsuvík	24.08.15		-35.2	-203	-29.0	-20.6		-3.2	
15-AS-02	Krýsuvík	24.08.15		-36.1	-200	-31.6				
15-AS-03	Kerlingarfjöll	25.08.15		-24.3	-196	-31.0			-3.2	
15-AS-04	Kerlingarfjöll	25.08.15		-24.3	-195	-30.7			-3.3	
15-AS-05	Kerlingarfjöll	26.08.15		-26.1	-200	-32.2			-3.1	
15-AS-06	Kerlingarfjöll	26.08.15		-25.6	-196	-32.5			-3.0	
15-AS-11	Námafjall	28.08.15		-34.3	-297	-32.0	-25.5			
16-AS-08	Námafjall	07.08.16		-33.5	-265	-24.2	-21.8		-3.0	-109
16-AS-09	Námafjall	07.08.16		-34.3	-267	-24.9	-21.4		-3.2	-108
16-AS-10	Hengill	09.08.16		-28.6	-236	-36.9	-34.6		-3.6	-65
16-AS-11	Hveragerdi	09.08.16		-32.8	-252	-41.8	-29.9		-3.5	-67
16-AS-12	Hveragerdi	09.08.16		-25.5	-185	-37.4	-29.1	-27.2	-3.1	-64
17-TORF-1	Torfajökull	07.08.17		-32.5	-230	-35.1	-28.2	-28.2	-6.5	
17-TORF-2	Torfajökull	07.08.17		-30.6	-210	-32.9	-25.5	-30.6		
17-KVE-1	Kverkfjöll	06.09.17		-33.6	-226	-44.1	-29.9	-24.2		
17-KVE-2	Kverkfjöll	06.09.17		-33.9	-219	-43.5	-30.5	-24.8		
17-ASK-1	Askja	07.09.17		-43.3	-320	-38.7	-27.2			
17-ASK-3	Askja	07.09.17		-39.2	-293	-37.5				
<b>Alaska</b>										
MGK1	Mageik	12.07.13	92	-30.5		-27.5	-26.3	-25.8	-8.8	
TRI1	Trident	16.07.13	94	-20.2		-23.8	-22.6		-11.0	
<b>Argentina</b>										
Bramadora	Domuyo	01.03.14	107	-29.6		-19.4	-19.7			
Anfiteatro	Copahue	11.03.14	94	-36.0		-23.4	-18.3		-6.5	
Las Maquintas	Copahue	04.03.14	131	-27.9		-21.7	-18.3	-18.2	-7.6	
Las Maquintas	Copahue	04.03.14	94	-26.4		-20.9	-18.8		-7.6	
Pedra de Copahue	Copahue	06.03.14	93	-27.0		-21.2	-19.5		-7.5	
Chancho-Co	Copahue	07.03.14	95	-29.6		-19.4			-8.8	

\* T<sub>v</sub> = Vent temperature

1 **Extended Data Tables**

2

3 **References**

- 4 44. Lopez, T. et al. Geochemical constraints on volatile sources and subsurface conditions at  
5 Mount Martin, Mount Mageik, and Trident Volcanoes, Katmai Volcanic Cluster, Alaska.  
6 *J. Volcanol. Geotherm. Res.* **347**, 64-81 (2017).
- 7 45. Tassi, F. et al. The hydrothermal system of the Domuyo volcanic complex (Argentina): A  
8 conceptual model based on new geochemical and isotopic evidences. *J. Volcanol.*  
9 *Geotherm. Res.* **328**, 198-209 (2016).
- 10 46. Tassi, F. et al. The 2012-2016 eruptive cycle at Copahue volcano (Argentina) versus the  
11 peripheral gas manifestations: hints from the chemical and isotopic features of fumarolic  
12 fluids. *Bull. Volcanol.* **79**: 69 (2017).
- 13 47. Caliro, S., Viveiros, F., Chiodini, G. & Ferreira, T. Gas geochemistry of hydrothermal  
14 fluids of the S. Miguel and Terceira Islands, Azores. *Geochim. Cosmochim. Acta* **168**,  
15 43-57 (2015).
- 16 48. Moore, R.B. Volcanic geology and eruption frequency, Sao Miguel, Azores. *Bull.*  
17 *Volcanol.* **52**, 602-614 (1990).
- 18 49. Chiodini, G. et al. Fluid geochemistry of Nisyros island, Dodecanese, Greece. *J.*  
19 *Volcanol. Geotherm. Res.* **56**, 95-112 (1993).
- 20 50. Brombach, T. et al. Geochemical evidence for mixing of magmatic fluids with seawater,  
21 Nisyros hydrothermal system, Greece. *Bull. Volcanol.* **65**, 505-516 (2003).
- 22 51. Fytikas, M. et al. Geothermal Research on Santorini. In: 'Thera and the Aegean  
23 World III', Volume Two: 'Earth Sciences', Proceedings of the Third International  
24 Congress. Santorini, Greece, 3-9 September 1989. Publisher: Thera Foundation,  
25 ISBN: 0950613371, pp. 241 – 249 (1989).
- 26 52. Stefánsson, A. et al. Isotope systematics of Icelandic thermal fluids. *J. Volcanol.*  
27 *Geotherm. Res.* **337**, 146-164 (2017).
- 28 53. Chiodini, G., Cioni, R., Marini, L. & Panichi, C. Origin of the fumarolic fluids of Vulcano  
29 Island, Italy and implications for volcanic surveillance. *Bull. Volcanol.* **57**, 99-110 (1995).
- 30 54. Keller, J. The island of Vulcano. *Rend. Soc. Ital. Min. Petrol.* **36**, 369-414 (1980).

- 31 55. Panichi, C. et al. Geothermal assessment of the island of Ischia (southern Italy) from  
32 isotopic and chemical composition of the delivered fluids. *J. Volcanol. Geotherm. Res.*  
33 **49**, 329-348 (1992).
- 34 56. Chiodini, G. et al. Fumarolic and diffuse soil degassing west of Mount Epomeo, Ischia,  
35 Italy. *J. Volcanol. Geotherm. Res.* **133**, 291-309 (2004).
- 36 57. Caliro, S. et al. The origin of the fumaroles of La Solfatara (Campi Flegrei, South Italy).  
37 *Geochim. Cosmochim. Acta* **71**, 3040-3055 (2007).
- 38 58. Caliro, S., Chiodini, G. & Paonita, A. Geochemical evidences of magma dynamics at  
39 Campi Flegrei (Italy). *Geochim. Cosmochim. Acta* **132**, 1-15 (2014).
- 40 59. Chiodini, G., Marini, L. & Russo, M. Geochemical evidence for the existence of high-  
41 temperature hydrothermal brines at Vesuvio volcano, Italy. *Geochim. Cosmochim. Acta*  
42 **65**, 2129-2147 (2001).
- 43 60. Parelo, F. et al. Isotope geochemistry of Pantelleria volcanic fluids, Sicily Channel rift: a  
44 mantle volatile end-member for volcanism in southern Europe. *Earth Planet. Sci. Lett.*  
45 **180**, 325-339 (2000).
- 46 61. Giggenbach, W. F. Variations in the chemical and isotopic composition of fluids  
47 discharged from the Taupo Volcanic Zone, New Zealand. *J. Volcanol. Geotherm. Res.*  
48 **68**, 89-116 (1995).
- 49 62. Christenson, B. W. et al. Ohaaki reservoir chemistry: characteristics of an arc-type  
50 hydrothermal system in the Taupo Volcanic Zone, New Zealand. *J. Volcanol.*  
51 *Geotherm. Res.* **115**, 53-82 (2002).
- 52 63. Sewell, S. M. et al. Rotokawa conceptual model update 5 years after commissioning  
53 of the 138 MWe NAP plant. *Proc. 37th New Zealand Geotherm. Workshop* (2015).
- 54 64. Chambefort, I. et al. Ngatamariki geothermal field, New Zealand: Geology, geophysics  
55 and conceptual model. *Geothermics* **59**, 266-280 (2016).
- 56 65. Melian, G. et al. A magmatic source for fumaroles and diffuse degassing from the  
57 summit crater of Teide Volcano (Tenerife, Canary Islands): a geochemical evidence for  
58 the 2004-2005 seismic-volcanic crisis. *Bull. Volcanol.* **74**, 1465-1483 (2012).

## 1 **Supplementary Information**

2 “Abiotic” n-alkanes displayed in Figures 1c and 2c comprise data from (ultra)mafic  
3 hydrothermal systems (Lost City<sup>5</sup>, unsedimented mid-ocean ridges<sup>66</sup> and Socorro<sup>67</sup>),  
4 continental volcanic-hydrothermal systems (Milos<sup>68</sup>), ophiolites (Zambales<sup>69</sup>, Chimaera<sup>70</sup>),  
5 inclusions in igneous rocks (Khibina<sup>71,72</sup>, Lovozero<sup>71</sup>), old cratons (Kidd Creek<sup>73</sup>, Driefontein<sup>73</sup>,  
6 Kloof<sup>73</sup>, Copper Cliff<sup>73</sup>, Mponeng<sup>73</sup>, Sudbury<sup>74</sup>, Elliott Lake<sup>74</sup>, Red Lake<sup>74</sup>, Juuka<sup>74</sup>, Pori<sup>74</sup>) and  
7 from cold (hyper)alkaline springs (Al Khoud Nizwa<sup>75</sup>, Genova<sup>76</sup>, Othrys<sup>77</sup>, Cabeco de Vide<sup>78</sup>,  
8 Happonen<sup>79</sup>, Al Farfar<sup>80</sup>, Ronda<sup>81</sup>). Craton gases and (hyper)alkaline spring gases with a  
9 predominant microbial contribution were excluded, as was previously done in the correlation  
10 plots of  $\delta D-CH_4$  vs  $\delta^{13}C-CH_4$  compiled by Etiope & Sherwood Lollar<sup>1</sup> and Etiope<sup>82</sup>.

11

## 12 **References**

- 13 66. McCollom, T. M. & Seewald, J. S. Abiotic synthesis of organic compounds in deep-sea  
14 hydrothermal environments. *Chem. Rev.* **107**, 382-401 (2007).
- 15 67. Taran, Y. A., Varley, N. R., Inguaggiato, S. & Cienfuegos, E. Geochemistry of H<sub>2</sub>- and  
16 CH<sub>4</sub>-enriched hydrothermal fluids of Socorro Island, Revillagigedo Archipelago, Mexico.  
17 Evidence for serpentinization and abiogenic methane. *Geofluids* **10**, 542-555 (2010).
- 18 68. Botz, R. et al. Hydrothermal gases offshore milos Island, Greece. *Chem. Geol.* **130**, 161-  
19 173 (1996).
- 20 69. Abrajano, T. et al. Methane-hydrogen gas seeps, Zambales Ophiolite, Philippines: Deep  
21 or shallow origin? *Chem. Geol.* **71**, 211-222 (1988).
- 22 70. Etiope, G., Schoell, M. & Hosgormez, H. Abiotic methane flux from the Chimaera seep  
23 and Tekirova ophiolites (Turkey): understanding gas exhalation from low temperature  
24 serpentinization and implications for Mars. *Earth Planet. Sci. Lett.* **310**, 96–104 (2011).
- 25 71. Potter, J., Rankin, A. H. & Treloar, P. J. Abiotic Fischer-Tropsch synthesis of  
26 hydrocarbons in alkaline igneous rocks; fluid inclusion, textural and isotopic evidence from  
27 the Lovozero complex, N. W. Russia. *Lithos* **75**, 311–330 (2004).
- 28 72. Potter, J. & Longstaffe, F. J. A gas-chromatograph, continuous flow-isotope ratio mass-  
29 spectrometry method for  $\delta^{13}C$  and  $\delta D$  measurement of complex fluid inclusion volatiles:  
30 Examples from the Khibina alkaline igneous complex, northwest Russia and the south  
31 Wales coalfields. *Chem. Geol.* **244**, 186-201 (2007).

- 32 73. Sherwood Lollar, B. et al. Unravelling abiogenic and biogenic sources of methane in the  
33 Earth's deep subsurface. *Geochim. Cosmochim. Acta* 226, 328-339 (2006).
- 34 74. Sherwood Lollar, B. et al. Abiogenic methanogenesis in crystalline rocks. *Geochim.*  
35 *Cosmochim. Acta* 57, 5087-5097 (1993).
- 36 75. Fritz, P. I. et al. Deuterium and <sup>13</sup>C evidence for low temperature production of hydrogen  
37 and methane in a highly alkaline groundwater environment in Oman. In: Proceed. 7th  
38 Intern. Symp. on Water–Rock Interaction: Low Temperature Environments. Editors: Y. K.  
39 Kharaka & A. S. Maest, vol. 1. pp. 793–796, Balkema, Rotterdam.
- 40 76. Boschetti, T., Etiope, G. & Toscani, L. Abiotic methane in the hyperalkaline springs of  
41 Genova, Italy. *Proc. Earth Planet. Sci.* 7, 248-251 (2013).
- 42 77. Etiope, G. et al. Methane flux and origin in the Othrys ophiolite hyperalkaline springs,  
43 Greece. *Chem. Geol.* 347, 161-174 (2013).
- 44 78. Etiope, G. et al. Methane in serpentinized ultramafic rocks in mainland Portugal. *Mar. Pet.*  
45 *Geol.* 45, 12-16 (2013).
- 46 79. Suda, K. et al. Origin of methane in serpentinite-hosted hydrothermal systems: The CH<sub>4</sub>-  
47 H<sub>2</sub>-H<sub>2</sub>O hydrogen isotope systematics of the Hakuba Happo hot spring. *Earth Planet. Sci.*  
48 *Lett.* 386, 112-125 (2014).
- 49 80. Etiope, G., Judas, J. & Whiticar, M. J. Occurrence of abiotic methane in the eastern United  
50 Arab Emirates ophiolite aquifer. *Arab. J. Geosci.* 8, 11345-11348 (2015).
- 51 81. Etiope, G. et al. Abiotic methane seepage in the Ronda peridotite massif, southern Spain.  
52 *Appl. Geochem.* 66, 101-113 (2016).
- 53 82. Etiope, G. Abiotic methane in continental serpentinization sites: an overview. *Proc. Earth*  
54 *Planet. Sci.* 17, 9-12 (2017).

# Extreme isotopic and chemical variations in light hydrocarbons in magmatic and hydrothermal gases from Vulcano Island (southern Italy): insights into deep source(s) and post-genetic processes

A. Ricci<sup>1</sup>, J. Fiebig<sup>2</sup>, F. Tassi<sup>3,4</sup>, C. Schreiber<sup>2</sup>, S. Hofmann<sup>2</sup>, F. Capecchiacci<sup>3,4</sup>, O. Vaselli<sup>3,4</sup>

<sup>1</sup> Department of Biological, Geological and Environmental Sciences, University of Bologna, Piazza di Porta San Donato 1, 40126 Bologna, Italy

<sup>2</sup> Institute of Geosciences, Goethe University, Altenhöferallee 1, 60438 Frankfurt/Main, Germany

<sup>3</sup> Department of Earth Sciences, University of Florence, Via La Pira 4, 50121 Florence, Italy

<sup>4</sup> CNR-IGG Institute of Geosciences and Earth Resources, Via La Pira 4, 50121 Florence, Italy

**Keywords:** Methane, hydrocarbons, stable isotopes, hydrothermal, volcanic gases, Vulcano Island

## Abstract

We have analyzed the carbon isotopic composition of CO<sub>2</sub>, CH<sub>4</sub> and C<sub>2</sub>–C<sub>4</sub> hydrocarbons, the hydrogen isotopic composition of CH<sub>4</sub>, H<sub>2</sub> and H<sub>2</sub>O as well as the chemical composition of gases from low-temperature ( $\leq 100^\circ\text{C}$ ) hydrothermal discharges (Levante beach) and high-temperature (up to  $400^\circ\text{C}$ ) fumaroles (La Fossa crater) located at Vulcano Island (Southern Italy). The main aim was to provide insights into (i) the source(s) of the organic volatiles and (ii) the role played by post-genetic supergene processes on determining the isotopic and chemical composition of light hydrocarbons. Investigations of fumarolic discharges at Vulcano Island revealed CH<sub>4</sub> with remarkable H-isotopic signatures ranging from uniquely low ( $< -657\text{‰}$  vs. V-SMOW) to relatively D-enriched values (up to  $-78\text{‰}$  vs. V-SMOW). This spread in the H-isotopic composition is accompanied by a similar noteworthy spread in the C-isotopic composition of methane, with  $\delta^{13}\text{C}\text{-CH}_4$  ranging from  $-30$  to  $-4.7\text{‰}$  vs. V-PDB. At Baia di Levante beach, methane and light hydrocarbons are produced by high temperature pyrolysis of marine organic matter at late stage cracking. This interpretation may explain the  $^{13}\text{C}$ -enriched isotopic composition of methane, the reverse carbon isotopic pattern of C<sub>1</sub>-C<sub>3</sub> n-alkanes, the average carbon isotopic composition of C<sub>2+</sub> n-alkanes and the high

$C_1/C_2$  ratios. The hydrogen isotopic composition of methane may be instead fixed by isotopic equilibrium with water at 300-400 °C within the deepest and hottest part of the hydrothermal system. However, in the southern sector of the Levante beach, where hydrothermal alteration of the volcanic rocks produces sediments saturated with acidic waters and mainly constituted by smectites, sulfides, sulfate, metal oxides and alumina-rich silicates, light hydrocarbons are highly affected by post-genetic processes. Alteration minerals and acidic conditions promote the dehydrogenation of normal-alkanes to alkenes and the aromatization of alkenes to benzene. The overall process, known as cyclomerization, strongly affects the molecular and isotopic signature of light hydrocarbons, completely masking the deep signature. At La Fossa crater, spatial and temporal changes of the chemical composition and stable isotopes of light hydrocarbons may be caused by contributions of different hydrothermal-type fluids supplied to the fumarolic conduits by the heterogeneous hydrothermal envelope surrounding the uprising magmatic gas. Uneven rock permeability regulates the fluid-rock interaction within the magmatic-hydrothermal system, developing highly variable contents of acidic species ( $SO_2$ ,  $H_2S$ ,  $HCl$  and  $HF$ ) in the gases. Methane and higher hydrocarbons in contact with large amounts of acidic species, are involved in irreversible transformation such as halogenation or sulfonation. These reactions are likely responsible for the observed  $^{12}C$ - and  $^1H$ -depleted carbon and hydrogen isotopic composition and for the variations of  $C_1$ - $C_2$  relative abundances. Where the hydrothermal fluids entering the volcanic conduit are relatively low in acidic species, the pristine chemical and isotopic composition of methane is mostly preserved. We suggest that extremely D-depleted methane may have formed by FT-type reaction under open-system conditions or by “bit-metamorphism”-like thermogenic process within the hydrothermal envelope and then added to the uprising magmatic gases.

## **1. Introduction**

Methane and light hydrocarbons are ubiquitous in the Earth's crust. These gas species have been recognized in continental and submarine hydrothermal fluids (Tassi et al., 2005; 2007; 2010; 2012a; 2012b; Cruse and Seewald, 2006; Fiebig et al., 2009; 2013; 2015; Taran et al., 2010a; Suda et al., 2014), deep fluids circulating in sedimentary basins and crystalline rocks (Sherwood-Lollar et al. 2002, 2006, 2008), fluids associated with inland and submarine serpentinized systems (Abrajano et al., 1988; Charlou et al., 2002; Proskurowski et al., 2008; Etiope et al., 2011, 2018) and fluid inclusions in minerals from ore deposits and igneous

intrusions (Potter et al., 2004, 2013; Ikorsky and Avedisyan, 2007; Nivin, 2011, 2016; McLin et al., 2012).

Fluids from low temperature ( $T \leq 100$  °C) subaerial hydrothermal emissions typically show CH<sub>4</sub> at concentrations <1 mol% on a H<sub>2</sub>O-free basis, associated with trace amounts of C<sub>2+</sub> volatile organic compounds (VOCs) mainly belonging to the alkane, alkene and aromatic groups (Darling, 1998; Capaccioni and Mangani, 2001; Capaccioni et al., 2004; Tassi et al., 2007; 2012a; 2012b). By contrast, these organic compounds in high temperature (> 200 °C) gases discharged by fumaroles from active volcanoes, were found at very low concentrations (ppb to sub-ppb by vol.) (Taran and Giggenbach 2003 and reference therein).

Despite VOCs are a minor component of volcanic-hydrothermal fluids, their occurrence stirred the interest of the scientific community especially in the framework of prebiotic chemistry of early Earth's atmosphere, emergence of life on Earth and other planets (Tobie et al., 2006; Atreya et al., 2007; Mousis et al., 2009; Mumma et al., 2009; Eigenbrode et al., 2018). In fact, several models for the origin and evolution of life invoked reactions, substrates, catalysts and conditions commonly encountered in subaerial volcanic-hydrothermal environments (e.g. Wächtershäuser, 1993; Zolotov and Shock, 2000; Miyakawa et al., 2002; Ferris, 2005; Mulkidjanian, 2009; Parker et al., 2011a; 2011b; de Aldecoa et al., 2013; Damer and Deamer, 2015; Shock and Boyd, 2015). Moreover, these compounds are also considered useful geochemical monitoring tools for volcanic surveillance (Capaccioni and Mangani, 2001; Capaccioni et al., 2004; Tassi et al., 2005; 2007).

Based on empirical and experimental observations, thermal decomposition of organic matter, dispersed in sedimentary rocks and/or supplied by the infiltrating recharging meteoric or marine waters, has been proposed as the dominant source of methane and light hydrocarbons in volcanic-hydrothermal systems (Des Marais et al., 1981). Likewise, Capaccioni et al. (1995; 2001) ascribed the formation of saturated, unsaturated and aromatic organic compounds mainly to cracking and reforming processes. Taran and Giggenbach (2003) reported a large and comprehensive compositional dataset of light hydrocarbons and suggested that thermal degradation of organic matter through stepwise hydrolytic disproportionation can play as primary source of VOCs in volcanic-hydrothermal fluids. Notwithstanding the hydrocarbons in volcanic-hydrothermal fluids are widely considered as exclusively produced by high temperature pyrolysis of organic matter (Fiebig et al., 2018), the availability of reactive surfaces of inorganic solid phases, extreme temperature gradients and extensive fluid-rock interaction make active volcanoes and geothermal systems suitable contexts for the efficient proceeding of abiogenic organic synthesis.

In the last three decades, laboratory experiments have shown that organic molecules can be successfully synthesized from inorganic substrates under hydrothermal conditions using metal and mineral catalysts (Foustoukos and Seyfried, 2004; Fu et al., 2007; McCollom and Seewald, 2006, 2007; Taran et al., 2007; 2010b; McCollom et al., 2010; McCollom, 2013; 2016; Zhang et al., 2013). The most commonly invoked abiotic genetic mechanism is the Fischer-Tropsch type (FTT) synthesis, i.e. the formation of CH<sub>4</sub> and higher hydrocarbons via catalytic hydrogenation of CO (or CO<sub>2</sub>; Sabatier reaction) at high temperatures (Fischer and Tropsch, 1926; Anderson, 1984). Other abiotic reactions include: thermal decomposition of carbonate minerals, methane polymerization, clay-catalyzed synthesis and organosulfur pathways (McCollom, 2013). However, despite many experimental evidences supported abiotic hydrocarbons formation in volcanic and geothermal contexts, the effective catalytic potential of most natural minerals and the influence of the steam/liquid ratio on the initiation and progression of chemical reactions involving organic molecules remain unclear (McCollom, 2016). It is also evident that there is strikingly little resemblance between the compositional make-up of hydrocarbons observed in experimental systems and those of organic compounds found in natural volcanic-hydrothermal fluids. Carbon and hydrogen isotope composition of CH<sub>4</sub>, carbon isotopic patterns of n-alkanes, isotopic composition of co-occurring species (e.g. CO<sub>2</sub>, H<sub>2</sub>, H<sub>2</sub>O), CH<sub>4</sub>/(C<sub>2</sub>H<sub>6</sub>+C<sub>3</sub>H<sub>8</sub>) ratios and Shultz-Flory molecular weight probability distribution were extensively used as interpretive tools to recognize the origin of hydrocarbons in order to discriminate between abiotic and biotic sources (Bernard et al., 1976; Schoell, 1980; 1988; Whiticar, 1999; Sherwood Lollar et al., 2008; Etiope and Sherwood Lollar, 2013). However, none of these parameters proved to be essential and reliable in unraveling the source(s) of hydrocarbons in natural fluids. On one hand, this is because the compositional features of a product gas (abiotic or biotic) strongly depend on the composition of the substrates/reactants and the conditions (e.g. temperature, pressure, time scale) under which the formation occurs. On the other hand, post-genetic processes (e.g. fluid mixing, diffusion/advection, hydration/dehydration, oxidation/reduction, heteroatomic substitution, biodegradation) may affect the chemical and isotopic composition of light hydrocarbons after their formation (Shock et al., 1998; Etiope et al., 2009; Shock et al., 2013; Gagliano et al., 2014; Tassi et al., 2015). In order to (i) clarify the controversial indications provided by the observations of natural systems, thermodynamic models and hydrothermal experiments and (ii) constrain the processes controlling the origin and behavior of light hydrocarbons at volcanic-hydrothermal conditions, the geochemistry of VOCs in fluids from two fumarolic fields (i.e. Levante beach and La Fossa crater) on Vulcano Island

(southern Italy) was investigated. At Vulcano Island, one of the most extensively studied active volcanoes of the world (e.g. Capasso et al., 1992; 1997; 1999; 2000; Chiodini et al., 1992; 1993; 1995; 1996, Paonita et al., 2002; 2013), gas discharges show the occurrence, although at relatively low concentration, of different VOCs, whose origin was tentatively ascribed to pyrolysis of organic matter buried in sediments or transported by circulating groundwater (Capaccioni et al., 2001; Tassi et al., 2012b) or, alternatively, abiogenic gas-phase reactions at high temperatures (Schwandner et al., 2004; 2013). The debate on the origin of methane and light hydrocarbons in the fluid discharges of the Island is still open likely because information from molecular abundances showed inconclusive diagnostic property and no carbon and hydrogen isotopes data on organic volatiles are available in the literature.

The study focuses on the isotopic composition of carbon in CH<sub>4</sub>, ethane, propane, ethylene, propylene, C<sub>4</sub> hydrocarbons (n-butane, iso-butane and butylene) and CO<sub>2</sub>, and hydrogen isotopic composition of CH<sub>4</sub>, H<sub>2</sub> and water vapor (H<sub>2</sub>O) of fluids from low-temperature ( $\leq 100$  °C) and hot ( $\leq 450$  °C) fluid discharges from Levante beach and La Fossa crater, respectively, at Vulcano Island. These data, coupled with the chemical composition of the main inorganic gases and light hydrocarbons, were investigated to provide insights into (i) source(s) of organic volatiles and (ii) the role played by primary formation mechanisms and post-genetic processes on determining the ultimate compositional features of these compounds. To the best of our knowledge, the <sup>13</sup>C/<sup>12</sup>C and D/H ratios on light hydrocarbons from La Fossa crater presented in this work are the first ones ever reported for high-temperature magmatic gases from subaerial active volcanoes. Eventually, the broad range of temperatures, redox states, gas chemistry and flow rate of fumarolic emissions at Vulcano offered the opportunity to investigate the behavior of VOCs at conditions resembling those suggested by several scenarios of prebiotic Earth.

## **2. Volcanic-Hydrothermal Setting of Vulcano Island**

### *2.1 Geological background*

Vulcano island is the southernmost island of the Aeolian Archipelago (Sicily, southern Italy) in the Tyrrhenian Sea. The Aeolian islands are the exposed summits of volcanic edifices which, together with the surrounding seamounts, constitute a volcanic arc related to the subduction of the Ionian slab underneath the Calabro-Peloritani terrain (Zanon et al., 2003). The current geomorphology of Vulcano Island was interpreted as the result of eruptive

periods of at least three volcanic complexes separated by volcano-tectonic events and major quiescence stages (De Astis et al., 2013). The volcanic activity started in the late Pleistocene and moved progressively from south to north. The last eruption occurred in 1888-1890 (Clocchiatti et al., 1994), characterized by the emission of pyroclastic material from La Fossa, a 391 m high stratocone (Arrighi et al., 2006). After that volcanic event, Vulcano Island was affected by ground deformation, shallow seismicity and intense and persistent fumarolic emission. The present fumarolic discharges mostly occur in a 0.045 km<sup>2</sup> wide area (Aiuppa et al., 2005) located in the northern sector and the inner slope of La Fossa summit crater where high temperature vents (up to 450 °C) emit steam and gases rich in CO<sub>2</sub> and acidic species (SO<sub>2</sub>, H<sub>2</sub>S, HCl and HF). Hydrothermal-type gases, rich in CO<sub>2</sub> and H<sub>2</sub>S with no detectable SO<sub>2</sub>, HCl and HF gases, are discharged from subaerial and submarine fumaroles, with outlet temperature ≤ 100 °C, mostly located close to the Faraglione tuff cone and along the Baia di Levante beach, the eastern side of a flat isthmus connecting Vulcano to Vulcanello at the foothill of La Fossa Cone. Strong diffuse degassing of CO<sub>2</sub> from the soil around the central volcanic edifice was also reported (Inguaggiato et al., 2012), whereas hot (up to 85 °C) water was discharged by wells drilled in the Vulcano Porto area (Capasso et al., 2001, 2014).

After the 1888-1890 eruptive phase, La Fossa crater experienced numerous episodes of increasing fumarolic activity characterized by rising outlet temperatures (Sicardi, 1941; Cannata et al., 2012; Harris et al., 2012) and volatile fluxes (Italiano et al., 1998, Granieri et al., 2006), expansion of the fumarolic field and strong and relatively quick changes in the chemical and isotopic composition of the discharged fluids (Chiodini et al., 1996; Capasso et al., 1997; Paonita et al., 2013). Despite geochemical and geophysical signals of renewed activity were recorded during these unrest periods, none of the volcanic crises culminated with paroxysmal events.

## *2.2 The volcanic-hydrothermal system of Vulcano: geochemical features and conceptual models*

During the last four decades, Vulcano Island has been the subject of several investigations focused on elaborating a reliable geochemical model of the fumarolic system, crucial factor in correctly interpreting geochemical signals as eruption precursors (e.g. Chiodini et al., 1995; Leeman et al., 2005 and Paonita et al., 2013). Among the different models proposed (Martini and Tonani, 1970; Martini et al., 1980; Carapezza et al., 1981; Cioni and D'Amore, 1984; Nuccio et al., 1999), there is a general consensus in considering the composition of crater

fumaroles as the result of a mixing between magmatic and hydrothermal fluids, generally based on the strong correlations between H<sub>2</sub>O, CO<sub>2</sub>, N<sub>2</sub>, Ar, He and δD. The magmatic component shows high CO<sub>2</sub>, N<sub>2</sub>, Ar and He, low H<sub>2</sub>O and  $-24‰ < \delta D < -14‰$  vs. V-SMOW (Chiodini et al., 2000) resembling the typical chemical features of a subduction-related andesitic water (Giggenbach, 1992). Tedesco and Scarsi (1999), Taran (2011) and Paonita et al. (2002, 2013) showed that this CO<sub>2</sub>-rich endmember also has high <sup>3</sup>He/<sup>4</sup>He ratios ( $R/R_a$  up to 6.0-6.2), slightly positive δ<sup>13</sup>C-CO<sub>2</sub> ( $+0.5‰$  V-PDB) and low <sup>40</sup>Ar/<sup>36</sup>Ar values ( $\approx 300$ ) close to that measured in fluid inclusions and in phenocrysts (augite and plagioclase) from recent eruptions (Magra and Pennisi, 1991, Magra and Ferrara, 1994). The hydrothermal component is characterized by high H<sub>2</sub>O ( $0.95 < X_{H_2O} < 0.97$  mol/mol), low CO<sub>2</sub> (3 mol%), lower <sup>13</sup>C/<sup>12</sup>C ratios of CO<sub>2</sub> ( $-6.5‰ < \delta^{13}C < -2‰$  vs. V-PDB), lower amounts of N<sub>2</sub> and noble gases, high N<sub>2</sub>/Ar values ( $\approx 1000$ ) and an excess of radiogenic isotopes (<sup>4</sup>He, <sup>40</sup>Ar, <sup>21</sup>Ne and <sup>22</sup>Ne) suggesting a marked crustal signature (Chiodini et al., 1995; Tedesco and Scarsi 1999; Paonita et al., 2002; 2013; Taran, 2011). Several authors Chiodini et al., 2000; Paonita et al. 2002; Leeman et al., 2005) pointed out that the hydrothermal component shows δD-H<sub>2</sub>O close to that of local seawater ( $+10‰$  vs. V-SMOW), corroborating the hypothesis that Mediterranean marine water infiltrates below La Fossa cone through fractures in volcanic rocks and undergoes several processes (e.g. boiling, water-rock interaction and isotopic equilibrium at high temperatures) that modify its O- and B-isotope signatures. Along with the magmatic and hydrothermal components, minor contributions from meteoric water have been recognized to occasionally contaminate the fumarolic gases (Chiodini et al., 1995; Capasso et al., 1997; Tedesco and Scarsi, 1999; Paonita et al., 2002; Taran, 2011).

Many studies highlighted that composition of crater's gases is highly variable over time. Fluctuation of magmatic activity and the structural response of the volcanic edifice, drove the evolution of the hydrothermal envelope from dry to wet conditions and vice versa over time, highly affecting the absolute and relative contents of soluble acidic species (SO<sub>2</sub>, H<sub>2</sub>S, HCl and HF) via bubble-liquid fractionation and gas-brine-rock interaction (Di Liberto et al., 2002). Accordingly, the envelope surrounding the central volcanic conduit has to be considered as an hydrothermal system characterized by temporally and spatially uneven pH, salinity, chemical composition and redox conditions (Chiodini et al., 1993; 1995; Di Liberto et al., 2002). Tassi et al. (2012b) suggested that volatile organic compounds are supplied to La Fossa crater fumarolic field by this hydrothermal envelope within which thermogenesis occurs. The fluid discharges at Baia di Levante have been interpreted as gas emissions fed by a seawater-dominated multilayerd boiling aquifer, having temperatures comprise from  $\approx 100$

°C at the surface and  $\approx 200$  °C at 185-236 m depth (Sommaruga, 1984), where steam condensation, vapor separation and gas-water-rock interaction chemically and thermally buffer the hydrothermal system.

### 3. Sample Collection and Analytical Methods

#### 3.1 Gas sampling

Samples were collected from fumarolic gas discharges located at two different areas: (1) the northern sector of La Fossa crater and (2) along the Levante beach at the foothill of La Fossa cone (Figure 1). Gas sampling was carried out in May 2015, June 2016, October 2016 and May 2017. Pre-evacuated 60 mL glass flasks, equipped with a Teflon stopcock and filled with 20 mL of 4 N NaOH and 0.15 Cd(OH)<sub>2</sub> suspension (Giggenbach, 1975; Montegrossi et al., 2001) were used in line with 1) a titanium tube and double-wall glass dewars and 2) silicone/tygon tubes connected to a plastic funnel, to sample gases from fumarolic vents and bubbling pools, respectively (Vaselli et al., 2006). During sampling, water vapor and acidic gas species (CO<sub>2</sub>, SO<sub>2</sub>, HCl and HF) dissolved in the soda solution, whereas H<sub>2</sub>S precipitates as insoluble CdS. Low-solubility gas compounds (N<sub>2</sub>, O<sub>2</sub>, CO, H<sub>2</sub>, He, Ar, CH<sub>4</sub> and light hydrocarbons) were concentrated in the sampling flask headspace. Steam condensates (for the analysis of the  $\delta D$  values of water) and dry gases (for the analysis of <sup>13</sup>C/<sup>12</sup>C ratio in CO<sub>2</sub> and D/H ratio in H<sub>2</sub>) were sampled from the fumarolic vents using a water-cooled condenser connected to the sampling line adopted for the soda flasks. At each sampling site, an additional gas sample was collected in 100-150 mL glass flasks filled with 40-50 mL of 4 N NaOH solution for the analysis of the  $\delta^{13}C$  value in CH<sub>4</sub> and C<sub>2+</sub> hydrocarbons and  $\delta D$  in CH<sub>4</sub>.

#### 3.2 Chemical and isotopic analysis of gases

The concentration of major and trace gases was determined at the Department of Earth Sciences of the University of Florence (Italy). The inorganic compounds stored in the sampling flask head-space, i.e., N<sub>2</sub>, Ar + O<sub>2</sub>, H<sub>2</sub>, CH<sub>4</sub>, He and CO, were analyzed by a Shimadzu 15A gas-chromatograph equipped with a thermal conductivity detector (TCD), using a 10 m long stainless-steel packed molecular sieve column and helium or argon (the latter being used for He analysis) as carrier gas. Argon and O<sub>2</sub> were analyzed using a Thermo Focus gas chromatograph Equipped with a 30 m long capillary molecular sieve column and a TCD. The caustic solution was separated from solid CdS by centrifugation, oxidized with

H<sub>2</sub>O<sub>2</sub>, and used for the analysis of: 1) CO<sub>2</sub> as CO<sub>3</sub><sup>2-</sup> by automatic titration with 0.1 N HCl and 2) HF, HCl and SO<sub>2</sub> as F<sup>-</sup>, Cl<sup>-</sup> and SO<sub>4</sub><sup>2-</sup>, respectively, by ion chromatography (Metrohm 761). Solid CdS was dissolved with H<sub>2</sub>O<sub>2</sub>, to analyze H<sub>2</sub>S as SO<sub>4</sub><sup>2-</sup> by IC. The analytical errors for GC analyses were better than 5%.

The carbon isotopic composition of CO<sub>2</sub> was analyzed using a Flash-EA 1112 (Thermo) according to the protocol provided by Fiebig et al. (2004, 2007). Reproducibility was better than ±0.2‰. Carbon isotope analysis of CH<sub>4</sub> and light hydrocarbons were performed using analytical setups and protocols described by Fiebig et al., 2015. External precision was ±0.5‰. The adopted column was unable to chromatographically resolve the iso-butane and butene peaks, providing a single peak given by the superimposition of the two. Capaccioni et al. (2001) measured relatively high contents of iso-butene in the gas emissions at Baia di Levante, with concentrations often equal or higher than those of co-discharged iso-butane. For this reason, we have reported the carbon isotopic composition and relative abundance of the sum of iso-C<sub>4</sub>H<sub>10</sub> and C<sub>4</sub>H<sub>8</sub> [ $\Sigma(\text{i-C}_4\text{H}_{10}+\text{C}_4\text{H}_8)$ ]. Concentrations of C<sub>2</sub>-C<sub>4</sub> hydrocarbons relative to methane were determined from mass spectrometric chromatograms. Analytical precision for hydrocarbon distribution ratios was ≤ ±10%. For the analysis of hydrogen isotopic composition of CH<sub>4</sub>, a sample preconcentration line was connected to a GC-C-II (Thermo) equipped with a Poropack Q column. Methane was separated from H<sub>2</sub> by cooling the GC column down to -30 °C and keeping it isothermal during measurements. External precision for δD-CH<sub>4</sub> analysis was ≤ ±5‰. Determination of D/H ratio in H<sub>2</sub> was carried out by expanding a variable amount of dry gas sample into a sample loop having a fixed volume (100 µl) through a pre-evacuated injection line. The sample was then transferred towards the GC column (Molecular sieve 5A) by means of an He carrier gas flow. H<sub>2</sub> was separated from the other gas compounds by holding the column at -50 °C. Hydrogen isotope ratios were then determined from the 3/2 intensity ratios (HD/H<sub>2</sub>) of sample H<sub>2</sub> compared to that of a working standard with known isotopic composition, calibrated against the primary reference standard VSMOW. In order to be able to correct for small fractionations, different H<sub>2</sub>-standards with known isotopic composition were analyzed along with the samples [133.7 ‰ (OzTech), -366 ‰ (OzTech) and -710 ‰]. A further correction was applied to remove the mass 3 contribution from H<sub>3</sub><sup>+</sup>-ion produced in the source (Sharp, 2007; Sessions et al., 2001). The reproducibility was better than ± 5 ‰ (1σ). Analyses of the H-isotopic composition of H<sub>2</sub>O were performed using a high temperature conversion/element analyzer (Thermo), coupled with a MAT 253 (TC/EA-MS). The external precision was below ± 3 ‰ (1σ). Carbon and

hydrogen stable isotope analysis were carried out at the Laboratory of Stable Isotopes of the Goethe University of Frankfurt.

## 4. Results

### 4.1 Gas temperature and chemical composition

The outlet temperatures, the steam concentrations (expressed in % by vol.) and the chemical composition of the dry gas fraction of the fumarolic gas discharges analyzed in the present study is reported in Table 1. The gas discharges from La Fossa cone of Vulcano Island consist of fumarolic-like vents whose outlet temperature varies from 99 up to 387 °C. At Levante beach, the outlet temperature of the gases emerging along the shoreline and from the sea ranges from the boiling point of water at the sea level ( $\approx 100$  °C) to the temperature of the surrounding seawater ( $\approx 20$  °C). The crater fumaroles show dominant water vapor (up to 91.2% by vol.), followed by CO<sub>2</sub> (up to 948 mmol/mol), acidic gases (SO<sub>2</sub>, H<sub>2</sub>S, HCl and HF: up to 98, 58.8, 3.6 and 0.087 mmol/mol, respectively), N<sub>2</sub> (up to 36 mmol/mol) and H<sub>2</sub> (up to 1.1 mmol/mol). Atmospheric gases (O<sub>2</sub> and Ar) and CO are <0.1 mmol/mol. CH<sub>4</sub> contents are relatively low, ranging from 0.0007 to 0.0055 mmol/mol. Concentrations of C<sub>2</sub>H<sub>6</sub> and C<sub>2</sub>H<sub>4</sub> are 8.3-20.9 and 1.8-143.3 nmol/mol, respectively. Ethylene dominates over ethane (C<sub>2</sub>H<sub>4</sub>/C<sub>2</sub>H<sub>6</sub> molar ratios up to 8.8) in all investigated gases with the exception of F27 (C<sub>2</sub>H<sub>4</sub>/C<sub>2</sub>H<sub>6</sub> = 0.2) and F202 (C<sub>2</sub>H<sub>4</sub>/C<sub>2</sub>H<sub>6</sub> = 0.7). Trace amounts of propane (0.7 nmol/mol) and propylene (1.4 nmol/mol) were determined for fumaroles F27 (May 2015). The beach gas exhalations are mainly composed of CO<sub>2</sub> (up to 983 mmol/mol), N<sub>2</sub> (up to 33 mmol/mol), H<sub>2</sub>S (up to 22 mmol/mol), H<sub>2</sub> (up to 9.5 mmol/mol) and CH<sub>4</sub> (up to 2.6 mmol/mol), whereas SO<sub>2</sub>, HCl and HF are lower than the instrumental detection limit. Oxygen, Ar and He concentrations are slightly higher than those of the crater fumaroles, whereas CO is up to three orders of magnitude lower. The values of the N<sub>2</sub>/Ar ratio, with the exception of sample FOM (June 2016), are generally higher (up to 463, VV–May 2017) than that of air (N<sub>2</sub>/Ar<sub>air</sub> = 83.6), suggesting that N<sub>2</sub> contents are partly related to an input from a non-atmospheric source, as commonly observed in volcanic gases along convergent plate boundaries (Giggenbach, 1996). Light hydrocarbons (C<sub>2</sub>-C<sub>3</sub> alkene-alkane pairs, C<sub>4</sub> compounds) are all present at trace levels, with  $\Sigma(\text{C}_2\text{-C}_4)$  not exceeding 2.5  $\mu\text{mol/mol}$ . The volatile organic compounds (VOCs) composition is mainly dominated by normal-alkanes (in decreasing order of concentration: ethane, propane and n-butane) but relatively high contents of alkenes (up to 46% of the C<sub>2</sub>-C<sub>4</sub> fraction at VI–June 2016) and iso-butane + butene (up to 49% of the C<sub>2</sub>-C<sub>4</sub>

fraction at VIE–May 2017) were also detected. The chemical composition of inorganic and organic constituents of the gas discharges from both La Fossa crater and Levante beach are consistent with those reported by previous work (Chiodini et al., 1995; Capasso et al., 1997; Capaccioni et al., 2001; Giggenbach et al., 2001; Paonita et al., 2002; Tassi et al., 2012b).

#### 4.2 Carbon isotopic composition of CO<sub>2</sub> and C<sub>1</sub>-C<sub>4</sub> hydrocarbons

The  $\delta^{13}\text{C}$  values of CO<sub>2</sub>, C<sub>1</sub>-C<sub>4</sub> hydrocarbons and benzene in the Vulcano gas samples are reported in Table 2. The crater fumaroles and the Baia di Levante gas emissions show  $\delta^{13}\text{C}$ -CO<sub>2</sub> values (‰ vs. V-PDB) ranging from -1.2‰ to -0.3‰ and from -4.4‰ to -2.5‰, respectively. Low-temperature gases discharged at the beach show a C-isotopic composition of CH<sub>4</sub> significantly enriched in <sup>13</sup>C with  $\delta^{13}\text{C}$  values spanning in a narrow range between -10.4 and -4.7‰ vs. V-PDB. On the contrary, the  $\delta^{13}\text{C}$ -CH<sub>4</sub> values of the crater fumaroles vary considerably, both spatially and temporally, by  $\approx 20\%$  (from -29.7 to -9.4 ‰ vs. V-PDB). At Levante beach, the carbon isotopic composition of C<sub>2</sub>-C<sub>4</sub> n-alkanes ranges between -26.6 and -14.3 ‰ vs. V-PDB, with ethane exhibiting the largest variation in  $\delta^{13}\text{C}$  (-24 to -14.3‰) followed by propane (-26.4 to -17.4‰) and n-butane (-26.6 to -18‰). Within the abovementioned isotopic range, the carbon isotopes of the C<sub>2</sub>-nC<sub>4</sub> gas fraction show both direct (FIM, FOM and FUM) and inverse (VI, VIC, VIE, VV and FM) distribution patterns. The <sup>13</sup>C/<sup>12</sup>C isotope ratio of  $\Sigma(\text{i-C}_4\text{H}_{10}+\text{C}_4\text{H}_8)$  shows values ranging from -28.2 to -21‰. The  $\delta^{13}\text{C}$  of ethylene and propylene ranges from -33 to -25.2‰ and from -30.4 to -20.6‰, respectively. The crater gases have  $\delta^{13}\text{C}$  of C<sub>2</sub>H<sub>6</sub> and C<sub>2</sub>H<sub>4</sub>, ranging from -28.5 to -13‰ vs. V-PDB and from -31.4 to -16.6‰ vs. V-PDB, respectively. The only measured  $\delta^{13}\text{C}$  values of C<sub>3</sub>H<sub>8</sub> and C<sub>3</sub>H<sub>6</sub> are broadly equal ( $-31.4 \pm 0.3\%$  vs. V-PDB) and slightly more negative than those of co-discharged methane.

#### 4.3 Hydrogen isotopic composition of H<sub>2</sub>O, H<sub>2</sub> and CH<sub>4</sub>

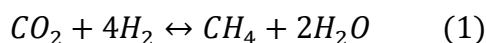
The  $\delta\text{D}$  values of water vapor, H<sub>2</sub> and CH<sub>4</sub> in the Vulcano gas samples are reported in Table 2. The hydrogen isotopic compositions of most condensates of La Fossa crater are between -1 and 12‰ vs. V-SMOW whereas those of gases (VIE and VV) exhalating at Baia di Levante are slightly lower, with values around  $-12.5 \pm 5.5\%$  vs. V-SMOW. FZIO, the only low-temperature (99 °C) crater fumarole sampled, shows significantly more negative  $\delta\text{D}$ -H<sub>2</sub>O values of around  $-32.5 \pm 5.5\%$  vs. V-SMOW. The hydrogen isotopic composition of H<sub>2</sub> discharged from the crater fumaroles exhibits values ranging from -638 to -525‰ vs. V-

SMOW, whereas beach gases show  $\delta D$ -values of  $H_2$  spanning in a small range between  $-610$  and  $-540\text{‰}$  vs. V-SMOW. The hydrogen stable isotopes ratios of  $CH_4$  emitted at the crater vary considerably between  $-658$  and  $-116\text{‰}$  vs. V-SMOW. On the contrary,  $\delta D$  values of  $CH_4$  at Baia di Levante are unusually heavy, clustering between  $-102$  and  $-78\text{‰}$  vs. V-SMOW.  $\delta D-CH_4$  values more negative than  $-450\text{‰}$  have never been reported before for methane associated to natural sources (Etiope and Sherwood Lollar, 2013).

## 5. Discussion

### 5.1 Baia di Levante beach: light hydrocarbons under hydrothermal conditions

Geothermal exploration carried out during the 1950's in an area close to the Baia di Levante beach revealed the existence of a layered hydrothermal system comprising of (i) a shallow (at 7-14 m depth) water body at  $\approx 100$  °C, (ii) an intermediate (at 90-95 m depth) level at  $\approx 136$  °C, and (iii) and a slightly acidic ( $4.3 \leq \text{pH} \leq 5.4$ ) seawater-like (salinity  $\approx 38$  g/L) deep (at 185-236 m depth) water body at 194-200 °C (Sommaruga, 1984). On the basis of geochemical measurements, Chiodini and Marini (1998) suggested that subaerial and submerged fumaroles, occurring at Baia di Levante beach, are fed by vapors separated from the deepest hydrothermal aquifer at 180-230 °C and partially affected by steam condensation. Possible redox conditions in this hydrothermal environment, are satisfactorily approximated by either the Giggenbach "rock buffer" [(FeO)-(FeO<sub>1.5</sub>)] (Giggenbach, 1987) or the empirical relationship of D'Amore and Panichi (1980). While kinetically fast reactive species ( $H_2$  and CO) re-equilibrate at these T-P-redox conditions,  $CH_4$ , one of the kinetically slowest gas species to equilibrate (Giggenbach, 1991) can be used to investigate the deepest hydrothermal parental liquid (Fiebig et al., 2013). Assuming that  $CH_4$  is entirely produced within the hydrothermal system by reduction of  $CO_2$ , in line with the Sabatier reaction:



$\log(X_{CH_4}/X_{CO_2})$  in the liquid phase, considering that  $\log(f_{H_2O}) = 5.4620 - 2046.69/T$  (3 m NaCl solution; Chiodini et al., 2001), is a function of temperature and redox conditions according to:

$$\log\left(\frac{X_{CH_4}}{X_{CO_2}}\right)_L = 4R_H + 1.259 + 4727.62/T - \log(B_{CH_4}/B_{CO_2}) \quad (2)$$

where T is in K,  $X_{CH_4}$  and  $X_{CO_2}$  are the molar fractions of  $CH_4$  and  $CO_2$ , respectively,  $R_H$  is  $\log(X_{H_2}/X_{H_2O})$  (Giggenbach, 1980) whereas  $B_{CH_4}$  and  $B_{CO_2}$  are the vapor/liquid distribution

coefficients of CH<sub>4</sub> and CO<sub>2</sub>, respectively (Chiodini and Marini, 1998). Assuming that the fayalite-hematite-quartz (FHQ, Giggenbach “rock buffer”) correctly describes redox conditions underneath Baia di Levante, measured data implies that CH<sub>4</sub>/CO<sub>2</sub> equilibrates within a liquid phase with 3 m NaCl salinity at temperatures of 350 ± 25 °C. These temperatures closely agree with the maximum temperatures (350-419 °C) directly measured at 1-2 km depth in two geothermal boreholes, VU-IS.V.1 and VU-1DIR (Faraone et al., 1986), drilled in the 1980’s by AGIP-EMS-ENEL, southwest of La Fossa crater.

Comparison of observed and equilibrium isotopic fractionations among CH<sub>4</sub>-H<sub>2</sub>-H<sub>2</sub>O and CH<sub>4</sub>-CO<sub>2</sub> can provide useful information on the origin of methane in hydrothermal systems (Fiebig et al., 2004; 2007; 2013; Proskurowski et al., 2006; Bradley and Summons, 2010; Suda et al., 2014). Figure 2 shows the correlation between ε(H<sub>2</sub>-H<sub>2</sub>O) and ε(CH<sub>4</sub>-H<sub>2</sub>O) values. In the H<sub>2</sub>-H<sub>2</sub>O subsystem, the equilibrium temperatures for Baia di Levante gases are between 130 and 150 °C. These temperatures are all higher than the measured vent temperatures, which were found to be ≤102 °C, and in good agreement with the temperatures of the intermediate hydrothermal aquifer. The temperature discrepancy can be explained by rapid cooling of the fluid compared to the rate of isotopic exchange reactions (Proskurowski et al., 2006). The δD-H<sub>2</sub> values decrease with the increase of the distance of the vents from the Faraglione tuff cone. Steam condensation and re-equilibration of H<sub>2</sub> with cold surficial seawater could be responsible for the observed trend, indicating that gas emissions located in the northern sector of Levante beach are more affected by secondary processes. The ε(CH<sub>4</sub>-H<sub>2</sub>O), by applying the Horibe and Craig (1995) fractionation factors corrected for the vapor-density isotope effect (Driesner, 1997) values indicate equilibrium temperature between H<sub>2</sub>O and CH<sub>4</sub> higher than those estimated for the H<sub>2</sub>-H<sub>2</sub>O subsystem. Isotopic exchange between CH<sub>4</sub> and H<sub>2</sub>O is known to be slower than that between H<sub>2</sub> and H<sub>2</sub>O. Thus, two possible explanations could be invoked: (i) CH<sub>4</sub> and H<sub>2</sub>O are in isotopic disequilibrium or (ii) CH<sub>4</sub> and H<sub>2</sub>O attained hydrogen isotopic equilibrium at temperature of ≈400 °C and the ε(CH<sub>4</sub>-H<sub>2</sub>O) quenched during the upflow and cooling of the deep hydrothermal fluids. It is worth to highlight that the inferred CH<sub>4</sub>-H<sub>2</sub>O equilibration temperatures are a maximum estimation since the isotopic composition of the steam at Baia di Levante is affected by vapor-liquid re-equilibration at lower temperatures, fractionation by condensation and meteoric water addition (Chiodini et al., 1995; 2000; Capasso et al., 1997). All these processes move the δD-H<sub>2</sub>O towards more negative values, which in turn causes an increase of the ε(CH<sub>4</sub>-H<sub>2</sub>O). Assuming a δD of the parental deep water close to that of local seawater (+10‰ vs-VSMOW; Chiodini et al., 1995), this would increase the ε(CH<sub>4</sub>-H<sub>2</sub>O) of ≈20, leading to lower

equilibration temperatures of around 300 °C, in general agreement with the apparent chemical equilibration temperature indicated by  $\log(X_{\text{CH}_4}/X_{\text{CO}_2})$ .

In contrast, the C-isotopic fractionation between CO<sub>2</sub>, and CH<sub>4</sub> is clearly at disequilibrium. In fact, by using fractionation factors of Horita (2001), the available carbon isotope data ( $1 \leq \epsilon(\text{CO}_2\text{-CH}_4) \leq 6.74$ ) indicate equilibration temperatures  $\gg 900$  °C, values unrealistically too high for a volcanic-hydrothermal system.

These evidences suggest that CH<sub>4</sub>, despite in apparent chemical equilibrium with CO<sub>2</sub>, did not approach the <sup>13</sup>C-isotopic equilibrium in the hydrothermal environments. Giggenbach (1997) stated that the rate of attainment of isotopic equilibrium between CH<sub>4</sub> and CO<sub>2</sub> is 400 times slower than that of chemical equilibration. Therefore, kinetic barriers could have prevented the attainment of CO<sub>2</sub>-CH<sub>4</sub> isotopic equilibrium. Another possible explanation is that methane is not primarily produced by CO<sub>2</sub> reduction but it is instead formed by thermal decomposition of organic matter buried with sediments or transported in the meteoric or marine waters circulating throughout the rocks. After its formation, methane could have eventually approached chemical equilibrium with CO<sub>2</sub> and isotopic equilibrium with H<sub>2</sub>O, with sluggish reaction rate instead preventing carbon isotopic re-equilibration. A third scenario is that, regardless of the source of methane, its isotopic composition and concentration in the discharged gases are totally controlled by post-genetic processes such as methane production/consumption by microbial activity (i.e. methanotrophy and methanogenesis) at shallow depth within waters and soils (Etiope et al., 2009).

The shallow seeps, wells and vents in and around the Baia di Levante have yielded more genera of hyperthermophiles than any other hydrothermal environment. In fact of the more than two dozen known hyperthermophilic genera from continental and marine systems worldwide, at least 10 are represented at Vulcano. (Stetter, 1982; 1988; 1996; Zillig et al., 1983; Fiala & Stetter, 1986; Fiala et al., 1986; Huber et al., 1986; Stetter et al., 1990; Hafenbradl et al., 1996; Deckert et al., 1998; Amend et al., 2003a). Amend et al. (2003b) by computing the overall Gibbs free energy of 90 redox reactions in ten sites (seeps, wells and vents) at Levante beach, showed that microbial metabolisms based on CO<sub>2</sub> or CO reduction to CH<sub>4</sub> or disproportionation of CO to CO<sub>2</sub> and CH<sub>4</sub>, are slightly thermodynamically favorable, suggesting that methanogenesis exerts a negligible effect on chemical and isotopic composition of investigated gas emissions. Moreover, Gagliano (2013) observed that microbial methane oxidation rates within the hydrothermalized soils of Vulcano Island are very low, possibly due to high temperatures and low pH of interstitial water. So, microbial

processes affecting methane at near-surface depth seem to be weakly active or completely absent at punctual gas emissions of Levante beach.

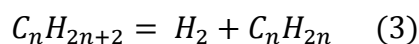
CH<sub>4</sub> in samples from Baia di Levante, exhibits relative consistent C- and H-isotopic values with  $-10.4$  to  $-4.7$  ‰ vs. V-PDB and  $-102$  to  $-78$  ‰ vs. V-SMOW, respectively. Accordingly, in the  $\delta^{13}\text{C}$  vs  $\delta\text{D}$  diagram (Figure 3), data plot right to the upper thermogenic field, within the compositional field traditionally referred to abiotic methane.

In almost all laboratory experiments designed to investigate the occurrence of abiotic methane production via FTT-reactions under hydrothermal conditions and to characterize the chemical and isotopic signatures of reaction's products,  $^{13}\text{C}$  depletions (up to 49‰) of methane relative to the carbon source occurred (Hu et al., 1998; Fu et al., 2007; Taran et al., 2007; 2010b; McCollom et al., 2010; Zhang et al., 2013). Given that the  $\epsilon(\text{CO}_2\text{-CH}_4)$  for all gases from Baia di Levante is greater than or equal to 1, catalytic hydrogenation of CO<sub>2</sub> as the sole source of methane seems unlikely. Observed enriched carbon and hydrogen isotope signatures compared to the thermogenic trend may be explained with thermal degradation of a highly matured organic substrate. Recently, Fiebig et al. (2018) pointed out that in hydrothermal systems methane from marine organic matter may have the potential to become highly enriched in  $^{13}\text{C}$  during the late stage of thermal cracking, when the fraction of generated CH<sub>4</sub> approached 1. The layered hydrothermal system existing underneath the Levante beach, is mostly recharged by local seawater, which can provide considerable amounts of labile organic matter for thermogenesis. Accordingly, previous studies (Capaccioni et al., 2001; Tassi et al. 2012b) ascribed the occurrence of light hydrocarbons in low-temperature gas discharges from Levante beach to thermogenic processes. High ( $>100$ ) CH<sub>4</sub>/( $\Sigma\text{C}_2\text{-C}_4$  n-alkanes) values such as those measured in all the analyzed gas samples (Figure 4) are consistent with those measured in late mature gases from sedimentary basins (Bernard et al., 1976; Whiticar, 1994), corroborating the thermogenic hypothesis.

On the basis of the relative contents of alkanes, alkenes and aromatics, Capaccioni et al. (2001), observed that gas discharges from the northern sector of Baia di Levante were enriched in alkanes, while those from the southern sector were relatively enriched in alkenes and benzene. Accordingly, inspection of Figure 3 and Figure 4, shows that gases from these two sectors are characterized by different CH<sub>4</sub>/( $\Sigma\text{C}_2\text{-C}_4$  n-alkanes) ratios,  $\delta^{13}\text{C-CH}_4$  and  $\delta\text{D-CH}_4$  values. Gas emissions from the southern sector (FM, VIE, VI, VIC and VV) have CH<sub>4</sub>/( $\Sigma\text{C}_2\text{-C}_4$ )  $>5000$ ,  $\delta^{13}\text{C-CH}_4$  of around  $-5.3$ ‰ and  $\delta\text{D-CH}_4$  of  $-83$ ‰, while gases discharged at the northern sector (FOM and FUM) exhibit CH<sub>4</sub>/( $\Sigma\text{C}_2\text{-C}_4$ ) ratios,  $\delta^{13}\text{C-CH}_4$  and  $\delta\text{D-CH}_4$  of  $\approx 1100$ ,  $-10$ ‰ and  $-100$ ‰, respectively. Finally, FIM, a low flux submerged

fumarole, shows compositional features intermediate between those of southern and northern sector gases. Mixing process between two distinct sources could be invoked to explain the observed data distribution in Figure 4. However, methane concentration in all the investigated gases is fairly constant (Table 1) and no correlation between its concentration and the total amount of heavier hydrocarbons is observed. Therefore, a mixing model would imply the existence of two sources of organic compounds having extremely different concentration of C<sub>2+</sub> hydrocarbons but the same methane concentration. However, previous works (Chiodini et al., 1995; Capasso et al., 1997; Capaccioni et al., 2001; Tassi et al., 2012b) and our chemical gas composition of inorganic species did not highlight any spatial distribution ascribable to two-components mixing process, pointing instead to a common hydrothermal source for all gases exhaled at Levante beach.

As observed by Capaccioni et al. (2001), gases from the southern sector of Baia di Levante are enriched in alkene compounds. As highlighted by Seewald (1994; 2001) in a series of laboratory experiments at 300° to 350°C and 350 bars pressure, alkane-alkene pair with the same carbon number attained metastable thermodynamic equilibrium states. Hence, relative amounts of the two hydrocarbons are regulated by a redox-controlled reversible equilibrium reaction, as follows:



The equilibrium constants of reaction (Eq 3) for ethene-ethane and propene-propane pairs can be approximated as follows:

$$\log K_{eq} (n = 2) = 7.73 - \frac{7809}{T} \quad (4)$$

$$\log K_{eq} (n = 3) = 7.15 - \frac{6600}{T} \quad (5)$$

For the dehydrogenation (oxidation) of alkanes and the formation of alkenes more oxidized conditions, higher temperatures and lower pressures are preferable. Owing to their redox and temperature dependence, dehydrogenation reactions have been extensively utilized for evaluating deep temperatures in geothermal and volcanic systems (e.g. Capaccioni and Mangani, 2001; Capaccioni et al., 2004; Tassi et al., 2005; 2007; 2009; 2010; 2011; 2016). Assuming that FHQ correctly describes the redox buffer system of hydrothermal fluids from Levante beach, measured  $\log(C_2H_4/C_2H_6)$  and  $\log(C_3H_6/C_3H_8)$  give equilibration temperatures comprise between 500 and 950 °C, values too high to actually reflect the thermal conditions at depth in the hydrothermal system. In the  $\log(C_2H_4/C_2H_6)$  vs.  $\log(C_3H_6/C_3H_8)$  diagram (Figure

5a) gases from the southern sector exhibit the highest values of alkene/alkane ratios [ $-0.7 < \log(C_2H_4/C_2H_6) < 0$ ;  $0 < \log(C_3H_6/C_3H_8) < 1$ ] which are, to the best of our knowledge, the highest ever recorded in gases associated to hydrothermal systems and geothermal areas. Measured high  $\log(C_3H_6/C_3H_8)$  values are associated with  $^{13}C$ -depleted isotopic composition of  $\delta^{13}C-\Sigma C_3$  (Figure 5b), which were defined as follows:

$$\delta^{13}C-\Sigma C_n = X_{C_nH_{2n+2}} * \delta^{13}C_{C_nH_{2n+2}} + (1 - X_{C_nH_{2n}}) * \delta^{13}C_{C_nH_{2n}} \quad (6)$$

$$X_{C_nH_{2n+2}} = \frac{x_{C_nH_{2n+2}}}{x_{C_nH_{2n+2}} + x_{C_nH_{2n}}} \quad (7)$$

where  $x$  is the molar concentration. The same correlation was also observed for  $\delta^{13}C_{\Sigma C_2}-\log(C_2H_4/C_2H_6)$  and  $\delta^{13}C_{\Sigma C_4}-\log((i-C_4H_{10}+C_4H_8)/n-C_4H_{10})$  couples. In fact, gases from southern sector are characterized by values of  $\delta^{13}C_{\Sigma C_2}$ ,  $\delta^{13}C_{\Sigma C_3}$  and  $\delta^{13}C_{\Sigma C_4}$  as negative as  $-26.3\%$ ,  $-29\%$  and  $-27.8\%$ , respectively (Figure 6). Simple dehydrogenation or hydrogenation (alkane reforming) reactions alter the alkene/alkane ratios without causing any changes of  $\delta^{13}C_{\Sigma C_n}$ ; an horizontal displacement in the  $\log(\text{alkene/alkane})$  vs.  $\delta^{13}C_{\Sigma C_n}$  space. However,  $\delta^{13}C_{\Sigma C_n}$  for the investigated gases is inversely correlated with  $\log(\text{alkene/alkane})$  (Figure 5b), suggesting that chemical and isotopic composition of alkenes and alkanes is controlled by other processes rather than redox reactions or by several mechanisms simultaneously affecting these compounds.

As mentioned above, benzene is one of the main constituents of the organic fraction of gases discharged at Baia di Levante, eventually being the most abundant non-methane hydrocarbon in gas emissions from the southern sector (Capaccioni et al., 2001). On average, taking into account the concentration data for benzene in fumaroles from Levante beach available in the literature (Capaccioni et al., 1995; 2001; Tassi et al., 2012b), emissions from southern and northern sectors display an ethane/benzene ratio of 0.1 and 35, respectively. Accordingly, applying these ratios to the average ethane measured concentrations, we estimated that benzene content in gases from southern and northern sectors is 1057 and 57 nmol/mol, respectively. Likewise total estimated  $C_2-C_6$  contents are 1490 (southern sector) and 1280 (northern sector) nmol/mol. Hence, despite showing different relative abundances of alkane-alkene-aromatic compounds, gases discharged at Baia di Levante have a basically constant total amount of  $C_{2+}$  hydrocarbons (Figure 7). The occurrence of benzene in volcanic-hydrothermal fluids is likely related to the high stability of the aromatic ring under a large range of temperature and redox conditions (Katritzky et al., 1990). Therefore, assuming that differences of alkane-alkene-aromatic relative abundance are related to the effect of post-

genetic processes rather than different primary sources of hydrocarbons or T-P-redox conditions, alkanes-rich gases from the northern sector seems to have retained the deep chemical and isotopic signature. On the contrary, organic compounds at southern sector underwent significant supergene alteration, able to strongly modify the deep compositional signal. In this view, benzene is the final product of a multi-step reaction constituted by (i) dehydrogenation of normal alkanes followed by (ii) reforming processes, i.e. ring closure and aromatization. This mechanism, known in organic chemistry as dehydrocyclization (Bragin et al., 1974; 1983), is commonly used in petroleum refining processes to transform paraffins into aromatics. Zeolites, clay minerals (e.g. montmorillonite, saponite, illite), alumina, metal oxides and metal sulfides are extensively deployed as catalysts in order to speed up the alkanes-aromatics conversion and control the product distribution sensitivity (Solymosi and Széchenyi, 2004; Wang et al., 2014). Indeed, Fulignati et al. (1997) observed that interaction of original volcanic rocks with acidic ( $2 < \text{pH} < 4$ ) hydrothermal fluids produced clay minerals sulfates, sulfides and iron oxides (mainly hematite) in the surroundings of the Faraglione cone. Clays- S-rich sediments saturated with acid waters may promote dehydrocyclization of normal-alkanes to produce benzene and intermediate products such as  $\text{C}_2$ ,  $\text{C}_3$  and  $\text{C}_4$  alkenes and iso-butane. The proposed scenario perfectly matches with that suggested by Capaccioni et al. (2001).

In this respect, the observed  $^{12}\text{C}$ -enrichment of  $\delta^{13}\text{C}_{\Sigma\text{C}_n}$ , may be ascribed to the preferential incorporation of  $^{13}\text{C}$  into benzene possibly because heavier isotopes are favored with respect to the lighter ones into the rigid and chemically stable structure of the aromatic ring in virtue of their lower vibrational frequency.

### *5.2 La Fossa crater: light hydrocarbons under magmatic-hydrothermal conditions*

La Fossa crater fumarolic field is the surficial expression of a classic magmatic-hydrothermal system where magmatic volatiles, degassed from a magma body, mix with hydrothermal fluids seeping towards the central open-system depressurized volcanic conduit and getting vaporized at high-temperature and low-pressure conditions. Minor reactive species ( $\text{H}_2$  and  $\text{CO}$ ) re-equilibrate under the redox conditions governed by the  $\text{H}_2\text{S}/\text{SO}_2$  magmatic gas buffer (Giggenbach, 1987), at temperatures and pressures close to those of the surface vent. On the contrary, the  $\text{CH}_4$ - $\text{CO}_2$  pair was far from the equilibrium conditions suggested by the  $\text{CO}$ - $\text{CO}_2$ - $\text{H}_2$ - $\text{H}_2\text{O}$  system. In fact, at the high temperatures and oxidizing redox conditions indicated by the  $\text{H}_2/\text{H}_2\text{O}$  and  $\text{CO}/\text{CO}_2$  molar ratios, equilibrated  $\text{CH}_4$  should be present in concentrations lower than 4-5 orders of magnitude with respect to those measured in the fluid

discharges. The occurrence of a CH<sub>4</sub>-excess would imply CH<sub>4</sub> addition from an “external” source. Taran and Giggenbach (2003) stated that concentration of methane in subduction-related volcanic fumaroles depends on the mixing proportions from CH<sub>4</sub>-free magmatic volatiles and CH<sub>4</sub>-bearing fluids which are generated within the hydrothermal envelope surrounding the central conduit most likely through thermal decomposition of organic matter. At La Fossa crater fumaroles, mixing proportions between hydrothermal and magmatic components can be successfully investigated by using the H<sub>2</sub>O-CO<sub>2</sub>-S<sub>tot</sub> system, as suggested by Chiodini et al. (1993; 1995) which proposed the existence of a deep magmatic component (DMC), a shallow H<sub>2</sub>O-rich hydrothermal component (SHC1) and a shallow hydrothermal component (SHC2) rich in acidic species, notably SO<sub>2</sub>, H<sub>2</sub>S, HCl and HF. On the basis of CO<sub>2</sub>/S<sub>tot</sub> vs. H<sub>2</sub>O relation, all investigated samples, with the exception of fumaroles affected by elemental sulfur precipitation, suggest a percentage of DMC ranging from 40 to 60%, values consistent with those reported by Leeman et al. (2005) for the “hybrid mixed fluid” (EM2). Methane concentration in the hydrothermal endmember can be calculated by applying the estimated DMC/SHC mixing ratios to our measured log(CH<sub>4</sub>/CO<sub>2</sub>) ratios. Assuming a CH<sub>4</sub>-free DMC, we obtained a log(CH<sub>4</sub>/CO<sub>2</sub>)<sub>SHC</sub> of -4.5. Estimated log(CH<sub>4</sub>/CO<sub>2</sub>)<sub>SHC</sub> ratio may be attributed to an hydrothermal CH<sub>4</sub> in chemical equilibrium with CO<sub>2</sub> in a vapor-liquid-halite system at high temperatures (>400 °C) under redox conditions controlled by FHQ or PPM mineral buffer. Alternatively, methane content in the SHC may be governed by the rate of degradation of organic matter within the surrounding hydrothermal envelope, not reflecting equilibrium conditions. Further indications on the origin of methane can be obtained by looking at its isotopic composition. In δ<sup>13</sup>C-CH<sub>4</sub> vs. δD-CH<sub>4</sub> diagram (Figure 3), investigated fumaroles show isotopic composition ranging from extremely depleted to extremely enriched in deuterium and <sup>13</sup>C. As far as known, δD-CH<sub>4</sub> values below -450‰ have not been related to natural sources yet. However, they were mentioned in connection with artificial or “bit metamorphic” CH<sub>4</sub> (Whiticar, 1989) and with experimental laboratories of FTT-synthesis under hydrothermal conditions (Taran et al., 2010b; McCollom et al., 2010). The former may be related to cracking of oil-based drilling mud under high temperatures and pressures (Jeffrey and Kaplan, 1988; Faber et al., 1999; Wenger et al., 2009). Accordingly, it may be possible that similar deuterium depleted CH<sub>4</sub> is formed owing to hydrothermal alteration of organic matter at elevated temperature and pressure. However, several pyrolysis experiments do not agree with this scenario, albeit experimental conditions including used organic substrates probably differ to magmatic-hydrothermal conditions (e.g. Berner et al., 1995; Lewan et al., 2008; Gao et al., 2018). Moreover, Vulcano is so far the only known

volcanic-hydrothermal area discharging such D-depleted CH<sub>4</sub>. In Figure 2 La Fossa crater samples plot similar to several FTT-experiments, with  $\epsilon(\text{CH}_4\text{-H}_2)$  values around 0. Additionally, also  $\Delta^{13}\text{C}_{\text{CH}_4\text{-CO}_2}$  (about -30‰) and  $\Delta^{13}\text{C}_{\text{CH}_4\text{-C}_2\text{H}_6}$  (about 0‰) are consistent with FTT experiments (Taran et al., 2010b; McCollom et al., 2010). In Figure 3, distribution of investigated gases from La Fossa crater, except for FNB, depicts a trend having an angular coefficient, expressed as  $\Delta\text{H}/\Delta\text{C}$ , of 29. According to Etiope et al. (2009), values greater than 20 are commonly associated with “abiogenic” CH<sub>4</sub> oxidation. Accordingly, samples showing heavier isotopic composition, have lower CH<sub>4</sub> contents (Figure 8a) and lower C<sub>1</sub>/C<sub>2</sub> ratios (Figure 8b), possibly indicating methane degradation processes. Furthermore, these gases display higher content of acidic species (SO<sub>2</sub>, H<sub>2</sub>S and HCl) with respect to those having D-depleted hydrogen isotopic composition of methane. Tassi et al. (2012b) and Schwandner et al. (2013) found ppb concentrations of CS<sub>2</sub>, CH<sub>2</sub>Cl<sub>2</sub> and CHCl<sub>3</sub> in gases discharged by high-temperature fumaroles at La Fossa crater and ascribed their formation to reaction of methane with SO<sub>2</sub>, H<sub>2</sub>S and Cl<sub>2</sub> in the gas phase. Accordingly, methane in gases rich in acidic species may undergo sulfonation and halogenation causing a D- <sup>13</sup>C- enrichment of the residual unreacted fraction. Positive correlation of  $\delta^{13}\text{C}\text{-CH}_4$ ,  $\delta^{13}\text{C}\text{-C}_2\text{H}_6$  and  $\delta^{13}\text{C}\text{-C}_2\text{H}_4$ , suggest that ethane and ethylene are affected as well by similar heteroatomic reactions producing a comparable <sup>13</sup>C-enrichment of residual reactants (Figure 9). Peripheral fumaroles (FNB and FZIO) partially depart from the observed trends, possibly suggesting that the effect of other secondary processes, such as subsurface interaction of uprising gases with acidic steam condensates flowing downwards from the top of the crater rim, may have changed the deep chemical and isotopic signature.

## 6. Conclusions

Investigating the organic geochemistry of gases discharged by vents at Vulcano Island, offered the unique opportunity of studying the primary origin and fate of methane and light hydrocarbons under a wide spectrum of temperatures, redox states and chemistry of the gas phase. At Levante Beach, two distinct sectors were distinguished on the basis of molecular and isotopic composition of hydrocarbons. At the northern sector, the carbon isotopic composition of the discharged methane, the negative carbon isotope fractionation between ethane and methane, as well as the lack of carbon isotope fractionation between ethane, propane and n-butane is compatible with the n-alkanes deriving from marine organic source where primary cracking proceeds under open system conditions at a late stage cracking. At

southern sector, clay minerals, sulfides and oxides possibly catalyze organic reactions, in particular the reaction of cyclomerization of alkanes, resulting in high contents of alkenes and benzene. These findings imply that post-genetic processes can effectively regulate the molecular and isotopic composition of light hydrocarbons under hydrothermal conditions, completely masking the deep signature and leading to erroneous interpretations. Sites like the southern sector of Levante beach are perfect candidate to investigate mineral-assisted organic reaction pathways which can have the potential to abiotically form the building blocks of life. Hydrocarbons from high-temperature magmatic-hydrothermal gases discharged at La Fossa crater, show unique molecular and isotopic composition. In SO<sub>2</sub>-, H<sub>2</sub>S- and HCl-rich gas phases methane and C<sub>2</sub>-compunds are irreversibly transformed into CS<sub>2</sub> and organohalogens through halogenation and sulfonation processes. Gases having lower concentrations of acidic species show higher methane contents, higher C<sub>1</sub>/C<sub>2</sub> ratios and an extremely <sup>13</sup>C- and D-depleted carbon and hydrogen composition of methane. Accordingly, those gases have retained the original composition being less affected by heteroatomic reactions. In this respect, we propose that methane is formed by (i) open-system catalytic hydrogenation of C-bearing inorganic gaseous species (e.g. CO<sub>2</sub>, CO) or (ii) high temperature “bit-metamorphism”-like thermal decomposition of organic matter. The former hypothesis would imply that active volcanoes may be suitable environments for abiotic methane formation on Earth.

### **Acknowledgments**

The Deep Carbon Observatory (DCO) and the Deep Energy Community (DEC) are acknowledged for funding the project. Furthermore, this work was financially supported by the laboratories of Fluid and Rock Geochemistry and Stable Isotope Geochemistry of the Department of Earth Sciences, the Institute of Geosciences and Earth Resources of the National Research Council of Italy (IGG-CNR) of Florence and the German Science Foundation.

## References

- Abrajano T. A., Sturchio N. C., Bohlke J. K., Lyon G. L., Poreda R. J., Stevens C. M. (1988). Methane-hydrogen gas seeps, Zambales Ophiolite, Philippines: deep or shallow origin? *Chemical Geology*, 71, 211–222, [http://dx.doi.org/10.1016/0009-2541\(88\)90116-7](http://dx.doi.org/10.1016/0009-2541(88)90116-7).
- Aiuppa A., Federico C., Giudice G., Gurrieri S. (2005): Chemical mapping of a fumarolic field: La Fossa Crater, Vulcano Island (Aeolian Islands, Italy). *Geophysical Research Letters*, 32, L13309, doi:10.1029/2005GL023207.
- Amend J. P., D'arcy R., Sheth S. N., Zolotova N., Amend A. C. (2003a). *Palaeococcus helgesonii* sp. nov., a facultatively anaerobic, hyperthermophilic archaeon from a geothermal well on Vulcano Island, Italy. *Archives of microbiology*, 179(6), 394-401.
- Amend J. P., Rogers K. L., Shock E. L., Gurrieri S., Inguaggiato S. (2003b). Energetics of chemolithoautotrophy in the hydrothermal system of Vulcano Island, southern Italy. *Geobiology*, 1(1), 37-58.
- Anderson R. B. (1984). *The Fischer–Tropsch Synthesis*. Academic Press, London.
- Arrighi S., Tanguy J.-C., Rosi M., (2006). Eruptions of the last 2200 years at Vulcano and Vulcanello (Aeolian Islands, Italy) dated by high-accuracy archeomagnetism. *Physics of the Earth and Planetary Interiors*, 159, 225–233, doi: 10.1016/j.pepi.2006.07.010.
- Atreya S.K., Mahaffy P.R., Wong A.-S. (2007). Methane and related trace species on Mars: Origin, loss, implications for life, and habitability. *Planetary Space Science*, 55, 358–369, <http://dx.doi.org/10.1016/j.pss.2006.02.005>.
- Bernard B. B., Brooks J. M. Sackett W. M. (1976). Natural gas seepage in the Gulf of Mexico. *Earth and Planetary Science Letters*, 31, 48–54.
- Berner U., Faber E., Scheeder G., Panten D. (1995). Primary cracking of algal and landplant kerogens: kinetic models of isotope variations in methane, ethane and propane. *Chemical geology* 126, 3-4, 233–245.
- Bradley A. S., Summons R. E. (2010). Multiple origins of methane at the Lost City Hydrothermal Field. *Earth and Planetary Science Letters*, 297(1-2), 34-41.
- Bragin O. V., Preobrazhenskii A. V., Liberman A. L. (1974). Catalytic cyclotrimerization of ethylene to benzene. *Bulletin of the Academy of Sciences of the USSR, Division of chemical science*, 23(12), 2654-2659.
- Bragin O. V., Vasina T. V., Preobrazhensky A. V., Palishkina N. V. (1983). Aromatization of ethylene, ethane and methanol on metal-oxide and zeolite-catalysts, *Welterdölkongreß* (London).

- Cannata A., Diliberto S., Alparone S., Gambino S., Gresta S., Liotta M., Madonia P., Milluzzo V., Aliotta M., Montalto P. (2012). Multiparametric approach in investigating volcanohydrothermal systems: the case study of Vulcano (Aeolian Islands, Italy). *Pure and Applied Geophysics*, 169, 167–182, <http://dx.doi.org/10.1007/s00024-011-0297-z>.
- Capaccioni B., and Mangani F. (2001). Monitoring of active but quiescent volcanoes using light hydrocarbon distribution in volcanic gases: the results of 4 years of discontinuous monitoring in the Campi Flegrei (Italy). *Earth and Planetary Science Letters*, 188 (3-4), 543–555, doi:10.1016/S0012-821X(01)00338-7
- Capaccioni B., Martini M., Mangani F. (1995). Light hydrocarbons in hydrothermal and magmatic fumaroles: hints of catalytic and thermal reactions. *Bulletin of Volcanology*, 56 (8), 593–600.
- Capaccioni B., Taran Y., Tassi F., Vaselli O., Mangani G., Macias J. L. (2004). Source conditions and degradation processes of light hydrocarbons in volcanic gases: an example from El Chichón volcano (Chiapas State, Mexico). *Chemical Geology*, 206 (1-2), 81–96, doi: 10.1016/j.chemgeo.2004.01.011
- Capaccioni B., Tassi F., Vaselli O. (2001). Organic and inorganic geochemistry of low temperature discharges at the Baia di Levante beach, Vulcano Island, Italy. *Journal of Volcanology and Geothermal Research*, 108, 173–185.
- Capasso G., D'Alessandro W., Favara R., Inguaggiato S., Parello F. (2001). Interaction between the deep fluids and the shallow groundwaters on Vulcano island (Italy). *Journal of Volcanology and Geothermal Research*, 108, 187–198.
- Capasso G., Dongarra G., Haiser S., Favara R., Valenza M. (1992). Isotope composition of rain water, well water and fumarolic steam on the island of Vulcano, and their implications for volcanic surveillance. *Journal of Volcanology and Geothermal Research*, 49, 147–155, [http://dx.doi.org/10.1016/0377-0273\(92\)90010-B](http://dx.doi.org/10.1016/0377-0273(92)90010-B).
- Capasso G., Favara R., Francofonte S., Inguaggiato S. (1999). Chemical and isotopic variations in fumarolic discharge and thermal waters at Vulcano Island (Aeolian Islands, Italy) during 1996: evidence of resumed volcanic activity. *Journal of Volcanology and Geothermal Research*, 88, 167–175.
- Capasso G., Favara R., Inguaggiato S. (1997). Chemical features and isotopic composition of gaseous manifestations on Vulcano Island, Aeolian Islands, Italy: An interpretative model of fluid circulation. *Geochimica et Cosmochimica Acta*, 61, 16, 3425–3440.

- Capasso G., Favara R., Inguaggiato S. (2000). Interaction between fumarolic gases and thermal groundwaters at Vulcano Island (Italy): evidences from chemical composition of dissolved gases in waters. *Journal of Volcanology and Geothermal Research*, 102, 309–318.
- Capasso G., Federico C., Madonia P., Paonita A. (2014). Response of the shallow aquifer of the volcano-hydrothermal system during the recent crises at Vulcano Island (Aeolian Archipelago, Italy). *Journal of Volcanology and Geothermal Research*, 273, 70–80.
- Carapezza M., Nuccio P. M., Valenza M. (1981). Genesis and evolution of the fumaroles of Vulcano (Aeolian Islands, Italy): a geochemical model. *Bulletin of Volcanology*, 44, 547–563.
- Charlou J. L., Donval J. P., Fouquet Y., Jean-baptiste P., Holm, N. (2002). Geochemistry of high H<sub>2</sub> and CH<sub>4</sub> vent fluids issuing from ultramafic rocks at the Rainbow hydrothermal field (36° 14' N, MAR). *Chemical Geology*, 191, 345–359.
- Chiodini G, Frondini F., Raco B. (1996). Diffuse emission of CO<sub>2</sub> from the Fossa crater, Vulcano Island (Italy). *Bulletin of Volcanology*, 58, 41–50.
- Chiodini G., Marini L. (1998). Hydrothermal gas equilibria: the H<sub>2</sub>O-H<sub>2</sub>-CO<sub>2</sub>-CO-CH<sub>4</sub> system. *Geochimica et Cosmochimica Acta*, 62(15), 2673-2687.
- Chiodini G., Marini L., Russo M. (2001). Geochemical evidence for the existence of high-temperature hydrothermal brines at Vesuvio volcano, Italy. *Geochimica et Cosmochimica Acta*, 65(13), 2129-2147.
- Chiodini G., Allard P., Caliro S., Parello F. (2000). <sup>18</sup>O exchange between steam and carbon dioxide in volcanic and hydrothermal gases: implications for the source of water. *Geochimica et Cosmochimica Acta*, 64, 2479–2488, [http://dx.doi.org/10.1016/S0016-7037\(99\)00445-7](http://dx.doi.org/10.1016/S0016-7037(99)00445-7).
- Chiodini G., Cioni R., Falsaperla S., Montalto A., Guidi M., Marini L. (1992). Geochemical and seismological investigations at Vulcano (Aeolian Islands) during 1978–1989. *Journal of Geophysical Research*, 97, 11,025–11,032.
- Chiodini G., Cioni R., Marini L. (1993) Reactions governing the chemistry of crater fumaroles from Vulcano Island, Italy, and implications for volcanic surveillance. *Applied Geochemistry*, 8, 357–371.
- Chiodini G., Cioni R., Marini L., Panichi C. (1995). Origin of the fumarolic fluids of Vulcano Island, Italy and implication for volcanic surveillance. *Bulletin of Volcanology*, 57, 99–110.
- Chiodini G., Cioni R., Raco B., Taddeucci G. (1991) Gas geobarometry applied to evaluate phreatic explosion hazard at Vulcano Island (Sicily, Italy). *Acta Vulcanol.* 1, 193–198.
- Cioni R. and D'Amore F. (1984). A genetic model for the crater fumaroles of Vulcano Island (Sicily, Italy). *Geothermics*, 13, 375–384, [http://dx.doi.org/10.1016/0375-6505\(84\)90051-8](http://dx.doi.org/10.1016/0375-6505(84)90051-8).

- Clocchiatti R., Del Moro A., Gioncada A., Joron J.L., Mosbah M., Pinarelli L., Sbrana A. (1994). Assessment of a shallow magmatic system: the 1888-90 eruption, Vulcano Island, Italy. *Bulletin of Volcanology*, 56, 466–486.
- Cruse A. M., and Seewald J. S. (2006). Geochemistry of low-molecular weight hydrocarbons in hydrothermal fluids from Middle Valley, northern Juan de Fuca Ridge. *Geochimica et Cosmochimica Acta*, 70 (8), 2073–2092, doi:10.1016/j.gca.2006.01.015
- Damer B and Deamer D. (2015). Coupled Phases and Combinatorial Selection in Fluctuating Hydrothermal Pools: A Scenario to Guide Experimental Approaches to the Origin of Cellular Life. *Life*, 5, 872–887, doi:10.3390/life5010872.
- D'Amore F., Panichi C. (1980). Evaluation of deep temperature of hydrothermal systems by a new gas-geothermometer. *Geochim. Cosmochim. Acta* 44, 549–556.
- Darling, W. G. (1998). Hydrothermal hydrocarbon gases: 1, Genesis and geothermometry. *Applied Geochemistry*, 13 (7), 815–824. doi: 10.1016/S0883-2927(98)00013-4
- De Aldecoa A. L. I., Roldan F. V., Menor-Salvan C. (2013). Natural Pyrrhotite as a Catalyst in Prebiotic Chemical Evolution. *Life*, 3, 502–517; doi:10.3390/life3030502.
- De Astis G., La Volpe L., Peccerillo A., Civetta L. (1997). Volcanological and petrological evolution of Vulcano island (Aeolian Arc, southern Tyrrhenian Sea). *Journal of Geophysical Research*, 102, B4, 8021–8050.
- Deckert G., Warren P. V., Gaasterland T., Young W. G., Lenox A. L., Graham D. E., Overbeek R., Snead M. A., Keller M., Aujay M., Huber R., Feldman R. A., Short J. M., Olsen G. J., Swanson R. V. (1998) The complete genome of the hyperthermophilic bacterium *Aquifex aeolicus*. *Nature* 392, 353–358.
- Des Marais D. J., Donchin J. H., Nehring N. L., Truesdell A. H. (1981). Molecular carbon isotopic evidence for the origin of geothermal hydrocarbons. *Nature*, 292, 826–828.
- Di Liberto V., Nuccio P.M., Paonita A. (2002). Genesis of chlorine and sulphur in fumarolic emissions at Vulcano Island (Italy): assessment of pH and redox conditions in the hydrothermal system. *Journal of Volcanology and Geothermal Research*, 116, 137–150.
- Driesner T. (1997). The effect of pressure on deuterium-hydrogen fractionation in high-temperature water. *Science*, 277(5327), 791-794.
- Eigenbrode, J. L., Summons, R. E., Steele, A., Freissinet, C., Millan, M., Navarro-González, R., Sutter B., McAdam A. C., Franz H. B., Glavin D. P., Archer Jr P. D., Mahaffy P. R., Conrad P. G., Hurowitz J. A., Grotzinger J P., Gupta S., Ming D. W., Sumner D. Y., Szopa C., Malespin C., Buch A., Coll, P. (2018). Organic matter preserved in 3-billion-year-old

mudstones at Gale crater, Mars. *Science*, 360, 6393, 1096–1101.  
<http://science.sciencemag.org/content/360/6393/1096.abstract>.

Etiopio G. and Sherwood Lollar B. (2013). Abiotic methane on Earth. *Reviews of Geophysics*, 51 (2), 276–299, doi: 10.1002/rog.20011

Etiopio G., Feyzullayev A., Milkov A. V., Waseda A., Mizobe K., Sun, C. H. (2009). Evidence of subsurface anaerobic biodegradation of hydrocarbons and potential secondary methanogenesis in terrestrial mud volcanoes. *Marine and Petroleum Geology*, 26(9), 1692–1703, doi:10.1016/j.marpetgeo.2008.12.002

Etiopio G., Fridriksson T., Italiano F., Winiwarter W., Theloke J. (2007). Natural emissions of methane from geothermal and volcanic sources in Europe. *Journal of Volcanology and Geothermal Research*, 165, 76–86, doi: 10.1016/j.jvolgeores.2007.04.014.

Etiopio G., Ifandi E., Nazzari M., Procesi M., Tsikouras B., Ventura G., Steele A., Tardini R., Szatmari P. (2018). Widespread abiotic methane in chromitites. *Scientific Reports*, 8:8728, DOI:10.1038/s41598-018-27082-0.

Etiopio G., Schoell M., Hosgörmez H. (2011). Abiotic methane flux from the Chimaera seep and Tekirova ophiolites (Turkey): Understanding gas exhalation from low temperature serpentinization and implications for Mars. *Earth and Planetary Science Letters*, 310 (1-2), 96–104, doi:10.1016/j.epsl.2011.08.001.

Faber E., Whiticar M. J., Gerling P. (1999) Comparison of hydrocarbons from unconventional sources: KTB, EPR and bit metamorphism. *Geol. Jb. D107*, 175-194.

Faraone D., Silvano A., Verdiani G. (1986). The monzogabbroic intrusion in the island of Vulcano, Aeolian Archipelago, Italy. *Bulletin of volcanology*, 48(5), 299-307.

Ferris J. P. (2005). Mineral catalysis and prebiotic synthesis: montmorillonite-catalyzed formation of RNA. *Elements*, 1, 145–149.

Fiala G., Stetter K. O. (1986) *Pyrococcus furiosus* sp. nov. represents a novel genus of marine heterotrophic archaeobacteria growing optimally at 100 °C. *Archives of Microbiology* 145, 56–61.

Fiala G., Stetter K. O., Jannasch H. W., Langworthy T. A., Madon J. (1986) *Staphylothermus marinus* sp. nov. represents a novel genus of extremely thermophilic submarine heterotrophic archaeobacterial growing to 98 °C. *Systematic and Applied Microbiology* 8, 106–113.

Fiebig J., Chiodini G., Caliro S., Rizzo A., Spangenberg J., Hunziker J. C. (2004). Chemical and isotopic equilibrium between CO<sub>2</sub> and CH<sub>4</sub> in fumarolic gas discharges: Generation of CH<sub>4</sub> in arc magmatic-hydrothermal systems. *Geochimica et Cosmochimica Acta*, 68 (10), 2321–2334, doi:10.1016/j.gca.2003.10.035

- Fiebig J., Stefánsson, A., Ricci A., Tassi F., Viveiros F. V., Silva C., Lopez T M., Schreiber C., Hofmann C., Mountain B. W. (2018). Abiotic hydrocarbons in Earth's crust: a phantom. Manuscript submitted for publication.
- Fiebig J., Tassi F., D'Alessandro W., Vaselli O., Woodland A. B. (2013). Carbon-bearing gas geothermometers for volcanic-hydrothermal systems. *Chemical Geology*, 351, 66–75, doi:10.1016/j.chemgeo.2013.05.006
- Fiebig J., Tassi F., D'Alessandro W., Vaselli O., Woodland A. B. (2015). Isotopic patterns of hydrothermal hydrocarbons emitted from Mediterranean volcanoes. *Chemical Geology*, 396, 152–163, <http://dx.doi.org/10.1016/j.chemgeo.2014.12.030>.
- Fiebig J., Woodland A. B., D'Alessandro W., Puttmann W. (2009). Excess methane in continental hydrothermal emissions is abiogenic. *Geology*, 37(6), 495–498, doi:10.1130/G25598A.1
- Fiebig J., Woodland A. B., Spangenberg J., Oschmann W. (2007). Natural evidence for rapid abiogenic hydrothermal generation of CH<sub>4</sub>. *Geochimica et Cosmochimica Acta*, 71 (12), 3028–3039, doi:10.1016/j.gca.2007.04.010
- Fischer F. and Tropsch H. (1926). The synthesis of petroleum at atmospheric pressures from the gasification products of coal. *Brennst. Chem.*, 7, 97.
- Foustoukos D. I. and Seyfried W. E. (2004). Hydrocarbons in hydrothermal vent fluids: the role of chromium-bearing catalysts. *Science*, 304 (5673), 1002–1005, doi:10.1126/science.1096033
- Fu Q., Sherwood Lollar B., Horita J., Lacrampe-Couloume G., Seyfried W. E. (2007). Abiotic formation of hydrocarbons under hydrothermal conditions: Constraints from chemical and isotope data. *Geochimica et Cosmochimica Acta*, 71(8), 1982–1998, doi:10.1016/j.gca.2007.01.022.
- Gagliano A. L. (2013). Gaseous emissions from geothermal and volcanic areas: focus on methane and methanotrophs (Doctoral dissertation, PhD thesis, University of Palermo).
- Gagliano A. L., D'Alessandro W., Tagliavia M., Parello F., Quatrini P. (2014). Methanotrophic activity and diversity of methanotrophs in volcanic geothermal soils at Pantelleria (Italy). *Biogeosciences*, 11, 5865–5875, doi: 10.5194/bg-11-5865-2014.
- Gao J., Liu J., Ni Y. (2018). Gas generation and its isotope composition during coal pyrolysis: The catalytic effect of nickel and magnetite. *Fuel*, 222, 74-82.
- Giggenbach W. F. (1975). A simple method for collection and analysis of volcanic gases. *Bulletin of Volcanology*, 39, 1, 132–145.

- Giggenbach W. F. (1980). Geothermal gas equilibria. *Geochimica et Cosmochimica Acta*, 44(12), 2021-2032.
- Giggenbach W. F. (1987). Redox processes governing the chemistry of fumarolic gas discharges from White Island, New Zealand. *Applied Geochemistry*, 2(2), 143-161.
- Giggenbach W. F. (1991). Chemical techniques in geothermal exploration. In: *Application of Geochemistry in Geothermal Reservoir Development*. (ed. F. D'Amore), UNITAR, 119–144.
- Giggenbach W. F. (1992). Isotopic shift in waters from geothermal and volcanic systems along convergent plate boundaries and their origin. *Earth and Planetary Science Letters*, 113, 495–510
- Giggenbach W. F. (1996). Chemical composition of volcanic gases. In: *Monitoring and Mitigation of Volcano Hazards*. Springer Verlag, Berlin, pp. 222–256.
- Giggenbach W. F. (1997). Relative importance of thermodynamic and kinetic processes in governing the chemical and isotopic composition of carbon gases in high-heatflow sedimentary basins. *Geochimica et Cosmochimica Acta*, 61(17), 3763-3785.
- Giggenbach W. F., Tedesco D., Sulistiyo Y., Caprai A., Cioni R., Favara R., Fischer T. P., Hirabayashi J.-I., Korzhinsky M., Martini M., Menyailov I., Shinohara H. (2001). Evaluation of results from the fourth and fifth IAVCEI field workshops on volcanic gases, Vulcano island, Italy and Java, Indonesia. *Journal of Volcanology and Geothermal Research*, 108, 157–172.
- Granieri D., Carapezza M. L., Chiodini G., Avino R., Caliro S., Ranaldi M., Ricci T. and Tarchini L. (2006). Correlated increase in CO<sub>2</sub> fumarolic content and diffuse emission from La Fossa crater (Vulcano, Italy): evidence of volcanic unrest or increasing gas release from a stationary deep magma body? *Geophysical Research Letters*, 33, L13316, <http://dx.doi.org/10.1029/2006GL026460>.
- Hafenbradl D., Keller M., Dirmeier R., Rachel R., Rossnagel P., Burggraf S., Huber H., Stetter K. O. (1996) *Ferroglobus placidus* gen. nov., sp. nov., a novel hyperthermophilic archaeum that oxidizes Fe<sup>2+</sup> at neutral pH under anoxic conditions. *Archives of Microbiology* 166, 308–314.
- Harris A., Alparone S., Bonforte A., Dehn J., Gambino S., Lodato L., Spampinato L. (2012). Vent temperature trends at the Vulcano Fossa fumarole field: the role of permeability. *Bulletin of Volcanology*, 74, 1293–1311, <http://dx.doi.org/10.1007/s00445-012-0593-1>.
- Horibe Y., Craig H. (1995). DH fractionation in the system methane-hydrogen-water. *Geochimica et Cosmochimica Acta*, 59(24), 5209-5217.

- Horita J. (2001). Carbon isotope exchange in the system CO<sub>2</sub>-CH<sub>4</sub> at elevated temperatures. *Geochimica et Cosmochimica Acta*, 65(12), 1907-1919.
- Hu G., Ouyang Z.Y., Wang X., Wen Q. (1998). Carbon isotopic fractionation in the process of Fischer–Tropsch reaction in primitive solar nebula. *Science in China (Series D)* 41, 202–207.
- Huber R, Langworthy TA, König H, Thomm M, Woese CR, Sleytr UB, Stetter KO (1986) *Thermotoga maritima* sp. nov. represents a new genus of unique extremely thermophilic eubacteria growing up to 90 °C. *Archives of Microbiology* 144, 324–333.
- Ikorsky S. V., Avedisyan A. A. (2007). Hydrocarbon gases and helium isotopes in the Paleozoic alkaline-ultramafic massifs of the Kola Peninsula. *Geochemistry International*, 45, 62–69.
- Inguaggiato S., Mazot A., Diliberto I. S., Inguaggiato C., Madonia P., Rouwet D., Vita F. (2012). Total CO<sub>2</sub> output from Vulcano island (Aeolian Islands, Italy). *Geochemistry Geophysics Geosystems*, 13, 2, 1–19, doi: 10.1029/2011GC003920.
- Italiano F., Pecoraino G., Nuccio P. M. (1998). Steam output from fumaroles of an active volcano: tectonic and magmatic-hydrothermal controls on the degassing system at Vulcano (Aeolian arc). *Journal of Geophysical Research*. 103 (B12), 29829–29842.
- Jeffrey A. W. A., Kaplan I. R. (1988). Hydrocarbons and inorganic gases in the Gravberg-1 well, Siljan Ring, Sweden. *Chemical Geology*, 71(1-3), 237-255.
- Katritzky, A. R., Balasubramanian, M., & Siskin, M. (1990). Aqueous high-temperature chemistry of carbo- and heterocycles. 2. Monosubstituted benzenes: Benzyl alcohol, benzaldehyde and benzoic acid. *Energy & Fuels*, 4(5), 499-505.
- Leeman W. P., Tonarini S., Pennisi M., Ferrara G. (2005). Boron isotope variations in fumarolic condensates and thermal waters from Vulcano Island, Italy: implications for evolution of volcanic fluids. *Geochimica et Cosmochimica Acta*, 69, 143–163, <http://dx.doi.org/10.1016/j.gca.2004.04.004>.
- Lewan M., Kotarba M., Więclaw D., Piestrzyński, A. (2008). Evaluating transition-metal catalysis in gas generation from the Permian Kupferschiefer by hydrous pyrolysis. *Geochimica et Cosmochimica Acta*, 72, 16, 4069–4093.
- Martini M, Piccardi G, Cellini Legittimo P (1980). Geochemical surveillance of active volcanoes: data on the fumaroles of Vulcano (Aeolian Islands, Italy). *Bulletin of Volcanology*, 43, 255–263
- Martini M. and Tonani F. (1970). *Risultati del rilevamento geochimico: Vulcano 1969*. Palermo.

- McCollom T. M. (2013). Laboratory simulations of abiotic hydrocarbon formation in Earth's deep subsurface. *Review Mineral Geochem* 75, 467–494.
- McCollom T. M. (2016). Abiotic methane formation during experimental serpentinization of olivine. *PNAS*, [www.pnas.org/cgi/doi/10.1073/pnas.1611843113](http://www.pnas.org/cgi/doi/10.1073/pnas.1611843113).
- McCollom T. M. and Seewald J. S. (2006). Carbon isotope composition of organic compounds produced by abiotic synthesis under hydrothermal conditions. *Earth and Planetary Science Letters*, 243 (1-2), 74–84, doi:10.1016/j.epsl.2006.01.027
- McCollom T. M. and Seewald J. S. (2007). Abiotic Synthesis of Organic Compounds in Deep-Sea Hydrothermal Environments, *Chemical Review*, 107, 382–401.
- McCollom T. M., Sherwood Lollar B., Lacrampe-Couloume G., Seewald J. S. (2010). The influence of carbon source on abiotic organic synthesis and carbon isotope fractionation under hydrothermal conditions. *Geochimica et Cosmochimica Acta*, 74 (9), 2717–2740, doi: 10.1016/j.gca.2010.02.008
- McLin K. S., Moore J. N., Bowman J. R., McCulloch J. E. (2012). Mineralogy and fluid inclusion gas chemistry of production well mineral scale deposits at the Dixie Valley geothermal field, USA. *Geofluids*, 12, 216–227.
- Miyakawa S., Yamanashi H., Kobayashi K., Cleaves H. J., Miller S. L. (2002). Prebiotic synthesis from CO atmospheres: Implications for the origins of life. *PNAS*, 99, 23, 14628–14631, [www.pnas.org/cgi/doi/10.1073/pnas.192568299](http://www.pnas.org/cgi/doi/10.1073/pnas.192568299).
- Montegrossi G., Tassi F., Vaselli O., Buccianti A., Garofalo K. (2001). Sulphur species in volcanic gases. *Analytical Chemistry*, 73(3), 709–715.
- Mousis O., Lunine J. I., Waite H., Lewis W. S., Mandt K. E., Marquer D., Cordier D. (2009). Formation conditions of Enceladus and origin of its methane reservoir. *The Astrophysical Journal Letters*, 701, L39–L42, doi:10.1088/0004-637X/701/1/L39
- Mulkidjanian A. Y. (2009). On the origin of life in the Zinc world: 1. Photosynthesizing, porous edifices built of hydrothermally precipitated zinc sulfide as cradles of life on Earth. *Biology Direct*, 4:26, doi:10.1186/1745-6150-4-26.
- Mumma M. J., Villanueva G. L., Robert E., Novak R. E., Hewagama T., Boncho P., Bonev B. P., DiSanti M. A., Mandell A. M., Michael D., Smith M. D. (2009). Strong release of methane on Mars in northern summer 2003. *Science*, 323, 1041–1045, doi:10.1126/science.1165243.
- Nivin V. A. (2011). Variations in the composition and origin of hydrocarbon gases from inclusions in minerals of the Khibiny and Lovozero plutons, Kola Peninsula, Russia. *Geology of Ore Deposits*, 53, 699–707.

- Nivin V. A. (2016). Free hydrogen-hydrocarbon gases from the Lovozero loparite deposit (Kola Peninsula, NW Russia). *Applied Geochemistry*, 74, 44–55.
- Nuccio P. M. and Paonita A. (2001). Magmatic degassing of multicomponent vapours and assessment of magma depth: application to Vulcano Island (Italy). *Earth and Planetary Science Letters*, 193, 467–481, [http://dx.doi.org/10.1016/S0012-821X\(01\)00512-X](http://dx.doi.org/10.1016/S0012-821X(01)00512-X).
- Paonita A., Favara R., Nuccio P. M., Sortino F. (2002). Genesis of fumarolic emissions as inferred by isotope mass balances: CO<sub>2</sub> and water at Vulcano Island, Italy. *Geochimica et Cosmochimica Acta*, 66, 759–772.
- Paonita A., Federico C., Bonfanti P., Capasso G., Inguaggiato S., Italiano F., Madonia P., Pecoraino G., Sortino F. (2013). The episodic and abrupt geochemical changes at La Fossa fumaroles (Vulcano Island, Italy) and related constraints on the dynamics, structure, and compositions of the magmatic system. *Geochimica et Cosmochimica Acta*, 120, 158–178, <http://dx.doi.org/10.1016/j.gca.2013.06.015>.
- Parker E. T., Cleaves H. J., Callahan M. P., Dworkin J. P., Glavin D. P., Lazcano A., Bada J. L. (2011). Prebiotic Synthesis of Methionine and Other Sulfur-Containing Organic Compounds on the Primitive Earth: A Contemporary Reassessment Based on an Unpublished 1958 Stanley Miller Experiment. *Origin of Life and Evolution of Biospheres*, 41, 201–212, DOI 10.1007/s11084-010-9228-8.
- Parker E. T., Cleaves H. J., Dworkin J. P., Callahan M. P., Aubrey A., Lazcano A., Bada J. L. (2011). Primordial synthesis of amines and amino acids in a 1958 Miller H<sub>2</sub>S-rich spark discharge experiment. *PNAS*, 108, 14, 5526–5531, [www.pnas.org/cgi/doi/10.1073/pnas.1019191108](http://www.pnas.org/cgi/doi/10.1073/pnas.1019191108).
- Potter J., Rankin A. H., Treloar P. J. (2004). Abiogenic Fischer-Tropsch synthesis of hydrocarbons in alkaline igneous rocks; fluid inclusion, textural and isotopic evidence from the Lovozero complex, N.W. Russia. *Lithos*, 75 (3-4), 311–330, doi:10.1016/j.lithos.2004.03.003
- Potter J., Salvi S., Longstaffe F. J. (2013). Abiogenic hydrocarbon isotopic signatures in granitic rocks: Identifying pathways of formation. *Lithos*, 182-183, 114–124, <http://dx.doi.org/10.1016/j.lithos.2013.10.001>.
- Proskurowski G., Lilley M. D., Kelley D. S., Olson E. J. (2006). Low temperature volatile production at the Lost City Hydrothermal Field, evidence from a hydrogen stable isotope geothermometer. *Chemical Geology*, 229(4), 331-343.

- Proskurowski G., Lilley M. D., Seewald J. S., Früh-Green G. L., Olson E. J., Lupton J. E., Kelley D. S. (2008). Abiogenic hydrocarbon production at Lost City hydrothermal field. *Science* (New York, N.Y.), 319 (5863), 604–7, doi:10.1126/science.1151194.
- Schoell M. (1983). Genetic characterization of natural gases. *AAPG Bulletin*, 67, 2225–2238.
- Schoell M. (1988). Multiple origins of methane in the Earth. *Chemical Geology*, 71, 1–10.
- Schoell, M. (1980). The hydrogen and carbon isotopic composition of methane from natural gases of various origins. *Geochimica et Cosmochimica Acta*, 44, 649-661, doi: 10.1016/0016-7037(80)90155-6
- Schwandner F. M., Seward T. M., Gize A. P., Hall A., Dietrich V. J. (2013). Halocarbons and other trace heteroatomic organic compounds in volcanic gases from Vulcano (Aeolian Islands, Italy). *Geochimimica et Cosmochimica Acta*, 101, 191–221, doi: 10.1016/j.gca.2012.10.004.
- Schwandner F. M., Seward T. M., Gize A. P., Hall P. A., Dietrich V. J. (2004). Diffuse emission of organic trace gases from the flank and crater of a quiescent active volcano (Vulcano, Aeolian Islands, Italy). *Journal of Geophysical Research*, D 109, D04301, <http://dx.doi.org/10.1029/2003JD003890>.
- Seewald J. S. (1994). Evidence for metastable equilibrium between hydrocarbons under hydrothermal conditions. *Nature* 370, 285–287.
- Seewald J. S. (2001). Aqueous geochemistry of low molecular weight hydrocarbons at elevated temperatures and pressures: constraints from mineral buffered laboratory experiments. *Geochimica et Cosmochimica Acta*, 65(10), 1641-1664.
- Sherwood Lollar B., Lacrampe-Couloume G., Slater G. F., Ward J., Moser D. P., Gihring T. M., Onstott T. C. (2006). Unravelling abiogenic and biogenic sources of methane in the Earth's deep subsurface. *Chemical Geology*, 226 (3-4), 328–339, doi: 10.1016/j.chemgeo.2005.09.027
- Sherwood Lollar B., Lacrampe-Couloume G., Voglesonger K., Onstott T. C., Pratt L. M., Slater G. F. (2008). Isotopic signatures of CH<sub>4</sub> and higher hydrocarbon gases from Precambrian Shield sites: A model for abiogenic polymerization of hydrocarbons. *Geochimica et Cosmochimica Acta*, 72 (19), 4778–4795, doi: 10.1016/j.gca.2008.07.004
- Sherwood Lollar B., Westgate T. D., Ward J. A., Slater G. F., Lacrampe-Couloume G. (2002). Abiogenic formation of alkanes in the Earth's crust as a minor source for global hydrocarbon reservoirs. *Nature*, 416(6880), 522–4, doi:10.1038/416522a
- Shock E. L. and Boyd E. S. (2015). Principles of geobiochemistry. *Elements*, 11, 395–401, doi: 10.2113/gselements.11.6.395.

- Shock E. L. and Schulte M. D. (1998). Organic synthesis during fluid mixing in hydrothermal systems. *Journal of Geophysical Research*, 103, E12, 28513–28527.
- Shock E. L., Canovas P., Yang Z., Boyer G., Johnson K., Robinson K., Fecteau K., Windman T., Cox A. (2013). Thermodynamics of organic transformations in hydrothermal fluids. *Rev. Mineral. Geochem.*, 76, 311–350, doi: 10.2138/rmg.2013.76.9.
- Sicardi L. (1941). Il recente ciclo dell'attività fumarolica dell'isola di Vulcano. *Bullettino Vulcanologico*, 7, 85–140.
- Solymosi F., Szechenyi A. (2004). Aromatization of isobutane and isobutene over Mo<sub>2</sub>C/ZSM-5 catalyst. *Applied Catalysis A: General*, 278(1), 111-121.
- Sommaruga C. (1984). Le ricerche geotermiche svolte a Vulcano negli anni '50. *Rendiconti Società Italiana Mineralogia e petrologia*, 39, 355–366.
- Stetter K. O. (1982) Ultrathin mycelia-forming organisms from submarine volcanic areas having an optimum growth temperature of 105 °C. *Nature* 300, 258–260.
- Stetter K. O. (1988) *Archaeoglobus fulgidus* gen. nov., sp. nov. a new taxon of extremely thermophilic archaeobacteria. *Systematic and Applied Microbiology* 10, 172–173.
- Stetter K. O. (1996) Hyperthermophilic procaryotes. *FEMS Microbiology Reviews* 18, 149–158.
- Stetter K. O., Fiala G., Huber G., Huber R., Seegerer A. (1990) Hyperthermophilic microorganisms. *FEMS Microbiology Reviews* 75, 117–124.
- Suda K., Ueno Y., Yoshizaki M., Nakamura H., Kurokawa K., Nishiyama E., Maruyama S. (2014). Origin of methane in serpentinite-hosted hydrothermal systems: The CH<sub>4</sub>–H<sub>2</sub>–H<sub>2</sub>O hydrogen isotope systematics of the Hakuba Happo hot spring. *Earth and Planetary Science Letters*, 386, 112–125, doi:10.1016/j.epsl.2013.11.001
- Taran Y. (2011). N<sub>2</sub>, Ar, and He as a tool for discriminating sources of volcanic fluids with application to Vulcano, Italy. *Bulletin of Volcanology*, 73, 395–408, <http://dx.doi.org/10.1007/s00445-011-0448-1>.
- Taran Y. A., and Giggenbach W. F. (2003). *Geochemistry of Light Hydrocarbons in Subduction-Related Volcanic and Hydrothermal Fluids*. Society of Economic Geologists, Special Publication 10, 61–74.
- Taran Y. A., Kliger G. A., Cienfuegos E., Shuykin A. N. (2010b). Carbon and hydrogen isotopic compositions of products of open-system catalytic hydrogenation of CO<sub>2</sub>: Implications for abiogenic hydrocarbons in Earth's crust. *Geochimica et Cosmochimica Acta*, 74 (21), 6112–6125, doi:10.1016/j.gca.2010.08.012

- Taran Y. A., Kliger G. A., Sevastianov V. S. (2007). Carbon isotope effects in the open-system Fischer–Tropsch synthesis. *Geochimica et Cosmochimica Acta*, 71(18), 4474–4487, doi:10.1016/j.gca.2007.06.057
- Taran Y.A., Varley N.R., Inguaggiato S., Cienfuegos E. (2010a). Geochemistry of H<sub>2</sub>- and CH<sub>4</sub>-enriched hydrothermal fluids of Socorro Island, Revillagigedo Archipelago, Mexico. Evidence for serpentinization and abiogenic methane. *Geofluids*, 10, 542–555, doi:10.1111/j.1468-8123.2010.00314.x.
- Tassi F., Martinez C., Vaselli O., Capaccioni B., Viramonte J. (2005). Light hydrocarbons as redox and temperature indicators in the geothermal field of El Tatio (northern Chile). *Applied Geochemistry*, 20 (11), 2049–2062, doi:10.1016/j.apgeochem.2005.07.013
- Tassi F., Vaselli O., Capaccioni B., Montegrossi G., Barahona F., Caprai A. (2007). Scrubbing process and chemical equilibria controlling the composition of light hydrocarbons in natural gas discharges: An example from the geothermal fields of El Salvador. *Geochemistry, Geophysics, Geosystems*, 8 (5), doi:10.1029/2006GC001487
- Tassi F., Montegrossi G., Vaselli O., Liccioli C., Moretti S., Nisi B. (2009). Degradation of C<sub>2</sub>–C<sub>15</sub> volatile organic compounds in a landfill cover soil. *Science of the Total Environment*, 407(15), 4513-4525.
- Tassi F., Montegrossi G., Capecchiacci F., Vaselli O. (2010) Origin and distribution of thiophenes and furans in gas discharges from active volcanoes and geothermal systems. *International Journal of Molecular Science*, 1434–1457. <http://dx.doi.org/10.3390/ijms11041434>.
- Tassi F., Aguilera, F., Vaselli O., Darrah T., Medina E. (2011). Gas discharges from four remote volcanoes in northern Chile (Putana, Olca, Irruputuncu and Alitar): a geochemical survey. *Annals of Geophysics*, 54(2).
- Tassi F., Fiebig J., Vaselli O., Nocentini M. (2012a). Origins of methane discharging from volcanic-hydrothermal, geothermal and cold emissions in Italy. *Chemical Geology*, 310-311, 36–48, doi: 10.1016/j.chemgeo.2012.03.018
- Tassi F., Capecchiacci F., Cabassi J., Calabrese S., Vaselli O., Rouwet D., Pecoraino G., Chiodini G. (2012b). Geogenic and atmospheric sources for volatile organic compounds in fumarolic emissions from Mt. Etna and Vulcano Island (Sicily, Italy). *Journal of Geophysical Research*, 117, D17305, doi: 10.1029/2012JD017642.
- Tassi F., Nisi B., Cardellini C., Capecchiacci F., Donnini M., Vaselli O., Avino R., Chiodini G. (2013a). Diffuse soil emission of hydrothermal gases (CO<sub>2</sub>, CH<sub>4</sub>, C<sub>6</sub>H<sub>6</sub>) at Solfatara crater

(Campi Flegrei, southern Italy). *Applied Geochemistry*, 35, 142–153, doi: 10.1016/j.apgeochem.2013.03.020.

Tassi F., Capecchiacci F., Giannini L., Vougioukalakis G.E., Vaselli O. (2013b). Volatile organic compounds (VOCs) in air from Nisyros Island (Dodecanese Archipelago, Greece): Natural versus anthropogenic sources. *Environmental Pollution*, 180, 111-121, doi: 10.1016/j.envpol.2013.05.023

Tassi F., Venturi S., Cabassi J., Capecchiacci F., Nisi B., Vaselli O. (2015). Volatile organic compounds (VOCs) in soil gases from Solfatara crater (Campi Flegrei, southern Italy): Geogenic source(s) vs. biogeochemical processes. *Applied Geochemistry*, 56, 37–49, doi: 10.1016/j.apgeochem.2015.02.005.

Tassi F., Aguilera F., Benavente O., Paonita A., Chiodini G., Caliro S., ... Caselli A. (2016). Geochemistry of fluid discharges from Peteroa volcano (Argentina-Chile) in 2010–2015: Insights into compositional changes related to the fluid source region (s). *Chemical Geology*, 432, 41-53.

Tedesco D. and Scarsi P. (1999). Intensive gas sampling of noble gases and carbon at Vulcano (Southern Italy). *Journal of Geophysical Research*, 104, 10499–10510, <http://dx.doi.org/10.1029/1998JB900066>.

Tobie G., Lunine J. I., Sotin C. (2006). Episodic outgassing as the origin of atmospheric methane on Titan. *Nature*, 440, 61–64, doi:10.1038/nature04497.

Vaselli O., Tassi F., Montegrossi G., Capaccioni B., Giannini L. (2006). Sampling and analysis of fumarolic gases. *Acta Vulcanologica*, 1-2, 65-76.

Wächtershäuser G. (1993). The cradle chemistry of life – on the origin of natural-products in a pyrite-pulled chemoautotrophic origin of life. *Pure Applied Chemistry*, 65, 1343–1348.

Wang G., Li C., Shan H. (2014). Highly efficient metal sulfide catalysts for selective dehydrogenation of isobutane to isobutene. *ACS Catalysis*, 4(4), 1139-1143.

Wenger L. M., Pottorf R. J., Macleod G., Otten G., Dreyfus S., Justwan H. K., Wood E. S. (2009). Drill bit metamorphism: Recognition and impact on show evaluation. In: *SPE Annual Technical Conference and Exhibition*. Society of Petroleum Engineers. <https://doi.org/10.2118/125218-MS>

Whiticar M. J. (1990). A geochemical perspective of natural gas and atmospheric methane. *Organic Geochemistry*, 16(1-3), 531-547.

Whiticar M. J. (1994). Correlation of natural gases with their sources. In: Magoon, L., Dow, W. Eds., *The Petroleum System - From Source to Trap*. AAPG Memoir 60, 261–284.

- Whiticar M. J. (1999). Carbon and hydrogen isotope systematics of bacterial formation and oxidation of methane. *Chemical Geology*, 161, 291–314.
- Zanon V., Frezzotti M. L., Peccerillo A. (2003). Magmatic feeding system and crustal magma accumulation beneath Vulcano Island (Italy): evidence from CO<sub>2</sub> fluid inclusions in quartz xenoliths. *Journal of Geophysical Research*, 108(B6), 2298. <http://dx.doi.org/10.1029/2002JB002140>.
- Zhang S., Mi J. and He K. (2013). Synthesis of hydrocarbon gases from four different carbon sources and hydrogen gas using a gold-tube system by Fischer-Tropsch method. *Chemical Geology*, 349–350, 27–35.
- Zillig W, Holz I, Janekovic D, Schäfer W, Reiter WD (1983) The archaeobacterium *Thermococcus celer* represent a novel genus within the thermophilic branch of the Archaeobacteria. *Systematic and Applied Microbiology* 4, 88–94.
- Zolotov M. Y. and Shock E. L. (2000). A thermodynamic assessment of the potential synthesis of condensed hydrocarbons during cooling and dilution of volcanic gases. *Journal of Geophysical Research*, 105(B1), 539–59, <http://www.ncbi.nlm.nih.gov/pubmed/11543291>.

## Table captions

**Table 1.** Outlet temperatures (°C) steam fraction (expressed in % by vol.) and chemical composition of the dry gas fraction of the investigated gases from La Fossa crater and Levante beach of Vulcano Island. Gas concentration data for common gas constituents in mmol/mol, for hydrocarbons higher than methane in nmol/mol.  $\Sigma C_4$  expresses the sum of iso-butane and butylene. Abbreviations: not available (na), below detection limit (bdl).

**Table 2.** Carbon isotopic composition (expressed as  $\delta^{13}C$  ‰ vs. V-PDB) of  $CO_2$ , methane, ethane, propane, n-butane,  $\Sigma C_4$  (sum of iso-butano and butylene), ethylene and propylene and hydrogen isotopic composition ( $\delta D$  ‰ vs. V-SMOW) of methane, molecular hydrogen and water vapor from Vulcano Island vents. Abbreviations: not analyzed (na), below detection limit (bdl).

## Figure captions

**Figure 1.** Location of Vulcano Island and sampling sites; A = La Fossa crater; B = Levante Beach

**Figure 2.**  $H_2$ - $H_2O$ - $CH_4$  H-isotope systematics (after Suda et al., 2014). In contrast Suda et al. (2014),  $\epsilon$  represents the enrichment factor instead of  $1000 \ln \alpha$ . The green line is the curve recommended by Horibe and Craig (1995). The dashed part indicates the fractionation after correction for vapor-density isotope effects (Driesner, 1997). Grey dashed lines exhibit  $CH_4$ - $H_2$  equilibrium fractionation at the given temperature. Besides field data, also experimental studies in bacterial cultures and FTT syntheses are considered.

**Figure 3.**  $\delta^{13}C$  vs  $\delta D$  diagram of methane

**Figure 4.** Isotopic composition of methane vs. concentration ratios of n-alkanes. Colors as in Figure 3

**Figure 5.**  $C_3$  alkene/alkane ratios vs.  $C_2$  alkene/alkane ratios (a) and carbon isotopic composition of  $\Sigma C_3$

**Figure 6.** Carbon isotopic composition of  $\Sigma C_4$  vs carbon isotopic composition of  $\Sigma C_2$  and  $\Sigma C_3$

**Figure 7.** Average concentration ratios for Southern and Northern sectors

**Figure 8.** Carbon isotopic composition of methane vs. concentration of methane in the total gas (expressed in ppm) (a) and vs.  $C_1/C_2$  ratios (b).

**Figure 9.** Carbon isotopic composition of methane vs. carbon isotopic composition of ethane and ethylene.

Sample	Date	T <sub>vent</sub>	CO <sub>2</sub>	HCl	HF	SO <sub>2</sub>	H <sub>2</sub> S	N <sub>2</sub>	Ar	O <sub>2</sub>	H <sub>2</sub>	He	CO	CH <sub>4</sub>	C <sub>2</sub> H <sub>6</sub>	C <sub>3</sub> H <sub>8</sub>	n-C <sub>4</sub> H <sub>10</sub>	ΣC <sub>4</sub>	C <sub>2</sub> H <sub>4</sub>	C <sub>3</sub> H <sub>6</sub>	Steam	
<i>Levante beach</i>																						
VI	may-15	87	971	bdl	bdl	bdl	11	15	0.063	0.015	2.9	0.019	0.00027	2.1	76.8	19.7	8.6	42.8	61.4	65.0	na	
VI	jun-16	na	968	bdl	bdl	bdl	11	16	0.058	0.011	4.2	0.013	0.00019	2.2	202.8	101.4	59.6	298.2	na	na	na	
VIC	oct-16	102	956	bdl	bdl	bdl	21	16	0.055	0.060	6.3	0.012	0.00025	2.1	200.5	118.0	59.0	235.9	80.2	118.0	na	
VIE	oct-16	100	966	bdl	bdl	bdl	13	13	0.051	0.015	8.1	0.015	0.00022	1.8	111.0	39.6	22.0	242.3	33.3	79.3	na	
VIE	may-17	100	956	bdl	bdl	bdl	15	24	0.071	0.095	4.6	0.012	0.000061	2.6	101.9	34.0	16.2	226.5	40.8	44.2	na	
VV	oct-16	100	956	bdl	bdl	bdl	16	18	0.084	0.011	9.5	0.025	0.00015	1.4	41.2	8.6	3.1	101.2	28.9	66.1	na	
VV	may-17	100	949	bdl	bdl	bdl	17	25	0.054	0.28	8.7	0.015	0.000052	1.5	48.1	12.3	4.4	88.1	28.9	50.6	na	
FM	may-17	103	959	bdl	bdl	bdl	13	21	0.059	0.19	6.9	0.018	0.000057	1.9	63.5	6.0	1.7	29.4	19.0	19.4	na	
FIM	jun-16	na	983	bdl	bdl	bdl	0.45	15	0.13	0.12	0.86	0.012	0.000088	1.1	266.4	43.0	10.7	43.0	2.7	8.6	na	
FIM	may-17	48	960	bdl	bdl	bdl	3.6	33	0.28	0.69	2.3	0.011	0.000022	1.4	583.1	97.2	24.3	170.1	11.7	19.4	na	
FOM	may-15	na	968	bdl	bdl	bdl	13	13	0.064	0.022	5.5	0.016	0.00023	1.8	1207.2	208.1	50.8	30.5	7.2	12.5	na	
FOM	jun-16	na	974	bdl	bdl	bdl	15	8.1	0.096	0.031	2.5	0.008	0.000056	0.85	602.4	103.9	26.0	46.7	6.0	7.3	na	
FOM	oct-16	87	970	bdl	bdl	bdl	11	15	0.041	0.015	3.6	0.033	0.00018	1.4	969.5	167.2	41.8	46.0	8.7	11.7	na	
FOM	may-17	76	949	bdl	bdl	bdl	22	22	0.11	0.87	5.5	0.021	0.000062	2.3	1960.8	350.1	87.5	87.5	15.7	21.0	na	
FUM	oct-16	27	977	bdl	bdl	bdl	3.3	19	0.058	0.013	0.87	0.018	0.00011	1.7	1117.0	189.3	47.3	52.1	4.5	5.7	na	
<i>La Fossa crater</i>																						
F202	may-17	202	891	2.9	0.046	56	28	21	0.0074	0.0009	0.86	0.0016	0.088	0.0036	10.4	bdl	bdl	bdl	7.3	bdl	bdl	89.2
F27	may-15	222	913	3.2	0.026	33	26	24	0.013	0.0067	0.85	0.0031	0.014	0.0021	8.8	0.7	bdl	bdl	1.8	1.4	86.9	88.3
F27	may-17	199	842	3.1	0.068	68	51	36	0.0091	0.0012	0.77	0.0022	0.077	0.0015	bdl	bdl	bdl	bdl	bdl	bdl	89	
FNA	may-15	387	895	1.2	0.017	49	38	16	0.025	0.0038	1.1	0.0025	0.0095	0.0045	9.3	bdl	bdl	bdl	10.2	bdl	bdl	89
FNA	jun-16	na	880	2.1	0.085	58	41	18	0.0087	0.0007	0.41	0.0034	0.022	0.0011	8.3	bdl	bdl	bdl	20.7	bdl	bdl	86.4
FNA	may-17	340	902	2.2	0.036	44	33	18	0.0077	0.0011	0.58	0.0021	0.071	0.0021	12.3	bdl	bdl	bdl	bdl	bdl	bdl	87.9
FNB	oct-16	220	925	1.3	0.015	26	25	22	0.0078	0.0024	0.11	0.0026	0.061	0.0021	16.3	bdl	bdl	bdl	143.3	bdl	bdl	87.5
FNB	may-17	325	901	2.5	0.042	51	26	19	0.0061	0.0008	0.41	0.0029	0.075	0.0033	bdl	bdl	bdl	bdl	bdl	bdl	90.5	
F5	oct-16	362	887	2.8	0.036	56	31	23	0.0093	0.0057	1	0.0044	0.034	0.0055	9.3	bdl	bdl	bdl	15.7	bdl	bdl	89.2
F5	may-17	351	923	2.9	0.051	36	22	16	0.0069	0.0013	0.29	0.0015	0.078	0.0049	bdl	bdl	bdl	bdl	bdl	bdl	87.5	
F11	jun-16	na	826	2.9	0.034	98	59	14	0.0099	0.0010	0.57	0.0082	0.013	0.00073	7.4	bdl	bdl	bdl	34.0	bdl	bdl	89.3
F11	may-17	299	878	3.6	0.087	61	34	22	0.0086	0.0011	0.77	0.0013	0.069	0.0013	bdl	bdl	bdl	bdl	bdl	bdl	88.8	
FZIO	jun-16	99	942	1.9	0.023	13	13	29	0.0078	0.0011	0.61	0.0029	0.011	0.0016	19.3	bdl	bdl	bdl	32.8	bdl	bdl	90.9
FZIO	oct-16	99	944	1.6	0.022	11	12	31	0.0065	0.0041	0.21	0.0018	0.055	0.0017	17.9	bdl	bdl	bdl	39.4	bdl	bdl	91.2
FZIO	may-17	99	948	1.8	0.021	16	11	23	0.0088	0.0019	0.24	0.0027	0.058	0.0019	20.9	bdl	bdl	bdl	23.0	bdl	bdl	90.5

Table 1.

Sample	Date	$\delta^{13}\text{C} \text{‰ V-PDB}$								$\delta\text{D} \text{‰ V-SMOW}$		
		$\text{CO}_2$	$\text{CH}_4$	$\text{C}_2\text{H}_6$	$\text{C}_3\text{H}_8$	n- $\text{C}_4\text{H}_{10}$	$\Sigma\text{C}_4$	$\text{C}_2\text{H}_4$	$\text{C}_3\text{H}_6$	$\text{CH}_4$	$\text{H}_2$	$\text{H}_2\text{O}$
<b><i>Levante beach</i></b>												
VI	may-15	na	-5.5	-20.8	-26.4	-26.0	-27.0	-32.8	-28.2	-78	na	na
VI	jun-16	-2.90	-5.2	-21.9	-26.2	-26.6	-28.2	-33.0	-30.4	-82	na	na
VIC	oct-16	-3.10	-5.4	-24.0	-24.7	-25.5	-25.9	-32.1	-25.6	-84	-584	na
VIE	oct-16	-3.60	-5.2	-19.7	-23.5	-18.8	-23.9	-25.2	-27.0	-84	-565	-7
VIE	may -17	-3.70	-4.7	-20.2	-21.3	-24.7	-21.8	-28.6	-22.5	-82	-558	-11
VV	oct-16	-3.60	-4.8	-17.1	-25.4	-24.5	-24.7	-30.1	-29.5	-85	-578	-11
VV	may -17	-4.40	-5.4	-20.0	-20.9	-23.2	-22.7	-30.0	-21.7	-83	-574	-18
FM	may -17	-3.60	-6.2	-14.3	-21.9	-23.9	-22.3	-28.4	-25.1	-83	-540	na
FIM	jun-16	-3.30	-6.0	-23.5	-21.0	-20.5	-24.1	-32.5	-25.7	-91	na	na
FIM	may -17	-3.50	-8.0	-21.1	-18.3	-18.4	-23.4	-30.2	-24.0	-90	bdl	na
FOM	may-15	na	-10.4	-21.0	-20.1	-20.4	-24.2	-28.2	-25.4	-98	na	na
FOM	jun-16	-2.50	-9.0	-20.0	-18.1	-18.6	-23.4	-26.7	-23.5	-99	na	na
FOM	oct-16	-3.20	-9.4	-20.3	-18.1	-18.4	-22.5	-26.2	-24.0	-99	bdl	na
FOM	may -17	-3.50	-10.1	-20.3	-17.4	-18.1	-21.7	-28.1	-22.9	-102	-610	na
FUM	oct-16	-3.10	-9.8	-20.5	-18.0	-18.0	-21.9	-26.9	-20.6	-97	bdl	na
<b><i>La Fossa crater</i></b>												
F202	may -17	-0.5	-27.2	-28.3	bdl	bdl	bdl	bdl	bdl	-646	-627	8
F27	may-15	na	-27.7	-28.5	-31.1	bdl	bdl	-31.4	-31.7	na	na	na
F27	may -17	-0.5	-9.4	bdl	bdl	bdl	bdl	bdl	bdl	-116	bdl	1
FNA	may-15	-0.9	-28	-27.4	bdl	bdl	bdl	-28.6	bdl	na	na	na
FNA	jun-16	-0.8	-19.6	-20.8	bdl	bdl	bdl	-26.1	bdl	-394	na	na
FNA	may -17	-0.4	-26.1	-21.1	bdl	bdl	bdl	bdl	bdl	-586	na	4
FNB	oct-16	-0.8	-11.5	-13.6	bdl	bdl	bdl	-24.4	bdl	-214	-553	1
FNB	may -17	-0.3	-21.7	bdl	bdl	bdl	bdl	bdl	bdl	-257	-592	12
F5	oct-16	-1.1	-29	-27.3	bdl	bdl	bdl	-26.7	bdl	-657	-525	-1
F5	may -17	-0.7	-29.7	bdl	bdl	bdl	bdl	bdl	bdl	na	na	6
F11	jun-16	-1.1	-11.2	-13	bdl	bdl	bdl	-16.6	bdl	-143	na	na
F11	may -17	-0.9	-23.2	bdl	bdl	bdl	bdl	bdl	bdl	na	-638	2
FZIO	jun-16	-1.2	-23.6	-22.5	bdl	bdl	bdl	-26	bdl	na	na	na
FZIO	oct-16	-1.1	-12.9	-15.1	bdl	bdl	bdl	-24.2	bdl	-147	bdl	-27
FZIO	may -17	-0.9	-21.4	bdl	bdl	bdl	bdl	bdl	bdl	-185	bdl	-38

**Table 2.**

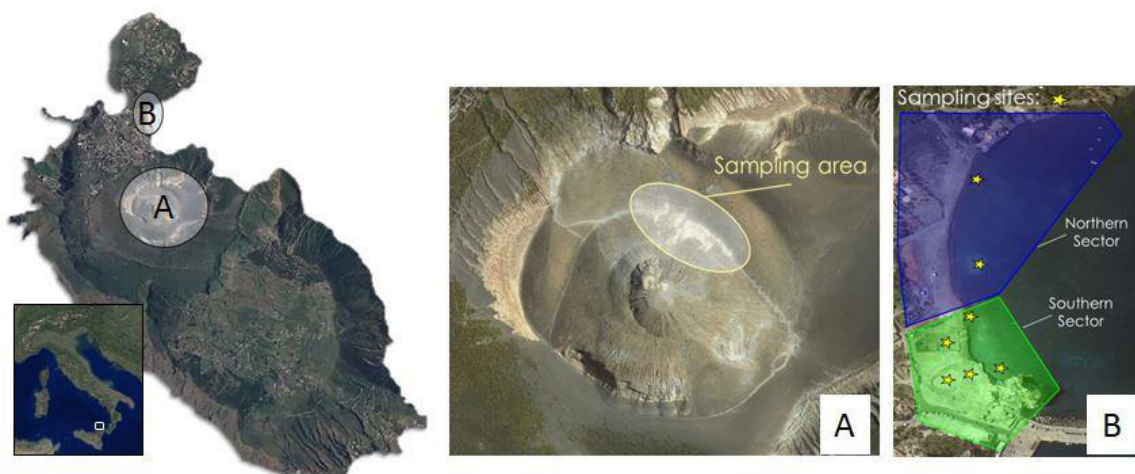


**Fig.1.**

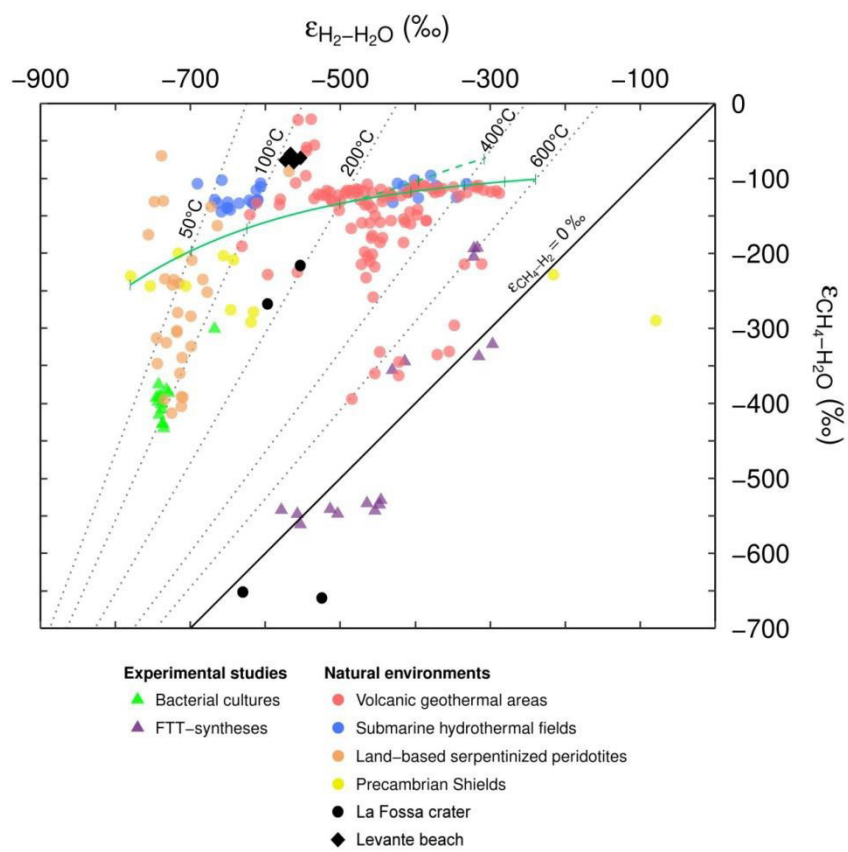


**Fig.2.**

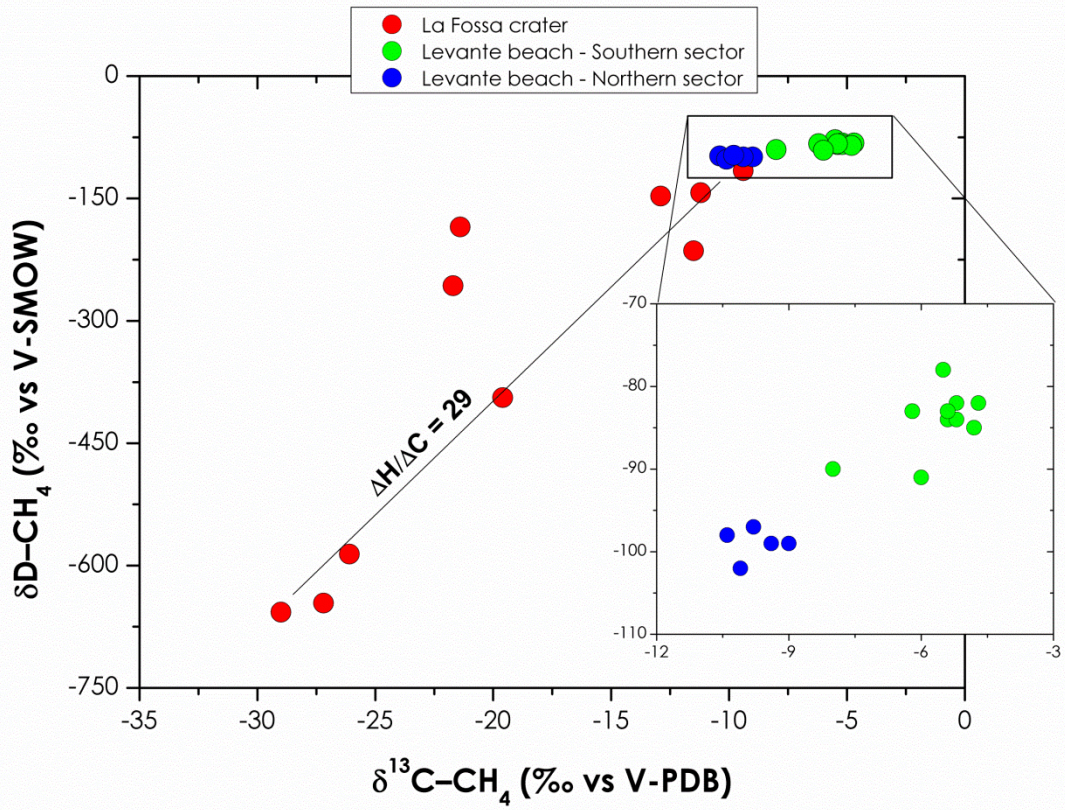


Fig.3.

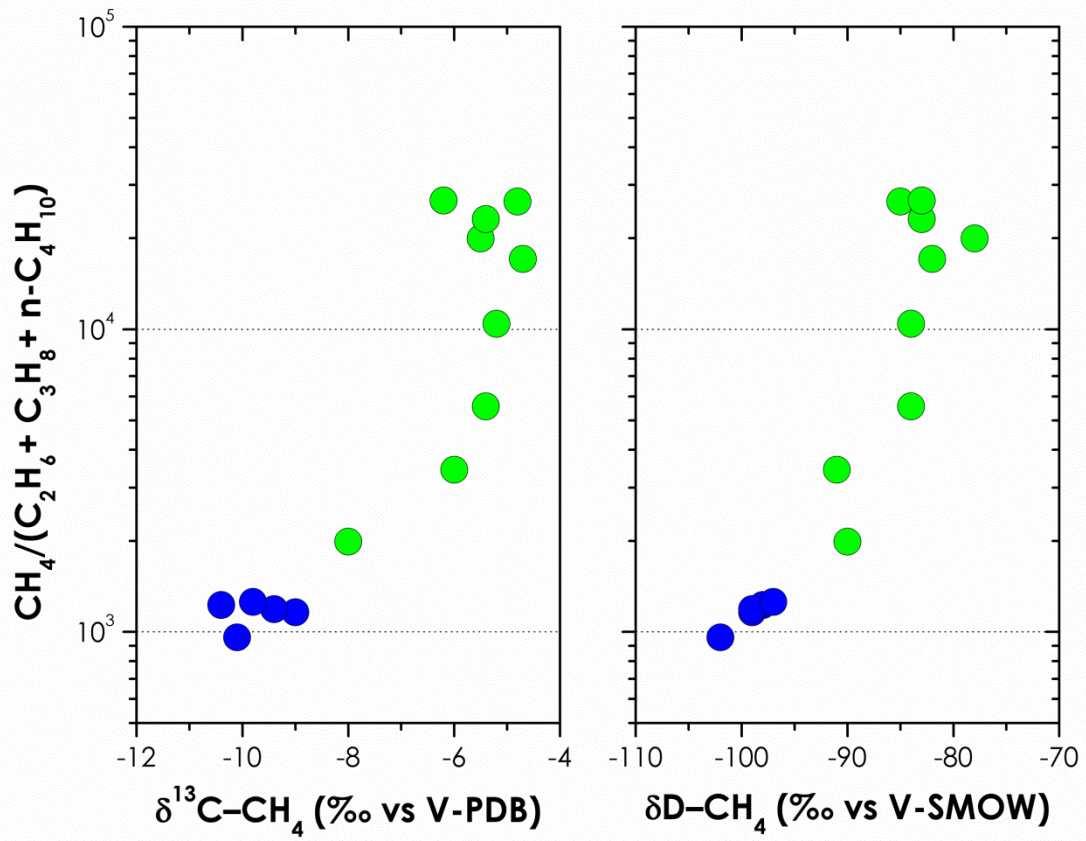
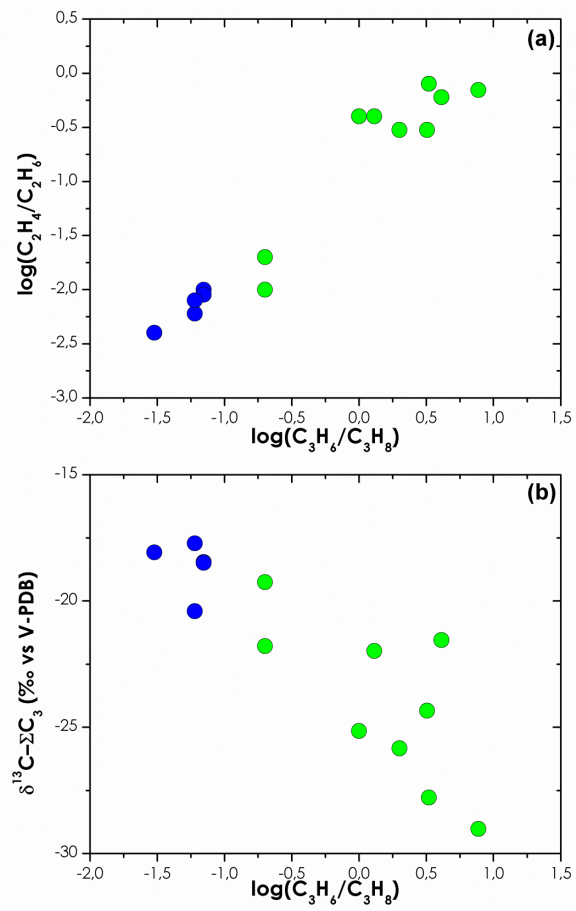


Fig.4.



**Fig.5.**

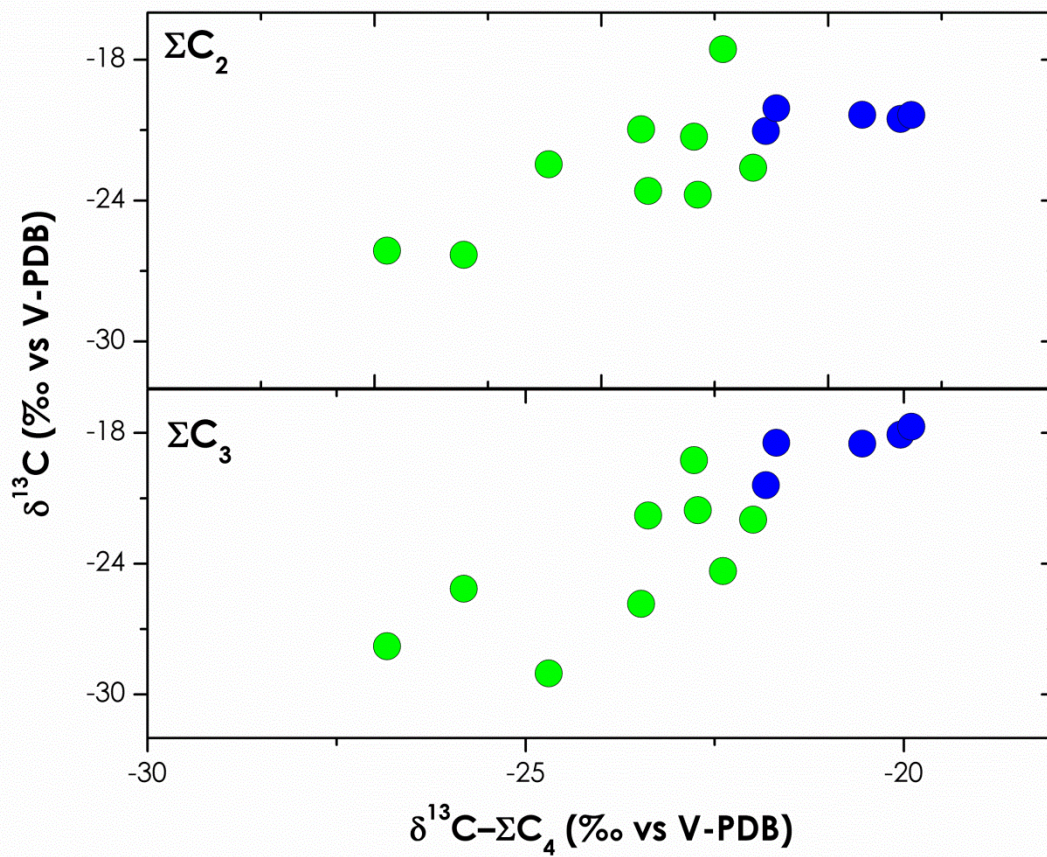


Fig.6.

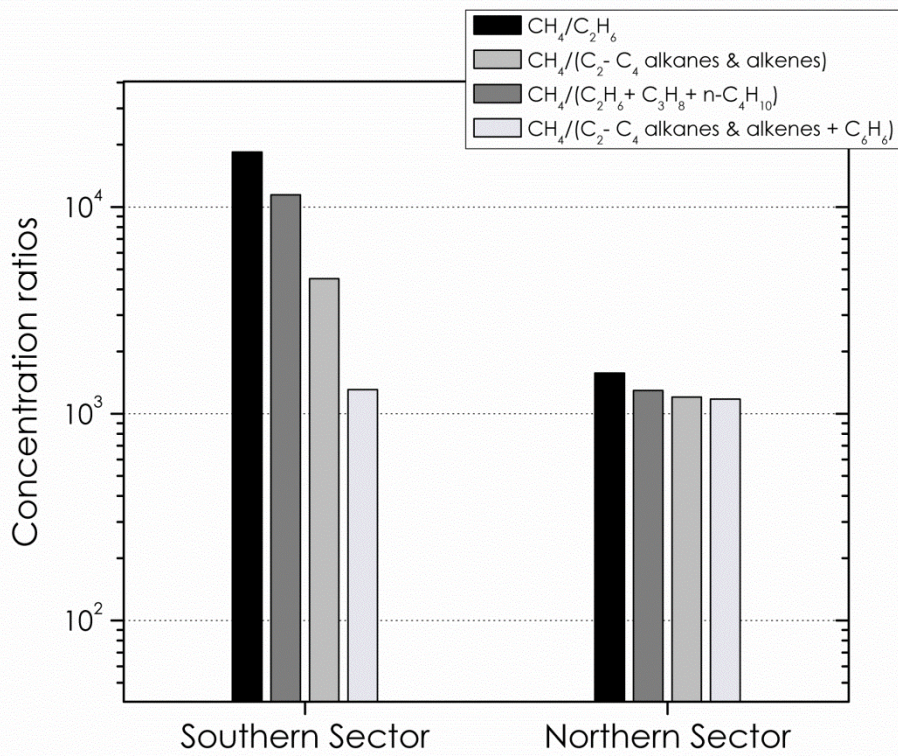


Fig.7.

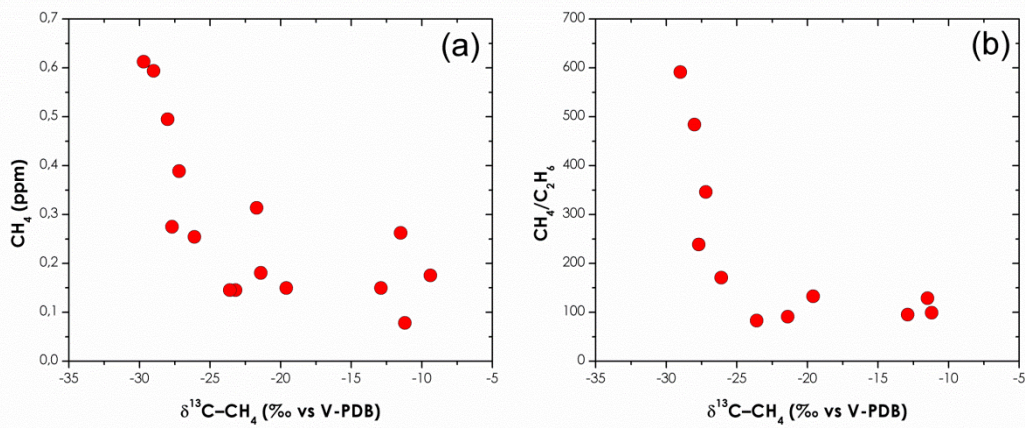


Fig.8.

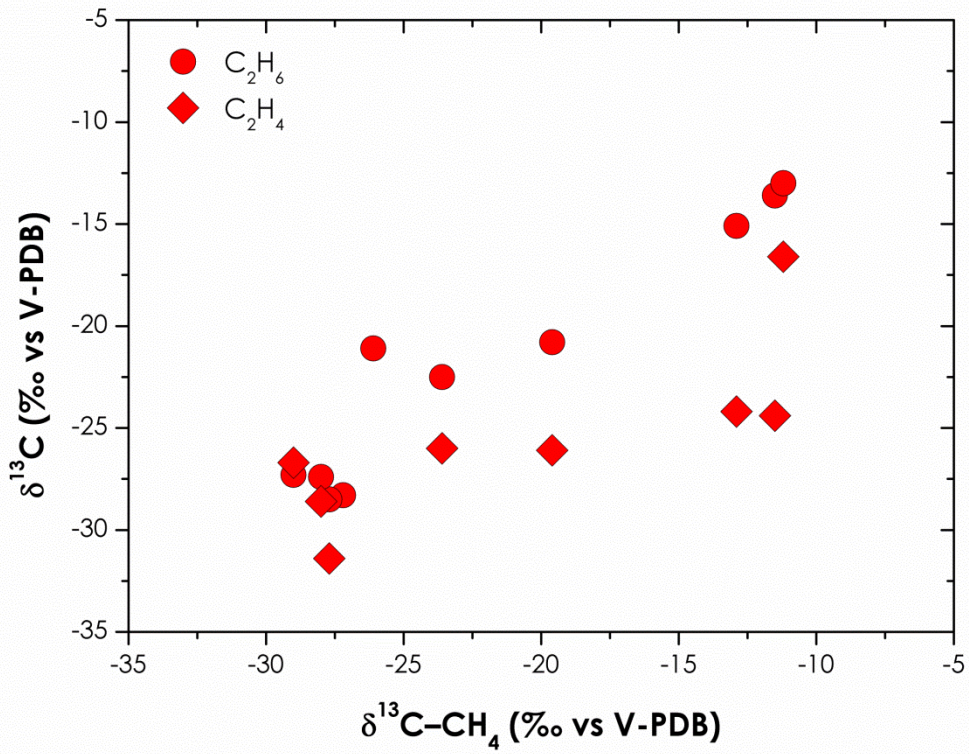


Fig.9.



## Fractionation processes affecting the stable carbon isotope signature of thermal waters from hydrothermal/volcanic systems: The examples of Campi Flegrei and Vulcano Island (southern Italy)



Stefania Venturi<sup>a,b,\*</sup>, Franco Tassi<sup>a,b</sup>, Gabriele Bicchocchi<sup>a</sup>, Jacopo Cabassi<sup>a,b</sup>, Francesco Capecciacci<sup>a,b</sup>, Giorgio Capasso<sup>c</sup>, Orlando Vaselli<sup>a,b</sup>, Andrea Ricci<sup>d</sup>, Fausto Grassa<sup>c</sup>

<sup>a</sup> Dipartimento di Scienze della Terra, Università di Firenze, Via G. La Pira 4, 50121 Firenze, Italy

<sup>b</sup> Istituto di Geoscienze e Georisorse (IGG), Consiglio Nazionale delle Ricerche (CNR), Via G. La Pira 4, 50121 Firenze, Italy

<sup>c</sup> Istituto Nazionale di Geofisica e Vulcanologia (INGV), Sezione Palermo, Via Ugo La Malfa 153, 90146 Palermo, Italy

<sup>d</sup> Dipartimento di Scienze Biologiche, Geologiche ed Ambientali, Università di Bologna, Porta S. Donato 1, 40127 Bologna, Italy

### ARTICLE INFO

#### Article history:

Received 10 April 2017

Received in revised form 2 August 2017

Accepted 2 August 2017

Available online 4 August 2017

#### Keywords:

Thermal waters

Carbon isotopes

Dissolved CO<sub>2</sub>

TDIC

Volcanic-hydrothermal systems

Secondary fractionation processes

### ABSTRACT

The carbon isotopic composition of dissolved C-bearing species is a powerful tool to discriminate the origin of carbon in thermal waters from volcanic and hydrothermal systems. However, the  $\delta^{13}\text{C}$  values of dissolved CO<sub>2</sub> and TDIC (Total Dissolved Inorganic Carbon) are often different with respect to the isotopic signature that characterizes the potential carbon primary sources, i.e. deep hydrothermal reservoirs, magmatic gases and organic activity. The most commonly invoked explanation for such isotopic values is related to mixing processes between deep and shallow end-members. Nevertheless, experimental and empirical investigations demonstrated that isotopic fractionation due to secondary processes acting on the uprising fluids from the hydrothermal reservoirs is able to reproduce the measured isotopic values. In this paper, we investigated the chemistry of thermal waters, collected at Campi Flegrei and Vulcano Island (southern Italy), whose origin is related to interaction processes among magmatic gases, meteoric water, seawater and hosting rocks. A special focus was dedicated to the  $\delta^{13}\text{C}$  values of dissolved CO<sub>2</sub> ( $\delta^{13}\text{C}_{\text{CO}_2(\text{aq})}$ ) and total dissolved inorganic carbon ( $\delta^{13}\text{C}_{\text{TDIC}}$ ). The  $\delta^{13}\text{C}_{\text{CO}_2(\text{aq})}$  and  $\delta^{13}\text{C}_{\text{TDIC}}$  values in the water samples from both these systems ranged from (i) those measured in fumarolic gases, likely directly related to the deep hydrothermal-magmatic reservoir, and (ii) those typically characterizing biogenic CO<sub>2</sub>, i.e. produced by microbially-driven degradation of organic matter. A simple mixing model of the two end-members, apparently explaining these intermediate carbon isotopic values, contrasts with the chemical composition of the dissolved gases. On the contrary, isotopic fractionation due to secondary processes, such as calcite precipitation, affecting hydrothermal fluids during their underground circulation, seems to exhaustively justify both the chemical and isotopic data. If not recognized, these processes, which frequently occur in volcanic and hydrothermal systems, may lead to an erroneous interpretation of the carbon source, causing an underestimation of the contribution of the hydrothermal/magmatic fluids to the dissolved carbon species. These results pose extreme caution in the interpretation of intermediate  $\delta^{13}\text{C}_{\text{CO}_2(\text{aq})}$  and  $\delta^{13}\text{C}_{\text{TDIC}}$  values for the assessment of the carbon budget of hydrothermal-volcanic systems.

© 2017 Elsevier B.V. All rights reserved.

### 1. Introduction

Fluids from volcanic and hydrothermal systems significantly contribute to the global carbon cycle, since they discharge huge amounts

\* Corresponding author at: Dipartimento di Scienze della Terra, Via G. La Pira 4, 50121 Firenze, Italy.

E-mail addresses: [stefania.venturi@unifi.it](mailto:stefania.venturi@unifi.it) (S. Venturi), [franco.tassi@unifi.it](mailto:franco.tassi@unifi.it) (F. Tassi), [gabriele.bicchocchi@unifi.it](mailto:gabriele.bicchocchi@unifi.it) (G. Bicchocchi), [jacopo.cabassi@igg.cnr.it](mailto:jacopo.cabassi@igg.cnr.it) (J. Cabassi), [francesco.capecciacci@unifi.it](mailto:francesco.capecciacci@unifi.it) (F. Capecciacci), [giorgio.capasso@ingv.it](mailto:giorgio.capasso@ingv.it) (G. Capasso), [orlando.vaselli@unifi.it](mailto:orlando.vaselli@unifi.it) (O. Vaselli), [andrea.ricci34@unibo.it](mailto:andrea.ricci34@unibo.it) (A. Ricci), [fausto.grassa@ingv.it](mailto:fausto.grassa@ingv.it) (F. Grassa).

<http://dx.doi.org/10.1016/j.jvolgeores.2017.08.001>  
0377-0273/© 2017 Elsevier B.V. All rights reserved.

of CO<sub>2</sub> to the atmosphere through active vents (open conduit craters and fumaroles) and diffuse soil degassing (e.g. Chiodini et al., 1998; Aiuppa et al., 2013; Burton et al., 2013; Conde et al., 2014). A significant portion of volcanic/hydrothermal CO<sub>2</sub> dissolves into subsurface waters as HCO<sub>3</sub><sup>-</sup> and CO<sub>3</sub><sup>2-</sup>, as a function of pH, and is discharged from springs and/or shallow wells (e.g. D'Alessandro et al., 1997; Inguaggiato et al., 2005; Chiodini et al., 2015a). The isotopic signature ( $\delta^{13}\text{C}$ ) of dissolved CO<sub>2</sub> and total dissolved inorganic carbon (TDIC) are useful tools to discriminate the different sources of carbon in thermal waters, when a gas-free phase does not occur (e.g. Chiodini et al., 2000, 2004). Distinct  $\delta^{13}\text{C}_{\text{CO}_2(\text{aq})}$  and  $\delta^{13}\text{C}_{\text{TDIC}}$  values can indeed be recognized in C-bearing

dissolved species that derive from CO<sub>2</sub> generated by different processes, such as: 1) mantle/magmatic degassing, producing CO<sub>2</sub> typically showing  $\delta^{13}\text{C}$  values around  $-6\text{‰}$  vs. V-PDB (Rollinson, 1993; Sano and Marty, 1995; Hoefs, 2009), i.e. similar to the isotopic value of atmospheric CO<sub>2</sub> (ca.  $-8\text{‰}$  vs. V-PDB; Scripps CO<sub>2</sub> Program); 2) degradation of organic matter, characterized by CO<sub>2</sub> with  $\delta^{13}\text{C} < -20\text{‰}$  vs. V-PDB (Degens, 1969; Rollinson, 1993; Sano and Marty, 1995); 3) thermometamorphic reactions on carbonate rocks, producing isotopically heavy CO<sub>2</sub> ( $\delta^{13}\text{C} = 0 \pm 5\text{‰}$  vs. V-PDB; Sano and Marty, 1995; Clark, 2015). Despite the isotopic fractionation of CO<sub>2</sub> to form CO<sub>2(aq)</sub> and (bi)carbonates species (e.g. Bottinga, 1968; Deines et al., 1974; Mook et al., 1974), this widely accepted classification is not consistent with the isotopic signature of a number of thermal waters from volcanic and hydrothermal areas, which show  $\delta^{13}\text{C}_{\text{CO}_2(\text{aq})}$  values ranging from  $-18\text{‰}$  to  $-9\text{‰}$  vs. V-PDB (e.g. D'Alessandro et al., 1997; Caliro et al., 1999; Federico et al., 2002; Taran et al., 2002; Inguaggiato et al., 2005; Grassa et al., 2006; Yamada et al., 2011; Ruzié et al., 2013; Marrero-Diaz et al., 2015; Morikawa et al., 2016). In most cases, these isotopic values, which are intermediate with respect to those related to mantle/magmatic and biogenic CO<sub>2</sub>, were interpreted as due to mixing processes between deep and shallow/marginal end-members (e.g. Italiano et al., 2009; Fourré et al., 2011; Ruzié et al., 2013). However, other studies demonstrated the strong influence of isotopic fractionation on the  $\delta^{13}\text{C}_{\text{CO}_2(\text{aq})}$  and  $\delta^{13}\text{C}_{\text{TDIC}}$  values, which were related to multi-step CO<sub>2</sub> dissolution (e.g. Weinlich, 2005; Gilfillan et al., 2009; Güleç and Hilton, 2016) and carbonate precipitation/dissolution (e.g. Ohwada et al., 2007; Gilfillan et al., 2009; Barry et al., 2014; Güleç and Hilton, 2016). These secondary chemical processes are considered to commonly affect thermal fluids from volcanic and hydrothermal areas (Simmons and Christenson, 1994 and references therein). Hence, they may represent a valuable alternative explanation for  $\delta^{13}\text{C}_{\text{CO}_2(\text{aq})}$  and  $\delta^{13}\text{C}_{\text{TDIC}}$  values not consistent with the primary CO<sub>2</sub> sources.

In the present study, we report a complete dataset, consisting of major ion chemistry, chemical composition of dissolved gases and carbon isotopes ( $\delta^{13}\text{C}_{\text{CO}_2(\text{aq})}$  and  $\delta^{13}\text{C}_{\text{TDIC}}$ ), measured in thermal waters from two volcanic systems in Italy: Campi Flegrei (Naples, southern Italy) and Vulcano Island (Aeolian Archipelago, southern Italy) (e.g. Boschetti et al., 2003 and references therein; Valentino and Stanzione, 2003 and references therein). The main aim is to investigate the mechanisms controlling the  $\delta^{13}\text{C}_{\text{CO}_2(\text{aq})}$  and  $\delta^{13}\text{C}_{\text{TDIC}}$  values in these fluids, in order to provide insights into the role played by the secondary chemical processes that may affect the estimation of hydrothermal/magmatic CO<sub>2</sub> contribution to the global carbon budget.

## 2. Geological features and hydrothermal/magmatic systems of the study areas

### 2.1. Campi Flegrei

The Campi Flegrei caldera (Fig. 1a) is an active volcanic complex occupying  $\sim 100 \text{ km}^2$  of the Campanian Plain, NW of Naples (southern Italy). The caldera structure formed during two large eruptions, which produced (i) the Campanian Ignimbrite (39 ka; De Vivo et al., 2001) and (ii) the Neapolitan Yellow Tuff (14.9 ka; Deino et al., 2004). The volcanic system developed within the Campanian graben, where volcanic deposits (K-basalts, trachybasalts, latites, trachytes, alkali-trachytes and phonolites), marine and continental sediments overlie the Mesozoic carbonate basement located at 4 km depth. The last historical eruptive event occurred in 1538 CE (Di Vito et al., 1987), which originated the monogenic tuff cone of Monte Nuovo (Fig. 1a), after about 3000 years of quiescence.

The hydrothermal system of the Campi Flegrei caldera, which is related to fluids released from a magma chamber located at about 5 km below the town of Pozzuoli (e.g. Gottsmann et al., 2006), is responsible for frequent episodes of ground uplift and subsidence (*bradyseism*)

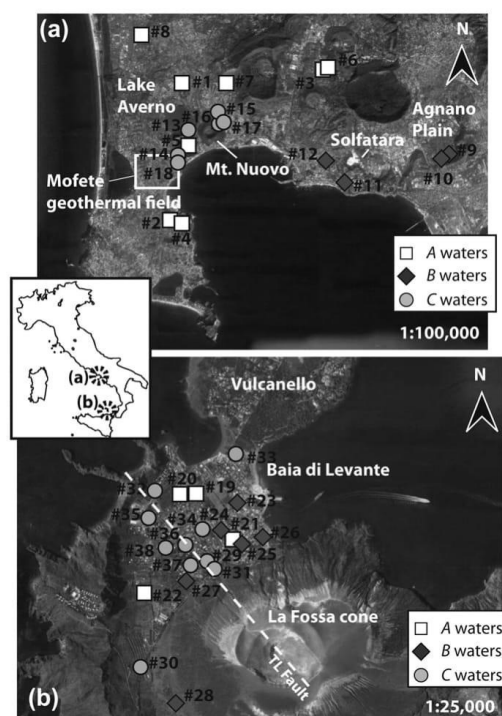


Fig. 1. Satellite photos of (a) Campi Flegrei caldera and (b) Vulcano Island. The sampling sites of thermal waters are reported. Symbols are according to the three groups of waters distinguished on the basis of the dissolved CO<sub>2</sub> isotopic composition, as follows: group A = white squares; group B = dark grey diamonds; group C = light grey circles (see the text for details). The Tindari-Letojanni (LT) Fault is shown in Fig. 1b (white dashed line).

accompanied by seismic activity (e.g. Bonafede and Mazzanti, 1998; Chiodini et al., 2003, 2012, 2015b; Gottsmann et al., 2006).

Two distinct hydrothermal reservoirs, located within the volcanic cover, were recognized in the area: (i) a seawater-contaminated shallow reservoir (depth  $< 2 \text{ km}$ ) diluted by meteoric waters, and (ii) a deep hydrothermal reservoir ( $> 2 \text{ km}$ ) of hypersaline waters (Caprarello et al., 1997; Valentino and Stanzione, 2003). The surficial expression of the hydrothermal activity within the caldera mostly consists of submarine and inland fumarolic vents, anomalous diffuse soil degassing (e.g. Chiodini et al., 2001; Todesco et al., 2003; Caliro et al., 2007; Vaselli et al., 2011; Passaro et al., 2016), and thermal water discharges and wells (e.g. Valentino and Stanzione, 2003, 2004).

### 2.2. Vulcano Island

Vulcano Island is the southernmost island of the Aeolian Archipelago (southern Italy), a subduction-related volcanic arc in the Southern Tyrrhenian Sea (Fig. 1b). It consists of a main edifice, mostly developed during the Pleistocene and Holocene through several stages of stratocone building and caldera collapse (Keller, 1980; De Astis et al., 1997), and a smaller island (Vulcanello), made of lavas and pyroclastic cones formed by nearly continuous activity between 1000 and 1250 CE (Arrighi et al., 2006). The last eruptive event occurred in 1888–1890 (Clocchiatti et al., 1994) from La Fossa, a 391 m high cone (Fig. 1b) having a base diameter of 1 km. La Fossa summit crater is

currently characterized by intense fumarolic activity, mostly occurring in its NW sector. The fumaroles are characterized by outlet temperatures up to 450 °C and a typical magmatic composition, with a dry gas fraction dominated by CO<sub>2</sub> and relatively high concentrations of HCl, SO<sub>2</sub>, H<sub>2</sub>S and HF (e.g. Capasso et al., 1997, 1999; Inguaggiato et al., 2012). Subaerial and submerged fumaroles, with outlet temperatures <100 °C, occur at Baia di Levante, the bay delimiting the eastern side of a flat isthmus that connects Vulcano to Vulcanello (Fig. 1b). These fluid discharges, which show relatively high CH<sub>4</sub> and H<sub>2</sub>S contents and the virtual absence of high-temperature magmatic gases (SO<sub>2</sub>, HCl and HF), are fed by a shallow hydrothermal source heated by the uprising hot magmatic fluids (Capaccioni et al., 2001). According to the geochemical measurements carried out on fluids from a geothermal well drilled in the 1950s near the Baia di Levante beach (Sommaruga, 1984), the hydrothermal system consists of multilevel water bodies, as follows: (i) a shallow aquifer (at 7–14 m depth) at ~100 °C, (ii) an intermediate aquifer (at 90–95 m depth) having a temperature of ~136 °C, and (iii) a deep aquifer (at 185–236 m depth) at ~200 °C, the latter showing a seawater-like chemical composition. Strong soil degassing affects both the surroundings of the volcanic edifice and some portions of the Vulcano Porto plain located NW of La Fossa cone (Carapezza et al., 2011; Inguaggiato et al., 2012), where several domestic thermal wells were drilled.

### 3. Materials and methods

#### 3.1. Water and dissolved gas sampling

Water and dissolved gas samples were collected during three field campaigns in 2013 and 2015 from (i) 17 wells and the bottom of Lake Averno (33 m depth) in the Campi Flegrei caldera (Fig. 1a), and (ii) 20 wells located within the area of Vulcano Porto village at Vulcano Island (Fig. 1b).

Three water aliquots were collected at each sampling site, as follows: (1) one aliquot in a 125 mL polyethylene bottle, for the determination of main anions, (2) one filtered (0.45 μm) aliquot in a 50 mL polyethylene bottle containing 0.5 mL of 30% Suprapur HCl, for the analysis of main cations, and (3) a third aliquot, sampled in evacuated glass vials containing 2 mL of anhydrous phosphoric acid, for isotope analyses of total dissolved inorganic carbon ( $\delta^{13}\text{C}_{\text{TDIC}}$ ; Salata et al., 2000). Temperature (°C) and pH were measured in the field.

The sample from the bottom of Lake Averno, a volcanic crater lake located a few hundred meters NW of the Monte Nuovo cone (Fig. 1a), was collected using a sampling equipment consisting of a Rilsan® tube (6 mm in diameter), lowered to the sampling depth, and an 150 mL syringe equipped with a three-way valve to pump the water up to the surface. The water sample was collected after the displacement of a water volume double that of the inner volume of the tube (Cabassi et al., 2013 and references therein).

The dissolved gas samples were collected into pre-evacuated 250 mL glass flasks, equipped with a Teflon stopcock, that were submerged into the water or connected to the Rilsan® tubes. The stopcock was opened to fill the vial of water up to about three quarters of its inner volume (Tassi et al., 2008, 2009).

#### 3.2. Chemical and isotopic ( $\delta^{13}\text{C}_{\text{TDIC}}$ ) analysis of waters

The main ionic species were analyzed by ion chromatography (IC), using an 861 Advanced Compact IC-Metrohm for cations (Na, NH<sub>4</sub>, K, Mg, Ca) and a 761 Compact IC-Metrohm for anions (F, Cl, Br, NO<sub>3</sub>, SO<sub>4</sub>). The HCO<sub>3</sub> concentrations were determined by acidimetric titration (AT) with 0.01 N HCl using a Basic Titrimo 794-Metrohm autotitrator. The analytical errors for IC and AT were <5%.

The analysis of  $\delta^{13}\text{C}_{\text{TDIC}}$  (expressed in ‰ vs. V-PDB) was carried out with a Finnigan Delta Plus XL mass spectrometer on the CO<sub>2</sub> recovered after the reaction of 3 mL of water sample with 2 mL of anhydrous

phosphoric acid in vacuo (Salata et al., 2000). The recovered CO<sub>2</sub> was analyzed after a two-step extraction and purification procedure on the gas mixture by using a N<sub>2</sub> and trichloroethylene solid-liquid mixture (e.g. Vaselli et al., 2006). The analytical error and the reproducibility for  $\delta^{13}\text{C}_{\text{TDIC}}$  analysis were ±0.05‰ and ±0.1‰, respectively.

#### 3.3. Chemical and isotopic ( $\delta^{13}\text{C}_{\text{CO}_2(\text{aq})}$ ) analysis of dissolved gases

Inorganic gases (CO<sub>2</sub>, N<sub>2</sub>, O<sub>2</sub>, Ar and H<sub>2</sub>) stored in the headspace of the sampling flasks were analyzed using a Shimadzu 15A and a Thermo Focus gas chromatographs equipped with Thermal Conductivity Detectors (TCD). Methane was analyzed using a Shimadzu 14A gas chromatograph equipped with a Flame Ionization Detector (FID). The chemical composition of the dissolved gas compounds was computed by considering the measured concentrations of gases stored in the headspace on the basis of: (i) headspace gas pressure and volume, (ii) volume of water in the flask and (iii) solubility coefficients of each gas compound (Whitfield, 1978).

The isotopic composition of dissolved CO<sub>2</sub> ( $\delta^{13}\text{C}_{\text{CO}_2(\text{aq})}$ , expressed in ‰ vs. V-PDB) was determined on the basis of the <sup>13</sup>C/<sup>12</sup>C ratio measured in CO<sub>2</sub> from the sampling flask headspace ( $\delta^{13}\text{C}_{\text{CO}_2\text{strip}}$ ). The  $\delta^{13}\text{C}_{\text{CO}_2\text{strip}}$  was analyzed by using a Finnigan Delta Plus XL mass spectrometer after a two-step extraction and purification procedure, as described for the determination of the  $\delta^{13}\text{C}_{\text{TDIC}}$  values. Both internal (Carrara and San Vincenzo marbles) and international (NBS18 and NBS19) standards were used in order to estimate the external precision. The analytical error and the reproducibility were ±0.05‰ and ±0.1‰, respectively. The  $\delta^{13}\text{C}_{\text{CO}_2(\text{aq})}$  values were calculated from the measured  $\delta^{13}\text{C}_{\text{CO}_2\text{strip}}$  on the basis of the enrichment factor ( $\epsilon_1$ ) for gas-water isotope equilibrium proposed by Zhang et al. (1995):

$$\epsilon_1 = \delta^{13}\text{C}_{\text{CO}_2(\text{aq})} - \delta^{13}\text{C}_{\text{CO}_2\text{strip}} = (0.0049 \times t) - 1.31 \quad (1)$$

where  $t$  (°C) is the temperature.

## 4. Results

### 4.1. Campi Flegrei

#### 4.1.1. Water geochemistry

The waters collected from the Campi Flegrei caldera showed heterogeneous physicochemical features (Table 1), with temperatures from 10 (#1) to 77 °C (#18), pH values from 6.20 (#10) to 8.27 (#13), TDS values from 722 (#8) to 19,066 mg/L (#18), and distinct geochemical facies, including Ca-HCO<sub>3</sub>, Na-HCO<sub>3</sub>, Na-Cl and Ca-Cl compositions (Fig. 2a).

The Ca-HCO<sub>3</sub> (#3 and #6) and Ca-Cl waters (#2) were characterized by low temperature ( $\leq 23$  °C) and TDS values (<1000 mg/L), whereas the Na-HCO<sub>3</sub> waters (#1, #4, #5, #7, #8, #9, and #12; Fig. 2a) displayed wide range of temperatures (from 10 to 63 °C) and TDS (from 795 to 4330 mg/L).

The Na-Cl waters (#10, #11, #13, #14, #15, #16, #17, and #18; Fig. 2a) had relatively high temperatures ( $\geq 25$  °C), with the exception of #13 (12 °C), and TDS values (>1000 mg/L) (Table 1).

#### 4.1.2. Chemical composition of dissolved gases

Atmospheric gases (PN<sub>2</sub>: from 215 to 1231 mbar; PO<sub>2</sub>: from b.d.l. to 139 mbar; PAr: from 2.6 to 14 mbar), and carbon dioxide (PCO<sub>2</sub> varying from 0.8 to 54 mbar) dominate the chemical composition of the dissolved gases (Table 2; Fig. 3a). Methane and H<sub>2</sub> were relatively low (up to 0.12 and 0.14 mbar, respectively) with the exception of #13 (i.e. the sample from the bottom of Lake Averno) that was CH<sub>4</sub>-rich (936 mbar) and characterized by the highest PH<sub>2</sub> value (9.8 mbar) among the whole Campi Flegrei water suite. Setting aside #4, all the waters with relatively high TDS values (>2000 mg/L) were enriched in PCO<sub>2</sub> (from 4.7 to 54 mbar) (Table 2).

**Table 1**  
Chemical composition of the main solutes (anions and cations, in mg/L), temperature (°C), pH and salinity (expressed as TDS, in mg/L) of water samples collected from Campi Flegrei and Vulcano Island.

Study area	E (UTM)	N (UTM)	ID	Name	Group	T	pH	TDS	HCO <sub>3</sub> <sup>-</sup>	F <sup>-</sup>	Cl <sup>-</sup>	Br <sup>-</sup>	NO <sub>3</sub> <sup>-</sup>	SO <sub>4</sub> <sup>2-</sup>	Ca <sup>2+</sup>	Mg <sup>2+</sup>	Na <sup>+</sup>	K <sup>+</sup>	NH <sub>4</sub> <sup>+</sup>	Li <sup>+</sup>	
Campi Flegrei	422236	4522378	1	Vivai e Pianta	A	10	7.99	795	253	11.52	104	0.22	59	107	20	1.8	210	27	0.27	0.41	
	421823	4518191	2	Agriturismo di Baia	A	11	7.12	997	195	0.97	180	0.53	120	191	119	22	122	45	0.31	0.15	
	426565	4522770	3	Catone	A	19	7.30	851	337	4.40	63	1.14	60	141	97	9.2	84.0	54	0.61	0.19	
	422131	4518162	4	Castello di Baia	A	21	7.07	3027	862	4.04	435	1.53	383	408	150	72	623	88	0.16	0.34	
	422368	4520460	5	Costagliola	A	22	7.20	1163	366	5.72	194	0.52	66	169	48	8.7	245	60	0.11	0.36	
	426651	4522845	6	Rist. Edera	A	23	7.32	802	385	3.75	66	0.97	5.60	109	91	7.5	80.0	52	1.3	0.27	
	423664	4522351	7	Parco Delta	A	30	7.58	1056	226	2.95	131	0.31	211	177	104	15	160	28	0.24	0.21	
	421045	4523852	8	Parco Enea	A	37	6.77	722	344	12.1	97	0.86	0.01	44	12	1.4	182	28	0.63	0.26	
	430331	4520074	9	Agnano Marte	B	21	6.46	2317	1064	4.65	314	0.85	1.6	212	121	30	450	116	2.9	0.46	
	430259	4520013	10	Agnano De Pisis	B	55	6.20	7866	1488	2.74	3009	11	0.92	448	279	75	2209	330	9.5	2.6	
	427172	4519315	11	Terme Puteolane	B	58	6.90	7904	2196	4.96	1944	5.12	31	984	46	67	2434	186	4.5	1.2	
	426602	4519946	12	Tortorelli	B	63	7.16	4330	1699	14.73	253	0.42	7.0	972	11	2.0	1187	182	0.15	1.9	
	422375	4521003	13	Averno Lake	C	12	8.27	1753	405	9.07	510	1.17	0.94	193	25	13	536	60	0.44	0.64	
	422151	4520287	14	Samuele	C	25	7.46	2104	636	7.19	543	1.00	2.13	193	82	17	520	103	0.12	0.43	
	423382	4521520	15	Esposito	C	36	7.55	2158	601	5.62	457	1.35	108	236	70	13	541	124	0.25	0.50	
	423323	4521164	16	Ippico	C	36	7.78	1979	533	7.40	413	0.63	120	247	34	14	484	125	0.29	0.29	
	423436	4521232	17	Damiani	C	46	7.45	2216	552	8.36	565	2.02	94	212	36	8.6	611	127	0.23	0.31	
	422057	4519983	18	Stufe di Nerone	C	77	6.55	19,066	373	17.02	10,227	36	89	683	301	45	7094	193	1.5	6.7	
	Vulcano Island	495989	4251957	19	Casa con Pesci	A	21.5	7.32	1020	272	7.36	220	0.32	39	173	74	28	167	38	0.97	
		495858	4251946	20	Casa Rosa	A	21.7	7.31	1139	305	13.6	266	0.44	8.6	185	85	27	195	53	0.42	
496281		4251585	21	Piscio'	A	37.8	6.46	3274	234	5.01	356	0.58	23	1651	404	48	395	157	0.61		
495582		4251164	22	Lentia	A	47.1	7.49	3987	889	16	579	1.82	10	1157	35	24	926	347	2.2	0.37	
496316		4251873	23	Bambara	B	24.6	5.61	1260	247	6.77	181	0.48	135	296	189	21	130	51	2.4		
496193		4251663	24	Casamento	B	26.3	5.87	970	454	4.28	73.3	0.02	36	98	73	26	126	79	0.75		
496347		4251557	25	Rifici	B	30	7.14	3454	128	4.94	236	0.36	120	1942	730	80	111	101	0.8	0.17	
496520		4251604	26	Rimessa	B	38.7	5.89	3863	344	4.85	360	0.58	0.24	2018	679	91	206	158	1.4	0.35	
495922		4251252	27	Camping Sicilia	B	51.8	8.1	6245	510	11.3	1760	4.27	1.89	1790	95	95	1487	488	2.2	0.77	
495826		4250287	28	Discarica	B	47.2	6.86	4589	2503	11.5	116	0.19	0.28	748	104	326	404	375	0.93		
496088		4251418	29	Genovese	C	46	7.12	2319	398	11	261	0.46	35	869	110	25	417	192	0.22		
495547		4250587	30	Eas	C	46.5	6.66	17,634	1604	12.3	8463	28	1.4	1425	500	921	4327	332	15	5.2	
496132		4251385	31	Chantal	C	48.5	6.98	5130	350	6.06	1062	2.24	3.4	1936	216	87	1099	366	1.6	0.82	
495661		4251985	32	Eden Park	C	23.9	7.01	1296	167	22	411	0.78	32	219	69	29	243	102	0.68	0.16	
496305		4252264	33	Eros	C	24	6.94	6024	703	14.2	2316	7.4	0.75	974	295	182	1311	211	9	0.44	
496037		4251674	34	Le Palme	C	25.2	7.13	1520	503	14.6	189	0.36	148	215	107	32	195	93	23	0.07	
495615		4251769	35	Orsa Maggiore	C	27.1	7.29	3142	297	15.3	967	1.65	105	671	159	76	663	184	2.3	0.56	
495896		4251556	36	Davanti Casa Schmidt	C	27.4	8.27	2896	407	12.1	591	1.15	32	860	60	24	653	254	1.4		
495940		4251396	37	Le Calette	C	38.9	6.98	2135	269	8.4	431	1.1	52	688	170	50	314	150	1.3	0.3	
495748		4251530	38	Bonanno	C	40.3	7.69	2686	380	13.7	669	1.46	3.66	707	82	44	596	187	2.3	0.37	

#### 4.1.3. $\delta^{13}C_{TDIC}$ and $\delta^{13}C_{CO2(aq)}$ values

The isotopic composition of dissolved CO<sub>2</sub> ( $\delta^{13}C_{CO2(aq)}$ ) varied from -23.7 (♯6) to -5.0 (♯10) ‰ vs. V-PDB (Table 3). Such a relatively large isotopic interval allowed to distinguish three groups of waters (Table 4), as follows: A waters (from ♯1 to ♯8), i.e. those characterized by strongly negative  $\delta^{13}C_{CO2(aq)}$  values ( $\leq -19.7\%$  vs. V-PDB) and low PCO<sub>2</sub> values ( $\leq 2.3$  mbar; Fig. 3a); the isotopically heavy ( $\delta^{13}C_{CO2(aq)} \geq -7.6\%$  vs. V-PDB) B waters (from ♯9 to ♯12), characterized by high TDS and PCO<sub>2</sub> values (up to 7904 mg/L and 21 mbar, respectively) and Na-HCO<sub>3</sub> and Na-Cl compositions, and C waters (from ♯13 to ♯18), clustering in the Monte Nuovo area (Fig. 1a), with intermediate  $\delta^{13}C_{CO2(aq)}$  values (from -15.9 to -11.8‰ vs. V-PDB) with respect to those measured in the A and B waters.

The  $\delta^{13}C_{TDIC}$  values (Table 3) were consistent with those of  $\delta^{13}C_{CO2(aq)}$ : strongly negative values (from -16.2 to -12.8‰ vs. V-PDB) were measured in the A waters, whereas the highest  $\delta^{13}C_{TDIC}$  values (from -1.6 to +0.4‰ vs. V-PDB) were related to the B waters (Table 4). The waters from the Monte Nuovo area (C waters) showed intermediate  $\delta^{13}C_{TDIC}$  values (from -8.6 to -7.1‰ vs. V-PDB).

## 4.2. Vulcano Island

### 4.2.1. Water geochemistry

Similarly to the Campi Flegrei waters, those from Vulcano Island showed a relatively large range in temperature, pH and TDS varying

from 21.5 (♯19) to 51.8 °C (♯27), from 5.61 (♯23) to 8.27 (♯36), and from 970 (♯24) to 17,634 mg/L (♯30), respectively (Table 1).

The two samples (♯24 and ♯34) showing a Na-HCO<sub>3</sub> composition had relatively low temperatures and TDS values ( $\leq 26.3$  °C and  $\leq 1520$  mg/L, respectively), whereas the Mg-HCO<sub>3</sub> water (♯28; Fig. 2b) was at 47.2 °C and had a TDS of 4589 mg/L. Those waters showing a Na-SO<sub>4</sub> composition (♯22, ♯29, ♯31, ♯36, and ♯37; Fig. 2b) were characterized by temperatures and TDS values ranging from 27.4 to 48.5 °C and from 2135 to 5130 mg/L, respectively (Table 1). Temperature and TDS values of the Ca-SO<sub>4</sub> waters (♯21, ♯23, ♯25, and ♯26; Fig. 2b) varied from 24 to 38.7 °C and from 1260 to 3863 mg/L, respectively (Table 1), whereas the Na-Cl waters (♯19, ♯20, ♯27, ♯30, ♯32, ♯33, ♯35, and ♯38; Fig. 2b) showed wide ranges of temperature (from 21.5 to 51.8 °C) and TDS values (from 1020 to 17,634 mg/L).

### 4.2.2. Chemical composition of dissolved gases

Dissolved gases in the Vulcano waters (Table 2) mostly consisted of N<sub>2</sub> (from 215 to 1017 mbar), O<sub>2</sub> (from 0.73 to 79 mbar), CO<sub>2</sub> (from 1.6 to 20 mbar) and Ar (from 1.3 to 12 mbar) (Fig. 3b). Most dissolved gases showed the presence of H<sub>2</sub>, which reached 4.9 mbar at ♯23. PCH<sub>4</sub> was  $\leq 0.14$  mbar. The dissolved gas composition showed no clear relation with the water physicochemical features.

### 4.2.3. $\delta^{13}C_{TDIC}$ and $\delta^{13}C_{CO2(aq)}$ values

The  $\delta^{13}C_{CO2(aq)}$  values of dissolved gases from Vulcano Island ranged from -21.8 (♯22) to -4.0 (♯23) ‰ vs. V-PDB (Table 3). As observed for

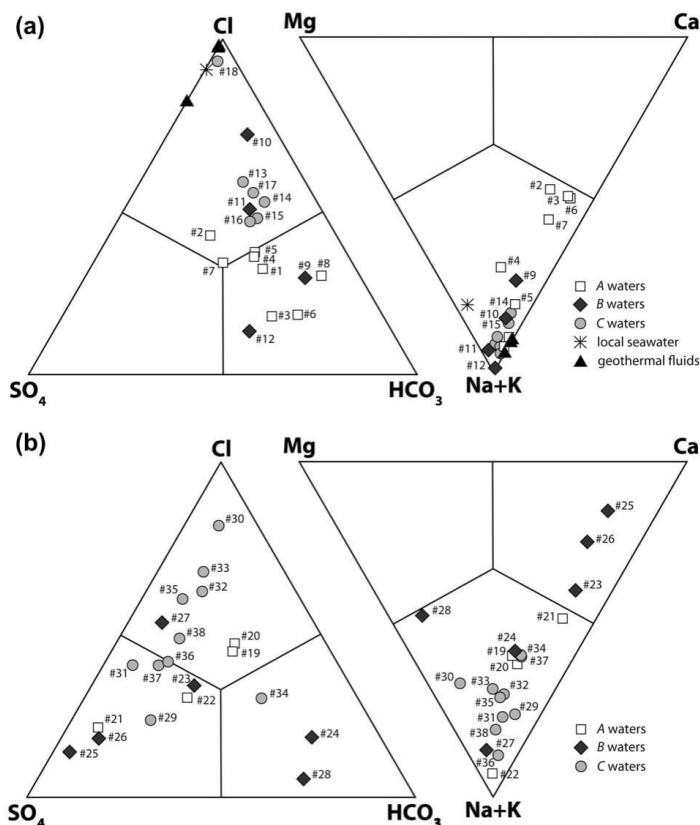


Fig. 2. Ternary diagrams for the main anions ( $\text{HCO}_3$ ,  $\text{Cl}$ ,  $\text{SO}_4$ ) and cations ( $\text{Ca}$ ,  $\text{Mg}$ ,  $\text{Na} + \text{K}$ ) from (a) Campi Flegrei caldera and (b) Vulcano Island. In Fig. 2a, the composition of local seawater (black asterisk) and geothermal fluids from Mofete drillings (black triangles) at Campi Flegrei (Fig. 1a), as reported by Guglielminetti (1986), is also shown.

the Campi Flegrei samples, three different groups of waters were also distinguished at Vulcano (Table 4), as follows: isotopically light A waters (from #19 to #22), having the lowest  $\text{PCO}_2$  values ( $\leq 2.3$  mbar; Fig. 3b) and  $\delta^{13}\text{C}_{\text{CO}_2(\text{aq})}$  values ranging from  $-21.8$  to  $-20.9\%$  vs. V-PDB; B waters (from #23 to #28), mainly located at the base of La Fossa cone, characterized by  $\text{PCO}_2$  values  $\geq 13$  mbar and  $\delta^{13}\text{C}_{\text{CO}_2(\text{aq})}$  from  $-6.0$  to  $-4.0\%$  vs. V-PDB; C waters (from #29 to #38), with  $\delta^{13}\text{C}_{\text{CO}_2(\text{aq})}$  values, ranging from  $-16.5$  to  $-9.1\%$  vs. V-PDB, and  $\text{PCO}_2$  values similar to those of the B waters (Table 2; Fig. 3b). The latter group of samples was collected both at the base of the volcanic edifice and in the northern and western portions of the Vulcano Porto Plain (Fig. 1a).

Similar to what observed at Campi Flegrei, the  $\delta^{13}\text{C}_{\text{TDIC}}$  (Table 3) and the  $\delta^{13}\text{C}_{\text{CO}_2(\text{aq})}$  values were strongly related, the former ranging from  $-17.5$  to  $-14.5\%$  vs. V-PDB, from  $-1.8$  to  $+1.9\%$  vs. V-PDB, and from  $-11.3$  to  $-4.8\%$  vs. V-PDB in the A, B, and C waters, respectively (Table 4).

## 5. Discussion

### 5.1. Campi Flegrei

#### 5.1.1. Origin of waters and dissolved gases

The wide variation of chemical features characterizing the waters collected from the Campi Flegrei study area was interpreted as

produced by mixing of fluids from different sources: (i) shallow aquifer(s) fed by meteoric water, (ii) seawater and (iii) deep geothermal brine (e.g. Baldi et al., 1975; Cortecci et al., 1978; Duchi et al., 1995; Valentino et al., 1999; Valentino and Stanzione, 2003, 2004). The chemical composition of meteoric water permeating through the carbonates cropping out on the Apennine Chain (Duchi et al., 1995 and references therein; Valentino and Stanzione, 2003) varied from  $\text{Ca-HCO}_3$  to  $\text{Na-HCO}_3$  due to interaction with volcanic deposits. Close to the coastline (Fig. 1a), seawater contamination produced the  $\text{Ca-Cl}$  (#2) and  $\text{Na-Cl}$  (#4) waters characterized by low  $\text{PCO}_2$  values (Table 2; Fig. 3a) and strongly negative  $\delta^{13}\text{C}$  values of both  $\text{CO}_2(\text{aq})$  and TDIC, approaching those related to microbial activity (Degens, 1969). Seawater inflow also affected the chemistry of #11, although for this water addition of deep  $\text{Na-Cl}$  fluids was also recognized (Valentino and Stanzione, 2003). A significant contribution of heat and fluids from the magmatic system was also characterizing the waters from the areas close to the Solfatara Crater (#12), Agnano (#9 and #10) and Monte Nuovo (from #13 to #18), as shown by their high  $\text{PCO}_2$  values and the less negative carbon isotopic signatures (Tables 2 and 3). The relatively high  $\text{HCO}_3$  concentrations measured in these waters were likely originated by dissolution of deep-sourced  $\text{CO}_2$ , whereas their enrichment in  $\text{NH}_4$  and  $\text{Li}$  (Table 1) indicate relatively high temperatures and prolonged water-rock interactions, respectively (Nicholson, 1993). Accordingly, their  $\text{Li/Cl}$  ratios points to those of the geothermal fluids exploited from wells

**Table 2**  
Chemical composition of the main gases dissolved in waters (partial pressures in mbar) from Campi Flegrei and Vulcano Island.

Study area	ID	group	PCO <sub>2</sub>	PN <sub>2</sub>	PO <sub>2</sub>	PAr	PCH <sub>4</sub>	PH <sub>2</sub>	Ptotal
Campi Flegrei	1	A	1.5	931	139	11	0.039		1082
	2	A	2.3	988	117	11	0.026		1118
	3	A	1.6	945	124	11	0.039		1081
	4	A	1.0	945	117	11	0.032		1073
	5	A	1.2	1031	60	12	0.12		1104
	6	A	1.2	888	102	9.3	0.026		1000
	7	A	2.0	959	124	10	0.019		1095
	8	A	0.80	974	109	11	0.032		1094
	9	B	21	243	16	2.7	0.045		283
	10	B	21	458	10	5.2	0.006	0.050	495
	11	B	4.7	745	38	8.6	0.032	0.100	796
	12	B	15	544	88	6.2	0.019	0.038	653
	13	C	40	1231		14	936	9.8	2231
	14	C	34	272	9.5	3.3	0.058	0.100	319
	15	C	5.4	988	29	11	0.032		1034
	16	C	20	215	8.0	2.6	0.078	0.063	246
	17	C	16	702	18	7.3	0.071	0.075	742
	18	C	54	315	12	3.7	0.026	0.14	385
Vulcano Island	19	A	1.8	945	63	11	0.14		1022
	20	A	2.3	1017	59	12	0.084		1090
	21	A	2.1	988	65	11	0.078		1066
	22	A	1.6	1017	52	11	0.097		1081
	23	B	18	372	1.5	3.3	0.019	4.9	400
	24	B	13	702	8.0	8.0	0.032	0.96	732
	25	B	18	458	8.0	5.3	0.006	1.2	491
	26	B	17	215	0.73	1.3	0.013	2.4	236
	27	B	18	344	4.4	4.0	0.058	3.4	374
	28	B	16	558	5.8	4.6	0.039	0.74	585
	29	C	18	458	14	4.6	0.006	1.1	496
	30	C	17	487	9.5	4.6	0.032	0.85	519
	31	C	15	587	57	4.6	0.013	0.61	664
	32	C	20	501	12	4.6	0.013	1.2	539
	33	C	17	472	13	4.6	0.013	0.96	508
	34	C	16	587	19	6.6	0.026	0.74	630
	35	C	20	401	12	4.0	0.006	0.36	437
	36	C	17	644	79	5.3	0.013	0.51	746
	37	C	11	802	47	8.6	0.019	0.44	869
	38	C	20	415	18	4.0	0.032	0.64	458

**Table 3**  
 $\delta^{13}\text{C}$  (in ‰ vs. V-PDB) of dissolved CO<sub>2</sub> and TDIC in waters from Campi Flegrei and Vulcano Island.

Study area	ID	Group	$\delta^{13}\text{C}_{\text{CO}_2(\text{aq})}$	$\delta^{13}\text{C}_{\text{TDIC}}$
Campi Flegrei	1	A	-19.7	-12.8
	2	A	-21.3	-15.7
	3	A	-22.9	-14.0
	4	A	-23.4	-16.2
	5	A	-23.0	-16.1
	6	A	-23.7	-14.8
	7	A	-23.0	-15.1
	8	A	-21.5	-13.3
	9	B	-5.8	-1.6
	10	B	-5.0	-0.8
	11	B	-6.8	0.3
	12	B	-7.6	0.4
	13	C	-12.5	-8.6
	14	C	-15.4	-8.0
	15	C	-15.2	-7.6
	16	C	-15.9	-8.2
	17	C	-11.8	-7.1
	18	C	-14.2	-7.6
Vulcano Island	19	A	-21.0	-14.5
	20	A	-21.1	-14.6
	21	A	-20.9	-15.6
	22	A	-21.8	-17.5
	23	B	-4.0	1.9
	24	B	-6.0	0.3
	25	B	-4.4	0.0
	26	B	-5.7	0.4
	27	B	-4.7	-1.8
	28	B	-5.4	-1.8
	29	C	-9.3	-5.2
	30	C	-9.1	-5.4
	31	C	-9.2	-5.5
	32	C	-11.4	-5.2
	33	C	-14.7	-8.0
	34	C	-11.1	-4.9
	35	C	-11.1	-5.3
	36	C	-10.8	-4.8
	37	C	-16.5	-11.3
	38	C	-12.8	-8.8

drilled in the Mofete area (Guglielminetti, 1986) (Fig. 4). The relevant influence of the deep fluid source on the chemistry of #12 water was also supported by geophysical measurements showing that the Solfatara Crater corresponds to the major gas upflow zone of the Campi Flegrei hydrothermal system (Afanasyev et al., 2015). These data showed that the uprising of hot geothermal fluids is also affecting the Agnano Plain (De Siena et al., 2010), as confirmed by the chemical features of the hot and brackish #10 water (Table 1). Eventually, a highly permeable zone was recognized at the Monte Nuovo area (De Siena et al., 2010; Petrillo et al., 2013), where the last eruptive event of the Campi Flegrei

system occurred and the hottest and most saline water (#18) was found.

#### 5.1.2. Processes regulating the $\delta^{13}\text{C}_{\text{CO}_2(\text{aq})}$ and $\delta^{13}\text{C}_{\text{TDIC}}$ values

The wide-ranging carbon isotopic compositions observed at Campi Flegrei likely result from varying source contributions to the analyzed waters.

Both the  $\delta^{13}\text{C}_{\text{CO}_2(\text{aq})}$  and  $\delta^{13}\text{C}_{\text{TDIC}}$  values and the low PCO<sub>2</sub> values in the A waters were consistent with those of interstitial soil water in areas not affected by degassing of deep-originated fluids (Degens,

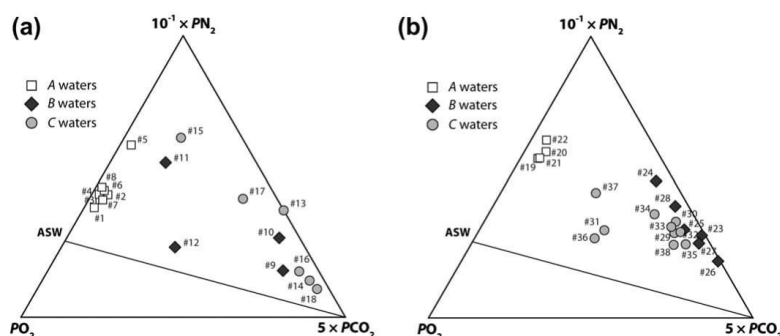


**Fig. 3.** PCO<sub>2</sub>-PN<sub>2</sub>-PO<sub>2</sub> ternary diagrams for dissolved gases in waters from (a) Campi Flegrei caldera and (b) Vulcano Island. The straight line corresponds to the N<sub>2</sub>/O<sub>2</sub> ratio in Air Saturated Water (ASW).

**Table 4**

Ranges of isotopic and chemical signatures of the three water groups (A, B and C) distinguished among samples from Campi Flegrei and Vulcano Island.

Study area	Group	$PCO_2$ (mbar)		$\delta^{13}C_{CO_2(aq)}$ (‰ vs. V-PDB)		TDIC (mmol/L)		$\delta^{13}C_{TDIC}$ (‰ vs. V-PDB)	
		Min	Max	Min	Max	Min	Max	Min	Max
Campi Flegrei	A	0.8	2.3	-23.7	-19.7	3.29	14.17	-16.2	-12.8
	B	4.7	21	-7.6	-5.0	18.26	36.18	-1.6	0.4
	C	5.4	54	-15.9	-11.8	8.19	11.76	-8.6	-7.1
Vulcano Island	A	1.6	2.3	-21.8	-20.9	3.92	14.63	-17.5	-14.5
	B	13	18	-6.0	-4.0	2.81	41.64	-1.8	1.9
	C	11	20	-16.5	-9.1	3.53	26.95	-11.3	-4.8

1969; Faure, 1986; Clark, 2015). Consistently, the chemical composition of these waters, which are randomly distributed within the study area, pointed to a shallow (or marginal to the volcanic-hydrothermal system) source for the dissolved carbon species. Accordingly, they plotted close to the biogenic field in Fig. 5a, with  $\delta^{13}C_{CO_2(aq)}$  values approaching those expected for water interaction with biogenic  $CO_2$  (Fig. 5b).

On the other hand, the chemical composition and the relatively high temperature, TDS and  $PCO_2$  values shown by the B and C waters from the Solfatara, Agnano Plain, and Monte Nuovo areas clearly indicated a dominant contribution from hydrothermal fluids.

The  $\delta^{13}C_{TDIC}$  vs. TDIC binary diagram (Fig. 5a) reports the theoretical field of the geothermal fluids that was drawn considering (i) the TDIC values of deep reservoir fluids collected from the Mofete geothermal wells (from 431 to 1209 mmol/L; Allard et al., 1991 and references therein) and (ii) the  $\delta^{13}C$  values of the fumarolic emissions in the Solfatara, Agnano Plain, and Monte Nuovo areas (from -1.9 to -0.6‰ vs. V-PDB; Vaselli et al., 2011; Tassi et al., 2015), assuming the isotopic composition of TDIC to be equal to that of  $CO_{2(g)}$ . The latter assumption is supported by the fact that in the deep geothermal fluids feeding the fumarolic emissions the amount of dissolved  $CO_2$  largely exceeds that of  $HCO_3^-$  (Allard et al., 1991). Consequently, considering the  $HCO_3^-$  in solution as being negligible with respect to  $CO_{2(aq)}$ , a significant isotopic difference should not be expected between dissolved carbon and gaseous  $CO_2$  in the hydrothermal system. Moreover, hydrothermal calcite, characterized by  $\delta^{13}C$  values ranging from -3.1 to -2.4‰ vs. V-PDB, was found in the Mofete drilling cores (Carella and Guglielminetti, 1983;

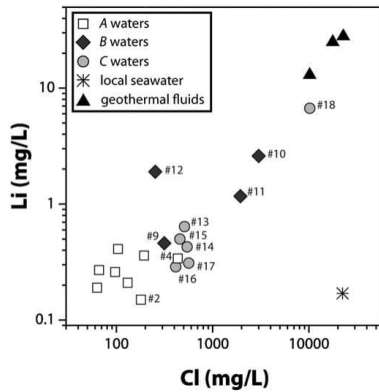


**Fig. 4.** Li vs. Cl (in mg/L) binary diagram for waters from Campi Flegrei caldera. Symbols as in Fig. 2a.

Rosi and Sbrana, 1987; De Vivo et al., 1989; Caprarello et al., 1997; Mormone et al., 2015). Considering an isotopic enrichment factor of about 2‰ between  $CO_{2(g)}$  and calcite at the temperature measured in the geothermal wells (Bottinga, 1968), the precipitation of calcite under closed-system conditions in the deep hydrothermal reservoir would be related to gaseous  $CO_2$  with  $\delta^{13}C_{CO_2(g)}$  values from -1.1 to -0.4‰ vs. V-PDB, which were consistent with those measured in the fumarolic gases (e.g. Vaselli et al., 2011; Tassi et al., 2015).

Noteworthy, the B waters displayed  $\delta^{13}C_{TDIC}$  values similar to those of the geothermal end-member (Fig. 5a), supporting the hypothesis that the chemistry of these waters was mainly controlled by the deep fluid source. Accordingly, these waters were collected from the central part of the caldera, where upwardly convecting fluid from the deep magmatic-hydrothermal system is particularly efficient.

The effects on  $\delta^{13}C_{CO_2(aq)}$  and  $\delta^{13}C_{TDIC}$  values of a simple gaseous  $CO_2$  dissolution in a two-phase system can be checked by computing theoretical isotopic values of the C-bearing compounds in the liquid and gas phases. Initially, as gaseous  $CO_2$  uprising from the deep reservoir dissolves into the shallow aquifers feeding the sampled wells, the produced  $CO_{2(aq)}$  is expected to be enriched in  $^{12}C$  relative to  $CO_{2(g)}$ , according to the equilibrium isotopic enrichment factor  $\epsilon_{CO_2(aq)-CO_2(g)}$  defined by Deines et al. (1974), as follows:

$$\epsilon_{CO_2(aq)-CO_2(g)} = \frac{6300}{T^2} - 0.91 \quad (2)$$

where T is in K. Subsequently,  $CO_{2(aq)}$  is converted to  $HCO_3^-$ , causing a further isotope fractionation, according to the isotopic enrichment factor  $\epsilon_{HCO_3-CO_2(aq)}$  whose dependence on temperature was described by Mook et al. (1974), as follows:

$$\epsilon_{HCO_3-CO_2(aq)} = \frac{9866}{T} - 24.12 \quad (3)$$

Assuming (i) TDIC and  $HCO_3^-$  to be entirely derived from  $CO_{2(g)}$  dissolution and  $CO_{2(aq)}$  conversion, respectively, and (ii) the attainment of isotopic equilibrium between gaseous and dissolved carbon species, the isotope mass balance can be used to define the  $\delta^{13}C$  values of TDIC and  $CO_{2(aq)}$  resulting from  $CO_{2(g)}$  dissolution ( $\delta^{13}C_{TDIC\_dis}$  and  $\delta^{13}C_{CO_2(aq)\_dis}$ , respectively), as follows:

$$\delta^{13}C_{TDIC\_dis} = \epsilon_{CO_2(aq)-CO_2(g)} + \delta^{13}C_{CO_2(g)} \quad (4)$$

$$\delta^{13}C_{CO_2(aq)\_dis} = \delta^{13}C_{TDIC\_dis} - \frac{\epsilon_{HCO_3-CO_2(aq)} \times HCO_3}{TDIC} \quad (5)$$

where  $HCO_3^-$  and TDIC are in mmol/L.

Using the  $\delta^{13}C_{CO_2(g)}$  values of the fumarolic emissions in Eq. (4), the theoretical  $\delta^{13}C_{TDIC\_dis}$  values expected for hydrothermal  $CO_2$  dissolution range from -2.8 to -1.5‰ vs. V-PDB, whereas the theoretical  $\delta^{13}C_{CO_2(aq)\_dis}$  values derived from Eq. (5) at increasing  $HCO_3^-/CO_{2(aq)}$  ratios (i.e. proceeding of the  $CO_{2(aq)}$  to  $HCO_3^-$  conversion; expressed in log values for graphical convenience) are depicted in Fig. 5b. These values were consistent with those measured in the B waters. In particular, the  $\delta^{13}C_{CO_2(aq)}$  value measured in the #12 sample, from the surroundings of the Solfatara Crater where the most intense hydrothermal gas upflow occurs, is to be considered the most intensely affected by carbon isotope fractionation caused by water-gas interaction processes. A shift towards values slightly higher than those expected for theoretical  $\delta^{13}C_{CO_2(aq)\_dis}$  was displayed by the #10 water, likely due to the occurrence of dissolved carbon species from both the uprising hydrothermal gases and the hot brine, an hypothesis supported by the relatively high contents of Cl, Li and  $NH_4$  measured in this water.

Differently, the  $\delta^{13}C_{CO_2(aq)}$  and  $\delta^{13}C_{TDIC}$  values in the C waters from the Monte Nuovo area were not consistent with a simple gas dissolution into shallow aquifers and were markedly lower than those measured in waters from both Solfatara and Agnano Plain areas. A mixing between

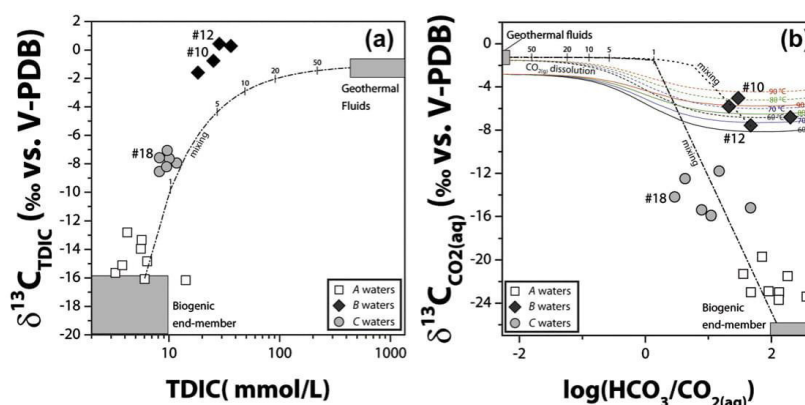


Fig. 5. (a)  $\delta^{13}\text{C}_{\text{TDIC}}$  vs. TDIC (in mmol/L) and (b)  $\delta^{13}\text{C}_{\text{CO}_2(\text{aq})}$  vs.  $\log(\text{HCO}_3^-/\text{CO}_2(\text{aq}))$  binary diagrams for waters from Campi Flegrei caldera. The mixing line between a biogenic end-member and deep geothermal fluids is shown (black dash dot line) in both (a) and (b). The fraction (in percentage) of the geothermal fluids involved in the mixture is reported. Note that the mixing between biogenic and geothermal end-members, although apparently compatible with waters distribution in (a), is not a viable explanation for the chemical composition of C waters (see text for details). In (b), the mixing line between the #12 sample and geothermal fluids (black dot line) is also shown. The  $\delta^{13}\text{C}_{\text{CO}_2(\text{aq})}$  values at increasing conversion of  $\text{CO}_2(\text{aq})$  to  $\text{HCO}_3^-$  for waters with  $\delta^{13}\text{C}_{\text{TDIC}}$  derived from dissolution of hydrothermal  $\text{CO}_2$ , i.e.  $\delta^{13}\text{C}_{\text{TDIC,dis}}$  from  $-2.8$  to  $-1.5\%$  vs. V-PDB (straight and dash lines, respectively), are depicted in (b) for different temperatures (60 °C = black lines; 70 °C = blue lines; 80 °C = green lines; 90 °C = red lines).

geothermal fluids and the A waters, as suggested by Caliro (2004) and apparently representing the most reliable explanation for the distribution of the C waters in Fig. 5a and b, is not consistent with the physico-chemical features of #18. In fact, assuming (i) a shallow (or marginal) end-member having TDIC and  $\text{CO}_2(\text{aq})$  of 6 and 0.05 mmol/L, respectively, and  $\delta^{13}\text{C}_{\text{TDIC}}$  and  $\delta^{13}\text{C}_{\text{CO}_2(\text{aq})}$  of  $-16$  and  $-25.8\%$  vs. V-PDB, respectively, and (ii) deep fluids with TDIC and  $\text{CO}_2(\text{aq})$  of 431 and 430 mmol/L, respectively, and  $\delta^{13}\text{C}_{\text{TDIC}}$  and  $\delta^{13}\text{C}_{\text{CO}_2(\text{aq})}$  of  $-1.25\%$  vs. V-PDB, the  $\delta^{13}\text{C}_{\text{CO}_2(\text{aq})}$  and  $\delta^{13}\text{C}_{\text{TDIC}}$  values of the #18 water would imply a low geothermal fluid contribution (<2%) that is not consistent with the chemical features of this water (Fig. 4), being the hottest and most saline among the analyzed samples. More likely, the negative shift observed in the C waters suggests that the uprising hydrothermal fluids were affected by secondary processes able to cause a  $^{13}\text{C}$ - $^{12}\text{C}$  fractionation. Such processes, although widely occurring at different degrees throughout the caldera, were particularly efficient in the Monte Nuovo area, i.e. at the margin of the main hydrothermal fluids uplift area, where enhanced water-rock interaction, e.g. alteration of Ca-Al-silicates (Giggenbach, 1984), able to induce widespread calcite precipitation (Simmons and Christenson, 1994) occurs, as follows:



Chiodini et al. (2015a) suggested that the conversion of Ca-Al silicates into hydrothermal calcites (Eq. (6)) is actually responsible for a significant  $\text{CO}_2$  sequestration in the Campi Flegrei caldera, as also supported by the already mentioned occurrence of hydrothermal calcite in the Mofete drillings.

The isotopic fractionation caused by calcite precipitation occurring during hydrothermal fluid circulation under open-system conditions can be described as a Rayleigh-type fractionation process, as follows:

$$\delta^{13}\text{C}_{\text{TDIC, res}} = \left[ (\delta^{13}\text{C}_{\text{TDIC, ini}} + 1000) \times f^{(\alpha_{\text{calcite-TDIC}} - 1)} \right] - 1000 \quad (7)$$

where  $\delta^{13}\text{C}_{\text{TDIC, ini}}$  is the initial isotopic composition of TDIC in the hydrothermal fluid,  $\delta^{13}\text{C}_{\text{TDIC, res}}$  is the isotopic composition of the residual TDIC after calcite precipitation,  $f$  is the fraction of residual TDIC and  $\alpha_{\text{calcite-TDIC}}$

is the isotopic fractionation factor between calcite and TDIC computed, as follows:

$$\begin{aligned} \alpha_{\text{calcite-TDIC}} - 1 &= \frac{\epsilon_{\text{calcite-TDIC}}}{1000} = \frac{\epsilon_{\text{calcite-CO}_2(\text{g})} - \epsilon_{\text{TDIC-CO}_2(\text{g})}}{1000} \quad (8) \\ &= [\epsilon_{\text{calcite-CO}_2(\text{g})} - \left( \frac{\text{CO}_2(\text{aq})}{\text{TDIC}} \times \epsilon_{\text{CO}_2(\text{aq})-\text{CO}_2(\text{g})} \right) \\ &\quad + \left( \frac{\text{HCO}_3^-}{\text{TDIC}} \times \epsilon_{\text{HCO}_3-\text{CO}_2(\text{g})} \right)] \times 10^{-3} \end{aligned}$$

The  $\epsilon_{\text{CO}_2(\text{aq})-\text{CO}_2(\text{g})}$  value was calculated as in Eq. (2), whereas  $\epsilon_{\text{HCO}_3-\text{CO}_2(\text{g})}$  and  $\epsilon_{\text{calcite-CO}_2(\text{g})}$  were calculated using the equations proposed by Deines et al. (1974), as follows:

$$\epsilon_{\text{HCO}_3-\text{CO}_2(\text{g})} = \delta^{13}\text{C}_{\text{HCO}_3} - \delta^{13}\text{C}_{\text{CO}_2(\text{g})} = \frac{1099000}{T^2} - 4.54 \quad (9)$$

$$\epsilon_{\text{calcite-CO}_2(\text{g})} = \delta^{13}\text{C}_{\text{calcite}} - \delta^{13}\text{C}_{\text{CO}_2(\text{g})} = \frac{1194000}{T^2} - 3.63 \quad (10)$$

The theoretical  $\delta^{13}\text{C}_{\text{TDIC, res}}$  values were computed according to the following assumptions: (i) the  $\delta^{13}\text{C}_{\text{TDIC, ini}}$  value was equal to that of the  $\delta^{13}\text{C}_{\text{CO}_2(\text{g})}$  reported for the Monte Nuovo fumarole ( $-1.4\%$  vs. V-PDB; Vaselli et al., 2011), (ii) fixed near-neutral pH conditions, consistent with those reported for geothermal brines at depth (Carella and Guglielminetti, 1983), and (iii) temperatures ranging from 80 to 100 °C. As shown in Fig. 6, progressive calcite precipitation efficiently decreases the  $\delta^{13}\text{C}_{\text{TDIC, res}}$  values. Hence, a Rayleigh-type fractionation process induced by calcite precipitation from hydrothermal fluids under open-system conditions can explain the  $\delta^{13}\text{C}_{\text{CO}_2(\text{aq})}$  and  $\delta^{13}\text{C}_{\text{TDIC}}$  values of the C waters. Accordingly, although affected by secondary processes, the dissolved carbon species of the #18 sample likely had a hydrothermal origin, in contrast with the low hydrothermal contribution (<2%) estimated on the basis of the mixing model (Fig. 5a) between geothermal fluids and shallow waters.

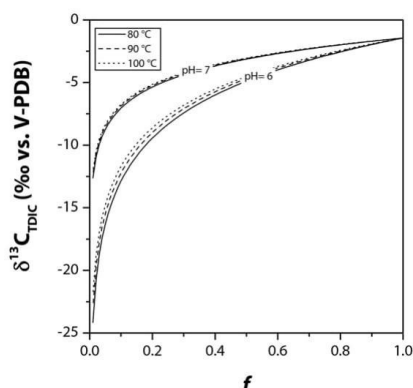


Fig. 6. Theoretical  $\delta^{13}\text{C}_{\text{TDIC}}$  values produced by calcite precipitation ( $f$  = fraction of residual TDIC after precipitation) computed for different temperatures (80 °C = solid line; 90 °C = dashed line; 100 °C = dot line) and fixed pH values.

### 5.2. Evidences from Vulcano Island

The hydrogeological setting in Vulcano Island is characterized by discontinuous shallow aquifers, complex vertical and horizontal flow paths and different fluid sources (meteoric water, seawater, uprising geothermal waters and volcanic steam) (e.g. Capasso et al., 1999, 2001; Cortecchi and Boschetti, 2001; Cortecchi et al., 2001; Boschetti et al., 2003; Federico et al., 2010; Madonia et al., 2015), producing strongly differing geochemical features in the well waters (Table 1).

Similar to what was observed at Campi Flegrei, the A waters displayed both chemical (relatively low TDS, dissolved gases dominated by  $\text{N}_2$ ,  $\text{PCO}_2$  values in the range of soil  $\text{CO}_2$ ) and isotopic ( $\delta^{13}\text{C}\text{-CO}_{2(\text{aq})}$  and  $\delta^{13}\text{C}_{\text{TDIC}}$  values consistent with those of organic-derived carbon) features compatible with aquifers fed by meteoric waters with a negligible influence of volcanic gases (Fig. 7a and b).

Conversely, the chemistry of the B waters, including most wells from the base of La Fossa cone, were interpreted as produced by interaction of uprising hot steam and mature geothermal fluids (Capasso et al., 1999, 2000, 2001; Boschetti et al., 2003). A relevant contribution from

volcanic condensates was recognized in #27 well, where temporal variations in  $\text{PCO}_2$  values were found to be strikingly related to changes in La Fossa crater fumarolic activity (Capasso et al., 1999, 2000). Accordingly, the supply of volcanic fluids was highlighted by the presence of a piezometric high (Madonia et al., 2015) and anomalous  $\text{CO}_2$  soil degassing (Capasso et al., 2000) in this area. Similarly, the relatively high temperature, the TDS values of Cl- and  $\text{SO}_4$ -rich waters from Baia di Levante (#23, #25, #26) and the peculiarly high  $\text{HCO}_3$  contents measured in the #28 water (Table 1; Capasso et al., 2000, 2001; Boschetti et al., 2003) were likely originated by interaction processes with volcanic condensates or  $\text{CO}_2$ -rich steam phase. Accordingly, both the measured (i)  $\delta^{13}\text{C}_{\text{TDIC}}$  values (Fig. 7a), which approached those of the  $\delta^{13}\text{C}_{\text{CO}_2}$  in fumarolic and bubbling gases at La Fossa crater and Baia di Levante (from -3.4 to +0.7‰ vs. V-PDB; Capasso et al., 1997), and (ii)  $\delta^{13}\text{C}_{\text{CO}_2(\text{aq})}$  values, which were consistent with the theoretical  $\delta^{13}\text{C}_{\text{CO}_2(\text{aq})\text{-dis}}$  values derived from Eqs. (4) and (5) assuming dissolution of gaseous  $\text{CO}_2$  with  $\delta^{13}\text{C}$  values in the fumarolic range (Fig. 7b), confirmed a strong interaction of the B waters with high temperature fluids from the deep volcanic system. Indeed, the foot of the volcanic cone and Baia di Levante represent zones of structural weakness where volcanic and hydrothermal fluids are mainly drained by fracture/faulting systems, resulting in both fumarolic discharges and intense  $\text{CO}_2$  soil degassing at the surface.

Noteworthy, most C waters were similarly located along a NE-oriented alignment corresponding to the Tindari-Letojanni fault (Fig. 1b; Billi et al., 2006), i.e. the main tectonic discontinuity in this region, where an upflow of volcanogenic fluids was inferred on the basis of an anomalous elevation of the water table recognized in this area (Inguaggiato et al., 2012; Madonia et al., 2015). The remaining C waters (#30 and #33), characterized by high Cl, Br,  $\text{NH}_4$  and Li contents (Table 1) and Na/Cl and Cl/Br mass ratios (0.51 and 302 in #30 and 0.57 and 313 in #33, respectively) similar to those of seawater (Na/Cl = 0.56, Cl/Br = 292), likely intercepted a seawater-contaminated water body affected by hydrothermal contribution (Federico et al., 2010).

Despite the well-assessed contribution from hydrothermal fluids, the values of TDIC and  $\text{CO}_{2(\text{aq})}$  measured in the C waters were ascribable to neither pure dissolution of deep-derived  $\text{CO}_2$  into shallow aquifers, as shown in Fig. 7b, nor simple mixing model between hydrothermal fluids and biogenic carbon sources. This would not indeed be consistent with the relatively high  $\text{PCO}_2$  and TDIC values and the high Cl, Br,  $\text{NH}_4$  and Li contents (up to 8463, 28, 15 and 5.2 mg/L, respectively; Table 1) of these waters, which are unequivocal hints of a relevant contribution from hydrothermal fluids. As previously demonstrated for the

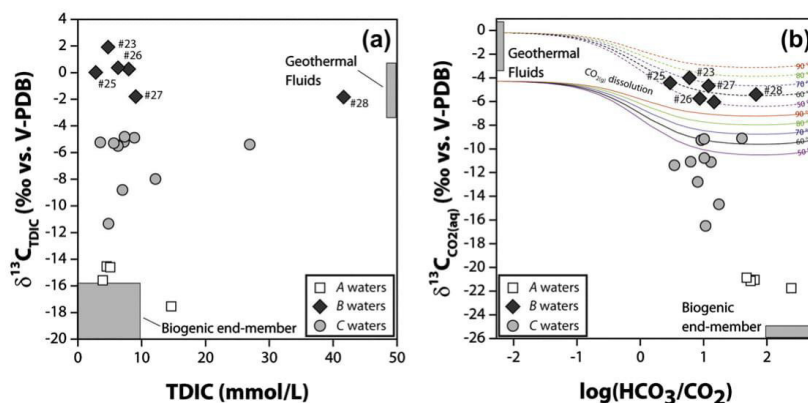


Fig. 7. (a)  $\delta^{13}\text{C}_{\text{TDIC}}$  vs. TDIC (in mmol/L) and (b)  $\delta^{13}\text{C}_{\text{CO}_2(\text{aq})}$  vs.  $\log(\text{HCO}_3/\text{CO}_2)$  binary diagrams for waters from Vulcano Island. The  $\delta^{13}\text{C}_{\text{CO}_2(\text{aq})\text{-dis}}$  values at increasing conversion of  $\text{CO}_{2(\text{aq})}$  to  $\text{HCO}_3$  for waters with  $\delta^{13}\text{C}_{\text{TDIC}}$  derived from dissolution of hydrothermal  $\text{CO}_2$ , i.e.  $\delta^{13}\text{C}_{\text{TDIC}\text{-dis}}$  from -4.26 to -0.15‰ vs. V-PDB (straight and dash lines, respectively), are depicted in (b) for different temperatures (50 °C = purple lines; 60 °C = black lines; 70 °C = blue lines; 80 °C = green lines; 90 °C = red lines).

case study of Campi Flegrei, a strong isotopic fractionation can be easily produced by a Rayleigh-type calcite precipitation affecting the uprising deep fluids (Fig. 6). The occurrence of calcite precipitation, coupled with steam condensation and multi-step boiling processes, was already suggested by Federico et al. (2010) to explain the wide variations in major ions, dissolved gases and stable isotopes in thermal waters from the island. Although such process is not expected to occur only along the Tindari-Letojanni fault, local conditions may play a key role in determining the isotopic composition of dissolved carbon species in thermal waters. In particular, (i) decreasing temperature and salinity (Madonia et al., 2015) at increasing distance from the volcanic edifice and (ii) absence of CO<sub>2</sub> soil degassing anomalies in this area (Inguaggiato et al., 2012) revealed a less intense supply of volcanic/hydrothermal fluids into shallow ground waters, which, consistently with what observed at the Campi Flegrei, likely allowed secondary isotopic fractionation processes to overwhelm the typical signature of the deep-derived carbon.

## 6. Conclusions

The chemical and isotopic compositions of the main solutes and dissolved gases in thermal and cold waters collected from wells located at Campi Flegrei and Vulcano Island were investigated to elucidate the processes controlling the  $\delta^{13}\text{C}_{\text{CO}_2(\text{aq})}$  and  $\delta^{13}\text{C}_{\text{TDIC}}$  values. The occurrence of hydrothermal-magmatic CO<sub>2</sub>, possibly affected by a relatively low isotopic fractionation due to dissolution in shallow water, exhaustively explains the chemical features of the wells located in the proximity of the areas interested by the highest deep fluid upflow, corresponding to the Solfatara crater and La Fossa cone at Campi Flegrei and Vulcano Island, respectively. In some cases (e.g. the well waters from Agnano Plain), the involvement of both hydrothermal gases and geothermal brine should be invoked to reconcile the measured and theoretical data.

Waters dominantly fed by shallow meteoric aquifers were occurring in the two volcanic systems and characterized by dissolved CO<sub>2</sub> and TDIC showing the typical chemical and isotopic features of interstitial soil waters. Water samples with intermediate  $\delta^{13}\text{C}_{\text{CO}_2(\text{aq})}$  and  $\delta^{13}\text{C}_{\text{TDIC}}$  values from both areas are the main point of interest of this study, since their chemistry is not consistent with a simple mixing between deep and shallow end-members. Instead, assuming a dominant deep source for the C-bearing species of these waters, we demonstrated that the strong isotope fractionation (>5‰) necessary to explain the measured isotopic values can be obtained through Rayleigh-type calcite precipitation. This excludes a significant contribution from the shallow source, as dictated by the classical mixing model that would lead to a strong underestimation of the deep CO<sub>2</sub> fraction. At Campi Flegrei, these waters were only found at Monte Nuovo. The cause of this peculiar relationship between the spatial distribution and the chemical features of these waters, although intriguing, is not clear and deserves further investigation. Notwithstanding, it is worth noting that calcite precipitation is commonly observed in volcanic and hydrothermal systems, hence the hypothesized secondary <sup>13</sup>C-<sup>12</sup>C fractionation process can be considered to play a fundamental role in controlling the isotopic signature of carbon in dissolved CO<sub>2</sub> and TDIC at a global scale. These findings imply that intermediate  $\delta^{13}\text{C}_{\text{CO}_2(\text{aq})}$  and  $\delta^{13}\text{C}_{\text{TDIC}}$  values are to be interpreted with extreme caution for the assessment of the carbon budget of hydrothermal-volcanic systems. As assessed for the Campi Flegrei waters, the attribution of such carbon isotopic values to mixing between shallow ground waters and deep-originated fluids could be misleading, determining a substantial underestimation of the hydrothermal contribution to dissolved carbon species in thermal waters.

## Acknowledgments

This work was financially supported by the Department of the Civil Protection (DPC) and the laboratories of Fluid and Rock Geochemistry and Stable Isotope Geochemistry of the Department of Earth Sciences

and CNR-IGG of Florence. E. Calvi (CNR-IGG Pisa) is kindly acknowledged for his help during the measurement of the isotopic composition of dissolved CO<sub>2</sub>. Many thanks are due to local people for kindly providing their permission to collect the waters from their private wells.

## References

- Afanasyev, A., Costa, A., Chiodini, G., 2015. Investigation of hydrothermal activity at Campi Flegrei caldera using 3D numerical simulations: extension to high temperature processes. *J. Volcanol. Geotherm. Res.* 299:68–77. <http://dx.doi.org/10.1016/j.jvolgeores.2015.04.004>.
- Aiuppa, A., Tamburello, G., Di Napoli, R., Cardellini, C., Chiodini, G., Giudice, G., Grassa, F., Pedone, M., 2013. First observations of the fumarolic gas output from a restless caldera: implications for the current period of unrest (2005–2013) at Campi Flegrei. *Geochim. Geophys. Res.* 14 (10):4153–4169. <http://dx.doi.org/10.1002/ggge.20261>.
- Allard, P., Maiorani, A., Tedesco, D., Correcchi, G., Turi, B., 1991. Isotopic study of the origin of sulfur and carbon in Solfatara fumaroles, Campi Flegrei caldera. *J. Volcanol. Geotherm. Res.* 48, 139–159.
- Arrighi, S., Tanguy, J.-C., Rosi, M., 2006. Eruptions of the last 2200 years at Vulcano and Vulcanello (Aeolian Islands, Italy) dated by high-accuracy archeomagnetism. *Phys. Earth Planet. Inter.* 159:225–233. <http://dx.doi.org/10.1016/j.pepi.2006.07.010>.
- Baldi, P., Ferrara, G.C., Panichi, C., 1975. Geothermal research in western Campania (southern Italy): chemical and isotopic studies of thermal fluids in the Campi Flegrei. *Proc. 2nd U.N. Symp. on Development and Use of Geothermal Resources*, San Francisco, CA, 20–29 May 1975, pp. 687–697.
- Barry, P.H., Hilton, D.R., Füre, E., Halldórsson, S.A., Grönvold, K., 2014. Carbon isotope and abundance of Icelandic geothermal gases, fluids and subglacial basalts with implications for mantle plume-related CO<sub>2</sub> fluxes. *Geochim. Cosmochim. Acta* 134:74–99. <http://dx.doi.org/10.1016/j.gca.2014.02.038>.
- Billi, A., Barberi, G., Faccenna, C., Neri, G., Pepe, F., Sulli, A., 2006. Tectonics and seismicity of the Tindari Fault System, southern Italy: crustal deformations at the transition between ongoing contractional and extensional domains located above the edge of a subducting slab. *Tectonics* 25 (2), TC2006. <http://dx.doi.org/10.1029/2004TC001763>.
- Bonafede, M., Mazzanti, M., 1998. Modelling gravity variations consistent with ground deformation in the Campi Flegrei caldera (Italy). *J. Volcanol. Geotherm. Res.* 81, 137–157.
- Boschetti, T., Correcchi, G., Bolognesi, L., 2003. Chemical and isotopic compositions of the shallow groundwater system of Vulcano Island, Aeolian Archipelago, Italy: an update. *GeoActa* 2, 1–34.
- Bottinga, Y., 1968. Calculation of fractionation factors for carbon and oxygen isotopic exchange in the system calcite-carbon dioxide-water. *J. Phys. Chem.* 72, 800–808.
- Burton, M.R., Sawyer, G.M., Granieri, D., 2013. Deep carbon emissions from volcanoes. *Rev. Mineral. Geochim.* 75:323–354. <http://dx.doi.org/10.2138/rmg.2013.75.11>.
- Cabassi, J., Tassi, F., Vaselli, O., Fiebig, J., Nocentini, M., Capecciacci, F., Rouwet, D., Biccocchi, G., 2013. Biogeochemical processes involving dissolved CO<sub>2</sub> and CH<sub>4</sub> at Albano, Averno, and Monticchio meromictic volcanic lakes (Central-Southern Italy). *Bull. Volcanol.* 75:683. <http://dx.doi.org/10.1007/s00445-012-0683-0>.
- Caliro, S., 2004. Volcanic and Non-volcanic Degassing in Campania Region (Southern Italy). Ph. D. Thesis. Università degli Studi di Napoli “Federico II”, Naples (177 pp).
- Caliro, S., Panichi, C., Stanzone, D., 1999. Variation in the total dissolved carbon isotope composition of thermal waters of the Island of Ischia (Italy) and its implications for volcanic surveillance. *J. Volcanol. Geotherm. Res.* 90, 219–240.
- Caliro, S., Chiodini, G., Moretti, R., Avino, R., Granieri, D., Russo, M., Fiebig, J., 2007. The origin of the fumaroles of La Solfatara (Campi Flegrei, South Italy). *Geochim. Cosmochim. Acta* 71:3040–3055. <http://dx.doi.org/10.1016/j.gca.2007.04.007>.
- Capaccioni, B., Tassi, F., Vaselli, O., 2001. Organic and inorganic geochemistry of low temperature discharges at the Baia di Levante beach, Vulcano Island, Italy. *J. Volcanol. Geotherm. Res.* 108, 173–185.
- Capasso, G., Favara, R., Inguaggiato, S., 1997. Chemical features and isotopic composition of gaseous manifestations on Vulcano Island, Aeolian Islands, Italy: an interpretative model of fluid circulation. *Geochim. Cosmochim. Acta* 61 (16), 3425–3440.
- Capasso, G., Favara, R., Francofonte, S., Inguaggiato, S., 1999. Chemical and isotopic variations in fumarolic discharge and thermal waters at Vulcano Island (Aeolian Islands, Italy) during 1996: evidence of resumed volcanic activity. *J. Volcanol. Geotherm. Res.* 88, 167–175.
- Capasso, G., Favara, R., Inguaggiato, S., 2000. Interaction between fumarolic gases and thermal groundwaters at Vulcano Island (Italy): evidences from chemical composition of dissolved gases in waters. *J. Volcanol. Geotherm. Res.* 102, 309–318.
- Capasso, G., D’Alessandro, W., Favara, R., Inguaggiato, S., Parello, F., 2001. Interaction between the deep fluids and the shallow groundwaters on Vulcano island (Italy). *J. Volcanol. Geotherm. Res.* 108, 187–198.
- Caprarello, G., Tsutsumi, M., Turi, B., 1997. Chemical and isotopic signatures of the basement rocks from the Campi Flegrei geothermal field (Naples, southern Italy): inferences about the origin and evolution of its hydrothermal fluids. *J. Volcanol. Geotherm. Res.* 76, 63–82.
- Carapezza, M.L., Barberi, F., Ranaldi, M., Ricci, T., Tarchini, L., Barrancos, J., Fischer, C., Perez, N., Weber, K., Di Piazza, A., Gattuso, A., 2011. Diffuse CO<sub>2</sub> soil degassing and CO<sub>2</sub> and H<sub>2</sub>S concentrations in air and related hazards at Vulcano Island (Aeolian arc, Italy). *J. Volcanol. Geotherm. Res.* 207:130–144. <http://dx.doi.org/10.1016/j.jvolgeores.2011.06.010>.
- Carella, R., Guglielminetti, M., 1983. Multiple reservoirs in the Mofete Field, Naples, Italy. *Proceedings Ninth Workshop Geothermal Reservoir Engineering*, Stanford University, Stanford, California, December 1983.

- Chiodini, G., Cioni, R., Guidi, M., Raco, B., Marini, L., 1998. Soil CO<sub>2</sub> flux measurements in volcanic and geothermal areas. *Appl. Geochem.* 13 (5), 543–552.
- Chiodini, G., Frondini, F., Cardellini, C., Parello, F., Peruzzi, L., 2000. Rate of diffuse carbon dioxide Earth degassing estimated from carbon balance of regional aquifers: the case of central Apennine, Italy. *J. Geophys. Res.* 105 (B4), 8423–8434.
- Chiodini, G., Frondini, F., Cardellini, C., Granieri, D., Marini, L., Ventura, G., 2001. CO<sub>2</sub> degassing and energy release at Solfatara volcano, Campi Flegrei, Italy. *J. Geophys. Res.* 106 (B8), 16213–16221.
- Chiodini, G., Todesco, M., Caliro, S., Del Gaudio, C., Macedonio, G., Russo, M., 2003. Magma degassing as a trigger of bradyseismic events: the case of Phlegrean fields (Italy). *Geophys. Res. Lett.* 30 (8):1434. <http://dx.doi.org/10.1029/2002GL016790>.
- Chiodini, G., Cardellini, C., Amato, A., Boschi, E., Caliro, S., Frondini, F., Ventura, G., 2004. Carbon dioxide Earth degassing and seismogenesis in central and southern Italy. *Geophys. Res. Lett.* 31, L07615. <http://dx.doi.org/10.1029/2004GL019480>.
- Chiodini, G., Caliro, S., De Martino, P., Avino, R., Gherardi, F., 2012. Early signals of new volcanic unrest at Campi Flegrei caldera? Insights from geochemical data and physical simulations. *Geology* 40:943–946. <http://dx.doi.org/10.1130/G33251.1>.
- Chiodini, G., Pappalardo, L., Aiuppa, A., Caliro, S., 2015a. The geological CO<sub>2</sub> degassing history of a long-lived caldera. *Geology* 43 (9):767–770. <http://dx.doi.org/10.1130/G36905.1>.
- Chiodini, G., Vandemeulebrouck, J., Caliro, S., D'Auria, L., De Martino, P., Mangiacapra, A., Petrillo, Z., 2015b. Evidence of thermal-driven processes triggering the 2005–2014 unrest at Campi Flegrei caldera. *Earth Planet. Sci. Lett.* 414:58–67. <http://dx.doi.org/10.1016/j.epsl.2015.01.012>.
- Clark, I., 2015. *Groundwater Geochemistry and Isotopes*. CRC Press, Boca Raton (FL), p. 456.
- Clocchiatti, R., Del Moro, A., Gioncada, A., Joron, J.L., Mosbah, M., Pinarelli, L., Sbrana, A., 1994. Assessment of a shallow magmatic system: the 1888–90 eruption, Vulcano Island, Italy. *Bull. Volcanol.* 56, 466–486.
- Conde, V., Robidoux, P., Avard, G., Galle, B., Aiuppa, A., Muñoz, A., Giudice, G., 2014. Measurements of volcanic SO<sub>2</sub> and CO<sub>2</sub> fluxes by combined DOAS, multi-GAS and FTIR observations: a case study from Turrialba and Telica volcanoes. *Int. J. Earth Sci. (Geol. Rundsch.)* <http://dx.doi.org/10.1007/s00531-014-1040-7>.
- Cortecci, G., Boschetti, T., 2001. Geochemical model of the phreatic system of Vulcano (Aeolian Islands, Italy). In: Cidu (Ed.), *Water-rock Interaction 2001*. Swets & Zeitlinger, Lisse, pp. 795–798.
- Cortecci, G., Noto, P., Panichi, C., 1978. Environmental isotopic study of the Campi Flegrei (Naples, Italy) geothermal field. *J. Hydrol.* 36, 143–159.
- Cortecci, G., Dinelli, E., Bolognesi, L., Boschetti, T., Ferrara, G., 2001. Chemical and isotopic compositions of water and dissolved sulfate from shallow wells on Vulcano Island, Aeolian Archipelago, Italy. *Geothermics* 30, 69–91.
- D'Alessandro, W., De Gregorio, S., Dongarrà, G., Gurrieri, S., Parello, F., Parisi, B., 1997. Chemical and isotopic characterization of the major element composition of deep groundwater in the Kii Peninsula, southern Japan. *Geochim. Cosmochim. Acta* 182: 173–196. <http://dx.doi.org/10.1016/j.gca.2016.03.017>.
- De Astis, G., La Volpe, L., Peccerillo, A., Civetta, L., 1997. Volcanological and petrological evolution of Vulcano island (Aeolian Arc, southern Tyrrhenian Sea). *J. Geophys. Res.* 102 (B4), 8021–8050.
- De Siena, L., Del Pezzo, E., Bianco, F., 2010. Seismic attenuation imaging of Campi Flegrei: evidence of gas reservoirs, hydrothermal basins, and feeding systems. *J. Geophys. Res.* 115, B09312. <http://dx.doi.org/10.1029/2009JB006938>.
- De Vivo, B., Belkin, H.E., Barbieri, M., Chelini, W., Lattanzi, P., Lima, A., Tolomeo, L., 1989. The Campi Flegrei (Italy) geothermal system: a fluid inclusion study of the Mofete and San Vito fields. *J. Volcanol. Geotherm. Res.* 36, 303–326.
- De Vivo, B., Rolandi, G., Gans, P.B., Calvert, A., Bohson, W.A., Spera, F.J., Belkin, H.E., 2001. New constraints on the pyroclastic eruptive history of the Campanian volcanic Plain (Italy). *Mineral. Petrol.* 73:47–65. <http://dx.doi.org/10.1007/s007100170010>.
- Degens, E.T., 1969. *Biogeochemistry of stable carbon isotopes*. In: Eglinton, G., Murphy, M.T.J. (Eds.), *Organic Geochemistry*. Springer, Berlin-Heidelberg-New York, pp. 194–208.
- Deines, P., Langmuir, D., Herman, R.S., 1974. Stable carbon isotope ratio and the existence of a gas phase in the evolution of carbonate groundwaters. *Geochim. Cosmochim. Acta* 38, 1147–1164.
- Deino, A.L., Orsi, G., de Vita, S., Piochi, M., 2004. The age of the Neapolitan Yellow Tuff caldera-forming eruption (Campi Flegrei caldera – Italy) assessed by <sup>40</sup>Ar/<sup>39</sup>Ar dating method. *J. Volcanol. Geotherm. Res.* 133:157–170. [http://dx.doi.org/10.1016/S0377-0273\(03\)00396-2](http://dx.doi.org/10.1016/S0377-0273(03)00396-2).
- Di Vito, M., Lirer, L., Mastrolorenzo, G., Rolandi, G., 1987. The 1538 Monte Nuovo eruption (Campi Flegrei, Italy). *Bull. Volcanol.* 49, 608–615.
- Duchi, V., Minissale, A., Vaselli, O., Ancillotti, M., 1995. Hydrogeochemistry of the Campanian region in southern Italy. *J. Volcanol. Geotherm. Res.* 67, 313–328.
- Faure, G., 1986. *Inorganic Geochemistry*. Macmillan Pub. Com., p. 627.
- Federico, C., Aiuppa, A., Allard, P., Bellomo, S., Jean-Baptiste, P., Parello, F., Valenza, M., 2002. Magma-derived gas influx and water-rock interactions in the volcanic aquifer of Mt. Vesuvius, Italy. *Geochim. Cosmochim. Acta* 66 (6), 963–981.
- Federico, C., Capasso, G., Paonita, A., Favara, R., 2010. Effects of steam-heating processes on a stratified volcanic aquifer: stable isotopes and dissolved gases in thermal waters of Vulcano Island (Aeolian archipelago). *J. Volcanol. Geotherm. Res.* 192:178–190. <http://dx.doi.org/10.1016/j.jvolgeores.2010.02.020>.
- Fouarré, E., Di Napoli, R., Aiuppa, A., Parello, F., Gaubi, E., Jean-Baptiste, P., Allard, P., Calabrese, S., Ben, Mamou, A., 2011. Regional variations in the chemical and helium-carbon isotope composition of geothermal fluids across Tunisia. *Chem. Geol.* 288: 67–85. <http://dx.doi.org/10.1016/j.chemgeo.2011.07.003>.
- Giggenbach, 1984. Mass transfer in hydrothermal alteration systems – a conceptual approach. *Geochim. Cosmochim. Acta* 48 (12), 2693–2711.
- Gillfillan, S.M.V., Sherwood, Lollar, B., Holland, G., Blagburn, D., Stevens, S., Schoell, M., Cassidy, M., Ding, Z., Zhou, Z., Lacrampe-Couloume, G., Ballentine, C., 2009. Solubility trapping in formation water as dominant CO<sub>2</sub> sink in natural gas fields. *Nature* 458: 614–618. <http://dx.doi.org/10.1038/nature07852>.
- Gottsmann, J., Rymer, H., Berrino, G., 2006. Unrest at the Campi Flegrei caldera (Italy): a critical evaluation of source parameters from geodetic data inversion. *J. Volcanol. Geotherm. Res.* 150:132–145. <http://dx.doi.org/10.1016/j.jvolgeores.2005.07.002>.
- Grassa, F., Capasso, G., Favara, R., Inguaggiato, S., 2006. Chemical and isotopic composition of waters and dissolved gases in some thermal springs of Sicily and adjacent Volcanic Islands, Italy. *Pure Appl. Geophys.* 163:781–807. <http://dx.doi.org/10.1007/s00024-006-0043-0>.
- Guglielminetti, M., 1986. Mofete geothermal field. *Geothermics* 15 (5/6), 781–790.
- Gülec, N., Hilton, D.R., 2016. Turkish geothermal fields as natural analogues of CO<sub>2</sub> storage sites: gas geochemistry and implications for CO<sub>2</sub> trapping mechanisms. *Geothermics* 64:96–110. <http://dx.doi.org/10.1016/j.geothermics.2016.04.008>.
- Hoefs, J., 2009. *Stable Isotope Geochemistry*. 6th Edition. Springer, Berlin, p. 285.
- Inguaggiato, S., Martin-Del-Pozzo, A.L., Aguayo, A., Capasso, G., Favara, R., 2005. Isotopic, chemical and dissolved gas constraints on spring water from Popocatepetl volcano (Mexico): evidence of gas-water interaction between magmatic component and shallow fluids. *J. Volcanol. Geotherm. Res.* 141:91–108. <http://dx.doi.org/10.1016/j.jvolgeores.2004.09.006>.
- Inguaggiato, S., Mazot, A., Diliberto, I.S., Inguaggiato, C., Madonia, P., Rouwet, D., Vita, F., 2012. Total CO<sub>2</sub> output from volcano island (Aeolian Islands, Italy). *Geochim. Geophys. Res.* 13 (2):1–19. <http://dx.doi.org/10.1029/2011GC003920>.
- Italiano, F., Bonfanti, P., Ditta, M., Petri, R., Slejko, F., 2009. Helium and carbon isotopes in dissolved gases of Friuli Region (NE Italy): geochemical evidence of CO<sub>2</sub> production and degassing over a seismically active area. *Chem. Geol.* 266:76–85. <http://dx.doi.org/10.1016/j.chemgeo.2009.05.022>.
- Keller, J., 1980. The island of Vulcano. *Rend. Soc. Ital. Mineral. Petrol.* 36, 369–414.
- Madonia, P., Capasso, G., Favara, R., Franconforte, S., Tommasi, P., 2015. Spatial distribution of field physico-chemical parameters in the Vulcano Island (Italy) coastal aquifer: volcanological and hydrogeological implications. *Watermark* 7:3206–3224. <http://dx.doi.org/10.3390/w7073206>.
- Marrero-Diaz, R., López, D., Perez, N.M., Custodio, E., Sumino, H., Melián, G.V., Padrón, E., Hernandez, P.A., Calvo, D., Barrancos, J., Padilla, G., Sortino, F., 2015. Carbon dioxide and helium dissolved gases in groundwater at central Tenerife Island, Canary Islands: chemical and isotopic characterization. *Bull. Volcanol.* 77:86. <http://dx.doi.org/10.1007/s00445-015-0969-0>.
- Moore, W.G., Bemmerson, J.C., Steverman, W.H., 1974. Carbon isotope fractionation between dissolved bicarbonate and gaseous carbon dioxide. *Earth Planet. Sci. Lett.* 22, 169–176.
- Morikawa, N., Kazahaya, K., Takahashi, M., Inamura, A., Takahashi, H.A., Yasuhara, M., Ohwada, M., Sato, T., Nakama, A., Handa, H., Sumino, H., Nagao, K., 2016. Widespread distribution of ascending fluids transporting mantle helium in the fore-arc region and their upwelling processes: noble gas and major element composition of deep groundwater in the Kii Peninsula, southern Japan. *Geochim. Cosmochim. Acta* 182: 173–196. <http://dx.doi.org/10.1016/j.gca.2016.03.017>.
- Mormone, A., Troise, C., Piochi, M., Balassone, G., Joachimski, M., De Natale, G., 2015. Mineralogical, geochemical and isotopic features of tuffs from the CFDDP drill hole: hydrothermal activity in the eastern side of the Campi Flegrei volcano (southern Italy). *J. Volcanol. Geotherm. Res.* 290:39–52. <http://dx.doi.org/10.1016/j.jvolgeores.2014.12.003>.
- Nicholson, K., 1993. *Geothermal Fluids. Chemistry and Exploration Techniques*. Springer-Verlag, Berlin Heidelberg, p. 263.
- Ohwada, M., Satake, H., Nagao, K., Kazahaya, K., 2007. Formation processes of thermal waters in Green Tuff: a geochemical study in the Hokuriku district, central Japan. *J. Volcanol. Geotherm. Res.* 168:55–67. <http://dx.doi.org/10.1016/j.jvolgeores.2007.07.009>.
- Passaro, S., Tamburrino, S., Vallefuoco, M., Tassi, F., Vaselli, O., Giannini, L., Chiodini, G., Caliro, S., Sacchi, M., Rizzo, A.L., Ventura, G., 2016. Seafloor doming driven by degassing processes unveils sprouting volcanism in coastal areas. *Sci Rep* 6:22448. <http://dx.doi.org/10.1038/srep22448>.
- Petrillo, Z., Chiodini, G., Mangiacapra, A., Caliro, S., Capuano, P., Russo, G., Cardellini, C., Avino, R., 2013. Defining a 3D physical model for the hydrothermal circulation at Campi Flegrei caldera (Italy). *J. Volcanol. Geotherm. Res.* 264:172–182. <http://dx.doi.org/10.1016/j.jvolgeores.2013.08.008>.
- Rollinson, H., 1993. *Using Geochemical Data*. Longman, London, UK, p. 352.
- Rosi, M., Sbrana, A. (Eds.), 1987. *Phlegrean Fields*. Consiglio Nazionale delle Ricerche, Quaderni Ricerca Scientifica, 114, p. 175.
- Ruziè, L., Aubaud, C., Moreira, M., Agrinier, P., Dessert, C., Gréau, C., Crispi, O., 2013. Carbon and helium isotopes in thermal springs of La Soufrière volcano (Guadeloupe, Lesser Antilles): implications for volcanological monitoring. *Chem. Geol.* 359:70–80. <http://dx.doi.org/10.1016/j.chemgeo.2013.09.008>.
- Salata, G.G., Roelke, L.A., Cifuentes, L.A., 2000. A rapid and precise method for measuring stable carbon isotope ratios of dissolved inorganic carbon. *Mar. Chem.* 69 (1–2): 153–161. [http://dx.doi.org/10.1016/S0304-4203\(99\)00102-4](http://dx.doi.org/10.1016/S0304-4203(99)00102-4).
- Sano, Y., Marty, B., 1995. Origin of carbon in fumarolic gas from island arcs. *Chem. Geol. Isot. Geosci.* 119, 265–274.
- Scripps CO<sub>2</sub> Program, d. Scripps Institution of Oceanography UC San Diego <http://scrippsco2.ucsd.edu>.
- Simmons, S.F., Christenson, B.W., 1994. Origins of calcite in a boiling geothermal system. *Am. J. Sci.* 294, 361–400.
- Sommaruga, C., 1984. Le ricerche geotermiche svolte a Vulcano negli anni '50. *Rendiconti Società Italiana Mineralogia e petrologia*, 39 pp. 355–366.
- Taran, Y., Inguaggiato, S., Varley, N., Capasso, G., Favara, R., 2002. Helium and carbon isotopes in thermal waters of the Jalisco block, Mexico. *Geofis. Int.* 41 (4), 459–466.
- Tassi, F., Vaselli, O., Luchetti, G., Montegrossi, G., Minissale, A., 2008. Metodo per la determinazione dei gas disciolti in acque naturali. 10450. *Int Rep CNR-IGG, Florence*, p. 11.

- Tassi, F., Vaselli, O., Tedesco, D., Montegrossi, G., Darrah, T., Cuoco, E., Mapendano, M.Y., Poreda, R., Delgado, Huertas A., 2009. Water and gas chemistry at Lake Kivu (DRC): geochemical evidence of vertical and horizontal heterogeneities in a multi-basin structure. *Geochem. Geophys. Geosyst.* 10 (2). <http://dx.doi.org/10.1029/2008GC002191>.
- Tassi, F., Venturi, S., Cabassi, J., Capecciacci, F., Nisi, B., Vaselli, O., 2015. Volatile organic compounds (VOCs) in soil gases from Solfatara crater (Campi Flegrei, southern Italy): geogenic source(s) vs. biogeochemical processes. *Appl. Geochem.* 56:37–49. <http://dx.doi.org/10.1016/j.apgeochem.2015.02.005>.
- Todesco, M., Chiodini, G., Macedonio, G., 2003. Monitoring and modelling hydrothermal fluid emission at La Solfatara (Phlegrean Fields, Italy). An interdisciplinary approach to the study of diffuse degassing. *J. Volcanol. Geotherm. Res.* 125:57–79. [http://dx.doi.org/10.1016/S0377-0273\(03\)00089-1](http://dx.doi.org/10.1016/S0377-0273(03)00089-1).
- Valentino, G.M., Stanzione, D., 2003. Source processes of the thermal waters from the Phlegrean Fields (Naples, Italy) by means of the study of selected minor and trace elements distribution. *Chem. Geol.* 194, 245–274.
- Valentino, G.M., Stanzione, D., 2004. Geochemical monitoring of the thermal waters of the Phlegrean Fields. *J. Volcanol. Geotherm. Res.* 133:261–289. [http://dx.doi.org/10.1016/S0377-0273\(03\)00402-5](http://dx.doi.org/10.1016/S0377-0273(03)00402-5).
- Valentino, G.M., Cortecchi, G., Franco, E., Stanzione, D., 1999. Chemical and isotopic compositions of minerals and waters from the Campi Flegrei volcanic system, Naples, Italy. *J. Volcanol. Geotherm. Res.* 91, 329–344.
- Vaselli, O., Tassi, F., Montegrossi, G., Capaccioni, B., Giannini, L., 2006. Sampling and analysis of volcanic gases. *Acta Vulcanol.* 18 (1–2), 65–76.
- Vaselli, O., Tassi, F., Tedesco, D., Poreda, J.R., Caprai, A., 2011. Submarine and inland gas discharges from the Campi Flegrei (southern Italy) and the Pozzuoli Bay: geochemical clues for a common hydrothermal-magmatic source. *Proc. Earth Planet. Sci.* 4: 57–73. <http://dx.doi.org/10.1016/j.proeps.2011.11.007>.
- Weinlich, F.H., 2005. Isotopically light carbon dioxide in nitrogen rich gases: the gas distribution pattern in the French Massif Central, the Eifel and the western Eger Rift. *Ann. Geophys.* 48 (1), 19–31.
- Whitfield, M., 1978. Activity coefficients in natural waters. In: Pytkowicz, R.M. (Ed.), *Activity Coefficients in Electrolyte Solutions*. CRC Press, Boca Raton, pp. 153–300.
- Yamada, M., Oshawa, S., Kazahaya, K., Yasuhara, M., Takahashi, H., Amita, K., Mawatari, H., Yoshikawa, S., 2011. Mixing of magmatic CO<sub>2</sub> into volcano groundwater flow at Aso volcano assessed combining carbon and water stable isotopes. *J. Geochem. Explor.* 108:81–87. <http://dx.doi.org/10.1016/j.gexplo.2010.10.007>.
- Zhang, J., Quay, P.D., Wilbur, D.O., 1995. Carbon isotope fractionation during gas-water exchange and dissolution of CO<sub>2</sub>. *Geochim. Cosmochim. Acta* 59 (1), 107–114.



## Carbon isotopic signature of interstitial soil gases reveals the potential role of ecosystems in mitigating geogenic greenhouse gas emissions: Case studies from hydrothermal systems in Italy



S. Venturi<sup>a,\*</sup>, F. Tassi<sup>a,b</sup>, F. Magi<sup>b</sup>, J. Cabassi<sup>a</sup>, A. Ricci<sup>c</sup>, F. Capecciacci<sup>b</sup>, C. Caponi<sup>b</sup>, B. Nisi<sup>d</sup>, O. Vaselli<sup>a,b</sup>

<sup>a</sup> Institute of Geosciences and Earth Resources (IGG), National Research Council of Italy (CNR), Via G. La Pira 4, 50121 Florence, Italy

<sup>b</sup> Department of Earth Sciences, University of Florence, Via G. La Pira 4, 50121 Florence, Italy

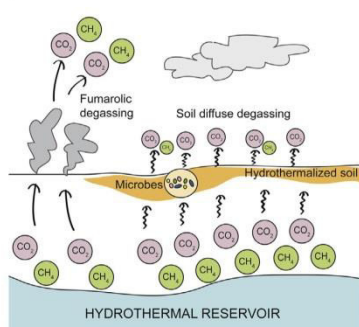
<sup>c</sup> Department of Biological, Geological and Environmental Sciences, University of Bologna, Porta S. Donato 1, 40127 Bologna, Italy

<sup>d</sup> Institute of Geosciences and Earth Resources (IGG), National Research Council of Italy (CNR), Via G. Moruzzi 1, 56124 Pisa, Italy

### HIGHLIGHTS

- Greenhouse gases are released from hydrothermal systems through diffuse degassing.
- Carbon in CO<sub>2</sub> from soil gases is isotopically heavier than that from fumaroles.
- CO<sub>2</sub>/CH<sub>4</sub> ratios in soil gases are higher than those measured in fumarolic emissions.
- Autotrophs and methanotrophs mitigate the release of geogenic greenhouse gases.
- Microbes contribute to regulate CH<sub>4</sub> (and CO<sub>2</sub>) emissions from hydrothermal areas.

### GRAPHICAL ABSTRACT



### ARTICLE INFO

#### Article history:

Received 13 August 2018

Received in revised form 18 November 2018

Accepted 20 November 2018

Available online 22 November 2018

Editor: Mae Sexauer Gustin

#### Keywords:

Volcanic and hydrothermal systems

Greenhouse gases

CH<sub>4</sub> consumption

Carbon isotopes

Soil gases

### ABSTRACT

Volcanic and hydrothermal areas largely contribute to the natural emission of greenhouse gases to the atmosphere, although large uncertainties in estimating their global output still remain. Nevertheless, CO<sub>2</sub> and CH<sub>4</sub> discharged from hydrothermal fluid reservoirs may support active soil microbial communities. Such secondary processes can control and reduce the flux of these gases to the atmosphere. In order to evaluate the effects deriving from the presence of microbial activity, chemical and carbon (in CO<sub>2</sub> and CH<sub>4</sub>) isotopic composition of interstitial soil gases, as well as diffuse CO<sub>2</sub> fluxes, of three hydrothermal systems from Italy were investigated, i.e. (i) Solfatara crater (Campi Flegrei), (ii) Monterotondo Marittimo (Larderello geothermal field) and (iii) Baia di Levante in Vulcano Island (Aeolian Archipelago), where soil CO<sub>2</sub> fluxes up to 2400, 1920 and 346 g m<sup>-2</sup> day<sup>-1</sup> were measured, respectively. Despite the large supply of hydrothermal fluids, <sup>13</sup>C<sub>2</sub> enrichments were observed in interstitial soil gases with respect to the fumarolic gas discharges, pointing to the occurrence of autotrophic CO<sub>2</sub> fixation processes during the migration of deep-sourced fluids towards the soil-air interface. On the other hand, (i) the δ<sup>13</sup>C-CH<sub>4</sub> values (up to -48‰ vs. V-PDB higher than those measured at the fumarolic emissions) of the interstitial soil gases and (ii) the comparison of the CO<sub>2</sub>/CH<sub>4</sub> ratios between soil gases and fumarolic

\* Corresponding author.

E-mail addresses: [stefania.venturi@igg.cnr.it](mailto:stefania.venturi@igg.cnr.it) (S. Venturi), [franco.tassi@unifi.it](mailto:franco.tassi@unifi.it) (F. Tassi), [francesco.magi@unifi.it](mailto:francesco.magi@unifi.it) (F. Magi), [jacopo.cabassi@igg.cnr.it](mailto:jacopo.cabassi@igg.cnr.it) (J. Cabassi), [andrea.ricci34@unibo.it](mailto:andrea.ricci34@unibo.it) (A. Ricci), [francesco.capecciacci@unifi.it](mailto:francesco.capecciacci@unifi.it) (F. Capecciacci), [chiara.caponi@unifi.it](mailto:chiara.caponi@unifi.it) (C. Caponi), [barbara.nisi@igg.cnr.it](mailto:barbara.nisi@igg.cnr.it) (B. Nisi), [orlando.vaselli@unifi.it](mailto:orlando.vaselli@unifi.it) (O. Vaselli).

<https://doi.org/10.1016/j.scitotenv.2018.11.293>  
0048-9697/© 2018 Elsevier B.V. All rights reserved.

emissions suggested that the deep-sourced CH<sub>4</sub> was partly consumed by methanotrophic activity, as supported by isotope fractionation modeling. These findings confirmed the key role that methanotrophs play in mitigating the release of geogenic greenhouse gases from volcanic and hydrothermal environments.

© 2018 Elsevier B.V. All rights reserved.

## 1. Introduction

Carbon dioxide and methane are considered among the main greenhouse gases responsible for the current global warming (e.g. IPCC, 2007a). Concentrations of these gases in the atmosphere have roughly doubled since the late 18th century (Ciais et al., 2013), reaching 404 ppmv and 1859 ppbv in October 2018, respectively (data from the NOAA/ESRL Global Monitoring Division; [www.esrl.noaa.gov/gmd](http://www.esrl.noaa.gov/gmd)). Whilst the main reason for the rapid increment in the low atmosphere of CO<sub>2</sub> and CH<sub>4</sub> must be sought in anthropogenic activities related to the massive exploitation (and burning) of fossil fuels since the beginning of the industrial era, their quantification from natural sources at a global scale still suffers from large degrees of uncertainty (e.g. Burton et al., 2013; Mörner and Etiope, 2002). Among geogenic sources, degassing from volcanic and associated hydrothermal areas is responsible for a large fraction of the natural CO<sub>2</sub> emissions (e.g. Holloway et al., 2007), with a global subaerial volcanic CO<sub>2</sub> flux estimated at  $540 \times 10^{12}$  g/yr (Burton et al., 2013). Carbon dioxide discharged from fumarolic vents and diffuse soil degassing was recognized as an important mechanism for gas release from volcanoes (Mörner and Etiope, 2002), which at a local scale may exceed that emitted from volcanic plumes (e.g. Baubron et al., 1991; Chiodini et al., 1998; Italiano et al., 1998). Areas characterized by intense diffuse degassing significantly (and persistently) contribute to the total gas emissions from volcanic/hydrothermal systems (Cardellini et al., 2003; Chiodini et al., 2004; Granieri et al., 2010; Tassi et al., 2013; Viveiros et al., 2010), with associated CO<sub>2</sub> fluxes that are often larger than those related to the fumarolic vents occurring in the same areas (e.g. D'Alessandro et al., 2006; Pecoraino et al., 2005; Chiodini et al., 2010; Aiuppa et al., 2013).

Despite the fact that the Global Warming Potential (GWP) of CH<sub>4</sub> is 25 times higher than that of CO<sub>2</sub> (IPCC, 2007b), the global CH<sub>4</sub> output from volcanic and hydrothermal areas is still largely unknown (Mörner and Etiope, 2002). In general, whilst contributions from the biosphere to atmospheric CH<sub>4</sub> are relatively well characterized, accounting for  $345 \times 10^{12}$  g CH<sub>4</sub>/yr (Etiope and Klusman, 2002), few data are available for those released from geogenic sources, which, according to Etiope and Klusman (2002), should account for  $30\text{--}70 \times 10^{12}$  g CH<sub>4</sub>/yr. Geogenic CH<sub>4</sub> contributions are expected to be relevant within peculiar geological settings (e.g. Cardellini et al., 2003; Castaldi and Tedesco, 2005; D'Alessandro et al., 2009, 2011; Tassi et al., 2013, 2015a), such as those that characterize the Italian peninsula, where the numerous volcanic and hydrothermal areas discharge up to  $0.043 \times 10^{12}$  g CH<sub>4</sub>/yr (Etiope et al., 2007), i.e. an amount comparable to that emitted from the European geothermal areas (about  $10^{11}$  g CH<sub>4</sub>/yr). Nevertheless, the CO<sub>2</sub>/CH<sub>4</sub> ratio from diffuse degassing is generally higher than that measured in the fumarolic discharges from the same areas, suggesting that CH<sub>4</sub> is partially lost as the deep-seated gas flows through the soil (D'Alessandro et al., 2009).

Soil is considered the largest biological sink for atmospheric CH<sub>4</sub>, responsible for a global uptake of about  $22 \times 10^{12}$  g CH<sub>4</sub>/yr (Dutaur and Verchot, 2007). More than 50% of CH<sub>4</sub> permeating the soil is consumed by methanotrophs before being emitted to the atmosphere (Reeburgh, 2003). These bacteria use CH<sub>4</sub> as energy source producing CO<sub>2</sub> (e.g. Conrad, 1996; Hanson and Hanson, 1996; Op den Camp et al., 2009). Until ten years ago, all the known species of methanotrophs were affiliated to the bacterial phylum *Proteobacteria*, in the classes Gamma- and Alpha-proteobacteria, which, being characterized by an optimum growth temperature below 60 °C and pH >4 (Op den Camp et al., 2009 and references therein), were not expected to thrive in hot and acidic

conditions occurring in soils from volcanic and hydrothermal areas. Nevertheless, CH<sub>4</sub> oxidation in laboratory tests on soils from Solfatara crater (southern Italy) with pH down to 1.8 suggested the occurrence of methanotrophic activity even under hotter (up to 70 °C) and more acidic conditions (Castaldi and Tedesco, 2005). Finally, in 2007–2008, non-proteobacterial thermoacidophilic methanotrophs, belonging to the phylum *Verrucomicrobia*, were identified in soils and acidic hot springs from hydrothermal areas (Dunfield et al., 2007; Islam et al., 2008; Pol et al., 2007). Recent studies highlighted the presence of methanotrophic microbial communities in volcanic and hydrothermal soils based on microbiological analyses (e.g. Gagliano et al., 2014, 2016; Sharp et al., 2014) and novel species were identified able to thrive under a variety of harsh conditions, suggesting that methanotrophs likely have a wider distribution in hydrothermal environments than that previously supposed (e.g. Carere et al., 2017; van Teeseling et al., 2014). Accordingly, methanotrophic activity in hydrothermal soils was inferred on the basis of geochemical tracers, such as soil CO<sub>2</sub> and CH<sub>4</sub> flux measurements and chemical and isotopic analysis of interstitial soil gases (e.g. Castaldi and Tedesco, 2005; D'Alessandro et al., 2009, 2011; Tassi et al., 2015b).

On the other hand, both field and experimental studies (e.g. Beulig et al., 2015; Khadem et al., 2011; Nowak et al., 2015; Oppermann et al., 2010) suggested that high CO<sub>2</sub> concentrations, such as those characterizing soil gases in diffuse degassing areas, may favor microbial carbon fixation via autotrophic pathways, leading to a significant incorporation of geogenic CO<sub>2</sub> into the microbial carbon pool. The capability of microbes to incorporate CO<sub>2</sub> and oxidize CH<sub>4</sub> in the soil system before these gases are released to the atmosphere renders these communities particularly appealing in terms of bioremediation technologies and mitigation of greenhouse gas emissions (e.g. Farhan Ul Haque et al., 2018; Oppermann et al., 2010; Semrau, 2011; Strong et al., 2015; Trotsenko et al., 2009). Since microbiological investigations are generally quite expensive, extensive sampling surveys are rarely carried out. Geochemical tracers offer the opportunity to widen our knowledge on the distribution and effectiveness of microbial consumption of greenhouse gases in soils affected by geogenic CO<sub>2</sub> and CH<sub>4</sub> fluxes in natural environments.

In this paper, we reported (i) soil CO<sub>2</sub> flux measurements, (ii) chemical analysis of interstitial soil gases, and (iii) carbon isotopic analysis of interstitial soil CO<sub>2</sub> and CH<sub>4</sub> carried out in three hydrothermal systems from southern and central Italy, i.e. Solfatara crater (Campi Flegrei, Naples), Monterotondo Marittimo (within the Larderello geothermal field, Tuscany), and Baia di Levante at Vulcano Island (Aeolian Archipelago). The main aim was to investigate the contribution of these diffuse degassing areas to the output of greenhouse gases and the potential role that the soil ecosystems can play in mitigating CO<sub>2</sub> and CH<sub>4</sub> emissions to the atmosphere.

## 2. Study areas

### 2.1. Solfatara crater

Solfatara crater is a tuff cone located NW of Naples along the Tyrrhenian coast close to the town of Pozzuoli, in southern Italy (Fig. 1a, b). It was formed about 4000 yr BP within the Campi Flegrei caldera, an active volcanic complex of about 100 km<sup>2</sup> that was built during two main eruptive events, i.e. (i) the Campanian Ignimbrite (39 ka; De Vivo et al., 2001) and (ii) the Neapolitan Yellow Tuff (14.9 ka; Deino et al., 2004). The caldera shows strong hydrothermal activity, consisting of thermal springs, steam-heated pools, and fumaroles (e.g. Caliro et al.,

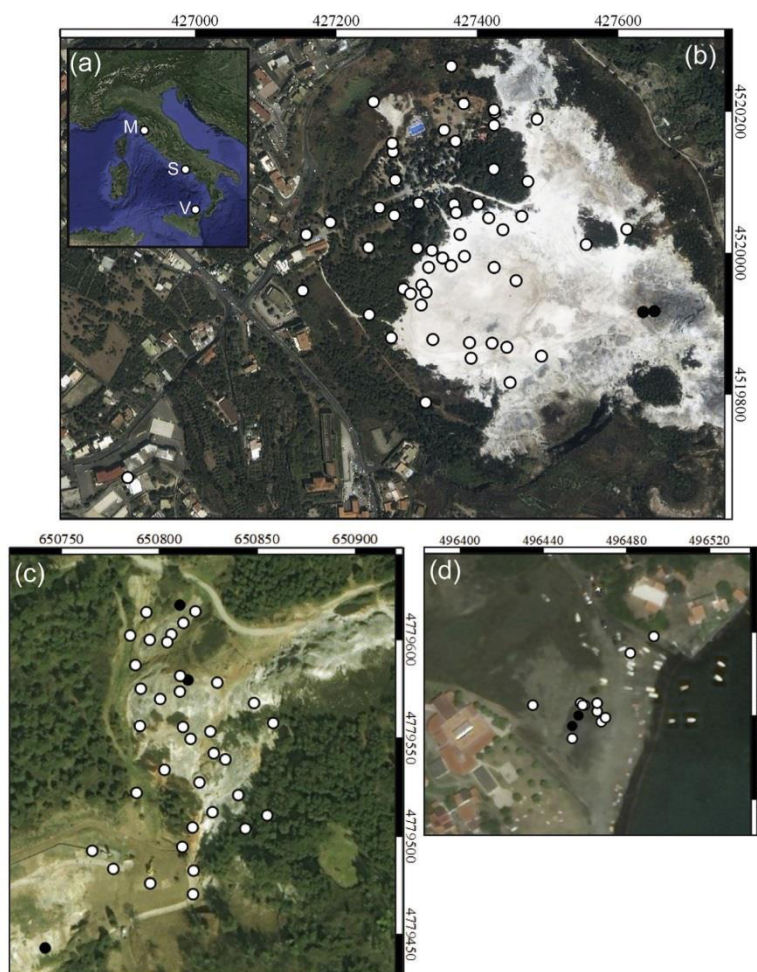


**Fig. 1.** (a) Location of Solfatara crater (S), Monterotondo M.mo (M) and Vulcano Island (V) in Italy. The location of the interstitial soil (white circles) and fumarolic (black circles) gas sampling sites at (b) Solfatara crater, (c) Monterotondo M.mo and (d) Vulcano Island is shown.

2007; Chiodini et al., 2001; Passaro et al., 2016; Todesco et al., 2003; Valentino and Stanzione, 2003, 2004; Vaselli et al., 2011; Venturi et al., 2017). The Solfatara crater hosts one of the largest fumarolic discharges worldwide, mostly located in the NE and SE portions of the crater, with a related thermal energy flux of ~100 MW (Chiodini et al., 2001) and is characterized by a widespread soil diffuse degassing emitting about  $79 \times 10^6$  g CO<sub>2</sub>/day and  $1.04 \times 10^3$  g CH<sub>4</sub>/day from the hydrothermalized bottom area (Tassi et al., 2013). The central part of the Solfatara crater hosts three bubbling acidic mud pools (named *Fangaia*) fed by rainwater, steam condensation, and continuous inputs of hydrothermal gases. Eventually, Mediterranean maquis shrubland covers the Solfatara crater to NW where diffuse degassing is mainly dominated by soil respiration (Tassi et al., 2013).

The fluid source of the CO<sub>2</sub>-rich gas emissions at Solfatara crater consists of a 1.5–2 km deep column of ascending magmatic (about 26%) and hydrothermal (about 74%) fluids (e.g. Caliro et al., 2007;

Cardellini et al., 2017; Chiodini et al., 2001, 2015;) originated by (i) a degassing magma chamber at ~5 km depth (Gottsmann et al., 2006) and (ii) boiling of the overlying aquifer(s). The magmatic fluids mix with meteoric-originated hydrothermal liquids in the lowest part of the hydrothermal system (2–2.5 km depth), generating vapors at temperatures  $\geq 360$  °C and pressures of 200–250 bar (Caliro et al., 2007). Below this mixing zone, magmatic conditions, i.e. high temperatures and presence of magmatic acidic species (i.e. SO<sub>2</sub>, HCl, HF), prevail. Hydrothermal conditions dominate in the upper zone where the reduced gas species (e.g. CH<sub>4</sub> and H<sub>2</sub>S) are formed and the most acidic and oxidizing magmatic compounds are scrubbed (Caliro et al., 2007). According to Caliro et al. (2007), the central column of the ascending fluids is characterized by the presence of a separated vapor phase that moves from the high temperature injection zone to a shallow single phase gas zone at temperatures ranging from 190 to 230 °C and at 100–300 m depths.

## 2.2. Monterotondo Marittimo

Monterotondo Marittimo (hereafter, Monterotondo M.mo; Fig. 1a, c) belongs to the Larderello-Travale geothermal area that spans between the districts of Pisa and Grosseto (Tuscany, Central Italy), in the inner portion of the Apennine orogenic belt. Larderello is the largest and most important geothermal system in Italy and one of a few superheated geothermal systems in the world, together with “The Geysers” in California (Romagnoli et al., 2010). The area is characterized by (i) an anomalous heat flow (1000 mW/m<sup>2</sup>) (Baldi et al., 1995), (ii) a thermal gradient up to 300 °C/km, and (iii) the occurrence of thermal springs, acidic and boiling steam-heated pools, mud pools (here called “*lagoni*”), and steam vents (Duchi et al., 1986, 1992), related to the emplacement, during the Mio-Pliocene post-orogenic magmatism, of granitic intrusives (3.8–2.25 Ma; Dini et al., 2005; Gianelli and Laurenzi, 2001; Villa and Puxeddu, 1994) at depths comprised between 3 and 8 km (K-horizon bright spot; Batini et al., 2003, and references therein). The stratigraphic sequence of the Larderello-Travale area is made up of (Batini et al., 2003, and references therein): (i) Neogene (Late Miocene) and Quaternary continental to marine deposits; (ii) allochthonous Ligurian Complex l.s., consisting of Jurassic oceanic crust remnants (ophiolitic sequences, characterized by gabbros, pillow basalts and serpentinites), and a Jurassic-Eocene sedimentary cover (flysch units); (iii) a Late Triassic-Early Miocene sedimentary carbonate-evaporite sequence (Tuscan Nappe); and (iv) the Tuscan Metamorphic Complex (Permian-Triassic) that includes the upper Monticiano-Roccastrada Unit and the lower Gneiss Complex.

The Larderello geothermal field is mainly fed by meteoric waters, although thermo-metamorphic and magmatic fluids were also recognized (D'Amore and Bolognesi, 1994; Minissale, 1991). Two main geothermal reservoirs occur, as follows: (i) a shallow aquifer (500–1500 m), hosted in the Mesozoic carbonate-evaporite sequence pertaining to the Tuscan Nappe and showing a temperature of 220–260 °C and a pressure of 30–60 bar and (ii) a deep aquifer (<3000 m) within the Paleozoic metamorphic rocks at 300–350 °C and 40–70 bar (Barelli et al., 1995; Bertani et al., 2005).

## 2.3. Vulcano Island

Vulcano Island is located at the southernmost edge of the subduction-related Aeolian volcanic arc (southern Italy), in the Southern Tyrrhenian Sea (Fig. 1a). The island consists of (i) a main edifice developed during the last 130 ky through several phases of stratocone building and caldera collapses (De Astis et al., 1997; Keller, 1980) and (ii) a smaller island (Vulcanello), consisting of lavas and pyroclastic deposits, formed between 1000 and 1250 CE (Arrighi et al., 2006). La Fossa crater represents the presently active volcanic center where the last eruptive event took place in 1888–1890 (e.g. Clocchiatti et al., 1994). Fumarolic activity occurs at both La Fossa crater and the bay delimiting the eastern side of the isthmus that connects Vulcano to Vulcanello (Baia di Levante; Fig. 1d). The gas emissions at La Fossa crater show outlet temperatures up to 450 °C and a typical magmatic composition, with a dry gas fraction dominated by CO<sub>2</sub> and relatively high concentrations of SO<sub>2</sub>, H<sub>2</sub>S, HCl and HF (e.g. Capasso et al., 1997, 1999; Inguaggiato et al., 2012). The Baia di Levante subaerial and submerged fumaroles are characterized by outlet temperatures <100 °C and a typical hydrothermal composition, consisting of H<sub>2</sub>O, CO<sub>2</sub> and H<sub>2</sub>S with relatively high CH<sub>4</sub> contents (Capaccioni et al., 2001), the latter two gases likely produced by interactions between deep originated fluids and a shallow aquifer (Capasso et al., 1997, 2001a; Chiodini et al., 1995). Geothermal exploratory wells drilled near Baia di Levante (AGIP-Sommaruga, 1984; Todesco, 1995) suggested the presence of the multi-layer hydrothermal system, which consists of (i) a shallow aquifer (at 7–14 m depth) at ~100 °C, (ii) an intermediate aquifer (at ~100 m depth) with a temperature of ~136 °C, and (iii) a deep aquifer at ~200 m depth and nearly ~200 °C with a seawater-like chemical composition.

## 3. Materials and methods

### 3.1. Soil CO<sub>2</sub> flux measurements

Soil CO<sub>2</sub> flux measurements were carried out following the accumulation chamber (AC) method (Chiodini et al., 1998). A cylindrical chamber (basal area 200 cm<sup>2</sup>; inner volume: 3060 cm<sup>3</sup>) was placed firmly on the ground and the gas was continuously pumped from the chamber, using a low-flux pump (20 mL/s), to an Infra-Red (IR) spectrophotometer (Licor® Li-820; measurement range: 0–20,000 ppm; accuracy: 4%). Once passed through the detector, the gas was injected back into the chamber to minimize the disturbance of the gas flux. An analog-to-digital (AD) converter allowed to visualize the increase in time of the CO<sub>2</sub> concentration inside the chamber (dC<sub>CO2</sub>/dt) on a palmtop computer equipped with a dedicated software. The CO<sub>2</sub> flux from the soil (ΦCO<sub>2</sub>) was then determined, as follows (Chiodini et al., 1998):

$$\Phi\text{CO}_2 = cf \times d\text{C}_{\text{CO}_2}/dt \quad (1)$$

where *cf* is a constant factor, which depends on (i) the geometry of the measuring equipment and (ii) the air temperature and pressure (Chiodini et al., 1998). The proportionality (*cf*) between dC<sub>CO2</sub>/dt and ΦCO<sub>2</sub> was determined by laboratory tests, during which the ΦCO<sub>2</sub> values from soil were simulated by injecting CO<sub>2</sub> at different known fluxes into the accumulation chamber. Several measurements were performed in the range from 10 to 10,000 g m<sup>-2</sup> day<sup>-1</sup> by checking the imposed flux by means of a precision flowmeter (accuracy 1.5%).

### 3.2. Sampling and analytical procedures for fumarolic fluids and interstitial soil gases

Fumarolic gases were collected by inserting a Titanium tube into the fumarolic vent and then, connected to a sampling line consisting of a series of dewared glass tubes (Vaselli et al., 2006), which conveyed the gas into (i) a pre-evacuated 60 mL glass flask, equipped with a Thorion® valve, containing a 4 M NaOH and 0.15 M Cd(OH)<sub>2</sub> suspension (Montegrossi et al., 2001), or (ii) a Graham type condenser connected, through a PTFE three-way valve, to a 12 mL Labco Exetainer® glass vial for the sampling of the dry gas fraction (Tassi et al., 2015a).

A stainless-steel tube (inner diameter 0.4 cm) was inserted at 5 to 20 cm depth to collect interstitial soil gases. The tube was then connected, through a PTFE three-way valve, to a 60 mL plastic syringe used for pumping the gas from the tube, and to (i) a 12 mL glass vial, equipped with a pierceable rubber septum (Labco Exetainer®), for chemical analyses, and (ii) a 1 L Supelco's Tedlar® gas sampling bag, equipped with a push/pull lock valve, for isotopic analyses (Tassi et al., 2015a, 2015b). Soil temperature was determined by inserting a thermocouple in the soil down to the sampling depth.

Gas analyses were carried out by Gas-Chromatography (GC) using (i) a Shimadzu 15A GC equipped with a Thermal Conductivity Detector (TCD) and either a 10 m long 5A Molecular Sieve column (for N<sub>2</sub>, O<sub>2</sub>, Ar and H<sub>2</sub> both in the headspace of the glass flasks and in the glass vials for fumarolic and interstitial soil gases, respectively), or a 3 m long column filled with 80/100 mesh Porapak Q (for CO<sub>2</sub> and H<sub>2</sub>S in the interstitial soil gases), (ii) a Shimadzu 14A GC equipped with a Flame Ionization Detector (FID) and a 10 m long stainless steel column filled with 23% SP 1700 on Chromosorb PAW (80/100 mesh) for the analysis of light hydrocarbons (C<sub>1</sub>–C<sub>3</sub>), and (iii) Thermo Trace Ultra GC coupled with a Thermo DSQ Quadrupole Mass Spectrometer (MS) for the analysis of C<sub>4+</sub> VOCs in fumarolic and soil gases. Sample injection into the GC-MS was carried out after exposing the gas samples collected in the glass vials to a 2 cm long DiVinylBenzene – Carboxen – PolyDiMethylSiloxane fiber (Supelco; Bellefonte, PA, USA) for 30 min at 20 °C (Solid Phase Micro Extraction, SPME; Arthur and Pawliszyn, 1990). The analytes absorbed on the fiber were then desorbed into the GC column headspace at 220 °C (Tassi et al., 2012a, 2015a, 2015b). Carbon dioxide

and H<sub>2</sub>S, dissolved into the alkaline solution of the sampling flasks, were analyzed as CO<sub>3</sub><sup>2-</sup> by automatic titration (AT; Metrohm 794 Basic Titrino) using a 0.5 M HCl solution, and SO<sub>4</sub><sup>2-</sup> by ionic chromatography (IC; Metrohm 761 Compact) after oxidation with H<sub>2</sub>O<sub>2</sub>, respectively (Montegrossi et al., 2001; Vaselli et al., 2006). Analytical errors for AT, IC and GC were <5%.

The carbon isotopic composition of CO<sub>2</sub> and CH<sub>4</sub> ( $\delta^{13}\text{C-CO}_2$  and  $\delta^{13}\text{C-CH}_4$ , expressed as ‰ vs. V-PDB) was analyzed by Cavity Ring-Down Spectroscopy (CRDS) using a Picarro G2201-i Analyzer. In order to avoid interferences, the instrument inlet line was equipped with (i) a Drierite trap and (ii) a copper trap to remove water vapor and H<sub>2</sub>S, respectively. According to the operative ranges of the Picarro G2201-i instrument, gas samples showing CO<sub>2</sub> and CH<sub>4</sub> concentrations higher than 2000 ppmv and 500 ppmv, respectively, were diluted with high purity chromatographic air. Gas samples with CO<sub>2</sub>/CH<sub>4</sub> ratios higher than those of the operative ranges were treated by using a bubbler partially filled with a 4 M NaOH solution to remove carbon dioxide prior the CRDS analysis. Internal standards consisting of CO<sub>2</sub> and CH<sub>4</sub> (Air Liquide), with  $\delta^{13}\text{C-CO}_2$  and  $\delta^{13}\text{C-CH}_4$  of  $-28$  and  $-60$ ‰ vs. V-PDB were used to calibrate and test the reproducibility of the Picarro measurements. The analytical error for  $\delta^{13}\text{C-CO}_2$  and  $\delta^{13}\text{C-CH}_4$  was 0.16 and 1.15‰, respectively, whilst the concentrations of CO<sub>2</sub> and CH<sub>4</sub> were differing of <5% and 10%, respectively, when compared to those measured by GC.

## 4. Results

### 4.1. Solfatara crater

#### 4.1.1. Chemical composition of fumarolic gases

Fumarolic gases were collected from Bocca Grande (SF1) and Bocca Nuova (SF2) vents, located in the eastern portion of the crater (Fig. 1b). The chemical composition of fumarolic dry gases (SF1 and SF2; Table S11; Fig. 1b) was largely dominated by CO<sub>2</sub> (up to 983 mmol/mol), followed by H<sub>2</sub>S (up to 15 mmol/mol), N<sub>2</sub> and H<sub>2</sub> (up to 3.1 and 2.3 mmol/mol, respectively). Minor amounts of CH<sub>4</sub> (up to 66  $\mu\text{mol/mol}$ ) and C<sub>2</sub>H<sub>6</sub> (up to 3.9  $\mu\text{mol/mol}$ , respectively) were also measured. Molecular oxygen (O<sub>2</sub>) and Ar were present at low concentrations ( $\leq 4.1$  and 3.6  $\mu\text{mol/mol}$ , respectively). Benzene (C<sub>6</sub>H<sub>6</sub>), C<sub>3</sub>H<sub>8</sub> and iC<sub>4</sub>H<sub>8</sub> were up to 1.9, 0.81 and 0.75  $\mu\text{mol/mol}$ , respectively.

The isotopic composition of CO<sub>2</sub> at SF1 and SF2 were from  $-1.3$  to  $-1.1$ ‰, whilst those of CH<sub>4</sub> were from  $-18.7$  and  $-18.5$ ‰, respectively (Table S11). These values are consistent with those reported from previous studies carried out for the Solfatara fumaroles, i.e.  $\delta^{13}\text{C-CO}_2$  from  $-2$  to  $-0.95$ ‰ (Chiodini et al., 2008; Tassi et al., 2015a; Vaselli et al., 2011) and  $\delta^{13}\text{C-CH}_4$  from  $-18.1$  to  $-17.8$ ‰ (Tassi et al., 2012b).

#### 4.1.2. Soil temperatures, diffuse CO<sub>2</sub> fluxes from the soil and chemical composition of interstitial soil gases

Soil temperature and  $\Phi\text{CO}_2$  measurements, and soil gas sampling were carried out at 54 sites (Fig. 1b). Soil temperatures at 20 cm depth ranged from 25.3 to 72.7 °C (Table S11). The highest temperatures were measured in the surroundings of the Fangai mud pool, in agreement with those reported by other investigations (e.g. Byrdina et al., 2014; Chiodini et al., 2001; Montanaro et al., 2017; Tassi et al., 2013), although relatively high temperatures (up to 53.4 °C) were also recorded on the NW inner flank of the crater. Differently, temperatures in the vegetated portion of the crater and outside the crater were  $<35$  °C.

Diffuse CO<sub>2</sub> fluxes from the soil varied over a wide range, i.e. from 5.0 to 2400 g m<sup>-2</sup> day<sup>-1</sup> (Table S11), the highest values ( $>200$  g m<sup>-2</sup> day<sup>-1</sup>) being generally detected in those areas showing relatively high soil temperatures, whereas lower  $\Phi\text{CO}_2$  values ( $<50$  g m<sup>-2</sup> day<sup>-1</sup>) were measured where Mediterranean maquis shrubland occurred.

The chemical composition of interstitial soil gases collected at 20 cm depth (Table S11) varied from CO<sub>2</sub>-dominated to N<sub>2</sub>-dominated. The former had CO<sub>2</sub>/N<sub>2</sub> ratios ranging from 1.1 to 28 whilst the latter had

CO<sub>2</sub>/N<sub>2</sub> ratios from 0.04 to 0.72. The CO<sub>2</sub>-dominated soil gases, collected from sites with  $\Phi\text{CO}_2$  values ranging from 213 to 2400 g m<sup>-2</sup> day<sup>-1</sup> and temperatures from 31.0 to 72.7 °C, were characterized by CO<sub>2</sub> concentrations between 517 and 965 mmol/mol and relevant concentrations of H<sub>2</sub>S and H<sub>2</sub> (up to 0.94 and 0.81 mmol/mol, respectively). In these samples, the concentrations of CH<sub>4</sub> varied from 1.5 to 29  $\mu\text{mol/mol}$ , whilst those of C<sub>2</sub>H<sub>6</sub> and C<sub>6</sub>H<sub>6</sub> were up to 3.9 and 2.6  $\mu\text{mol/mol}$ , respectively. Minor amounts of C<sub>3</sub>H<sub>8</sub> and iC<sub>4</sub>H<sub>8</sub> ( $\geq 0.19$  and  $\geq 0.15$   $\mu\text{mol/mol}$ , respectively) were also measured. The concentrations of N<sub>2</sub>, O<sub>2</sub> and Ar were relatively low ( $\leq 480$ ,  $\leq 10$ , and  $\leq 3.3$  mmol/mol, respectively). The N<sub>2</sub>-dominated soil gases, collected from sites with  $\Phi\text{CO}_2$  values ranging from 5 to 440 g m<sup>-2</sup> day<sup>-1</sup> and temperatures from 25.3 to 57.6 °C, showed concentrations of N<sub>2</sub>, O<sub>2</sub>, and Ar up to 923, 99 and 12 mmol/mol, respectively, whilst those of CO<sub>2</sub> were from 33 to 418 mmol/mol. Relatively low contents of H<sub>2</sub>S, H<sub>2</sub> ( $\leq 0.23$  and  $\leq 0.25$  mmol/mol, respectively), C<sub>2</sub>H<sub>6</sub>, C<sub>6</sub>H<sub>6</sub>, C<sub>3</sub>H<sub>8</sub> and iC<sub>4</sub>H<sub>8</sub> ( $\leq 1.3$ ,  $\leq 0.76$ ,  $\leq 0.26$  and  $\leq 0.25$   $\mu\text{mol/mol}$ , respectively) were measured, whilst CH<sub>4</sub> varied over a wide range, i.e. from 1.7 to 55  $\mu\text{mol/mol}$ .

The isotopic composition of CO<sub>2</sub> ranged from  $-0.76$  to 2.28‰ in the CO<sub>2</sub>-dominated gases, whereas a wider range of  $\delta^{13}\text{C-CO}_2$  values were measured in those interstitial gases dominated by N<sub>2</sub>, i.e. from  $-14.0$  to 1.18‰ (Table S11). Differently, the  $\delta^{13}\text{C-CH}_4$  values showed large variations in both CO<sub>2</sub>- and N<sub>2</sub>-dominated gases, since they were ranging from  $-47.1$  to 27.5‰ and from  $-43.6$  to 10.9‰, respectively (Table S11).

### 4.2. Monterotondo M.mo

#### 4.2.1. Chemical composition of fumarolic gases

The field survey focused on a fumarolic and hydrothermally altered area ( $\sim 0.01$  km<sup>2</sup>; Fig. 1c) located in close proximity to the Lagoni geothermal power plant ("Nuova Monterotondo" ENEL Ltd.), inside "Le Biancane" Natural Park, north of Monterotondo M.mo village. The chemical composition of the dry gases from the fumarolic discharges (Fig. 1c; Table S12) was dominated by CO<sub>2</sub> (from 849 to 870 mmol/mol), followed by N<sub>2</sub> (from 107 to 131 mmol/mol), H<sub>2</sub>S (from 7.6 to 8.5 mmol/mol), H<sub>2</sub> (from 7.3 to 8.1 mmol/mol), and CH<sub>4</sub> (from 4200 to 4650  $\mu\text{mol/mol}$ ). Concentrations of O<sub>2</sub> and Ar were  $\leq 1.9$  and  $\leq 0.76$  mmol/mol, respectively. Among VOCs, C<sub>2</sub>H<sub>6</sub> and C<sub>6</sub>H<sub>6</sub> were the most abundant species (ranging from 6.3 to 7.7  $\mu\text{mol/mol}$  and from 2.7 to 3.2  $\mu\text{mol/mol}$ , respectively), whereas C<sub>3</sub>H<sub>8</sub> and iC<sub>4</sub>H<sub>8</sub> had lower contents ( $\leq 1.6$  and  $\leq 1.9$   $\mu\text{mol/mol}$ , respectively).

The isotopic composition of CO<sub>2</sub> and CH<sub>4</sub> ranged from  $-3.5$  to  $-3.2$ ‰ and from  $-27.1$  to  $-25.5$ ‰, respectively (Table S12), in agreement with the  $\delta^{13}\text{C-CO}_2$  and  $\delta^{13}\text{C-CH}_4$  values (from  $-7.1$  to  $-1.4$  and from  $-31.7$  to  $-20.9$ ‰) reported for hydrothermal fluids from geothermal wells (Gherardi et al., 2005) and fumarolic discharges (Tassi et al., 2012b) in the Larderello geothermal field.

#### 4.2.2. Soil temperatures, diffuse CO<sub>2</sub> fluxes from the soil and chemical composition of interstitial soil gases

Soil temperatures,  $\Phi\text{CO}_2$  measurements and soil gas sampling were carried out in 35 sites (Fig. 1c). Soil temperatures varied from 28.8 to 94.9 °C (Table S12). The highest temperatures were recorded in the northernmost and southernmost edges of the study area. Soil CO<sub>2</sub> fluxes showed a large variability: from 1.2 to 1920 g m<sup>-2</sup> day<sup>-1</sup> (Table S12), and the highest  $\Phi\text{CO}_2$  values were measured in the proximity of the fumarolic emissions (Fig. 1c).

Interstitial soil gases collected at depths ranging from 10 to 20 cm were characterized by CO<sub>2</sub>- or N<sub>2</sub>-dominated compositions (Table S12). The CO<sub>2</sub>-dominated gases were associated with  $\Phi\text{CO}_2$  values ranging from 271 to 1920 g m<sup>-2</sup> day<sup>-1</sup> and temperatures from 47.7 to 94.5 °C, with CO<sub>2</sub> concentrations from 555 to 912 mmol/mol, whilst those of N<sub>2</sub> and Ar were  $\leq 428$  and  $\leq 4.5$  mmol/mol, respectively. Concentrations of O<sub>2</sub> varied over 2 orders of magnitude: from 0.21 to 13 mmol/mol. Hydrogen sulfide and H<sub>2</sub> showed contents ranging from 0.07 to 0.56

mmol/mol and from 0.05 to 0.24 mmol/mol, respectively, whilst those of CH<sub>4</sub> ranged from 2.3 to 355 μmol/mol. Light alkanes, i.e. C<sub>2</sub>H<sub>6</sub> and C<sub>3</sub>H<sub>8</sub>, were characterized by concentrations varying from 1.1 to 5.5 μmol/mol and from 0.21 to 0.95 μmol/mol, respectively, whilst those of C<sub>6</sub>H<sub>6</sub> and iC<sub>4</sub>H<sub>8</sub> ranged from 0.74 to 3.1 μmol/mol and from 0.22 to 1.3 μmol/mol, respectively. The N<sub>2</sub>-dominated gases, collected from sites with φCO<sub>2</sub> values ranging from 1.2 to 94 g m<sup>-2</sup> day<sup>-1</sup> and temperatures from 28.8 to 94.9 °C, were characterized by N<sub>2</sub> and CO<sub>2</sub> concentrations ≥773 and ≤215 mmol/mol, respectively. Argon and O<sub>2</sub> contents varied from 8.2 to 14 mmol/mol and from 2.1 to 123 mmol/mol, respectively. Hydrogen sulfide and H<sub>2</sub> were sporadically detected at concentrations ≤0.16 and ≤0.11 mmol/mol, respectively, whilst those of CH<sub>4</sub> varied from 1.50 to 58 μmol/mol. Other VOCs, including C<sub>2</sub>H<sub>6</sub>, C<sub>6</sub>H<sub>6</sub>, C<sub>3</sub>H<sub>8</sub> and iC<sub>4</sub>H<sub>8</sub>, were occasionally detected in few samples at concentrations ≤0.88, ≤0.56, ≤0.21 and ≤0.25 μmol/mol, respectively.

The δ<sup>13</sup>C-CO<sub>2</sub> and δ<sup>13</sup>C-CH<sub>4</sub> values in the CO<sub>2</sub>- and N<sub>2</sub>-dominated gases spanned quite largely, i.e. from -16.1 to 3.52‰ and from -43.9 to 21.9‰, respectively (Table S12).

#### 4.3. Vulcano Island

##### 4.3.1. Chemical composition of fumarolic gases

Carbon dioxide dominated the chemical composition of the dry gases from fumarolic discharges (978 mmol/mol; Table S13) collected from two vents at Baia di Levante (Fig. 1d), followed by N<sub>2</sub> and H<sub>2</sub>S (from 12 to 13 and from 3.2 to 4.8 mmol/mol, respectively). The fourth most abundant compound was CH<sub>4</sub>, with concentrations ranging from 3.1 to 3.3 mmol/mol, followed by those of H<sub>2</sub> (up to 2.2 mmol/mol), whilst those of Ar and O<sub>2</sub> were up to 0.25 and 0.019 mmol/mol. Among VOCs, C<sub>2</sub>H<sub>6</sub> was the most abundant species, with concentrations up to 6.80 μmol/mol, whilst those of C<sub>3</sub>H<sub>8</sub>, C<sub>6</sub>H<sub>6</sub> and iC<sub>4</sub>H<sub>8</sub> were up to 0.71, 0.43 and 0.11 μmol/mol, respectively.

The δ<sup>13</sup>C-CO<sub>2</sub> and δ<sup>13</sup>C-CH<sub>4</sub> values were from -2.3 to -2.1‰ and from -8.1 to -7.5‰ (Table S13). Similar values were reported for δ<sup>13</sup>C-CO<sub>2</sub> (from -3.1 to -1.7‰) by Capasso et al. (1997) and for δ<sup>13</sup>C-CH<sub>4</sub> (from -7.3 to -5.0‰) by Panichi and Noto (1992) and Nerozzi (2016).

##### 4.3.2. Soil temperatures, diffuse CO<sub>2</sub> fluxes from the soil and chemical composition of interstitial soil gases

Eleven sites were selected at Baia di Levante (Fig. 1d) for temperature and φCO<sub>2</sub> measurements and soil gas sampling at 10 cm depth (except for site V11 where a thick and hard carapace did not allow to reach depths >5 cm) and 30 cm depth (except for sites where the soil gas sampling was impeded by the shallowness of the marine water table). Soil temperatures measured at 5 and 10 cm depths ranged from 21.5 to 37.5 °C, whereas they varied from 27 to 30.9 °C at 30 cm depth (Table S13). Diffuse CO<sub>2</sub> fluxes ranged from 2.6 to 346 g m<sup>-2</sup> day<sup>-1</sup> (Table S13). Nitrogen was the most abundant gaseous species of the interstitial soil gases, ranging from 537 to 981 mmol/mol and decreasing with increasing sampling depth (Table S13). Ar and O<sub>2</sub> concentrations varied from 6.2 to 15 mmol/mol and from 2.9 to 51 mmol/mol, respectively, at shallow depths and from 7.5 to 15 mmol/mol and 3.1 to 29 mmol/mol, respectively, at 30 cm depth. The CO<sub>2</sub> concentrations, inversely correlated to those of N<sub>2</sub>, varied from 3.2 to 411 mmol/mol at shallow depths and showed a direct correlation with the sampling depth, with concentrations at 30 cm depth (from 15 to 216 mmol/mol) from 3.1 to 5.8 times higher than those measured at 10 cm depth at the same sites (Table S13). Similar trends were shown by the CH<sub>4</sub> concentrations that ranged from 1.7 to 3.9 μmol/mol at 5 and 10 cm depths and from 4.2 to 7.5 μmol/mol at 30 cm depth. Hydrogen sulfide (≤0.58 mmol/mol), H<sub>2</sub> (≤0.44 mmol/mol), C<sub>2</sub>H<sub>6</sub> (≤0.84 μmol/mol), C<sub>6</sub>H<sub>6</sub> (≤0.23 μmol/mol) and C<sub>3</sub>H<sub>8</sub> (≤0.22 μmol/mol) were sporadically detected.

The δ<sup>13</sup>C-CO<sub>2</sub> and δ<sup>13</sup>C-CH<sub>4</sub> values ranged from -15.5 to 1.44‰ and from -47.7 to 6.47‰, respectively, with no clear trend with respect to sampling depth (Table S13).

## 5. Discussion

Carbon dioxide was the dominant gas species in the investigated hydrothermal fluids. Accordingly, the uprising of CO<sub>2</sub>-rich fluids from the deep hydrothermal systems produced anomalous φCO<sub>2</sub> values in the investigated areas, i.e. up to 2400 g m<sup>-2</sup> day<sup>-1</sup>, 1920 g m<sup>-2</sup> day<sup>-1</sup> and 346 g m<sup>-2</sup> day<sup>-1</sup> at Solfatara crater, Monterotondo M.mo and Vulcano Island, respectively. High φCO<sub>2</sub> values were generally associated with (i) high soil temperatures (Fig. 2a), produced by steam condensation at relatively shallow depths, and (ii) high concentrations of CO<sub>2</sub> in interstitial soil gases (Fig. 2b), coupled with relevant concentrations of other hydrothermal-derived gases (H<sub>2</sub>S, H<sub>2</sub> and VOCs) and inversely correlated to air-related species (N<sub>2</sub>, O<sub>2</sub> and Ar; Fig. 2c).

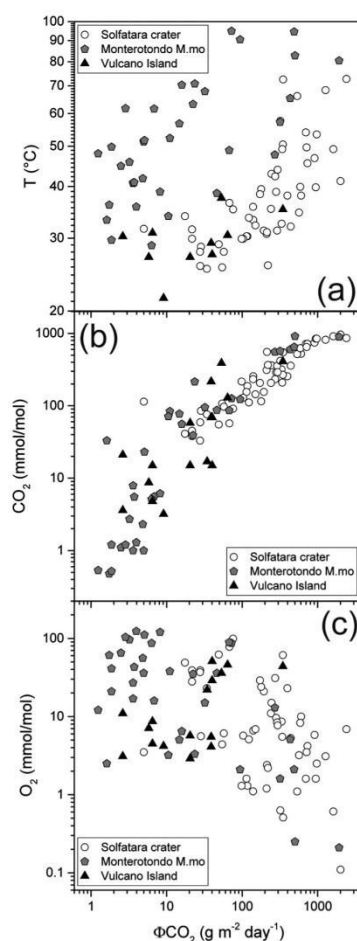


Fig. 2. (a) Soil temperature, (b) soil CO<sub>2</sub> content and (c) soil O<sub>2</sub> concentration vs. φCO<sub>2</sub> binary diagrams for interstitial soil gases from Solfatara crater (white circles), Monterotondo M.mo (grey pentagons) and Vulcano Island (black triangles).

The isotopic composition of CO<sub>2</sub> from the interstitial soil gases approached the δ<sup>13</sup>C-CO<sub>2</sub> values of the fumarolic discharges at increasing CO<sub>2</sub> concentrations (Fig. 3) and ΦCO<sub>2</sub> values. On the other hand, soil gases with relatively low CO<sub>2</sub> contents, collected from sites characterized by ΦCO<sub>2</sub> values approaching typical background soil CO<sub>2</sub> effluxes fed by biogenic sources in the soil (<50 g m<sup>-2</sup> day<sup>-1</sup>; e.g. Chiodini et al., 2008 and references therein), displayed significantly negative δ<sup>13</sup>C-CO<sub>2</sub> values, pointing to an end-member characterized by isotopically light CO<sub>2</sub>. The latter can be identified with a biogenic component, related to soil respiration, characterized by δ<sup>13</sup>C-CO<sub>2</sub> values ≤ -20‰ (Cheng, 1996; Chiodini et al., 2008; Degens, 1969; Viveiros et al., 2010). As evidenced in Fig. 3, the distribution of the measured data is approximately consistent with the theoretical mixing trend between hydrothermal and biogenic CO<sub>2</sub>, coherently with the compositional features of interstitial soil gases.

Nevertheless, the mixing process between hydrothermal and biogenic components does not exhaustively explain the distribution of the measured data, since δ<sup>13</sup>C-CO<sub>2</sub> values higher than those reported for the deep end-member were recorded in all the study areas (Fig. 3). This was clearly evidenced at Solfatara crater (Fig. 3a), where soil gases, characterized by intermediate ΦCO<sub>2</sub> values (up to 972 g m<sup>-2</sup> day<sup>-1</sup>) and CO<sub>2</sub> contents up to 845 mmol/mol, displayed δ<sup>13</sup>C-CO<sub>2</sub> values up to 2.28‰, i.e. significantly heavier than the carbon isotopic values measured at the fumarolic gas discharges.

Different hypotheses can be invoked to explain the observed anomalously high δ<sup>13</sup>C-CO<sub>2</sub> values, as follows: (i) isotope fractionation related to gas diffusion, (ii) partial dissolution of CO<sub>2</sub> in steam condensate, (iii) microbial consumption at shallow depths.

Whilst the upward motion of hydrothermally-derived CO<sub>2</sub> is mainly driven by pressure and temperature gradients (advection) within the CO<sub>2</sub>-enriched soil layer, the gas migration in the shallowest CO<sub>2</sub>-depleted portions of the soil is mainly controlled by diffusion, i.e. a transport mechanism controlled by concentration gradients. Advection is expected to produce negligible isotopic fractionation (e.g. Etiope et al., 2009 and references therein; Kayler et al., 2010), and accordingly, CO<sub>2</sub>-rich soil gases from sites with ΦCO<sub>2</sub> values ≥ 1275 g m<sup>-2</sup> day<sup>-1</sup> at Solfatara crater displayed δ<sup>13</sup>C-CO<sub>2</sub> values similar to those recorded in the fumarolic gas discharges (Fig. 3a). Conversely, diffusion through the soil is able to induce a fractionation effect due to the faster kinetics of <sup>12</sup>CO<sub>2</sub> escaping towards the atmosphere, producing an increase of δ<sup>13</sup>C-CO<sub>2</sub> values within the shallow CO<sub>2</sub>-depleted soil layers (e.g. Cerling and

Quade, 1993; Capasso et al., 1997, 2001b; Di Martino et al., 2016; Etiope et al., 2009 and references therein; Federico et al., 2010; Kayler et al., 2010). Nevertheless, even though it was not possible to develop a diffusion-enrichment model to be compared with field data due to the lack of δ<sup>13</sup>C-CO<sub>2</sub> measurements systematically performed along vertical profiles within the soil, the hypothesis of a <sup>13</sup>C enrichment induced by gas diffusion does not agree with the high ΦCO<sub>2</sub> values (up to 972 g m<sup>-2</sup> day<sup>-1</sup>) and CO<sub>2</sub> contents (>800 mmol/mol) characterizing soil gases, whose δ<sup>13</sup>C-CO<sub>2</sub> values were up to 3‰ higher than those measured in fumarolic discharges.

Steam condensation related to hydrothermal fluids upward motion largely occurs at Solfatara crater, producing a water-saturated layer that emerges from the *Fangaia* mud pool (Chiodini et al., 2001; Bruno et al., 2007; De Landro et al., 2017; Gresse et al., 2017). The isotope fractionation effect related to the dissolution of gaseous CO<sub>2</sub> into the aqueous solution is expected to produce a relative enrichment in <sup>13</sup>C in the residual gas, according to the isotopic enrichment factor ε<sub>CO<sub>2</sub>(aq)-CO<sub>2</sub>(g)</sub> defined by Deines et al. (1974), as follows:

$$\epsilon_{\text{CO}_2(\text{aq})-\text{CO}_2(\text{g})} = \frac{6300}{T^2} - 0.91 \quad (2)$$

where T is the temperature in K. Isotope fractionation related to partial dissolution of CO<sub>2</sub> into steam condensate was indeed previously invoked to explain δ<sup>13</sup>C values recorded in soil gas CO<sub>2</sub> from Iwojima volcano (Japan), which were up to ~6‰ higher than those in fumarolic fluids (Notsu et al., 2005). The partial dissolution of deep-sourced CO<sub>2</sub> into the steam condensate at relatively shallow depths can be modeled as a Rayleigh-type fractionation process under open-system conditions, as follows:

$$\delta^{13}\text{C}-\text{CO}_{2,\text{res}} = \left[ (\delta^{13}\text{C}-\text{CO}_{2,\text{ini}} + 1000) \times f^{\left(\frac{\epsilon_{\text{CO}_2(\text{aq})-\text{CO}_2(\text{g})}}{1000}\right)} \right] - 1000 \quad (3)$$

where δ<sup>13</sup>C-CO<sub>2,ini</sub> is the isotopic composition of CO<sub>2</sub> in the uprising hydrothermal fluids (assumed as equal to the average value measured in fumarolic gases), whilst f and δ<sup>13</sup>C-CO<sub>2,res</sub> are the fraction and isotopic composition of the residual CO<sub>2</sub> after the interaction with condensates, respectively. Accordingly, an enrichment of 3‰ of δ<sup>13</sup>C-CO<sub>2</sub> values in soil gases would require a dissolution of ~95% of the deep-sourced CO<sub>2</sub>. However, such an intense CO<sub>2</sub> scrubbing is compatible neither

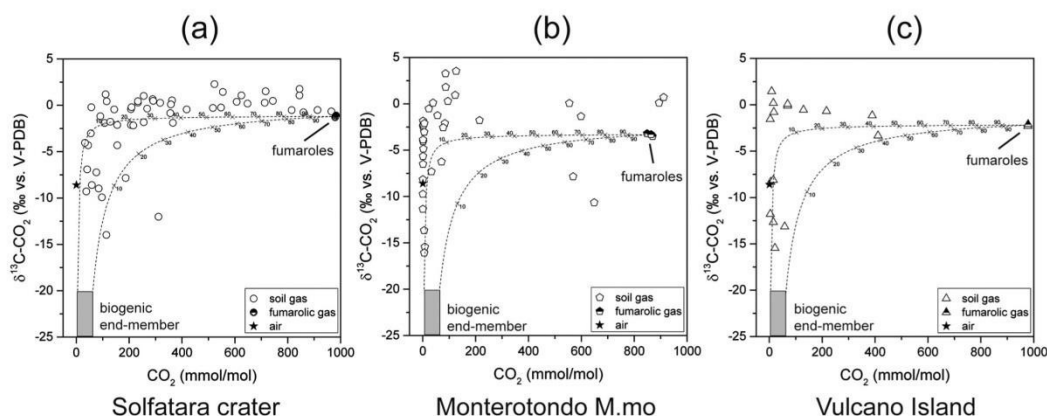


**Fig. 3.** δ<sup>13</sup>C-CO<sub>2</sub> vs. CO<sub>2</sub> binary diagrams for interstitial soil gases from (a) Solfatara crater, (b) Monterotondo M.mo and (c) Vulcano Island. Fumarolic discharges (black and white symbols) and air (black star; Keeling et al., 2005) are reported. The mixing lines between (i) a hydrothermal component, with CO<sub>2</sub> and δ<sup>13</sup>C-CO<sub>2</sub> corresponding to the average values measured in fumarolic gases from each study area, and (ii) a biogenic component, with CO<sub>2</sub> concentrations from 5 to 50 mmol/mol and δ<sup>13</sup>C-CO<sub>2</sub> values ranging from -25 to -20‰, are shown. The fraction (in percentage) of the hydrothermal component involved in the mixture is reported.

with the acidic conditions of the steam condensate (pH values at Fangaia mud pool were  $\leq 1.8$ ; Crognale et al., 2018; Rouwet et al., 2018) nor with the high  $\phi\text{CO}_2$  values measured at sites displaying  $^{13}\text{C}$  enriched soil gases.

Accordingly, biological  $\text{CO}_2$  uptake and fixation processes, which are expected to produce a  $^{13}\text{C}$ -rich residual  $\text{CO}_2$  in interstitial soil gases (e.g. Freude and Blaser, 2016 and references therein; Tassi et al., 2015b and references therein), are the most likely responsible for the heavier  $\delta^{13}\text{C}\text{-CO}_2$  values. Accordingly, autotrophic bacteria were isolated from terrestrial solfataric fields (e.g. Huber et al., 2000; Stetter, 1999), including Solfataria crater (Crognale et al., 2018), where the occurrence of autotrophic  $\text{CO}_2$  fixation in hydrothermal deposits was also confirmed based on the  $\delta^{13}\text{C}$  value of organic carbon (Glamoclija et al., 2004).

In fact, most extremophiles adapted to live in solfataric fields exhibit a chemolithoautotrophic metabolism (Stetter, 2006). Chemosynthetic microbes gain energy for the conversion of  $\text{CO}_2$  or other carbon-containing molecules into organic matter from the oxidation of inorganic compounds, such as  $\text{H}_2$ ,  $\text{H}_2\text{S}$  and  $\text{CH}_4$  (e.g. Carere et al., 2017; Mohammadi et al., 2017), which are largely supplied by the uprising hydrothermal fluids. Accordingly, soil gases from the investigated areas were generally characterized by  $\text{CO}_2/\text{H}_2$ ,  $\text{CO}_2/\text{H}_2\text{S}$  and  $\text{CO}_2/\text{CH}_4$  ratios largely higher than those measured in fumarolic fluids, suggesting the involvement of the deep-sourced reduced gaseous compounds in shallow oxidation processes.

Differently from  $\text{CO}_2$ , the  $\text{CH}_4$  concentrations in fumarolic gases showed large differences among the study areas ( $\sim 65$   $\mu\text{mol/mol}$  at Solfataria crater;  $\sim 4450$   $\mu\text{mol/mol}$  at Monterotondo M.mo;  $\sim 3200$   $\mu\text{mol/mol}$  at Vulcano Island), likely related to the different temperature and redox conditions characterizing the three hydrothermal systems. The  $\text{CH}_4$  concentrations from soil gases were up to 55, 355 and 7.5  $\mu\text{mol/mol}$  at Solfataria crater, Monterotondo M.mo and Vulcano Island, respectively, and inversely correlated to  $\text{O}_2$  (Fig. 4), suggesting that aerobic conditions may limit the  $\text{CH}_4$  levels within the soil pores. On the other hand, differently from other VOCs, especially  $\text{C}_6\text{H}_6$ ,  $\text{iC}_4\text{H}_8$  and even short-chain  $\text{C}_{2-3}$  alkanes, which were strictly correlated to the hydrothermal fluid supply, no evident correlation between  $\text{CH}_4$  and  $\text{CO}_2$  was observed, suggesting that these gas species undergo different processes during fluids uprising towards the surface. In particular, interstitial soil gases were mostly characterized by  $\text{CO}_2/\text{CH}_4$  ratios higher than those recorded in fumarolic fluids, evidencing that methanotrophy is able to significantly affect  $\text{CH}_4$  in the soil.

Wide variations in the isotopic composition of  $\text{CH}_4$  in interstitial soil gases were observed, since  $\delta^{13}\text{C}\text{-CH}_4$  values ranging from  $-47.1$  to  $27.5\%$  at Solfataria crater, from  $-43.9$  to  $21.9\%$  at Monterotondo M.

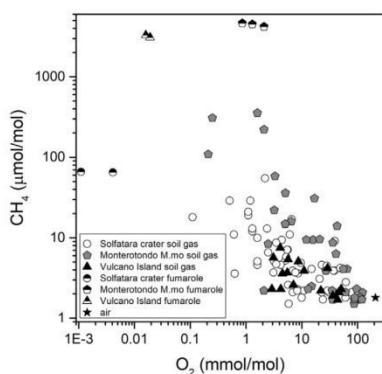


Fig. 4.  $\text{CH}_4$  vs.  $\text{O}_2$  binary diagrams for interstitial soil gases and fumarolic gases (black and white symbols) from (a) Solfataria crater, (b) Monterotondo M.mo and (c) Vulcano Island. The composition of air (black star) is also reported.

mo, from  $-47.7$  to  $6.47\%$  at Vulcano Island were registered. These values significantly differ with respect to those of the fumarolic gases for which a narrower range was observed: from  $-18.7$  to  $-18.5\%$  at Solfataria crater; from  $-27.1$  to  $-25.5\%$  at Monterotondo M.mo; from  $-8.1$  to  $-7.5\%$  at Vulcano Island.

In Fig. 5, the  $\delta^{13}\text{C}\text{-CH}_4$  values from the interstitial soil gases are plotted vs. the  $\text{CH}_4$  contents for Solfataria (Fig. 5a), Monterotondo M.mo (Fig. 5b) and Vulcano Island (Fig. 5c), together with the curves of mixing of the deep hydrothermal end-member (i.e. average fumarolic  $\text{CH}_4$  and  $\delta^{13}\text{C}\text{-CH}_4$  values) with (i) air ("mixing 1"), characterized by  $\text{CH}_4$  and  $\delta^{13}\text{C}\text{-CH}_4$  values of  $\sim 1.8$   $\mu\text{mol/mol}$  and  $\sim -47\%$ , respectively (Nisbet et al., 2016 and references therein), and (ii) a shallow biogenic end-member ("mixing 2"). The latter was assumed to be represented by the soil gas from each study area characterized by (i)  $\delta^{13}\text{C}\text{-CH}_4$  values approaching those of typical microbial  $\text{CH}_4$ , i.e.  $\leq -50$  ‰ (e.g. McCollom and Seewald, 2007; Schoell, 1980; Whiticar, 1999) and (ii) isotopically light  $\text{CO}_2$ . As shown in Fig. 5, the distribution of most values does not follow the depicted mixing trends. Accordingly, secondary processes occurring during hydrothermal fluids upward motion in diffuse degassing areas largely control the isotopic composition of  $\text{CH}_4$ . Despite the clear contribution from hydrothermal fluids revealed by  $\delta^{13}\text{C}\text{-CO}_2$  values within the fumarolic range and relatively high soil  $\text{CO}_2$  fluxes,  $\text{CH}_4$ -rich soil gases with low  $\delta^{13}\text{C}\text{-CH}_4$  values ( $\sim -40\%$ ) were observed at both Solfataria crater and Monterotondo M.mo (Fig. 5a, b). These soil gases were characterized by a difference between  $\delta^{13}\text{C}\text{-CO}_2$  and  $\delta^{13}\text{C}\text{-CH}_4$  values of  $\sim -35\%$  (Tables S11, S12), similar to the carbon isotopic fractionation values obtained by Valentine et al. (2004) during experimental studies on  $\text{H}_2/\text{CO}_2$  methanogenesis. Accordingly, methanogenic activity may partially contribute to the production of  $\text{CH}_4$  under the reducing conditions characterizing the deeper soil layers. On the other hand, the markedly high  $\delta^{13}\text{C}\text{-CH}_4$  values characterizing soil gases with relatively low  $\text{CH}_4$  contents could be related to the occurrence of  $\text{CH}_4$  consumption driven by microbial activity at shallow depths (methanotrophy). In fact,  $^{12}\text{CH}_4$  tends to be oxidized faster than  $^{13}\text{CH}_4$  by methanotrophs, favoring the formation of  $^{13}\text{C}$ -rich residual methane (e.g. Whiticar, 1999).

The isotope fractionation effect related to methanotrophy was depicted on Fig. 5 considering a Rayleigh-type fractionation process, as follows:

$$\delta^{13}\text{C}\text{-CH}_{4,\text{res}} = \left[ (\delta^{13}\text{C}\text{-CH}_{4,\text{ini}} + 1000) \times f^{\left(\frac{1}{\alpha_{\text{CH}_4\text{-CH}_3\text{OH}}}\right)} \right] - 1000 \quad (4)$$

where  $\delta^{13}\text{C}\text{-CH}_{4,\text{ini}}$  is the isotopic composition of  $\text{CH}_4$  in the uprising hydrothermal fluids (assumed as equal to the average value measured in fumarolic gases or, alternatively, to the  $\delta^{13}\text{C}\text{-CH}_4$  value of  $\text{CH}_4$ -rich soil gases likely related to methanogenesis),  $\delta^{13}\text{C}\text{-CH}_{4,\text{res}}$  is the isotopic composition of the residual  $\text{CH}_4$  after the microbial uptake,  $f$  is the fraction of residual  $\text{CH}_4$  and  $\alpha_{\text{CH}_4\text{-CH}_3\text{OH}}$  is the carbon isotope fractionation factor for aerobic bacterial first oxidation of  $\text{CH}_4$  ranging from 1.005 to 1.035 (Templeton et al., 2006). The resulting curves agreed relatively well with the measured data (Fig. 5), suggesting that methanotrophic activity in the soil can partially reduce the emissions of deep-sourced (either thermogenic or biogenic)  $\text{CH}_4$  from solfataric fields. The widest shifts in  $\delta^{13}\text{C}\text{-CH}_4$  values of soil gases relative to fumarolic discharges ( $\sim 46\%$ ) were observed at Solfataria crater and Monterotondo M.mo (Fig. 5a, b), in sites (S49 and M33) characterized by temperatures and  $\text{O}_2$  contents of  $72$  °C and  $6.9$  mmol/mol and  $49$  °C and  $89$  mmol/mol, respectively. During methanotrophy, the oxidation of  $\text{CH}_4$  results in a decrease of  $\text{CH}_4$  concentrations, an increase of  $\text{CO}_2$  contents and a shift of  $\delta^{13}\text{C}$  of residual  $\text{CH}_4$  towards heavier values. Accordingly, a progressive increase in the measured  $\delta^{13}\text{C}\text{-CH}_4$  values was associated with increasing  $\text{CO}_2/\text{CH}_4$  ratios in the interstitial soil gases (Fig. 6a), further supporting the hypothesis of  $\text{CH}_4$  consumption in the soil. As evidenced in Fig. 6b, the isotopic shift of  $\delta^{13}\text{C}\text{-CH}_4$  towards positive values was also

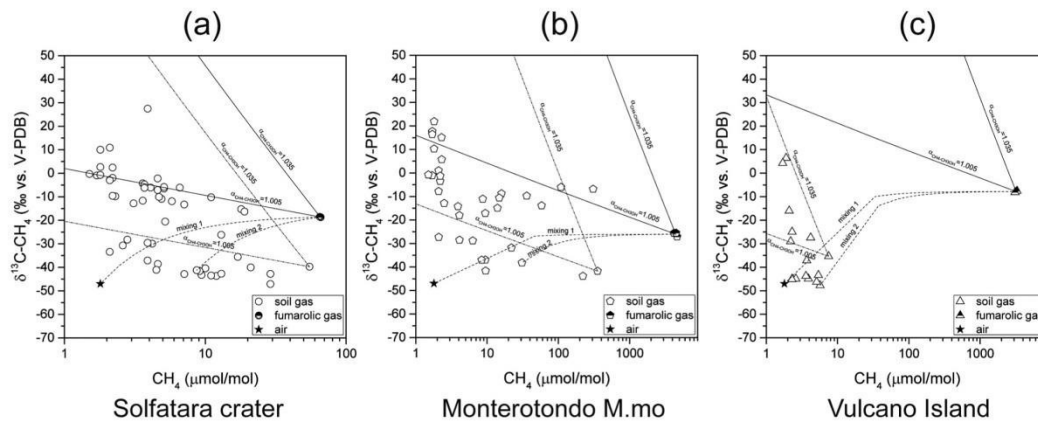


Fig. 5.  $\delta^{13}\text{C-CH}_4$  vs.  $\text{CH}_4$  binary diagrams for interstitial soil gases from (a) Solfatara crater, (b) Monterotondo M.mo and (c) Vulcano Island. Fumarolic gases (black and white symbols) and air (black star) are reported together with mixing lines and Rayleigh fractionation evolution curves, as described in the text.

recorded in interstitial soil gases from sites characterized by relatively high  $\Phi_{\text{CO}_2}$  values, particularly at Solfatara crater (Fig. 6b), where the most positive  $\delta^{13}\text{C-CH}_4$  value (27.5‰), associated with a  $\text{CO}_2/\text{CH}_4$  ratio ~15 times higher than that measured in fumarolic emissions, was recorded in one soil gas collected from a site characterized by a  $\text{CO}_2$  flux of  $2400 \text{ g m}^{-2} \text{ day}^{-1}$ . This evidence suggests that, differently to what observed by Tassi et al. (2013) on the basis of  $\Phi_{\text{CO}_2}$  and  $\Phi_{\text{CH}_4}$  measurements at Solfatara crater, methanotrophy is potentially able to mitigate  $\text{CH}_4$  emissions from hydrothermalized areas also under high diffuse soil flux conditions. If confirmed by further analysis, this scenario would open interesting perspectives in terms of quantification of the impact of natural greenhouse gas sources and development of effective strategies for the abatement of anthropogenic emissions.

6. Conclusions

Diffuse degassing from volcanic-hydrothermal areas largely contributes to the emission of greenhouse gases released to the atmosphere, as shown by the soil fluxes of  $\text{CO}_2$  measured in this study at Solfatara crater

(up to  $2400 \text{ g m}^{-2} \text{ day}^{-1}$ ), Monterotondo M.mo ( $1920 \text{ g m}^{-2} \text{ day}^{-1}$ ) and Baia di Levante at Vulcano Island (up to  $346 \text{ g m}^{-2} \text{ day}^{-1}$ ). The chemical and isotopic compositions of interstitial soil gases from these areas also suggested that secondary processes occurring during fluids uprising towards the surface largely affected  $\text{CO}_2$  and  $\text{CH}_4$ . In particular, interstitial soil gases showed a large variability in terms of  $\delta^{13}\text{C-CH}_4$  due to the presence of significant microbial  $\text{CH}_4$  consumption, even in presence of high soil  $\text{CO}_2$  fluxes and relatively low  $\text{O}_2$ . Methanotrophic activity is apparently characterizing all the investigated areas, though at different extent, as a function of  $\text{CH}_4$  availability in deep sourced gases. This implies that methanotrophy has to be considered a common process in diffuse degassing areas. The comparison between  $\text{CO}_2/\text{CH}_4$  ratios from soil gases and fumarolic discharges suggests that microbial activity in the soil likely contributes to regulate the emission of  $\text{CH}_4$  and, though to a lesser extent, that of  $\text{CO}_2$  from natural environments. Therefore, microbial communities inhabiting soil in hydrothermal diffuse degassing areas play a key role in mitigating climate change by reducing geogenic greenhouse gas emissions (e.g. Gupta et al., 2014; Singh et al., 2010).

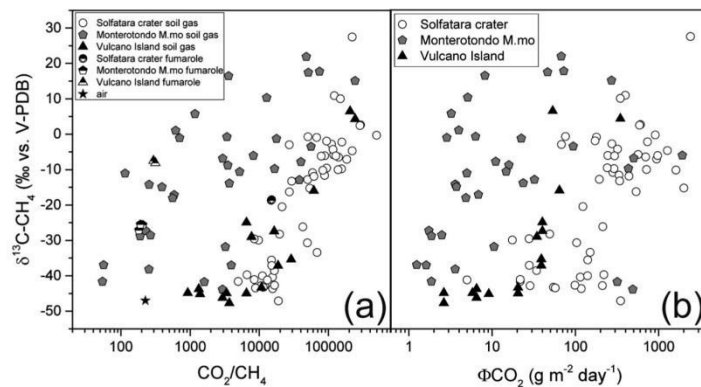


Fig. 6.  $\delta^{13}\text{C-CH}_4$  vs. (a)  $\text{CO}_2/\text{CH}_4$  ratios and (b)  $\Phi_{\text{CO}_2}$  binary diagrams for interstitial soil gases from Solfatara crater, Monterotondo M.mo and Vulcano Island. In (a) fumarolic gases (black and white symbols) and air (black star) are also reported.

## Acknowledgments

This work was financially supported by the laboratories of Fluid and Rock Geochemistry and Stable Isotope Geochemistry of the Department of Earth Sciences and CNR-IGG of Florence. F. Di Binnardo, A. Randazzo, G. Picchi, R. Fani, C. Fagorzi and C. Chiellini are kindly acknowledged for their help during the sampling campaigns. This work largely benefited by detailed, useful and helpful comments of three anonymous reviewers who greatly improved an early version of the manuscript.

## Appendix A. Supplementary data

Supplementary data to this article can be found online at <https://doi.org/10.1016/j.scitotenv.2018.11.293>.

## References

- Aiuppa, A., Tamburello, G., Di Napoli, R., Cardellini, C., Chiodini, G., Giudice, G., Grassa, F., Pedone, M., 2013. First observations of the fumarolic gas output from a restless caldera: implications for the current period of unrest (2005–2013) at Campi Flegrei. *Geochim. Geophys. Geosyst.* 14 (10), 4153–4169. <https://doi.org/10.1002/ggge.20261>.
- Arrighi, S., Tanguy, J.-C., Rosi, M., 2006. Eruptions of the last 2200 years at Vulcano and Vulcanello (Aeolian Islands, Italy) dated by high-accuracy archeomagnetism. *Phys. Earth Planet. Inter.* 159, 225–233. <https://doi.org/10.1016/j.pepi.2006.07.010>.
- Arthur, C.L., Pawliszyn, J., 1990. Solid phase microextraction with thermal desorption using fused silica optical fibers. *Anal. Chem.* 62, 2145–2148.
- Baldi, P., Bellani, S., Ceccarelli, A., Fiordelisi, A., Squarci, P., Taffi, L., 1995. Geothermal anomalies and structural features of southern Tuscany. *World Geothermal Congress Proceedings*, Florence, Italy, May 1995, pp. 1287–1291.
- Barelli, A., Cappetti, G., Stefani, G., 1995. Results of deep drilling in the Larderello-Travale/Radicondoli geothermal area. *World Geothermal Congress Proceedings*, Florence, Italy, May 1995, pp. 1275–1278.
- Batini, F., Brogi, A., Lazzarotto, A., Liotta, D., Pandeli, E., 2003. Geological features of Larderello-Travale and Mt. Amiata geothermal areas (southern Tuscany, Italy). *Episodes* 26 (3), 239–244.
- Baubron, J.C., Allard, P., Toutain, J.P., 1991. Gas hazard on Vulcano Island. *Nature* 350, 26–27.
- Bertani, R., Bertini, G., Cappetti, G., Fiordelisi, A., Marocco, B.M., 2005. An update of the Larderello-Travale/Radicondoli deep geothermal system. *World Geothermal Congress Proceedings*, Antalya, Turkey, 2005, p. 6.
- Beulig, F., Heuer, V.B., Akob, D.M., Viehweger, B., Elvert, M., Herrmann, M., Hinrichs, K.U., Küsel, K., 2015. Carbon flow from volcanic CO<sub>2</sub> into soil microbial communities of a wetland mofette. *ISME J.* 9, 746–759. <https://doi.org/10.1038/ismej.2014.148>.
- Bruno, P.P., Ricciardi, G.P., Pettrillo, Z., Di Fiore, V., Troiano, A., Chiodini, G., 2007. Geophysical and hydrogeological experiments from a shallow hydrothermal system at Solfatara Volcano, Campi Flegrei, Italy: response to caldera unrest. *J. Geophys. Res.* 112, B06201. <https://doi.org/10.1029/2006JB004383>.
- Burton, M.R., Sawyer, G.M., Granieri, D., 2013. Deep carbon emissions from volcanoes. *Rev. Mineral. Geochim.* 75, 323–354. <https://doi.org/10.2138/rmg.2013.75.11>.
- Byrdina, S., Vandemeulebrouck, J., Cardellini, C., Legas, A., Camerlynck, C., Chiodini, G., Lebourg, T., Gresse, M., Bascou, P., Motos, G., Carrier, A., Caliro, S., 2014. Relations between electrical resistivity, carbon dioxide flux, and self-potential in the shallow hydrothermal system of Solfatara (Phlegrean Fields, Italy). *J. Volcanol. Geotherm. Res.* 283, 172–182. <https://doi.org/10.1016/j.jvolgeores.2014.07.010>.
- Caliro, S., Chiodini, G., Moretti, R., Avino, R., Granieri, D., Russo, M., Fiebig, J., 2007. The origin of the fumaroles of La Solfatara (Campi Flegrei, South Italy). *Geochim. Cosmochim. Acta* 71, 3040–3055. <https://doi.org/10.1016/j.gca.2007.04.007>.
- Capaccioni, B., Tassi, F., Vaselli, O., 2001. Organic and inorganic geochemistry of low temperature discharges at the Baia di Levante beach, Vulcano Island, Italy. *J. Volcanol. Geotherm. Res.* 108, 173–185.
- Capasso, G., Favara, R., Inguaggiato, S., 1997. Chemical features and isotopic composition of gaseous manifestations on Vulcano Island, Aeolian Islands, Italy: an interpretative model of fluid circulation. *Geochim. Cosmochim. Acta* 61 (16), 3425–3440.
- Capasso, G., Favara, R., Francoforte, S., Inguaggiato, S., 1999. Chemical and isotopic variations in fumarolic discharge and thermal waters at Vulcano Island (Aeolian Islands, Italy) during 1996: evidence of resumed volcanic activity. *J. Volcanol. Geotherm. Res.* 88, 167–175.
- Capasso, G., D'Alessandro, W., Favara, R., Inguaggiato, S., Parello, F., 2001a. Interaction between the deep fluids and the shallow groundwaters on Vulcano island (Italy). *J. Volcanol. Geotherm. Res.* 108, 187–198.
- Capasso, G., D'Alessandro, W., Favara, R., Inguaggiato, S., Parello, F., 2001b. Kinetic isotope fractionation of CO<sub>2</sub> carbon due to diffusion processes through the soil. *Water-Rock Interaction*, 10. Swets & Zeitlinger, Lisse, pp. 1497–1499.
- Cardellini, C., Chiodini, G., Frondini, F., Granieri, D., Lewicki, J., Peruzzi, L., 2003. Accumulation chamber measurements of methane fluxes: application to volcanic-geothermal areas and landfills. *Appl. Geochem.* 18, 45–54.
- Cardellini, C., Chiodini, G., Frondini, F., Avino, R., Bagnato, E., Caliro, S., Lelli, M., Rosiello, A., 2017. Monitoring diffuse volcanic degassing during volcanic unrests: the case of Campi Flegrei (Italy). *Sci. Rep.* 7 (1), 6757. <https://doi.org/10.1038/s41598-017-06941-2>.
- Carere, C.R., Hards, K., Houghton, K.M., Power, J.F., McDonald, B., Collet, C., Gapes, D.J., Sparling, R., Boyd, E.S., Cook, G.M., Greening, C., Stott, M.B., 2017. Mixotrophy drives niche expansion of verrucocomicrobial methanotrophs. *ISME J.* 11, 2599–2610. <https://doi.org/10.1038/ismej.2017.112>.
- Castaldi, S., Tedesco, D., 2005. Methane production and consumption in an active volcanic environment of Southern Italy. *Chemosphere* 58, 131–139. <https://doi.org/10.1016/j.chemosphere.2004.08.023>.
- Cerling, T.E., Quade, J., 1993. Stable carbon and oxygen isotopes in soil carbonates. In: Swart, P., McKenzie, J.A., Lohman, K.C. (Eds.), *American Geophysical Union Monograph*, vol. 78, pp. 217–231.
- Cheng, W., 1996. Measurement of rhizosphere respiration and organic matter decomposition using natural <sup>13</sup>C. *Plant Soil* 183, 263–268.
- Chiodini, G., Cioni, R., Marini, L., Panichi, C., 1995. Origin of the fumarolic fluids of Vulcano Island, Italy and implications for volcanic surveillance. *Bull. Volcanol.* 57, 99–110.
- Chiodini, G., Cioni, R., Guidi, M., Raco, B., Marini, L., 1998. Soil CO<sub>2</sub> flux measurements in volcanic and geothermal areas. *Appl. Geochem.* 13 (5), 543–552.
- Chiodini, G., Frondini, F., Cardellini, C., Granieri, D., Marini, L., Ventura, G., 2001. CO<sub>2</sub> degassing and energy release at Solfatara volcano, Campi Flegrei, Italy. *J. Geophys. Res.* 106 (B8), 16,213–16,221.
- Chiodini, G., Avino, R., Brombach, T., Caliro, S., Cardellini, C., De Vita, S., Frondini, F., Granieri, D., Marotta, E., Ventura, G., 2004. Fumarolic and diffuse soil degassing west of Mount Epomeo, Ischia, Italy. *J. Volcanol. Geotherm. Res.* 133, 291–309. [https://doi.org/10.1016/S0377-0273\(03\)00403-7](https://doi.org/10.1016/S0377-0273(03)00403-7).
- Chiodini, G., Caliro, S., Cardellini, C., Avino, R., Granieri, D., Schmidt, A., 2008. Carbon isotopic composition of soil CO<sub>2</sub> efflux, a powerful method to discriminate different sources feeding soil CO<sub>2</sub> degassing in volcanic-hydrothermal areas. *Earth Planet. Sci. Lett.* 274, 372–379. <https://doi.org/10.1016/j.epsl.2008.07.051>.
- Chiodini, G., Caliro, S., Cardellini, C., Granieri, D., Avino, R., Baldini, A., Donnini, M., Minopoli, C., 2010. Long-term variations of the Campi Flegrei, Italy, volcanic system as revealed by the monitoring of hydrothermal activity. *J. Geophys. Res.* 115, B03205. <https://doi.org/10.1029/2008JB006258>.
- Chiodini, G., Vandemeulebrouck, J., Caliro, S., D'Auria, L., De Martino, P., Mangiacapra, A., Pettrillo, Z., 2015. Evidence of thermal-driven processes triggering the 2005–2014 unrest at Campi Flegrei caldera. *Earth Planet. Sci. Lett.* 414, 58–67. <https://doi.org/10.1016/j.epsl.2015.01.012>.
- Ciais, P., Sabine, C., Bala, G., Bopp, L., Brovkin, V., Canadell, J., Chhabra, A., Defries, R., Galloway, J., Heimann, M., Jones, C., Le Quéré, C., Myneni, R.B., Piao, S., Thornton, P., 2013. Carbon and other biogeochemical cycles. In: Stocker, T.F., Qin, D., Plattner, G.-K., Tignor, M., Allen, S.K., Boschung, J., Nauels, A., Xia, Y., Bex, V., Midgley, P.M. (Eds.), *Climate Change 2013: The Physical Science Basis. Contribution of Working Group I to the Fifth Assessment Report of the Intergovernmental Panel on Climate Change*. Cambridge University Press, Cambridge, United Kingdom and New York, NY, USA.
- Clocchiatti, R., Del Moro, A., Gioncada, A., Joron, J.L., Moshah, M., Pinarelli, L., Sbrana, A., 1994. Assessment of a shallow magmatic system: the 1888–90 eruption, Vulcano Island, Italy. *Bull. Volcanol.* 56, 466–486.
- Conrad, R., 1996. Soil microorganisms as controllers of atmospheric trace gases (H<sub>2</sub>, CO, CH<sub>4</sub>, OCS, N<sub>2</sub>O, and NO). *Microbiol. Rev.* 60 (4), 609–640.
- Crognale, S., Venturi, S., Tassi, F., Rossetti, S., Rashed, H., Cabassi, J., Capecciacci, F., Nisi, B., Vaselli, O., Morrison, H.G., Sogin, M.L., Fazi, S., 2018. Microbiome profiling in extremely acidic soils affected by hydrothermal fluids: the case of the Solfatara Crater (Campi Flegrei, southern Italy). *FEMS Microbiol. Ecol.* 94 (12), fty190. <https://doi.org/10.1093/femsec/fty190>.
- D'Alessandro, W., Brusca, L., Kyriakopoulos, K., Rotolo, S., Michas, G., Minio, M., Papadakis, G., 2006. Diffuse and focused carbon dioxide and methane emissions from the Soufaki geothermal system, Greece. *Geophys. Res. Lett.* 33, L05307. <https://doi.org/10.1029/2006GL025777>.
- D'Alessandro, W., Bellomo, S., Brusca, L., Fiebig, J., Longo, M., Martelli, M., Pecoraino, G., Salerno, F., 2009. Hydrothermal methane fluxes from the soil at Pantelleria island (Italy). *J. Volcanol. Geotherm. Res.* 187, 147–157. <https://doi.org/10.1016/j.jvolgeores.2009.08.018>.
- D'Alessandro, W., Brusca, L., Kyriakopoulos, K., Martelli, M., Michas, G., Papadakis, G., Salerno, F., 2011. Diffuse hydrothermal methane output and evidence of methanotrophic activity within the soils at Soufaki (Greece). *Geofluids* 11, 97–107. <https://doi.org/10.1111/j.1468-8123.2010.00322.x>.
- D'Amore, F., Bolognesi, L., 1994. Isotopic evidence for a magmatic contribution to fluids of the geothermal systems of Larderello, Italy and The Geysers, California. *Geothermics* 23 (1), 21–32.
- De Astis, G., La Volpe, L., Peccerillo, A., Civetta, L., 1997. Volcanological and petrological evolution of Vulcano island (Aeolian Arc, southern Tyrrhenian Sea). *J. Geophys. Res.* 102 (B4), 8021–8050.
- De Landro, G., Serlenga, V., Russo, G., Amoroso, O., Festa, G., Bruno, P.P., Gresse, M., Vandemeulebrouck, J., Zollo, A., 2017. 3D ultra-high resolution seismic imaging of shallow Solfatara crater in Campi Flegrei (Italy): new insights on deep hydrothermal fluid circulation processes. *Sci. Rep.* 7, 3412. <https://doi.org/10.1038/s41598-017-03604-0>.
- De Vivo, B., Rolandi, G., Gans, P.B., Calvert, A., Bohrsen, W.A., Spera, F.J., Belkin, H.E., 2001. New constraints on the pyroclastic eruptive history of the Campanian volcanic Plain (Italy). *Mineral. Petrol.* 73, 47–65. <https://doi.org/10.1007/s007100170010>.
- Degens, E.T., 1969. Biogeochemistry of stable carbon isotopes. In: Eglinton, G., Murphy, M.T.J. (Eds.), *Organic Geochemistry*, Berlin-Heidelberg-New York: Springer, pp. 194–208.
- Deines, P., Langmuir, D., Herman, R.S., 1974. Stable carbon isotope ratio and the existence of a gas phase in the evolution of carbonate groundwaters. *Geochim. Cosmochim. Acta* 38, 1147–1164.
- Deino, A.L., Orsi, G., de Vita, S., Piochi, M., 2004. The age of the Neapolitan Yellow Tuff caldera-forming eruption (Campi Flegrei caldera - Italy) assessed by <sup>40</sup>Ar/<sup>39</sup>Ar dating

- method. *J. Volcanol. Geotherm. Res.* 133, 157–170. [https://doi.org/10.1016/S0377-0273\(03\)00396-2](https://doi.org/10.1016/S0377-0273(03)00396-2).
- Di Martino, R.M.R., Capasso, G., Camarda, M., 2016. Spatial domain analysis of carbon dioxide from soils on Vulcano Island: implications for CO<sub>2</sub> output evaluation. *Chem. Geol.* 444, 59–70. <https://doi.org/10.1016/j.chemgeo.2016.09.037>.
- Dini, A., Gianelli, G., Puxeddu, M., Ruggieri, G., 2005. Origin and evolution of Pliocene–Pleistocene granites from the Larderello geothermal field (Tuscan Magmatic Province, Italy). *Lithos* 81, 1–31.
- Duchi, V., Minissale, A., Rossi, R., 1986. Chemistry of thermal springs in the Larderello-Travale geothermal region, southern Tuscany, Italy. *Appl. Geochem.* 1 (6), 659–667.
- Duchi, V., Minissale, A., Manganelli, M., 1992. Chemical composition of natural deep and shallow hydrothermal fluids in the Larderello geothermal field. *J. Volcanol. Geotherm. Res.* 49, 313–328.
- Dunfield, P.F., Yuryev, A., Senin, P., Smirnova, A.V., Stott, M.B., Hou, S., Ly, B., Saw, J.H., Zhou, Z., Ren, Y., Wang, J., Mountain, B.W., Crowe, M.A., Weatherby, T.M., Bodelier, P.L.E., Liesack, W., Feng, L., Wang, L., Alam, M., 2007. Methane oxidation by an extremely acidophilic bacterium of the phylum Verrucomicrobia. *Nature* 450, 879–882.
- Dutaur, L., Verchot, L.V., 2007. A global inventory of the soil CH<sub>4</sub> sink. *Glob. Biogeochem. Cycles* 21, GB4013. <https://doi.org/10.1029/2006GB002734>.
- Etiopie, G., Klusman, R.W., 2002. Geologic emissions of methane to the atmosphere. *Chemosphere* 49, 777–789.
- Etiopie, G., Fridriksson, T., Italiano, F., Winiwarer, W., Theloke, J., 2007. Natural emissions of methane from geothermal and volcanic sources in Europe. *J. Volcanol. Geotherm. Res.* 165, 76–86. <https://doi.org/10.1016/j.jvolgeores.2007.04.014>.
- Etiopie, G., Feyzullayev, A., Milkov, A.V., Waseda, A., Mizobe, K., Sun, C.H., 2009. Evidence of subsurface anaerobic biodegradation of hydrocarbons and potential secondary methanogenesis in terrestrial mud volcanoes. *Mar. Pet. Geol.* 26, 1692–1703. <https://doi.org/10.1016/j.marpetgeo.2008.12.002>.
- Farhan Ul Haque, M., Crombie, A.T., Ensminger, S.A., Baciu, C., Murrell, J.C., 2018. Facultative methanotrophs are abundant at terrestrial natural gas seeps. *Microbiome* 6, 118. <https://doi.org/10.1186/s40168-018-0500-x>.
- Federico, C., Corso, P.P., Fioridino, E., Cardellini, C., Chiodini, G., Parello, F., Pisciotta, A., 2010. CO<sub>2</sub> degassing at La Solfatara volcano (Phlegrean Fields): processes affecting δ<sup>13</sup>C and δ<sup>18</sup>O of soil CO<sub>2</sub>. *Geochim. Cosmochim. Acta* 74, 3521–3538. <https://doi.org/10.1016/j.gca.2010.03.010>.
- Freude, C., Blaser, M., 2016. Carbon isotope fractionation during catabolism and anabolism in acetogenic bacteria growing on different substrates. *Appl. Environ. Microbiol.* 82 (9), 2728–2737. <https://doi.org/10.1128/AEM.03502-15>.
- Gagliano, A.L., D'Alessandro, W., Tagliavia, M., Parello, F., Quatrini, P., 2014. Methanotrophic activity and diversity of methanotrophs in volcanic geothermal soils at Pantelleria (Italy). *Biogeosciences* 11, 5865–5875. <https://doi.org/10.5194/bg-11-5865-2014>.
- Gagliano, A.L., Tagliavia, M., D'Alessandro, W., Franzetti, A., Parello, F., Quatrini, P., 2016. So close, so different: methanotrophic flux shapes divergent soil microbial communities at neighbouring sites. *Geobiology* 14, 150–162. <https://doi.org/10.1111/gbi.12167>.
- Gherardi, F., Panichi, C., Gonfiantini, R., Magro, G., Scandifoglio, G., 2005. Isotope systematics of C-bearing gas compounds in the geothermal fluids of Larderello, Italy. *Geothermics* 34, 442–470. <https://doi.org/10.1016/j.geothermics.2004.09.005>.
- Gianelli, G., Laurenzi, M.A., 2001. Age and cooling rate of the geothermal system of Larderello. *Geoth. Res. Counc. Trans.* 25, 731–735.
- Glamoclija, M., Garrel, L., Berthon, J., López-García, P., 2004. Biosignatures and bacterial diversity in hydrothermal deposits of Solfatara crater, Italy. *Microbiol. J.* 21 (8), 529–541. <https://doi.org/10.1080/01490450490888235>.
- Gottsmann, J., Rymner, H., Berrino, G., 2006. Unrest at the Campi Flegrei caldera (Italy): a critical evaluation of source parameters from geodetic data inversion. *J. Volcanol. Geotherm. Res.* 150, 132–145. <https://doi.org/10.1016/j.jvolgeores.2005.07.002>.
- Granieri, D., Avino, R., Chiodini, G., 2010. Carbon dioxide diffuse emission from the soil: ten years of observations at Vesuvio and Campi Flegrei (Pozzuoli), and linkages with volcanic activity. *Bull. Volcanol.* 72, 103–118. <https://doi.org/10.1007/s00445-009-0304-8>.
- Gresse, M., Vandemeulebrouck, J., Byrdina, S., Chiodini, G., Revil, A., Johnson, T.C., Ricci, T., Vilaro, G., Mangiacapra, A., Lebourg, T., Grangeon, J., Bascou, P., Metral, L., 2017. Three-dimensional electrical resistivity tomography of the Solfatara Crater (Italy): implication for the multiphase flow structure of the shallow hydrothermal system. *J. Geophys. Res. Solid Earth* 122. <https://doi.org/10.1002/2017JB014389>.
- Gupta, C., Prakash, D., Gupta, S., 2014. Role of microbes in combating global warming. *Int. J. Pharm. Sci. Lett.* 4 (2), 359–363.
- Hanson, R.S., Hanson, T.E., 1996. Methanotrophic bacteria. *Microbiol. Rev.* 60 (2), 439–471.
- Holloway, S., Pearce, J.M., Hards, V.L., Ohsumi, T., Gale, J., 2007. Natural emissions of CO<sub>2</sub> from the geosphere and their bearing on the geological storage of carbon dioxide. *Energy* 32, 1194–1201. <https://doi.org/10.1016/j.energy.2006.09.001>.
- Huber, R., Huber, H., Stetter, K.O., 2000. Towards the ecology of hyperthermophiles: biotopes, new isolation strategies and novel metabolic properties. *FEMS Microbiol. Rev.* 24, 615–623.
- Inguaggiato, S., Mazot, A., Diliberto, I.S., Inguaggiato, C., Madonia, P., Rouwet, D., Vita, F., 2012. Total CO<sub>2</sub> output from Vulcano island (Aeolian Islands, Italy). *Geochim. Geophys. Res.* 17, 1–19. <https://doi.org/10.1029/2011GC003920>.
- IPCC, 2007a. Climate change 2007: mitigation. In: Metz, B., Davidson, O.R., Bosch, P.R., Dave, R., Meyer, L.A. (Eds.), Contribution of Working Group III to the Fourth Assessment Report of the Intergovernmental Panel on Climate Change. Cambridge University Press, Cambridge, United Kingdom and New York, NY, USA, p. 851.
- IPCC, 2007b. Climate change 2007: the physical science basis. In: Solomon, S., Qin, D., Manning, M., Chen, Z., Marquis, M., Averyt, K.B., Tignor, M., Miller, H.L. (Eds.), Contribution of Working Group I to the Fourth Assessment Report of the Intergovernmental Panel on Climate Change. Cambridge University Press, Cambridge, United Kingdom, p. 996.
- Islam, T., Jensen, S., Reigstad, L.J., Larsen, O., Birkeland, N.K., 2008. Methane oxidation at 55 °C and pH 2 by a thermoacidophilic bacterium belonging to the Verrucomicrobia phylum. *Proc. Natl. Acad. Sci. U. S. A.* 105, 300–304.
- Italiano, F., Nuccio, M., Pecoraino, G., 1998. Steam output from fumaroles of an active volcano: tectonic and magmatic hydrothermal controls on the degassing system at Vulcano (Aeolian arc). *J. Geophys. Res.* 103 (12), 29829–29841.
- Kayler, Z.E., Sulzman, E.W., Ruzh, W.D., Mix, A.C., Bond, B.J., 2010. Characterizing the impact of diffusive and advective soil gas transport on the measurement and interpretation of the isotopic signal of soil respiration. *Soil Biol. Biochem.* 42, 434–444. <https://doi.org/10.1016/j.soilbio.2009.11.022>.
- Keeling, C.D., Piper, S.C., Bacastow, R.B., Wahlen, M., Whorf, T.P., Heimann, M., Meijer, H.A., 2005. Atmospheric CO<sub>2</sub> and <sup>13</sup>C exchange with the terrestrial biosphere and oceans from 1978 to 2000: observations and carbon cycle implications. In: Ehleringer, J.R., Cerling, T.E., Dearing, M.D. (Eds.), *A History of Atmospheric CO<sub>2</sub> and its Effects on Plants, Animals, and Ecosystems*. Springer Verlag, New York, pp. 83–113.
- Keller, J., 1980. The island of Vulcano. *Rend. Soc. Ital. Mineral. Petrol.* 36, 369–414.
- Khadem, A.F., Pol, A., Wiecezorek, A., Mohammadi, S.S., Francoijs, K.J., Stunnenberg, H.G., Jetten, M.S.M., Op den Camp, H.J.M., 2011. Autotrophic methanotrophy in Verrucomicrobia: *Methylacidiphilum fumarolicum* SolV uses the Calvin-Benson-Bassham cycle for carbon dioxide fixation. *J. Bacteriol.* 193 (17), 4438–4446. <https://doi.org/10.1128/JB.00407-11>.
- McCormick, T.M., Seewald, J.S., 2007. Abiotic synthesis of organic compounds in deep-sea hydrothermal environments. *Chem. Rev.* 107, 382–401. <https://doi.org/10.1021/cr0503660>.
- Minissale, A., 1991. The Larderello geothermal field: a review. *Earth-Sci. Rev.* 31, 133–151.
- Mohammadi, S., Pol, A., van Alen, T.A., Jetten, M.S.M., Op den Camp, H.J.M., 2017. *Methylacidiphilum fumarolicum* SolV, a thermoacidophilic 'Knallgas' methanotroph with both an oxygen-sensitive and -insensitive hydrogenase. *ISME J.* 11, 945–958. <https://doi.org/10.1038/ismej.2016.171>.
- Montanaro, C., Mayer, K., Ischia, R., Gresse, M., Scheu, B., Yilmaz, T.I., Vandemeulebrouck, J., Ricci, T., Dingwell, D.B., 2017. Hydrothermal activity and subsoil complexity: implication for degassing processes at Solfatara crater, Campi Flegrei caldera. *Bull. Volcanol.* 79, 83. <https://doi.org/10.1007/s00445-017-1167-z>.
- Montegrossi, G., Tassi, F., Vaselli, O., Buccianti, A., Garofalo, K., 2001. Sulphur species in volcanic gases. *Anal. Chem.* 73, 3709–3715. <https://doi.org/10.1021/ac001429b>.
- Mörner, N.A., Etiopie, G., 2002. Carbon degassing from the lithosphere. *Glob. Planet. Chang.* 33, 185–203.
- Neruzzi, A., 2016. L'origine del metano nei sistemi vulcanici attivi: l'esempio di Vulcano. (Unpublished thesis), University of Florence.
- Nisbet, E.G., Dlugokencky, E.J., Manning, M.R., Lowry, D., Fisher, R.E., France, J.L., Michel, S.E., Miller, J.B., White, J.W.C., Vaughn, B., Bousquet, P., Pyle, J.A., Warwick, N.J., Cain, M., Brownlow, R., Zazzeri, G., Lanoisellé, M., Manning, A.C., Gloor, E., Worthy, D.E.J., Brunke, E.G., Labuschagne, C., Wolff, E.W., Ganesan, A.L., 2016. Rising atmospheric methane: 2007–2014 growth and isotopic shift. *Glob. Biogeochem. Cycles* 30, 1356–1370. <https://doi.org/10.1002/2016GB005406>.
- Notsu, K., Sugiyama, K., Hosoe, M., Uemura, A., Shimoiike, Y., Tsunomori, F., Sumino, H., Yamamoto, J., Mori, T., Hernández, P.A., 2005. *J. Volcanol. Geotherm. Res.* 139, 147–161. <https://doi.org/10.1016/j.jvolgeores.2004.08.003>.
- Nowak, M.E., Beulig, F., von Fischer, J., Muhr, J., Küsel, K., Trumbore, S.E., 2015. Autotrophic fixation of geogenic CO<sub>2</sub> by microorganisms contributes to soil organic matter formation and alters isotope signatures in a wetland mofette. *Biogeosciences* 12, 7169–7183. <https://doi.org/10.5194/bg-12-7169-2015>.
- Op den Camp, H.J.M., Islam, T., Stott, M.B., Harhangi, H.R., Hynes, A., Schouten, S., Jetten, M.S.M., Birkeland, N.K., Pol, A., Dunfield, P., 2009. Environmental, genetic and taxonomic perspectives on methanotrophic Verrucomicrobia. *Environ. Microbiol. Rep.* 1 (5), 293–306. <https://doi.org/10.1111/j.1758-2229.2009.00022.x>.
- Oppermann, B.L., Michaelis, W., Blumenberg, M., Frerichs, J., Schutz, H.M., Schippers, A., Beaubien, S.E., Krüger, M., 2010. Soil microbial community changes as a result of long-term exposure to a natural CO<sub>2</sub> vent. *Geochim. Cosmochim. Acta* 74, 2697–2716. <https://doi.org/10.1016/j.gca.2010.02.006>.
- Panichi, C., Noto, P., 1992. Isotopic and chemical composition of water, steam and gas samples of the natural manifestations of the island of Vulcano (Aeolian Arc, Italy). *Acta Vulcanol.* 2, 297–312.
- Passaro, S., Tamburrino, S., Vallefucio, M., Tassi, F., Vaselli, O., Giannini, L., Chiodini, G., Caliro, S., Sacchi, M., Rizzo, A.L., Ventura, G., 2016. Seafloor doming driven by degassing processes unveils sprouting volcanism in coastal areas. *Sci. Rep.* 6, 22448. <https://doi.org/10.1038/srep22448>.
- Pecoraino, G., Brusca, L., D'Alessandro, W., Giammanco, S., Inguaggiato, S., Longo, M., 2005. Total CO<sub>2</sub> output from Ischia Island volcano (Italy). *Geochim. J.* 39, 451–458. <https://doi.org/10.2343/geochemj.39.451>.
- Pol, A., Heijmans, K., Harhangi, H.R., Tedesco, D., Jetten, M.S.M., 2007. Methanotrophy below pH 1 by a new Verrucomicrobia species. *Nature* 450, 874–878.
- Reeburgh, W.S., 2003. Global methane biogeochemistry. In: Keeling, R.F., Holland, H.D., Turekian, K.K. (Eds.), *Treatise on Geochemistry*, Vol. 4: The Atmosphere. Elsevier-Pergamon, Oxford, UK, pp. 65–89.
- Romagnoli, P., Arias, A., Barelli, A., Cei, M., Casini, M., 2010. An updated numerical model of the Larderello-Travale geothermal system, Italy. *Geothermics* 39, 292–313.
- Rouwet, D., Tamburello, G., Scarra, A., Ricci, T., Caliro, S., 2018. The Fangaia mud pool, Solfatara (Campi Flegrei, Italy): the effect of scrubbing on CO<sub>2</sub> and H<sub>2</sub>S degassing. *Geophys. Res. Abstr.* 20 (EGU2018-14058, EGU General Assembly 2018).
- Schoell, M., 1980. The hydrogen and carbon isotopic composition of methane from natural gases of various origins. *Geochim. Cosmochim. Acta* 44 (5), 649–661.
- Semrau, J.D., 2011. Bioremediation via methanotrophy: overview of recent findings and suggestions for future research. *Front. Microbiol.* 2, 209. <https://doi.org/10.3389/fmicb.2011.00209>.

- Sharp, C.E., Smirnova, A.V., Graham, J.M., Stott, M.B., Khadka, R., Moore, T.R., Grasby, S.E., Strack, M., Dunfield, P.F., 2014. Distribution and diversity of Verrucomicrobia methanotrophs in geothermal and acidic environments. *Environ. Microbiol.* 16 (6), 1867–1878. <https://doi.org/10.1111/1462-2920.12454>.
- Singh, B.K., Bardgett, R.D., Smith, P., Reay, D.S., 2010. Microorganisms and climate change: terrestrial feedbacks and mitigation options. *Natl. Rev.* 8, 779–790. <https://doi.org/10.1038/nrmicro2439>.
- Sommaruga, C., 1984. Le ricerche geotermiche svolte a Vulcano negli anni '50. *Rend. Soc. Ital. Mineral. Petrol.* 39, 355–366.
- Stetter, K.O., 1999. Extremophiles and their adaptation to hot environments. *FEBS Lett.* 452, 22–25.
- Stetter, K.O., 2006. Hyperthermophiles in the history of life. *Philos. Trans. R. Soc. B* 361, 1837–1843. <https://doi.org/10.1098/rstb.2006.1907>.
- Strong, P.J., Xie, S., Clarke, W.P., 2015. Methane as a resource: can the methanotrophs add value? *Environ. Sci. Technol.* 49, 4001–4018. <https://doi.org/10.1021/es504242n>.
- Tassi, F., Capecciacci, F., Buccianti, A., Vaselli, O., 2012a. Sampling and analytical procedures for the determination of VOCs released into air from natural and anthropogenic sources: a comparison between SPME (Solid Phase Micro Extraction) and ST (Solid Trap) methods. *Appl. Geochem.* 27, 115–123. <https://doi.org/10.1016/j.apgeochem.2011.09.023>.
- Tassi, F., Fiebig, J., Vaselli, O., Nocentini, M., 2012b. Origins of methane discharging from volcanic-hydrothermal, geothermal and cold emissions in Italy. *Chem. Geol.* 310–311, 36–48. <https://doi.org/10.1016/j.chemgeo.2012.03.018>.
- Tassi, F., Nisi, B., Cardellini, C., Capecciacci, F., Donnini, M., Vaselli, O., Avino, R., Chiodini, G., 2013. Diffuse soil emission of hydrothermal gases (CO<sub>2</sub>, CH<sub>4</sub>, C<sub>2</sub>H<sub>6</sub>) at Solfatara crater (Campi Flegrei, southern Italy). *Appl. Geochem.* 35, 142–153. <https://doi.org/10.1016/j.apgeochem.2013.03.020>.
- Tassi, F., Venturi, S., Cabassi, J., Capecciacci, F., Nisi, B., Vaselli, O., 2015a. Volatile organic compounds (VOCs) in soil gases from Solfatara crater (Campi Flegrei, southern Italy): Geogenic source(s) vs. biogeochemical processes. *Appl. Geochem.* 56, 37–49. <https://doi.org/10.1016/j.apgeochem.2015.02.005>.
- Tassi, F., Venturi, S., Cabassi, J., Gelli, I., Cinti, D., Capecciacci, F., 2015b. Biodegradation of CO<sub>2</sub>, CH<sub>4</sub> and volatile organic compounds (VOCs) in soil gases from the Vicano-Cimino hydrothermal system (central Italy). *Org. Geochem.* 86, 81–93. <https://doi.org/10.1016/j.orggeochem.2015.06.004>.
- Templeton, A.S., Chu, K.H., Alvarez-Cohen, L., Conrad, M.E., 2006. Variable carbon isotope fractionation expressed by aerobic CH<sub>4</sub>-oxidizing bacteria. *Geochim. Cosmochim. Acta* 70, 1739–1752. <https://doi.org/10.1016/j.gca.2005.12.002>.
- Todesco, M., 1995. Modeling of the geothermal activity at Vulcano (Aeolian Islands, Italy). *Proc. World Geothermal Congress, 1995. 2. Int. Geotherm. Assoc.*, pp. 1309–1314.
- Todesco, M., Chiodini, G., Macedonio, G., 2003. Monitoring and modelling hydrothermal fluid emission at La Solfatara (Phlegrean Fields, Italy). An interdisciplinary approach to the study of diffuse degassing. *J. Volcanol. Geotherm. Res.* 125, 57–79. [https://doi.org/10.1016/S0377-0273\(03\)00089-1](https://doi.org/10.1016/S0377-0273(03)00089-1).
- Trotsenko, Y.A., Medvedkova, K.A., Khmelina, V.N., Eshinimayev, B.Ts., 2009. Thermophilic and thermotolerant aerobic methanotrophs. *Microbiology* 78 (4), 387–401. <https://doi.org/10.1134/S0026261709040018>.
- Valentine, D.L., Chidthaisong, A., Rice, A., Reeburgh, W.S., Tyler, S.C., 2004. Carbon and hydrogen isotope fractionation by moderately thermophilic methanogens. *Geochim. Cosmochim. Acta* 68 (7), 1571–1590. <https://doi.org/10.1016/j.gca.2003.10.012>.
- Valentino, G.M., Stanzione, D., 2003. Source processes of the thermal waters from the Phlegrean Fields (Naples, Italy) by means of the study of selected minor and trace elements distribution. *Chem. Geol.* 194, 245–274.
- Valentino, G.M., Stanzione, D., 2004. Geochemical monitoring of the thermal waters of the Phlegrean Fields. *J. Volcanol. Geotherm. Res.* 133, 261–289. [https://doi.org/10.1016/S0377-0273\(03\)00402-5](https://doi.org/10.1016/S0377-0273(03)00402-5).
- van Teeseling, M.C.F., Pol, A., Harhangi, H.R., van der Zwart, S., Jetten, M.S.M., Op den Camp, H.J.M., van Niftrik, L., 2014. Expanding the Verrucomicrobial methanotrophic world: description of three novel species of *Methylacidimicrobium* gen. nov. *Appl. Environ. Microbiol.* 80 (21), 6782–6791. <https://doi.org/10.1128/AEM.01838-14>.
- Vaselli, O., Tassi, F., Montegrossi, G., Capaccioni, B., Giannini, L., 2006. Sampling and analysis of volcanic gases. *Acta Vulcanol.* 18 (1–2), 65–76.
- Vaselli, O., Tassi, F., Tedesco, D., Poreda, J.R., Caprai, A., 2011. Submarine and inland gas discharges from the Campi Flegrei (southern Italy) and the Pozzuoli Bay: geochemical clues for a common hydrothermal-magmatic source. *Prog. Earth Planet Sci.* 4, 57–73. <https://doi.org/10.1016/j.proeps.2011.11.007>.
- Venturi, S., Tassi, F., Biccocchi, G., Cabassi, J., Capecciacci, F., Capasso, G., Vaselli, O., Ricci, A., Grassa, F., 2017. Fractionation processes affecting the stable carbon isotope signature of thermal waters from hydrothermal/volcanic systems: the examples of Campi Flegrei and Vulcano Island (southern Italy). *J. Volcanol. Geotherm. Res.* 345, 46–57. <https://doi.org/10.1016/j.jvolgeores.2017.08.001>.
- Villa, L., Puxeddu, M., 1994. Geochronology of the Larderello geothermal field: new data and the 'closure temperature' issue. *Contrib. Mineral. Petrol.* 315, 415–426.
- Viveiros, F., Cardellini, C., Ferreira, T., Caliro, S., Chiodini, G., Silva, C., 2010. Soil CO<sub>2</sub> emissions at Furnas Volcano, São Miguel Island, Azores archipelago: volcano monitoring perspectives, geomorphologic studies, and land use planning application. *J. Geophys. Res.* 115 (B12208). <https://doi.org/10.1029/2010JB007555>.
- Whiticar, M.J., 1999. Carbon and hydrogen isotope systematics of bacterial formation and oxidation of methane. *Chem. Geol.* 161, 291–314.

# Methane in groundwaters of Emilia Plain (northern Italy): sources and sinks

Andrea Ricci<sup>1\*</sup>, Stefano Cremonini<sup>1</sup>, Paolo Severi<sup>2</sup>, Franco Tassi<sup>3,4</sup>, Orlando Vaselli<sup>3,4</sup>, Jens Fiebig<sup>5</sup>, Andrea Luca Rizzo<sup>6</sup>, Fausto Grassa<sup>6</sup>, Bruno Capaccioni<sup>1</sup>

<sup>1</sup>*Department of Biological, Geological and Environmental Sciences, University of Bologna, Piazza di Porta S. Donato 1, 40127 Bologna (Italy)*

<sup>2</sup>*Geological, Seismic and Soil Survey of the Emilia-Romagna Region, Viale della Fiera 8, 40127 Bologna (Italy)*

<sup>3</sup>*Department of Earth Sciences, University of Florence, Via G. La Pira 4, 50121 Florence (Italy)*

<sup>4</sup>*CNR – Institute of Geosciences and Georesources, Via G. La Pira 4, 50121 Florence (Italy)*

<sup>5</sup>*Institut für Geowissenschaften, Goethe-Universität, Altenhöferallee 1, 60438 Frankfurt am Main (Germany)*

<sup>6</sup>*Istituto Nazionale di Geofisica e Vulcanologia (INGV), Sezione Palermo, Via Ugo La Malfa 153, 90146 Palermo (Italy)*

\* Corresponding author. Andrea Ricci (andrea.ricci34@unibo.it)

**Keywords:** Methane, Methanogenesis, Methanotrophy, Biogeochemistry, Emilia-Romagna Region, Po Plain

## Abstract

The occurrence of methane in the deep subsurface of Po Plain is a widespread phenomenon. Origin and evolution of deep hydrocarbons reservoirs in this region are relatively well constrained, thanks to data of numerous wells drilled in the last century for oil and natural gas exploration. In shallow geological domains, methane-rich fluids were frequently found. However, their origin and the link between deep and shallow reservoirs are poorly known. This paper presents new chemical and isotopic data on gases from deep oil and gas field, bubbling gases, dissolved gases in groundwaters and dry seeps in order to (i) identify the source(s) of methane in the shallow environment, (ii) describe the biogeochemical sinks of methane and (iii) clarify the relation between deep and shallow reservoirs. Results of our investigation highlighted that three main deep sources of methane (and higher hydrocarbons) occur in the Po Plain: (i) biogenic/diagenetic gases from marine Pliocene-Pleistocene sediments; (ii) Miocene thermogenic gases and (iii) early mature thermogenic gases from Triassic carbonates. Methane in shallow domains originates mainly within the Plio-Quaternary marine sediments by CO<sub>2</sub>-reduction, then migrates toward the surface. On the

contrary, thermogenic hydrocarbons are stored in deep structural and stratigraphic traps and do not migrate towards the surface. In aerobic soils, oxic water and anoxic waters, microbial consumption regulates the output of fossil Plio-Quaternary methane. Furthermore, our investigation suggested that heat release through the exothermic oxidation of methane mediated by methanotrophic bacteria under aerobic conditions, is the processes responsible for the episodes of water temperature increase in phreatic water wells (Warm Water Wells, WWW) in the Po Plain. Where structural geometry of the sedimentary prism allows further migration, methane can be ultimately discharged into the atmosphere from surficial gas emissions (bubbling gases and dry seeps).

## **1. Introduction**

Methane is the most abundant hydrocarbon in the atmosphere, where it plays a fundamental role in the tropospheric chemistry. The globally-averaged surface dry air mole fraction of CH<sub>4</sub> in June 2018 was  $\approx 1851$  ppb ([https://www.esrl.noaa.gov/gmd/ccgg/trends\\_ch4/](https://www.esrl.noaa.gov/gmd/ccgg/trends_ch4/)), about 2.7 times the CH<sub>4</sub> concentration in the atmosphere during the early 18<sup>th</sup> century prior to the Industrial Revolution. Nowadays, about 60 % of the methane global emissions are anthropogenic, making CH<sub>4</sub> the second most important human-induced greenhouse gas after CO<sub>2</sub>. Human industrial activities, such as agriculture, landfills and fossil fuels usage, have a strong impact on the global methane cycle. Although the global CH<sub>4</sub> emission, estimated at  $\sim 558$  Tg/y for the 2003-2012 decade (Saunio et al., 2016), are only 5 % of the global CO<sub>2</sub> emissions, methane has contributed 20% of the additional radiative forcing accumulated in the lower atmosphere since 1750 (Ciais et al., 2013). In fact, despite having a short lifetime in the atmosphere ( $\approx 9$  years, Prather et al., 2012), the global warming potential of methane is  $\sim 28$  times greater than that of CO<sub>2</sub> (Myhre et al., 2013). Beyond having a direct heating effect, methane breaks down into carbon dioxide and water vapor by radical hydroxylation reactions in the troposphere and stratosphere, increasing the greenhouse effect and depleting the ozone layer.

Natural methane sources include wetlands, wild animals, wildfires, termites, terrestrial permafrost geological sources (seeps, microseepage, mud volcanoes, geothermal areas, active volcanoes and marine seepages), oceans as well as other water bodies (lakes, ponds and rivers). Many sources were recognized but their magnitude and variability remain uncertain (USEPA, 2010; Kirschke et al., 2013). Geological sources have long been considered to play a minor role in the global CH<sub>4</sub> cycle but recent studies, providing more accurate estimation, highlighted their importance for the methane budget. Sedimentary basins account for 90%

(Etiope and Klusman, 2002) of the total geogenic CH<sub>4</sub> emission. In rapidly subsiding basins, deposition and accumulation of sediments, eroded from high-relief areas, form km-thickness sedimentary sequences. Organic matter buried with sediments is biodegraded by metabolic activity of microbial consortia (biogenesis) and thermochemically transformed by heat and pressure through cracking and reforming reactions (thermogenesis). Methane is produced by either mechanisms with biogenic gases exhibiting significantly higher CH<sub>4</sub>/(C<sub>2</sub>H<sub>6</sub> + C<sub>3</sub>H<sub>8</sub>) ratios and lighter (<sup>13</sup>C-depleted) δ<sup>13</sup>C-CH<sub>4</sub> than thermogenic gases (Whiticar, 1999). Microbial activity and maturation of organic matter lead to the formation of methane (and higher hydrocarbons) accumulations in the subsurface. After gas formation and accumulation in a reservoir, and during its migration to the surface, a series of post-genetic processes such as biodegradation and diffusion/advection-related fractionation may affect its molecular and isotopic composition (Etiope et al., 2009a) and regulates the total carbon input into the atmosphere. Microbial oxidation of methane occurs in both oxic (e.g. soils and water column) and anoxic (e.g. marine sediments) environments, and represents the most important process in which methane is removed from the environment before reaching the atmosphere (e.g., Valentine and Reeburgh, 2000; Hinrichs and Boetius, 2002; Valentine, 2002; Lieberman and Rosenzweig, 2004; Reeburgh, 2007; McDonald et al., 2008; Conrad, 2009; Knittel and Boetius, 2009). In tectonically active environments, systems of fractures and faults highly enhance channeling and vertical migration of CH<sub>4</sub>-rich fluids from the source zone to reservoirs (Mucciarelli et al., 2015). High fluxes prevent the complete microbial consumption of uprising methane, ultimately allowing its extrusion from terrestrial and submarine vents (Etiope, 2009b; Capaccioni et al., 2015). Surface seepage of methane, light hydrocarbons and oil is a widespread phenomenon along the Alpine-Himalayan Orogen where mud volcanoes, dry gas vents and brackish/salt water seeps, mostly occurring in correspondence of suture zones between the converging plates (e.g. Gulf of Cadiz, Mediterranean Ridge, Makran, Northern Apennines, Carpathians, Caucasus, Black Sea and Caspian Sea) discharge large volumes of CH<sub>4</sub> and C<sub>2+</sub> volatile organic compounds (VOCs) into the atmosphere (Baciu et al., 2007; Bonini et al., 2013; Delisle et al., 2002; Kopf et al., 2001; 2003; Somoza et al., 2003). These surficial seeps are intimately linked to subsurface hydrocarbon accumulations and the tectonic regime (Bonini, 2007; 2013; Capozzi and Picotti, 2002). Inland and offshore natural seeps of biogenic and thermogenic gases have been documented in Italy where they punctuate the Apennine orogenic front from the Po Plain to Sicily. Surface seepages in the southern Po River Basin (Emilia-Romagna Region, Italy), a syntectonic sedimentary wedge forming the infill of the Pliocene-Pleistocene foredeep of the Northern Apennine, are

characterized by diffuse emission of CH<sub>4</sub>-rich gases, CH<sub>4</sub>-saturated shallow aquifers and gas bubbling in water wells (Martinelli et al 2012a and reference therein; Capaccioni et al., 2015). The core of the main buried thrust groups, i.e.: i) Pedeappenninic folds (Reggio, Modena, Bologna, etc.); ii) intermediate folds (Minerbio, Budrio, Cotignola, etc.); iii) Dorsale Ferrarese inner arc (Correggio, Mirandola, Cento, Argenta, Ravenna); iv) Dorsale Ferrarese outer arc (Poggio Rusco, Bondeno, Ferrara, Comacchio) still preserve major hydrocarbons reservoirs (Casero, 2004; Martinelli et al., 2012a), presently exploited by oil and gas companies (e.g. ENI S. p. A., Gas Plus S. p. a.). According to Mattavelli et al. (1983), 80% of the deep hydrocarbon reservoirs in the Po Plain subsurface has a biogenic origin, whereas thermogenic (10%) and mixed (10%) gases account for the remaining percentage. The outermost buried front of the Northern Apennine orogenic thrust belt (Ferrara arc) is likely still active in response to the general compressive stress field dating from the middle Pleistocene. The most recent seismic sequence struck the eastern Po Plain in May 2012, causing 27 fatalities and widespread damages to infrastructure, economy and cultural heritage. After the two main seismic occurred on May 20th and 29th 2012, unusual geological phenomena (UGP), such as sudden temperature increases of water from wells (up to 53°C), as well as extrusions of mud-sand-fluid mix and shallow fracturing of soils, have been reported to occur mostly within the epicentral region, located between the municipalities of Ferrara and Mirandola (Bonzi et al., 2017). Presently, six years after the May-June 2012 Emilia earthquake, heating events of groundwaters in domestic wells are still registered with an unchanged frequency, raising concern in the population. Recently, Capaccioni et al. (2015), investigating a farming area (“Warm Earths of Medolla”) located in proximity of the town of Medolla (Mirandola, Modena, Emilia-Romagna Region, Italy) and characterized by warm soils (51.8 °C, Sciarra et al., 2017), linked the increases in ground temperature to the heat release through the exothermic oxidation of methane, diffusively uprising from deeper layers, by methanotrophic bacteria under aerobic conditions (Cappelletti et al., 2016). However, it has not been yet clarified in the literature whether the same phenomenon is responsible for the increase of the water temperature in wells. Co-seismic and post-seismic occurrence of gas-related UGP, renewed the interest for the origin and fate of methane and light hydrocarbons in the Po Plain. In this study we have investigated the chemical and isotopic composition of dissolved gases and waters by coupling direct sampling and continuous monitoring of phreatic water wells for which a heating episodes was documented in the past. The main aim is to provide insights into the mechanism timing of temperature increases. Furthermore, gases and waters from deep exploitation wells of natural gas fields, CH<sub>4</sub>-rich waters from artesian wells

and bubbling gases from deep abandoned borehole and phreatic wells were geochemically characterized to investigate the possible link between heating episodes, surficial CH<sub>4</sub>-rich gas seepage, shallow and deep hydrocarbon reservoirs and structural context of the Emilia Plain (Emilia-Romagna Region, Italy). A comprehensive conceptual model of the CH<sub>4</sub>-rich fluids pathways in the Po Plain subsurface was also produced.

## 2. Geological settings

Po River sedimentary basin (Figure 1) is a complex physiographic and sedimentary system representing the foreland basin of both the Alps and Apennine mountain chains (Fantoni and Franciosi, 2010). The Apennine chain is the domain of the Alpine orogen generated during the last (*Neo-Alpine*) phase of the orogenesis (Vai, 2001), linked to the collisional overthrusting of the Sardinia and Corsica continental block onto the African Apulia (Castellarin et al., 1992). After the Burdigalian and Messinian tectonic phases (Castellarin, 2001; Ghielmi et al., 2010) a fast NEward migration of the northern Apennine chain front toward the present location, occurred in the Lower Pliocene (Cerrina Ferroni et al., 2002). The continuation of the orogen tectonic evolution, during the Late Pliocene and Pleistocene (post-collisional phase) was due to a slab-retreat mechanism (e.g. Scrocca et al., 2007; Picotti and Pazzaglia, 2008; Martelli et al., 2017a, therein references; Martelli et al., 2017b) that induced a frontal area shortening and a back-arc area extension (Doglioni et al., 1999). These tectonic actions shaped a still evolving thrust-and-fold chain whose last, youngest foredeep basin is the Po valley sedimentary prism. The chain shows two fronts 50 km distant one another. The inner front raises above the regional alluvial plain whereas the outermost one is still buried beneath the Po plain. The former defines the geomorphologic features of the foothill (Boccaletti and Martelli, 2004; Boccaletti et al., 2011) and coincides with the Pedepenninic Thrust Front (PTF) (Boccaletti et al., 1985) resting, in turn, upon a first group of buried folds and thrusts very close to the PTF (Pedepenninic folds). The latter, buried front is composed of three groups of main faulted folds, each coupled with a huge back syncline, from Northwest to Southeast: i) Emilia Folds, ii) Ferrara (and Romagna) Folds, iii) Adriatic Folds (Pieri and Groppi, 1981; Bigi et al., 1990; Turrini et al., 2014). The second fold group, named *Dorsale Ferrarese*, is located in the central part of Emilia Romagna Region and its front is the most protracted in the foreland area. The compressive field stress causing the thrusting maintained the entire Apennine orogen below the coeval sea bottom up to the end of the Lower Pliocene. During the Middle-Late Pliocene (ca. 3.9-3.3 My: *Intrazanclean*) and the

Lower Pleistocene (ca.2.4-2.2 My: *Gelasian*) tectonic phases (Di Dio, 1998) the chain began to uplift and generated an embryonal emerged topography. Concomitantly with these tectonic phases the three buried structural arches of the Emilia-Ferrara-Adriatic Folds were activated (Ghielmi et al., 2013), highlighting a tectonic *jump* of the chain front (Martelli et al., 2017b). At the end of the Lower Pleistocene the generalized uplifting of the chain began to trigger a quick forced marine regression all over the Po Valley moving from western toward eastern areas (Muttoni et al., 2003; Gunderson et al., 2014). In such a way, an important stratigraphic body (Po valley *Prograding Complex*) was generated that with its upper coastal sands (0.8-0.65 My BP) marked also in Emilia Region (Di Dio, 1998) the definitive physiographic change of the Po valley area from a marine to a prevailing continental environment. At the same time also the emerged chain front established itself at the present location (Bartolini, 2003). Finally, from the Middle Pleistocene up to the Holocene, the mainly continental sedimentation, conventionally comprised in the *Emiliano-Romagnolo Supersyntheme* (e.g. Di Dio, 1998; R.ER., 2003; Boccaletti et al., 2011), recorded both alluvial environment and transitional-shallow marine facies (Martelli et al., 2017b) laterally and vertically organized according to the transgressive-regressive glacio-eustatic cyclicity (Amorosi et al., 2008; 2016; Campo et al., 2017). Their fine-grained sequences are attributed to both interglacial and glacial ages. A transversal tectonic faulting of the buried thrusts (Nardon et al., 1991; ISPRA, 2015) and a one order of magnitude decrease of the compressional deformation during the Pleistocene are known (Boccaletti et al., 2011) coupled with a prevailing vertical motion of buried structural highs during the Middle-Upper Pleistocene (Ghielmi et al., 2013), in particular around 250-230 ky BP (Martelli et al., 2017b). In the last 1.4 My BP the uplifting rate of the external buried front decreased from 0.53 to 0.16 mm/y (Scrocca et al., 2007) whereas the emerged morphologic front of the chain is now uplifting at a rate of 1 mm/y (D'Anastasio, et al. 2006; Carminati and Valditacca, 2010a) and the geologic subsidence rates of the Po alluvial basin in the same period is in the range of 0.5-2 mm/y (Carminati and Martinelli, 2002). Due to these movements the thrusts' top of the *Dorsale Ferrarese* at places now are lying buried at around 100 m of depth beneath the today topographic surface (RER and ENI-AGIP, 1998; Capaccioni et al., 2015). GPS data show that the crustal shortening still occurs along the buried chain front (Devoti et al., 2010; Carminati et al., 2010a) as well as the thrusting activity (Di Bucci and Angeloni, 2013; Vannoli et al. 2014) that was stressed by the May 2012 Emilia seismic sequence (Galli et al., 2012; Cesca et al., 2013; Ventura and Di Giovambattista, 2013; Martelli et al., 2017b; Nespoli et al., 2018) responsible for positive vertical displacements ranging between 73 and 150 mm (Devoti, 2012; Borgatti et al., 2012)

and related crustal shortening between 30 and 40 mm (Galli et al., 2012) recorded in the epicentral area

### *2.1 Hydrogeological and hydrochemical setting*

The Po River sedimentary basin is a system where buried marine sediments with fossil saltwater and overlying freshwaters-bearing continental sediments are still mutually interplaying (Castellarin et al., 2006; Martinelli et al., 2016). The hydrostratigraphic frame of the Emilia foreland basin was derived by the interpretation of industrial seismic sections, hydrocarbon and water wells throughout the recognition of a repeated alternance of fine-grained aquiclude/aquitard bodies and relatively coarse-grained aquifers (RER and ENI-AGIP, 1998; Teatini et al., 2006). In the SER the aquifers are the sum of the continental river channel bodies with related subfacies (hydrostratigraphic unit A and B in RER and ENI-AGIP, 1998) and of the Pleistocene coastal sands (hydrostratigraphic unit C in RER and ENI-AGIP, 1998), whereas in the paleo-marine domain lying beneath the SER aquifers are mainly represented by the coarse grained term of the turbidite sequences. In principle, the former have got a more irregular geometry and contain freshwater whereas the latter are more regular and contain brackish or salt waters. As a matter of fact, the hydrostratigraphic boundaries between freshwaters and saltwaters cuts diagraphically the boundaries of the three main aquifer Groups A, B, and C schematically drawn in Figure 2 in a very simple way. In fact, the deepest aquifer C, corresponding to the last marine deposits and to the transitional complex, now is often bearing freshwater rather than the original marine connate saltwater, thus suggesting water displacement phenomena. The elevation of the buried freshwater/saltwater boundary changes from place to place mainly according to the local tectonic features, being deepest in synclines and highest in anticline-top areas (IRSA and CNR, 1982; RER and ENI-AGIP, 1998; Molinari et al., 2007). Anyway, the elevation of this boundary is higher along the today back-coastal Adriatic areas, due to the presence of the recent connate marine water. Somewhere the occurrence of other brackish water uprisings in areas lying in the inner alluvial plain, far from the sea, coinciding with buried structural highs as well as sinclines is recorded (Castellarin et al., 2006) leaving open questions concerning the water uprising mechanisms and pathways. According to RER and ENI-AGIP (1998) the aquifer Group A is characterized by Ca-HCO<sub>3</sub> (Ca-bicarbonate) waters with the exception of two areas: i) the easternmost part of the Region together with the *Dorsale Ferrarese* top where Na-HCO<sub>3</sub> groundwaters are recorded; and ii) the highest culminations of the *Dorsale Ferrarese* thrust

hosting Na-Cl waters. The underlying aquifer Group B is not completely known and this explains the uncertainties in the sketch of Figure 2. In the central-eastern part of the Region it shows Na-HCO<sub>3</sub> groundwaters whereas in the western part the existence of predominantly Ca-HCO<sub>3</sub> groundwaters is poorly known. In the C Group the existence of Na-HCO<sub>3</sub> and/or Ca-HCO<sub>3</sub> groundwaters is likely due to a displacement of a possible original Na-Cl hydrochemical facies. In Na-HCO<sub>3</sub> groundwaters the Na excess is due to ionic exchanges between meteoric waters and Na-rich clay minerals together with the mediation of CO<sub>2</sub> mainly deriving from the organic matter degradation (RER and ENI-AGIP 1998) and/or the Na-Ca exchange with clays (Martinelli et al., 2014). Na-Cl groundwaters result from the mixing of Quaternary transgressive saltmarsh and lagoonal or Pliocene marine waters and meteoric waters (Martinelli et al., 2014). In Figure 2 simplified, ideal sketch of the groundwater chemical facies distribution is proposed according to the evidences from recent surveys (e.g. Moggia, 2016). Isotopical analyses show that the maximum age of the ancient A Group and B Group groundwaters is in the order of 30 ky BP (Martinelli et al., 2014) but the ages can result renewed by the severe artificial water withdrawal (ENI-AGIP, 1998). Notwithstanding this, it is accepted that the Po basin deeply buried Pliocene sediments are still experiencing an active dewatering process highlighted by the expulsion of brackish waters (*salt plumes*) from the buried thrusts front (Martinelli et al., 2016). Furthermore it was also recognized that in the central-eastern part of the Emilia plain the deep confined aquifers not recharged by modern infiltration circuits are characterized by a high hydraulic head possibly linked to the active tectonic compression (Martinelli et al., 2016) as suggested for the Hungarian Plain (Toth and Almasi, 2001).

## 2.2 Unusual geological phenomena in the Emilia-Romagna Region

In May-June 2012, the Emilia-Romagna Region has been struck by an intense seismic sequence, affecting a 50-km wide area located at the southern edge of the Po river alluvial plain. The sequence started on May 20, with a  $M_L$  5.9 earthquake followed by thousands of earthquakes, six of them with  $M_L \geq 5.0$ . Immediately after the start of the seismic sequence, several anomalous events, presently known as unusual geological phenomena (UGP) have been observed and reported by the local population (Bonzi et al., 2014; 2017). In the period from June 2012 to September 2018, 88 UGP have been documented, the majority of whom occurred in correspondence of the epicentral area of the seismic swarm, while only a small percentage is located in peripheral areas such as the municipality of Bologna and the eastern

sector of the Po Plain (Figure 3). These UGP have been grouped into six categories: (i) occurrence of warm water in phreatic wells (41); (ii) gas bubbling in water wells (24); (iii) surficial fractures and ground deformations (9); (iv) fast water-wells level changes (2); (v) death of fishes in small lakes and canals (4) and (vi) sand and mud volcanoes (8). Most of the UGP listed above concern the increase of water temperature, up to 55 °C, in phreatic wells less than 10 meters deep and mainly located in the northern part of the Modena province. These events have been called “Warm Water Wells” and the acronym WWW will be used from now on to refer to these phenomena. Some of this WWW are surely due to an anthropogenic reason such as the malfunctioning of the water well pump (Bonzi et al., 2017). An online database (<http://ambiente.regione.emilia-romagna.it/geologia/temi/geologia/fenomeni-geologici-particolari>) have been created by the Geological, Seismic and Soil Survey of the Emilia-Romagna Region in order to collect all the information regarding the UGP and to make them available to the scientific community and public. Less than one UGP per year has been reported before the seismic sequence of May-June 2012, hence these phenomena can be classified as co-seismic or post-seismic events. Accordingly, historical documentation reported the occurrence of luminous phenomena, changes of water’s characteristics in wells and soil liquefaction after great seismic shocks that struck Italy before 1990 (Boschi et al., 1995; 1997). However, Martinelli et al. (2016) suggest that no influence on the UGP can be assigned to seismicity, in particular, to that experienced in May 2012 with the only exception of the progressive water table rising of the deepest aquifers. Notwithstanding, two evidences cannot be denied: i) the most of these phenomena is located in the core of the 2012 seismic swarm epicentral area; ii) the clear increase in the number of UGP occurred after the earthquakes in Emilia-Romagna Region seems to point to the existence of a relationship, although still not clarified, between seismotectonic and UGP.

### **3. Materials and methods**

#### *3.1 Study sites and methodology*

The study sites are located in the Southern Po River basin, most of whom within the Modena province. Waters and gases from domestic phreatic and artesian wells (15), abandoned natural gas wells (3), gas seepages (3) and wells from five oil and gas field have been investigated. At W4, W6, W7, W8, W10, W11, W16, W17 and W18 at least one episode of water temperature increase has been documented after the seismic sequence of May-June 2012. The basic information concerning the surveyed sites are summarized in Table 1. Their location with

respect to the buried tectonic setting is also reported. As for the G-wells also the studied W-wells gas seepages are mostly located on structural high (Figure 1) but a small group is located in syncline areas. The Cavone field (G1) (Pieri and Groppi, 1981; Nardon et al., 1991; ENI, 1994) produces oil from a structural trap lying in the Dorsale Ferrarese inner arc. The reservoir is hosted in Mesozoic carbonate formations (*Brecce di Cavone and Calcari Grigi di Noriglio*) at around 3000 m depth. Its economic importance and the key location in the 2012 earthquake epicentral area triggered a wide debate concerning the possible relationships between the field exploitation and seismicity (Lavecchia et al. 2015; Mucciarelli et al. 2015). Spilamberto (G2) (ANL, 1959) and S. Martino gas fields (G3) (ENI, 1994) lie upon the Pedepenninic folds group. At Spilamberto the gas pool was intercepted at 1242 m depth, lying at the bottom of Pliocene clayey seal (ANL 1959), and another productive level was at 1460 m depth (Scicli, 1972). The Sillaro field (G4) found gas at 2100 m depth in several horizons hosted in the Pliocene suite (Energy-pedia, 2010). The reservoir of Dosso Angeli (G5) (ENI, 1972) is hosted in an anticline structural trap in Pliocene sandy deposits. It consists of 8 pools with the gas-water contact lying between 2885 and 3839 m depth (Simeoni et al., 2017) but the three most important levels lie between 3033 to 3232 m depth (Bertoni et al., 1995). Well W1 (Vallalta) was originally created as a natural gas well but today it is out of service and delivers gases (mostly methane) coming from Miocene geological formations together with water mainly supplied by the uppermost 250 m of Quaternary sedimentary cover (Martinelli et al., 2016). W2 (Diamantina) is one of 24 abandoned gas wells drilled up to an average thickness of 200 m between 1948 and 1963 m depth (Scicli, 1972). This well erupted gas and brackish water in 2014 after the degraded sealing disruption. In the Coccabile geographic area, to which Ambrogio village pertains, between years 1944 and 1969 24 gas wells were drilled up to 350 m average depth (Scicli, 1972). In 2013 one of these wells (W3) erupted warm, brackish water and gases as the result of sealing wear. Water wells (W4-W18) have depth not exceeding 350 m and are located in the Holocenic sedimentary suite (<20 m) and within sediments dating back to middle-upper Pleistocene (20-350 m). They intercept the A and, to a lesser extent, the B regional aquifers.

### 3.2 Water and gas sampling

Water and dissolved gas samples from phreatic wells were collected using sampling equipment consisting of a Rilsan<sup>®</sup> tube (6 mm in diameter), lowered to half of the water column, and a 150 mL syringe equipped with a three-way valve to pump the water up to the

surface. Waters and gases from artesian wells were sampled using a submerged electric pump. Water samples were collected after the displacement of a water volume double than the inner volume of the tube (Cabassi et al., 2013 and references therein). To minimize the dissolved gas loss, the water discharging from the Rilsan<sup>®</sup> tube was flushed into a bucket where the pre-evacuated 250 mL glass flasks equipped with a Teflon stopcock used for the sampling were submerged and opened, allowing the water entering up to about three quarters of the flask inner volume (Tassi et al., 2009). Gases naturally bubbling in water wells were collected using a funnel up-side-down positioned and connected to the sampling flasks. At W4, W5, W8, W9, W10, W11 and W12, water and gas sampling were performed every two months in the period 2015-2016, in order to detect temporal compositional variations and trends. Waters from deep exploitation wells were collected at the water-gas separator, while gases were sampled by connecting the sampling line to the pressure-control valve of the production wells. At each exploitation wells, two gas aliquots were collected, as follows: (1) one 60 mL glass flask for the determination of major compounds concentrations and isotopic composition of C<sub>1</sub>-C<sub>4</sub> n-alkanes and (2) one 12 mL glass vials equipped with a silicone rubber porous septum for the analysis of C<sub>5</sub>-C<sub>10</sub> VOCs. At eight selected wells, a third gas aliquot for the measurement of isotopic composition of noble gases (He and Ar) was also collected in a stainless-steel flask to prevent helium losses by diffusion after sampling. Water temperature (°C), electrical conductivity, pH and Eh were measured in the field. Three water aliquots were collected at each sampling site, as follows: (1) one aliquot in a 125 mL polyethylene bottle, for the determination of main anions, (2) one filtered (0.45 µm) aliquot in a 50 mL polyethylene bottle containing 0.5 mL of 30 % Suprapur HCl, for the analysis of main cations, and (3) a third aliquot in glass bottles with the addition of HgCl<sub>2</sub> for the isotope analysis of water (δD and δ<sup>18</sup>O) and total dissolved inorganic carbon (δ<sup>13</sup>C–TDIC).

### *3.3 Continuous monitoring techniques*

Temporal changes of water temperature (T), electrical conductivity (EC) and level (WL) were monitored in four phreatic wells (W4, W8, W10 and W11) by placing a multi-parameter probe close to the bottom of the water column. Data stored in the data loggers were downloaded every two-three months. At W4, W8 and W11, all three parameters (T, EC and WL) were monitored by means of a Seba Hydrometrie Dipper PTEC high-performance 32 bit measurement data collector (T, EC, WL sensor accuracy of ± 0.1 °C, ± 1 mS/cm and ± 0.1 %, respectively) while at W10, temperature and water-level were monitored using an integrated

pressure sensor OTT Orpheus Mini (accuracy for temperature and water-level measurements were  $\pm 0.5$  °C and  $\pm 0.05$  %, respectively).

### *3.4 Chemical and isotopic analysis of waters*

The main ionic species were analyzed by ion chromatography (IC), using an 861 Advanced Compact IC-Metrohm for cations (Na, NH<sub>4</sub>, K, Mg, Ca) and a 761 Compact IC-Metrohm for anions (F, Cl, Br, NO<sub>3</sub>, SO<sub>4</sub>). The HCO<sub>3</sub> concentrations were determined by acidimetric titration (AT) with 0.01 N HCl using a Basic Titrino 794-Metrohm. The analytical errors for IC and AT were < 5%.

The <sup>18</sup>O/<sup>16</sup>O and <sup>2</sup>H/<sup>1</sup>H isotopic ratios (expressed as  $\delta^{18}\text{O}$  and  $\delta^2\text{H}$  ‰ vs V-SMOW) in water samples were determined by using a Finnigan Delta PlusXL mass spectrometer according to standard protocols. Oxygen isotopes were analyzed using the CO<sub>2</sub>–H<sub>2</sub>O equilibration method proposed by Epstein and Mayeda (1953). Hydrogen isotopic ratios were measured on H<sub>2</sub> after the reaction of 10 mL of water with metallic zinc at 500 °C (Coleman et al., 1982). The experimental error was +0.1‰ and +1‰ for  $\delta^{18}\text{O}$  and  $\delta^2\text{H}$  values, respectively, using EEZ-3 and EEZ-4 as internal standards that were previously calibrated versus V-SMOW and SLAP reference standards. The values of  $\delta^{13}\text{C}$ -TDIC were analyzed with a Finnigan Delta Plus XL mass spectrometer after the reaction of 3 mL of water with 2 mL of anhydrous phosphoric acid in vacuo (Salata et al., 2000). The recovered CO<sub>2</sub> was analyzed after a two-step extraction and purification procedures of the gas mixtures by using liquid N<sub>2</sub> and a solid-liquid mixture of liquid N<sub>2</sub> and trichloroethylene (Evans et al., 1998; Vaselli et al., 2006). The analytical error for  $\delta^{13}\text{C}$ -TDIC was  $\pm 0.05$  ‰.

### *3.5 Chemical and isotopic analysis of gases*

Inorganic gases (CO<sub>2</sub>, N<sub>2</sub>, O<sub>2</sub>, and Ar) stored in the sampling glass flasks were analyzed using a Shimadzu 15A and a Thermo Focus gas chromatographs equipped with Thermal Conductivity Detectors (TCD). Methane and light alkanes (C<sub>2</sub>H<sub>6</sub>, C<sub>3</sub>H<sub>8</sub>, iso-C<sub>4</sub>H<sub>10</sub>, n-C<sub>4</sub>H<sub>10</sub>) were analyzed using a Shimadzu 14A gas chromatograph equipped with a Flame Ionization Detector (FID). The composition of dissolved gas compounds was calculated on the basis of the Henry's law constants, regulating the liquid-gas equilibrium for each volatile compound (Vaselli et al., 2006; Tassi et al., 2008). The C<sub>4+</sub> hydrocarbons were analyzed by GC–MS (Gas Chromatography coupled with Mass Spectrometry) using the Solid Phase Micro-Extraction (SPME) technique (Arthur and Pawliszyn, 1990) to extract volatile organic

compounds (VOCs) from the gas mixture and inject them in the GC–MS (Davoli et al., 2003; Mangani et al., 2003; Florez Menendez et al., 2004). Quantitative analyses were performed using an external standard calibration procedure on the basis of calibration curves constructed measuring the instrumental signal of Accustandard® standard mixtures of compounds pertaining to the following functional groups, cyclic compounds, aromatic compounds (Tassi et al., 2011). The values of the Relative Standard Deviation (RSD), calculated from five replicate analyses of the gas mixture in which the compounds of interest are present at a concentration of 50 ppbv, were  $\leq 5\%$ . The limit of quantification (LOQ) was determined by linear extrapolation from the lowest standard in the calibration curve using the area of a peak having a signal/noise ratio of 5 (Mangani et al., 2003). The  $^{13}\text{C}/^{12}\text{C}$  ratios of dissolved  $\text{CO}_2$  ( $\delta^{13}\text{C}-\text{CO}_{2(\text{aq})}$ ) were determined on the basis of those measured in the separated gas phase stored in the headspace of the dissolved gas flasks. The  $^{13}\text{C}/^{12}\text{C}$  values (expressed as  $\delta^{13}\text{C}-\text{CO}_2$  Vienna Pee Dee Belemnite (VPDB)‰) were analyzed by mass spectrometry (Finnigan Delta S), after a two-step extraction and purification procedures of the gas mixtures by using liquid  $\text{N}_2$  and a solid-liquid mixture of liquid  $\text{N}_2$  and trichloroethylene. Internal (Carrara and San Vincenzo marbles) and international (National Bureau of Standards (NBS) 18 and NBS 19) standards were used to estimate external precision. The analytical uncertainty and the reproducibility were  $\pm 0.05\%$  and  $\pm 0.1\%$ , respectively. The analyses of the  $^{13}\text{C}/^{12}\text{C}$  and  $^2\text{H}/^1\text{H}$  ratios of  $\text{CH}_4$  (expressed as  $\delta^{13}\text{C}-\text{CH}_4$  ‰ vs V-PDB and  $\delta\text{D}-\text{CH}_4$  ‰ vs V-SMOW, respectively) were performed by mass spectrometry (Varian MAT 250) according to the procedure described by Schoell (1980). Analytical error was  $\pm 0.15\%$ . The analysis of the  $\delta^{13}\text{C}$  and  $\delta\text{D}$  of  $\text{CH}_4$ ,  $\text{C}_2\text{H}_6$ ,  $\text{C}_3\text{H}_8$ ,  $n\text{-C}_4\text{H}_{10}$  and  $i\text{-C}_4\text{H}_{10}$  in the gas samples from deep natural gas wells were carried out at the Goethe University in Frankfurt following the methods outlined by Fiebig et al. (2015). External analytical precision was  $\pm 0.5\%$ .

The He-isotope composition and the  $^4\text{He}/^{20}\text{Ne}$  ratio were determined by separately introducing He and Ne into a split-flight-tube mass spectrometer (GVI Helix SFT) after performing standard purification procedures (e.g., Correale et al., 2012). The values of the  $^3\text{He}/^4\text{He}$  ratio are expressed as  $\text{R}/\text{Ra}$  (where  $\text{Ra}$  is the  $^3\text{He}/^4\text{He}$  ratio of air, which is equal to  $1.39 \times 10^{-6}$ ); the analytical error was generally less than 1%. The  $\text{R}/\text{Ra}$  values were corrected for atmospheric contamination based on the  $^4\text{He}/^{20}\text{Ne}$  ratio. The Ar-isotope composition was measured in a multi-collector mass spectrometer (GVI Argus), for which the analytical uncertainty was generally less than 0.5%. The uncertainty in the determinations of He, Ne, and Ar elemental contents was less than 5%.

## 4. Results

### 4.1 Water geochemistry

Temperatures, EC, TDS (Total Dissolved Solids), pH, Eh, concentrations of the main solutes (in mg/L) and isotopic composition of water and TDIC (Total Dissolved Inorganic Carbon) are reported in Table 2. Waters from Cavone (G1), Spilamberto (G2), Sillaro (G4), Dosso Angeli (G5) gas fields and abandoned gas wells (W1, W2 and W3) have a Na-Cl composition (Figure 4a), high TDS (4.5-71 g/L) and circumneutral pH (from 6.7 to 7.7), while waters of S. Martino (G3) have a Ca-HCO<sub>3</sub> composition and low TDS (594 mg/L). In the Cl vs. Na diagram (Figure 4b), these waters show a Na/Cl ratio close to the seawater value (Na/Cl = 0.85, atomic ratio), whereas brackish and saline waters (W1, W2, W3, G1, G2, G4 and G5) exhibit lower Cl/Br ratio lower (427 to 520). thus excluding the dissolution of Triassic or Messinian evaporitic minerals as the main source of Na, Cl and Br. The high concentrations of bromine may be instead ascribed to the decomposition of organic matter (Conti et al., 2000; Toscani et al. 2007; Boschetti et al., 2011; Sciarra et al., 2013). The  $\delta D$  and  $\delta^{18}O$  values, measured in seven water samples from gas fields (G1-G5) and abandoned gas wells (W2 and W3), range from  $-69.2\text{‰}$  to  $+3.7\text{‰}$  and from  $-10\text{‰}$  to  $+7.7\text{‰}$  vs. V-SMOW, respectively. As shown in Figure 5, W-waters plot close to the GMW (Craig, 1961) and LMW (Longinelli and Selmo, 2003) lines, while G-waters deviate from the meteoric lines, plotting on a meteoric-seawater mixing trend. Waters of G1 show a moderate shift to highly positive  $\delta^{18}O$  values ( $+7.7\text{‰}$ ), suggesting that the early isotopic composition of the water was modified by high temperature ( $>100^{\circ}C$ ) interaction with carbonate rocks (Morad et al., 2003). Waters from the upper unconfined A-aquifer (W4-W18) have temperatures and TDS ranging from  $10.1^{\circ}C$  to  $53.6^{\circ}C$  and from  $0.7\text{ g/L}$  to  $3\text{ g/L}$ , respectively and are neutral to weakly basic (pH = 6.9-8.1). Eh values are highly variable, ranging from  $-378\text{ mV}$  to  $+271\text{ mV}$ . These waters mostly have a Ca-HCO<sub>3</sub> composition (Figure 4a), which is typical of meteoric waters circulating at shallow depth within sedimentary rocks (Martinelli et al., 1998; Duchi et al., 2005). Waters from Mirabello area (W16-W18) show high contents of sulfate (294-783 mg/L), which may be attributed to H<sub>2</sub>S<sub>(aq)</sub> oxidation or anthropogenic sources (e.g. agricultural fungicides). As shown in Figure 4b, W-waters plot close to the dilution line between shallow meteoric waters and seawater, suggesting that the relatively high concentrations of Na and Cl observed in some samples may be ascribed to contributions from fluids trapped in marine sediments (RER and ENI-AGIP, 1998; Martinelli et al., 1998;

Boschetti et al., 2011; Sciarra et al., 2013). Carbon isotopic composition of TDIC of the analyzed waters ranges from  $-26.9\text{‰}$  to  $-5\text{‰}$  vs. V-PDB.

#### 4.2 Chemical gas composition

The concentration of the main constituents ( $\text{CO}_2$ ,  $\text{N}_2$ , Ar,  $\text{O}_2$ ,  $\text{CH}_4$  and  $\text{C}_2\text{--C}_4$  alkanes) of dissolved and free gases is shown in Table 3 (W and S sites) and Table 4 (G-sites). The chemical gas composition of the W and S samples is highly variable. On the basis of  $\text{CH}_4$  content (% v/v), two groups can be distinguished: i)  $\text{CH}_4$ -rich gases (W1, W2, W5, W9, W13, W14, W15, S2 and S3); and ii)  $\text{CH}_4$ -poor gases (W4, W6, W7, W8, W10, W11, W12, W16, W17 and W18). Gases of the former group are dominated by  $\text{CH}_4$  ( $>50\%$  v/v) followed by  $\text{N}_2$  (up to  $32.5\%$  v/v),  $\text{CO}_2$  (up to  $12.4\%$  v/v),  $\text{O}_2$  (not exceeding  $4.5\%$  v/v) and Ar ( $0.06\text{--}0.8\%$  v/v). The  $\text{CH}_4$ -poor gases are instead characterized by low ( $<50\%$  v/v) or absent contents of  $\text{CH}_4$ , high concentrations of atmospheric gases and highly variable  $\text{CO}_2$  concentrations (from  $<1.7\%$  to  $87\%$  v/v).  $\text{C}_2\text{--C}_4$  alkanes (ethane, propane, n-butane and iso-butane) were detected in all  $\text{CH}_4$ -rich gases and in the W11 dissolved gases, at total concentrations ranging from  $0.59$  to  $1.76$  mmol/L. Gases from G-sites are dominated by  $\text{CH}_4$  that ranges from  $64.5$  to  $99.98\%$  v/v. At G1, propane is the most abundant alkane of the  $\text{C}_2\text{--C}_4$  fraction, while at the other sites ethane dominates. Up to 70 different  $\text{C}_4\text{--C}_{10}$  hydrocarbons, pertaining to the alkane (33 compounds), cyclic (29 compounds), aromatic (6 compounds) and organosulfur (2 compounds) groups were recognized and quantified in the G-gases (Table 5). The  $\text{C}_{4+}$  hydrocarbons mainly consist of alkanes and cyclics, while relatively high contents of aromatics were detected only at G1. Cyclics having  $\text{C}_5$ ,  $\text{C}_6$ ,  $\text{C}_7$  and  $\text{C}_8$  rings are mostly tri-, di- and mono-methylated, although cyclopentane and cyclohexane represents a significant fraction ( $12\%$  and  $22\%$ , respectively at G1) of the total cyclic abundance in some gases. Few cyclics showing ethyl, propyl branches and polycyclic compounds were detected and their concentrations are lower than those of not-branched and methylated compounds. Benzene and toluene are the most abundant aromatic compounds. Organosulfur group includes dimethylsulfide and carbondisulfide, both present at trace levels in all investigated gases.

#### 4.3 Isotopic composition of $\text{CO}_2$ , $\text{CH}_4$ , $\text{C}_2\text{--C}_4$ alkanes and noble gases (He and Ar)

The  $\delta^{13}\text{C}\text{--CO}_2$ ,  $\delta^{13}\text{C}\text{--CH}_4$  and  $\delta\text{D}\text{--CH}_4$  values in the W and S gases (Table 3) vary within wide ranges, comprised between  $-73.2$  and  $-15.5\text{‰}$  vs. V-PDB,  $-79$  and  $-20.7\text{‰}$  vs. V-PDB and  $-225$  and  $-58\text{‰}$  vs. V-SMOW, respectively. Both the  $\delta^{13}\text{C}\text{--CH}_4$  and  $\delta\text{D}\text{--CH}_4$  values for

the G-gases are clustered in a narrow range, from  $-71.7$  to  $-54.5$  ‰ vs. V-PDB and from  $-210$  to  $-171$  ‰ vs. V-SMOW, respectively. Relative variations in  $\delta^{13}\text{C}$  values decrease in the order ethane, propane, n-butane and iso-butane, the latter having a carbon isotopic composition ranging from  $-21.6$  to  $-30$  ‰ vs. V-PDB. The isotopic composition of helium and argon were measured in 9 G-samples.  $R_{\text{C}}/R_{\text{A}}$  ratio varies within a narrow range, from 0.014 to 0.04. The  $^{40}\text{Ar}/^{36}\text{Ar}$  and  $^{38}\text{Ar}/^{36}\text{Ar}$  ratios range from 292 to 317 and from 0.1871 to 0.1897, respectively. The  $^4\text{He}/^{20}\text{Ne}$  ratios vary from 5 to 727, i.e. largely higher than the atmospheric background ( $^4\text{He}/^{20}\text{Ne} = 0.318$ ).

#### *4.4 Temperature, electrical conductivity and water level temporal series*

Temperature (T), electrical conductivity (EC) and water level (WL) time series were obtained for four warm water wells (WWW), i.e. W4, W8, W10 and W11. At W10, EC was not recorded. During the continuous measurement period, ranging from September 2016 to November 2017, no significant changes in the monitored parameters were observed at W4. The evolution over time of the water temperature (Figure 6) shows minimum values in correspondence of the winter months and maximum values during summer, indicating that the water temperature is affected by the seasonal variation of the external air's temperature. EC values remained mostly constant throughout the monitoring period. Water level changed over time, with abrupt decreases punctuating the whole period caused by the pumping for agricultural purposes. T, EC and WL data of W8 well were recorded from October 2015 to August 2018. At W8 well the water temperature reached  $55$  °C few days after the installation of the multi-parametric probe and then exponentially declined to normal values. After the temperature peak registered in 2015, the temperature remained stable, varying following an asymmetric sinusoidal pattern typical of shallow aquifers. The evolution over time of the EC and WL was marked by four episodes of concomitant increase of the two parameters. This phenomenon may be ascribed to the arrival of saltier waters from underlying levels. Accordingly, during the first EC peak (2016) an increase in the contents of chloride and sodium were observed at W8 and W9 (Table 2). However, EC-WL peaks were not associated to temperature increase, suggesting the existence of different triggering processes. As for W4, abrupt decreases of WL marked pumping episodes. At W10 well, monitored from May 2016 to May 2017, water temperature followed the same trend observed at W8, but the maximum recorded value was  $33$  °C. W11 well has the most peculiar temperature's time sequence. In fact, the evolution of the well, monitored from September 2012 to August 2018, was punctuated by several episodes of temperature increase, with the highest temperature recorded

of 36 °C. The minimum water temperature of W11 well for the 2012-2015 period has never dropped below 15 °C, almost 2 °C higher than the average value of the minimum temperature of a typical phreatic well (Sciarra et al., 2013). Notwithstanding, frequency and magnitude of heating episodes at W8 well are decreasing over time.

## 5. Discussion

### 5.1 *CH<sub>4</sub>-rich fluids physical pathways in the sedimentary prism of Emilia plain*

Processes involved in methane seeping and related migration pathways are mutually tightly related. For this reason dealing with them as separated realms or entities can be a very difficult task but it is anyhow a convenient way. Furthermore, a tight link between gaseous phase and circulating groundwater solutions exists (Burst, 1969; Cahill et al., 2017; Capaccioni et al., 2017).

The gas generation is a process developing through time at any depth level (see below) according to varying rates depending on the original synsedimentary amount of available organic matter, its conservation or consumption resting on the biogeochemistry of the buried environment at various depth. The primary migration of gas, that is its first progressive upward removal from the original genetic *locus/site* (Burst, 1969), can mainly use the primary permeability of the hosting sediment, i.e. that depending on the grain size related effective porosity. Furthermore, gas can move itself as a free (dry gas) or groundwater-dissolved phase thus possessing different flow speed (Cahill et al., 2017). If a physical permeability threshold (e.g. a clayey aquiclude) exists then gas accumulation generates a pressure increase up to the overcoming of the local lithostatic/hydrostatic pressure threshold.

The secondary migration, moving gas from first location to final reservoir/trap (Wood and Saney 2016), depends on the free volume exhaustion of the former location and on its 3D geometrical characteristics. In both lateral and vertical gas migration the main role is played by grain size anisotropies, packing of coarse sedimentary bodies, up-dip diffusion and secondary permeability due to various fracture kinds afflicting the volume of gas-bearing sediment. According to the geological setting characteristics (see above),

gas sources can be deep marine turbiditic environment, prodeltaic and lagoonal materials as well as alluvial basin sediments with or without peaty layers. The role of primary gas-hosting sediment in marine realm is played by each sandy term of the Bouma turbiditic sequence whereas in the continental environment its equivalent is the riverbed and crevasse channels network. For these reasons, referring in particular to Emilia plain foreland basin (Figure 7),

the structural traps collected the gas in a suite of superimposed pools hosted in marine Pliocene suite (e.g. Dosso Angeli Field) whose huge total volume available for feeding the reservoirs largely exceeds that of the overlying continental Pleistocene suite nourishing the buried paleo-riverbeds network.

If the up-dip secondary migration of natural gas in buried syncline contexts (Oppo et al., 2015) is continuous through time then also around the crestal area of the eroded, buried thrusts' folds this advection must be assumed as an effective mechanism of gas seep from the structural high top. This could have been the origin the carbonatic cemented horizons often recorded at the base of the sediments directly overlying the eroded tops (eg. Capaccioni et al., 2017), thus possibly being Methane-derived Autigenic Carbonates (Capozzi et al 2012; Oppo et al. 2015). Furthermore, upon these eroded structural highs top the existence of brackish groundwaters is recorded resulting from the mixing of Na-Cl connate water and surrounding Ca/Na-HCO<sub>3</sub> groundwaters (Figure 2). In Pleistocene and Holocene buried riverbeds net gas collects by means of a prominent sub-horizontal migration along sand body axis and finally can vertically seep at every place where the effectiveness of the stratigraphic seals is missing due to stratigraphic pinch-outs or secondary discontinuities (Capaccioni et al., 2015; Idem, 2017; Cahill et al., 2017). The complex interconnection net of the permeable sedimentary bodies scattered in uppermost part of the local syntheme (Amorosi et al., 2017) is due to the channel size greater than present and to the character of monocursal or anabranching riverbed of paleo-Po during the glacial periods as well as its freely wandering behaviour. In this sense, if a direct outcropping of buried fault planes in the plain is excluded, the most recent (Holocene) fluvial network sedimentation is the most important driving factor for establishing the topographic location of surficial gas seep. The wide areal diffusion all over the plain, even in the main syncline areas, of the typical subcircular features (Figure 8), such as the ones found at Warm Grounds of Medolla (WGM), suggests that a considerable percent of the diffuse gas seepage is possibly due to methane generated by very young sedimentary deposits. Nonetheless, the role of secondary permeability in the whole buried sedimentary prism is of primary importance for gas vertical migration, in particular at shallow depth, although the literature dealing with this topic is much more abundant for submarine environmental setting than for continental one. The fractures are of different origin (tectonic and not) and scale: i) tear/wrench faults orthogonally intersecting the first order thrust arc (e.g. Figure 1b) (Nardon et al., 1991; ISPRA, 2015); ii) normal faults often located on the thrusts back-side (Bigi et al., 1990) (Figure 1) and sometimes in the syncline depocentral area (e.g. Castellarin et al., 2006); extradossal faults located on thrusts top above the fold neutral surface (Lisle et al., 2009;

Carminati et al., 2010b); iii) faults originating by sediment differential compaction around the thrusts' top (Carminati et al. 2010b); iv) polygonal faults (Cartwright et al., 2003; Goult, 2001; Allen et al., 2013; Morgan et al., 2015; Gay, 2017) or incipient sub-surficial dewatering faults (Burst, 1969; Scherer, 1989) and conical faults/fluid pipes (Gay, 2017); v) seismically induced surficial faults (Pratt, 1998; Obermeier et al., 2001). Furthermore, a secondary porosity enhancement can be generated in the sedimentary cover lying above the blind fault tip (Mandl, 1988; Abe et al., 2008). Finally, the aerated surficial zone characterizing the today topographic surface as well as the large number of man-made water wells represents the end-members of an extremely complex network able to deliver gas at seep location. In addition to these disjunction elements other minor structures of seal-breaching (faults, intrusions and pipes) exist allowing fluids vertical migration (Cartwright et al., 2007). Even if all of them would be lacking a fluid could be carried through an impermeable seal in short (less than a century) events of expulsion when the fluid pressure becomes higher than 85% of the local lithostatic pressure (Roberts and Nunn, 1995).

The most of these features are ideally summarized in Figure 7 to suggest the possible complexity of physical pathways available for gas and groundwater flow in Po Valley as well as in other settings (Wood and Sanei, 2016). Furthermore, these pathways can be responsible also for the mixing of old and young gas original convoys as sometimes recognized (Cremonini et al., 2008). Part of those features, such as volumes of enhanced porosity above the fault tip, extradossal fractures as well as polygonal fault systems (PFS), cannot yet be recognizable in the up to date available seismic sections (ISPRA, 2015) due to their low resolution character. Nonetheless, in some cases fractures/faults buried at medium depth (50-300 m or more) are recorded that do not appear directly linked to the local tectonic contexts (e.g. Castellarin et al., 2006; Cremonini et al., 2010b; Borgatti et al., 2012) thus possibly suggesting the existence of PFS or incipient dewatering fault systems. Other minor but pervasive features such as pipes or small chimneys were recognized in the uppermost thousands metres of the Po plain sedimentary prism (Cremonini et al., 2010b; Cremonini et al., 2010a). In Figure 7 is also reported the suggestion that an aliquot of methane can be produced by the bacterial activity in groundwaters slowly circulating through organic matter rich aquifers (Martinelli et al., 2016). Finally, in the same figure surficial peats combustion phenomena linked to methane seep are also indicated according to literature (Cremonini et al., 2008; Martinelli et al., 2012b; Idem, 2015).

## *5.2 Deep hydrocarbon sources in the Po Plain*

The occurrence of methane in surficial dry seeps, bubbling gases and dissolved gases in groundwater is a widespread phenomenon in the Po Plain. The compositional characteristics of the sampled gases are investigated and compared to those of gases from oil and gas wells (G1-G5) from Emilia-Romagna Region reported in literature (Mattavelli et al., 1983; Elliot et al., 1993; Tassi et al., 2012; Oppo et al., 2013), in order to recognize the source(s) of methane in the shallow geological domains of the study area

The high  $^4\text{He}/^{20}\text{Ne}$  ratios shows that helium mostly derives from an extra-atmospheric source, likely related to the decay of radiogenic elements within the crust, as indicated by the relatively low  $R_C/R_A$  measured at all G-sites. The high  $^{40}\text{Ar}/^{36}\text{Ar}$  ratios of G1 and G2 indicate a significant  $^{40}\text{Ar}$  radiogenic contribution, while the other sampled gases show air-like values. As suggested by Elliot et al. (1993) for Dosso Angeli (G5), preferential production and release of  $^4\text{He}$  over  $^{40}\text{Ar}$  from the sites of their production to the reservoirs have to be invoked in order to explain  $^4\text{He}$ -enrichment without any shift from the atmospheric  $^{40}\text{Ar}/^{36}\text{Ar}$  ratios. The “Schoell”  $\delta^{13}\text{C}-\text{CH}_4$  vs.  $\delta\text{D}-\text{CH}_4$  diagram (Schoell, 1980) (Figure 9a) suggest that  $\text{CH}_4$  in G3, G4 and G5 gases has a biogenic origin, likely through microbial  $\text{CO}_2$  reduction, while G1 and G2 gases are characterized by thermogenic and thermogenic-biogenic  $\text{CH}_4$ , respectively.

These indications are supported by the “Bernard”  $\text{CH}_4/\text{C}_2\text{H}_6$  vs.  $\delta^{13}\text{C}-\text{CH}_4$  diagram (Bernard et al., 1978) (Figure 9b) the G4 and G5 gases, whose reservoir is likely hosted in Pliocene sediments, plot within the field of microbial hydrocarbon production, whereas the G2 and G3 samples seem to be related to mixing between microbial and Tertiary thermogenic fluids. The latter gas source is similar to that recognized for the Cortemaggiore gases that are produced by thermal decomposition of organic matter hosted in the Marnoso Arenacea Formation, a Miocene flysch sequence (Riva et al., 1986; Mattavelli and Novelli, 1990). Gases from Cavone oil field (G1) show remarkably high contents of  $\text{C}_{2+}$  alkanes and  $\text{C}_1/\text{C}_2$  ratio  $<10$ . These features indicate that Cavone hydrocarbon accumulation is a thermogenic gas produced by cracking of kerogen hosted in Triassic carbonates (Mattavelli et al., 1983; Riva et al., 1986). These data are in agreement with those reported by Mattavelli et al. (1983) which claimed that 80% of gases from the Po Plain subsurface consists of biogenic/diagenetic gases while the remaining percentage is equally distributed between thermogenic (10%) and mixed origin (10%) gases.

Carbon isotopic distribution pattern of light hydrocarbons is a useful indicator of gas origin and maturity (Chung et al., 1988; Clayton, 1991; Rooney et al., 1995; Prinzhofner et al., 2000; Berner and Faber, 1996; Lorant et al., 1998). Thermogenic gases produced by primary

cracking of organic matter are typically characterized by the positive order of  $\delta^{13}\text{C}_1 < \delta^{13}\text{C}_2 < \delta^{13}\text{C}_3 < \delta^{13}\text{C}_4$  (Dai, 1992; Boreham and Edwards, 2008; Dai et al., 2016).

As shown in Figure 10, all gases show a direct isotopic pattern, indicating a thermogenic origin of light hydrocarbons. However,  $\delta^{13}\text{C}-\text{C}_2\text{H}_6 < -40\text{‰}$  for the G4 and G5 gases suggest a biogenic/diagenetic input of  $\text{C}_{2+}$  hydrocarbons. Oil-associated gas originating in sapropelic source rock is characterized by  $\delta^{13}\text{C}_2$  values less than  $-28\text{‰}$  (Dai, 1992), and coal-derived gas originating in humic source rock is characterized by  $\delta^{13}\text{C}_2$  values greater than  $-28\text{‰}$ . In this respect, the G1 gases seems to originate by cracking of type I kerogen, while the G2 gases show  $\delta^{13}\text{C}-\text{C}_2\text{H}_6$  values ascribable to both sapropelic and humic source rocks. This feature is most likely related to the heterogeneity of the organic matter in the turbiditic clastic rock unit forming the Marnoso Arenacea Formation (Riva et al., 1986). The G3 gases share several features with the G2 gases, possibly indicating a common origin of the thermogenic endmember. However, the G3 gases are more affected by mixing with biogenic gases and biodegradation of  $\text{C}_{2+}$  with respect to the G2 gases.

The compositional features of  $\text{C}_7$  hydrocarbons are strongly related to: biological sources and diagenetic processes (Duan, 2000; Duan and Ma, 2001; Duan et al., 2004). Among  $\text{C}_7$  hydrocarbons, enrichments of methylcyclohexane are found to occur in oils from terrigenous source material (e.g. lignin, fiber and saccharide of higher plants), whereas dimethylcyclopentane with different structures, deriving mainly from lipids of aquatic organisms, is a typical feature of light hydrocarbons of marine-derived oils (Leythaeuser et al., 1979; Dai, 1993; Wang and Zhang, 2008). Source of normal heptane ( $\text{nC}_7$ ) is comparatively complex and mainly comes from bacteria and algae, or chain lipid of higher plant. The cyclic and chain lipid of different structures are the main components of sapropelic organic matter (type I and type II kerogen) with hydrogen-rich structure, with the relative content influenced by maturity. According to these considerations, in the ternary diagram of  $\text{C}_7$  light hydrocarbon compounds can identify the sources of natural gases. In the ternary diagram of components of MCH,  $\Sigma\text{DMCP}$  and  $\text{nC}_7$  (Figure 11), the G1, G4 and G5 gases show a MCH-poor composition suggesting that type I kerogen is the main source of light hydrocarbons. Conversely, the G2 and G3 gases are enriched in methylcyclohexane, strengthening the idea of thermal decomposition of terrigenous organic matter as the main gas source. In Figure 12, where the concentrations of cyclic compounds with respect to the total cyclic abundances is shown for the G1-G5 gases are reported, three main patterns can be distinguished: (i) enrichment in  $\text{C}_6$  cyclic compounds (cyclohexane and methycyclopentane) observed for the G1 gases; (ii) enrichment in not-branched, mono- and di-methylated

cyclohexane and minor enrichment in branched cyclopentane in the G2 and G3 gases and (iii) enrichment in dimethylcyclopentane and trimethylcyclohexane in the G4 and G5 gases. Paucity of methylated species at G1 gases could be caused by the progressive expulsion of methyl groups from the cyclic rings at increasing maturity of the source rock or be inherited by the primary composition of organic matter. Degradation of carotenoids during the early stage of organic matter transformation into kerogen could be responsible for the high concentrations of trimethylcyclohexane in the G4 and G5 gases. Carotenoids are abundant in marine organic matter and their early diagenetic products mainly consists of tri-methylated cyclohexenyl moieties that undergo subsequent hydrogenation to form cycloalkanes having three methyl groups attached (Sinninghe and Koopmaans, 1997). The disposition of the methyl groups around the C<sub>6</sub> ring may be used to infer the type of the pre-existing carotenoid structure. The G4 and G5 gases are dominated by 1,1,3 trimethylcyclohexane, a common product of degradation of β-carotene (Jiang and Fowler, 1986), a carotenoid typically associated to halotolerant marine algae (e.g. *Dunaliella salina* and *Dunaliella bardawil*) (Soto, 2015). This is consistent with the Na-Cl composition of the saline (TDS >60 g/L) waters at G4 and G5 sites and the geological information available on the source rock consisting of sandy sediments deposited in marine-lagoonal environment during the Pliocene. Summarizing, three main types of gases can be found in the “deep” subsurface of the southern Po Plain: (i) biogenic/diagenetic gases (e.g. G4 and G5) in marine Pliocene-Pleistocene sediments; (ii) Miocene thermogenic gases (Cortemaggiore-like gases; Mattavelli et al., 1983) formed within the Marnoso Arenacea Formation at great depth (at least 3 km; Tassi et al., 2012); and (iii) thermogenic gases, showing G1-like composition, predominantly produced in Triassic carbonate rocks and commonly associated with oil (Riva et al., 1986). This subdivision is in accordance with the general conceptual model of the architecture of the petroleum systems in the Po Plain proposed by previous papers (Mattavelli and Novelli, 1990; Lindquist, 1999, Martinelli et al., 2012a). Gases of the second group are presently found mainly in Messinian-Lower Pliocene reservoirs mixed with in situ produced biogenic gases (Mattavelli et al., 1983), suggesting that these gases migrated from the source rocks and formed gas accumulation in structural traps.

### 5.3 Shallow occurrences of methane in the Po plain: origin and biogeochemical processes

As shown in the O<sub>2</sub>-Ar-N<sub>2</sub> ternary plot (Figure 13a), the average value of N<sub>2</sub>/Ar ratios of the investigated gases does not significantly deviate from that of the air saturated water

[(N<sub>2</sub>/Ar)<sub>ASW</sub> = 38], suggesting that both N<sub>2</sub> and Ar have an atmospheric origin. Only two gases (W2 and W5-11/2016) show N<sub>2</sub>-excess (N<sub>2</sub>/Ar ratios of 55 and 50, respectively) with respect to the ASW composition, likely caused by nitrate denitrification or anaerobic ammonium oxidation (Korom, 1992; Dalsgaard et al., 2005). Oxygen concentration is highly variable within the data set. The CH<sub>4</sub>-rich gases (dissolved and free) show very low content of oxygen, with the exception of W13, W14, S2 and S3 gases which have higher contents presumably due to air contamination. The chemical composition of warm water wells (WWW) ranges from that of W12, ASW-like reference gas to that of CH<sub>4</sub>-rich waters. To investigate the reason of O<sub>2</sub>-depletion in the WWW samples, O<sub>2</sub> has been plotted in a ternary diagram (Figure 13b) versus two extra-atmospheric gas species, CO<sub>2</sub> and CH<sub>4</sub>. WWW gases does not plot along a mixing line between ASW and CH<sub>4</sub>-rich waters, indicating that O<sub>2</sub> consumption is the cause of its depletion. Moreover, the distribution of the samples shows that WWW waters are also characterized by the occasional appearance of CO<sub>2</sub> and CH<sub>4</sub>. During quiescent periods, meteoric water seems to be the sole contribution that feeds the studied warm water wells and the composition of the dissolved gas phase is dominated by atmospheric species (N<sub>2</sub>, Ar, and O<sub>2</sub>). Similar to that of ASW. The results of our geochemical survey highlighted that the water heating episodes affected the dissolved gas phase since significant concentrations of CH<sub>4</sub> and subordinate contents of CO<sub>2</sub> occurred, which were also accompanied by an abrupt O<sub>2</sub> decrease. On the contrary, the water chemistry did not show any substantial change in time (Figure 6). Moreover, the dissolved CH<sub>4</sub> of WWW shows a relatively heavy isotopic composition ( $\delta^{13}\text{C}$  and  $\delta\text{D}$  up to -20.7 ‰ and -58.5 ‰, respectively), strongly different from that recorded within the deep reservoirs of natural gas and shallow CH<sub>4</sub>-rich waters. Contribution of warm water from the underlying marine formations as the cause of the temperature increase seems unlikely due to both the low local geothermal gradient ( $\leq 25^\circ\text{C}/\text{km}$ ) and the absence of any major changes in the water chemistry. Presently, the most reliable explanation is the exothermic oxidation of diffusively uprising methane by methanotrophic bacteria under aerobic conditions at very shallow depths within the water column. The same process was recently invoked for explaining the anomalous high temperature in the soils from “Terre Calde di Medolla” (literally, “Warm Grounds of Medolla”, WGM), a site located in a farming area close to some of the monitored water wells. This hypothesis rises several questions concerning how and where methane, both in WWW and shallow CH<sub>4</sub>-rich waters, is actually produced.

The  $\delta^{13}\text{C}\text{-CH}_4$  and  $\delta\text{D}\text{-CH}_4$  values measured in the bubbling gases and CH<sub>4</sub>-rich shallow aquifers (Figure 14a) ranged from -79 to -65 ‰ vs. V-PDB and from -225 to -130 ‰ vs. V-

SMOW, respectively, suggesting a prevailing microbial origin of CH<sub>4</sub>. Carbonate reduction and acetate fermentation are the two main metabolic pathways leading to the formation of biogenic methane (Whiticar, 1999). The former process dominates in marine and saline environments, while the latter is typical of freshwater environments where plant root exudates and fresh OM provide a ready supply of labile OM to the bacteria (Whiticar, 1999). All the  $\delta\text{D}-\text{CH}_4$  data lie around  $-180\text{‰}$  vs. V-SMOW, indicating that CH<sub>4</sub> was produced by carbonate reduction. The  $\delta^{13}\text{C}-\text{CH}_4$  vs.  $\delta^{13}\text{C}-\text{CO}_2$  diagram (Fig. 14b) shows that in low temperature freshwater environments, in which acetate fermentation dominates over carbonate reduction, the carbon isotope ratios of these gases are considered to be largely determined by kinetics, rather than thermodynamic equilibrium (e.g., Rosenfeld and Silverman, 1959; Nakai, 1960; Claypool and Kaplan, 1974). However, the CO<sub>2</sub>-CH<sub>4</sub> fractionation of gas formed in marine sediments through CO<sub>2</sub>-reduction was found to closely approach thermodynamic equilibrium (e.g., Whiticar et al., 1986). Moreover, lab-culture experiments reported by Botz et al. (1996) showed that, during the stationary phase, methanogen cultures fractionated carbon isotopes close to the thermodynamic equilibrium between CH<sub>4</sub> and CO<sub>2</sub> in the temperature range 35-85 °C. Most data from CH<sub>4</sub>-rich waters show a carbon isotope fractionation factor between  $\delta^{13}\text{C}-\text{CH}_4$  and  $\delta^{13}\text{C}-\text{CO}_2$ , expressed as  $\alpha_{\text{CO}_2-\text{CH}_4}$ ,  $\geq 1.06$ , i.e. a value typically associated with methane produced by CO<sub>2</sub>-reduction (Whiticar, 1999; Bogard et al., 2014). Assuming that CO<sub>2</sub>-CH<sub>4</sub> are in thermodynamic equilibrium, this would yield to formation temperatures of around 45 °C, 30-35 °C higher than temperatures directly measured in the CH<sub>4</sub>-rich shallow waters (Table 2). Temperatures not significantly exceeding 50 °C were found at depths ranging from 750 to 2000 m in correspondence of the *Dorsale Ferrarese* tectonic fold where the occurrence of gas and salty waters was also reported (Capaccioni et al., 2015).

These evidences suggest that methane in shallow domains originates within the Plio-Quaternary marine sediments by CO<sub>2</sub>-reduction, then migrates toward the surface and gets stored in shallow anoxic aquifers. Where structural architecture of the sedimentary prism allows further migration (Figure 7), methane can be discharged from bubbling wells and dry seeps and foster methanotrophic communities in aerated soils (WGM) and oxic waters (WWW). Minor methane contributions from fermentation of methyl-compounds within near-surface peaty layers cannot be totally excluded. For example, isotopic composition of gases from the W16-18 sites (Figure 14a) could be the result of partial microbial oxidation of methane produced by acetate fermentation coupled with CO<sub>2</sub>-reduction. Where structural architecture of the sedimentary prism allow further migration (Figure 7), methane can be

discharged from bubbling wells and dry seeps and foster methanotrophic communities in aerated soils (WGM) and oxic waters (WWW) In Figure 14a, the distribution of methane isotopic data from shallow methane occurrences in the Po plain, depicts two major trends of  $^{13}\text{C}$ -D-enrichment, characterized by distinct angular coefficients, expressed as  $\Delta\text{H}/\Delta\text{C}$  ratio. Several authors (Coleman et al., 1981; Whiticar, 1999; Kinnaman et al., 2007) attributed values of  $\Delta\text{H}/\Delta\text{C}$  ranging from 5.9 to 13 to microbial oxidation that leaves residual methane enriched in both  $^{13}\text{C}$  and D. Few sites, both anoxic aquifers (e.g. W9) and soils from WGM, lie on a trend having a  $\Delta\text{H}/\Delta\text{C}$  (7.3) consistent with the range suggested by the literature. This feature may be the result of anaerobic oxidation of methane (AOM) that occurred in  $\text{O}_2$ -depleted horizons of soil and within  $\text{CH}_4$ -rich aquifers. The other trend has a  $\Delta\text{H}/\Delta\text{C}$  value ranging from 1.5 to 2.7 and is outlined mostly by data from WGM and WWW. According to Sciarra et al. (2017),  $\text{CH}_4$  and  $\text{CO}_2$ , diffusively emitted from the soil at WGM, are supplied by two sources: (i) deep (> 3000 m) Mesozoic thermogenic source and (ii) shallow (200-900 m depth) Plio-Pleistocene microbial source. Those authors claimed that the two-components mixing caused the observed trend in the  $\delta^{13}\text{C}$ - $\delta\text{D}$  space. The Cavone oil and gas field (G1) is the exploitation area located in proximity of WGM and most WWW and sourced by a >3000 meters depth Mesozoic thermogenic reservoir. As shown in Figure 14a, isotopic composition of methane from Cavone does not match the one of the thermogenic endmember inferred by Sciarra et al. (2017), having a  $\delta^{13}\text{C}$ - $\text{CH}_4$  and  $\delta\text{D}$ - $\text{CH}_4$  of  $-56.2$  ‰ and  $-210$  ‰, respectively. Thus, our isotopic dataset does not support the hypothesis of mixing of deep fluids from neither the Mesozoic nor the Miocene reservoirs with younger microbial gas as the cause of data distribution on the “Schoell” plot. A more convincing explanation is that methane is likely supplied to WGM and WWW by gases escaping from the  $\text{CH}_4$ -rich groundwaters of the Plio-Quaternary succession and then oxidized by methanotrophic bacteria.

Templeton et al. (2006) suggested that the  $\alpha_{\text{CO}_2\text{-CH}_4}$  fractionation factor caused by aerobic  $\text{CH}_4$ -oxidizing bacteria strongly correlates to the cell density under constant flow conditions. At low cell densities, low concentrations of methane monooxygenase (MMO) limit the amount of  $\text{CH}_4$  oxidized, while at higher cell densities, the overall rates of  $\text{CH}_4$  oxidation increase. Thus, the residual methane is more fractionated at low cell densities than at high cell densities. At WGM, gases having low methane concentrations show a  $^{13}\text{C}$ - and D-enriched isotopic signature, whereas at increasing methane concentrations weak carbon and hydrogen isotopic fractionation is observed. Consequently, data previously interpreted as thermogenic are instead the result of aerobic microbial methane consumption at low cell density. Communities constituted by a small number of individuals could develop during the early

stages of growth of a bacterial colony under a constant nutrient supply condition, within zones where the nutrients are scarce but constantly provided or in environments characterized by cycles of starvation periods and short-lasting pulses of nutrients. The second and third scenarios most likely represent the situation present in some sites at WGM and during the heating episodes of waters from phreatic wells.

Summarizing, microbial consumption of uprising methane by methanotrophic bacteria is a widespread phenomenon in the Po Plain, able to bio-sequestering huge amounts of methane in the form of CO<sub>2</sub> and biomass. Warm grounds occurred at Medolla (WGM) can be regarded as biogeochemical system in steady state where microbes are almost constantly fed by biogenic CH<sub>4</sub>. Heating episodes in water wells instead record the arrival of discrete amounts of methane into oxic shallow aquifers. W11 warm well stands alone among the WWW since methane and CO<sub>2</sub> are always present, indicating the CH<sub>4</sub> consumption is constantly balanced by CH<sub>4</sub> input. Where the gas flux is high enough to break the methanotrophic biofilter, methane can be discharged into the atmosphere by gas emissions such as CH<sub>4</sub>-rich bubbling gases in water wells (W1, W2, W13 and W14).

The heat release is probably the most peculiar feature of WGM and WWW. Capaccioni et al. (2015) provided a solution for the longstanding debate concerning the high temperatures of the grounds at WGM, but a high heat production is not a common feature of methanotrophs found in natural environments worldwide. The more Gibbs' free energy is dissipated, the less will be available for biomass or product yield. Under nutrient-limited conditions bacteria can consume higher amounts of energy without concomitant biomass production. In this growth-independent reaction, energy sources were converted to heat (Russell, 1986), i.e., as Westerhoff (1983) theorized: "thermodynamic efficiency may be sacrificed to make the process run faster". Therefore, for example, heat release would be expected to happen in response of a pulse of nutrients after a starvation period. Another explanation can be that wasting of energy source as heat is used for denying substrate to competing organisms or to make environmental temperature unfavorable for the growth of other species (Russel, 1986). The former hypothesis seems to be more consistent with the general view of the nutrients supplying systems at WGM and especially at WWW, but evolutionary reasons cannot be ruled out.

## 6. Conclusions

The chemical and isotopic composition of light hydrocarbons of deep gas wells investigated in the present study evidences three main types of gases in the “deep” subsurface of the southern Po Plain: (i) biogenic/diagenetic CH<sub>4</sub>-rich gases in marine Pliocene-Pleistocene sediments; (ii) Miocene thermogenic gases (Cortemaggiore-like gases) formed within the Marnoso Arenacea Formation at great depth (at least 3 km); and (iii) early mature thermogenic gases, showing Cavone-like composition, predominantly produced in Triassic carbonate rocks and commonly associated with oil. Methane in shallow domains originates mainly within the Plio-Quaternary marine sediments by CO<sub>2</sub>-reduction, then migrates toward the surface and gets stored in shallow anoxic aquifers. Where structural geometry of the sedimentary prism allows further migration, methane can be ultimately discharged from bubbling wells and dry seeps. Heating episodes in water wells (Warm Water Wells, WWW) record the arrival of discrete amounts of methane into oxic shallow aquifers which readily undergoes exothermic microbial oxidation mediated by methanotrophs under aerobic conditions. Hence, methane is likely supplied to WGM (Warm Grounds of Medolla) and WWW by gases escaping from the CH<sub>4</sub>-rich groundwaters of the Plio-Quaternary succession. No evidence of migration of Miocene and Triassic gases from the reservoirs to the surface, has been found. Geochemical data from WGM, previously interpreted as arrival of Mesozoic thermogenic gases, are instead more consistent with aerobic microbial methane consumption at low cell density conditions. Summarizing, the occurrence of methane-rich fluids and the microbial consumption of uprising methane by methanotropic bacteria are widespread phenomena in the Po Plain. The latter is able to bio-sequestering huge amounts of methane in the form of CO<sub>2</sub> and biomass. Where gas flux is high enough to break the methanotropic biofilter, methane can be discharged into the atmosphere by gas emissions such as CH<sub>4</sub>-rich bubbling gases in water wells and dry seeps. In tectonically active foreland basin such as the Po Plain, huge amounts of methane can migrate from the reservoirs/sources to shallower geological domains, thanks to faults and fractures. At shallow levels, methane can be stored in groundwaters or ultimately reach the atmosphere. Biogeochemical processes, such as methanotrophy, are able indeed to sequestered large quantities of carbon as biomass both in soils and waters.

### **Acknowledgments**

This work was financially supported by the Department of Biological, Geological and Environmental Sciences of University of Bologna (Bologna), the laboratories of Fluid and

Rock Geochemistry and Stable Isotope Geochemistry of the Department of Earth Sciences and CNR-IGG of Florence. We are very grateful to the oil and gas companies (ENI, Gas Plus s. p. a. and Northsun for providing us with the access to the exploitation fields, for allowing us to collect water and gas samples from production wells and finally, for giving us the authorization to use and publish analyzed data. Many thanks are due to local people for kindly providing their permission to collect water and gas samples from their private wells. This paper is dedicated to the memory of Prof. Bruno Capaccioni, brilliant colleague and dear friend, who left us too early.

## References

- Abe S. van Gent H. Urai J. L. Holland M. (2008). Discrete element simulations of the formation of open fractures during normal faulting of cohesive materials. *Boll. Geof. Teor. Appl.*, 49, Suppl. 2, 298-309.
- AGIP, 1977. Temperature sotterranee. Inventario dei dati raccolti dall'AGIP durante la ricerca e la produzione di idrocarburi in Italia. Segrate, 1390 p.
- Allen C.C., Oehler D.Z., Etiope G., Van Rensbergen P., Baciù C., Feyzullayev A., Martinelli G., Tanaka K., Van Rooij D., 2013. Fluid expulsion in terrestrial sedimentary basins: A process providing potential analogs for giant polygons and mounds in the martian lowlands. *Icarus*, 224, 424–432.
- Amorosi A., Bruno L., Cleveland D. M., Morelli A., Hong W., 2017. Paleosols and associated channel-belt sand bodies from a continuously subsiding late Quaternary system (Po Basin, Italy): new insights into continental sequence stratigraphy. *GSA Bulletin*, 129, 3/4, 449–463; doi: 10.1130/B31575.1
- Amorosi A., Maselli V., Trincardi F., 2016. Onshore to offshore anatomy of a late Quaternary source-to-sink system (Po Plain–Adriatic Sea, Italy). *Earth-Science Reviews*, 153, 212–237.
- Amorosi, A., Pavesi, M., Ricci Lucchi, M., Sarti, G., Piccin, A. 2008. Climatic signature of cyclic fluvial architecture from the Quaternary of the central Po Plain, Italy. *Sedimentary Geology* 209, 58–68.
- Arthur C. L., Pawliszyn J., 1990. Solid phase microextraction with thermal desorption using fused silica optical fibers. *Analytical Chemistry* 62, 2145–2148.
- Baciù C., Caracausi A., Etiope G., Italiano F., 2007. Mud volcanoes and methane seeps in Romania: main features and gas flux. *Annals of Geophysics* 50, 501-511.

- Bartolini C., 2003. When did the Northern Apennine become a mountain chain? *Quaternary International*, 101-102, 75-80.
- Bernard B. B., Brooks J. M., Sackett W. M., 1978. A geochemical model for characterization of hydrocarbon gas sources in marine sediments. *Offshore Technology Conference*, Houston, USA, 435–438.
- Berner U., Faber E., (1996). Empirical carbon isotope/maturity relationships for gases from algal kerogens and terrigenous organic matter, based on dry, open-system pyrolysis. *Organic Geochemistry*, 24(10-11), 947-955.
- Bigi G., Cosentino D., Parotto M. Sartori R. Scandone, P. Carrozzo, M.T. Luzio D., Margiotta C., Quarta T., 1990. Structural model of Italy and gravity map (1:500.000). *Prog. Final. Geodinamica (Public. n.114, 6 sheets)*.
- Boccaletti M., Coli M., Eva C., Ferrari G., Giglia G., Lazzaretto A., Merlanti F., Nicolich R., Papani G., Post pischhl D.,1985. Considerations on the seismotectonics of the Northern Apennines. *Tectonophysics*, 117, 7-38.
- Boccaletti M., Corti G., Martelli L., 2011. Recent and active tectonics of the external zone of the Northern Apennines (Italy). *Int.J. Earth Sci (Geol. Rundsch)*,100,1331-1348; DOI 10.1007/s00531-010-0545-y.
- Boccaletti M., Martelli L. (Eds.), 2004. *Note illustrative della Carta sismotettonica della Regione Emilia-Romagna, scala 1:250.000. Firenze, 60 pp.*
- Bogard M. J., Del Giorgio P. A., Boutet L., Chaves M. C. G., Prairie Y. T., Merante A., Derry A. M., 2014. Oxidic water column methanogenesis as a major component of aquatic CH<sub>4</sub> fluxes. *Nature communications*, 5, 5350.
- Bonini M., 2007. Interrelations of mud volcanism, fluid venting, and thrust-anticline folding: examples from the external northern Apennines (Emilia–Romagna, Italy). *Journal of Geophysical Research* 112, B08413. <http://dx.doi.org/10.1029/2006JB004859>.
- Bonini M., Tassi F., Feyzullaev A.A., Aliyev C.S., Capecchicci F., Minissale A., 2013. Deep gas discharged from mud volcanoes of Azerbaijan: New geochemical evidence. *Marine and Petroleum Geology* 43, 450–463, <http://dx.doi.org/10.1016/j.marpetgeo.2012.12.003>.
- Bonzi L. Ferrari V., Martinelli G. and Severi P., 2014. Fenomeni geologici inusuali accaduti in occasione della sequenza sismica dell’Emilia nel 2012. In: *Poster 2.2, 33<sup>rd</sup> Convegno Nazionale Gruppo Nazionale di Geofisica della Terra Solida, Bologna, Italy.*

- Bonzi L., Ferrari V., Martinelli G., Norelli E., Severi P., 2017. Unusual geological phenomena in the Emilia-Romagna plain (Italy): gas emissions from wells and the ground, hot water wells, geomorphological variations. A review and an update of documented reports. *Bollettino di Geofisica Teorica ed Applicata* 58 (2), 87–102, DOI 10.4430/bgta0193
- Boreham C. J., Edwards D. S., 2008. Abundance and carbon isotopic composition of neopentane in Australian natural gases. *Organic Geochemistry* 39, 550–566.
- Borgatti L., Bracci E. A., Cremonini S., Martinelli G., 2012. Looking for the effects of the May-June 2012 Emilia seismic sequence (Italy): medium-depth deformation structures at the periphery of the epicentral area. *Annals of Geophysics*, 55, 717-725. doi: 10.4401/ag-6131. (on line available at: <http://www.annalsofgeophysics.eu/index.php/annals>)
- Boschi E., Ferrari G., Gasperini P., Guidoboni E., Smriglio G. and Valensise G., 1995. *Catalogo dei forti terremoti in Italia dal 461 a.C. al 1980*. ING-SGA, Roma, Italy, 973 pp.
- Boschi E., Guidoboni E., Ferrari G., Valensise G. and Gasperini P., 1997. *Catalogo dei forti terremoti in Italia dal 461 a.C. al 1990*. ING-SGA, Roma, Italy, 644 pp.
- Botz R., Pokojski H. D., Schmitt M., Thomm M., 1996. Carbon isotope fractionation during bacterial methanogenesis by CO<sub>2</sub> reduction. *Organic Geochemistry*, 25(3-4), 255-262.
- Burst J.F., 1969. Diagenesis of Gulf Coast clayey sediments and its possible relation to petroleum migration. *AAPG Bulletin*, 53, 73-93.
- Cabassi J., Tassi F., Vaselli O., Fiebig J., Nocentini M., Capecchiacci F., Rouwet D., Bicocchi G., 2013. Biogeochemical processes involving dissolved CO<sub>2</sub> and CH<sub>4</sub> at Albano, Averno, and Monticchio meromictic volcanic lakes (Central-Southern Italy). *Bulletin of Volcanology*, 75, 683, doi: 10.1007/s00445-012-0683-0.
- Cahill A.G., Steelman C.M., Forde O., Kuloyo O., Ruff S.E., Mayer B. Mayer K.U., Strous M., Ryann M. C., Cherry J.A., Parker B.L., 2017. Mobility and persistence of methane in groundwater in a controlled-release field experiment. *Nature Geoscience*. Articles published online: 27 march 2017 | doi: 10.1038/ngeo2919, 8 p.
- Campo B., Amorosi A., Vaiani S.C., 2017. Sequence stratigraphy and late Quaternary paleoenvironmental evolution of the Northern Adriatic coastal plain (Italy). *Palaeogeography, Palaeoclimatology, Palaeoecology*, 466, 265–278.
- Capaccioni B., Coltorti M., Todesco M., Cremonini S., Di Giuseppe D., Faccini B., Tessari U., 2017. Sand volcano generated by a violent degassing from methane-saturated

- aquifers: The case study of Medolla (Modena, Italy). *Engineering Geology*, 221, 91–103.
- Capaccioni B., Tassi F., Cremonini S., Sciarra A. and Vaselli O., 2015. Ground heating and methane oxidation processes at shallow depth in Terre Calde di Medolla (Italy): observations and conceptual model. *Journal of Geophysical Research, Solid earth*, 120, 3048-3064, doi:10.1002/2014JB011635.
- Capozzi R. and Picotti V., 2002. Fluid migration and origin of a mud volcano in the Northern Apennines (Italy): the role of deeply rooted normal faults. *Terra Nova* 14, 363–370.
- Capozzi R., Guido F.L., Oppo D., Gabbianelli G., 2012. Methane-Derived Authigenic Carbonates (MDAC) in northern-central Adriatic Sea: relationships between reservoir and methane seepages. *Marine Geology*, 332–334. 174–188.
- Cappelletti M., Ghezzi D., Zannoni D., Capaccioni B., Fedi S., 2016. Diversity of Methane-Oxidizing Bacteria in Soils from “Hot Lands of Medolla” (Italy) Featured by Anomalous High-Temperatures and Biogenic CO<sub>2</sub> Emission. *Microbes and Environments* 31 (4), 369–377, doi:10.1264/jsme2.ME16087
- Carminati E., Martinelli G., 2002. Subsidence rates in the Po Plain, northern Italy: The relative impact of natural and anthropogenic causation. *Eng. Geol.*, 66, 241–255, doi:10.1016/S0013-7952(02)00031-5.
- Carminati, E., Scrocca D., Doglioni C., 2010b. Compaction-induced stress variations with depth in an active anticline: Northern Apennines, Italy, *J. Geophys. Res.*, 115, B02401, doi:10.1029/2009JB006395.
- Carminati, E., Valditacca, L., 2010a. Two- and three-dimensional numerical simulations of the stress field at the thrust front of the northern Apennines, Italy. *J. Geophys. Res.* 115, 21 p. <http://dx.doi.org/10.1029/2010JB007870>.
- Cartwright J., Huuse M., Aplin A., 2007. Seal bypass systems. *AAPG Bulletin*, 91, (8), 1141-1166.
- Cartwright J., James D., Bolton A., 2003. The genesis of polygonal faults: a review. *Geol Soc. London Spec. Publ.*, 216, 223-244.
- Casero P., 2004. Structural setting of petroleum exploration plays in Italy. In: Crescenti V., D’Offizi S., Merlino S., Sacchi L., (Eds.), *Geology of Italy*, Special volume of the Italian Geological Society for the IGC 32 Florence-2004, 189-199.
- Castellarin A., 2001. Alps-Apennines and PoPlain-Frontal Apennines relationships. In: Vai G. B. and Martini I. P. (Eds.), *Anatomy of an Orogen. The Apennines and adjacent Mediterranean Basins*, London, Kluwer, 177-196.

- Castellarin A., Cantelli L., Fesce A.M., Mercier J.L., Ricotti V., Pini G.A., Prosser G., Selli L., 1992. Alpine compressional tectonics in the Southern Alps. Relationships with the N-Appennines. *Annales Tectonicae*, 6, 62-94.
- Castellarin A., Rabbi E., Cremonini S., Martelli L., Piattoni F., 2006. New insights into the underground hydrology of the eastern Po Plain (northern Italy). *Boll. Geof. Teor. Appl.*, 47, 271-298.
- Cerrina Ferroni A., Martelli L., Martinelli P., Ottria G., Catanzariti R., 2002. Note illustrative della Carta geologico-strutturale dell'Appennino emiliano-romagnolo 1:250.000. Firenze, 112 p, 1 Sheet.
- Cesca S., Braun T., Maccaferri F., Passatelli L., Rivalta E., Dahm T., 2013. Source modelling of the M5-6 Emilia-Romagna, Italy, earthquakes (2012 May 20-29). *Geophys. J. Int.*, 193, 1658-1672.
- Chung H. M., Gormly J. R., Squires R. M., 1988. Origin of gaseous hydrocarbons in subsurface environments: theoretical considerations of carbon isotope distribution. *Chemical Geology*, 71(1-3), 97-104.
- Ciais P., Sabine C., Bala G., Bopp L., Brovkin V., Canadell J., Chhabra A., DeFries R., Galloway J.M.H., Jones C., Le Quéré C., Myneni R.B., Piao S., Thornton P., 2013. Carbon and Other Biogeochemical Sycles, in: *Climate Change 2013: The Physical Science Basis. Contribution of Working Group I to the Fifth Assessment Report of IPCC*, edited by: Stocker T.F., Qin D., Plattner G.-K., Tignor M., Allen S.K., Boschung J., Nauels A., Xia Y., Bex V., and Midgley P. M., Cambridge University Press, Cambridge, UK.
- Claypool G. E., Kaplan I. R., 1974. The origin and distribution of methane in marine sediments. In: *Natural gases in marine sediments*, Springer, Boston, 99-139.
- Clayton C., 1991. Carbon isotope fractionation during natural gas generation from kerogen. *Marine and petroleum geology*, 8(2), 232-240.
- Coleman D. D., Risatti J. B., Schoell M., 1981. Fractionation of carbon and hydrogen isotopes by methane-oxidizing bacteria. *Geochimica et Cosmochimica Acta*, 45(7), 1033-1037.
- Coleman M. L., Sheperd T. J., Rouse J. E., Moore G. R., 1982. Reduction of water with zinc for hydrogen isotope analysis, *Anal. Chem.*, 54, 993-995, doi:10.1021/ac00243a035.
- Conrad R., 2009. The global methane cycle: recent advances in understanding the microbial processes involved. *Environmental Microbiology Reports* 1, 285-292.
- Correale A., Paonita A., Martelli M., Rizzo A., Rotolo S. G., Corsaro R. A., Di Renzo V., 2014. A two-component mantle source feeding Mt. Etna magmatism: insights from the

geochemistry of primitive magmas. *Lithos* 184:243–258,  
<https://doi.org/10.1016/j.lithos.2013.10.038>.

- Craig H., 1961. Isotopic variations in meteoric waters. *Science* 133, 1702–1703.
- Cremonini S., 2010a. Can subaerial pockmarks exist? Atti del 2° Workshop Internazionale sui fenomeni di sinkhole “I sinkholes. Gli sprofondamenti catastrofici nell'ambiente naturale ed in quello antropizzato”, Roma, 3-4 Dicembre 2009, ISPRA. Roma, 29-34.
- Cremonini S., 2010b. A preliminary overview of sinkholes in the Emilia-Romagna Region (Italy). Atti del 2° Workshop Internazionale sui fenomeni di sinkhole “*I sinkholes. Gli sprofondamenti catastrofici nell'ambiente naturale ed in quello antropizzato*”, Roma, 3-4 Dicembre 2009, ISPRA. Roma 2010, 257-281.
- Cremonini S., Etiope G., Italiano F., Martinelli G., 2008, Evidence of possibile enhanced peat burning by deep-originated methane in the Po River delta plain. *Journ. Geol.*, 116, pp. 401-413.
- Dalsgaard T., Thamdrup B., Canfield D. E., 2005. Anaerobic ammonium oxidation (anammox) in the marine environment. *Research in Microbiology*, 156(4), 457-464.
- Dai J. X., 1992. Identification and distinction of various alkane gases. *Science in China (Series B)* 35, 185–193.
- Dai J. X., 1993. Identification of coal formed gas and oil type gas by light hydrocarbons. *Petroleum Exploration and Development* 20 (5), 26–32.
- Dai J. X., Ni Y. Y., Huang S.P., Gong D. Y., Liu D., Feng Z. Q., Peng W.L., Han W.X., 2016. Secondary origin of negative carbon isotopic series in natural gas. *Journal of Natural Gas Geoscience* 27, 1–7.
- D’Anastasio E., De Martini P. M., Selvaggi G., Pantosti D., Marchioni A., Maseroli R., 2006. Short-term vertical velocity field in the Apennines (Italy) revealed by geodetic levelling data. *Tectonophysics*, 418, 219-234.
- Davoli E., Gangai M. L., Morselli L., Tonelli D., 2003. Characterization of odorants emissions from landfills by SPME and GC/MS. *Chemosphere* 51, 357–368.
- Delisle G., von Rad U., Andrleit H., von Daniels C., Tabrez A., Inam A., 2002. Active mud volcanoes on- and offshore eastern Makran, Pakistan. *Int. J. Earth Sci.* 91, 93–110.
- Devoti R., 2012. Combination of coseismic displacement fields: a geodetic perspective. *Annals of Geophysics*, 55 (4); doi:10.4401/ag-6119
- Devoti, R., G. Pietrantonio, A. Pisani, F. Riguzzi, and E. Serpelloni 2010. Present day kinematics of Italy, *J. Virtual Explorer*, 36, doi:10.3809/jvirtex.2009.00237.

- Di Bucci D., Angeloni P., 2013. Adria seismicity and seismotectonics: Review and critical discussion. *Marine and Petroleum Geology*, 42, 182-190.
- Di Dio G., 1998. Inquadramento geologico della pianura emiliano-romagnola e del margine appenninico padano, in: Regione Emilia-Romagna & ENI-AGIP, Riserve idriche sotterranee della Regione Emilia-Romagna – Relazione tecnica. Firenze, p. 120.
- Doglioni C., Harabaglia P., Merlini S., Monelli F., Peccerillo A., Piromallo A. 1999. Orogens and slab vs. their direction of subduction. *Earth Sci. Rev.*, 45, 167–208, doi:10.1016/S0012-8252(98)00045-2.
- Duan Y., 2000. Organic geochemistry of recent marine sediments from the Nansha Sea, China. *Organic Geochemistry* 31, 159–167.
- Duan T., Ma L.H., 2001. Lipid geochemistry in a sediment core from Ruorgai Marsh deposit (Eastern Qinghai – Tibet plateau, China). *Organic Geochemistry* 32, 1429–1442.
- Duan Y., Wu B., Zheng G., Zhang H., Zheng C., 2004. The specific carbon isotopic compositions of branched and cyclic hydrocarbons from Fushun oil shale. *Chinese Science Bulletin* 49, 369–373.
- Duchi V., Venturelli G., Boccasavia I., Bonicolini F., Ferrari C., Poli D., 2005. Studio geochimico dei fluidi dell'Appennino Tosco-Emiliano-Romagnolo. *Boll. Soc. Geol. It.* 124, 475–491.
- Elliot T., Ballantine C.J., O'Nions R. K., Ricchiuto T., 1993. Carbon, helium, neon and argon isotopes in a Po Basin (northern Italy) natural gas field. *Chem. Geol.* 106, 429–440.
- Energy-pedia, 2010. Italy: Po Valley commences production from the Sillaro gas field (online available at: <https://www.energy-pedia.com/news/italy/po-valley-commences-production-from-the-sillaro-gas-field>).
- ENI (Ente Nazionale Idrocarburi), 1972. Acque dolci sotterranee. Inventario dei dati raccolti dall'AGIP durante la ricerca di idrocarburi in Italia. Roma, 914 p.
- ENI (Ente Nazionale Idrocarburi), 1994. Acque dolci sotterranee. Inventario dei dati raccolti dall'AGIP durante la ricerca di idrocarburi in Italia dal 1971 al 1990. Roma, 524 pp.
- Epstein S., and Mayeda T. K., 1953. Variation of the  $^{18}\text{O}/^{16}\text{O}$  ratio in natural waters, *Geochim. Cosmochim. Acta*, 4, 213–224, doi:10.1016/0016-7037(53)90051-9.
- Etiopie G. and Klusman R.W., 2002. Geologic emissions of methane to the atmosphere, *Chemosphere*, 49, 777–789.
- Etiopie G., 2009b. Natural emissions of methane from geological seepage in Europe, *Atmospheric Environment*, 43, 1430–1443.

- Etiopio G., Feyzullayev A., Milkov A.V., Waseda A., Mizobe K., Sun C.H., 2009a. Evidence of subsurface anaerobic biodegradation of hydrocarbons and potential secondary methanogenesis in terrestrial mud volcanoes. *Marine and Petroleum Geology* 26, 1692–1703.
- Evans W. C., Kling G. W., Tuttle M. L., Tanyileke G., White L. D., 1993. Gas build-up in Lake Nyos, Cameroon: The recharge process and its consequences, *Appl. Geochem.*, 8, 207–221, doi:10.1016/0883-2927(93)90036-G.
- Fantoni R., Franciosi R., 2010. Mesozoic extension and Cenozoic compression in Po Plain and Adriatic foreland. *Rend. Fis. Acc. Lincei*, 21, 197–209.
- Fiebig J., Hofmann S., Tassi F., D'Alessandro W., Vaselli O., Woodland A. B., 2015. Isotopic patterns of hydrothermal hydrocarbons emitted from Mediterranean volcanoes. *Chem. Geol.* 396, 152–163.
- Florez Menendez, J.C., Fernandez Sanchez, M.L., Fernandez Martinez, E., Sanchez Uria, J.E., Sanz-Mendez, A., 2004. Static headspace versus head space solid-phase microextraction (HS-SPME) for the determination of volatile organochlorine compounds in landfill leachates by gas chromatography. *Talanta* 63, 809–814
- Galli P., Castenetto S., Peronace E., 2012. May 2012 Emilia Earthquakes (MW 6, Northern Italy): Macroseismic effects distribution and seismotectonic implications. *Alpine and Mediterranean Quaternary*, 25 (2), 105-123.
- Gay A., 2017. Are polygonal faults the keystones for better understanding the timing of fluid migration in sedimentary basins? *EPJ Web of Conferences*, 140, 12009. DOI: 10.1051/epjconf/201714012009.
- Ghielmi M., Minervini M., Nini C., Rogledi S., Rossi M., 2013. Late Miocene–Middle Pleistocene sequences in the Po Plain—Northern Adriatic Sea (Italy): the stratigraphic record of modification phases affecting a complex foreland basin. *Marine and Petroleum Geology*, 42, 50–81.
- Ghielmi, M., Minervini M., Nini C., Rogledi S., Rossi M., Vignolo A. 2010. Sedimentary and tectonic evolution in the eastern Po-Plain and northern Adriatic Sea area from Messinian to middle Pleistocene (Italy), in *Nature and Geodynamics of the Northern Adriatic Lithostere*. *Rend. Fis. Acc. Lincei*, vol. 21/1, 131–166.
- Goult N.R., 2001. Polygonal fault networks in fine grained sediments. *First Break*, 19, 69-73.
- Gunderson K.L., Pazzaglia F.J., Picotti V., Anastasio D.A., Kodama K.P., Rittenour T., Frankel K.F., Ponza A., Berti C., Negri A., Sabbatici A., 2014. Unraveling tectonic

- and climatic controls on synorogenic growth strata (Northern Apennines, Italy). *Geol. Soc. Am. Bull.*, doi: 10.1130/B30902.1 ([https://netfiles.uiuc.edu/tstark/website/Conference\\_Publications/CP45.pdf](https://netfiles.uiuc.edu/tstark/website/Conference_Publications/CP45.pdf)).
- Hinrichs K.U. and Boetius A., 2002. The anaerobic oxidation of methane: new insights in microbial ecology and biogeochemistry. In *Ocean Margin Systems* (eds. G. Wefer, D. Billet, D. Hebbeln, B. B. Jorgensen, M. Schluter and T. C. E. V. van Weering). Springer-Verlag, Berlin, pp. 457–477
- <http://ambiente.regione.emilia-romagna.it/geologia/temi/geologia/fenomeni-geologici-particolari>
- [https://www.esrl.noaa.gov/gmd/ccgg/trends\\_ch4/](https://www.esrl.noaa.gov/gmd/ccgg/trends_ch4/)
- Hu T. L., Ge B. X., Chang Y. J., Liu B., 1990. The development and application of fingerprint parameters for hydrocarbons absorbed by source rocks and light hydrocarbons in natural gas. *Petroleum Geology & Experiment* 12, 375–394.
- IRSA (Istituto Ricerca sulle Acque) and CNR (Consiglio Nazionale delle Ricerche), 1982. Indagine sulle falde acquifere profonde della pianura padana. *Quaderni Istituto di Ricerca sulle Acque*, 51 - 3/2, 5-70.
- ISPRA 2015. Assessing subsurface potentials of the Alpine Foreland Basins for sustainable planning and use of natural resources – Area Pilota italiana - Modello geologico 3D e geopotenziali della Pianura Padana centrale (Progetto GeoMol). Rapporto ISPRA, 234/2015, 104 p with appendix. (on line available at: <http://www.isprambiente.gov.it/it/pubblicazioni/statistiche-download>).
- Jiang Z. S., Fowler M. G., 1986. Carotenoid-derived alkanes in oils from northwestern China. *Organic Geochemistry*, 10(4-6), 831-839.
- Kinnaman F. S., Valentine D. L., Tyler S. C., 2007. Carbon and hydrogen isotope fractionation associated with the aerobic microbial oxidation of methane, ethane, propane and butane. *Geochimica et Cosmochimica acta*, 71(2), 271-283.
- Kirschke S., Bousquet P., Ciais P., Saunoy M., Canadell J.G., Dlugokencky E.J., Bergamaschi P., Bergmann D., Blake D.R., Bruhwiler L., Cameron-Smith P., Castaldi S., Chevallier F., Feng L., Fraser A., Heimann M., Hodson E.L., Houweling S., Josse B., Fraser P.J., Krummel P.B., Lamarque J.F., Langenfelds R.L., Le Quere C., Naik V., O’Doherty S., Palmer P.I., Pison I., Plummer, D., Poulter B., Prinn R.G., Rigby M., Ringeval B., Santini M., Schmidt M., Shindell D.T., Simpson I.J., Spahni R., Steele L.P., Strode S.A., Sudo K., Szopa S., van der Werf G. R., Voulgarakis A., van

- Weele M., Weiss, R.F., Williams J.E., Zeng G., 2013. Three decades of global methane sources and sinks, *Nature Geoscience*, 6, 813–823, doi:10.1038/ngeo1955
- Knittel K. and Boetius A., 2009. Anaerobic oxidation of methane: progress with an unknown process. *Annual Review of Microbiology* 63, 311–334.
- Kopf A., Deyhle A., Lavrushin V.Y., Polyak B.G., Buachidze G.I., Eisenhauer A., 2003. Isotopic evidence for deep gas and fluid migration from mud volcanoes in a zone of incipient continental collision (Caucasus, Russia). *International Journal of Earth Science* 92, 407–426.
- Kopf A., Klaeschen D., Mascle J., 2001. Extreme efficiency of mud volcanism in dewatering accretionary prisms. *Earth and Planetary Science Letters* 189, 295–313.
- Korom S. F., 1992. Natural denitrification in the saturated zone: a review. *Water resources research*, 28(6), 1657-1668.
- Leythaeuser D., Schaefer R. G., Cornford C. T., Weiner B., 1979. Generation and migration of light hydrocarbons (C<sub>2</sub>–C<sub>7</sub>) in sedimentary basins. *Organic Geochemistry*, 1(4), 191-204.
- Lieberman R.L. and Rosenzweig A.C., 2004. Biological methane oxidation: regulation, biochemistry, and active site structure of particulate methane monooxygenase. *Critical Review in Biochemistry and Molecular Biology* 39, 147–164.
- Lindquist S. J., 1999. Petroleum systems of the Po Basin province of northern Italy and the northern Adriatic Sea: Porto Garibaldi (biogenic), Meride/Riva di Solto (thermal), and Marnoso Arenacea (thermal). US Department of the Interior, US Geological Survey.
- Lisle R.J., Aller J., Bastida F., Bobillo-Ares N.C., Toimil N.C., 2009. Volumetric strains in neutral surface folding. *Terra Nova*, 21, 14–20.
- Longinelli A., Selmo E., 2003. Isotopic composition of precipitation in Italy: a first overall map. *J. Hydrol.* 270, 75–88.
- Lorant F., Prinzhofer A., Behar F., Huc A. Y., 1998. Carbon isotopic and molecular constraints on the formation and the expulsion of thermogenic hydrocarbon gases. *Chemical Geology*, 147(3-4), 249-264.
- Mandl G., 1988. *Mechanics of tectonic faulting. Models and basic concepts.* Amsterdam, 1988, 407 p.
- Mangani G., Berloni A., Maione M., 2003. “Cold” solid-phase microextraction method for the determination of volatile halocarbons present in the atmosphere at ultratrace levels. *Journal of Chromatography. A* 988, 167–175.

- Martelli L., Bonini M., Calabrese L., Corti G., Ercolessi G., Molinari F.C., Piccardi L., Pondrelli S., Sani F., Severi P., 2017b. Explanatory notes of the seismotectonic map of the Emilia-Romagna Region and surrounding areas. 93p. with a map.
- Martelli L., Bonini M., Calabrese L., Corti G., Ercolessi G., Molinari F.C., Piccardi L., Pondrelli S., Sani F., Severi P., 2017. Note illustrative della Carta sismotettonica della Regione Emilia Romagna ed aree limitrofe (Explanatory notes of the seismotectonic Map of the Emilia-Romagna Region and surrounding areas). Bologna, 93 p., 1 Sheet.
- Martelli L., Santulin M., Sani F., Tamaro A., Bonini M., Rebez A., Corti G., Slejko D., 2017a. Seismic hazard of the Northern Apennines based on 3D seismic sources. *J Seismol.*, 21, 1251–1275, DOI 10.1007/s10950-017-9665-1.
- Martinelli G., Minissale A., Verrucchi C., 1998. Geochemistry of heavily exploited aquifers in the Emilia-Romagna region (Po Valley, northern Italy). *Environ. Geol.* 36, 195–206.
- Martinelli G., Cremonini S., Samonati E., 2012a. Geological and geochemical setting of natural hydrocarbon emissions in Italy. In: Al-Megren H. (ed), *Adv. Nat. Gas Tech.*, pp. 79–120, <[www.intechopen.com/books/advances-in-natural-gas-technology/geological-and-geochemical-setting-of-natural-hydrocarbon-emissions-in-Italy](http://www.intechopen.com/books/advances-in-natural-gas-technology/geological-and-geochemical-setting-of-natural-hydrocarbon-emissions-in-Italy)>.
- Martinelli G., Cremonini S., Samonati E., 2012b. The Peat fires of Italy. Stracher G. B., Prakash A., Sokol E. V. (Eds.), *Coal & peat fires: a global perspective*, 2 (Photographs and Multimedia Tours), Elsevier, 205-216. (ISBN: 9780444594129).
- Martinelli G., Cremonini S., Samonati E., Stracher G.B., 2015. Italian peat and coal fires. Stracher G., Prakash A., Rein G. (Eds.), *Coal and Peat Fires: A Global Perspective. Volume 4: Peat – Geology, Combustion, and Case Studies*. Amsterdam, 39-73.
- Martinelli G., Dadomo A., Italiano F., Petrini R., Slejko F.F., 2016. Geochemical monitoring of the 2012 Po Valley seismic sequence: a review and update. *Chemical Geology*, 469, 147-162. <http://dx.doi.org/10.1016/j.chemgeo.2016.12.013>
- Martinelli, G., Chahoud, A., Dadomo, A., Fava, A., 2014. Isotopic features of Emilia-Romagna region (North Italy) groundwaters: environmental and climatological implications. *J. Hydrol.* 519, 1928–1938. <http://dx.doi.org/10.1016/j.jhydrol.2014.09.077>
- Mattavelli L., Ricchiuto T., Grignani D. and Schoell M., 1983. Geochemistry and habitat of natural gases in Po Basin, northern Italy. *American Association of Petroleum Geologists Bulletin*, 67, 2239–2254.

- Mattavelli L., Novelli L., 1990. Geochemistry and Habitat of the Oils in Italy (1). AAPG Bulletin, 74 (10), 1623-1639.
- McDonald I.R., Bodrossy L., Chen Y. and Murrell J.C., 2008. Molecular ecology techniques for the study of aerobic methanotrophs. Applied and Environmental Microbiology. 74, 1305–1315
- Moggia M., 2016. Caratteristiche idrochimiche delle acque di Occhiobello (RO). Tesi di laurea triennale. Corso di Laurea in Scienze Geologiche della Scuola di Scienze – Università di Bologna, Anno Accademico 2015-2016. Relatore proff. Capaccioni B. e Cremonini S. (inedita).
- Molinari F.C., Boldrini G., Severi P., Duroni G., Rapti Caputo D., Martinelli G., 2007. Risorse idriche sotterranee della Provincia di Ferrara. Firenze, 80 p, 5 sheets.
- Morgan D.A., Cartwright J.A., Imbert P., 2015. Perturbation of polygonal fault propagation by buried pockmarks and the implications for the development of polygonal fault systems. Marine and Petroleum Geology, 65, 157-171.
- Mucciarelli M., Donda F., Valensise G., 2015. Earthquakes and depleted gas reservoirs: which comes first? Natural Hazards and Earth System Sciences, 15 (10), 2201-2208.
- Muttoni G., Carcano, Garzanti E., Ghielmi M, Piccin A., Pini R., Rogledi S., Sciunnach D., 2003. Onset of major Pleistocene glaciations in the Alps. Geology, 31 (11), 989-992.
- Myhre G., Shindell D., Bréon F.-M., Collins W., Fuglestedt J., Huang J., Koch D., Lamarque J.-F., Lee D., Mendoza B., Nakajima T., Robock A., Stephens G., Takemura T., Zhang H., 2013. Anthropogenic and Natural Radiative Forcing, in: In Climate Change 2013: The Physical Science Basis. Contribution of Working Group I to the Fifth Assessment Report of the Intergovernmental Panel on Climate Change., edited by: Stocker T.F., Qin D., Plattner G.-K., Tignor M., Allen S.K., Boschung J., Nauels A., Xia Y., Bex V., Midgley P.M., Cambridge University Press, Cambridge, UK and New York, NY, USA.
- Nakai N., 1960. Carbon isotope fractionation of natural gas in Japan. The Journal of earth sciences, Nagoya University, 8(2), 174-180.
- Nardon, S., Marzorati D., Bernasconi A., Cornini S., Gonfalonni M., Mosconi S., Romano A., Terdich P., 1991. Fractured carbonate reservoir characterization and modeling a multidisciplinary case study from the Cavone oil field, Italy. First Break, 9, 553–565.
- Nespoli M., Belardinelli M. E., Gualandi A., Serpelloni E., Bonafede M., 2018. Poroelasticity and fluid flow modeling for the 2012 Emilia-Romagna earthquakes: hints from GPS and InSAR data. Geofluids, 15 p, <https://doi.org/10.1155/2018/4160570>

- Obermeier S. F., Pond, E. C., Olson, S.M., 2001. Paleoliquefaction studies in continental settings: geologic and geotechnical factors in interpretations and back-analysis. U.S. Geological Survey open-file Report 01-29-2001 (available at: [https://netfiles.uiuc.edu/tstark/website/Conference\\_Publications/CP45.pdf](https://netfiles.uiuc.edu/tstark/website/Conference_Publications/CP45.pdf)).
- Oppo D., Capozzi R., Picotti V. (2013). A new model of the petroleum system in the Northern Apennines, Italy. *Marine and Petroleum Geology*, 48, 57-76.
- Oppo D., Capozzi R., Picotti V., Ponza A., 2015. A genetic model of hydrocarbon-derived chimneys in shelfal fine-grained sediments: the Enza River field, Northern Apennines (Italy). Capozzi R., Negri A., Reitner J., Taviani M. (Eds.), *Carbonate conduits linked to hydrocarbon-enriched fluid escape. Marine Petroleum Geology special issue*, 555-556.
- Picotti V, and Pazzaglia F. J., 2008. A new active tectonic model for the construction of the Northern Apennines mountain front near Bologna (Italy), in “*Journal Geophysical Research*” 113, BO8412, doi:10.1029/2007JB005307, 2008.
- Pieri M., Groppi G., 1981. Subsurface geological structure of the Po Plain (Italy). C.N.R.-Progetto Finalizzato Geodinamica, Pubbl. n. 414, p. 13.
- Prather M.J., Holmes C.D., and Hsu J., 2012. Reactive greenhouse gas scenarios: Systematic exploration of uncertainties and the role of atmospheric chemistry, *Geophysical Research Letters*, 39, L09803, doi:10.1029/2012gl051440
- Pratt B.R., 1998. Syneresis cracks: subaqueous shrinkage in argillaceous sediments caused by earthquake-induced dewatering. *Sedimentary Geology*, 117. 1-10.
- Prinzhofer A., Mello M. R., Takaki T., 2000. Geochemical characterization of natural gas: a physical multivariable approach and its applications in maturity and migration estimates. *AAPG bulletin*, 84(8), 1152-1172.
- Reeburgh W.S., 2007. Oceanic methane biogeochemistry. *Chemical Reviews* 107, 486–513.
- RER (Regione Emilia-Romagna), 2003. Carta geologica d'Italia, foglio 223 – Ravenna. ISPRA, Servizio Geologico d'Italia – Regione Emilia-Romagna. System Card, Roma. 2 Sheets
- RER and ENI-AGIP, 1998. Riserve idriche sotterranee della Regione Emilia Romagna. Firenze, 120 p, 9 sheets.
- Riva A., Salvatori T., Cavaliere R., Ricchiuto T., Novelli L., 1986. Origin of oils in Po Basin, northern Italy. *Organic Geochemistry*, 10 (1-3), 391-400.
- Roberts S. J., Nunn J. A., 1995. Episodic fluid expulsion from geopressed sediments. *Marine and Petroleum Geology*, 12, 195-202.

- Rooney M. A., Claypool G. E., Chung H. M., 1995. Modeling thermogenic gas generation using carbon isotope ratios of natural gas hydrocarbons. *Chemical Geology*, 126(3-4), 219-232.
- Rosenfeld W. D., Silverman S. R., 1959. Carbon isotope fractionation in bacterial production of methane. *Science*, 130(3389), 1658-1659.
- Russell J. B., 1986. Heat production by ruminal bacteria in continuous culture and its relationship to maintenance energy. *Journal of bacteriology*, 168(2), 694-701.
- Salata, G. G., Roelke L. A., Cifuentes L. A., 2000. A rapid and precise method for measuring stable carbon isotope ratios of dissolved inorganic carbon, *Mar. Chem.*, 69, 153–161, doi:10.1016/S0304-4203(99)00102-4.
- Saunois M., Bousquet P., Poulter B., Peregon A., Ciais P., Canadell J.G., Dlugokencky E.J., Etiope G., Bastviken D., Houweling S., Janssens-Maenhout G., Tubiello F.N., Castaldi S., Jackson R. B., Alexe M., Arora V.K., Beerling D.J., Bergamaschi P., Blake D.R., Brailsford G., Brovkin V., Bruhwiler L., Crevoisier C., Crill P., Covey K., Curry C., Frankenberg C., Gedney N., Höglund-Isaksson L., Ishizawa M., Ito A., Joos F., Kim H.-S., Kleinen T., Krummel P., Lamarque J.-F., Langenfelds R., Locatelli R., Machida T., Maksyutov S., McDonald K.C., Marshall J., Melton, J. R., Morino I., Naik V., O'Doherty S., Parmentier F.-J.W., Patra P.K., Peng C., Peng S., Peters G.P., Pison I., Prigent C., Prinn R., Ramonet M., Riley W.J., Saito M., Santini M., Schroeder R., Simpson I.J., Spahni R., Steele P., Takizawa A., Thornton B.F., Tian H., Tohjima Y., Viovy, N., Voulgarakis A., van Weele M., van der Werf G.R., Weiss R., Wiedinmyer C., Wilton D.J., Wiltshire A., Worthy D., Wunch D., Xu X., Yoshida Y., Zhang B., Zhang Z., Zhu Q., 2016. The global methane budget 2000–2012, *Earth System Science Data*, 8, 697–751, <https://doi.org/10.5194/essd-8-697-2016>.
- Scherer G.W., 1989. Mechanics of syneresis I. Theory. *Journal of Non-Crystalline Solids*, 108, 18-27.
- Schoell M., 1980. The hydrogen and carbon isotopic composition of methane from natural gases of various origins. *Geochimica et Cosmochimica Acta* 44, 649–661.
- Sciarra A., Cinti D., Pizzino L., Procesi M., Voltattorni N., Mecozzi S., Quattrocchi F., 2013. Geochemistry of shallow aquifers and soil gas surveys in a feasibility study at the Rivara natural gas storage site (Po Plain, Northern Italy). *Applied geochemistry*, 34, 3-22.

- Sciarra A., Cantucci B., Coltorti M., 2017. Learning from soil gas change and isotopic signatures during 2012 Emilia seismic sequence. *Scientific Reports* 7: 14187, DOI:10.1038/s41598-017-14500-y.
- Scrocca D., Carminati E., Dogliosi C., Marcantoni D., 2007. Slab retreat and active shortening along the Central-Northern Apennine. In: Lacombe O., Lavè J., Roure F., Verges L. (Eds.), *Thrust belts and foreland basins: from fold kinematics to hydrocarbon systems*. *Frontiers in Earth Sciences*, 471-487.
- Sinninghe Damsté J., Koopmans M. P., 1997. The fate of carotenoids in sediments: an overview. *Pure and applied chemistry*, 69(10), 2067-2074.
- Somoza L., Diaz-del-Río V., León R., Ivanov M., Fernández-Puga M.C., Gardner J.M., Hernández-Molina F.J., Pinheiro L.M., Rodero J., Lobato A., Maestro A., Vázquez J.T., Medialdea T., Fernández-Salas L.M., 2003. Seabed morphology and hydrocarbon seepage in the Gulf of Cádiz mud volcano area: acoustic imagery, multibeam and ultra-high resolution seismic data. *Marine Geology* 195, 153–176.
- Soto J. O., 2015. *Dunaliella Identification Using DNA Fingerprinting Intron-Sizing Method and Species-Specific Oligonucleotides: New Insights on Dunaliella Molecular Identification*. In: *Handbook of Marine Microalgae*, 559-568.
- Tassi F., Capecchiacci F., Buccianti A., Vaselli O. 2011. Sampling and analytical procedures for the determination of VOCs released into Air from natural and anthropogenic sources: a comparison between SPME (Solid Phase Micro Extraction) and ST (Solid Trap) methods. *Applied Geochemistry*. doi:10.1016/j.apgeochem.2011.09.023.
- Tassi F., Vaselli O., Luchetti G., Montegrossi G., Minissale A., 2008. Metodo per la determinazione dei gas disciolti in acque naturali. *Int Rep CNR-IGG*, Florence, n° 10450:11.
- Tassi F., Vaselli O., Tedesco D., Montegrossi G., Darrah T., Cuoco E., Mapendano M.Y., Poreda R., Delgado Huertas A., 2009. Water and gas chemistry at Lake Kivu (DRC): geochemical evidence of vertical and horizontal heterogeneities in a multi-basin structure. *Geochemistry, Geophysics Geosystems* 10(2), doi: 10.1029/2008GC002191.
- Tassi F., Bonini M., Montegrossi G., Capecchiacci F., Capaccioni B., Vaselli O., 2012. Origin of hydrocarbons in gases from mud volcanoes and CH<sub>4</sub>-rich emissions. *Chem. Geol.* 294 (295), 113–126.
- Teatini P., Ferronato M., Gambolati G., Gonella M. 2006. Groundwater pumping and land subsidence in the Emilia-Romagna coastland, Italy: modeling the past occurrence and the future trend. *Water Resour. Res.*, 42, 19 p, W01406, doi:10.1029/2005WR004242.

- Templeton A. S., Chu K. H., Alvarez-Cohen L., Conrad M. E., 2006. Variable carbon isotope fractionation expressed by aerobic CH<sub>4</sub>-oxidizing bacteria. *Geochimica et Cosmochimica Acta*, 70(7), 1739-1752.
- Toth J., Almasi I., 2001. Interpretation of observed fluid potential patterns in a deep sedimentary basin under tectonic compression: Hungarian Great Plain, Pannonian Basin. *Geofluids*, 1, 11-36.
- Turrini C., Lacombe O., Roure F., 2014. Present –day 3D structural model of the Po Valley basin, Northern Italy. *Marine and Petroleum Geology*, 56, 266-289.
- USEPA: Office of Atmospheric Programs (6207J), Methane and Nitrous Oxide Emissions From Natural Sources, U.S. Environmental Protection Agency, EPA 430-R-10-001, Washington, D.C., 20460, available at: <http://nepis.epa.gov/> (last access: 10 November 2016), 2010
- Vai G. B., 2001. Structure and stratigraphy: an overview. IN: Vai G. B. and Martini I. P. (Eds.), *Anatomy of an Orogen. The Apennines and adjacent Mediterranean basins*. Kluwer Academic, Dordrecht, 15-31.
- Valentine D.L. and Reeburgh W.S., 2000. New perspectives on anaerobic methane oxidation. *Environmental Microbiology* 2, 477–484.
- Valentine D.L., 2002. Biogeochemistry and microbial ecology of methane oxidation in anoxic environments: a review. *Antonie van Leeuwenhoek* 81, 271–282.
- Vannoli P., Burrato P., Valensise G., 2014. The seismotectonics of the Po plain (Northern Italy): Tectonic diversity in a blind faulting domain. *Pure and Applied Geophysics*. DOI: 10.1007/s00024-014-0873-0
- Vaselli O., Tassi F., Montegrossi G., Capaccioni B., Giannini L., 2006. Sampling and analysis of volcanic gases, *Acta Vulcanol.*, 18, 65–76.
- Ventura G., Di Giovambattista, R., 2013. Fluid pressure, stress field and propagation style of coalescing thrusts from the analysis of the 20 May 2012 ML 5.9 Emilia earthquake (Northern Apennines, Italy), *Terra Nova*, 25, 72-78, doi:10.1111/ter.12007.
- Wang X., Zhang M., 2008. Compositional and geochemical characteristics of light hydrocarbons for typical marine oils and typical coal-generated oils in China. *Chinese Journal of Geochemistry* 27, 407–411.
- Westerhoff H. V., Hellingwerf K. J., Van Dam K., 1983. Thermodynamic efficiency of microbial growth is low but optimal for maximal growth rate. *Proceedings of the National Academy of Sciences*, 80(1), 305-309.

- Whiticar M.J., 1999. Carbon and hydrogen isotope systematics of bacterial formation and oxidation of methane. *Chemical Geology* 161, 291–314.
- Whiticar M. J., Faber E., 1986. Methane oxidation in sediment and water column environments—*isotope evidence*. *Organic geochemistry*, 10(4-6), 759-768.
- Wood J. M., Sanei H., 2016. Secondary migration and leakage of methane from a major tight-gas system. *Nature Communications*, 7(13614) doi:10.1038/ncomms13614 [www.nature.com/naturecommunications](http://www.nature.com/naturecommunications).

## Table captions

**Table 1.** Location of study sites. The geographical coordinates of G-points refer to a generic gas field baricentral point. Type, depth, details and location with respect to the tectonic setting of the investigated sites are reported. Details: A.1 = gas bubbling in brackish/salt water; A.2 = gas bubbling in freshwater; B = CH<sub>4</sub>-rich water; C = unaltered domestic phreatic well (reference point); D = dry gas seepage from soil; E = gas seepage from an human-induced sediments-fluid eruption; WWW = Warm Water Wells. Tectonic setting: PF = Pedepenninic folds; ITG = Intermediate thrust group; DFI = Dorsale Ferrarese inner frontal thrust group; DFO = Dorsale Ferrarese outer frontal thrust group; and IS = Interposed syncline.

**Table 2.** Chemical and isotopic ( $\delta\text{D-H}_2\text{O}$ ,  $\delta^{18}\text{O-H}_2\text{O}$  and  $\delta^{13}\text{C-TDIC}$ ) composition of waters from G and W sites. Concentration of major compounds are expressed in mg/L. na = not available; bdl = below detection limit

**Table 3.** Chemical and isotopic ( $\delta^{13}\text{C-CO}_2$ ,  $\delta^{13}\text{C-CH}_4$  and  $\delta\text{D-CH}_4$ ) composition of dissolved and free gases from W and S sites. Concentration of gas species is expressed in % v/v.

**Table 4.** Chemical (in % v/v) and isotopic composition of gases from oil and gas fields (G sites)

**Table 5.** Chemical composition of C<sub>4</sub>-C<sub>10</sub> hydrocarbons of gases from oil and gas fields (G sites) of Southern Po River Basin (Northern Italy). Gas concentration are in  $\mu\text{mol/mol}$ . nd = not detected.

## Figure captions

**Figure 1.** Main groups of buried tectonic structures of Emilia-Romagna Region. A, B, C) Detail of buried tectonic structures (after Cerrina Ferrosi et al., 2002; simplified) and study-points location. White areas are the major depocentral synclines and the padealpine monocline. The grey-tones areas highlight the various buried thrusts envelope and only poses a descriptive geometrical value.

**Figure 2.** Essential linedraw (not to scale) of hydrochemical facies and their hypothetical mutual relationships at depth in Emilia-Romagna alluvial plain (redrawn and modified after Moggia, 2016). The depth scale shows average values. Aquifer Complexes of Emilia Region are after RER and ENI-AGIP (1998). The thick yellow bank is the *Prograding Complex Auctorum*. The straight red segments suggest fractures or faults.

**Figure 3.** Unusual Geological Phenomena (UGP) location in Emilia-Romagna Region occurred between May 2012 and September 2018.

**Figure 4.** a) Langelier-Ludwig diagram for the collected waters. b)  $\text{Cl}^-$  vs  $\text{Na}^+$  correlation plots for the collected waters.  $\text{Na}/\text{Cl}$  ratio of seawater is shown for comparison.

**Figure 5.**  $\delta\text{D}-\delta^{18}\text{O}$  scatter plot for the collected waters. The dotted line delineates the Global Meteoric Water line ( $\delta\text{D} = 8*\delta^{18}\text{O} + 10$ ; Craig, 1961); the dashed line is the Local Meteoric Water Line for Northern Italy ( $\delta\text{D} = 7.7094*\delta^{18}\text{O} + 9.4034$ , Longinelli and Selmo, 2003).

**Figure 6.** Temperature (red line and y axis), electrical conductivity (black line and y axis) and water level (blue line and y axis) time series of W4, W8, W10 and W11 wells. The sudden drops in the EC observed in the time series of W8 and W11 are due to the emersion of the probe from the water caused by severe pumping.

**Figure 7.** Essential linedraw of the average ideal setting of tectonic structures buried beneath the Emilia region alluvial plain. A) The age of each single sedimentary body (Paleocene to Holocene) is shown: it also corresponds to the genesis age of related trapped gas. The section results from the merging a multiplicity of various subsection (e.g. C-C' section after Martelli et al. 2017).

B) Gather of physical discontinuities kinds possibly existing in the sedimentary prism of Emilia alluvial plain.

**Figure 8.** Methane surficial seep in Mirabello area near studied points W16 and W18. Each single seep point is highlighted by the vegetational cover reaction giving origin to the typical ground features (Gas Patterned-ground Marks). Satellite scene by GOOGLE-Earth ©, fly 6/9/2104.

**Figure 9.** Chemical and isotopic composition of light hydrocarbons in analyzed gases from oil and gas fields from Po Plain. Data from previous papers (gray points) are also shown for cross-comparison. **a)**  $\delta^{13}\text{C}-\text{CH}_4$  vs.  $\delta\text{D}-\text{CH}_4$  “Schoell plot” for gas from Emilia-Romagna Region. Compositional fields classically associated to microbial gases are reported. **b)** Natural gas interpretative diagram combining the molecular ( $\text{C}_1/\text{C}_2$  ratio) and isotope ( $\delta^{13}\text{C}-\text{CH}_4$ ) compositional information. Calculated mixing lines for possible gas bacterial/diagenetic and thermogenic mixtures. Isotope and molecular compositions of Cortemaggiore gas (Mattavelli et al., 1983) has been assumed as those of thermogenic endmember. Microbial gas endmembers show different  $\text{C}_1/\text{C}_2$  ratios (10000 and 5000, respectively) and  $\delta^{13}\text{C}-\text{CH}_4$  values ( $-78$  and  $-60$  ‰ vs. V-PDB). Mesozoic gases are associated to the Malossa oil field, located close to Milan (Northern Italy) and related to the Southern Alps thrust belts.

**Figure 10.** Carbon isotopic composition of methane and higher chain homologues for the collected gases from oil and gas fields.

**Figure 11.** Ternary plot of  $\text{C}_7$  compounds in natural gas from the Po Plain. The division of humic- and sapropelic-type gases is after Hu et al. (1990). The  $\text{C}_7$  compounds refer to heptanes and can be divided into n-heptane (n- $\text{C}_7$ ), methylcyclohexane (MCH) and dimethylcyclopentane (DMCP). The n- $\text{C}_7$  (%) value refers to the ratio of n- $\text{C}_7/(\text{n-}\text{C}_7 + \text{MCH} + \Sigma\text{DMCP})$ . The same applies for the ratios of MCH and  $\Sigma\text{DMCP}$ .

**Figure 12.** Concentrations of cyclic compounds with respect to the total cyclic abundance in the investigated gas samples from oil and gas fields of Po plain.

**Figure 13.** Ternary plots of chemical composition of dissolved and free gases from W wells and S seeps: **a)**  $\text{O}_2-\text{Ar}-\text{N}_2$ ; **b)**  $\text{CH}_4-\text{O}_2-\text{CO}_2$ .

**Figure 14.** Isotopic composition of shallow and surficial gases from the Po Plain: **a)**  $\delta^{13}\text{C}-\text{CH}_4$  vs.  $\delta\text{D}-\text{CH}_4$  diagram showing the data distribution,  $^{13}\text{C}$ -D-enrichment trends (black arrow) with relative slope expressed as  $\Delta\text{H}/\Delta\text{C}$ . Isotopic composition of Pliocene (light gray box), Miocene (dark gray box) and Triassic (G11) gases are also shown for comparison (see text for details).

ID	Place Name	Well type	WGS84-N; WGS84-E	Well/pool depth (m b. g. s.)	Details	Tectonic setting
G1	Cavone	Oil field	44°52'57.83"; 10°56'38.91"	4155 (main pool: 2900)	-	DFI
G2	Spilamberto	Gas field	44°32'25.14"; 11°01'27.83"	2420 (main pool: 1242)	-	PF
G3	S. Martino	Gas field	44°35'01.03"; 10°55'44.38"	na	-	PF
G4	Sillaro	Gas field	44°29'36.88; 11°41'48.06"	Main pool: 2100	-	ITG
G5	Dosso Angeli	Gas field	44°35'39.16"; 12°14'48.51"	2885-3839 (main pools: 3033-3232)	-	DFO
W1	Vallalta	Abandoned gas well	44°55'47.91"; 11°00'01.42"	1742	A.1	DFI
W2	Diamantina,	Abandoned gas well	44°53'08.39"; 11°30'33.90"	≈200	A.1	DFO
W3	Ambrogio	Abandoned gas well	44°54'32.27"; 11°53'44.60"	≈350	A.1	DFO
W4	Novi	Phreatic well	44°53'20.30"; 10°52'53.40"	8.5	WWW	DFI
W5	Novi	Artesian well	44°53'19.93"; 10°52'55.88"	25	B	DFI
W6	Sorbara	Phreatic well	44°44'40.04"; 11°00'16.53"	12	WWW	IS
W7	Bomporto	Phreatic well	44°43'32.64"; 11°02'31.02"	8	WWW	IS
W8	Camurana	Phreatic well	44°51'53.10"; 11°04'18.65"	10	WWW	DFI
W9	Camurana	Artesian well	44°51'52.29"; 11°04'19.37"	22	B	DFI
W10	Crevalcore	Phreatic well	44°43'28.96"; 11°08'42.88"	5.7	WWW	IS
W11	Camposanto	Phreatic well	44°47'14.99"; 11°09'12.06"	10	WWW	DFI
W12	Decima	Phreatic well	44°41'15.09"; 11°13'08.90"	7	C	IS
W13	Renazzo	Phreatic well	44°45'34.88"; 11°17'30.57"	6.5	A.2	DFI
W14	Corpo Reno (Casino del gas)	Phreatic well	44°45'22.38"; 11°18'09.03"	4.5	A.2	DFI
W15	Corpo Reno	Phreatic well	44°45'47.57"; 11°19'08.35"	5.5	A.2	DFI
W16	Mirabello (C7)	Phreatic well	44°49'33.91"; 11°27'56.63"	7	WWW	DFO
W17	Mirabello (C5bis)	Phreatic well	44°49'39.77"; 11°28'11.08"	4.5	WWW	DFO
W18	Mirabello (C5)	Phreatic well	44°49'39.77"; 11°28'11.08"	5	WWW	DFO
S1	Warm Grounds of Medolla	Gas seepage	44°51'13.41"; 11°05'09.22"	0	D	DFI
S2	Bruino (CPT)	Gas seepage	44°51'28.64"; 11°04'33.34"	24	E	DFI
S3	Bondeno (CPT)	Gas seepage	44°52'50.51"; 11°24'31.96"	20	E	DFO

**Table 1.**

ID	Sampling Date	T	pH	Eh	EC	TDS	HCO <sub>3</sub> <sup>-</sup>	F <sup>-</sup>	Cl <sup>-</sup>	Br <sup>-</sup>	NO <sub>3</sub> <sup>-</sup>	SO <sub>4</sub> <sup>2-</sup>	Na <sup>+</sup>	NH <sub>4</sub> <sup>+</sup>	K <sup>+</sup>	Mg <sup>2+</sup>	Ca <sup>2+</sup>	δD-H <sub>2</sub> O	δ <sup>18</sup> O-H <sub>2</sub> O	δ <sup>13</sup> C-TDIC
G1	04/04/2016	na	7.5	-324	49000	32692	542	3.9	18624	97	bdl	782	11943	bdl	161	153	323	3.7	7.7	-7
G2	04/04/2016	na	6.9	-88	75500	50966	58	1.4	30988	151	bdl	4.7	17171	bdl	188	899	1505	-9.8	-0.01	-5
G3	04/04/2016	na	6.7	-129	na	594	247	0.5	134	bdl	bdl	6	71	bdl	27	7	101	-33.9	-3.3	
G4	14/10/2016	na	7	-120	88900	63328	232	8.9	37434	189	bdl	9.8	21616	bdl	246	1244	2348	-4.1	1	
G5	03/02/2016	na	6.9	-118	na	71015	156	2.7	43291	218	bdl	157	23343	bdl	140	1102	2605	0.3	0.06	-13.1
W1	28/06/2017	18	7.7	-180	na	4475	610	0.6	2146	10.6	14.3	34	1434	43	10	104	69			
W2	11/07/2014	21	7.3	-192	na	6874	214	0.8	3765	20	bdl	7	2269	bdl	18	323	252	-69.2	-10	
W3	21/02/2013	25	7.4	-220	na	25590	381	2	15785	69	bdl	15	7768	50	36	901	582	-57.1	-8	
W4	23/03/2016	10.1	7	15	1135	1062	598	0.1	87	0.06	5.4	117	58	bdl	5	55	137			-16.7
	16/05/2016	15	7.2	-86	1000	1093	665	0.08	73	0.04	4.1	96	56	0.05	3	48	148			
	29/06/2016	14.9	7	127	1227	1007	552	0.11	91	0.03	8.3	100	59	0.15	6	52	138			
	02/09/2016	17.1	7	45	1160	1047	622	0.17	71	0.04	1.8	99	52	0.16	4	51	145			
	02/11/2016	15.3	7.2	79	1108	1032	610	0.11	63	0.04	4.2	92	52	0.43	7	56	147			
W5	16/05/2016	14.8	7.3	-191	1246	1445	961	0.29	74	0.1	1.5	69	30	1.07	3	73	232			-24.8
	29/06/2016	16.3	7.2	-230	1358	1043	701	0.12	66	0.16	bdl	39	29	0.24	3	63	142			
	02/09/2016	15	7.3	-228	1304	1256	854	0.17	62	0.07	0.2	48	28	0.79	3	64	195			
	02/11/2016	14.6	7.1	-225	1315	1279	866	0.25	59	0.08	0.1	39	33	0.91	4	69	208			
W6	02/09/2016	30.3	7.2	31	1632	1434	729	0.2	99	0.1	7	216	98	bdl	65	68	152			
W7	20/09/2016	22.2	7.2	52	1638	1466	800	0.22	153	0.17	1.5	114	90	1.27	118	82	106			
W8	22/10/2015	53.6	7.3	104	1429	1390	631	0.19	203	0.71	1.8	125	68	1.14	140	68	150			
	28/10/2015	32.7	7.3	100	1519	1436	658	0.3	206	0.67	1.7	132	69	1.33	145	71	151			
	23/03/2016	12.5	7.4	14	2060	1974	568	0.13	564	1.82	31.7	165	314	3.35	92	60	173			-17.2
	16/05/2016	14.6	7.1	80	2145	1934	756	0.15	383	1.44	18.4	168	279	bdl	69	60	198			
	29/06/2016	14.6	7.1	127	1963	1513	653	0.13	250	0.67	9.6	147	225	bdl	57	43	127			
	02/09/2016	15	7.2	66	1402	1221	644	0.85	109	0.23	1.1	120	67	0.24	95	58	126			
	02/11/2016	15.9	7.2	155	1320	1201	653	0.15	89	0.18	1.9	104	80	bdl	100	52	120			
W9	28/10/2015	14.7	7.3	-250	3031	2865	1165	0.61	753	3.35	0.5	76	540	10.45	7	120	188			
	23/03/2016	12.7	8.1	-367	2560	2422	753	0.16	883	3.54	2	7	488	9.16	7	116	153			-26.9
	16/05/2016	14.8	7.6	-306	2410	2471	1354	0.39	411	1.89	0.05	2	384	9.78	9	111	188			
	29/06/2016	15.2	7.4	-366	4180	3082	1051	bdl	955	3.95	bdl	125	613	9.94	10	122	192			
	02/09/2016	15.2	7.5	-323	3500	2676	1092	1.39	773	3.2	2.3	14	493	9.72	11	107	170			
W10	28/10/2015	31.4	7.6	54	1058	1000	574	0.3	48	0.18	29.9	69	50	1.34	62	47	119			
	23/03/2016	19.7	7.9	-14	811	702	359	0.17	39	0.09	60.7	61	46	0.04	41	29	66			-16.1
	03/05/2016	32.8	7.8	-24	899	805	382	0.2	69	0.12	66.2	62	45	bdl	43	36	102			-14.6
	11/05/2016	33.8	7.9	-88	910	854	454	1.22	39	0.12	56.2	68	46	0.23	49	37	103			-17.3
	29/06/2016	20.4	7.4	83	915	777	428	0.19	39	0.15	40.2	56	40	bdl	44	35	95			
	02/11/2016	18.7	7.1	84	1088	1030	647	0.15	54	0.21	6.6	48	47	0.3	63	52	113			
W11	23/03/2016	15.9	7	35	1948	1830	837	0.08	233	0.12	80.7	145	141	1.33	178	89	125			-19.2
	16/05/2016	17.6	7.2	29	1948	1978	930	0.97	203	0.21	85.2	171	146	0.82	197	83	160			
	29/06/2016	17.4	7.1	95	2130	1739	780	0.07	188	0.04	69.3	169	138	bdl	194	75	126			
	02/09/2016	21	6.9	27	2110	1898	992	1.63	171	0.2	25.9	151	129	1.01	180	85	162			
	02/11/2016	18.8	6.9	67	2020	1833	952	0.14	154	0.19	6.1	153	130	0.67	193	86	158			
W12	23/03/2016	11.3	7.3	-35	1280	1218	519	0.1	64	0.13	99.1	215	48	0.05	52	37	184			-16.4
	16/05/2016	14.3	7.4	-40	1114	1267	738	0.88	63	0.15	19	113	60	2.7	55	37	176			
	29/06/2016	16.8	7	94	1354	1213	689	0.09	61	0.08	4.7	125	66	0.07	53	40	175			
	02/09/2016	18.8	7.1	-184	1378	1288	775	0.1	61	0.06	0.1	117	63	1.39	51	41	179			
	02/11/2016	16.3	7	72	1350	1299	778	0.18	62	0.13	2.4	98	67	0.46	54	44	192			
W13	28/06/2017	17	7.1	44	na	1175	700	0.25	68	0.3	23.8	91	76	10.8	3	45	157			
W14	28/06/2017	16	7.6	24	na	960	610	0.4	85	0.28	8.8	17	97	3.5	15	44	79			
W15	21/11/2012	14.5	6.9	-156	980	932	537	0.18	36	0.04	8	74	47	bdl	101	24	105			
W16	29/06/2012	13	7.2	264	2690	2133	586	0.24	215	0.14	65	692	135	bdl	47	128	265			
	02/07/2012	20.7	7.2	100	2710	2300	598	0.25	254	0.15	65	783	134	bdl	43	129	294			
W17	02/07/2012	16.5	7.4	-351	3450	2865	1007	0.27	362	0.28	0.03	599	268	4	258	126	241			
	24/07/2012	16.5	7.5	-378	2990	2961	995	0.31	438	0.26	0.16	643	262	2.6	254	126	240			
W18	29/06/2012	17.2	7.1	271	3160	2533	1062	0.15	435	0.29	1.4	294	298	0.02	128	133	181			
	02/07/2012	16	7.3	181	3820	3080	1209	0.16	385	0.28	3.7	642	282	0.13	174	147	237			

Table 2.

ID	Date	CO <sub>2</sub>	N <sub>2</sub>	O <sub>2</sub>	Ar	CH <sub>4</sub>	C <sub>2</sub> H <sub>6</sub>	C <sub>3</sub> H <sub>8</sub>	nC <sub>4</sub> H <sub>10</sub>	iC <sub>4</sub> H <sub>10</sub>	Gas tot.	δ <sup>13</sup> C-CO <sub>2</sub>	δ <sup>13</sup> C-CH <sub>4</sub>	δD-CH <sub>4</sub>
W1	28/06/2017	2.3	11.5	0.1	0.3	85.8	0.016	0.0025	0.0087	0.0065			-75	
W2	11/07/2014	0.71	3.38	0.01	0.06	95.75	0.03	0.0019	0.00105	0.0013		-15.5	-78	
W3	21/02/2013													
W4	23/03/2016		85.5	12.4	2.1						0.85			
	16/05/2016		80.3	17.7	2.0						0.85			
	29/06/2016		86.5	11.3	2.2						0.87			
	02/09/2016		92.8	4.9	2.3						0.71			
	02/11/2016		87.6	10.3	2.1						0.72			
W5	16/05/2016	12.4	28.3	0.9	0.7	57.7	0.040	0.007	0.002	0.002	0.88		-65.6	
	29/06/2016	10.1	33.2	1.3	0.8	54.5	0.037	0.006	0.001	0.002	0.84			
	02/09/2016	9.6	25.9	0.7	0.6	63.0	0.038	0.007	0.001	0.002	0.81			
	02/11/2016	11.9	18.7	0.5	0.4	68.4	0.040	0.007	0.003	0.003	0.80			
W6	02/09/2016	1.7	83.5	3.9	2.0	8.8					0.64			
W7	20/09/2016		93.4	4.4	2.2						0.59			
W8	22/10/2015	7.5	76.6	13.9	1.8	0.16					0.96	-23.2	-23.2	-58
	28/10/2015	4.2	78.5	15.1	2.0	0.21					0.91	-23.5	-20.7	
	23/03/2016		65.7	32.8	1.5						0.94			
	16/05/2016		68.6	29.7	1.7						0.83			
	29/06/2016		66.9	31.4	1.7						0.99			
	02/09/2016		60.4	38.0	1.6						1.03			
	02/11/2016		66.8	31.5	1.7						0.76			
W9	28/10/2015	5.0	20.4	0.4	0.5	73.7	0.035	0.004	0.002	0.004	1.36	-32.8	-71.4	-130
	23/03/2016	5.3	28.7	0.5	0.7	65.2	0.041	0.006	0.001	0.002	1.34		-75.3	-177
	16/05/2016	5.8	27.2	0.5	0.6	65.8	0.039	0.006	0.001	0.002	1.14			
	29/06/2016	5.9	27.7	0.9	0.7	64.8	0.038	0.006	0.001	0.002	1.27			
	02/09/2016	1.8	32.5	0.7	0.8	63.5	0.032	0.004	0.001	0.002	1.28			
W10	28/10/2015		68.4	29.8	1.8						0.89			
	23/03/2016		93.9	3.9	2.2	0.03					0.78			
	03/05/2016		91.5	6.4	2.2						0.75			
	11/05/2016		94.2	3.6	2.2	0.05					0.69			
	29/06/2016		96.3	1.3	2.4	0.08					0.63			
	02/11/2016		95.4	2.1	2.4	0.11					0.53			
W11	23/03/2016	51.9	28.8	0.8	0.7	18.5	0.011	0.002	0.001	0.002	1.76		-55.8	-154
	16/05/2016	62.4	10.9	0.4	0.3	26.1	0.011	0.003	0.002	0.002	1.38			
	29/06/2016	60.5	17.1	0.5	0.4	21.5	0.013	0.002	0.001	0.002	1.35			
	02/09/2016	53.5	34.9	1.3	0.9	9.4	0.007	0.002	0.001	0.002	1.17			
	02/11/2016	56.4	18.8	0.5	0.4	23.8	0.020	0.003	0.003	0.003	1.38			
W12	23/03/2016		66.8	31.6	1.6						0.75			
	16/05/2016		66.9	31.6	1.5						0.79			
	29/06/2016		65.5	32.7	1.8						0.73			
	02/09/2016		64.5	33.9	1.6						0.92			
	02/11/2016		65.9	32.4	1.7						0.83			
W13	28/06/2017	1.1	7.4	1.2	0.2	90.1	0.021	0.0036	0.0015	0.0021			-65	
W14	28/06/2017	1.3	8.5	1.0	0.2	89.0	0.021	0.0011						
W15	21/11/2012	7.27	2.86	0.03	0.07	89.82						-20.7	-78.6	-198
W16	29/06/2012	8.2	63.9	1.2	1.5	25.3						-21.3	-50.8	-237
	02/07/2012	47.5	34.0	17.7	0.8	0.014								
W17	02/07/2012	9.13	45.11	1.63	1.09	43.04						-22.9	-51.6	-225
	24/07/2012	81.06	10.16	0.15	0.25	8.58								
W18	29/06/2012	7.48	56.48	1.48	1.37	33.19						-23.1	-56.4	-231
	02/07/2012	86.96	10.59	2.19	0.25	0.01								
S1	08/2015											-72	-68.2	-116
	08/2015											-73.2	-73.2	-156
S2	10/2014	1.99	17.43	4.54	0.40	75.69	0.041	0.0051	0.0021	0.0035		-24.6	-67.5	-188
	11/2015											-35.2	-67.5	-188
S3	08/2014	2.39	24.48	2.82	0.54	69.71	0.051	0.0056	0.0026	0.0041		-16.1	-79	

Table 3.

ID	Wells	CH <sub>4</sub>	C <sub>2</sub> H <sub>6</sub>	C <sub>3</sub> H <sub>8</sub>	n-C <sub>4</sub> H <sub>10</sub>	i-C <sub>4</sub> H <sub>10</sub>	δ <sup>13</sup> C-CH <sub>4</sub>	δ <sup>13</sup> C-C <sub>2</sub> H <sub>6</sub>	δ <sup>13</sup> C-C <sub>3</sub> H <sub>8</sub>	δ <sup>13</sup> C-nC <sub>4</sub> H <sub>10</sub>	δ <sup>13</sup> C-iC <sub>4</sub> H <sub>10</sub>	δD-CH <sub>4</sub>	R/R <sub>a</sub>	<sup>4</sup> He/ <sup>20</sup> Ne	R/R <sub>a</sub>	<sup>40</sup> Ar/ <sup>36</sup> Ar	<sup>38</sup> Ar/ <sup>36</sup> Ar
<b>G1</b>		64.50	11.12	15.89	5.561	2.927	-56.2	-35.6	-31.6	-30.1	-30	-210	0.044	76.91	0.040	317	0.1887
<b>G2</b>	A	97.82	1.37	0.53	0.118	0.171	-56.9	-28.8	-22.2	-18.9	-21.9	-189	0.023	197.12	0.021	312	0.1877
	B	97.45	1.55	0.64	0.153	0.206	-57	-28.3	-22.3	-19	-21.7	-187					
	C	97.54	1.52	0.61	0.139	0.191	-57.1	-28.4	-22.3	-18.9	-21.7	-187					
	D	96.16	2.35	0.98	0.242	0.276	-54.5	-26.7	-22.1	-18.9	-21.6	-184	0.035	89.51	0.031	304	0.1887
	E	97.65	1.49	0.57	0.122	0.167	-56.4	-28.4	-22.5	-18.8	-22.2	-187					
	F	96.97	1.85	0.77	0.185	0.225	-56.3	-27.7	-22.4	-18.8	-21.8	-186					
	G	97.28	1.62	0.70	0.167	0.225	-57.3	-28.2	-22.3	-18.9	-21.7	-187	0.031	727.03	0.031	309	0.1875
<b>G3</b>	A	99.81	0.16	0.01	0.005	0.011	-67.1	-37.9	-22.9	-21.3	-22.5	-188					
	B	99.74	0.18	0.05	0.006	0.020	-66.4	-36.3	-28	-21.5	-23	-190	0.028	56.86	0.022	294	0.1879
<b>G4</b>		99.77	0.09	0.10	0.004	0.024	-63.9	-42.8	-34.1	-27.2	-24.3	-196	0.076	5.42	0.018	297	0.188
<b>G5</b>	A	99.94	0.04	0.01	0.001	0.005	-71.1	-53.9	-34.7	-26	-25	-171	0.049	33.67	0.040	292	0.1871
	B	99.95	0.04	0.01	0.001	0.002	-71.7	-56.8	-35.7	-26	-24.8	-171	0.040	37.95	0.032	295	0.1873
	C	99.88	0.07	0.04	0.002	0.012	-69.1	-47	-32.9	-26.1	-25.1	-183	0.023	33.16	0.014	293	0.1897

**Table 4.**

Organic Compounds	G1	G2-A	G2-B	G2-C	G2-D	G2-E	G2-F	G2-G	G3-A	G3-B	G4	G5-A	G5-B	G5-C
Iso-Butane	29267	1710	2062	1905	2759	1673	2253	2252	112	203	240	46	22	116
Normal-Butane	55606	1179	1531	1385	2417	1220	1847	1671	53	64	42	10	5.5	23
Butane 2-Methyl	55319	4447	4910	4657	6613	4428	6118	5462	468	530	464	114	56	259
Pentane	56905	902	1093	1062	1863	961	1536	1294	62	56	30	8.2	5.2	21
Butane 2,2-Dimethyl	301	544	599	540	908	521	784	641	46	46	11	7.0	3.7	6.9
Butane 2,3-Dimethyl	nd	nd	nd	nd	nd	nd	nd	nd	nd	nd	nd	79	nd	146
Pentane 2-Methyl	32856	2375	2890	2725	4764	3117	4836	3426	427	308	331	nd	68	nd
Pentane 3-Methyl	16022	2249	2569	2519	3212	2632	3399	2620	435	302	84	19	53	32
Normal-Hexane	117706	1004	1500	1594	2471	1592	2753	1612	244	52	52	8.6	13	20
Pentane 2,2-Dimethyl	110	227	238	212	296	248	317	229	42	27	nd	5.3	6.8	6.1
Pentane 2,4-Dimethyl	948	252	294	247	328	352	357	243	81	50	23	17	11	14
Pentane 3,3-Dimethyl	131	199	272	233	320	256	329	232	56	28	nd	3.3	nd	nd
Pentane 2,3-Dimethyl	4021	767	898	945	1085	1179	1343	939	362	159	113	36	14	52
Hexane 3-Methyl	9336	1964	3001	2886	3320	2913	3580	2270	960	399	127	28	nd	57
Normal-Heptane	16817	382	941	865	1199	666	977	529	149	24	90	5.4	nd	28
Hexane 2,2-Dimethyl	75	42	82	58	135	70	63	46	11	5.0	nd	1.0	nd	nd
Hexane 2,5-Dimethyl	366	127	228	165	244	186	222	161	45	16	15	2.9	nd	5.6
Hexane 2,4-Dimethyl	454	105	183	134	225	161	192	122	34	15	19	5.4	nd	11
Hexane 3,3-Dimethyl	nd	5.9	11	6.7	7.5	6.3	8.6	6.1	2.5	1.4	nd	0.6	nd	2.3
Hexane 2,3-Dimethyl	349	75	157	100	150	118	125	72	32	10	nd	3.2	nd	17
Hexane 3,4-Dimethyl	94	19	46	30	38	31	33	21	9.2	2.7	nd	54	nd	108
Heptane 2-Methyl	2457	435	1018	696	1046	653	810	431	200	39	70	2.9	nd	22
Heptane 4-methyl	795	287	635	472	702	510	521	294	139	36	nd	10	3.8	21
Heptane 3-Methyl	1449	491	1115	691	1031	782	887	477	230	52	nd	1.7	nd	5
Normal-Octane	3137	90	354	270	509	227	330	107	75	11	25	1.6	nd	17
Heptane 2,2-Dimethyl	nd	67	123	71	113	82	77	60	37	nd	nd	nd	nd	nd
Heptane 2,4-Dimethyl	nd	53	144	133	270	168	152	106	28	nd	nd	nd	nd	nd
Heptane 3,5-Dimethyl	241	232	604	335	476	386	389	165	140	27	nd	4.6	nd	13
Octane 2-Methyl	537	213	524	295	382	305	333	156	134	29	112	10	nd	34
Octane 3-Methyl	137	107	246	91	80	167	166	61	52	14	nd	8.2	nd	22
Octane 4-Methyl	184	98	232	107	80	168	163	73	5.2	6.4	nd	nd	nd	1.0
Hexane 2,2,4-Trimethyl	232	48	42	132	59	41	nd	89	13	2.5	nd	nd	5.1	nd
Octane 3,6-Dimethyl	nd	nd	27	14	nd	32	25	nd	10	nd	nd	2.2	nd	9.4
Cyclopentane	5405	388	441	255	637	542	766	644	80	44	21	nd	nd	nd
Cyclopentane Methyl	13153	1721	2573	2280	3471	2346	3262	1981	558	335	275	24	38	73
Cyclopentane 1,3-Dimethyl cis	2559	517	838	880	960	782	1015	542	273	116	170	38	5.8	71
Cyclopentane 1,3-Dimethyl trans	1239	385	612	579	717	549	736	404	222	106	210	47	8.0	103
Cyclopentane 1,2-Dimethyl cis	2487	808	1254	1193	1278	1226	1577	850	440	200	338	22	3.1	58
Cyclopentane Ethyl	605	91	202	162	203	162	198	98	80	20	22	2	nd	6
Cyclopentane 1,2,4-Trimethyl	300	220	367	290	317	344	363	211	165	53	128	18	2.6	33
Cyclopentane 1,2,3-Trimethyl	323	359	438	438	548	403	574	514	192	44	242	16	1.9	24
Cyclohexane	9857	2260	3742	3424	4384	3113	4714	2698	994	352	66	11	7.8	24
Cyclohexane Methyl	5670	3164	4980	4439	6349	4940	5872	4693	3161	538	177	14	nd	64
Cyclohexane 1,3-Dimethyl cis	1343	1115	1325	1352	1614	1263	1540	1605	357	52	216	44	4.4	75
Cyclohexane 1,1-Dimethyl	nd	265	467	576	751	373	432	384	92	15	nd	nd	nd	nd
Cyclohexane 1,2-Dimethyl	632	421	473	485	548	489	603	570	144	21	125	9.3	nd	22
Cyclohexane 1,4-Dimethyl cis	108	201	251	226	302	226	266	259	68	10	50	5.2	nd	20
Cyclohexane Ethyl	224	199	311	263	318	247	302	226	85	7.3	nd	nd	nd	nd
Cyclohexane 1,1,3-Trimethyl	395	107	120	108	124	116	132	105	78	22	496	142	10.5	212
Cyclohexane 1,2,3-Trimethyl	69	9.4	13	8.9	12	11	12	9.4	8.3	2.1	50	1.7	nd	3.0
Cyclohexane 1,2,4-Trimethyl	148	38	48	38	38	43	54	38	25	3.4	25	2.2	nd	3.9
Cyclohexane 1,3,5-Trimethyl	nd	8.3	9.1	5.7	20	11	12	6.4	5.6	0.7	nd	1.2	nd	2.7
Cyclohexane 1-Ethyl, 3-Methyl	nd	17	30	36	53	22	24	14	11	1.8	nd	0.0	nd	nd
Cyclohexane 1-Ethyl, 4-Methyl	nd	14	15	8.8	4.4	17	19	10	7.7	1.7	nd	1.0	nd	2.5
Cyclohexane Propyl	nd	11	9.2	4.4	2.5	14	12	5.7	5.1	1.1	nd	0.5	nd	1.1
Cyclohexane 1,1,3,5-Tetramethyl	nd	5.4	4.1	4.8	nd	8.5	6.2	5.3	3.6	0.5	nd	1.3	nd	1.5
Cyclohexane 1,1,2,3-Tetramethyl	nd	nd	nd	1.6	nd	2.7	2.8	nd	2.4	0.9	20	1.7	nd	4.1
Cycloheptane Methyl	nd	nd	nd	nd	nd	nd	nd	nd	nd	nd	45	5.3	nd	13
Cyclooctane Methyl	nd	5.9	7.0	2.6	1.5	2.9	4.6	3.9	3.5	1.3	nd	nd	nd	nd
OctaHydro Pentalene	nd	2.2	7.4	6.5	5.1	6.3	8.2	2.7	4.0	nd	nd	nd	nd	nd
1-H Indene Octahydro	nd	8.8	9.3	4.1	nd	12	10	4.5	5.1	1.4	nd	1.2	nd	1.9
3-Carene	nd	nd	nd	4.6	nd	nd	nd	3.4	nd	nd	nd	nd	nd	nd
Benzene	18721	nd	83	229	404	95	139	14	nd	nd	17	7.3	nd	86
Toluene	10001	nd	421	381	1362	143	130	23	nd	nd	nd	nd	nd	30
EthylBenzene	302	nd	160	123	266	63	73	6	59	10	nd	nd	nd	26
p-Xylene	282	nd	nd	1.3	nd	23								
o-Xylene	nd	0.4	90	48	85	57	37	nd	41	nd	nd	nd	nd	3.9
Styrene	nd	0.7	47	50	403	44	20	nd	23	nd	nd	nd	nd	nd
Dimethylsulfide	nd	nd	10	9.4	5.4	3.0	17	nd	nd	nd	14	8.4	11	13
Carbondisulfide	nd	0.2	nd	7.2	nd	20	nd	nd	nd	nd	nd	0.5	nd	nd

Table 5.

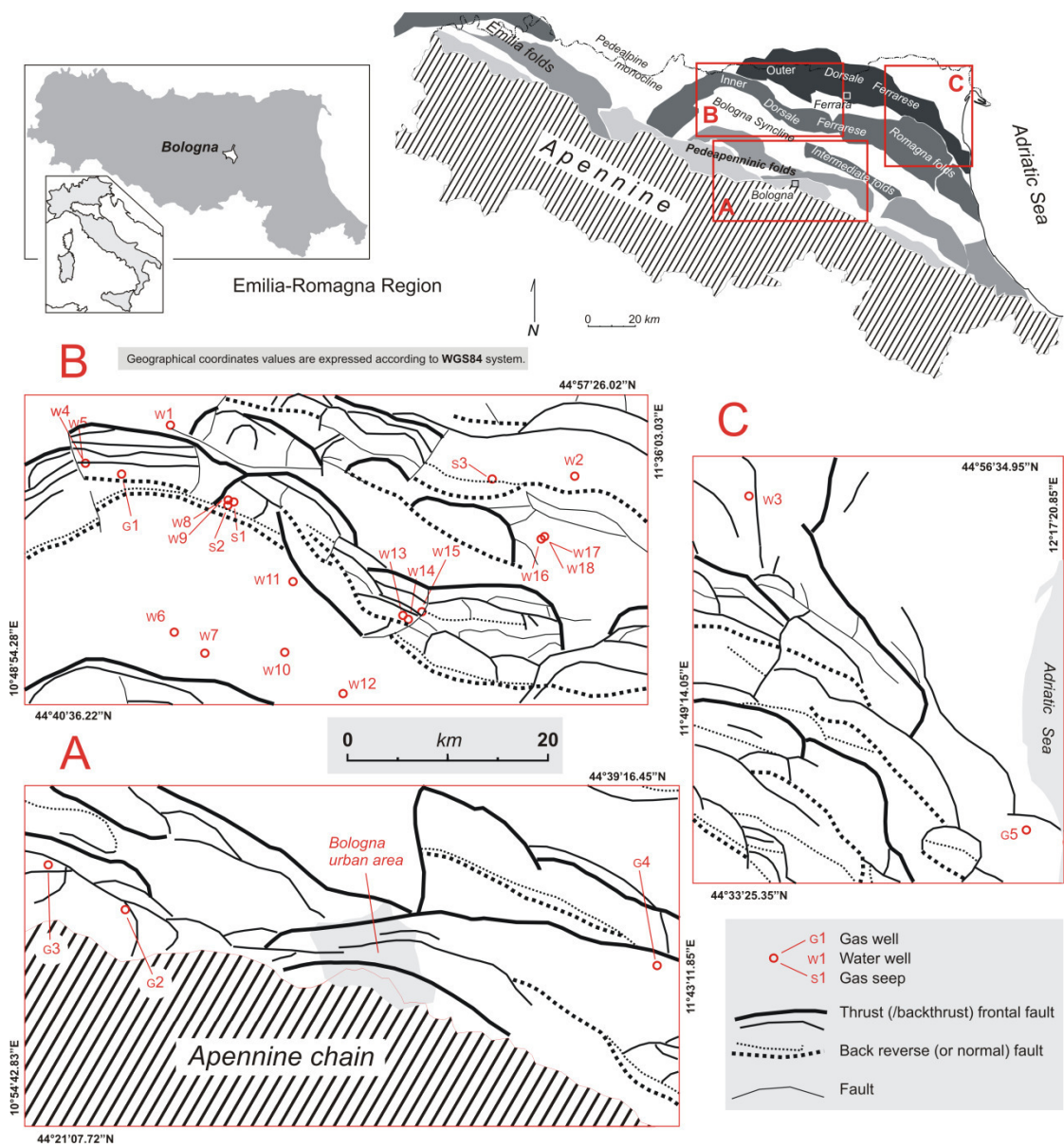


**Figure 1.**

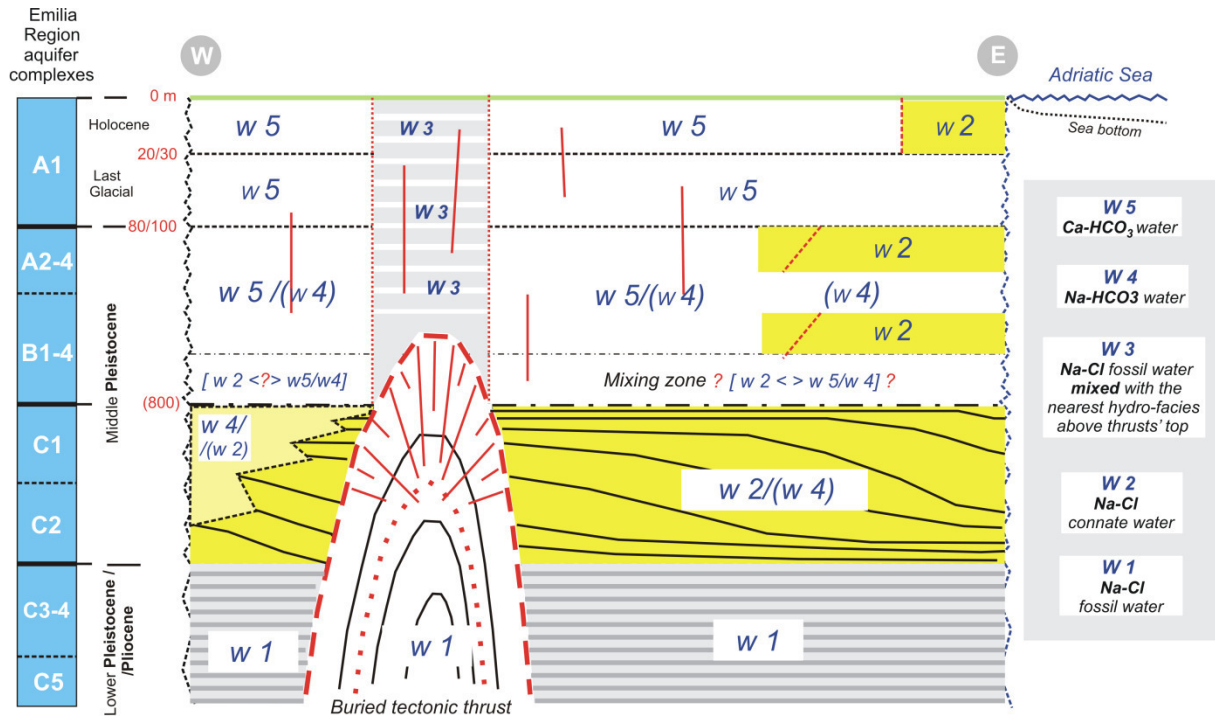


Figure 2.

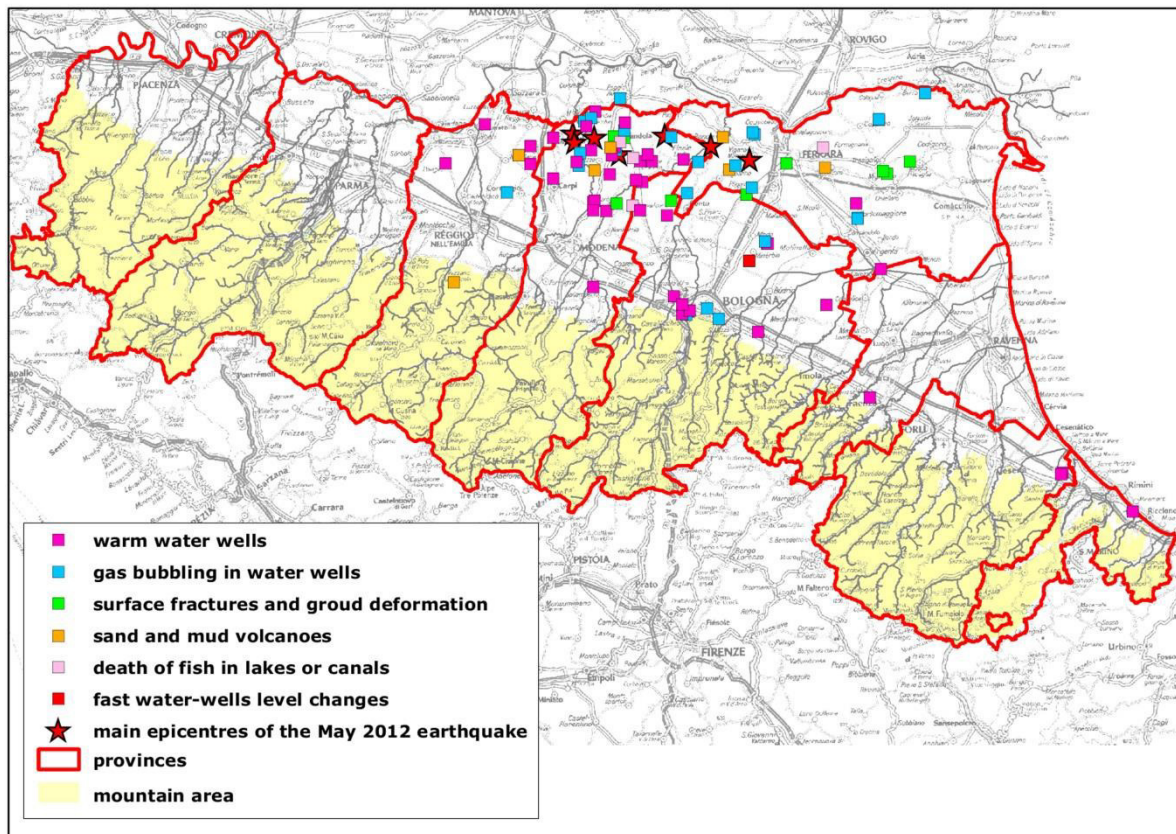


Figure 3

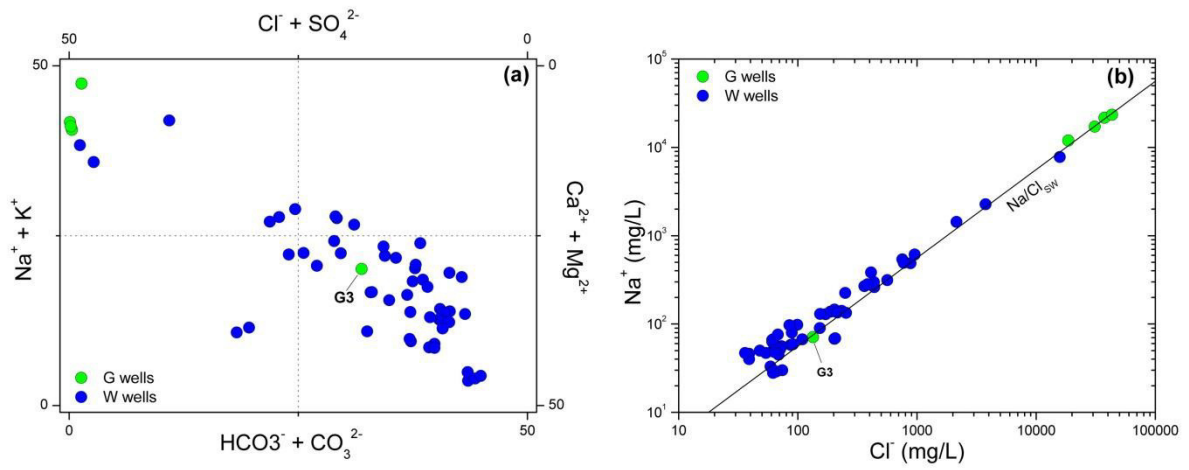


Figure 4

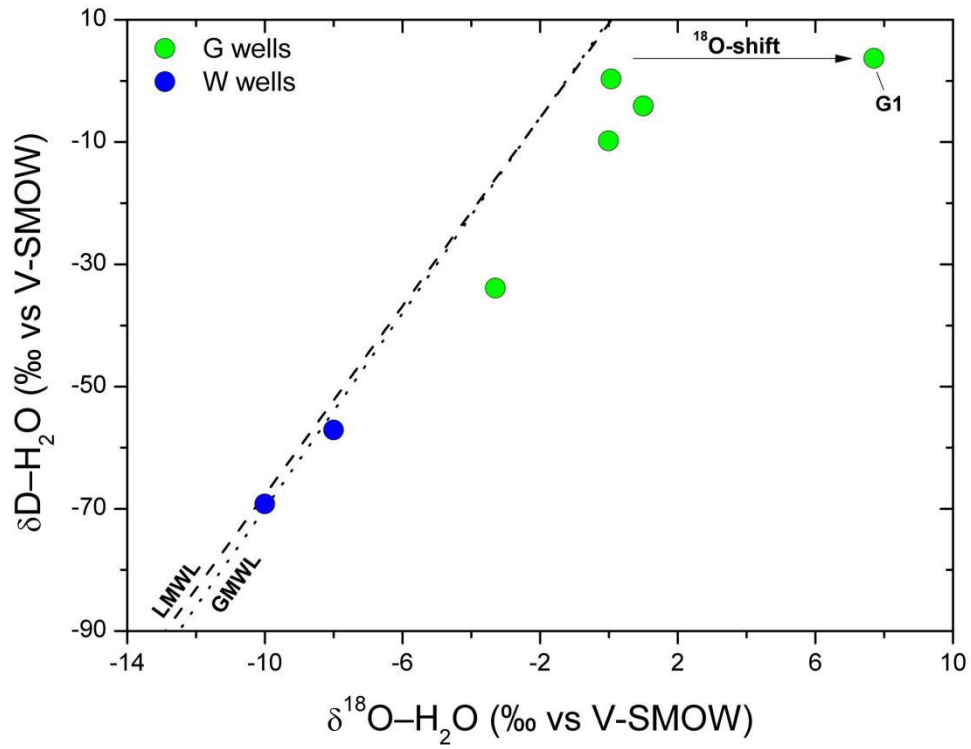


Figure 5

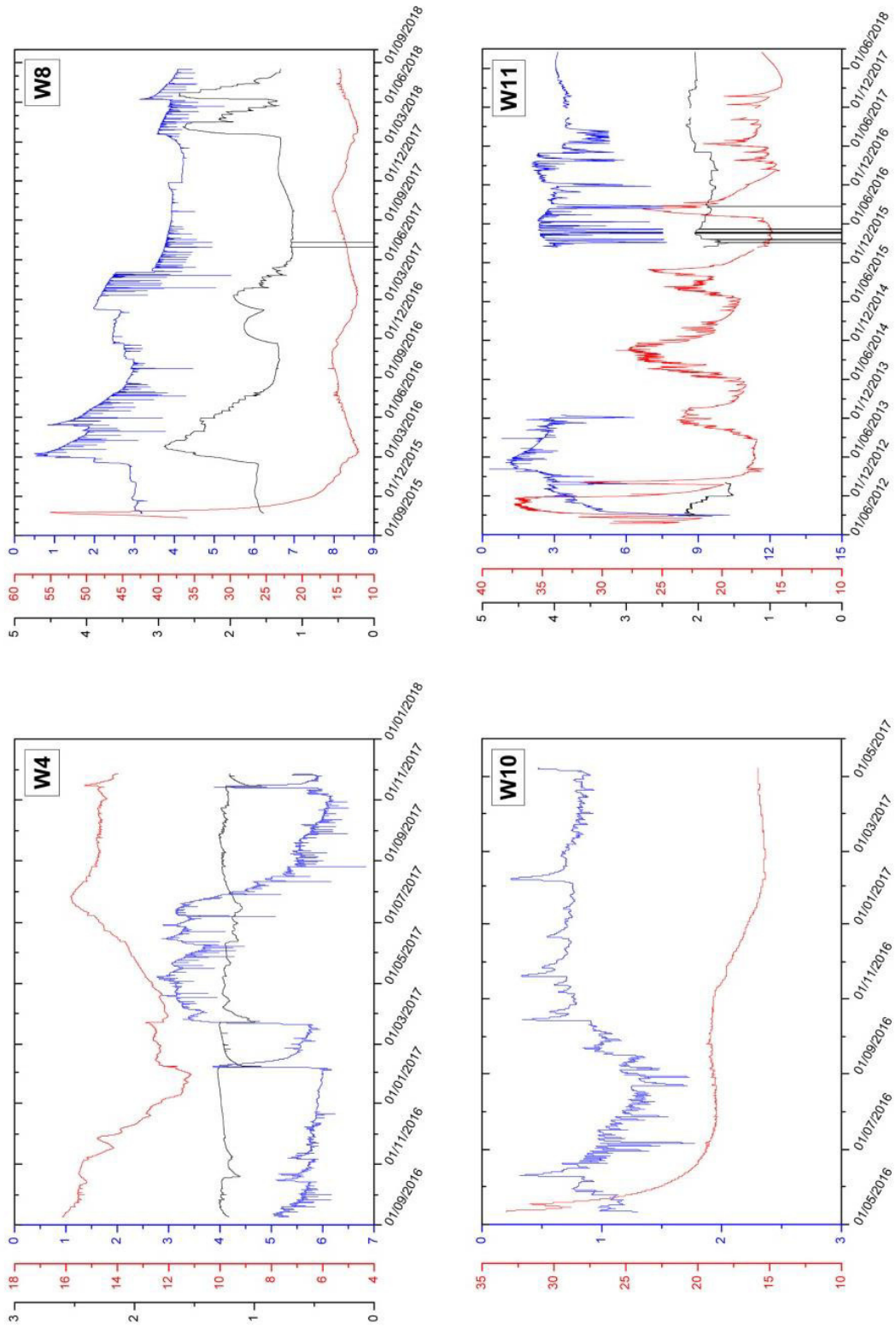
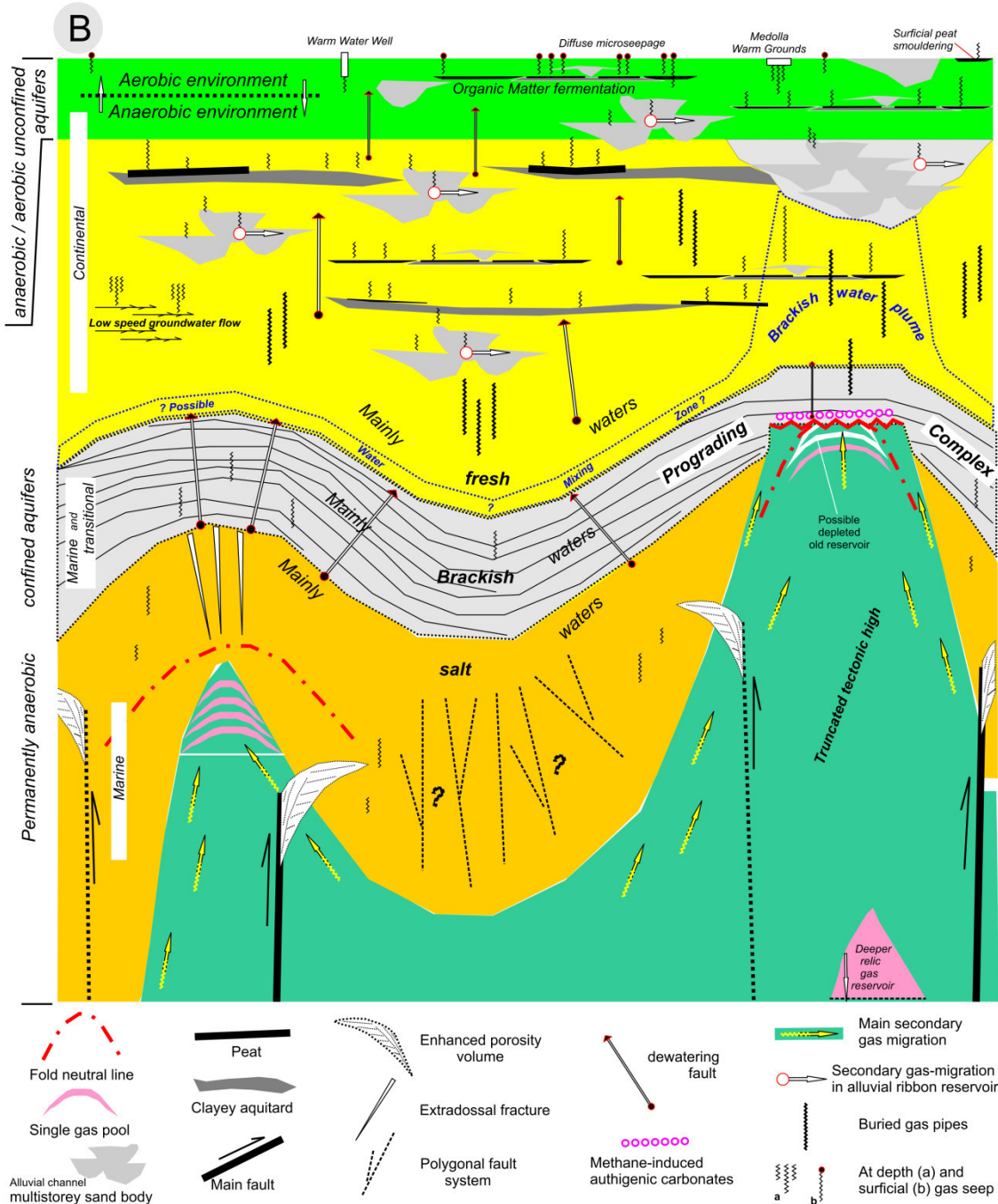
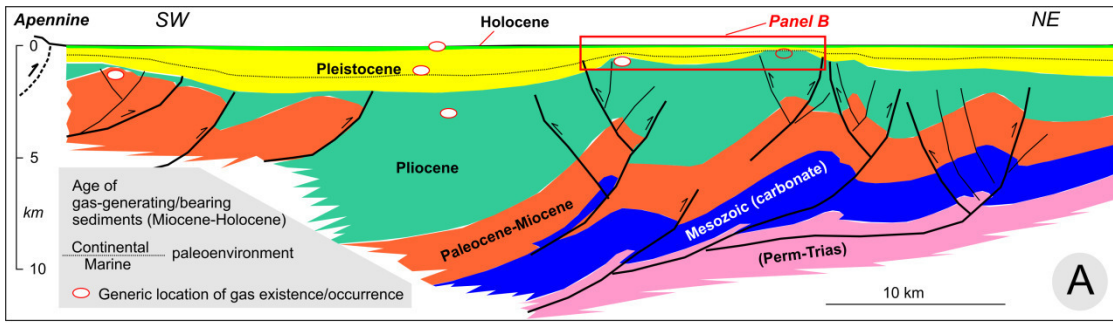
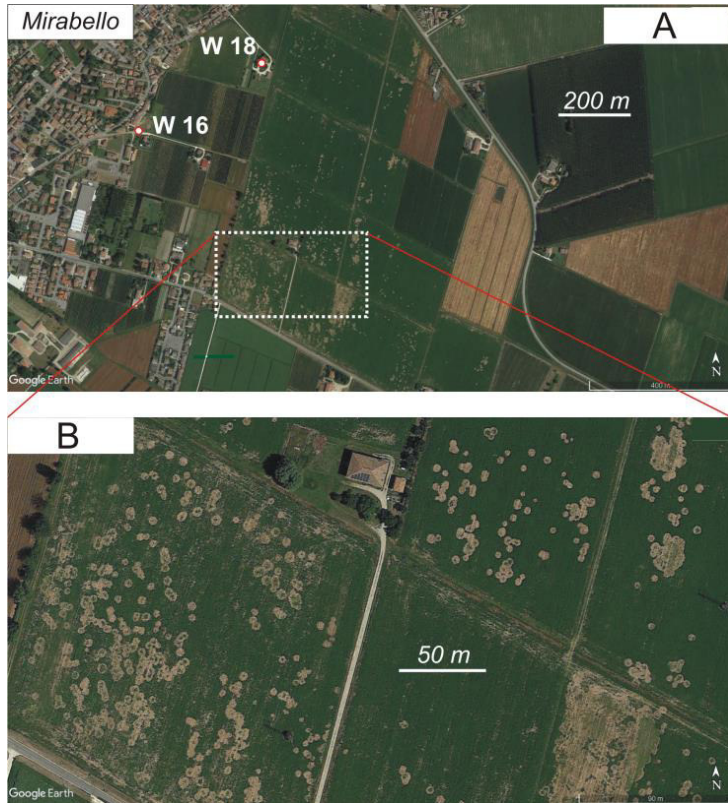


Figure 6.



**Figure 7.**



**Figure 8.**

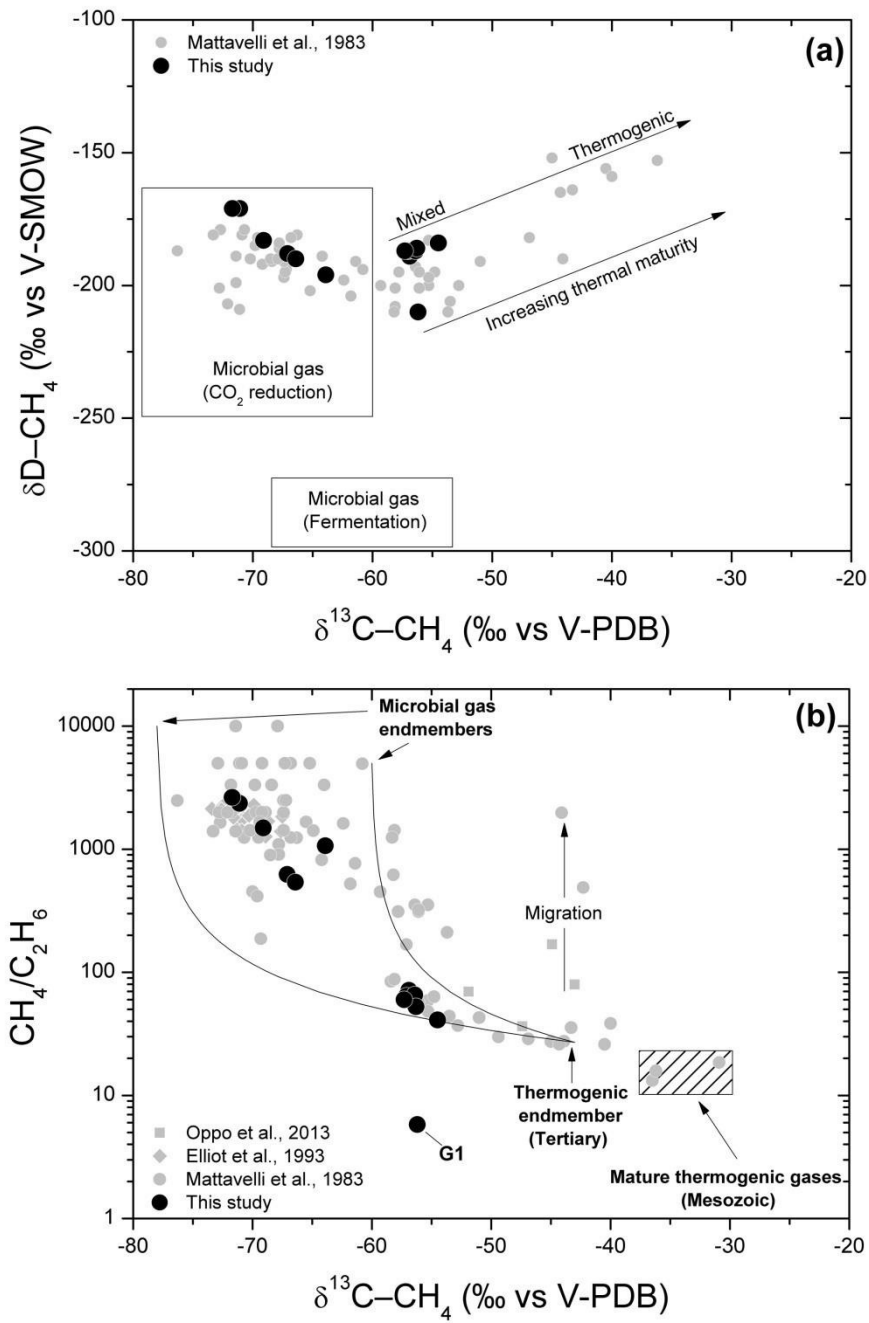


**Figure 9.**

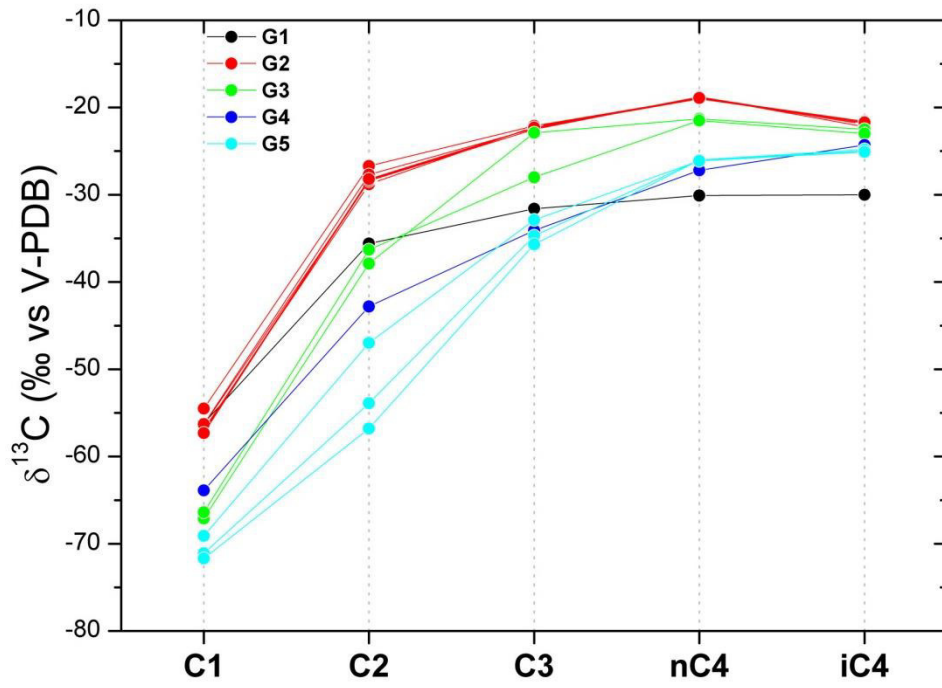


Figure 10.

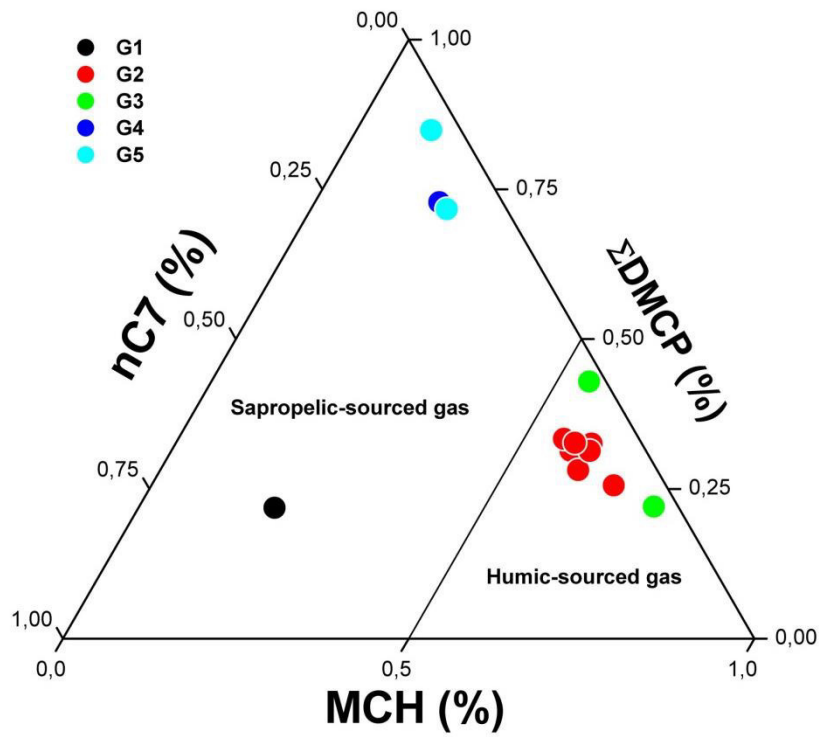


Figure 11.

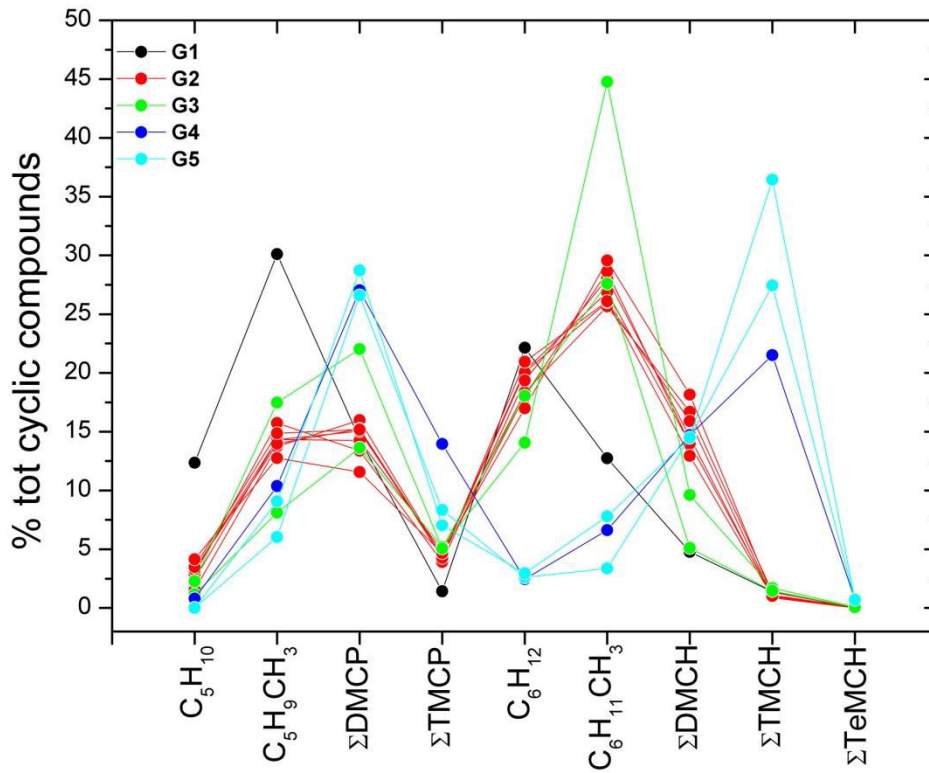


Figure 12.

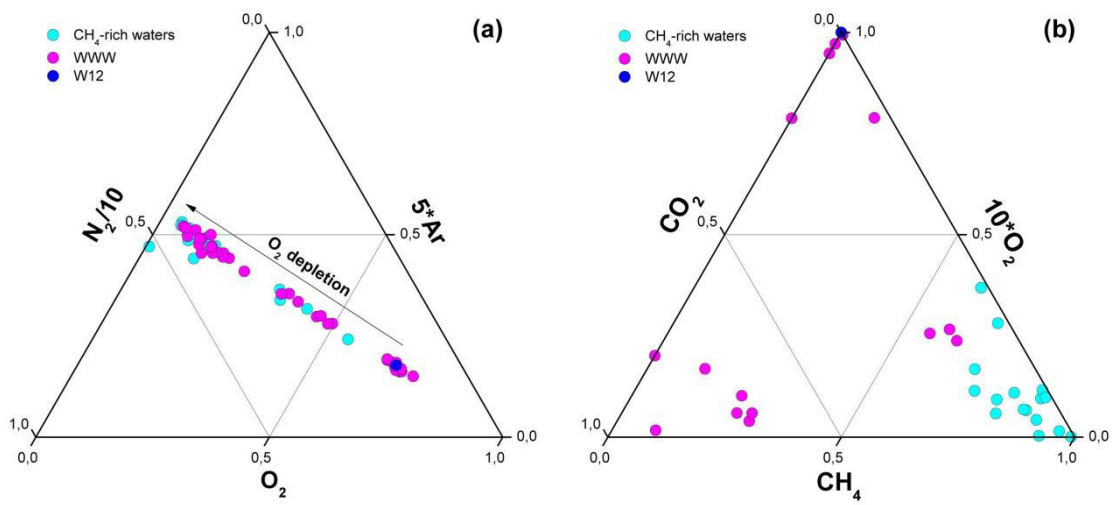


Figure 13.

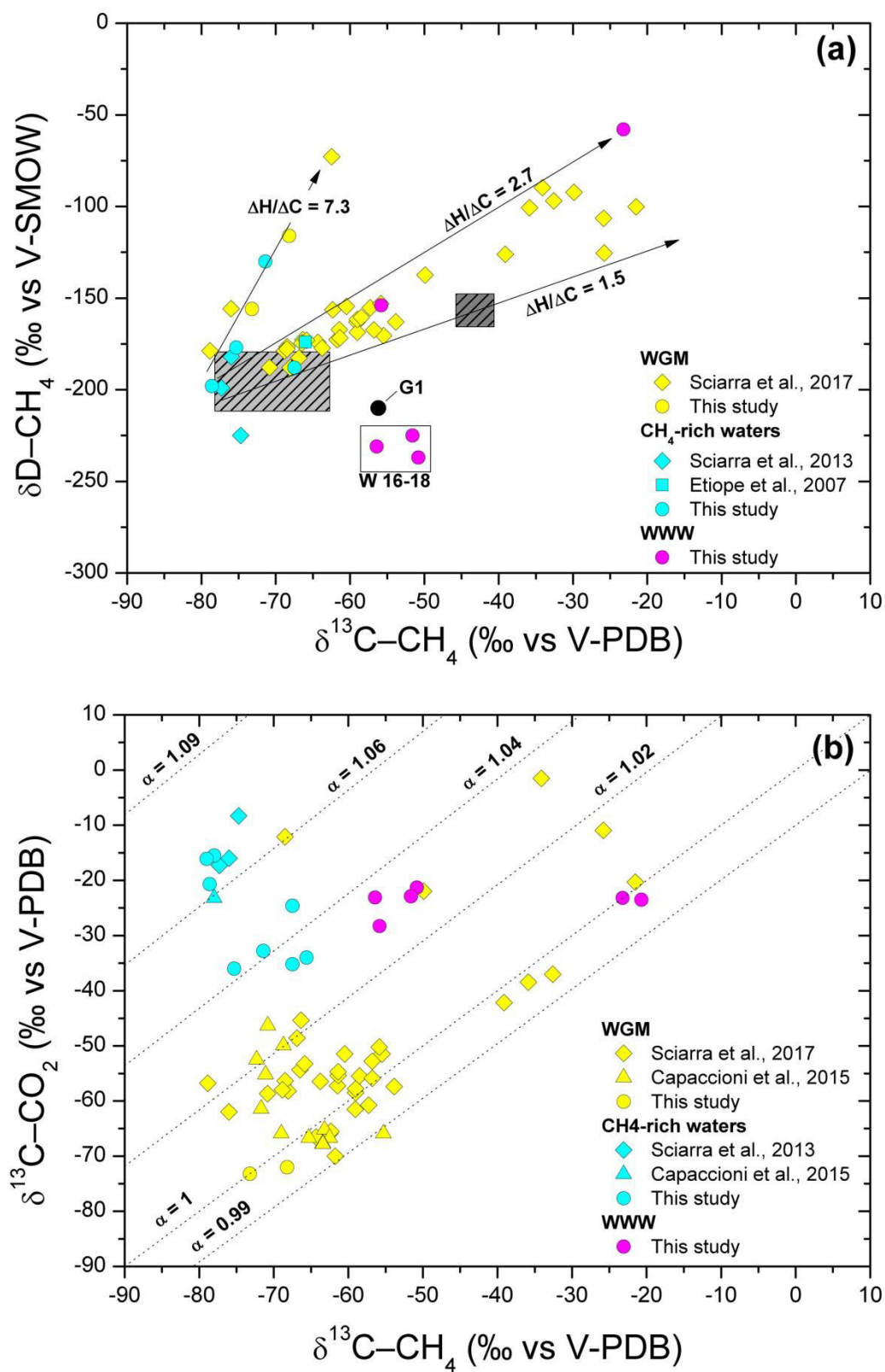


Figure 14.

## 8 Conclusions

Once formed through geological or biological processes in the subsurface, C-bearing gas compounds such as CO<sub>2</sub> and CH<sub>4</sub> may be transported within the Earth's crust as a free gas phases or dissolved in water, forming secondary carbon reservoirs, fostering shallow biosphere and ultimately being released into the atmosphere. Upon leaving the formation zone, C species may experience post-genetic processes during their geologic pathways throughout the crust, such as: dissolution of CO<sub>2</sub> into shallow aquifers and subsequent carbon segregation in carbonate minerals (e.g. Inguaggiato et al., 2005; Chiodini et al., 2015), microbial oxidation of methane in oxic and anoxic environments by methanotrophic activity (e.g. Templeton et al., 2006; Sivan et al., 2007) and biodegradation of C<sub>2+</sub> volatile organic compounds (e.g. Alexander, 1994). Accordingly, the chemical speciation of carbon in natural gas samples is the result of source and supergene processes and information about the primary source (genetic mechanism and physico-chemical conditions) can be totally or partially preserved or completely altered by secondary phenomena. The comprehension of both (i) the primary processes on C-bearing gas compounds occurring in deep reservoirs at crustal conditions and (ii) the secondary processes occurring during the uprising of fluids toward the surface, are crucial for a reliable estimation of the global carbon budget.

The latter processes have a limited effect on the pristine fluid composition when the uprising of the deep-originated C species is relatively fast. Hence, gases from high-flux natural emissions may be considered the best proxy of the deep reservoirs. However, CO<sub>2</sub>, CH<sub>4</sub> and light hydrocarbons are emitted not only through punctual degassing vents, but also diffusively through the Earth surface. Soil diffuse degassing significantly contributes to the atmospheric emissions of carbon (e.g. Cardellini et al., 2003; Chiodini et al., 2004; Granieri et al., 2010; Viveiros et al., 2010; Tassi et al., 2013). The chemical features of C species in interstitial soil gases from diffuse degassing areas are likely controlled by secondary processes as fluids are uprising towards the surface. Gas fluxes from soil, depending on the pressure gradient, and on the structure, porosity and permeability of the media encountered during the ascent towards the surface (e.g. Cardellini et al., 2003; Chiodini et al., 2010), is orders of magnitude lower than those characterizing punctual discharges (e.g. Aiuppa et al., 2013). Thus, it is reasonable to suppose that the composition of the gases released as diffuse emissions significantly depends on chemical and physical processes (e.g. oxidation reactions, water vapor condensation, interactions with shallow aquifers), favored by the strong changes in physico-

chemical conditions, which are particularly effective when fluids slowly approach the surface, i.e. within the soil (Tassi et al., 2013). Similarly, secondary processes driven by microorganisms (Bacteria and Archaea), inhabiting soils and aquifers at shallow depths, may affect the C-bearing compounds of fluids (e.g. Huber et al., 2000; Norris et al., 2002; D'Alessandro et al., 2011; Gagliano et al., 2014). The establishment of pathways of fluid migration in natural environments is particularly effective in volcanic and tectonic areas where structural configuration allows fluid channeling along faults and fracture enhancing the transport speed of carbon from deep to shallow reservoirs.

Investigating the geochemistry of C-bearing gas compounds in natural fluids can shed light on their origin and evolution and on the history of the transporting media but many aspects are still pending a solution. Hence, the overriding purpose of this thesis was to increase the scientific knowledge on the composition and behavior of C-bearing gas compounds in natural crustal fluids. The first goal of this PhD research project was to investigate the primary source(s) of CH<sub>4</sub> and light hydrocarbons in volcanic-hydrothermal gases under crustal conditions, whilst the second goal was to study the secondary processes affecting the composition of CO<sub>2</sub>, CH<sub>4</sub> and light hydrocarbons in natural fluids during their uprising from the deep reservoirs to the surface in different geologic setting, ranging from active volcanoes to sedimentary basins.

We demonstrated that hydrocarbons in hydrothermal fluids derive from biotic sources, i.e., predominantly from the thermal decomposition of organic matter. Meteoric waters and seawater circulating through the crust shuttle organic matter from Earth's surface into the reservoir rocks. There, high temperature pyrolysis of organic matter and open system degassing generates n-alkanes with isotopic compositions previously classified as being indicative for abiogenesis. These results led us to question the dogma of crustal production of abiotic hydrocarbons and highlighted the potential of n-alkanes to become sensitive indicators of life on habitable (exo)planets. Investigation of geochemistry of hydrocarbons in high-temperature magmatic-hydrothermal gases from Vulcano Island (southern Italy), an active stratovolcano, suggested that within hydrothermal systems in contact with hot uprising volcanic gases, physico-chemical conditions favorable for abiotic hydrocarbon formation may be achieved. The second goal was to study the secondary processes affecting the composition of CO<sub>2</sub>, CH<sub>4</sub> and light hydrocarbons in natural fluids during their uprising from the deep reservoirs to the surface in different geologic setting, ranging from active volcanoes to sedimentary basins. Chemical and isotopic composition of hydrocarbons from hot magmatic-hydrothermal vents of Vulcano Island, highlighted that these organic compounds may

undergo heteroatomic reactions and being irreversibly transformed. At hydrothermal conditions, we showed that mineral-assisted organic reactions strongly affect volatile organic compounds, drastically changing alkanes-alkenes-aromatics relative abundances and isotopic composition of C<sub>2</sub>-C<sub>4</sub> hydrocarbons. In peripheral areas of volcanic systems, characterized by diffuse degassing of CO<sub>2</sub>-rich gases, composition of CO<sub>2</sub> and CH<sub>4</sub> in soils and shallow aquifers are controlled by supergene mechanisms, such as calcite precipitation and biological processes. In particular, microbially-driven processes likely play a major role in modifying the composition of methane prior to its emission from soils in volcanic and hydrothermal systems. Finally, in tectonically active sedimentary basins, microbial processes at shallow depth strongly affect the composition of uprising CH<sub>4</sub> and CO<sub>2</sub>, primarily produced at depth by thermal or microbial degradation of organic matter, and regulate their ultimate release into the atmosphere.

# References

- Abrajano TA, Sturchio NC, Kennedy BM, Lyon GL, Muehlenbachs K, Bohlke JK (1990) Geochemistry of reduced gas related to serpentinization of the Zambales ophiolite, Philippines. *Appl Geochem* 5:625-630
- Agusto M., Tassi F., Caselli A.T., Vaselli O., Rouwet D., Capaccioni B., Caliro S., Chiodini G., Darrah T. (2013) Gas geochemistry of the magmatic-hydrothermal fluid reservoir in the Copahue-Caviahue Volcanic Complex (Argentina). *Journal of Volcanology and Geothermal Research*, 257, 44-56, doi: 10.1016/j.jvolgeores. 2013.03.003.
- Aiuppa A., Tamburello G., Di Napoli R., Cardellini C., Chiodini G., Giudice G., Grassa F., Pedone M., (2013) First observations of the fumarolic gas output from a restless caldera: Implications for the current period of unrest (2005-2013) at Campi Flegrei. *Geochem. Geophys. Geosyst.*, 14(10), 4153-4169, doi: 10.1002/ggge.20261.
- Akiya N., Savage P.E. (2001) Kinetics and mechanism of cyclohexanol dehydration in high-temperature water. *Ind. Eng. Chem. Res.*, 40, 1822-1831, doi: 10.1021/ie000964z.
- Alard O, Griffin WL, Lorand JP, Jackson SE, O'Reilly SY (2000) Non-chondritic distribution of the highly siderophile elements in mantle sulphides. *Nature* 407(6806):891-894
- Alexander M. (1994) Biodegradation and bioremediation. Academic Press Inc., San Diego, USA, pp. 302.
- Allison E., Boswell R. (2007) Methane hydrate, future energy within our grasp, an overview. DOE Overview Document <http://www.fossil.energy.gov/programs/oilgas/hydrates>
- Bahcall J. N., Pinsonneault M. H., Basu S. (2001) Solar models: Current epoch and time dependences, neutrinos, and helioseismological properties. *Astrophys J* 555:990, doi: 10.1086/321493
- Berndt ME, Allen DE, Seyfried WE (1996) Reduction of CO<sub>2</sub> during serpentinization of olivine at 300 °C and 500 bar. *Geology* 24:351-354
- Berner R. A. (1991) A model for atmospheric CO<sub>2</sub> over Phanerozoic time. *Am J Sci* 291:339-376, doi: 10.2475/ajs.291.4.339
- Berner R. A. (1999) A new look at the long-term carbon cycle. *GSA Today* 9(11):1-6
- Berner R. A., Lasaga A. C. (1989) Modeling the geochemical carbon cycle. *Sci Am* 260:74-81
- Berner RA (1994) 3GEOCARB II: A revised model for atmospheric CO<sub>2</sub> over Phanerozoic time. *Am J Sci* 294:56-91

- Berner RA (2004) *The Phanerozoic Carbon Cycle*. Oxford University Press, Oxford, UK
- Berner RA, Kothavala Z (2001) GEOCARB III: a revised model of atmospheric CO<sub>2</sub> over Phanerozoic time. *Am J Sci* 301:182-204
- Bischoff JL, Rosenbauer RJ (1985) An empirical equation of state for hydrothermal seawater (3.2 percent NaCl). *Am J Sci* 285:725-763
- Boswell R. (2009) Is gas hydrate energy within reach? *Science* 325:957-958
- Bradley A.S. and Summons R.E. (2010) Multiple origins of methane at the Lost City hydrothermal field. *Earth Planet Sci Lett* 297:34–41.
- Bradley AS, Summons RE (2010) Multiple origins of methane at the Lost City Hydrothermal Field. *Earth Planet Sci Lett* 297:34-41
- Brown T.E., LeMay H.E., Bursten B.E., Murphy C., Woodward P. (2012) *Chemistry: The Central Science*, 12th Edition. Prentice Hall, New Jersey, pp. 1200
- Brühl C., Lelieveld J., Crutzen P. J., Tost H. (2012) The role of carbonyl sulphide as a source of stratospheric sulphate aerosol and its impact on climate. *Atmos Chem Phys* 12:1239-1253, doi: 10.5194/acp-12-1239-2012
- Buffett B. A. (2000) Clathrate hydrates. *Ann Rev Earth Planet Sci* 28:477-507
- Burruss R.C. and Laughrey C.D. (2010) Carbon and hydrogen isotopic reversals in deep basin gas: evidence for limits to the stability of hydrocarbons. *Org Geochem* 41:1285–1296.
- Burton M., Allard P., Murè F., La Spina A. (2007) Depth of slug-driven strombolian explosive activity. *Science* 317:227-230
- Burton MR, Sawyer GM, Granieri D (2013) Deep carbon emissions from volcanoes. *Rev Mineral Geochem* 75:323-354
- Cadle R. D. (1980) A comparison of volcanic with other fluxes of atmospheric trace gas constituents. *Rev Geophys Space Phys* 18:746-752
- Campbell IH, O'Neill HSC (2012) Evidence against a chondritic Earth. *Nature* 483(7391):553-558
- Capaccioni B. Martini M., Mangani F. (1995) Light hydrocarbons in hydrothermal and magmatic fumaroles: hints of catalytic and thermal reactions. *B. Volcanol.*, 56, 593-600.
- Capaccioni B., Mangani F. (2001) Monitoring of active but quiescent volcanoes using light hydrocarbon distribution in volcanic gases: the results of 4 years of discontinuous monitoring in the Campi Flegrei (Italy). *Earth Planet. Sci. Lett.*, 188, 543-555.
- Capaccioni B., Martini M., Mangani F., Giannini L., Nappi G., Prati F. (1993) Light hydrocarbons in gas-emissions from volcanic areas and geothermal fluids. *Geochem. J.*, 27, 7-17.

- Capaccioni B., Taran Y., Tassi F., Vaselli O., Mangani G., Macias J.L. (2004) Source conditions and degradation processes of light hydrocarbons in volcanic gases: an example from El Chichón volcano (Chiapas State, Mexico). *Chem. Geol.*, 206, 81-96, doi: 10.1016/j.chemgeo.2004.01.011.
- Cardellini C., Chiodini G., Frondini F., Granieri D., Lewicki J., Peruzzi L., (2003) Accumulation chamber measurements of methane fluxes: application to volcanic geothermal areas and landfills. *Appl. Geochem.*, 18, 45-54.
- Caro G (2011) Early silicate earth differentiation. *Annu Rev Earth Planet Sci Lett* 39(1):31-58
- Chapelle F. H., O'Neill K., Bradley P. M., Methe B. A., Ciuffo S. A., Knobel L. L., Lovley D. R. (2002) A hydrogen-based subsurface microbial community dominated by methanogens. *Nature* 415:312-315
- Charlou JL, Donval JP, Fouquet Y, Jean-Baptiste P, Holm (2002) Geochemistry of high H<sub>2</sub> and CH<sub>4</sub> vent fluids issuing from ultramafic rocks at the Rainbow hydrothermal field (36° 14'N, MAR). *Chem Geol* 191:345-359
- Charlou JL, Donval JP, Konn C, Ondréas H, Fouquet Y (2010) High production and fluxes of H<sub>2</sub> and CH<sub>4</sub> and evidence of abiotic hydrocarbons synthesis by serpentinization in ultramafic-hosted hydrothermal systems on the Mid-Atlantic Ridge. *In: Diversity of Hydrothermal Systems on Slow Spreading Ocean Ridges*. Rona PA, Devey C, Dymont J, Murton BJ (eds). Am Geophys Union, Washington, DC, p 265-296
- Charlou JL, Fouquet Y, Donval JP, Auzende JM, Jean-Baptiste P, Stievenard M (1996) Mineral and gas chemistry of hydrothermal fluids on an ultrafast spreading ridge: East Pacific Rise, 17° to 19°S (Naudur cruise, 1993) phase separation processes controlled by volcanic and tectonic activity. *J Geophys Res* 101:15,899-15,919
- Chen JY, Jin LJ, Dong JP, Zheng HF (2008) *In situ* Raman spectroscopy study on dissociation of methane at high temperatures and at high pressures. *Chin Phys Lett* 25:780-782
- Chiodini G., Caliro S., Aiuppa A., Avino R., Granieri D., Moretti M., Parello F. (2011) First <sup>13</sup>C/<sup>12</sup>C isotopic characterisation of volcanic plume CO<sub>2</sub>. *Bull Volcanol* 73:531-542, doi: 10.1007/s00445-010-0423-2
- Chiodini G., Cardellini C., Amato A., Boschi E., Caliro S., Frondini F., Ventura G., (2004). Carbon dioxide Earth degassing and seismogenesis in central and southern Italy. *Geophys. Res. Lett.*, 31, L07615, doi: 10.1029/2004GL019480.
- Chiodini G., Cioni R., Guidi M., Raco B., Marini L., (2010) Soil CO<sub>2</sub> flux measurements in volcanic and geothermal areas. *Appl. Geochem.*, 13(5), 543-552.

- Chiodini G., Granieri D., Avino R., Caliro S., Costa A., Werner C. (2005) Carbon dioxide diffuse degassing and estimation of heat release from volcanic and hydrothermal systems, *J Geophys Res Solid Earth* 110:B08204, doi: 10.1029/2004JB003542
- Chiodini G., Pappalardo L., Aiuppa A., Caliro S., (2015) The geological CO<sub>2</sub> degassing history of a long-lived caldera. *Geology*, 43(9), 767-770, doi: 10.1130/G36905.1.
- Cody GD, Boctor NZ, Brandes JA, Filley TR, Hazen RM, Yoder HS (2004) Assaying the catalytic potential of transition metal sulfides for abiotic carbon fixation. *Geochim Cosmochim Acta* 68:2185-2196
- Colwell FS, D'Hondt S (2013) Nature and extent of the deep biosphere. *Rev Mineral Geochem* 75:547-574
- Crittendon R.C., Parsons E.J. (1994) Transformations of cyclohexane derivatives in supercritical water. *Organometallics*, 13, 2587-2591.
- Crossey L. J., Karlstrom K. E., Springer A. E., Newell D., Hilton D. R., Fischer T. (2009) Degassing of mantle-derived CO<sub>2</sub> and He from springs in the southern Colorado Plateau region-Neotectonic connections and implications for groundwater systems. *Geol Soc Am Bull* 121(7-8):1034-1053, doi: 10.1130/B26394.1
- Crutzen P. J. (1976) The possible importance of COS for the sulfate layer of the stratosphere. *Geophys Res Lett* 3:73-76
- D'Hondt S, Jørgensen BB, Miller DJ, Batzke A, Blake R, Cragg BA, Cypionka H, Dickens GR, Ferdelman T, Hinrichs K-U, Holm NG, Mitterer R, Spivack A, Wang G, Bekins B, Engelen B, Ford K, Gettemy G, Rutherford SD, Sass H, Skilbeck CG, Aiello IW, Guèrin G, House CH, Inagaki F, Meister P, Naehr T, Niitsuma S, Parkes RJ, Schippers A, Smith DC, Teske A, Wiegel J, Padilla CN, Acosta JLS (2004) Distributions of microbial activities in deep seafloor sediments. *Science* 306:2216-2221
- Dale Ortego J., Kowalska M., Cocke D.L. (1991) Interactions of montmorillonite with organic compounds - adsorptive and catalytic properties. *Chemosphere*, 22(8), 769-798.
- D'Alessandro W., Brusca L., Kyriakopoulos K., Martelli M., Michas G., Papadakis G., Salerno F., (2011) Diuse hydrothermal methane output and evidence of methanotrophic activity within the soils at Sousaki (Greece). *Geofluids*, 11, 97-107, doi: 10.1111/j.1468-8123.2010.00322.x.
- Dasgupta R, Chi H, Shimizu N, Buono A, Walker D (2013) Carbon solution and partitioning between metallic and silicate melts in a shallow magma ocean: implications for the origin and distribution of terrestrial carbon. *Geochim Cosmochim Acta* 102:191-212, doi: 10.1016/j.gca.2012.10.011

- Dasgupta R., Hirschmann M.M. (2006) Melting in the Earth's deep upper mantle caused by carbon dioxide. *Nature* 440:659-662
- Dasgupta R., Hirschmann M.M. (2010) The deep carbon cycle and melting in Earth's interior. *Earth Planet Sci Lett* 298:1-13, doi: 10.1016/j.epsl.2010.06.039
- Demaison GJ, Moore GT (1980) Anoxic environments and oil source bed genesis. *Bull Am Assoc Petrol Geol* 64:1179-1209
- Des Marais D.J., Donchin J.H., Nehring N.L., Truesdell A.H. (1981) Molecular carbon isotopic evidence for the origin of geothermal hydrocarbons. *Nature* 292:826–828.
- Dictor RA, Bell AT (1986) Fischer-Tropsch synthesis over reduced and unreduced iron oxide catalyst. *J Catal* 97:121-136
- Ehrenfreund P, Charnley SB (2000) Organic molecules in the interstellar medium, comets, and meteorites: A voyage from dark clouds to the early earth. *Ann Rev Astron Astrophys* 38:427-483
- Etiopie G, Ifandi E, Nazzari M, Procesi M, Tsikouras B, Ventura G, Steele A, Tardini R, Szatmari P (2018) Widespread abiotic methane in chromitites. *SCIENTIFIC REPORTS* 8:8728, DOI:10.1038/s41598-018-27082-0
- Etiopie G, Schoell M, Hosgormez H (2011) Abiotic methane flux from Chimaera seep and Tekirova ophiolites (Turkey): Understanding gas exhalation from low temperature serpentinization and implications for Mars. *Earth and Plan. Sci. Lett.* 310, 96-104, doi:10.1016/j.epsl.2011.08.001
- Etiopie G., Milkov A. V., Derbyshire E. (2008) Did geologic emissions of methane play any role in Quaternary climate change? *Global Planet Change* 61(1-2):79-88, doi:10.1016/j.gloplacha.2007.08.008
- Faiz M. and Hendry P. (2006) Significance of microbial activity in Australian coal bed methane reservoirs—A review. *Bull. Can. Pet. Geol.* 54(3), 261-272. [http://archives.datapages.com/data/cspg/data/054/054003/261\\_cspg540261.htm](http://archives.datapages.com/data/cspg/data/054/054003/261_cspg540261.htm)
- Ferris J.P. (2005) Mineral catalysis and prebiotic synthesis: montmorillonite-catalyzed formation of RNA. *Elements*, 1, 145-149.
- Feulner G. (2012) The faint young Sun problem. *Rev Geophys* 50:RG2006, doi: 10.1029/2011RG000375
- Fiebig J, Woodland AB, D'Alessandro W, Püttmann W (2009) Excess methane in continental hydrothermal emissions is abiogenic. *Geology* 37:495-498, doi:10.1130/G25598A.1
- Fiebig J, Woodland AB, Spangenberg J, Oschmann W (2007) Natural evidence for rapid abiogenic hydrothermal generation of CH<sub>4</sub>. *Geochim Cosmochim Acta* 71:3028-3039

- Fischer F, Tropsch H (1926) Über die direkte synthese von erdöl-kohlenwasserstoffen bei gewöhnlichem druck. *Berichte der Deutschen Chemischen Gesellschaft* 59:830-831
- Foustoukos DI, Seyfried WE (2004) Hydrocarbons in hydrothermal vent fluids: The role of chromium-bearing catalysts. *Science* 304:1002-1005
- French BM (1971) Stability relations of siderite (FeCO<sub>3</sub>) in the system Fe-C-O. *Am J Sci* 271:37-78
- Fritsche W., Hofrichter M. (2008) Aerobic degradation by microorganisms. In: Rehm H.J., Reed G. (eds.), *Biotechnology: Environmental Processes II*, Volume 11b, Second Edition, 144-167
- Frost BR (1985) On the stability of sulfides, oxides, and native metals in serpentinite. *J Petrol* 26:31-63
- Fu Q, Foustoukos DI, Seyfried WE (2008) Mineral catalyzed organic synthesis in hydrothermal systems: An experimental study using time-of-flight secondary ion mass spectrometry. *Geophys Res Lett* doi:10.1029/2008GL033389
- Fu Q, Sherwood Lollar B, Horita J, Lacrampe-Couloume G, Seyfried WE (2007) Abiotic formation of hydrocarbons under hydrothermal conditions: Constraints from chemical and isotope data. *Geochim Cosmochim Acta* 71:1982-1998
- Fu Q., Socki R.A., Niles P.B. (2011) Carbon isotope systematics in mineral-catalyzed hydrothermal organic synthesis processes at high temperatures and pressures [abstract 1057]. In 42nd Lunar and Planetary Science Conference Abstracts, Lunar and Planetary Institute, Houston.
- Gagliano A.L., D'Alessandro W., Tagliavia M., Parello F., Quatrini P., (2014) Methanotrophic activity and diversity of methanotrophs in volcanic geothermal soils at Pantelleria (Italy). *Biogeosciences*, 11, 5865-5875, doi: 10.5194/bg-11-5865-2014.
- Garcia, J.L. (1990). Taxonomy and ecology of methanogens. *FEMS Microbiol. Rev.* 87, 297–308.
- Gennadiev AN, Pikovskii YI, Tsibart AS, Smirnova MA, (2015). Hydrocarbons in soils: origin, composition, and behavior (review). *Eurasian Soil Sci+*, 48(10), 1076-1089, doi: 10.1134/S1064229315100026.
- Glasby GP (2006) Abiogenic origin of hydrocarbons: An historical overview. *Resour Geol* 56:83-96
- Gold T (1977) Rethinking the origins of oil and gas. *The Wall Street Journal* 8 June 1977
- Gold T (1992) The deep, hot biosphere. *Proc Natl Acad Sci USA* 89:6045-6049
- Gold T (1999) *The Deep Hot Biosphere*. Copernicus, New York

- Gold T, Soter S (1980) The deep earth gas hypothesis. *Sci Am* 242:155-161
- Gold T, Soter S (1982) Abiogenic methane and the origin of petroleum. *Energy Exploration Exploitation* 1:89-104
- Grace J., Collett T., Colwell F., Englezos P., Jones E., Mansell R., Meekison J. P., Ommer R., Pooladi-Darvish M., Riedel M., Ripmeester J. A., Shipp C., Willoughby E. (2008) Energy from gas hydrates—Assessing the opportunities and challenges for Canada. Report of the Expert Panel on Gas Hydrates, Council of Canadian Academies, September 2008
- Granieri D., Avino R., Chiodini G., (2010) Carbon dioxide diffuse emission from the soil: ten years of observations at Vesuvio and Campi Flegrei (Pozzuoli), and linkages with volcanic activity. *Bull. Volcanol.*, 72, 103-118, doi: 10.1007/s00445-009-0304-8.
- Guéret C., Daroux M., Billaud F. (1997) Methane pyrolysis: thermodynamics. *Chem. Eng. Sci.*, 52(2), 815-827.
- Guggenheim S., Koster van Groos A. F. K. (2003) New gas-hydrate phase: Synthesis and stability of clay–methane hydrate intercalate. *Geology* 31:653-656
- Gunter B.D.,(1978) C1-C4 hydrocarbons in hydrothermal gases. *Geochim. Cosmochim. Ac.*, 42, 137-139.
- Hayes JF, Waldbauer JR (2006) The carbon cycle and associated redox processes through time. *Phil Trans Royal Soc London B*361:931-950
- Hazen RM (2005) *Genesis: The Scientific Quest for Life's Origin*. Joseph Henry Press, Washington, DC
- Hazen RM, Downs RT, Jones AP, Kah L (2013) Carbon mineralogy and crystal chemistry. *Rev Mineral Geochem* 75:7-46
- Hazen RM, Hemley RJ, Mangum AJ (2012) Carbon in Earth's interior: storage, cycling, and life. *Eos Trans Am Geophys Union* 93:17-28
- He H., Zhong Y., Liang X., Tan W., Zhu J., Wang C.Y. (2015) Natural magnetite: an efficient catalyst for the degradation of organic contaminant. *Sci. Rep.*, 5:10139, doi: 10.1038/srep10139.
- Heinen W, Lauwers AM (1996) Organic sulfur compounds resulting from the interaction of iron sulfide, hydrogen sulfide and carbon dioxide in an anaerobic aqueous environment. *Orig Life Evol Biosphere* 26:161-150
- Higgs M. D. (1986) Laboratory studies into the generation of natural gas from coals. In *Habitat of Paleozoic Gas in N.W. Europe* (eds. J. Brooks). *Geol. Soc. Lond. Spec. Publ.* 23. pp. 113-120. <http://dx.doi.org/10.1144/GSL.SP.1986.023.01.08>

- Hinrichs K-U., Hayes J. M., Bach W., Spivack A. J., Hmelo L. R., Holm N. G., Johnson C. G., Sylva S. P. (2006) Biological formation of ethane and propane in the deep marine subsurface. *Proc Natl Acad Sci* 103:14684-14689
- Holland HD (1984) *The Chemical Evolution of the Oceans and Atmosphere*. Princeton University Press, Princeton, New Jersey
- Holloway JR (1984) Graphite-CH<sub>4</sub>-H<sub>2</sub>O-CO<sub>2</sub> equilibria at low-grade metamorphic conditions. *Geology* 12:455-458
- Holmen A., Olsvik O., Rokstad O.A. (1995) Pyrolysis of natural gas: chemistry and process concepts. *Fuel Process. Technol.*, 42, 249-267.
- Holser WT, Schidlowski M, MacKenzie FT, Maynard JB (1988) Geochemical cycles of carbon, and sulfur. *In: Chemical cycles in the evolution of the Earth*. Gregor MC, Garrels RM, Mackenzie FT, Maynard JB (eds) Wiley, New York, p 5-59.
- Horita J, Berndt ME (1999) Abiogenic methane formation and isotopic fractionation under hydrothermal conditions. *Science* 285:1055-1057
- Hornafius J. S., Quigley D., Luyendyk B. P. (1999) The world's most spectacular marine hydrocarbon seeps (Coal Oil Point, Santa Barbara Channel, California): quantification of emissions. *J Geophys Res* 104:20703-20711
- Hoyle F (1955) *Frontiers of Astronomy*. Heineman, London
- Hu G, Ouyang Z, Wang X, Wen Q (1998) Carbon isotopic fractionation in the process of Fischer-Tropsch reaction in primitive solar nebula. *Sci China Ser D* 41:202-207
- Huber R., Sacher M., Vollmann A., Huber H., Rose D., (2000) Respiration of arsenate and selenate by hyperthermophilic Archaea. *System. Appl. Microbiol.*, 23, 305-314.
- Hyndman R. D., Davis E. E. (1992) A mechanism for the formation of methane hydrate and sea-floor bottomsimulating reflectors by vertical fluid expulsion. *J Geophys Res-Solid Earth* 97:7025-7041
- Inagaki F., Hinrichs K.-U., Kubo Y., Bowles M. W., Heuer V. B., Hong W.-L., Hoshino T., Ijiri A., Imachi H., Ito M., Kaneko M., Lever M. A., Lin Y.-S., Methé B. A., Morita S., Morono Y., Tanikawa W., Bihan M., Bowden S. A., Elvert M., Glombitza C., Gross D., Harrington G. J., Hori T., Li K., Limmer D., Liu C.-H., Murayama M., Ohkouchi N., Ono S., Park Y.-S., Phillips S. C., Prieto-Mollar X., Purkey M., Riedinger N., Sanada Y., Sauvage J., Snyder G., Susilawati R., Takano Y., Tasumi E., Terada T., Tomaru H., Trembath-Reichert E., Wang D. T. and Yamada Y. (2015) Exploring deep microbial life in coal-bearing sediment down to ~ 2.5 km below the ocean floor. *Science* 349(6246), 420-424. <http://dx.doi.org/10.1126/science.aaa6882>

- Inguaggiato S., Martin-Del-Pozzo A.L., Aguayo A., Capasso G., Favara R., (2005) Isotopic, chemical and dissolved gas constraints on spring water from Popocatepetl volcano (Mexico): evidence of gas-water interaction between magmatic component and shallow fluids. *Journal of Volcanology and Geothermal Research*, 141, 91-108, doi: 10.1016/j.jvolgeores.2004.09.006.
- Insam H, Seewald MSA. (2010). Volatile organic compounds (VOCs) in soils. *Biol. Fertil. Soils*, 46, 199-213, doi: 10.1007/s00374-010-0442-3.
- Jarvie D. M., Hill R. J., Ruble T. E. and Pollastro R. M. (2007) Unconventional shale-gas systems: The Mississippian Barnett Shale of north-central Texas as one model for thermogenic shale-gas assessment. *AAPG Bull.* **91(4)**, 475-499. <http://dx.doi.org/10.1306/12190606068>
- Javoy M, Kaminski E, Guyot F, Andraut D, Sanloup C, Moreira M, Labrosse S, Jambon A, Agrinier P, Davaille A, Jaupart C (2010) The chemical composition of the Earth: Enstatite chondrite models. *Earth Planet Sci Lett* 293(3-4):259-268
- Javoy M, Pineau F, Allegre CJ (1982) Carbon geodynamic cycle. *Nature* 300:171-173, doi: 10.1038/300171a0
- Jenden P.D. (1993) Abiogenic hydrocarbons and mantle helium in oil and gas fields. In *The Future of Energy Gases*, U.S. Geological Survey Professional Paper 1570, edited by D.G. Howell, U.S. Geological Survey, Washington, DC, pp 31–56.
- Jones LC, Rosenbauer RJ, Goldsmith JJ, Oze C (2010) Carbonate controls of H<sub>2</sub> and CH<sub>4</sub> production in serpentinization systems at elevated P-Ts. *Geophys Res Lett* 37, doi:10.1029/2010GL043769
- Jorgensen B. B., Boetius A. (2007) Feast and famine--microbial life in the deep-sea bed. *Nat Rev Micro* 5:770- 781
- Kah LC, Bartley JK (2011) Protracted oxygenation of the Proterozoic biosphere. *Int Geol Rev* 53:1424-1442
- Kaschke M., Russell M.J., Cole W.J. (1994) [FeS/FeS<sub>2</sub>], a redox system for the origin of life. *Origins Life Evol. Biosphere*, 24, 43-56.
- Katritzky A.R., Allin S.M., Siskin M. (1996) Aquathermolysis: Reactions of organic compounds with superheated water. *Acc. Chem. Res.*, 29(8), 399-406.
- Katritzky A.R., Balasubramanian M., Siskin M. (1990) Aqueous high-temperature chemistry of carbo- and heterocycles. 2. Monosubstituted benzenes: benzyl alcohol, benzaldehyde, and benzoic acid. *Energ. Fuel.*, 4, 449-505.
- Kelley DS (1996) Methane-rich fluids in the oceanic crust. *J Geophys Res* 101:2943-2962

- Kelley DS, Karston JA, Früh-Green GL, Yoerger DR, Shank TM, Butterfield DA, Hayes JM, Schrenk MO, Olson EJ, Proskurowski G, Jakuba M, Bradley A, Larson B, Ludwig K, Glickson D, Buckman K, Bradley AS, Brazelton WJ, Roe K, Elend MJ, Delacour A, Bernasconi SM, Lilley MD, Baross JA, Summons RE, Sylva SP (2005) A serpentinite-hosted ecosystem: The Lost City hydrothermal field. *Science* 307:1428-1434
- Kenney JF, Shnyukov YF, Krayishkin VA, Tchabanenko II, Klochko VP (2001) Dismissal of claims of a biological connection for natural petroleum. *Energia* 22:26-34
- Killops S., Killops V. (2005) Introduction to organic geochemistry, Second Edition. Blackwell Publ., Malden, MA, pp. 393.
- Klein F, Bach W (2009) Fe-Ni-Co-O-S phase relations in peridotite-seawater interactions. *J Petrol* 50:37-59, doi:10.1093/petrology/egn071
- Koh C. A., Sloan E. D., Sum A. K., Wu D. T. (2011) Fundamentals and applications of gas hydrates. *Ann Rev Chem Biomolec Eng* 2:237-257
- Koh C. A., Sum A. K., Sloan E. D. (2009) Gas hydrates: Unlocking the energy from icy cages. *J Appl Phys* 106:061101-061114
- Kolesnikov A, Kutcherov VG, Goncharov AF (2009) Methane-derived hydrocarbons produced under uppermantle conditions. *Nat Geosci* 2:566-570, doi:10.1038/NGE0591
- Konig, H. (1992) Microbiology of methanogens. In: Vially, R. (Ed)..., *Bacterial Gas*. Editons Technip, Paris, pp. 3–12.
- Konn C., Charlou J.L., Holm N.G., Mousis O. (2015) The production of methane, hydrogen and organic compounds in ultramafic-hosted hydrothermal vents of the Mid-Atlantic Ridge. *Astrobiology*, 15(5), 381-399, doi: 10.1089/ast.2014.1198.
- Kudryatsev NA (1951) Against the organic hypothesis of the origin of petroleum. *Neftianoye Khozyaistvo* 9:17-29
- Kuramoto K (1997) Accretion, core formation, H and C evolution of the Earth and Mars. *Phys Earth Planet Inter* 100:3-20
- Kutcherov VG, Kolesnikov AY, Dyuzhheva TI, Kulikova LF, Nikolaev NN, Sazanova OA, Braghkin VV (2010) Synthesis of complex hydrocarbon systems at temperatures and pressures corresponding to the Earth's upper mantle conditions. *Dokl Phys Chem* 433:132-135
- Kvenvolden K. A. (1995) A review of the geochemistry of methane in natural gas hydrate. *Org Geochem* 23:997-1008
- Kwok S (2009) Organic matter in space: from star dust to the Solar System. *Astrophys Space Sci* 319:5-21

- Lancet MS, Anders EA (1970) Carbon isotope fractionation in the Fischer-Tropsch synthesis and in meteorites. *Science* 170:980-982
- Lazar C, McCollom TM, Manning CE (2012) Abiogenic methanogenesis during experimental komatiite serpentinization: Implications for the evolution of the early Precambrian atmosphere. *Chem Geol* 326-327:102-112
- Leif R.N., Simoneit B.R.T. (1995) Ketones in hydrothermal petroleums and sediment extracts from Guaymas Basin, Gulf of California. *Org. Geochem.*, 23(10), 889-904.
- Liebscher A, Heinrich CA (eds) (2007) Fluid-Fluid Interactions. *Reviews in Mineralogy and Geochemistry* Vol. 65. Mineralogical Society of America, Chantilly VA
- Lien P.J., Yang Z.H., Chang Y.M., Tu Y.T., Kao C.M. (2016) Enhanced bioremediation of TCE-contaminated groundwater with coexistence of fuel oil: Effectiveness and mechanism study. *Chem. Eng. J.*, 289, 525-536, doi: 10.1016/j.cej.2016.01.011.
- Little C.D., Palumbo A.Y., Herbes S.E., Lidstrom M.E., Tyndall R.L., Gilmer P.J. (1988) Trichloroethylene biodegradation by a methane-oxidizing bacterium. *Appl. Environ. Microbiol.*, 54(4), 951-956.
- Lodders K (2003) Solar system abundances and condensation temperatures of the elements. *Astrophys J* 591:1220-1247
- Loison A, Dubant S, Adam P, Albrecht P (2010) Elucidation of an iterative process of carbon-carbon bond formation of prebiotic significance. *Astrobiology* 10:973-988
- Low-Temperature Reaction of Ultramafic Rocks with Water. *Astrobiology* 16 (6), DOI: 10.1089/ast.2015.1382
- Mango F., Jarvie D., Herriman E. (2009) Natural gas at thermodynamic equilibrium. Implications for the origin of natural gas. *Geochem. Trans.*, 10(6), doi: 10.1186/1467-4866-10-6.
- Martin W, Baross J, Kelley D, Russell MJ (2008) Hydrothermal vents and the origin of life. *Nat Rev Microbiol* 6:805-814
- Marty B, Alexander CMO'D, Raymond SN (2013) Primordial origins of Earth's carbon. *Rev Mineral Geochem* 75:149-181
- Marty B., Tolstikhin I. N. (1998) CO<sub>2</sub> fluxes from mid-ocean ridges, arcs and plumes. *Chem Geol* 145:233-248
- Marty, D.G. (1992) Ecology and metabolism of methanogens. In: Vially, R. Ed., *Bacterial Gas*. Editons Technip, Paris, pp. 13–24

- Mason OU, Nakagawa T, Rosner M, Van Nostrand JD, Zhou J, Maruyama A, Fisk MR, Giovannoni SJ (2010) First investigation of the microbiology of the deepest layer of ocean crust. *PLoS ONE* 5:e15399
- Mathez EA (1984) Influence of degassing on oxidation states of basaltic magma. *Nature* 310:371-375
- Max M. D. (2003) *Natural Gas Hydrate in Oceanic and Permafrost Environments*. Kluwer Academic Publishers, Dordrecht
- McCullom TM (2003) Formation of meteorite hydrocarbons by thermal decomposition of siderite (FeCO<sub>3</sub>). *Geochim Cosmochim Acta* 67:311-317
- McCullom TM (2008) Observational, experimental, and theoretical constraints on carbon cycling in mid-ocean ridge hydrothermal systems. *In: Modeling Hydrothermal Processes at Oceanic Spreading Centers: Magma to Microbe*. Lowell RP, Seewald J, Perfit MR, Metaxas A (eds). Am Geophys Union, Washington, DC, p 193-213
- McCullom TM (2013) Laboratory simulations of abiotic hydrocarbon formation in Earth's deep subsurface. *Rev Mineral Geochem* 75:467-494
- McCullom TM (2016) Abiotic methane formation during experimental serpentinization of olivine. *PNAS*, [www.pnas.org/cgi/doi/10.1073/pnas.1611843113](http://www.pnas.org/cgi/doi/10.1073/pnas.1611843113)
- McCullom TM and Donaldson C (2016) Generation of Hydrogen and Methane during Experimental
- McCullom TM, Ritter G, Simoneit BR (1999) Lipid synthesis under hydrothermal conditions by Fischer-Tropsch-type reactions. *Orig Life Evol Biosph* 29:153-166
- McCullom TM, Seewald JS (2001) A reassessment of the potential for reduction of dissolved CO<sub>2</sub> to hydrocarbons during serpentinization of olivine. *Geochim Cosmochim Acta* 65:3769-3778
- McCullom TM, Seewald JS (2006) Carbon isotope composition of organic compounds produced by abiotic synthesis under hydrothermal conditions. *Earth Planet Sci Lett* 243:74-84
- McCullom TM, Seewald JS (2007) Abiotic synthesis of organic compounds in deep-sea hydrothermal environments. *Chem Rev* 107:382-401
- McCullom TM, Sherwood Lollar B, Lacrampe-Couloume G, and Seewald JS (2010) The influence of carbon source on abiotic organic synthesis and carbon isotope fractionation under hydrothermal conditions. *Geochim Cosmochim Acta* 74:2717-2740

- Megharaj M., Ramakrishnan B., Venkateswarlu K., Sethunathan N., Naidu R., (2011) Bioremediation approaches for organic pollutants: A critical perspective. *Environ. Int.*, 37(8), 1362-1375, doi: 10.1016/j.envint.2011.06.003
- Mendeleeev D (1877) L'origine du petrole. *Revue Scientifique* 8:409-416
- Menez B, Pasini V, Brunelli D (2012) Life in the hydrated suboceanic mantle. *Nature Geosci* 5:133-137
- Milkov A. V. (2004) Global estimates of hydrate-bound gas in marine sediments: how much is really out there? *Earth-Science Rev* 66:183-197
- Morbidelli A, Lunine JI, O'Brien DP, Raymond SN, Walsh KJ (2012) Building terrestrial planets. *Ann Rev Earth Planet Sci* 40(1):251-275
- Mori T., Notsu K. (1997) Remote CO, COS, CO<sub>2</sub>, SO<sub>2</sub>, HCl detection and temperature estimation of volcanic gas. *Geophys Res Lett* 24(16):2047-2050, doi: 10.1029/97GL52058
- Mörner N. A., Etiope G. (2002) Carbon degassing from the lithosphere. *Global Planet Change* 33:185-203
- Mukhopadhyay A. (2015) Tolerance engineering in bacteria for the production of advanced biofuels and chemicals. *Trends Microbiol.*, 23(8), 498-508, doi: 10.1016/j.tim.2015.04.008.
- Neubeck A, Duc NT, Bastviken D, Crill P, Holm NG (2011) Formation of H<sub>2</sub> and CH<sub>4</sub> by weathering of olivine at temperatures between 30 and 70 °C. *Geochem Trans* 12:6, <http://www.geochemicaltransactions.com/content/12/1/6>
- Nicewonger M. R., Verhulst K. R., Aydin M., Saltzman E. S. (2016) Preindustrial atmospheric levels inferred from polar ice cores: A constraint on the geologic sources of atmospheric ethane and methane. *Geophys Res. Lett.* 43, 214-221, doi: 10.1002/2015GL066854
- Norris T.B., Wraith J.M., Castenholz R.W., McDermott T.R., (2002) Soil microbial community structure across a thermal gradient following a geothermal heating event. *Appl. Environ. Microbiol.*, 68(12), 6300-6309, doi: 10.1128/AEM.68.12.-6300\_6309.2002.
- Oppenheimer C., Kyle P. R. (2008) Probing the magma plumbing of Erebus volcano, Antarctica, by openpath FTIR spectroscopy of gas emissions. *J Volcanol Geotherm Res* 177(3):743-754, doi: 10.1016/j.jvolgeores.2007.08.022

- Oze C, Jones LC, Goldsmith JI, Rosenbauer RJ (2012) Differentiating biotic from abiotic methane genesis in hydrothermally active planetary surfaces. *Proc Natl Acad Sci USA* 109:9750-9754, doi:10.1073/pnas.1205223109
- Pan C., Yu L., Liu J., and Fu J. (2006) Chemical and carbon isotopic fractionations of gaseous hydrocarbons during abiogenic oxidation. *Earth Planet Sci Lett* 246:70–89.
- Peñuelas J, Asensio D, Tholl D, Wenke K, Rosenkranz M, Piechulla B, Schnitzler JP (2014). Biogenic volatile emissions from the soil. *Plant Cell Environ.*, doi: 10.1111/pce.12340
- Pili E., Kennedy B. M., Conrad M. E., Gratier J-P. (2011) Isotopic evidence for the infiltration of mantle and metamorphic CO<sub>2</sub>-H<sub>2</sub>O fluids from below in faulted rocks from the San Andreas Fault system. *Chem Geol* 281(3-4):242-252, doi: 10.1016/j.chemgeo.2010.12.011
- Pineau F, Javoy M (1983) Carbon isotopes and concentrations in mid-ocean ridge basalts. *Earth Planet Sci Lett* 62:239-257
- Potter J, Konnerup-Madsen J (2003) A review of the occurrence and origin of abiogenic hydrocarbons in igneous rocks. *Geol Soc Spec Pubs* 214:151-173
- Potter J, Rankin AH, Treloar PJ (2004) Abiogenic Fischer-Tropsch synthesis of hydrocarbons in alkaline igneous rocks; fluid inclusion, textural and isotopic evidence from the Lovozero complex, N. W. Russia. *Lithos* 75:311-330
- Potter J, Salvi S, Longstaffe FJ (2013) Abiogenic hydrocarbon isotopic signatures in granitic rocks: Identifying pathways of formation. *Lithos*, <http://dx.doi.org/10.1016/j.lithos.2013.10.001>
- Proskurowski G, Lilley MD, Seewald JS, Früh-Green GL, Olson EJ, Lupton JE, Sylva SP, Kelley DS (2008) Abiogenic hydrocarbon production at Lost City Hydrothermal Field. *Science* 319:604-607
- Rice D. D. and Claypool G. E., (1981) Generation, accumulation, and resource potential of biogenic gas. *AAPG Bull.* 65(1), 5-25. <http://archives.datapages.com/data/bulletns/1980-81/data/pg/0065/0001/0000/0005.htm>
- Ronov AB, Yaroshevskiy AA (1976) A new model for the chemical structure of the Earth's crust. *Geochem Int* 13:89-121
- Roussel EG, Bonavita M-AC, Querellou J, Cragg BA, Webster G, Prieur D, Parkes RJ (2008) Extending the sub-sea-floor biosphere. *Science* 320:1046-1046
- Russell M.J. and Martin W., (2004) The rocky roots of the acetyl-CoA pathway. *Trends Biochem. Sci.*, 29(7), 358-363, doi: 10.1016/j.tibs.2004.05.007

- Safronov AF (2009) Vertical zoning of oil and gas formation: Historico-genetic aspects. *Russian Geol Geophys* 50:327-333
- Salvi S, Williams-Jones AE (1997) Fischer-Tropsch synthesis of hydrocarbons during sub-solidus alteration of the Strange Lake peralkaline granite, Quebec/Labrador, Canada. *Geochim Cosmochim Acta* 61:83-99
- Sano Y. and Marty B., (1995) Origin of carbon in fumarolic gas from island arcs. *Chem. Geol. (Isotope Geoscience Section)*, 119, 265-274.
- Satterfield CN, Hanlon RT, Tung SE, Zou Z, Papaefthymiou GC (1986) Initial behaviour of a reduced fusedmagnetite catalyst in the Fischer-Tropsch synthesis. *Ind Eng Chem Prod Res Dev* 25:401-407.
- Sawyer G. M., Carn S. A., Tsanev V. I., Oppenheimer C, Burton MR (2008) Investigation into magma degassing at Nyiragongo volcano, Democratic Republic of the Congo. *Geochem Geophys Geosyst* 9:Q02017, doi: 10.1029/2007GC001829
- Schoell M. (1983) Genetic characterization of natural gases. *Am Assoc Pet Geol Bull* 67:2225–2238.
- Schoell M. (1988) Multiple origins of methane in the Earth. *Chem Geol* 71:1–10.
- Schrenk MO, Brazelton WJ, Lang SQ (2013) Serpentinization, carbon, and deep life. *Rev Mineral Geochem* 75:575-606
- Schrenk MO, Huber JA, Edwards KJ (2010) Microbial provinces in the subseafloor. *Ann Rev Marine Sci* 2:279-304
- Scott HP, Hemley RJ, Mao H, Herschbach DR, Fried LE, Howard WM, Bastea S (2004) Generation of methane in the Earth's mantle: *In situ* high pressure-temperature measurements of carbonate reduction. *Proc Natl Acad Sci USA* 101:14,023-14,026, doi:10.1073/pnas.0405930101
- Seewald J.S. (1994) Evidence for metastable equilibrium between hydrocarbons under hydrothermal conditions. *Nature*, 370, 285-287.
- Seewald J.S. (2001) Aqueous geochemistry of low molecular weight hydrocarbons at elevated temperatures and pressures: Constraints from mineral buffered laboratory experiments. *Geochim. Cosmochim. Ac.*, 65(10), 1641-1664.
- Seewald J.S. (2003) Organic-inorganic interactions in petroleum-producing sedimentary basins. *Nature*, 426, 327-333. Semrau J.D., 2011. Bioremediation via methanotrophy: overview of recent findings and suggestions for future research. *Front. Microbiol.*, 2, 209, doi: 10.3389/fmicb.2011.00209.

- Seewald JS, Zolotov MY, McCollom TM (2006) Experimental investigation of single carbon compounds under hydrothermal conditions. *Geochim Cosmochim Acta* 70:446-460
- Selley RC (1985) *Elements of Petroleum Geology*. W.H. Freeman, San Francisco
- Sephton MA (2002) Organic compounds in carbonaceous meteorites. *Natural Product Reports* 19:292-311
- Sephton MA, Hazen RM (2013) On the origins of deep hydrocarbons. *Rev Mineral Geochem* 75:449-465
- Seyfried WE, Foustoukos DI, Fu Q (2007) Redox evolution and mass transfer during serpentinization: An experimental and theoretical study at 200 °C, 500 bar with implications for ultramafic-hosted hydrothermal systems at Mid-Ocean Ridges. *Geochim Cosmochim Acta* 71:3872-3886
- Sherwood Lollar B, Lacrampe-Couloume G, Slater GF, Ward J, Moser DP, Gihring TM, Lin L, Onstott TC (2006) Unravelling abiogenic and biogenic sources of methane in the Earth's deep subsurface. *Chem Geol* 226:328-339
- Sherwood Lollar B, Voglesonger K, Lin L-H, Lacrampe-Couloume G, Telling J, Abrajano TA, Onstott TC, Pratt LM (2007) Hydrogeologic controls on episodic H<sub>2</sub> release from Precambrian fractured rocks – Energy for deep subsurface life on Earth and Mars. *Astrobiology* 7:971-986, doi:10.1089/ast.2006.0096
- Sherwood Lollar B, Lacrampe-Couloume G, Voglesonger K, Onstott TC, Pratt LM, Slater GF (2008) Isotopic signatures of CH<sub>4</sub> and higher hydrocarbon gases from Precambrian Shield sites: A model for abiogenic polymerization of hydrocarbons. *Geochim Cosmochim Acta* 72:4778-4795
- Sherwood Lollar B, Westgate TD, Ward JA, Slater GF, Lacrampe-Couloume G (2002) Abiogenic formation of alkanes in the Earth's crust as a minor source for global hydrocarbon reservoirs. *Nature* 416:522-524
- Sherwood Lollar B. and McCollom T.M. (2006) Geochemistry: biosignatures and abiotic constraints on early life. *Nature* 444, doi:10.1038/nature05499.
- Sherwood Lollar B., (2004) Life's Chemical Kitchen. *Science*, 304, 972-973.
- Shi B, Jin C (2011) Inverse kinetic isotope effects and deuterium enrichment as a function of carbon number during formation of C-C bonds incobalt catalyzed Fischer-Tropsch synthesis. *Appl Catal A* 393:178-173
- Shipp J., Gould I.R., Herckes P., Shock E.L., Williams L.B., Hartnett H.E. (2013) Organic functional group transformations in water at elevated temperature and pressure:

- Reversibility, reactivity, and mechanisms. *Geochim. Cosmochim. Ac.*, 104, 194-209, doi: 10.1016/j.gca.2012.11.014.
- Shipp J., Gould I.R., Shock E.L., Williams L.B., Hartnett H.E. (2014) Sphalerite is a geochemical catalyst for carbon-hydrogen bond activation. *PNAS*, 111(32), 11642-11645, doi: 10.1073/pnas.1324222111.
- Shock E.L., Canovas P., Yang Z., Boyer G., Johnson K., Robinson K., Fecteau K., Windman T., Cox A. (2013) Thermodynamics of organic transformations in hydrothermal fluids. *Rev. Mineral. Geochem.*, 76, 311-350, doi: 10.2138/rmg.2013.76.9.
- Shock EL (1990) Geochemical constraints on the origin of organic compounds in hydrothermal systems. *Origins Life Evol Biosphere* 20:331-367
- Shock EL (1992) Chemical environments of submarine hydrothermal systems. *Origins Life Evol Biosphere* 22:67-107
- Siskin M., Katritzky A.R. (2000) A review of the reactivity of organic compounds with oxygen-containing functionality in superheated water. *J. Anal. Appl. Pyrolysis*, 54, 193-214.
- Sivan O., Schrag D.P., Murray R.W. (2007) Rates of methanogenesis and methanotrophy in deep-sea sediments. *Geobiology* 5, 141-151, DOI: 10.1111/j.1472-4669.2007.00098.x
- Sleep N. H., Zahnle K. (2001) Carbon dioxide cycling and implications for climate on ancient earth. *J Geophys Res* 106:1373-1399
- Sleep NH, Meibom A, Fridriksson T, Coleman RG, Bird DK (2004) H<sub>2</sub>-rich fluids from serpentinization: geochemical and biotic implications. *Proc Natl Acad Sci USA* 101:12818-12823
- Soma Y., Soma M. (1989) Chemical reactions of organic compounds on clay surfaces. *Environ. Health Perspect.*, 83, 205-214.
- Steele A, McCubbin FM, Fries MD, Golden DC, Ming DW, Benning LG (2012) Graphite in the Martian meteorite Allan Hills 84001. *Am Mineral* 97:1256-1259
- Suda, K., Ueno, Y., Yoshizaki, M., Nakamura, H., Kurokawa, K., Nishiyama, E., Yoshino, K., Hongoh, Y., Kawachi, K., Omori, S., Yamada, K., Yoshida, N., Maruyama, S., 2014. Origin of methane in serpentinite-hosted hydrothermal systems: the CH<sub>4</sub>-H<sub>2</sub>-H<sub>2</sub>O hydrogen isotope systematics of the Hakuba Happo hot spring. *Earth Planet. Sci. Lett.* 386, 112e125.
- Taran Y.A., Giggenbach W.F. (2003) Geochemistry of Light Hydrocarbons in Subduction-Related Volcanic and Hydrothermal Fluids. Society of Economic Geologists Special Publication, 10, 61-74.

- Taran YA, Kliger GA, Cienfuegos E, Shuykin AN (2010a) Carbon and hydrogen isotopic compositions of products of open-system catalytic hydrogenation of CO<sub>2</sub>: Implications for abiogenic hydrocarbons in Earth's crust. *Geochim Cosmochim Acta* 71:4474-4487
- Taran YA, Kliger GA, Sevastianov VS (2007) Carbon isotope effects in the open-system Fischer-Tropsch synthesis. *Geochim Cosmochim Acta* 71:4474-4487
- Taran YA, Varley NR, Inguaggiato S, Cienfuegos E (2010b) Geochemistry of H<sub>2</sub>- and CH<sub>4</sub>-enriched hydrothermal fluids of Socorro Island, Revillagigedo Archipelago, Mexico. Evidence for serpentinization and abiogenic methane. *Geofluids* 10:542-555, doi:10.1111/j.1468-8123.2010.00314.x
- Tassi F., Martinez C., Vaselli O., Capaccioni B., Viramonte J., (2005a). Light hydrocarbons as redox and temperature indicators in the geothermal field of El Tatio (northern Chile). *Appl. Geochem.*, 20, 2049-2062, doi: 10.1016/j.apgeochem.20-05.07.013.
- Tassi F., Nisi B., Cardellini C., Capecchiacci F., Donnini M., Vaselli O., Avino R., Chiodini G., (2013). Diurnal soil emission of hydrothermal gases (CO<sub>2</sub>, CH<sub>4</sub>, C<sub>2</sub>H<sub>6</sub>) at Solfatara crater (Campi Flegrei, southern Italy). *Appl. Geochem.*, 35, 142-153, doi: 10.1016/j.apgeochem.2013.03.020.
- Tassi F., Vaselli O., Capaccioni B., Giolito C., Duarte E., Fernandez E., Minissale A., Magro G., (2005b). The hydrothermal-volcanic system of Rincon de la Veja volcano (Costa Rica): A combined (inorganic and organic) geochemical approach to understanding the origin of the fluid discharges and its possible application to volcanic surveillance. *J. Volcanol. Geoth. Res.*, 148, 315-333, doi: 10.1016/j.jvolgeores.2005.05.001.
- Templeton A. S., Chu K.H., Alvarez-Cohen L., Conrad M. E., (2006) Variable carbon isotope fractionation expressed by aerobic CH<sub>4</sub>-oxidizing bacteria. *Geochim. Et Cosmochim. Acta* 70, 1739-1752.
- Troll V. R., Hilton D. R., Jolis E. M., Chadwick J. P., Blythe L. S., Deegan F. M., Schwarzkopf L. M., Zimmer M. (2012) Crustal CO<sub>2</sub> liberation during the 2006 eruption and earthquake events at Merapi volcano, Indonesia. *Geophys Res Lett* 39:L11302, doi: 10.1029/2012GL051307
- Ueno Y., Yamada K., Yoshida N., Maruyama S., Isozaki Y. (2006a) Evidence from fluid inclusions for microbial methanogenesis in the early Archaean era. *Nature* 440: 516–519.
- Ueno Y., Yamada K., Yoshida N., Maruyama S., Isozaki Y. (2006b) Geochemistry: biosignatures and abiotic constraints on early life (Reply). *Nature* 444:E18–E19.

- Van Zuilen MA, Lepland A, Arrhenius G (2002) Reassessing the evidence for the earliest traces of life. *Nature* 418:627-630
- Viveiros F., Cardellini C., Ferreira T., Caliro S., Chiodini G., Silva C., (2010) Soil O<sub>2</sub> emissions at Furnas Volcano, São Miguel Island, Azores archipelago: Volcano monitoring perspectives, geomorphologic studies, and land use planning application. *J. Geophys. Res.*, 115(B12208), doi: 10.1029/2010JB007555.
- Wächtershäuser G (1990) Evolution of the first metabolic cycles. *Proc Natl Acad Sci USA* 87:200-204
- Wächtershäuser G (1993) The cradle chemistry of life – on the origin of natural-products in a pyrite-pulled chemoautotrophic origin of life. *Pure Appl Chem* 65:1343-1348
- Wächtershäuser G., (1988) Before enzymes and templates: Theory of surface metabolism. *Micorbiol. Rev.*, 52(4), 452-484.
- Walker J. C. G. , Hays P. B., Kasting J. F. (1981) A negative feedback mechanism for the long-term stabilization of Earth's surface temperature. *J Geophys Res* 86:9776-9782, doi: 10.1029/JC086iC10p09776
- Wang W. C., Yung Y. L., Lacis A. A., Mo T., Hansen J. E. (1976) Greenhouse effects due to man-made perturbations of trace gases. *Science* 194(4266): 685-690
- Warren PH (2011) Stable-isotopic anomalies and the accretionary assemblage of the Earth and Mars: A subordinate role for carbonaceous chondrites. *Earth Planet Sci Lett* 311(1-2):93-100
- Watts S. F. (2000) The mass budgets of carbonyl sulfide, dimethyl sulfide, carbon disulfide and hydrogen sulfide. *Atmos Environ* 34:761-779
- Wei, L., Schimmelmann, A., Mastalerz, M., Lahann, R.W., Sauer, P.E., Drobnik, A., Strapoć, D., Mango, F.D. (2018) Catalytic generation of methane at 60 to 100 °C and 0.1 to 300 MPa from source rocks containing kerogen Types I, II, and III, *Geochimica et Cosmochimica Acta*, doi: <https://doi.org/10.1016/j.gca.2018.04.012>
- Whiticar M (1990) A geochemical perspective of natural gas and atmospheric methane. *Org Geochem* 16:531-54
- Williams LB, Canfield B, Vogelsonger KM, Holloway JR (2005) Organic molecules formed in a “primordial womb.” *Geology* 33:913-916
- Zeebe R. E., Caldeira K. (2008) Close mass balance of long-term carbon fluxes from ice-core CO<sub>2</sub> and ocean chemistry records. *Nature Geosci* 1:312-315

Zolotov MY, Shock EL (2000) An abiotic origin for hydrocarbons in the Allan Hills 84001 martian meteorite through cooling of magmatic and impact-generated gases. *Meteorit Planet Sci* 35:629-638